

Photocatalytic two-electron processes as alternatives to Barbier/Grignard-type reactions

Dissertation

Zur Erlangung des Doktorgrades der Naturwissenschaften

(Dr. rer. nat.)

an der Fakultät für Chemie und Pharmazie

der Universität Regensburg



vorgelegt von

Anna Berger

aus Regensburg

2019

This work has been carried out between November 2016 and November 2019 under the supervision of Prof. Dr. Burkhard König at the University of Regensburg, Institute of Organic Chemistry.

Date of submission: 31.10.2019

Date of colloquium: 17.12.2019

Board of examiners:	Prof. Dr. Patrick Nürnberger	(chair)
	Prof. Dr. Burkhard König	(1 st referee)
	Prof. Dr. Alexander Breder	(2 nd referee)
	Prof. Dr. Frank-Michael Matysik	(examiner)

"Erstzunehmende Forschung erkennt man daran, dass plötzlich zwei Problem existieren, wo es vorher nur eines gegeben hat."

Thorstein Bunde Veblen

TABLE OF CONTENTS

1	METHODS FOR THE PHOTOCATALYTIC GENERATION OF CARBANIONS ..	1
1.1	Introduction	3
1.2	Generation of carbanions after radical trapping	5
1.2.1	Intermolecular reactions with electrophiles	5
1.2.2	Intramolecular cyclisation reactions	6
1.2.3	Eliminations.....	7
1.3	Generation of carbanions <i>via</i> two consecutive one-electron transfer steps	8
1.4	Redox-neutral generation of carbanions from one starting material.....	10
1.5	Conclusion and outlook.....	12
1.6	References.....	13
2	PHOTOCATALYTIC ORGANOMETALLIC REACTIONS USING <i>IN SITU</i> GENERATED ZEROVALENT METALS	17
2.1	Introduction	19
2.2	Results and discussion	20
2.2.1	Photocatalytic generation of Zn(0)	20
2.2.2	Reformatsky reaction.....	22
2.2.3	Simmons-Smith cyclopropanation	23
2.2.4	Barbier reaction	26
2.2.5	Enhanced photocatalytic zinc generation using 4CzIPN	28
2.2.6	Two-step/one-pot Barbier-type reactions	31
2.2.7	Attempted formation of C(sp ²)-organozinc compounds.....	33
2.3	Conclusion	35
2.4	Experimental part	36
2.4.1	General information	36
2.4.2	General procedures.....	38
2.4.2.1	Synthesis of 4CzIPN.....	38

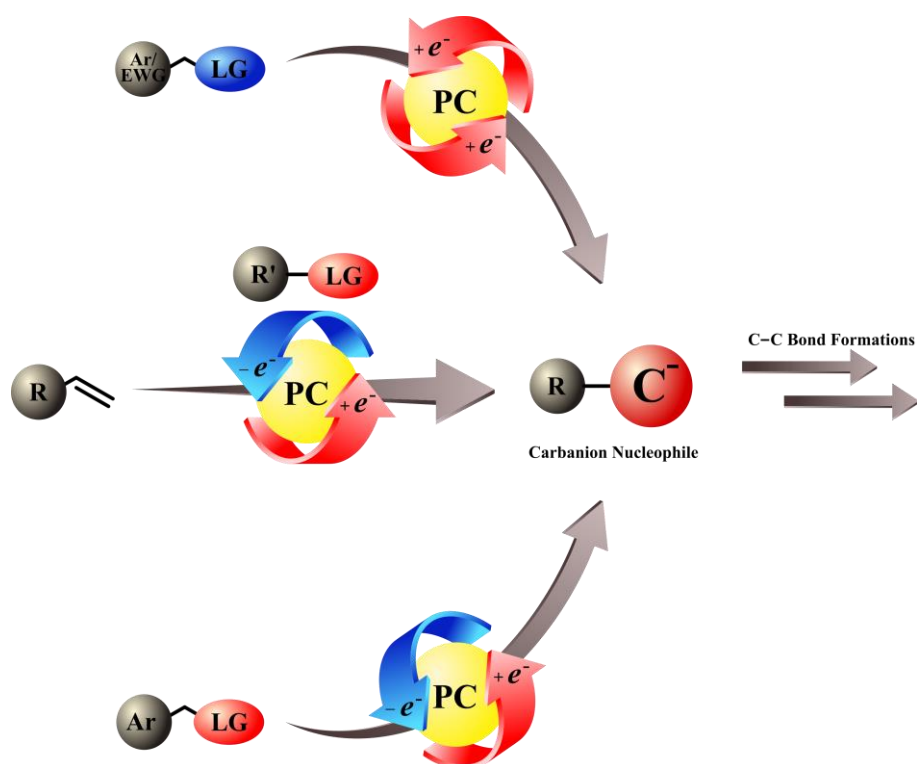
2.4.2.2	General procedure for the preparation of anhydrous ZnCl_2	38
2.4.2.3	General procedures for photocatalytic reactions	39
2.5	References.....	44
3	PHOTOCATALYTIC BARBIER REACTION - VISIBLE-LIGHT INDUCED ALLYLATION AND BENZYLATION OF ALDEHYDES AND KETONES.....	47
3.1	Introduction.....	49
3.2	Results and discussion	51
3.3	Conclusion	59
3.4	Experimental part.....	60
3.4.1	General information.....	60
3.4.2	General procedures	62
3.4.2.1	Synthesis of photocatalysts	62
3.4.2.2	Synthesis of starting materials	65
3.4.2.3	General procedure for the photocatalytic allylation of aldehydes and ketones	66
3.4.3	Detailed optimization of the reaction conditions	77
3.4.4	Mechanistic investigations.....	80
3.4.4.1	Fluorescence quenching experiments	82
3.4.4.2	Cyclic voltammetry measurements.....	86
3.4.4.3	UV/Vis measurements.....	88
3.4.4.4	Quantum yield determination	89
3.4.4.5	NMR-experiments	90
3.5	NMR-spectra	91
3.6	References.....	122
4	PHOTOCATALYTIC CARBANION GENERATION - BENZYLATION OF ALIPHATIC ALDEHYDES TO SECONDARY ALCOHOLS.....	125
4.1	Introduction.....	127
4.2	Results and discussion	129
4.3	Conclusion	135

4.4	Experimental part	136
4.4.1	General information.....	136
4.4.2	Synthetic procedures	138
4.4.2.1	Synthesis of photocatalysts	138
4.4.2.2	Synthesis of starting materials	141
4.4.3	Photocatalytic benzylation of aldehydes.....	142
4.4.4	Detailed reaction optimization process	158
4.4.5	Photocatalytic benzylation of acetone and use of potassium benzyl-trifluoroborate as a carbanion precursor.....	163
4.4.6	Attempted S _N 2 reactions with potassium benzyltrifluoroborate as a carbanion precursor.....	165
4.4.7	Mechanistic investigations	166
4.4.7.1	Photocatalytic benzylation with NBu ₄ PA (5) as carbanion precursor	166
4.4.7.2	Photo-degradation of 4CzIPN	167
4.4.7.3	Cyclic voltammetry measurement.....	172
4.4.7.4	Fluorescence quenching studies.....	174
4.4.7.5	<i>In situ</i> FT-IR measurements.....	177
4.4.7.6	Deuterium labeling studies.....	178
4.4.7.7	NMR <i>in-situ</i> irradiation studies	181
4.4.7.8	E1cb-elimination reactions	182
4.4.7.9	DFT-calculations.....	186
4.4.7.10	Photocatalytic benzylation of aromatic aldehydes	205
4.5	NMR-spectra	208
4.6	References.....	253
5	PHOTOCATALYTIC CARBANION GENERATION FROM C–H BONDS - REDUCTANT FREE BARBIER/GRIGNARD-TYPE REACTIONS.....	257
5.1	Introduction	259
5.2	Results and discussion	261
5.3	Conclusion	268

5.4	Experimental part.....	269
5.4.1	General information.....	269
5.4.2	General procedures	271
5.4.2.1	Synthesis of photocatalysts.....	271
5.4.2.2	Synthesis of starting materials	277
5.4.2.3	General procedure for the photocatalytic generation of carbanions from benzylic C–H bonds.....	279
5.4.3	Detailed optimization of the reaction conditions	301
5.4.3.1	Optimization process with ketones as electrophiles.....	301
5.4.3.2	Optimization process with aldehydes as electrophiles	306
5.4.4	Unsuccessful transformations.....	312
5.4.5	Mechanistic investigations.....	313
5.4.5.1	Reaction kinetics	313
5.4.5.2	Fluorescence quenching studies.....	314
5.4.5.3	Cyclic voltammetry measurements.....	316
5.4.5.4	Radical-radical homocoupling.....	317
5.4.5.5	Intramolecular ring closure using an ester as an electrophile	318
5.5	NMR-spectra	319
5.6	References.....	365
6	SUMMARY	371
7	ZUSAMMENFASSUNG	377
8	APPENDIX	383
8.1	Abbreviations.....	383
8.2	Curriculum Vitae	387
9	DANKSAGUNG	393

CHAPTER 1

1 Methods for the photocatalytic generation of carbanions



A. L. Berger and K. Donabauer wrote the manuscript. B. König supervised the project.

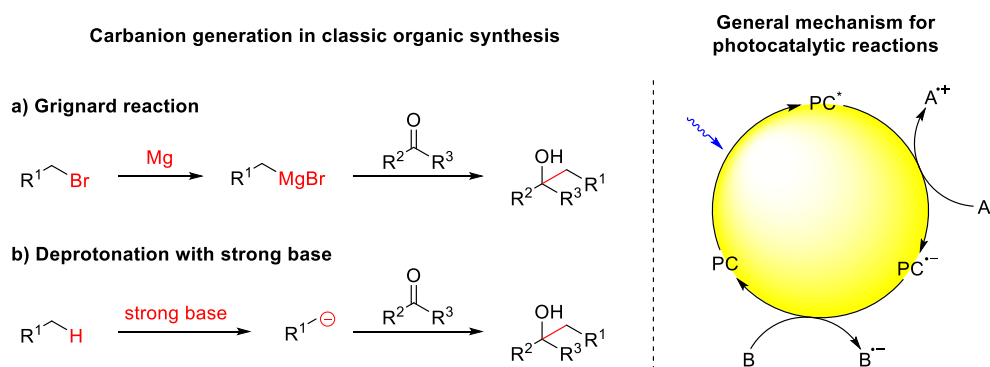
1.1 Introduction

Carbanions are among the most important intermediates in synthetic organic chemistry as they readily undergo reactions with various electrophiles and therefore enable the formation of new carbon–carbon or carbon–heteroatom bonds. Grignard and Barbier reactions are still among the most important C–C bond forming reactions in modern organic synthesis, although they have been first reported over a century ago.^[1] In these reactions, a zerovalent metal like magnesium or zinc is added to an organic halide to generate a highly nucleophilic organometal reagent, which is capable of reacting with electrophiles such as aldehydes, ketones, carbon dioxide, esters and several more, enabling the formation of a wide range of different products (Scheme 1-1a).^[2] Over the last years, the applicability of the Grignard and Barbier reaction has been further expanded, for example by the combination with metal-catalyzed cross-coupling reactions.^[3] The scope of viable substrates has been increased,^[4] and the reactions can be performed with high regio- and stereoselectivity^[5] and under mild reaction conditions.^[6] While these reactions are very versatile, they still have some disadvantages. The reactions require stoichiometric amounts of metals, which are converted to metal halide salts during the reaction, generating high amounts of waste products. In addition, they also require prefunctionalized organohalides as starting materials which are often not commercially available and need to be synthesized.^[7]

Another possible method for the formation of carbanions would be the direct deprotonation of C–H bonds, eliminating the need for prefunctionalized starting materials (Scheme 1-1b). However, in absence of stabilizing functional groups, C–H bonds in organic substrates usually have a very low acidity. Therefore their deprotonation would require the use of very active non-nucleophilic bases such as LDA ($pK_a = 36$ in THF) or *n*-BuLi ($pK_a = \text{approx. } 50$).^[8] The use of such strong bases limits the selectivity and functional group tolerance of the reaction and promotes the formation of side products. Additionally, most bases that are strong enough for these transformations are lithium-based causing the generation of stoichiometric amounts of metal salt waste products.

In recent years, photocatalysis has become increasingly popular, enabling a variety of many new transformations that could previously not be obtained with classical organic reactions.^[9] In photocatalysis, visible light is used to excite a catalyst which can either be metal-based or an organic dye. The excited state of this catalyst is capable of donating or accepting electrons to or from numerous substrates, generating radical cations, radical anions or neutral radicals as

intermediates which can subsequently undergo various reactions, e.g. trapping by alkenes,^[10] alkynes^[11] or arenes,^[12] radical-radical cross-couplings (Scheme 1-1, right side).^[13] New innovations, such as the dual-catalytic combination with metal- or organocatalysis,^[14] photocatalytic C–H bond activations,^[15] or the development of stereo- and enantioselective transformations^[16] have expanded the applicability of photocatalytic reactions in the last years. Despite these developments, all common photocatalytic reactions proceed *via* single electron transfer (SET) processes and are therefore limited to radical reactivity.



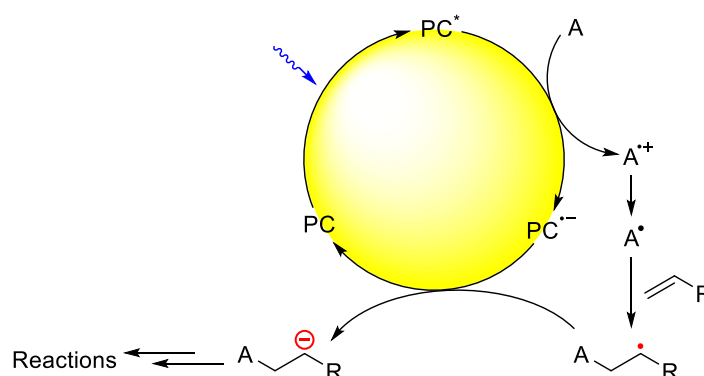
Scheme 1-1 – Left side: generation of carbanion intermediates in classic organic synthesis; right side: schematic mechanism for the formation of radical anions and radical cations in photoredox reactions, with A being an electron donor and B an electron acceptor.

The interest in the photocatalytic generation of carbanions, has increased recently and several groups have described the appearance of anionic intermediates in their reports. In most cases, the carbanion is formed during the regeneration of the photocatalyst to the ground state and is then only protonated to obtain the corresponding product.^[17] Utilizing a photocatalytically generated carbanion intermediate for a subsequent C–C bond formation has the potential to overcome the above mentioned downsides of Grignard-type reactions or classical carbanion generations, as the use of strong metal bases can be avoided. In this way, novel reaction pathways can be disclosed, in some cases employing simple, readily available, starting materials in high or even full atom economy under mild conditions.

This chapter will provide an overview of methods, in which photocatalytically generated carbanions have been used synthetically. Three different concepts for their photocatalytic generation will be introduced.

1.2 Generation of carbanions after radical trapping

So far, carbanions in photocatalysis have mainly been generated after trapping a previously formed radical with an alkene. The resulting, more stable radical species was then reduced again, forming a carbanion while regenerating the ground state of the photocatalyst and closing the catalytic cycle (Scheme 1-2). The resulting anion could then be used for several transformations, such as reactions with electrophiles, eliminations or intramolecular cyclisation reactions.



Scheme 1-2 – Schematic mechanism for the photocatalytic generation of carbanions after radical trapping with A being an electron donor and radical precursor and R being a group capable of stabilizing the radical intermediate (electron withdrawing or an aromatic group).

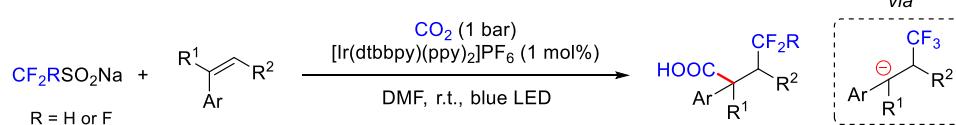
1.2.1 Intermolecular reactions with electrophiles

To our knowledge, the Martin group was the first that used this strategy for the generation of carbanions synthetically in their report on the intermolecular dicarbofunctionalization of styrenes with CO₂ (Scheme 1-3a).^[18] In this work, radical precursors such as sulfinates, trifluoroborates or oxalates were used to generate radical intermediates by photocatalytic oxidation. After trapping with styrenes the resulting benzylic radical was reduced to the corresponding carbanion which undergoes nucleophilic attacks with CO₂, generating carboxylic acids as products. Similar strategies were used by Wu *et al.* for the difunctionalization of alkenes with CO₂ and silanes,^[19] or by the Yu group in their report on the synthesis of β-phosphono carboxylic acids by the phosphonocarboxylation of alkenes with CO₂ (Scheme 1-3b).^[20] All of these examples use CO₂ as an electrophile to trap the carbanion and so far, reports using other electrophiles are scarce. In 2017 the Song group reported the thiotrifluoromethylation of alkenes with sodium trifluoromethanesulfinate as a precursor to generate a CF₃-radical which is trapped by terminal alkenes. After reduction to the carbanion

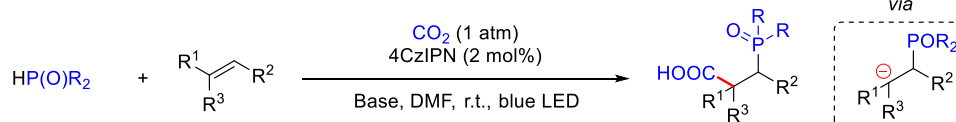
a reaction with benzenesulfonothioates takes place and the desired products are generated (Scheme 1-3c).^[21]

Generation of carbanions from radical + DB - Intermolecular reaction with electrophiles

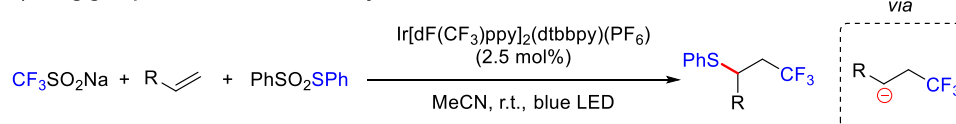
a) Martin group 2017: dicarbofunctionalization of styrenes



b) Yu group 2019: phosphonocarboxylation of alkenes



c) Song group 2017: thiotrifluoromethylation of alkenes



Scheme 1-3 – Examples for intermolecular reactions of carbanions generated by photocatalysis with electrophiles: a) dicarbofunctionalization of styrenes with CO₂,^[18] b) phosphonocarboxylation of alkenes with CO₂,^[20] c) thiotrifluoromethylation of terminal alkenes with sodium triflate and benzenesulfonothioates.^[21]

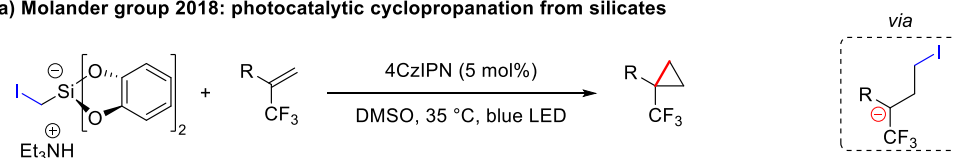
1.2.2 Intramolecular cyclisation reactions

Another reaction which has been widely used is the intramolecular cyclisation by a nucleophilic substitution. This strategy was first reported in 2018 by Molander *et al.* in their work on the redox-neutral cyclopropanation *via* radical/polar crossover (Scheme 1-4a).^[22] They use triethylammonium bis(catecholato)silicates as precursors to generate iodomethyl radicals by photocatalytic oxidation. After trapping by an alkene and subsequent reduction by the photocatalyst an anion is formed which can undergo a S_N2 reaction with iodide as a leaving group. The same concept was used for the cyclopropanation of α -substituted vinylphosphonates with chloromethyl silicates as methylene transfer reagents.^[23] Also in 2018, Aggarwal and co-workers reported a similar method for the synthesis of cyclopropanes using carboxylic acids as radical precursors, electron poor alkenes as trapping reagents and chloride as the leaving group (Scheme 1-4b).^[24] In contrast to the work of Molander, where the iodide is appended to the radical precursor, the chloride which is acting as a leaving group is attached to the alkene in this work, illustrating a different approach and yielding different products. Apart from carboxylic acids, this concept could also be applied for other radical precursors such as silicates, potassium trifluoroborates or dihydropyridines,^[25] as well as for the synthesis

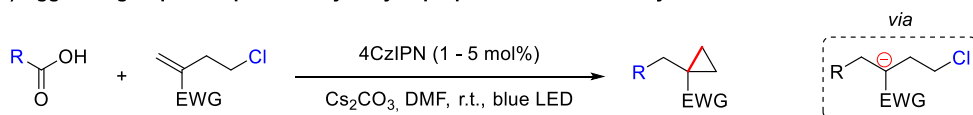
of cyclobutanes^[26] and saturated nitrogen heterocycles.^[27] Another notable application of this concept was reported by the group of Zhiwei Zuo (Scheme 1-4c).^[28] They use a combination of diphenylanthracene as a photo- and cerium(III) chloride as a hydrogen atom transfer (HAT) catalyst to enable the abstraction of hydroxy hydrogen atoms from cycloalkanols. The resulting oxygen radical quickly undergoes β -scission, leading to a ring opening and the generation of a carbon centered radical which is subsequently trapped by an electron deficient alkene. Analogously to the other reports, this radical is reduced to the corresponding carbanion by the photocatalyst, but in this case instead of a nucleophilic substitution, an intramolecular attack of a carbonyl group takes place, resulting in the formation of a seven membered ring.

Generation of carbanions from radical + DB - Intramolecular cyclisation reactions

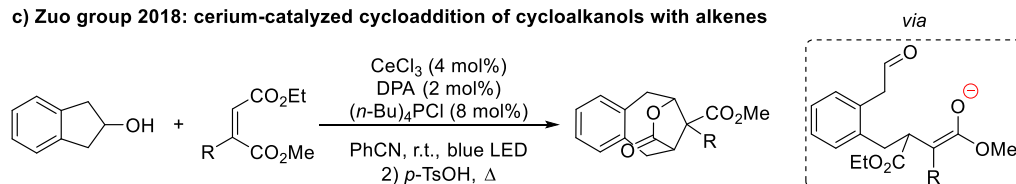
a) Molander group 2018: photocatalytic cyclopropanation from silicates



b) Aggarwal group 2018: photocatalytic cyclopropanation from carboxylic acids



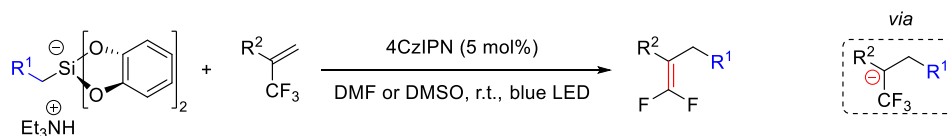
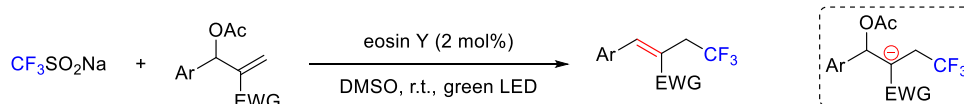
c) Zuo group 2018: cerium-catalyzed cycloaddition of cycloalkanols with alkenes



Scheme 1-4 – Examples for intramolecular cyclisation reactions using carbanions generated by photocatalysis: a) redox-neutral photocatalytic cyclopropanation,^[22] synthesis of functionalized cyclopropanes from carboxylic acids,^[24] c) cerium-catalyzed formal cycloaddition of cycloalkanols with alkenes through dual photoexcitation.^[28]

1.2.3 Eliminations

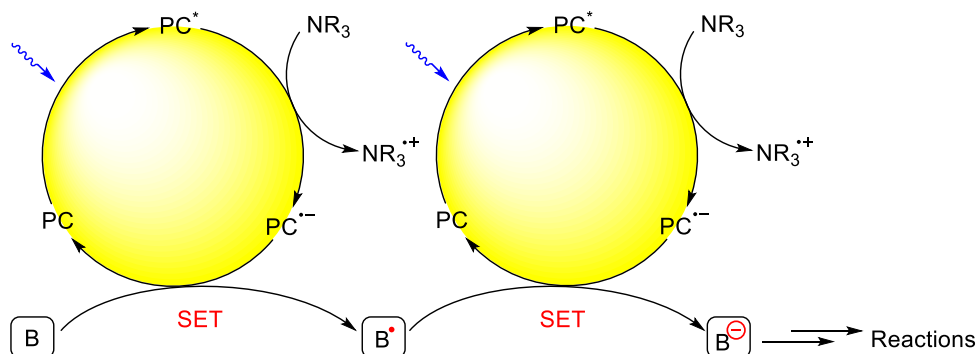
Another group of reactions using carbanions generated by photocatalysis in synthesis are E1cb eliminations, first reported by Molander and co-workers in 2017 (Scheme 1-5a).^[29] Silicates, potassium trifluoroborates or α -silylamines are used as precursors to generate radicals which are trapped by trifluoromethylalkenes. After reduction to the carbanion, a E1cb elimination of a fluoride takes place, generating the desired *gem*-difluoroalkenes. The same concept was used by Singh *et al.* for the γ -trifluoromethylation of Baylis-Hillman acetates. Sodium trifluoromethanesulfinate was used as a radical precursor, electron poor alkenes as trapping reagents and the desired product was obtained after the elimination of acetate (Scheme 1-5b).^[30]

Generation of carbanions from radical + DB - Eliminations**a) Molander group 2017: synthesis of 1,1-difluoroalkenes****b) Singh group 2019: γ -trifluoromethylation of Baylis-Hillman acetates**

Scheme 1-5 – Examples for elimination reactions using carbanions generated by photocatalysis: a) synthesis of 1,1-difluoroalkene carbonyl mimics,^[29] b) γ -trifluoromethylation of Baylis-Hillman acetates.^[30]

1.3 Generation of carbanions *via* two consecutive one-electron transfer steps

While the concept of redox-neutral carbanion-generation after radical trapping is already quite well established and has been used for many desirable reactions, it has the disadvantage that two separate molecules have to be combined first to enable the generation of a carbanion. While this might be beneficial for some applications it lacks the versatility of classic organic reactions such as the Grignard reactions, where almost any molecule with a suitable prefunctionalization can be transformed into an anionic intermediate. The most intuitive way to enable photocatalytic carbanion generations would be to replace the metal which is used for the twofold reduction of the neutral substrate in Barbier- or Grignard-type reactions by two subsequent photocatalytic single electron transfers (Scheme 1-6).

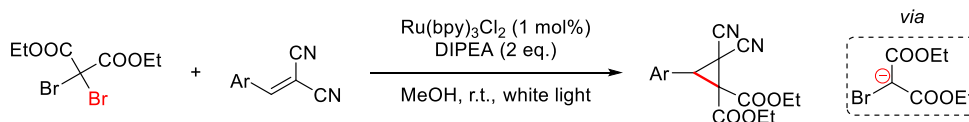


Scheme 1-6 – Schematic mechanism for the photocatalytic generation of carbanions *via* two subsequent one-electron reduction steps with B being an electron acceptor and precursor of a stabilized radical.

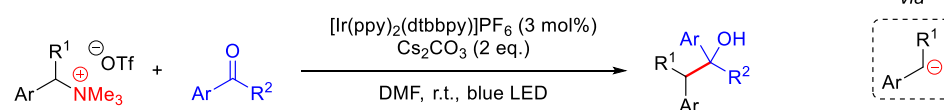
Although the two-step reduction of benzyl bromide to the corresponding benzylic anion using $\text{Ru}(\text{bpy})_3^{2+}$ as a photocatalyst has already been reported in 1984,^[31] reports where this concept is utilized for synthetic transformations are rare. In 2015, the group Guo reported the cyclopropanation of dibromomalonates with alkenes *via* double-SET (Scheme 1-7a).^[32] After the first reduction and subsequent bromide elimination of dibromomalonate, the resulting radical is reduced again, generating a carbanion which can add to an alkene, leading to an intramolecular cyclisation and yielding the desired cyclopropane product. Unfortunately, the scope of this method is extremely limited, as it is limited to strongly electron deficient dibromomalonates. In 2018, Yu *et al.* reported an elegant method for the coupling of tetraalkyl ammonium salts with various carbonyl compounds which proceeds without external reductants (Scheme 1-7b).^[33] In this work, benzylic tetraalkyl ammonium salts are reduced twice, yielding a benzylic radical which is capable of reacting with aromatic aldehydes or ketones and carbon dioxide. After the first photocatalytic SET, trimethylamine is cleaved from the starting material, enabling the regeneration of the photocatalyst without the addition of a sacrificial electron donor as an external reductant.

Generation of carbanions *via* two consecutive one-electron transfer steps

a) Guo group 2015: cyclopropanation of dibromomalonates with alkenes *via* two SET steps



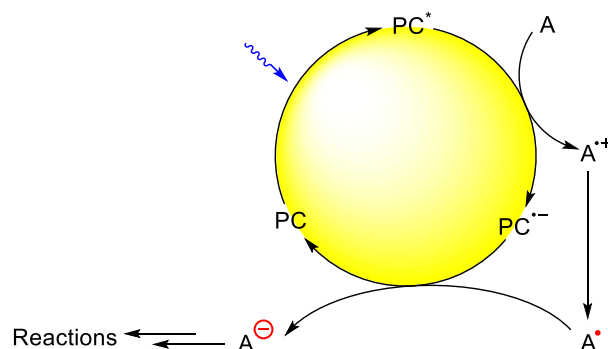
b) Yu group 2018: cross-electrophile couplings of tetraalkyl ammonium salts



Scheme 1-7 – Examples for reactions of carbanions generated by two subsequent photocatalytic reductions: a) cyclopropanation of dibromomalonates with alkenes *via* double-SET,^[32] b) external-reductant-free cross-electrophile couplings of tetraalkyl ammonium salts.^[33]

1.4 Redox-neutral generation of carbanions from one starting material

While the carbanion generation *via* two single electron transfer steps described above is mechanistically similar to conventional organometallic reactions, it also has the drawback of requiring sacrificial electron donors to close the catalytic cycle, leading to the formation of stoichiometric amounts of amine waste products. To circumvent these disadvantages, our group has developed a concept for the redox-neutral formation of carbanions by first generating a radical through photocatalytic oxidation, which is then directly reduced to the corresponding carbanion in the same catalytic cycle, without being trapped by an alkene first (Scheme 1-8). This concept enables the photocatalytic generation of carbanions from a single precursor molecule without the need for sacrificial electron donors.



Scheme 1-8 – Schematic mechanism for the redox-neutral photocatalytic generation of carbanions from a single substrate with A being an electron donor and precursor of a stabilized radical.

The first synthetic application of this concept has been published by our group in this year (Scheme 1-9a).^[34] Benzylic radicals are generated by the photocatalytic oxidation and subsequent CO₂ extrusion of carboxylic acids. The well-stabilized radicals are reduced again, closing the catalytic cycle and generating the desired benzylic carbanion, which could be trapped by aliphatic aldehydes to generate secondary alcohols as products. This method however still suffers from some drawbacks. While the use of external reductants is not necessary, stoichiometric amounts of base are required for the deprotonation of the carboxylic acid and CO₂ is released as a byproduct, diminishing the atom economy of the reaction. Furthermore, synthetically useful yields were only obtained for aldehydes as carbanion-traps while only traces of product were obtained for less active electrophiles, such as ketones, due to the competing protonation of the carbanionic intermediate. To overcome these limitations, we recently reported the carbanion generation from C–H bonds utilizing a dual-catalytic

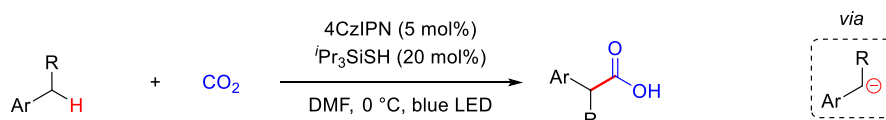
approach by combining photo- and hydrogen atom transfer catalysis (Scheme 1-9b and c).^[35] Instead of directly oxidizing a radical precursor to obtain the desired radical intermediate, a HAT catalyst is added, which - after oxidation by the photocatalyst – is capable of abstracting a hydrogen atom of a suitable unfunctionalized substrate. The thus generated radical is now reduced to the corresponding carbanion while the HAT catalyst is regenerated by deprotonation. This approach enables a redox-neutral, waste- and metal-free generation of carbanions in full atom economy. As a protonation of the carbanionic intermediate does not lead to the termination of the reaction, but rather to the regeneration of the starting material, the use of other electrophiles such as CO₂^[35a] or ketones^[35b] was also possible.

Redox-neutral generation of carbanions from one substrate

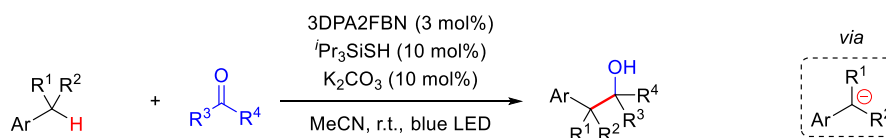
a) König group 2019: benzylation of aliphatic aldehydes to secondary alcohols



b) König group 2019: photocarboxylation of benzylic C-H bonds



c) König group 2019: activation of C-H bonds for the photocatalytic benzylation of ketones



Scheme 1-9 – Examples for reactions of carbanions generated by the redox-neutral oxidation and subsequent reduction of a radical precursor: a) photocatalytic carbanion generation from phenylacetic acids for the benzylation of aliphatic aldehydes to secondary alcohols,^[34] b) photocarboxylation of benzylic C–H bonds,^[35a] c) photocatalytic carbanion generation from C–H bonds for the benzylation of aldehydes and ketones.^[35b]

1.5 Conclusion and outlook

While carbanions have been occurring in photocatalytic cycles as intermediates to close the catalytic cycle after radical trapping for a while now, they have initially only been protonated to obtain the desired product. Starting in 2017, carbanions were generated as key intermediates in photocatalytic reactions and were used in synthesis. So far, three major strategies have been developed. Carbanions can be generated by reducing a radical that is formed after trapping a less stable photocatalytically generated radical with an alkene, by consecutively reducing one substrate twice in two photocatalytic cycles or by generating a radical oxidatively and subsequently reducing it in the same catalytic cycle. While these concepts already enable a wide variety of different transformations for various substrates, they are not yet capable of fully replacing the well-established anionic reactions known from conventional organic synthesis. Due to the nature of photocatalytic reactions, the choice of substrates is limited to compounds with suitable redox potentials. The occurrence of radicals, which are naturally rather unstable and short-lived, in the catalytic cycle often requires the use of starting materials containing stabilizing groups. However, the initial developments of the concept hold promise that further progress in the next years may eventually overcome some of the current limitations.

1.6 References

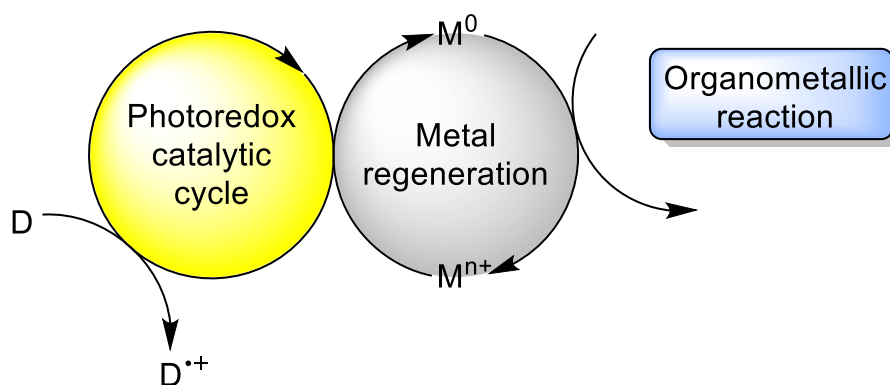
- [1] a) P. Barbier, *C. R. Acad. Sci.* **1899**, 128, 110-111; b) V. Grignard, *C. R. Acad. Sci.* **1900**, 130, 1322-1325.
- [2] a) C.-J. Li, *Tetrahedron* **1996**, 52, 5643-5668; b) G. S. Silverman, P. E. Rakita, *Handbook of Grignard Reagents*, Taylor & Francis, **1996**.
- [3] a) T. Hashimoto, T. Maruyama, T. Yamaguchi, Y. Matsubara, Y. Yamaguchi, *Adv. Synth. Catal.* **2019**, 361, 4232-4236; b) Q. Dai, B. Zhao, Y. Yang, Y. Shi, *Org. Lett.* **2019**, 21, 5157-5161; c) A. Piontek, W. Ochedzan-Siodlak, E. Bisz, M. Szostak, *Adv. Synth. Catal.* **2019**, 361, 2329-2336; d) G. Cahiez, G. Lefevre, A. Moyeux, O. Guerret, E. Gayon, L. Guillonnet, N. Lefevre, Q. Gu, E. Zhou, *Org. Lett.* **2019**, 21, 2679-2683.
- [4] a) A. Rizzo, D. Trauner, *Org. Lett.* **2018**, 20, 1841-1844; b) W. Xue, R. Shishido, M. Oestreich, *Angew. Chem. Int. Ed.* **2018**, 57, 12141-12145; c) W. Mao, W. Xue, E. Irran, M. Oestreich, *Angew. Chem. Int. Ed.* **2019**, 58, 10723-10726.
- [5] a) L. Keinicke, P. Fristrup, P. O. Norrby, R. Madsen, *J. Am. Chem. Soc.* **2005**, 127, 15756-15761; b) E. Lindbäck, Y. Zhou, L. Marinescu, C. M. Pedersen, M. Bols, *Eur. J. Org. Chem.* **2010**, 2010, 3883-3896; c) A. K. Srivastava, G. Panda, *Chem. Eur. J.* **2008**, 14, 4675-4688; d) F. Caprioli, A. V. Madduri, A. J. Minnaard, S. R. Harutyunyan, *Chem. Commun.* **2013**, 49, 5450-5452.
- [6] a) S. Li, J.-X. Wang, X. Wen, X. Ma, *Tetrahedron* **2011**, 67, 849-855; b) C.-J. Li, W.-C. Zhang, *J. Am. Chem. Soc.* **1998**, 120, 9102-9103; c) C. Petrier, J. L. Luche, *J. Org. Chem.* **1985**, 50, 910-912; d) F. Zhou, C. J. Li, *Nat. Commun.* **2014**, 5, 4254.
- [7] S. Ni, N. M. Padial, C. Kingston, J. C. Vantourout, D. C. Schmitt, J. T. Edwards, M. M. Kruszyk, R. R. Merchant, P. K. Mykhailiuk, B. B. Sanchez, S. Yang, M. A. Perry, G. M. Gallego, J. J. Mousseau, M. R. Collins, R. J. Cherney, P. S. Lebed, J. S. Chen, T. Qin, P. S. Baran, *J. Am. Chem. Soc.* **2019**, 141, 6726-6739.
- [8] K. Chatterjee, M. Miyake, L. M. Stock, *Energy Fuels* **1990**, 4, 242-248.
- [9] a) K. Zeitler, *Angew. Chem. Int. Ed.* **2009**, 48, 9785-9789; b) J. M. Narayanam, C. R. Stephenson, *Chem. Soc. Rev.* **2011**, 40, 102-113; c) N. A. Romero, D. A. Nicewicz, *Chem. Rev.* **2016**, 116, 10075-10166; d) L. Marzo, S. K. Pagire, O. Reiser, B. König, *Angew. Chem. Int. Ed.* **2018**, 57, 10034-10072.
- [10] a) T. Hering, D. P. Hari, B. König, *J. Org. Chem.* **2012**, 77, 10347-10352; b) A. U. Meyer, K. Straková, T. Slanina, B. König, *Chem. Eur. J.* **2016**, 22, 8694-8699; c) E. Fava, M. Nakajima, A. L. Nguyen, M. Rueping, *J. Org. Chem.* **2016**, 81, 6959-6964.
- [11] a) D. R. Heitz, K. Rizwan, G. A. Molander, *J. Org. Chem.* **2016**, 81, 7308-7313; b) D. P. Hari, T. Hering, B. König, *Org. Lett.* **2012**, 14, 5334-5337.
- [12] a) K. A. Margrey, A. Levens, D. A. Nicewicz, *Angew. Chem. Int. Ed.* **2017**, 56, 15644-15648; b) A. Ruffoni, F. Julia, T. D. Svejstrup, A. J. McMillan, J. J. Douglas, D. Leonori, *Nat. Chem.* **2019**, 11, 426-433.
- [13] a) J. L. Jeffrey, F. R. Petronijevic, D. W. MacMillan, *J. Am. Chem. Soc.* **2015**, 137, 8404-8407; b) A. L. Berger, K. Donabauer, B. König, *Chem. Sci.* **2018**; c) M. Nakajima, E. Fava, S. Loescher, Z. Jiang, M. Rueping, *Angew. Chem. Int. Ed.* **2015**, 54, 8828-8832; d) E. Fava, A. Millet, M. Nakajima, S. Loescher, M. Rueping, *Angew. Chem. Int. Ed.* **2016**, 55, 6776-6779.
- [14] a) K. L. Skubi, T. R. Blum, T. P. Yoon, *Chem. Rev.* **2016**; b) F. R. Petronijevic, M. Nappi, D. W. MacMillan, *J. Am. Chem. Soc.* **2013**, 135, 18323-18326; c) E. B. Corcoran, M. T. Pirnot, S. Lin, S. D. Dreher, D. A. DiRocco, I. W. Davies, S. L. Buchwald, D. W. MacMillan, *Science* **2016**, 353, 279-283; d) C. Le, T. Q. Chen, T. Liang, P. Zhang, D. W. C. MacMillan, *Science* **2018**, 360, 1010-1014.

- [15] a) P. L. Arnold, J. M. Purkis, R. Rutkauskaitė, D. Kovacs, J. B. Love, J. Austin, *ChemCatChem* **2019**, *11*, 3786-3790; b) D. F. Chen, J. C. K. Chu, T. Rovis, *J. Am. Chem. Soc.* **2017**, *139*, 14897-14900; c) L. Capaldo, D. Ravelli, *Eur. J. Org. Chem.* **2017**, 2017, 2056-2071; d) K. Qvortrup, D. A. Rankic, D. W. MacMillan, *J. Am. Chem. Soc.* **2014**, *136*, 626-629.
- [16] a) T. Roy, M. J. Kim, Y. Yang, S. Kim, G. Kang, X. Ren, A. Kadziola, H.-Y. Lee, M.-H. Baik, J.-W. Lee, *ACS Catal.* **2019**, *9*, 6006-6011; b) K. F. Biegasiewicz, S. J. Cooper, X. Gao, D. G. Oblinsky, J. H. Kim, S. E. Garfinkle, L. A. Joyce, B. A. Sandoval, G. D. Scholes, T. K. Hyster, *Science* **2019**, *364*, 1166-1169; c) T. R. Blum, Z. D. Miller, D. M. Bates, I. A. Guzei, T. P. Yoon, *Science* **2016**, *354*, 1391-1395; d) J. J. Murphy, D. Bastida, S. Paria, M. Fagnoni, P. Melchiorre, *Nature* **2016**, *532*, 218-222.
- [17] a) A. Noble, R. S. Mega, D. Pflasterer, E. L. Myers, V. K. Aggarwal, *Angew. Chem. Int. Ed.* **2018**, *57*, 2155-2159; b) A. Gualandi, D. Mazzearella, A. Ortega-Martínez, L. Mengozzi, F. Calcinelli, E. Matteucci, F. Monti, N. Armaroli, L. Sambri, P. G. Cozzi, *ACS Catal.* **2017**, *7*, 5357-5362; c) R. Zhou, H. Liu, H. Tao, X. Yu, J. Wu, *Chem. Sci.* **2017**, *8*, 4654-4659; d) A. J. Musacchio, L. Q. Nguyen, G. H. Beard, R. R. Knowles, *J. Am. Chem. Soc.* **2014**, *136*, 12217-12220; e) Y. Yasu, T. Koike, M. Akita, *Adv. Synth. Catal.* **2012**, *354*, 3414-3420; f) H. Huang, C. Yu, Y. Zhang, Y. Zhang, P. S. Mariano, W. Wang, *J. Am. Chem. Soc.* **2017**, *139*, 9799-9802; g) H. Yokoi, T. Nakano, W. Fujita, K. Ishiguro, Y. Sawaki, *J. Am. Chem. Soc.* **1998**, *120*, 12453-12458.
- [18] V. R. Yatham, Y. Shen, R. Martin, *Angew. Chem. Int. Ed.* **2017**, *56*, 10915-10919.
- [19] J. Hou, A. Ee, H. Cao, H. W. Ong, J. H. Xu, J. Wu, *Angew. Chem. Int. Ed.* **2018**, *57*, 17220-17224.
- [20] Q. Fu, Z. Y. Bo, J. H. Ye, T. Ju, H. Huang, L. L. Liao, D. G. Yu, *Nat. Commun.* **2019**, *10*, 3592.
- [21] W. Kong, H. An, Q. Song, *Chem. Commun.* **2017**, *53*, 8968-8971.
- [22] J. P. Phelan, S. B. Lang, J. S. Compton, C. B. Kelly, R. Dykstra, O. Gutierrez, G. A. Molander, *J. Am. Chem. Soc.* **2018**, *140*, 8037-8047.
- [23] T. Guo, L. Zhang, X. Liu, Y. Fang, X. Jin, Y. Yang, Y. Li, B. Chen, M. Ouyang, *Adv. Synth. Catal.* **2018**, *360*, 4459-4463.
- [24] C. Shu, R. S. Mega, B. J. Andreassen, A. Noble, V. K. Aggarwal, *Angew. Chem. Int. Ed.* **2018**, *57*, 15430-15434.
- [25] a) J. A. Milligan, J. P. Phelan, V. C. Polites, C. B. Kelly, G. A. Molander, *Org. Lett.* **2018**, *20*, 6840-6844; b) W. Luo, Y. Yang, Y. Fang, X. Zhang, X. Jin, G. Zhao, L. Zhang, Y. Li, W. Zhou, T. Xia, B. Chen, *Adv. Synth. Catal.* **2019**, *361*, 4215-4221.
- [26] C. Shu, A. Noble, V. K. Aggarwal, *Angew. Chem. Int. Ed.* **2019**, *58*, 3870-3874.
- [27] L. R. E. Pantaine, J. A. Milligan, J. K. Matsui, C. B. Kelly, G. A. Molander, *Org. Lett.* **2019**, *21*, 2317-2321.
- [28] A. Hu, Y. Chen, J. J. Guo, N. Yu, Q. An, Z. Zuo, *J. Am. Chem. Soc.* **2018**, *140*, 13580-13585.
- [29] S. B. Lang, R. J. Wiles, C. B. Kelly, G. A. Molander, *Angew. Chem. Int. Ed.* **2017**, *56*, 15073-15077.
- [30] A. K. Yadav, A. K. Sharma, K. N. Singh, *Org. Chem. Front.* **2019**, *6*, 989-993.
- [31] K. Hironaka, S. Fukuzumi, T. Tanaka, *J. Chem. Soc., Perkin Trans. 2* **1984**, 1705.
- [32] Y. Zhang, R. Qian, X. Zheng, Y. Zeng, J. Sun, Y. Chen, A. Ding, H. Guo, *Chem. Commun.* **2015**, *51*, 54-57.
- [33] L. L. Liao, G. M. Cao, J. H. Ye, G. Q. Sun, W. J. Zhou, Y. Y. Gui, S. S. Yan, G. Shen, D. G. Yu, *J. Am. Chem. Soc.* **2018**, *140*, 17338-17342.
- [34] K. Donabauer, M. Maity, A. L. Berger, G. S. Huff, S. Crespi, B. König, *Chem. Sci.* **2019**, *10*, 5162-5166.

- [35] a) Q. Y. Meng, T. E. Schirmer, A. L. Berger, K. Donabauer, B. König, *J. Am. Chem. Soc.* **2019**, *141*, 11393-11397; b) A. L. Berger, K. Donabauer, B. König, *Chem. Sci.* **2019**, *Manuscript submitted*.

CHAPTER 2

2 Photocatalytic organometallic reactions using *in situ* generated zerovalent metals

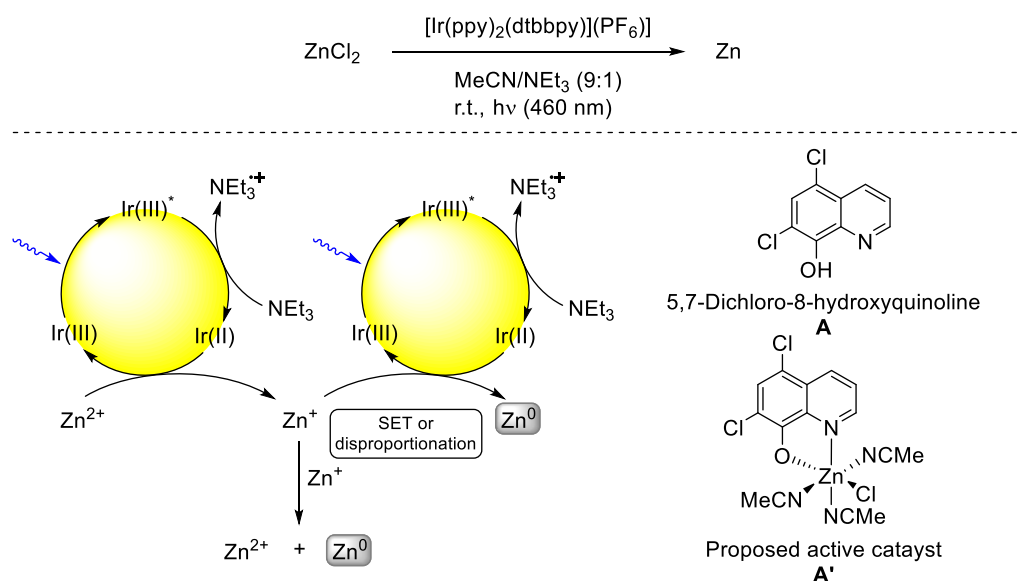


The experiments in this chapter have been conducted in cooperation with Karsten Donabauer and Saikat Das. A. L. Berger performed the experiments in section 2.2.2, 2.2.3 and a part of the experiments in section 2.2.1, 2.2.4 and 2.2.5. K. Donabauer performed the experiments in section 2.2.6 and a part of the experiments in section 2.2.1, 2.2.4 and 2.2.5. S. Das performed the experiments in section 2.2.7.

2.1 Introduction

Reactions involving the transfer of two electrons are an integral part of organic chemistry as they enable ionic reactions by the formation of anionic or cationic intermediates. The twofold reduction of organic starting materials to nucleophilic carbanion synthons with metals like zinc or magnesium is the key step in classic organometallic reactions like the Barbier or the Grignard reaction.^[1] While many transition metal catalyzed coupling reactions like Suzuki coupling,^[2] Heck reaction^[3] or Sonogashira coupling^[4] are already well established, require only small amounts of metal catalysts and work under mild reaction conditions, there are still many organometallic reactions that demand the use of stoichiometric amounts of the respective metal. In these reactions, the metal is used as a two-electron reductant to convert organic substrates into anionic intermediates, enabling a wide variety of nucleophilic reactions. During this process, the metal is oxidized which leads to the formation of stoichiometric amounts of undesired metal salt waste.

In 2013, the Bernhard group reported their work on the reduction of Zn(II) salts to zerovalent zinc using an iridium-based photocatalyst and triethylamine as sacrificial electron donor.^[5] The reaction likely proceeds either *via* two consecutive SET steps with Zn(I) as an intermediate which is stabilized by halide anions or *via* the disproportionation of two Zn(I) species, yielding Zn²⁺ and Zn(0) (Scheme 2-1, left). One year later, the same reaction was reported using the organic ligand 5,7-dichloro-8-hydroxyquinoline (**A**) which acts as the photocatalyst after forming a complex (**A'**) with ZnCl₂ *in situ* (Scheme 2-1, right).^[6]



Scheme 2-1 – Photocatalytic reduction of Zn(II) to Zn(0) as reported by Bernhard *et al.*^[5-6]

Zerovalent zinc is one of the most commonly applied reductants in organic chemistry and is used in numerous reactions like the defunctionalization of 1,2-dihalides^[7] or for the regeneration of other metals in many metal-catalyzed couplings.^[8] Additionally, Zn(0) is capable of inserting in certain carbon-halogen bonds, forming nucleophilic organozinc species which are key intermediates in many carbon-carbon bond formations such as the Barbier reaction,^[1a, 9] the Reformatzky reaction,^[10] the Simmons-Smith cyclopropanation^[11] or the Negishi coupling.^[12] While zinc(0) is an extremely versatile reagent with various applications, it has to be used in stoichiometric amounts for most transformations and zinc(II) salts are obtained as waste products after the reaction. Therefore, we envisioned that the combination of conventional organometallic reactions which usually require stoichiometric amounts of zinc with a suitable photocatalytic system for the reduction of Zn(II) to regenerate the zerovalent metal might be a new catalytic approach for many organometallic reactions.

2.2 Results and discussion

2.2.1 Photocatalytic generation of Zn(0)

The first step of this project was to find suitable conditions for the photocatalytic generation of zerovalent zinc (Table 2-1). When the reaction was performed using the reaction conditions reported by the Bernhard group, zinc formation could be observed with an iridium-based photocatalyst,^[5] as well as the organic dye 5,7-dichloro-8-hydroxyquinoline (**A**) (Table 2-1, entries 1 and 2).^[6] The reaction also worked when Ru(bpy)₃Cl₂, eosin Y or rhodamine 6G were used as photocatalysts (Table 2-1, entries 3-5), but no zinc was formed with rose bengal or riboflavin tetracetate (Table 2-1, entries 6 and 7).

Apart from photocatalysts, different solvents for the generation of zerovalent were also investigated (Table 2-2). With 5,7-dichloro-8-hydroxyquinoline (**A**) as a photocatalyst, only acetonitrile and ethyl acetate were viable solvents for the generation of Zn(0) (Table 2-2, entries 1 and 2). No reaction was observed when THF, DMF, DCM or methanol were used as solvents (Table 2-2, entries 3-6) and solvent mixtures containing acetonitrile also did not lead to any zinc formation (Table 2-2, entries 7 and 8).

After having found some viable conditions for the photocatalytic formation of Zn(0), the *in situ* use of the generated zerovalent metal in several reactions was tested.

Table 2-1 – Screening of different photocatalysts for the generation of Zn(0) from ZnCl₂.
$$\text{ZnCl}_2 \xrightarrow[\text{MeCN/NEt}_3 (9:1), \text{ r.t., 24 h, } h\nu]{\text{PC}} \text{Zn}$$

Entry	Photocatalyst (mol%)	Wavelength (nm)	Zinc formation
1	Ir(ppy) ₃ (1)	455	✓
2	5,7-Dichloro-8-hydroxyquinoline (5)	455	✓
3	Ru(bpy) ₃ Cl ₂ (2)	455	✓
4	Eosin Y (5)	535	✓
5	Rhodamine 6G (5)	455	✓
6	Rose Bengal (5)	535	X
7	Riboflavintetraacetate (5)	455	X

[a] The reactions were performed using 3 mmol ZnCl₂ in 3 mL degassed solvent mixture.

Table 2-2 – Screening of different solvents for the generation of Zn(0) from ZnCl₂.
$$\text{ZnCl}_2 \xrightarrow[\text{Solvent/NEt}_3 (9:1), \text{ r.t., 24 h, 455 nm}]{\text{5,7-Dichloro-8-hydroxyquinoline (5 mol\%)}} \text{Zn}$$

Entry	Solvent	Zinc formation
1	MeCN	✓
2	EtOAc	✓
3	THF	X
4	DMF	X
5	DCM	X
6	MeOH	X
7	DMF/MeCN	X
8	THF/MeCN	X

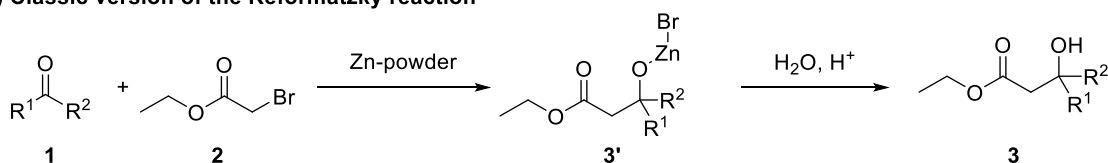
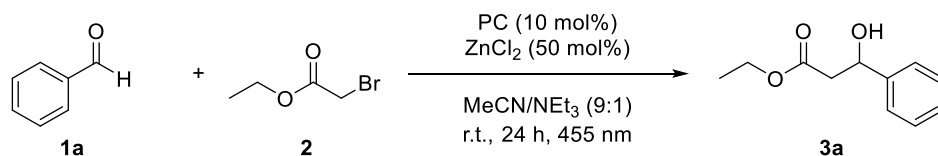
[a] The reactions were performed using 3 mmol ZnCl₂ in 3 mL degassed solvent mixture.

2.2.2 Reformatsky reaction

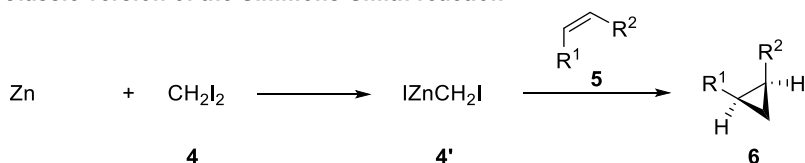
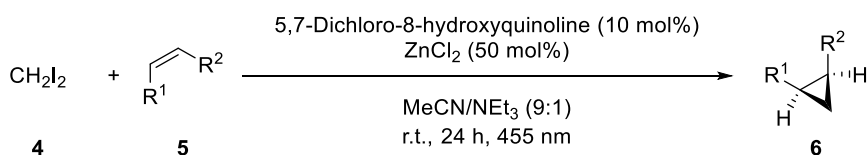
The Reformatsky reaction enables C–C bond formations between α -halogenated esters and aldehydes or ketones to form β -hydroxy esters using a stoichiometric amount of zinc powder.^[10] After the insertion of Zn(0) into the carbon-halogen bond, the newly formed nucleophilic carbon is capable of attacking an electrophilic ester (Scheme 2-2a). A photocatalytic version of the reaction was tested using benzaldehyde (**1a**) and ethyl bromoacetate (**2**) as starting materials, eosin Y or 5,7-dichloro-8-hydroxyquinoline as a photocatalyst, ZnCl₂ as a zinc source, triethylamine as a sacrificial electron donor and acetonitrile as a solvent (Scheme 2-2b). However, no formation of the desired product **3** could be observed in GC-MS. Using THF or a 9:1 mixture of MeCN and THF as a solvent did also not afford any product.

A possible problem in this reaction is, that no zinc formation was observed in the reaction mixture. This could either mean that the *in situ* formed Zn(0) is immediately reacting with the bromoacetate **2** to form an organozinc species, or that no zinc is generated at all in the reaction. However, as no product formation could be observed, it is more likely, that the photocatalytic formation of Zn(0) was suppressed under the reaction conditions.

Another reason why the photocatalytic approach of the Reformatsky reaction is not working might be that the desired product is obtained in a two-step reaction in the classic version of the reaction. After the oxidative addition of Zn(0) into the C-Br bond and the subsequent attack the electrophilic carbon of the aldehyde or ketone (**1**), the organozinc compound **3'** is formed as an intermediate. In the second reaction step an aqueous acidic workup is performed to remove zinc and form the β -hydroxy ester **3** and a zinc(II) salt (Scheme 2-2a). The first part of the reaction should in theory also be possible under the photocatalytic conditions. However, even if the reaction takes place and the organozinc intermediate **3'** is formed, the acidic workup step cannot be combined with the photocatalytic reaction and the reaction will stop after the first step. This not only means that the desired product cannot be formed, but also that the zinc(II) catalyst will not be regenerated. To enable a photocatalytic version of the Reformatsky reaction it would be necessary to find an alternative way to remove the zinc from intermediate **3'** without the acidic workup step.

a) Classic version of the Reformatsky reaction**b) Photocatalytic approach****Scheme 2-2** – a) Classical and b) photocatalytic version of the Reformatsky reaction.**2.2.3 Simmons-Smith cyclopropanation**

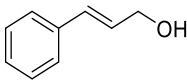
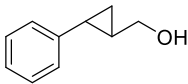
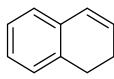
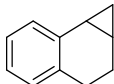
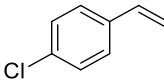
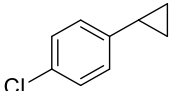
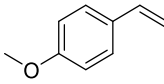
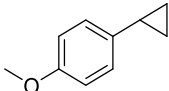
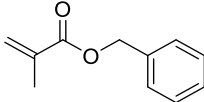
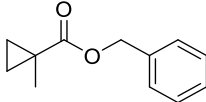
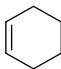
Another widely used reaction that requires the use of stoichiometric amounts of zinc powder is the Simmons-Smith cyclopropanation.^[11] In this reaction, Zn(0) and diiodomethane (4) are used to form iodomethylzinc iodide (4') *in situ* as the active reagent which is able to perform a cyclopropanation reaction of an alkene (5) yielding the desired product 6 (Scheme 2-3a). During this reaction, ZnI₂ is formed as a side product. For the photocatalytic approach of the Simmons-Smith reaction, 5,7-dichloro-8-hydroxyquinoline was used as a photocatalyst, ZnCl₂ as a zinc source, triethylamine as a sacrificial electron donor and acetonitrile as a solvent (Scheme 2-3b).

a) Classic version of the Simmons-Smith reaction**b) Photocatalytic approach****Scheme 2-3** – a) Classical and b) photocatalytic version of the Simmons-Smith reaction.

When the reaction was tested with various alkenes (**5**), traces of the desired products (**6**) were observed in GC-MS in most cases (Table 2-3). Of the tested alkenes, cyclohexene (**5f**) was the only one which did not yield any product formation (Table 2-3, entry 6). Although the formation of the desired products was observed in GC-MS, the conversions were extremely low which is why the isolation of the products was not possible. Attempting to increase the yield, different reaction conditions were tested using the reaction with cinnamyl alcohol (**4a**) as a test system. When eosin Y was used as a photocatalyst instead of 5,7-dichloro-8-hydroxyquinoline the same amount of product was obtained and neither increasing the amount of catalyst nor the use of other solvents such as DMF or DCE did lead to improved yields.

When the reaction was performed without ZnCl_2 traces of the product were also observed in GC-MS. Apparently, the reaction is not proceeding according to the mechanism of the classical Simmons-Smith reaction but instead *via* a purely photocatalytic process. At roughly the same time, a photocatalytic stereoconvergent cyclopropanation of styrenes with diiodomethane was published by Suero *et al.*^[13] In this reaction, $[\text{Ru}(\text{bpy})_3]\text{Cl}_2$ is used as a photocatalyst to reduce CH_2I_2 , yielding an iodomethyl radical which is able to undergo a cyclopropanation of various styrenes. Although with -1.44 V vs. SCE the redox potential of CH_2I_2 should be too low for the photocatalysts used in this reaction (Eosin Y: $\text{EY}/\text{EY}^{\bullet-} = -1.06\text{ V vs. SCE}$ in $\text{MeCN}/\text{H}_2\text{O}$ 1:1;^[14] 5,7-dichloro-8-hydroxyquinoline: $5,7\text{-dCl-Hq}/5,7\text{-dCl-Hq}^- = -0.91\text{ V vs. SCE}$ in MeCN .^[6]), it might still be possible that a small amount of diiodomethane is reduced photocatalytically to a iodomethyl radical. Another possibility is the purely photochemical formation of the cyclopropanation product, as it has been reported that a homolytic cleavage of the C–I bonds in diiodomethane is possible upon irradiation, forming a iodomethyl radical which is able to undergo cyclopropanation reactions with various alkenes.^[15]

Table 2-3 – Screening of different alkenes.^[a]

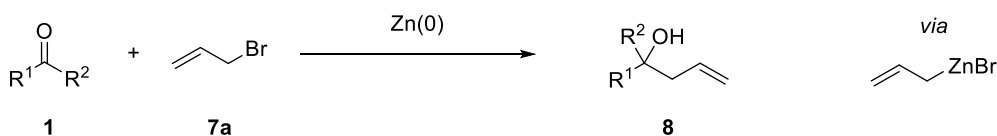
$\text{CH}_2\text{I}_2 + \text{R}^1\text{CH=CHR}^2 \xrightarrow[\text{MeCN/NEt}_3 (9:1), \text{ r.t., 24 h, } h\nu]{\text{PC (10 mol\%), ZnCl}_2 (50 \text{ mol\%})}$		
4	5	6
Entry	5	6 ^[b]
1	 5a	 6a
2	 5b	 6b
3	 5c	 6c
4	 5d	 6d
5	 5e	 6e
6	 5f	no product observed

[a] The reactions were performed using 1.5 eq. (0.3 mmol) **4** and 1 eq. (0.2 mmol) **5** in 2 mL degassed solvent. [b] Observed in GC-MS.

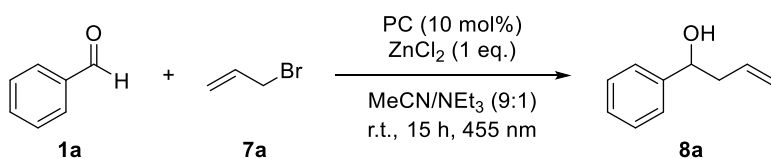
2.2.4 Barbier reaction

Zerovalent zinc is also a frequently used metal in the Barbier reaction which is one of the oldest C–C bond forming reactions and mechanistically similar to the better-known Grignard reaction. While the Grignard reaction is a two-step process where the organometallic reagent is formed prior to the addition of the electrophile, the Barbier reaction proceeds as a one-pot reaction with all reagents being present already at the beginning (Scheme 2-4a).^[1] For a photocatalytic approach of the Barbier reaction, benzaldehyde (**1a**) and allyl bromide (**7a**) were used as substrates, 5,7-dichloro-8-hydroxyquinoline (**A**) as photocatalyst, triethylamine as sacrificial electron donor and ZnCl₂ as a zinc source (Scheme 2-4b).

a) Classic version of the Barbier reaction



b) Photocatalytic approach



Scheme 2-4 – a) Classical and b) photocatalytic version of the Barbier reaction.

However, neither the desired product **8a** nor the formation of Zn(0) in the reaction mixture could be observed. As the photocatalytic generation of zerovalent zinc appears to be highly sensitive to changes, the reliability of the system in presence of various potential substrates and additives was tested (Table 2-4). Almost all tested substrates, including aldehydes (Table 2-4, entries 1 and 2), ketones (Table 2-4, entry 3), imines (Table 2-4, entry 4) and amines (Table 2-4, entries 6-8), inhibited the formation of zinc. The only tested additive which did not hinder the generation of Zn(0) was ethyl benzoate (Table 2-4, entry 5). This is in accordance with the observation, that ethyl acetate is a viable solvent for the photocatalytic reaction (Table 2-2, entry 2), indicating that the presence of ester groups seems to be tolerated by the system. However, while esters are viable electrophiles for Grignard-type reactions with

organomagnesium compounds, the corresponding zinc-based reagents are known to be generally incapable of reacting with esters under standard conditions.^[16]

Table 2-4 – Photocatalytic generation of Zn(0) in presence of various additives.^[a]

$\text{ZnCl}_2 \xrightarrow[\text{MeCN/NEt}_3 \text{ (9:1)}]{\text{5,7-dichloro-8-hydroxyquinoline (5 mol\%)} \atop \text{additive}} \text{Zn(0)}$ <p style="text-align: center;">r.t., 15 h, 455 nm</p>		
Entry	Additive (eq.)	Zinc formation
1	Benzaldehyde 1a (1)	X
2	Isovaleraldehyde (1)	X
3	Cyclohexanone (1)	X
4	<i>N</i> -Benzylideneaniline (1.5)	X
5	Ethyl benzoate (2.5)	✓
6	TMEDA (1)	X
7	EDTA (1)	X
8	2,2'-Bipyridine (2)	X

[a] The reactions were performed using 1 eq. ZnCl₂ (925 μmol) in 3 mL degassed solvent mixture.

As so far, none of the photocatalytic approaches for one-step organometallic reactions with *in situ* generated Zn(0) were successful, the use of zerovalent zinc generated by photocatalytic reduction from ZnCl₂ in a two-step process was tested. Directly adding the substrates **1a** and **7a** to the reaction mixture after zinc generation did not lead to any product formation (Table 2-5, entry 1). Surprisingly, even when the Zn(0) generated *via* photocatalytic reduction was washed, dried and subjected to reaction conditions which are known from literature to be suitable for Barbier reactions, the desired product **8a** could only be observed in traces using an aqueous protocol (Table 2-5, entry 2),^[17] and not at all under anhydrous conditions (Table 2-5, entries 3, 4 and 6),^[18] although the same protocol did afford product **8a** when commercial zinc powder was used, albeit in low yields (Table 2-5, entry 5). These observations suggest, that the zerovalent zinc which is formed in the photocatalytic reaction is not suitable for organometallic reactions, presumably due to a blocked and therefore inactive surface of the Zn(0).

Table 2-5 – Two-step process using photocatalytically generated Zn(0) for a classical Barbier reaction.^[a]

Entry	Preparation of Zn(0)	Solvent of Barbier reaction	Temperature [°C]	Yield
1	Direct addition of 1a and 7a to zinc suspension after photocatalytic reaction	MeCN/TEA (9:1)	25	–
2	Washed with MeCN two times, dried <i>in vacuo</i>	NH ₄ Cl(aq., sat.)/THF (5:1)	25	Traces ^[b]
3	Washed with MeCN two times, solvent residues removed <i>in vacuo</i> , flame dried	dry THF	25	–
4	Washed with MeCN two times, solvent residues removed <i>in vacuo</i> , flame dried	dry THF	60	–
5 ^[c]	Use of commercially available zinc powder	dry THF	25	10 ^[d]
6 ^[c]	Washed and flame dried zinc from several batches was collected	dry THF	25	–

[a] First step: The photocatalytic reaction was performed using 925 μmol ZnCl₂ 3 mL solvent mixture, second step: the Barbier reaction was performed using 1 eq. **1a** (0.2 mmol) and 1.5 eq. **7a**. [b] Observed in GC-FID. [c] A one- step Barbier reaction was performed using 1 eq. **1a** (40 mmol), 1.25 eq. and 1.9 eq. Zn(0) according to a literature procedure.^[18] [d] Isolated yield.

2.2.5 Enhanced photocatalytic zinc generation using 4CzIPN

The previous experiments revealed that the two main problems for the combination of light-induced zinc formation with classical organometallic reactions are the extreme sensitivity of the photocatalytic system for the reduction of Zn(II) and the low reactivity of the generated Zn(0). These problems could be solved by a more robust method for the generation of zerovalent zinc which works with various solvents, in presence of possible starting materials and generates a more reactive form of Zn(0) that is able to form organozinc reagents.

The use of the organic dye, 1,2,3,4-tetrakis(carbazole-9-yl)-5,6-dicyanobenzene (4CzIPN) as a photocatalyst has first been reported in 2016.^[19] Since then, 4CzIPN has proven to be a highly effective photocatalyst which enables reactions that could previously only be realized with

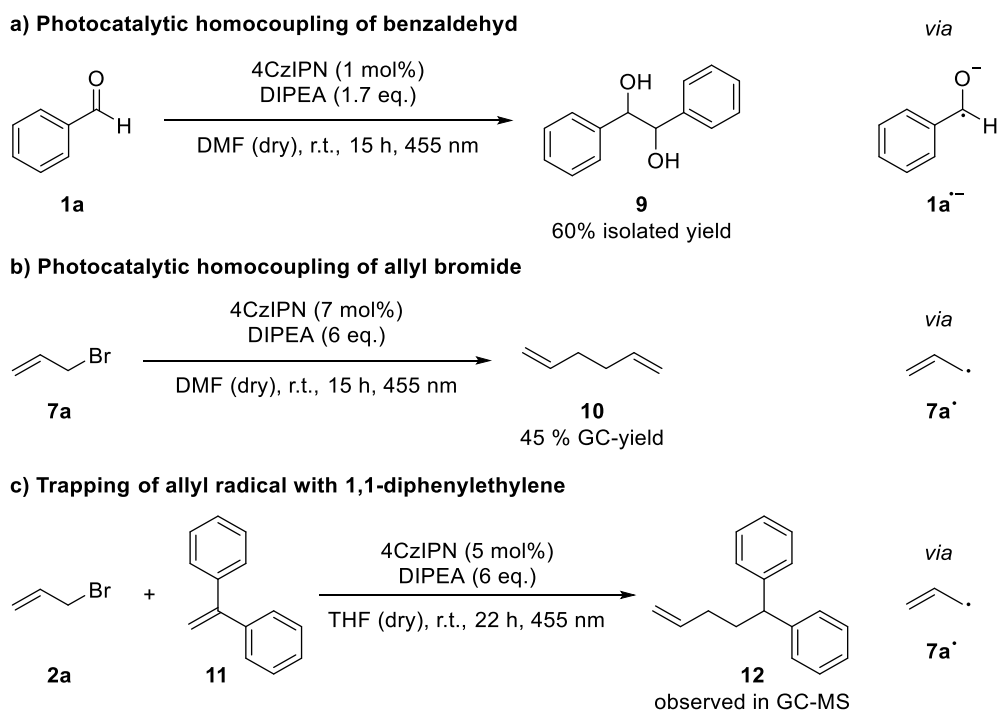
highly oxidizing or reducing iridium-based catalysts.^[20] When 4CzIPN was used as a photocatalyst for the photocatalytic reduction of ZnCl_2 to $\text{Zn}(0)$, the formation of zinc could not only be observed faster and in higher amounts than with the previously used hydroxyquinoline catalyst,^[21] but was also possible in different solvent and with various additives (Table 2-6). Apart from acetonitrile, the zinc generation also worked well in THF, DMF and a mixture of MeCN and THF (Table 2-6, entries 1-3 and 4) and small amounts of $\text{Zn}(0)$ were observed with ethanol as a solvent (Table 2-6, entry 4). Notably, apart from acetonitrile, none of these solvents were efficient for the zinc formation in the initial systems reported by Bernhard *et al.*^[5-6] With 4CzIPN as a photocatalyst, the reaction was also significantly less sensitive to the presence of possible substrates and additives. The generation of $\text{Zn}(0)$ now proceeded well when aliphatic aldehydes, ketones or bromides (Table 2-6, entries 7, 8 and 10) were added. Only small amounts of zinc were observed after the addition of ethylenediamine, presumably due to its ability to form complexes with Zn^{2+} (Table 2-6, entry 11). However, no zinc was produced when benzaldehyde **1a** or allyl bromide **7a** were added to the reaction mixture (Table 2-6, entries 6 and 9).

Table 2-6 – Photocatalytic generation of $\text{Zn}(0)$ with various solvents and additives using 4CzIPN as a photocatalyst.

$\text{ZnCl}_2 \xrightarrow[\text{Solvent/NEt}_3 \text{ (9:1)}]{\text{4CzIPN (1 mol\%)} \atop \text{additive (1 eq.)}} \text{Zn}$ <p style="text-align: center;">r.t., 24 h, 455 nm</p>			
Entry	Solvent	Additive	Zinc formation
1	MeCN ^[b]	—	✓
2	THF ^[b]	—	✓
3	DMF ^[b]	—	✓
4	EtOH	—	Small amount
5	MeCN/THF (1:1)	—	✓
6	MeCN or THF	Benzaldehyde 1a	X
7	THF	Isovaleraldehyde 1b	✓
8	THF or MeCN	Cyclohexanone 1c	✓
9	THF	Allyl bromide 7a	X
10	THF	1-Bromo propane 7b	✓
11	THF or MeCN	Ethylenediamine	Small amount
12	THF or MeCN	LiCl	X

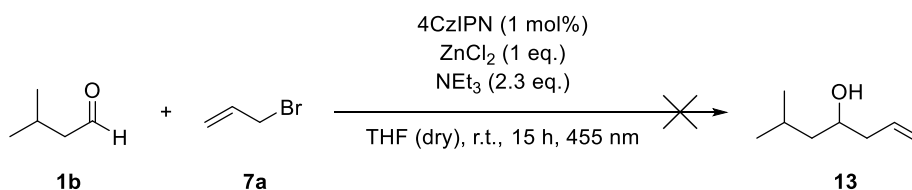
[a] The reactions were performed using 1 eq. ZnCl_2 (925 μmol) in 3 mL degassed solvent mixture. [b] Reaction also worked with DIPEA as an electron donor instead of TEA.

When **1a** was subjected to the conditions for the photocatalytic generation of zinc, the homocoupling product hydrobenzoin (**9**) could be observed instead of Zn(0) (Scheme 2-5a). In absence of ZnCl₂, **9** was obtained in 60% isolated yield while no homocoupling product was formed in the absence of 4CzIPN. This reaction likely proceeds *via* the homocoupling of the radical anion of benzaldehyde **1a^{•-}** which can be generated by the photocatalytic reduction of **1a**. A mechanistically similar photocatalytic pinacol reaction using iridium-based photocatalysts has been reported in 2016 by the Rueping group.^[22] So, when ZnCl₂ and benzaldehyde are both present in the reaction, 4CzIPN seems to reduce exclusively **1a** instead of Zn²⁺, thus preventing the generation of Zn(0). Zinc generation was also not observed in the presence of allyl bromide (**7a**). This might either be due to the possible *in situ* formation of an organozinc species by the insertion of Zn(0) into the C–Br bond, or due to the inhibition of the photocatalytic reduction of Zn²⁺ by the presence of **7a**. Control reactions have shown that in the absence of ZnCl₂ the homocoupling product 1,5-hexadiene (**10**) was obtained in a yield of 45% while only traces of **10** were observed without the photocatalyst (Scheme 2-5b). The reaction likely proceeds *via* the photocatalytic reduction of allyl bromide (**7a**) to the corresponding radical **7a[•]**. This assumption is further supported by the successful trapping of the allyl radical **7a[•]** by 1,1-diphenylethylene (Scheme 2-5c).



Scheme 2-5 – Side reactions observed by photocatalytic reduction of benzaldehyde **1a** and allyl bromide **7a** with 4CzIPN in absence of ZnCl₂.

An attempted one-pot Barbier reaction with photocatalytically generated Zn(0) using allyl bromide (**7a**) and isovaleraldehyde (**1b**), which does not interfere with the zinc generation, did not lead to the corresponding coupling product **13** (Scheme 2-6). This observation also indicates, that no zinc is generated in presence of **7a** as the formation of product **13** would be expected, if an organozinc species was formed *in situ* from Zn(0) and allyl bromide. Metallic zinc could be observed in the reaction mixture when alkyl bromides were added to the photocatalytic system (Table 2-6, entry 10), presumably because they cannot be reduced by the photocatalyst due to their significantly lower potential (1-bromo propane **7b**: $E_{1/2}^{\text{red}} = -2.1 \text{ V vs. SCE in DMSO}^{[23]}$ compared to allyl bromide **7a**: $E_{1/2}^{\text{red}} = -1.4 \text{ V vs. SCE in MeCN}^{[24]}$). However, this observation leads to the conclusion that the generated Zn(0) is not active enough to form the corresponding organozinc species. It is known from literature, that zinc needs further activation by additives such as LiCl to be able to insert into inactive C–Br bonds.^[16a] Therefore, the use of LiCl as a possible additive was tested, but no zinc formation could be observed when LiCl was added to the photocatalytic system (Table 2-6, entry 12).



Scheme 2-6 – Attempted photocatalytic coupling reaction of isovaleraldehyde **1b** and allyl bromide **7a**.

2.2.6 Two-step/one-pot Barbier-type reactions

As the possible substrates for Barbier-type reactions either inhibited the formation of zinc or did not lead to the formation of reactive organozinc intermediates, a two-step process was attempted with the improved photocatalytic system for zinc generation using 4CzIPN as a catalyst and DIPEA as a sacrificial electron donor (Table 2-7). When **1a** and **7a** were added directly to the reaction mixture after the completed photocatalytic reaction the zinc dissolved immediately, suggesting the formation of an organozinc intermediate by the oxidative addition of Zn(0) to allyl bromide. Surprisingly, no product was observed when acetonitrile was used as a solvent, and only traces of **8a** were formed when the reaction was performed in THF or DMF, although Zn(0) was fully consumed in all cases (Table 2-7, entries 1-3). We hypothesized, that the presence of water in the reaction mixture might quench the reactive

organozinc intermediate while forming the defunctionalization product propene and ZnBr(OH). As ZnCl₂ is known to be highly hygroscopic, it is likely the source of water in the reaction, which is why a literature known procedure for the synthesis of an anhydrous ZnCl₂ solution using thionyl chloride as a drying agent was employed.^[25] While the formation of **8a** was not observed when the reaction was performed with a solution of anhydrous ZnCl₂ in THF, the desired product could be isolated in a yield of 56% when DMF was used as a solvent instead (Table 2-7, entries 4 and 5). As expected, a control reaction without ZnCl₂ did not lead to the formation of product **8a**, indicating that the presence of Zn(0) is required for the reaction.

Table 2-7 – Development of a two-step/one-pot Barbier-type reaction using photocatalytically generated Zn(0).

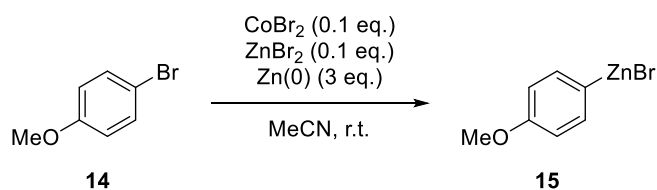
Entry	ZnCl ₂ source	Solvent	Yield
1	Commercial ZnCl ₂	MeCN/DIPEA	–
2	Commercial ZnCl ₂	THF (dry)/DIPEA	Traces ^[b]
3	Commercial ZnCl ₂	DMF (dry)/DIPEA	Traces ^[b]
4	Anhydrous ZnCl ₂ -solution ^[d]	THF (dry)/DIPEA (dry)	–
5	Anhydrous ZnCl ₂ -solution ^[d]	DMF (dry)/DIPEA (dry)	56 ^[d]
6	Without ZnCl ₂	DMF (dry)/DIPEA (dry)	–

[a] First step: The photocatalytic reaction was performed using 1 mmol ZnCl₂ in 3 mL degassed solvent mixture, second step: 1 eq. **1a** (0.1 mmol) and 2 eq. **7a** were added to the reaction mixture and stirred for 2 h in the dark. [b] Observed in GC-FID. [c] A 370 mM solution of anhydrous ZnCl₂ which was previously dried with thionyl chloride was used as a solvent and a ZnCl₂ source. [d] Isolated yield.

Although this approach for a two-step/one-pot Barbier reaction works reasonably well, it requires the stoichiometric use of ZnCl₂ as a catalytic process would only be possible in a one-step process. A stepwise process where the Zn(II) salt is regenerated in cycles after the organometallic reaction by irradiating the reaction mixture and therefore reinitiating the photocatalytic process is also not possible in this system, as the presence of benzaldehyde (**1a**) and allyl bromide (**7a**) prevents the generation of Zn(0).

2.2.7 Attempted formation of C(sp²)-organozinc compounds

As the previously attempted formations of C(sp³)-organozinc species have proven to be challenging, the generation of C(sp²)-organozinc compounds was targeted next. While zinc is known to be incapable of inserting into C(sp²)-Br bonds directly, a method for the preparation of aryl zinc species from the corresponding aryl bromides using catalytic amounts of a cobalt halide and zinc dust was reported by Gosmini and co-workers (Scheme 2-7).^[26]



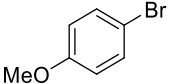
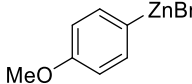
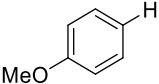
Scheme 2-7 – Cobalt catalyzed formation of aryl zinc species reported by Gosmini *et al.*

Their proposed mechanism includes the Zn(0)-induced reduction of Co(II) to Co(I) which can undergo oxidative addition into aromatic C–Br bonds, forming an aryl-Co(III) species. This intermediate is subsequently reduced to the corresponding aryl-Co(II) intermediate which can undergo transmetalation with ZnBr₂, generating the desired aryl zinc species **15**.

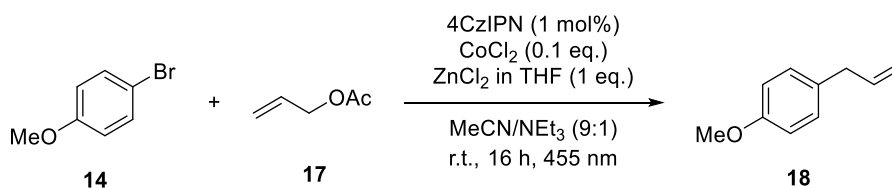
We hypothesized that a combination of our system with a Co(II) co-catalyst might enable the photocatalytic formation of aryl zinc species (Table 2-8). Unfortunately, regardless of the choice and combination of the Co(II) and Zn(II) sources, only the defunctionalization product anisole (**16**) could be obtained instead of the desired product **15**.

To investigate if the desired aryl zinc species **15** was not formed at all, or if it was generated and defunctionalized to product **16** *in situ* under our reaction conditions, a reaction of **14** with an allyl acetate (**17**) in presence of a Co(II) co-catalyst was attempted (Scheme 2-8). According to literature reports, aromatic organozinc intermediates should readily react with Co(II)-allyl species as electrophiles that are generated *in situ* from allyl acetates and the CoCl₂ co-catalyst.^[27]

Table 2-8 – Attempted reaction for the generation of aryl zinc species.^[a]

$ \begin{array}{ccc} \text{4CzIPN (1 mol\%)} \\ \text{CoX}_2 \text{ (0.1 eq.)} \\ \text{ZnX}_2 \text{ in THF (1 eq.)} \\ \hline \text{MeCN/NEt}_3 \text{ (9:1)} \\ \text{r.t., 16 h, 455 nm} \end{array} $			
 14	 15	+	 16
Entry	CoX ₂	ZnX ₂	Product
1	CoCl ₂	–	Traces of 16
2	CoBr ₂	–	Traces of 16
3	–	ZnCl ₂	–
4	–	ZnBr ₂	–
5	CoCl ₂	ZnCl ₂	Only 16
6	CoBr ₂	ZnBr ₂	Only 16

The reactions were performed using 1 eq. **14** (0.3 mmol), 1 mol% 4CzIPN, 10 mol% CoCl₂ or CoBr₂, 1 eq. ZnCl₂ (0.43 mL of a 0.7 M solution of anhydrous ZnCl₂ in THF) or 1 eq. ZnBr₂ in 1 mL degassed solvent mixture.


Scheme 2-8 – Attempted cobalt-catalyzed allylation of aryl bromides *via* the formation of aryl zinc species.

2.3 Conclusion

The goal of this project was the photocatalytic generation and subsequent *in situ* use of zerovalent zinc for various organometallic reactions that usually require the use of stoichiometric amounts of zerovalent metal. Eventually, this strategy was supposed to enable catalytic versions of many conventional organometallic reactions by constantly regenerating Zn(0) from catalytic amounts of Zn(II) salts.

Initially, the literature-reported procedure for the photocatalytic generation of zinc(0) has been reproduced and the combination with several well-known zinc-based reactions, such as the Reformatsky reaction, the Simmons-Smith cyclopropanation or the Barbier reaction was tested. However, due to the extreme sensitivity of the photocatalytic system towards changes in reaction conditions these approaches were not successful. Zinc formation only proceeded in acetonitrile which is not a suitable solvent for many organometallic reactions and the addition of potential substrates such as aldehydes, ketones or organohalides also inhibited the generation of Zn(0).

Therefore, the next step of this project was the development of a more robust photocatalytic method for the reduction of Zn^{2+} to Zn(0). A suitable system which enabled the formation of zinc in various solvents and in presence of several additives was found using 4CzIPN as a photocatalyst and DIPEA as an electron donor. With this system, a two-step/one-pot Barbier-type reaction could be realized where Zn(0) is generated photocatalytically from ZnCl_2 in the first step and subsequently used for a C–C coupling reaction in the second step by adding the respective substrates to the reaction mixture containing Zn(0). However, this system requires the use of stoichiometric amounts of ZnCl_2 .

So far, the development of a one-step process for the synthetic use and subsequent regeneration of catalytic amounts of Zn(0) generated by photocatalysis has not been possible. This is mainly due to the incompatibility of the reaction conditions required for organometallic reactions with the photocatalytic system. To circumvent these problems, purely photocatalytic methods that are capable of transferring two electrons and therefore mimic carbanionic reactivity were investigated in the following chapters.

2.4 Experimental part

2.4.1 General information

Starting materials and reagents were purchased from commercial suppliers (Sigma Aldrich, Alfa Aesar, Acros, Fluka, TCI or VWR) and used without further purification. Solvents were used as p.a. grade or dried and distilled according to literature known procedures.^[28] For automated flash column chromatography industrial grade of solvents was used. All reactions with oxygen- or moisture-sensitive reagents were carried out in glassware, which was dried before use by heating under vacuum. Dry nitrogen was used as inert gas atmosphere. Liquids were added via syringe, needle and septum techniques unless otherwise stated.

All NMR spectra were measured at room temperature using a Bruker Avance 300 (300 MHz for ¹H, 75 MHz for ¹³C, 282 MHz for ¹⁹F) or a Bruker Avance 400 (400 MHz for ¹H, 101 MHz for ¹³C, 376 MHz for ¹⁹F)^[29] NMR spectrometer. All chemical shifts are reported in δ -scale as parts per million [ppm] (multiplicity, coupling constant *J*, number of protons) relative to the solvent residual peaks as the internal standard.^[30] Coupling constants *J* are given in Hertz [Hz]. Abbreviations used for signal multiplicity: ¹H-NMR: b = broad, s = singlet, d = doublet, t = triplet, q = quartet, hept = heptet dd = doublet of doublets, dt = doublet of triplets, dq = doublet of quartets, and m = multiplet; ¹³C-NMR: (+) = primary/tertiary, (–) = secondary, (C_q) = quaternary carbon).

The mass spectrometrical measurements were performed at the Central Analytical Laboratory of the University of Regensburg. All mass spectra were recorded on a Finnigan MAT 95, ThermoQuest Finnigan TSQ 7000, Finnigan MAT SSQ 710 A or an Agilent Q-TOF 6540 UHD instrument.

GC measurements were performed on a GC 7890 from Agilent Technologies. Data acquisition and evaluation was done with Agilent ChemStation Rev.C.01.04. GC/MS measurements were performed on a 7890A GC system from Agilent Technologies with an Agilent 5975 MSD Detector. Data acquisition and evaluation was done with MSD ChemStation E.02.02.1431.A capillary column HP-5MS/30 m x 0.25 mm/0.25 μ M film and helium as carrier gas (flow rate of 1 mL/min) were used. The injector temperature (split injection: 40:1 split) was 280 °C, detection temperature 300 °C (FID). GC measurements were made and investigated via integration of the signal obtained. The GC oven temperature program was adjusted as follows: initial temperature 40 °C was kept for 3 minutes, the temperature was increased at a rate of

15 °C/min over a period of 16 minutes until 280 °C was reached and kept for 5 minutes, the temperature was again increased at a rate of 25 °C/min over a period of 48 seconds until the final temperature (300 °C) was reached and kept for 5 minutes. 1-Naphthol was used as an internal standard.

Analytical TLC was performed on silica gel coated alumina plates (MN TLC sheets ALUGRAM® Xtra SIL G/UV₂₅₄). Visualization was done by UV light (254 or 366 nm). If necessary, potassium permanganate, vanillin or ceric ammonium molybdate was used for chemical staining.

Purification by column chromatography was performed with silica gel 60 M (40-63 µm, 230-440 mesh, Merck) on a Biotage® Isolera™ Spektra One device.

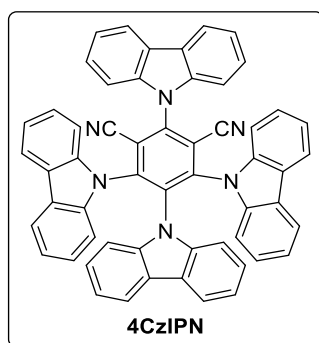
For irradiation with blue light OSRAM Oslon SSL 80 LDCQ7P-1U3U (blue, $\lambda_{\text{max}} = 455$ nm, $I_{\text{max}} = 1000$ mA, 1.12 W) was used. For irradiation with green light Cree XPEGRN L1 G4 Q4 (green, $\lambda_{\text{max}} = 535$ nm, $I_{\text{max}} = 1000$ mA, 1.12 W) was used.

2.4.2 General procedures

2.4.2.1 Synthesis of 4CzIPN

The photocatalyst was synthesized according to a literature procedure.^[19]

Under a nitrogen atmosphere, carbazole (1.67 g, 10 mmol, 5 eq.) was dissolved in dry THF (40 ml) at room temperature. Sodium hydride (60 % in paraffin oil, 0.6 g, 15 mmol, 6 eq.) was slowly added and the reaction mixture was stirred for 30 minutes at room temperature. Tetrafluoroisophthalonitrile (0.4 g, 2 mmol, 1 eq.) was added and the reaction was heated to 40 °C. After 12 h, the reaction mixture was quenched with water (2 ml), concentrated under vacuum and washed with water and EtOH. After recrystallization from hexane/DCM, the desired product 2,4,5,6-tetra(carbazole-9-yl)isophthalonitrile (4CzIPN) was obtained as a bright yellow powder (840 mg, 1.06 mmol, 53%).



¹H NMR (400 MHz, DMSO-*d*₆, δ_H) 8.35 (d, *J* = 7.7 Hz, 2H), 8.18 (d, *J* = 8.2 Hz, 2H), 7.91 – 7.83 (m, 4H), 7.78 – 7.71 (m, 6H), 7.59 – 7.42 (m, 6H), 7.19 – 7.04 (m, 8H), 6.80 (t, *J* = 7.4 Hz, 2H), 6.74 – 6.65 (m, 2H).

2.4.2.2 General procedure for the preparation of anhydrous ZnCl₂

ZnCl₂ has been dried according to a literature procedure.^[25]

Freshly distilled thionyl chloride (25 ml, 0.32 mol) was added to 10 g ZnCl₂ (0.07 mol) at room temperature in a schlenk flask. After gas evolution stopped, the suspension was refluxed for 2 h. The remaining thionyl chloride was removed under vacuum using a liquid nitrogen cold trap. The dry ZnCl₂ was dissolved in 200 ml dry solvent, 4Å molecular sieve was added and the solution was stored under nitrogen.

2.4.2.3 General procedures for photocatalytic reactions

General procedure for the photocatalytic generation of zinc

Procedure A:

A 5 mL crimp cap vial was equipped with ZnCl_2 (84 mg, 0.6 mmol, 1 equiv.), the photocatalyst (1-10 mol%) and a stirring bar. After adding the solvent mixture (solvent/electron donor 9:1, 2 mL) via syringe, the vessel was capped and degassed by three cycles of freeze pump thaw. The reaction mixture was stirred and irradiated using a blue LED (455 ± 15 nm) for 24 h at 25 °C, yielding the zerovalent zinc as a fine gray powder.

Procedure B:

A 5 mL crimp cap vial was equipped with the ZnCl_2 (126 mg, 0.925 mmol, 1 equiv.), the photocatalyst (1-10 mol%) and a stirring bar. After adding the solvent mixture (solvent/electron donor 9:1, 3 mL) via syringe, the vessel was capped and degassed by three cycles of freeze pump thaw. The reaction mixture was stirred and irradiated using a blue LED (455 ± 15 nm) for 15 h at 25 °C, yielding the zerovalent zinc as a fine gray powder.

General procedure for the photocatalytic Reformatsky reaction

A 5 mL crimp cap vial was equipped with benzaldehyde **1a** (20.3 μL , 0.2 mmol, 1 equiv.), ethyl bromoacetate **2** (66.5 μL , 0.6 mmol, 3 equiv.), ZnCl_2 (13.6 mg, 0.1 mmol, 0.5 equiv.), the photocatalyst (10 mol%) and a stirring bar. After adding the solvent (2 mL, MeCN/TEA 9:1) via syringe, the vessel was capped and degassed by three cycles of freeze pump thaw. The reaction mixture was stirred and irradiated using a blue ($455 \text{ nm} \pm 15 \text{ nm}$) or green LED ($535 \text{ nm} \pm 15 \text{ nm}$) for 20 h at 25 °C. The progress could be monitored by GC-FID and GC-MS analysis.

General procedure for the photocatalytic Simmons-Smith reaction

A 5 mL crimp cap vial was equipped with the alkene **5** (0.2 mmol, 1 equiv.), diiodomethane **4** (24.2 μL , 0.3 mmol, 1.5 equiv.), ZnCl_2 (13.6 mg, 0.1 mmol, 0.5 equiv.), the photocatalyst (10 mol%) and a stirring bar. After adding the solvent (2 mL, MeCN/ NEt_3 9:1) via syringe, the vessel was capped and degassed by three cycles of freeze pump thaw. The reaction mixture was stirred and irradiated using a blue ($455 \text{ nm} \pm 15 \text{ nm}$) or green LED ($535 \text{ nm} \pm 15 \text{ nm}$) for 20 h at 25 °C. The progress could be monitored by GC-FID and GC-MS analysis.

General procedure for the photocatalytic one-step Barbier reaction

A 5 mL crimp cap vial was equipped with benzaldehyde **1a** (20.3 μ L, 0.2 mmol, 1 equiv.), allyl bromide **7a** (66.5 μ L, 0.6 mmol, 3 equiv.), ZnCl_2 (13.6 mg, 0.1 mmol, 0.5 equiv.), the photocatalyst (10 mol%) and a stirring bar. After adding the solvent (2 mL, MeCN/ NEt_3 9:1) via syringe, the vessel was capped and degassed by three cycles of freeze pump thaw. The reaction mixture was stirred and irradiated using a blue (455 nm \pm 15 nm) or green LED (535 nm \pm 15 nm) for 20 h at 25 $^\circ\text{C}$. The progress could be monitored by GC-FID and GC-MS analysis.

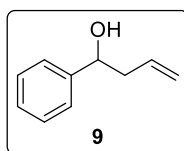
General procedure for the photocatalytic two-step/two-pot Barbier reaction

A 5 mL crimp cap vial was equipped with the ZnCl_2 (126 mg, 0.925 mmol, 1 equiv.), the photocatalyst (1-10 mol%) and a stirring bar. After adding the solvent mixture (solvent/electron donor 9:1, 3 mL) via syringe, the vessel was capped and degassed by three cycles of freeze pump thaw. The reaction mixture was stirred and irradiated using a blue LED (455 \pm 15 nm) for 15 h at 25 $^\circ\text{C}$. Afterwards, the zinc particles were allowed to deposit on the bottom of the vial and the liquid phase was removed *via* syringe. The remaining zinc powder was washed with 2 mL of MeCN twice and the remaining solvent was removed *in vacuo*. For anhydrous reactions the vial containing $\text{Zn}(0)$ was flame dried under vacuum. The solvent for the Barbier reaction (1 mL) and allyl bromide (**7a**, 26 μ L, 300 μ mol, 1.5 eq.) were added *via* syringe and the suspension was stirred for 1 h. Benzaldehyde (**1a**, 20 μ L, 200 μ mol, 1 eq.) was added and the mixture was stirred for 2 h. Afterwards, the reaction was quenched with saturated NH_4Cl solution (2 mL) and 1 mL THF was added. The reaction was analyzed by subjecting the organic phase to GC-FID or GC-MS.

Photocatalytic homocoupling of benzaldehyde (**1a**)^[22]

A 5 mL crimp cap vial was equipped with 4CzIPN (7.9 mg, 5 mol%) and a stirring bar. The vessel was capped and benzaldehyde (**1a**, 0.1 mL, 1 mmol, 1 eq.), DIPEA (0.3 mL, 1.7 mmol, 1.7 eq.) and 2.7 mL dry DMF were added via syringe under a nitrogen atmosphere. The reaction mixture was degassed by three cycles of freeze pump thaw and stirred and irradiated using a blue LED (455 ± 15 nm) at 25 °C. The progress could be monitored by GC-FID and GC-MS analysis.

The reaction mixture was diluted with water (10 ml), extracted with ethyl acetate (3 x 20 ml), washed with brine (1 x 20 ml) and dried over Na₂SO₄. The crude product was obtained by removing the solvents under reduced pressure. Purification was performed by automated flash column chromatography (PE/EtOAc, 0-50% EtOAc) yielding the corresponding product hydrobenzoin (**9**).

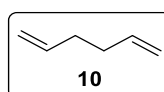


¹H-NMR (*dl* and *meso*) (400 MHz, DMSO-*d*₆, δ_{H}): 7.23-7.06 (m, 5H), 5.33 [5.18] (brs, 2H), 4.56 (s, 2H).

¹³C-NMR (*dl* and *meso*) (400 MHz, DMSO-*d*₆, δ_{H}): 143.3 (Cq), 142.3 (Cq), 127.4 (+), 127.2 (+), 127.2 (+), 127.1 (+), 126.7 (+), 126.6 (+), 77.6 (+), 77.0 (+).

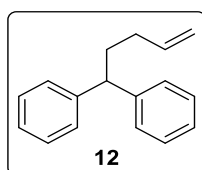
Photocatalytic homocoupling of allyl bromide (**7a**)

A 5 mL crimp cap vial was equipped with 4CzIPN (7.9 mg, 5 mol%) and a stirring bar. The vessel was capped and allyl bromide (**7a**, 12 μ L, 140 μ mol, 1 eq.), DIPEA (0.3 mL, 1.72 mmol, 12 eq.) and 2.7 mL dry DMF were added via syringe under a nitrogen atmosphere. The reaction mixture was degassed by three cycles of freeze pump thaw and stirred and irradiated using a blue LED (455 ± 15 nm) at 25 °C. The yield of the reaction was determined by GC analysis using *n*-decane as an internal standard. GC-yield of **10** was obtained over four experiments.



Radical trapping of allyl bromide (**7a**) with 1,1-diphenylethylene (**11**)

A 5 mL crimp cap vial was equipped with 4CzIPN (7.9 mg, 5 mol%) and a stirring bar. The vessel was capped and allyl bromide (**7a**, 20 μ L, 0.2 mmol, 1 eq.), 1,1-diphenylethylene (**11**, 177 μ L, 1 mmol, 5 eq.), DIPEA (0.2 mL, 1.15 mmol, 6 eq.) and 2.7 mL dry THF were added via syringe under a nitrogen atmosphere. The reaction mixture was degassed by three cycles of freeze pump thaw and stirred and irradiated using a blue LED (455 ± 15 nm) at 25 °C. The reaction progress was monitored by GC-FID and GC-MS analysis.

General procedure for the photocatalytic two-step/one-pot Barbier reaction

A flame dried 5 mL crimp cap vial was equipped with 4CzIPN (7.9 mg, 5 mol%) and a stirring bar. The vessel was capped and 2 mL of a 0.34 M solution of dry ZnCl_2 in DMF and DIPEA (200 μ L, 1.2 mmol, 6 eq.) were added via syringe under a nitrogen atmosphere. The reaction mixture was degassed by three cycles of freeze pump thaw and stirred and irradiated using a blue LED (455 ± 15 nm) at 25 °C. After irradiation for 18 h, an aldehyde or ketone (**1**, 0.2 mmol, 1 eq.) and an allyl or alkyl bromide (**7**, 0.2 mmol, 1 eq.) were added via syringe and the solution was stirred for 2 h at 25 °C in the dark. The progress could be monitored by TLC, GC analysis and GC-MS analysis.

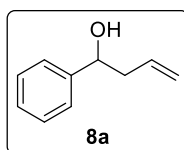
For isolation, the content of four batches was combined and saturated NH_4Cl solution (10 mL) was added. The mixture was extracted with DCM (3 x 10 mL), washed with brine (10 mL) and dried over Na_2SO_4 . The crude product was obtained by removing the solvents under reduced pressure. Purification was performed by automated flash column chromatography (PE/EtOAc, 0-20% EtOAc), yielding the corresponding product **8a**.

Synthesis of 4-phenyl-1-buten-4-ol (**8a**) with a classical Barbier-type reaction

The synthesis was performed according to a literature procedure.^[18]

A flask fitted with a dropping funnel and a condenser was flame dried. Zinc powder (5.0 g, 76.5 mmol, 1.9 eq.) was added under a nitrogen atmosphere and covered with dry THF (1 mL). A solution of **19a** (4.32 mL, 50.0 mmol, 1.25 eq.) in dry THF (3 mL) was slowly added to the stirred Zn-suspension to maintain a temperature of 25-30 °C and the reaction mixture was stirred for 1 h at room temperature after completed addition. Then, a solution of **1a** (4.08 mL, 40.0 mmol, 1 eq.) in dry THF (10 mL) was slowly added, and the resulting mixture was stirred for an additional hour. After completion, the mixture was hydrolyzed with NH₄Cl (aq., sat.) (10 mL). The aqueous phase was extracted with DCM (3 x 50 mL). The combined organic phases were washed with brine (2 x 50 mL), dried over MgSO₄, filtered and concentrated *in vacuo*. The crude product was purified by flash column chromatography (PE/EA, 20%). 4-Phenyl-1-buten-4-ol (**2a**) was obtained as colorless liquid (0.59 g, 3.98 mmol, 10%).

1-Phenyl-3-buten-1-ol (8a**)**^[31]



¹H-NMR (400 MHz, CDCl₃, δ_H): 7.38-7.27 (m, 5H), 5.87-5.77 (m, 1H), 5.20-5.13 (m, 2H), 4.76-4.73 (m, 1H), 2.58-2.46 (m, 2H).

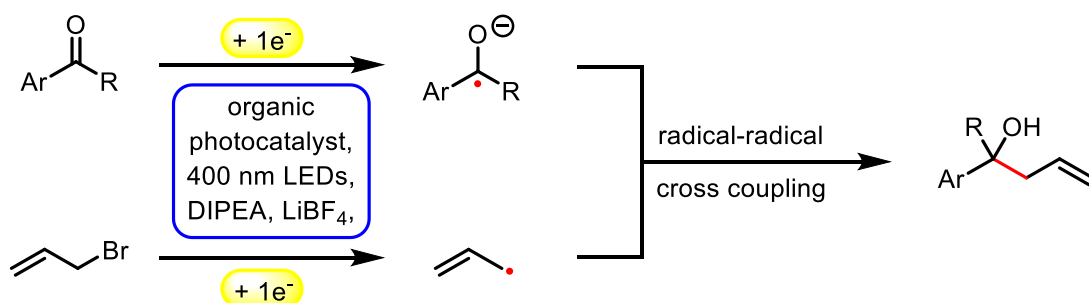
¹³C-NMR (101 MHz, CDCl₃, δ_C): 144.3 (Cq), 134.9 (+), 128.9 (+), 128.0 (+), 126.3 (+), 118.9 (-), 73.7 (+), 44.3 (-).

2.5 References

- [1] a) P. Barbier, *C. R. Acad. Sci.* **1899**, 128, 110-111; b) V. Grignard, *C. R. Acad. Sci.* **1900**, 130, 1322-1325.
- [2] N. Miyauchi, A. Suzuki, *Chem. Rev.* **1995**, 95, 2457-2483.
- [3] I. P. Beletskaya, A. V. Cheprakov, *Chem. Rev.* **2000**, 100, 3009-3066.
- [4] R. Chinchilla, C. Najera, *Chem. Rev.* **2007**, 107, 874-922.
- [5] A. C. Brooks, K. Basore, S. Bernhard, *Inorg. Chem.* **2013**, 52, 5794-5800.
- [6] A. C. Brooks, K. Basore, S. Bernhard, *Chem. Commun.* **2014**, 50, 5196-5199.
- [7] P. A. Tardella, L. Pellacani, *Tetrahedron Lett.* **1977**, 18, 4451-4454.
- [8] C. E. Knappke, S. Grupe, D. Gartner, M. Corpet, C. Gosmini, A. Jacobi von Wangelin, *Chemistry* **2014**, 20, 6828-6842.
- [9] G. W. Breton, J. H. Shugart, C. A. Hughey, B. P. Conrad, S. M. Perala, *Molecules* **2001**, 6, 655-662.
- [10] S. Reformatsky, *Ber. Dtsch. Chem. Ges.* **1887**, 20, 1210-1211.
- [11] H. E. Simmons, R. D. Smith, *J. Am. Chem. Soc.* **1958**, 80, 5323-5324.
- [12] a) A. O. King, N. Okukado, E.-i. Negishi, *J. Chem. Soc., Chem. Commun.* **1977**, 683; b) D. Haas, J. M. Hammann, R. Greiner, P. Knochel, *ACS Catal.* **2016**, 6, 1540-1552.
- [13] A. M. Del Hoyo, A. G. Herraiz, M. G. Suero, *Angew. Chem. Int. Ed.* **2017**, 56, 1610-1613.
- [14] D. P. Hari, B. König, *Chem. Commun.* **2014**, 50, 6688-6699.
- [15] a) D. C. Blomstrom, K. Herbig, H. E. Simmons, *J. Org. Chem.* **1965**, 30, 959-964; b) N. J. Pienta, P. J. Kropp, *J. Am. Chem. Soc.* **1978**, 100, 655-657; c) P. J. Kropp, N. J. Pienta, J. A. Sawyer, R. P. Polniaszek, *Tetrahedron* **1981**, 37, 3229-3236; d) P. J. Kropp, *Acc. Chem. Res.* **2002**, 17, 131-137.
- [16] a) A. Krasovskiy, V. Malakhov, A. Gavryushin, P. Knochel, *Angew. Chem. Int. Ed.* **2006**, 45, 6040-6044; b) A. D. Dilman, V. V. Levin, *Tetrahedron Lett.* **2016**, 57, 3986-3992.
- [17] a) C. Petrier, J. L. Luche, *J. Org. Chem.* **1985**, 50, 910-912; b) C.-J. Li, *Tetrahedron* **1996**, 52, 5643-5668.
- [18] F. X. Felpin, J. Lebreton, *J. Org. Chem.* **2002**, 67, 9192-9199.
- [19] J. Luo, J. Zhang, *ACS Catal.* **2016**, 6, 873-877.
- [20] E. Speckmeier, T. G. Fischer, K. Zeitler, *J. Am. Chem. Soc.* **2018**, 140, 15353-15365.
- [21] K. Donabauer, *Master Thesis* **2017**.
- [22] M. Nakajima, E. Fava, S. Loescher, Z. Jiang, M. Rueping, *Angew. Chem. Int. Ed.* **2015**, 54, 8828-8832.
- [23] A. J. Fry, R. L. Krieger, *J. Org. Chem.* **1976**, 41, 54-57.
- [24] A. J. Bard, A. Merz, *J. Am. Chem. Soc.* **1979**, 101, 2959-2965.
- [25] A. R. Pray, R. F. Heitmiller, S. Strycker, V. D. Aftandilian, T. Muniyappan, D. Choudhury, M. Tamres, *Inorg. Synth.* **1990**, 28, 321-323.
- [26] H. Fillon, C. Gosmini, J. Perichon, *J. Am. Chem. Soc.* **2003**, 125, 3867-3870.
- [27] C. Gosmini, A. Moncomble, *Isr. J. Chem.* **2010**, 50, 568-576.
- [28] S. Hünig, P. Kreitmeier, G. Märkl, J. Sauer, *Verlag Lehmanns* **2006**.
- [29] R. K. Harris, E. D. Becker, S. M. Cabral de Menezes, R. Goodfellow, P. Granger, *Magn. Reson. Chem.* **2002**, 40, 489-505.
- [30] G. R. Fulmer, A. J. M. Miller, N. H. Sherden, H. E. Gottlieb, A. Nudelman, B. M. Stoltz, J. E. Bercaw, K. I. Goldberg, *Organometallics* **2010**, 29, 2176-2179.
- [31] S. Kobayashi, K. Nishio, *J. Org. Chem.* **1994**, 59, 6620-6628.

CHAPTER 3

3 Photocatalytic Barbier reaction - visible-light induced allylation and benzylation of aldehydes and ketones



This chapter has been published in: A. L. Berger, K. Donabauer, B. König, *Chem Sci.* **2018**, 9, 7230-7235.

A. L. Berger and K. Donabauer developed the project, A. L. Berger carried out the reactions and wrote the manuscript. B. König supervised the project and is corresponding author.

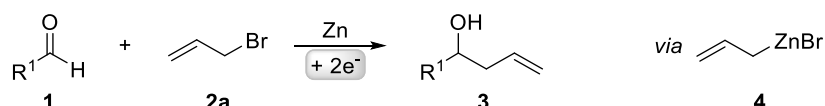
3.1 Introduction

Although first reported over a century ago, Barbier-type reactions are still important tools for carbon–carbon bond formations in organic synthesis today.^[1] In the classical Barbier reaction a metal, e.g. zinc^[2] or magnesium^[3] is able to insert in the carbon–halide bond of a reactive organic halide to form a nucleophilic organometallic intermediate **4** which can undergo a reaction with various electrophiles, like aldehydes or ketones to form the corresponding secondary or tertiary alcohols as products (Scheme 3-1a). One of the main application of Barbier reactions is the synthesis of allylic or benzylic alcohols from an aldehyde or ketone and allyl or benzyl bromide using a metal as reductant.^[4] Over the years, Barbier-type reactions have been developed further, and today they are known for many different substrates^[5] and with various metals e.g. tin^[6], indium,^[7] praseodymium^[8] or manganese.^[9] While these methods offer a wide variety of reaction conditions, they all are overall two-electron processes which is why they require the use of a stoichiometric amount of metal as a reductant. Using a photoredox catalyst to access an organic electron source instead of a metal would represent an interesting and more environmentally benign alternative. However, photoredox catalyzed two-electron processes are scarce, as photocatalytic reactions usually proceed *via* radical intermediates that are generated by a photoinduced single electron transfer (SET).^[10] To generate carbanion synthons with similar reactivity as the nucleophilic organometallic intermediate in classical Barbier-type reactions, two consecutive SETs would be required to generate a radical first followed by another reduction to the corresponding carbanion.^[11] Due to the high reactivity of most radicals and their low concentration in photocatalytic reactions this process is rather unlikely. Another strategy to enable photocatalytic two-electron processes would be a reductive radical-radical cross coupling where one electron is transferred to each starting material, generating two radical intermediates that can recombine to give the desired product (Scheme 3-1b).^[12] Photocatalytic reductions of aromatic aldehydes to the corresponding alcohols have been known since a report by Pac *et al.* in 1983^[13] and in 1990 the formation of diols as homocoupling products of ketyl radical anions has been observed.^[14]

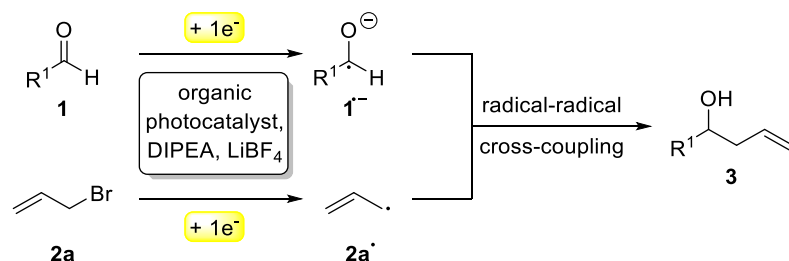
After having been used only rarely in photoredox catalysis for many years, there has been an increasing number of reports about photocatalytic reductions of aldehydes and ketones recently. Ketyl radicals have often been used for radical-radical coupling reactions,^[12, 15] e.g. in the work of Rueping and co-workers about a photoredox-catalyzed reductive dimerization of

aldehydes and ketones (Scheme 3-1c)^[15b] or in the reductive arylation of carbonyl derivatives by Xia *et al.* in 2017.^[12] Apart from radical-radical coupling reactions, it is also possible to use ketyl radicals for cyclization reactions^[16] or to trap them intermolecularly with alkenes.^[17] In the work of Chen and co-workers, hydroxymethyl radicals derived from the photocatalytic reduction of aldehydes or ketones are added to allyl sulfones (Scheme 3-1d) to form the corresponding homoallylic alcohols as products.^[17a] While this is an elegant method for the photocatalytic allylation of aldehydes and ketones, it is only possible for allyl sulfones with electron withdrawing CO₂Et-groups. A photochemical method for the allylation and benzylation of ketones and 1,2-diketones using organotrifluoroborate has been reported in 2009 by Nishigaichi *et al.*^[18] We developed a method for the direct photocatalytic synthesis of allylic and benzylic alcohols from ketones or aldehydes and allyl or benzyl bromides with an organic photocatalyst *via* a reductive radical-radical cross coupling.

a) Classical zinc mediated Barbier-type reaction



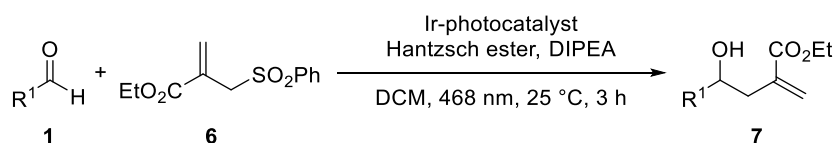
b) This work



c) Photoredox-catalyzed reductive coupling of aldehydes and ketones



d) Polarity-reversed allylation of aldehydes and ketones



Scheme 3-1 – a) Classical and b) photocatalytic version of the Barbier-type reaction; c and d) other photocatalytic reactions with ketyl radicals.

3.2 Results and discussion

For the optimization of the reaction conditions, we used the readily available substrates benzaldehyde (**1a**) and allyl bromide (**2a**) as starting materials. Initial experiments have shown that we could obtain 22% of the desired product **3a** when the reaction was performed in dry DMF with 4CzIPN (**A**) as a photocatalyst and DIPEA as sacrificial electron donor (Table 3-1, entry 1).

By using 3,7-di(4-biphenyl) 1-naphthalene-10-phenoxazine (**B**) as a photocatalyst^[19] the yield could be increased to 38% (Table 3-1 – entry 2) and by changing the irradiation wavelength from 455 to 400 nm and the solvent from DMF to DMA a yield of 54% could be obtained (Table 3-1 – entry 3). With the iridium-based photocatalyst **C** only 21% of **3a** was formed (Table 3-1 – entry 4). By adding 1.5 equivalents of LiBF₄ to the reaction mixture the formation of the diol homocoupling product of **1a** could be suppressed which further increased the yield to 64% (Table 3-1 – entry 5).^[15a] Reducing the reaction time from 18 to 2 hours only slightly decreased the yield (Table 3-1 – entry 6). While light and DIPEA are necessary for product formation (Table 3-1 – entries 7 and 8), the reaction also works in moderate yields without photocatalyst at 400 nm (46%, Table 3-1 – entry 9). However, the presence of the photocatalyst significantly accelerates the reaction as we already obtain complete conversion after 3 hours with 5 mol% of **B**, while only traces of **3a** were formed after the same time without photocatalyst (Table 3-1 – entry 10). When the reaction was performed at 455 nm without **B** no product formation could be observed (Table 3-1 – entry 11).

As shown in Table 1, varying amounts of the homocoupling products **5a** and **8a** are formed under all tested reaction conditions. Due to the use of an excess of allyl bromide (**2a**), the generation of **8a** has little influence on the yield of the reaction. In contrast, the formation of the diol homocoupling product **5a** decreases the yield of the desired product significantly, as two equivalents of the stoichiometric reagent **1a** are required to form one equivalent of **5a**.

Table 3-1 – Optimization of the reaction conditions.^[a]

Entry	PC (mol%, hv, [nm])	Solvent	DIPEA (eq.)	Additive (eq.)	t [h]	Yield 3a [%] ^[b]	Yield 5a [%] ^[c]	Yield 8a [%] ^[d]
1	A (5, 455)	DMF (dry)	6	–	18	22	15	31
2	B (5, 455)	DMF (dry)	6	–	18	38	8	17
3	B (5, 400)	DMA	6	–	18	54	14	23
4	C (2, 455)	DMA	6	–	18	21	19	43
5	B (5, 400)	DMA	6	LiBF ₄ (1.5)	18	64	13	23
6	B (5, 400)	DMA	6	LiBF ₄ (1.5)	2	59	12	28
7	B (5, 400)	DMA	–	LiBF ₄ (1.5)	18	0	0	0
8	B (5, dark)	DMA	6	LiBF ₄ (1.5)	18	0	0	0
9	– (400)	DMA	6	LiBF ₄ (1.5)	15	46	3	15
10	– (400)	DMA	6	LiBF ₄ (1.5)	4	3	2	6
11	– (455)	DMA	6	LiBF ₄ (1.5)	15	0	0	0

4CzIPN
A

B

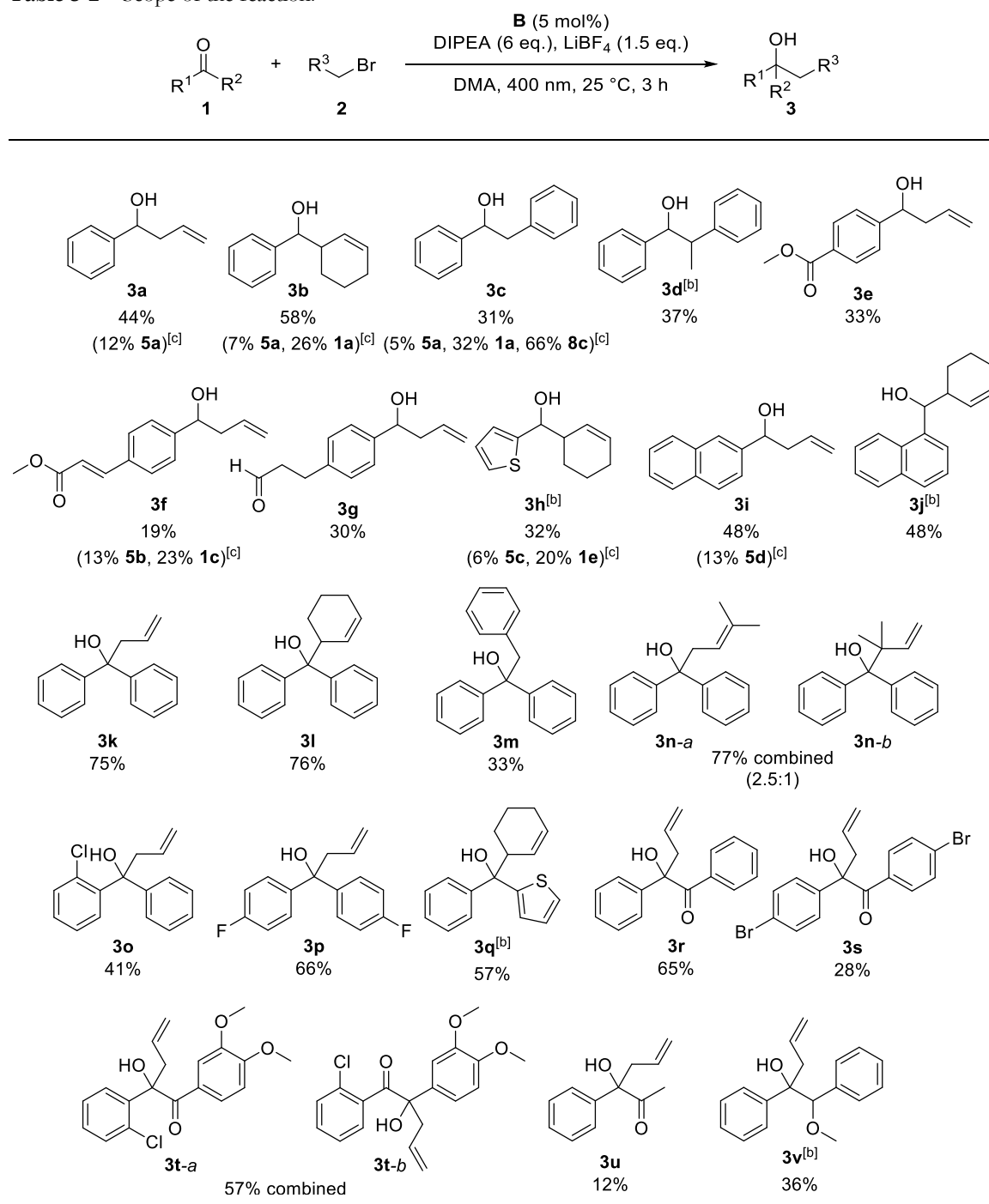
C

^[a] The reactions were performed using 1 eq. (0.2 mmol) **1a** and 2 eq. (0.4 mmol) **2a** in 2 mL degassed solvent under nitrogen, ^[b] yields were determined by GC analysis with 1-naphthol as an internal standard, ^[c] yields were determined by crude NMR with 1,3,5-trimethoxybenzene as an internal standard, ^[d] yields were determined by GC analysis with 1-naphthol as an internal standard.

The scope of the reaction was investigated using the optimized reaction conditions (Table 3-2). Apart from allyl bromide (**2a**) the reaction also worked in moderate to good yields with 3-bromo cyclohexene (**2b**), benzyl bromide (**2c**) (1-bromoethyl)benzene (**2d**). When 3,3-dimethylallyl bromide (**2e**) was used, a mixture of product **3n-a** and **3n-b** was obtained, with **3n-a** being the main product. Using alkyl or phenyl bromides did not lead to any product formation, probably because the radicals formed upon reduction and debromination are too unstable to undergo the coupling reaction. Aromatic aldehydes containing ester groups (**3e**, **3f**), or aliphatic aldehydes (**3g**) were also tolerated in the reaction with moderate yields. Notably, the reaction selectively takes place at the carbonyl group in benzylic position, while other carbonyl groups in the molecule remain unchanged. Apart from benzaldehydes which gave moderate yields (**3a-3g**) the reaction also works well with 1- and 2-naphthaldehyde (**3i**, **3j**) and with the heterocyclic 2-thiophenecarboxaldehyde (**3h**). Good yields were obtained when benzophenone was used (**3k-3n**) and 1,2-diketones (**3r-3u**) are also viable substrates. Using a non-symmetric diketone with an electron rich and an electron poor arene gave a mixture of product **3t-a** and **3t-b** with only a slight preference of the less electron rich position (**3t-a**). Product **3u** shows an important advantage over the classical Barbier reaction, as the reaction selectively takes place at the sterically more hindered ketone next to the aromatic system. Halogen substituted substrates (**3o**, **3p**, **3s**, **3t**) and substrates containing a methoxy group (**3v**) were also tolerated. Alkyl aldehydes and ketones did not yield any product as they have significantly lower reduction potentials and can therefore not be reduced by **B** ($E_{1/2}^{\text{red}}(\text{benzophenone } \mathbf{1e}) = -1.83 \text{ V vs SCE}^{[20]}$ compared to $E_{1/2}^{\text{red}}(\text{cyclohexanone } \mathbf{2m}) = -2.79 \text{ V vs SCE}^{[15a]}$). Additionally, an aromatic system in α -position to the carbonyl group seems to be required, probably due to the enhanced stability of the ketyl radical.

As moderate yields are obtained in many cases, the side products of the reaction were determined for selected examples (**3a**, **3b**, **3c**, **3f**, **3h**, **3i**). The diol homocoupling products **5** were observed in all examples. In some cases, remaining starting material was observed (**3b**, **3c**, **3f**, **3h**) which indicates an incomplete reaction. While the homocoupling of **2** did not have any influence on the yield in most cases, it seems to have significant effect when benzyl bromide (**2c**) was used. This can be seen in the case of **3c**, where 66% of the homocoupling product **8a** was formed.

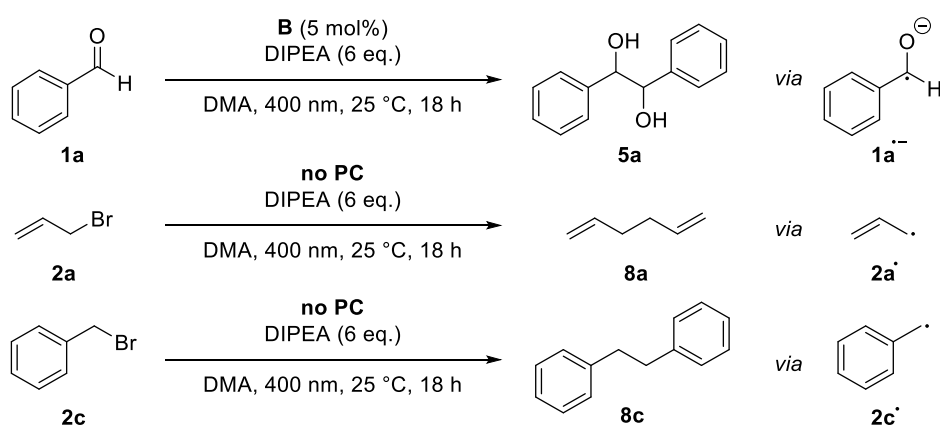
Table 3-2 – Scope of the reaction.^[a]



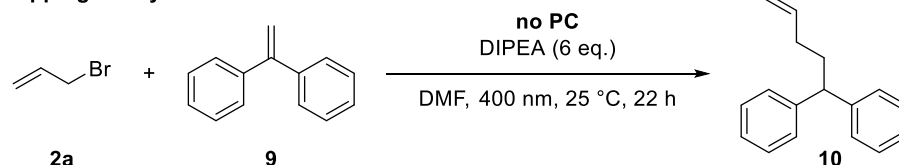
[a] The reactions were performed using 1 eq. (0.2 mmol) **1** and 2 eq. (0.4 mmol) **2** in 2 mL degassed DMA under nitrogen, all yields are of the isolated products, [b] a 1:1 mixture of the syn- and anti-product was obtained, [c] yields of the side products were determined by crude NMR with 1,3,5-trimethoxybenzene as an internal standard.

Control reactions have shown that under the reaction conditions the homocoupling products of benzaldehyde (**5a**) and allyl or benzyl bromide (**8**) could be observed (Scheme 3-2a). This confirms that the ketyl- (**1a^{•-}**) as well as the allyl- (**2a[•]**) or benzyl radical (**2c[•]**) are present in the reaction mixture and lead to product formation via a radical-radical cross-coupling reaction. Notably, the homocoupling products of **2a** and **2c** are formed also without photocatalyst just by irradiating a mixture of the bromide **2** and DIPEA with 400 nm while the photocatalyst is required for the formation of the diol **5a** from benzaldehyde. However, DIPEA and 400 nm light are both crucial for the formation of allyl radicals, as irradiating only **2a** at 400 nm as well as stirring a mixture of **2a** and DIPEA in the dark or at 455 nm did not lead to the formation of homocoupling product **8a**. It was also possible to trap the allyl radical, which was formed upon irradiation with 1,1-diphenylethylene (**9**) yielding product **10** (Scheme 3-2b).

a) Homocoupling products formed under the reaction conditions



b) Trapping of allyl radicals



Scheme 3-2 – Control reactions for radical-radical cross coupling.

Stern-Volmer fluorescence quenching experiments of photocatalyst **B** show that the excited state of **B** is quenched efficiently by benzaldehyde **1a**, but not by allyl bromide (**2a**) or DIPEA (Figure 3-1). These results are in accord with the prior observations, as they show that radical **1a[•]** is generated by a SET from **B** to **1a** while the allyl radical (**2a[•]**) is formed without photocatalyst.

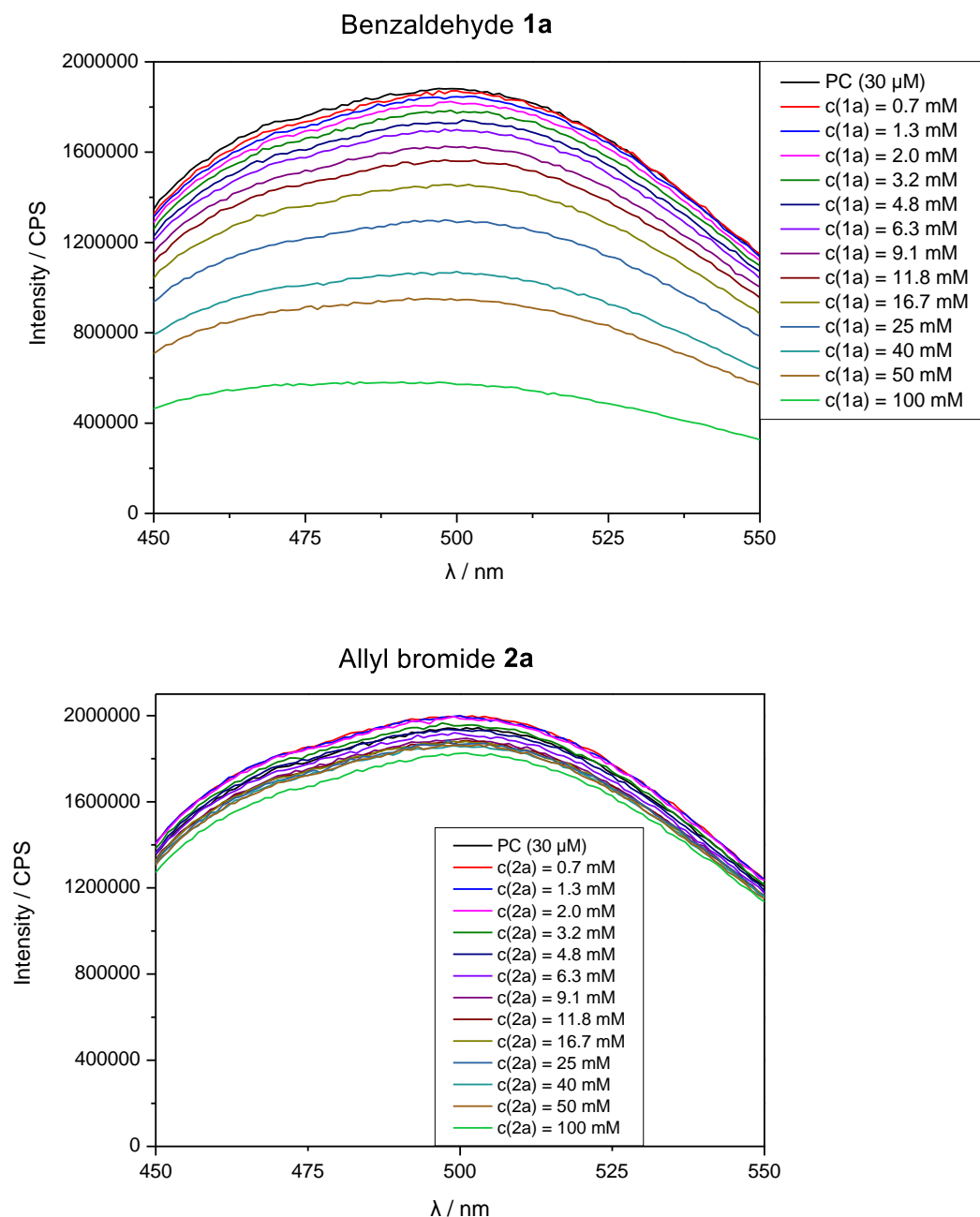


Figure 3-1 – Fluorescence quenching experiments of photocatalyst **B** upon addition of benzaldehyde (**1a**) and allyl bromide (**2a**)

According to cyclic voltammetry, benzaldehyde has a reduction potential of -2.0 V *vs.* SCE in DMF and should therefore not be in the range of photocatalyst **B** ($E^{0*} = -1.80$ V *vs.* SCE).^[19b, 19c] However, it is known that the potential of aldehydes and ketones can be lowered by activating the carbonyl group with Lewis acids^[15d] or with the oxidized form of the tertiary amine (DIPEA^{•+}).^[15b] Indeed, CV-measurements show, that the signal for the reduction of **1a** is clearly shifted to lower potentials upon addition of DIPEA and LiBF₄ (Figure 3-2). This effect could only be observed when both additives were present in the reaction mixture, which explains the role of LiBF₄ in the reaction.

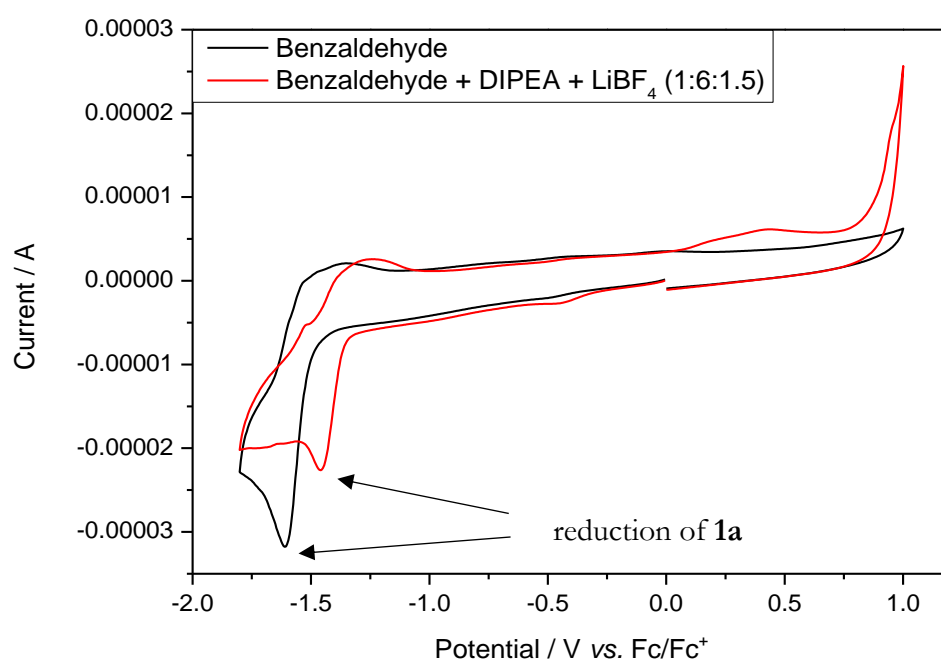


Figure 3-2 – Cyclic voltammograms of benzaldehyde (**1a**, black) and a mixture of **1a** (1 eq.), DIPEA (6 eq.) and LiBF₄ (1.5 eq.) (red); the peak that corresponds to the reduction of **1a** is shifted to lower potentials upon addition of DIPEA and LiBF₄.

Although the mixture of allyl bromide and DIPEA has no detectable absorbance at 400 nm, there seems to be a weak interaction between **2a** and DIPEA leading to the absorption of small amounts of light and initiating an electron transfer from the amine to **2a**. After a few minutes of irradiation, the absorption spectrum of the reaction mixture changes and an absorbance band with $\lambda_{\text{max, abs}} = 413$ nm arises, therefore enabling the efficient absorbance of 400 nm light and speeding up the reaction (Figure 3-3). To gain further insight, the quantum yield of the reaction was measured. While the determined value of $\varphi = 7.6$ % is rather high for photocatalytic reactions, it is in accordance with the fast reaction times.

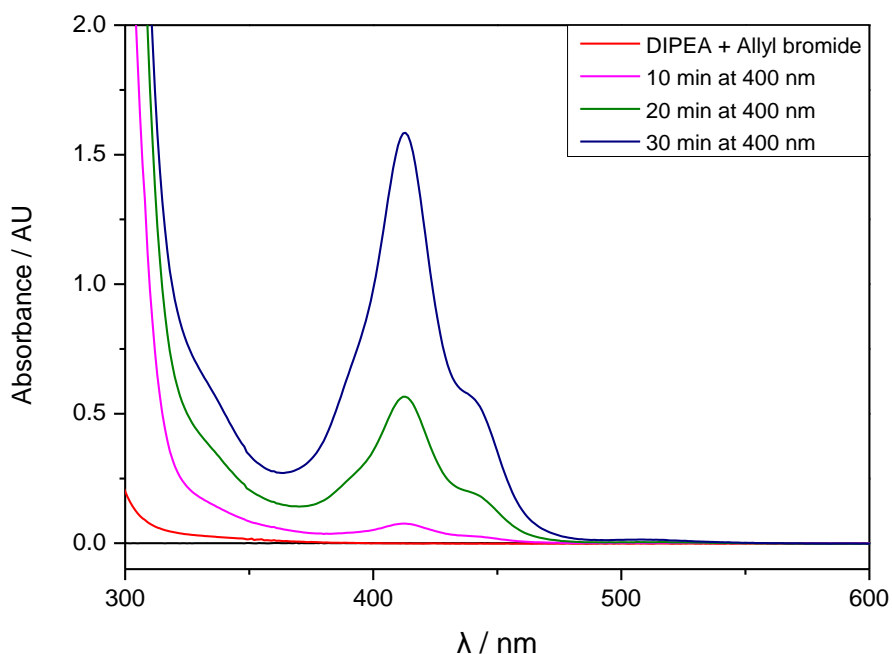
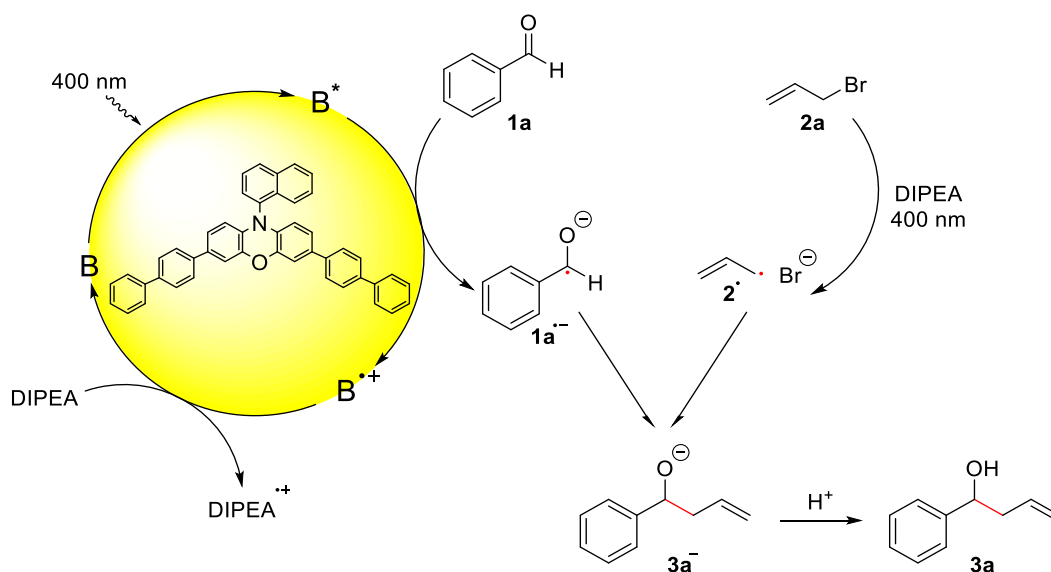


Figure 3-3 – UV/Vis absorption spectra of allyl bromide (**2a**, 1 eq.) and DIPEA (3 eq.) in DMA before irradiation and after 10, 20 and 30 minutes of 400 nm irradiation.

Based on these mechanistic investigations and recent literature reports,^[15, 21] we propose the reaction mechanism depicted in Scheme 3-4. Photocatalyst **B** is excited upon irradiation with 400 nm light and benzaldehyde (**1a**) can be reduced to the ketyl radical **1a^{•-}** by a SET from the excited photocatalyst **B^{*}**. DIPEA acts as a sacrificial electron donor to regenerate the photocatalyst from its oxidized form **B⁺⁺** to the ground state **B**. Irradiation of allyl bromide and DIPEA initiates an electron transfer, which after the cleavage of Br⁻, leads to the formation of the allyl radical **2a[•]**. The more persistent ketyl radical **1a^{•-}**^[21] and the transient allyl radical **2a[•]**^[22] recombine in a radical-radical cross-coupling, which is in accordance with the persistent radical effect,^[21, 23] and after protonation, the desired product **3a** is formed.



Scheme 3-3 – Proposed reaction mechanism.

3.3 Conclusion

In summary, we have developed a photocatalytic version of the Barbier-type reaction, which generates homoallylic or -benzylic alcohols from aldehydes or ketones and allyl- or benzyl bromides under mild conditions *via* a radical-radical cross-coupling. Instead of using stoichiometric amounts of zerovalent metal as a reductant to generate an organometallic carbanion synthon, we use an organic photocatalyst, a tertiary amine and visible light to reduce both substrates to the corresponding radicals. The cross-coupling of these radicals leads to the desired product and enables a photocatalytic two electron process.

3.4 Experimental part

3.4.1 General information

Starting materials and reagents were purchased from commercial suppliers (Sigma Aldrich, Alfa Aesar, Acros, Fluka, TCI or VWR) and used without further purification. Solvents were used as p.a. grade or dried and distilled according to literature known procedures.^[24] For automated flash column chromatography industrial grade of solvents was used. All reactions with oxygen- or moisture-sensitive reagents were carried out in glassware, which was dried before use by heating under vacuum. Dry nitrogen was used as inert gas atmosphere. Liquids were added via syringe, needle and septum techniques unless otherwise stated.

All NMR spectra were measured at room temperature using a Bruker Avance 300 (300 MHz for ^1H , 75 MHz for ^{13}C , 282 MHz for ^{19}F) or a Bruker Avance 400 (400 MHz for ^1H , 101 MHz for ^{13}C , 376 MHz for ^{19}F)^[25] NMR spectrometer. All chemical shifts are reported in δ -scale as parts per million [ppm] (multiplicity, coupling constant J , number of protons) relative to the solvent residual peaks as the internal standard.^[26]

Coupling constants J are given in Hertz [Hz]. Abbreviations used for signal multiplicity: ^1H -NMR: b = broad, s = singlet, d = doublet, t = triplet, q = quartet, hept = heptet dd = doublet of doublets, dt = doublet of triplets, dq = doublet of quartets, and m = multiplet; ^{13}C -NMR: (+) = primary/tertiary, (–) = secondary, (C_q) = quaternary carbon).

The mass spectrometrical measurements were performed at the Central Analytical Laboratory of the University of Regensburg. All mass spectra were recorded on a Finnigan MAT 95, ThermoQuest Finnigan TSQ 7000, Finnigan MAT SSQ 710 A or an Agilent Q-TOF 6540 UHD instrument.

GC measurements were performed on a GC 7890 from Agilent Technologies. Data acquisition and evaluation was done with Agilent ChemStation Rev.C.01.04. GC/MS measurements were performed on a 7890A GC system from Agilent Technologies with an Agilent 5975 MSD Detector. Data acquisition and evaluation was done with MSD ChemStation E.02.02.1431.A capillary column HP-5MS/30 m x 0.25 mm/0.25 μm film and helium as carrier gas (flow rate of 1 mL/min) were used. The injector temperature (split injection: 40:1 split) was 280 °C, detection temperature 300 °C (FID). GC measurements were made and investigated via integration of the signal obtained. The GC oven temperature program was adjusted as follows: initial temperature 40 °C was kept for 3 minutes, the temperature was increased at a rate of

15 °C/min over a period of 16 minutes until 280 °C was reached and kept for 5 minutes, the temperature was again increased at a rate of 25 °C/min over a period of 48 seconds until the final temperature (300 °C) was reached and kept for 5 minutes. 1-Naphthol was used as an internal standard.

Analytical TLC was performed on silica gel coated alumina plates (MN TLC sheets ALUGRAM® Xtra SIL G/UV₂₅₄). Visualization was done by UV light (254 or 366 nm). If necessary, potassium permanganate, vanillin or ceric ammonium molybdate was used for chemical staining.

Purification by column chromatography was performed with silica gel 60 M (40-63 µm, 230-440 mesh, Merck) on a Biotage® Isolera™ Spektra One device.

For irradiation with blue light OSRAM Oslon SSL 80 LDCQ7P-1U3U (blue, $\lambda_{\text{max}} = 455$ nm, $I_{\text{max}} = 1000$ mA, 1.12 W) was used. For irradiation with green light Cree XPEGRN L1 G4 Q4 (green, $\lambda_{\text{max}} = 535$ nm, $I_{\text{max}} = 1000$ mA, 1.12 W), and for irradiation with 400 nm Edison EDEV-SLC1-03 ($\lambda_{\text{max}} = 400$ nm, $I_{\text{max}} = 700$ mA, 400 mW) was used.

CV measurements were performed with the three-electrode potentiostat galvanostat PGSTAT302N from Metrohm Autolab using a glassy carbon working electrode, a platinum wire counter electrode, a silver wire as a reference electrode and TBATFB 0.1 M as supporting electrolyte. The potentials were achieved relative to the Fc/Fc⁺ redox couple with ferrocene as internal standard.^[27] The control of the measurement instrument, the acquisition and processing of the cyclic voltammetric data were performed with the software Metrohm Autolab NOVA 1.10.4. The measurements were carried out as follows: a 0.1 M solution of TBATFB in acetonitrile was added to the measuring cell and the solution was degassed by argon purge for 5 min. After recording the baseline the electroactive compound was added (0.01 M) and the solution was again degassed a stream of argon for 5 min. The cyclic voltammogram was recorded with one to three scans. Afterwards ferrocene (2.20 mg, 12.0 µmol) was added to the solution which was again degassed by argon purge for 5 min and the final measurement was performed with three scans.

Fluorescence spectra were measured on a HORIBA FluoroMax®-4 Spectrofluorometer at room temperature. Gas tight 10 mm Hellma® quartz fluorescence cuvettes with a screw cap with PTFE-coated silicon septum were used. FluorEssence Version 3.5.1.20 was used as a software for measurement and analysis. UV-Vis absorption spectroscopy was performed at 25 °C on a Varian Cary 100 Spectrometer with a 10 mm quartz cuvette.

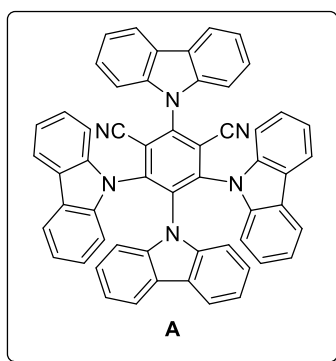
3.4.2 General procedures

3.4.2.1 Synthesis of photocatalysts

2,4,5,6-Tetra(carbazole-9-yl)isophthalonitrile (4CzIPN, A)

The photocatalysts were synthesized according to a literature procedure.^[28]

Under a nitrogen atmosphere, carbazole (1.67 g, 10 mmol, 5 eq.) was dissolved in dry THF (40 ml) at room temperature. Sodium hydride (60 % in paraffin oil, 0.6 g, 15 mmol, 6 eq.) was slowly added and the reaction mixture was stirred for 30 minutes at room temperature. Tetrafluoroisophthalonitrile or tetrafluorophthalonitrile (0.4 g, 2 mmol, 1 eq.) was added and the reaction was heated to 40 °C. After 12 h, the reaction mixture was quenched with water (2 ml), concentrated under vacuum and washed with water and EtOH. After recrystallization from hexane/DCM, the desired products were obtained.



¹H NMR (400 MHz, CDCl₃, δ_H) 8.22 (d, *J* = 7.7 Hz, 2H), 7.78 – 7.65 (m, 8H), 7.52 – 7.47 (m, 2H), 7.33 (d, *J* = 7.8 Hz, 2H), 7.25 – 7.18 (m, 4H), 7.16 – 7.00 (m, 8H), 6.82 (td, *J* = 8.2, 1.1 Hz, 4H), 6.63 (td, *J* = 7.6, 1.2 Hz, 2H).

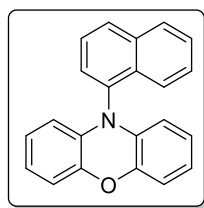
¹³C NMR (101 MHz, CDCl₃, δ_C) 145.3 (C_q), 144.7 (C_q), 140.1 (C_q), 138.3 (C_q), 137.1 (C_q), 134.9 (C_q), 127.1 (+), 125.9 (+), 125.1 (C_q), 124.9 (C_q), 124.7 (+), 124.0, 122.5 (+), 122.1 (+), 121.5 (+), 121.1 (+), 120.6 (+), 119.8 (+), 116.5 (C_q), 111.8 (C_q), 110.1 (+), 109.6 (+), 109.6 (+).

3,7-Di(4-biphenyl) 1-naphthalene-10-phenoxazine

The photocatalysts was synthesized according to a literature procedure.^[19a-c]

1-Naphthalene-10-phenoxazine^[19b]

A flame dried schlenk flask was equipped with phenoxazine (2.0 g, 10.9 mmol, 1 eq.), NaO^tBu (2.1 g, 21.8 mmol, 2 eq.), RuPhos (131.2 mg, 0.32 mmol, 3 mol%), RuPhos precatalyst (229.5 mg, 0.32 mmol, 3 mol%), 1-bromonaphthalene (3.1 ml, 21.8 mmol, 2 eq.) and 12 ml dry dioxane. The reaction mixture was stirred at 130 °C for 48 h. After cooling to room temperature DCM (20 ml) was added and the solution was washed with water (3 x 20 ml), brine (1 x 20 ml) and dried over MgSO₄. After removing the solvents under reduced pressure, the crude product was obtained. It was purified by recrystallization from DCM. After recrystallization, the solution was layered with hexane at -25 °C and the product was obtained as a light-yellow powder.



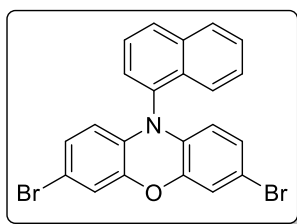
¹H NMR (400 MHz, CDCl₃, δ_H) 8.08 (d, *J* = 8.4 Hz, 1H), 8.02 – 7.94 (m, 2H), 7.68 – 7.60 (m, 1H), 7.59 – 7.52 (m, 2H), 7.51 – 7.44 (m, 1H), 6.78 – 6.69 (m, 2H), 6.63 (t, *J* = 7.6 Hz, 2H), 6.49 (dt, *J* = 7.7, 1.5 Hz, 2H), 5.70 (dd, *J* = 8.0, 1.5 Hz, 2H).

¹³C NMR (101 MHz, CDCl₃, δ_C) 144.1 (C_q), 135.7 (C_q), 135.2 (C_q), 134.4 (C_q), 131.5 (C_q), 129.3 (+), 129.1 (+), 128.9 (+), 127.4 (+), 127.0 (+), 126.9 (+), 123.5 (+), 123.5 (+), 121.4 (+), 115.5 (+), 113.5 (+).

Yield: 78%

3,7-Dibromo 1-naphthalene-10-phenoxazine

In a flask which was covered in aluminum foil to block out light, 1-naphthalene-10-phenoxazine (1.6 g, 5.2 mmol, 1 eq.) was dissolved in 160 ml chloroform. 160 ml of glacial acetic acid was added to the solution. *N*-Bromosuccinimide (1.9 mg, 10.6 mmol, 2.1 eq.) was added to the stirred reaction mixture in small portions in the dark. After stirring at room temperature for 2 h, the solvents were removed under reduced pressure. The solid residue was dissolved in chloroform, washed with water (3 x 20 ml), brine (1 x 20 ml) and dried with MgSO₄ and the product was collected as a brown powder.



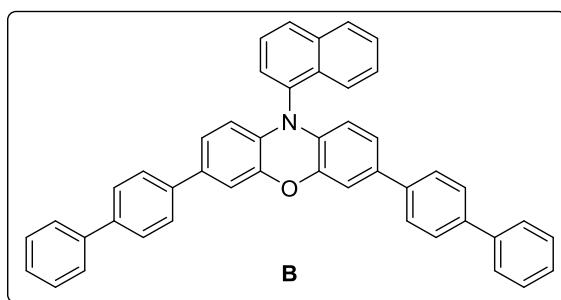
^1H NMR (400 MHz, Benzene- d_6 , δ_{H}) δ 7.82 (d, J = 8.3 Hz, 1H), 7.57 (dd, J = 18.9, 8.1 Hz, 2H), 7.21 – 7.18 (m, 1H), 7.15 – 7.10 (m, 2H), 6.90 (dd, J = 7.3, 1.2 Hz, 1H), 6.84 (d, J = 2.2 Hz, 2H), 6.36 (dd, J = 8.5, 2.2 Hz, 2H), 5.31 (d, J = 8.5 Hz, 2H).

^{13}C NMR (101 MHz, Benzene- d_6 , δ_{C}) 144.6 (C_{q}), 135.9 (C_{q}), 134.6 (C_{q}), 133.4 (C_{q}), 131.2 (C_{q}), 129.6 (+), 129.1 (+), 128.8 (+), 127.3 (+), 127.0 (+), 126.9 (+), 123.2 (+), 119.1 (+), 114.(+), 113.4 (+), 110.4 (C_{q}).

Yield: 77%

3,7-Di(4-biphenyl) 1-naphthalene-10-phenoxazine **B**

In a flame dried schlenk flask 3,7-dibromo 1-naphthalene-10-phenoxazine (1.1 g, 2.2 mmol, 1 eq.) and 4-biphenylboronic acid (1.9 g, 9.7 mmol, 4 eq.) were dissolved in 90 ml THF. 27 ml of a 2 M solution of K_2CO_3 in water was added to the solution and the reaction mixture was stirred at 80 °C for 20 minutes. After that, a solution of palladium tetrakis(triphenylphosphine) (420 mg, 0.4 mmol, 15 mol%) in 90 ml THF was added and the mixture was refluxed at 100 °C for 24 h. After cooling to room temperature, the solvents were removed under reduced pressure. The solid residue was dissolved in DCM, washed with water (2 x 20 ml), brine (1 x 20 ml) and dried with MgSO_4 . The crude product was purified by recrystallization in DCM/Methanol and the product was obtained as a light tan powder.



^1H NMR (400 MHz, DMSO- d_6 , δ_{H}) 8.18 (dd, J = 14.5, 8.0 Hz, 2H), 8.02 (d, J = 8.2 Hz, 1H), 7.81 – 7.76 (m, 2H), 7.72 – 7.7 (m, 14H), 7.46 (t, J = 7.8 Hz, 4H), 7.38 – 7.33 (m, 2H), 7.21 (d, J = 2.1 Hz, 2H), 6.98 (dd, J = 8.4, 2.1 Hz, 2H), 5.73 (d, J = 8.3 Hz, 2H).

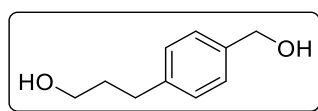
Yield: 80%

3.4.2.2 Synthesis of starting materials

3-(4-(Hydroxymethyl)phenyl)propan-1-ol^[29]

The substrate was synthesized according to a literature procedure.^[30]

Lithium aluminium hydride (2.4 g, 61.8 mmol, 6 eq) was added to a solution of 4-(2-carboxethyl)benzoic acid (2 g, 10.3 mmol, 1 eq) in 120 mL anhydrous THF. The reaction mixture was stirred at room temperature for 3 h and quenched by addition of aqueous KOH (80 mL, 5 wt%). The resulting solution was extracted with ethyl acetate. The organic layer was washed twice with brine, dried over MgSO₄ and the solvent was removed in vacuum. The crude product was purified by automated flash column chromatography (PE/EtOAc 1:1) to provide the desired product as a colorless oil.



¹H NMR (400 MHz, CDCl₃, δ_H) 7.30 – 7.26 (m, 2H), 7.21 – 7.17 (m, 2H), 4.65 (s, 2H), 3.66 (t, J = 6.4 Hz, 2H), 2.73 – 2.68 (m, 2H), 1.92 – 1.84 (m, 2H), 1.69 (s, 2H).

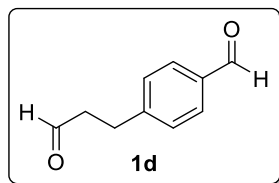
¹³C NMR (101 MHz, CDCl₃, δ_C) 141.5 (C_q), 138.6 (C_q), 128.8 (+), 127.4 (+), 65.3 (–), 62.3 (–), 34.3 (–), 31.9 (–).

Yield: 64%

4-(3-Oxopropyl)benzaldehyde^[31]

The substrate was synthesized according to a literature procedure.^[32]

Pyridinium chlorochromate (1.8 g, 8.58 mmol, 3 eq.) was added to a solution of 3-(4-(hydroxymethyl)phenyl) propan-1-ol (1 g, 2.86 mmol, 1 eq.) in THF (30ml) and stirred at 75 °C for 16 h. After cooling, the solution was filtered and evaporated. The product was purified by automated flash column chromatography (DCM/MeOH, 20:1) to give compound **1d**.



¹H NMR (300 MHz, CDCl₃, δ_H) 9.81 (s, 1H), 9.70 – 9.64 (m, 1H), 7.68 – 7.63 (m, 2H), 7.26 – 7.19 (m, 2H), 2.91 – 2.85 (m, 2H), 2.76 – 2.64 (m, 2H).

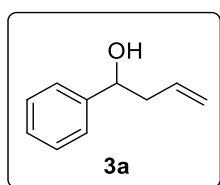
¹³C NMR (75 MHz, CDCl₃, δ_C) 200.8 (+), 191.9 (+), 147.8 (C_q), 134.7 (C_q), 130.1 (+), 129.0 (+), 44.6 (–), 28.1 (–).

3.4.2.3 General procedure for the photocatalytic allylation of aldehydes and ketones

A 5 mL crimp cap vial was equipped with the aldehyde/ketone **1** (0.2 mmol, 1 equiv.), an allyl or benzyl bromide **2** (0.4 mmol, 2 equiv.), DIPEA (200 μ l, 1.2 mmol, 6 equiv.), LiBF₄ (28.1 mg, 0.3 mmol, 1.5 eq.) the photocatalyst (5 mol%) and a stirring bar. After adding the solvent (2 mL DMA) via syringe, the vessel was capped and degassed by three cycles of freeze pump thaw. The reaction mixture was stirred and irradiated using a 400 nm (\pm 10 nm) LED for 2 – 6 h at 25 °C. The progress could be monitored by TLC, GC analysis and GC-MS analysis.

The reaction mixture was diluted with water (10 ml), extracted with ethyl acetate (3 x 20 ml), washed with brine (1 x 20 ml) and dried over Na₂SO₄. The crude product was obtained by removing the solvents under reduced pressure. Purification was performed by automated flash column chromatography (PE/EtOAc, 0-20% EtOAc or DCM/MeOH, 0-5% MeOH) yielding the corresponding product **3**.

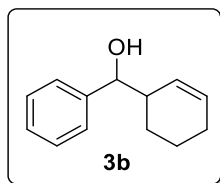
1-Phenyl-3-buten-1-ol (**3a**)^[33]



¹H NMR (400 MHz, CDCl₃, δ_{H}) 7.40 – 7.32 (m, 4H), 7.31 – 7.24 (m, 1H), 5.88 – 5.74 (m, 1H), 5.21 – 5.11 (m, 2H), 4.74 (dd, J = 7.6, 5.4 Hz, 1H), 2.58 – 2.45 (m, 2H), 2.07 (s, 1H).

¹³C NMR (101 MHz, CDCl₃, δ_{C}) 144.0 (C_q), 134.6 (+), 128.5 (+), 127.7 (+), 125.9 (+), 118.5 (–), 73.4 (+), 43.9 (–).

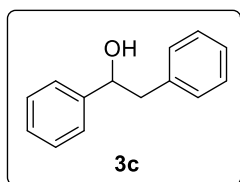
Yield: 44%

Cyclohex-2-enyl(phenyl)methanol (3b)^[34]

¹H NMR (300 MHz, CDCl₃, δ_H) 7.39 – 7.26 (m, 10H), 5.85 (s, 2H), 5.84 – 5.77 (m, 1H), 5.44 – 5.34 (m, 1H), 4.58 (d, *J* = 6.6 Hz, 1H), 4.46 (d, *J* = 7.0 Hz, 1H), 2.57 – 2.42 (m, 2H), 2.02 – 1.96 (m, 5H), 1.80 – 1.69 (m, 3H), 1.57 – 1.44 (m, 4H), 1.37 – 1.23 (m, 2H).

¹³C NMR (75 MHz, CDCl₃, δ_C) 143.6 (C_q), 143.0 (C_q), 130.5 (+), 129.9 (+), 128.4 (+), 128.3 (+), 128.1 (+), 127.5 (+), 127.5 (+), 127.2 (+), 126.6 (+), 126.4 (+), 78.1 (+), 77.49 (+), 43.1 (+), 42.9 (+), 26.4 (–), 25.4 (–), 25.3 (–), 24.0 (–), 21.6 (–), 21.2 (–).

Yield: 58 % (mixture syn/anti 1:1)

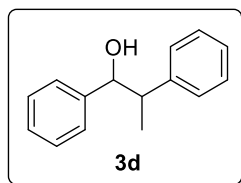
1,2-Diphenylethanol (3c)^[35]

¹H NMR (400 MHz, DMSO-*d*₆, δ_H) 7.34 – 7.12 (m, 10H), 5.26 (s, 1H), 4.80 – 4.69 (m, 1H), 2.94 – 2.82 (m, 2H).

¹³C NMR (101 MHz, DMSO-*d*₆, δ_C) 145.7 (C_q), 139.1 (C_q), 129.5 (+), 127.8 (+), 127.8 (+), 126.7 (+), 126.0 (+), 125.8 (+), 73.7 (+), 45.7 (–).

Yield: 31 %

1,2-Diphenyl-1-propanol (**3d**)^[2c]

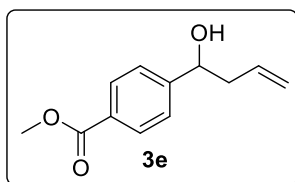


¹H NMR (400 MHz, CDCl₃, δ_H) 7.41 – 7.13 (m, 20H), 4.82 (d, *J* = 5.7 Hz, 1H), 4.67 (d, *J* = 8.7 Hz, 1H), 3.17 – 3.09 (m, 1H), 3.08 – 2.98 (m, 1H), 1.93 (s, 1H), 1.90 (s, 1H), 1.33 (d, *J* = 7.0 Hz, 3H), 1.10 (d, *J* = 7.1 Hz, 3H).

¹³C NMR (101 MHz, CDCl₃, δ_C) 143.7 (C_q), 143.5 (C_q), 143.0 (C_q), 142.7 (C_q), 128.8 (+), 128.4 (+), 128.4 (+), 128.2 (+), 128.2 (+), 128.1 (+), 127.9 (+), 127.3 (+), 127.1 (+), 127.0 (+), 126.6 (+), 126.4 (+), 79.8 (+), 78.8 (+), 48.3 (+), 47.3 (+), 18.5 (+), 15.1 (+).

Yield: 37 % (mixture syn/anti 1:1)

Methyl 4-(1-hydroxybut-3-en-1-yl)benzoate (**3e**)^[36]

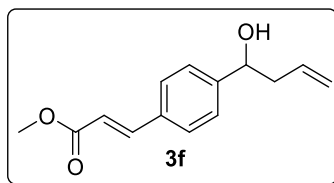


¹H NMR (300 MHz, CDCl₃, δ_H) 8.05 – 7.96 (m, 2H), 7.45 – 7.39 (m, 2H), 5.87 – 5.70 (m, 1H), 5.20 – 5.12 (m, 2H), 4.80 (dd, *J* = 7.8, 4.9 Hz, 1H), 3.90 (s, 3H), 2.58 – 2.41 (m, 2H), 2.18 (s, 1H).

¹³C NMR (75 MHz, CDCl₃, δ_C) 167.1 (C_q), 149.1 (C_q), 133.9 (+), 129.9 (+), 129.4 (C_q), 125.9 (+), 119.2 (–), 72.9 (+), 52.2 (+), 44.0 (–).

HRMS (APCI) (*m/z*): [MH⁺] (C₁₂H₁₅O₃⁺) calc.: 207.1016, found: 207.1018.

Yield: 33%

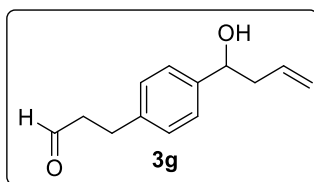
Methyl 3-(4-(1-hydroxybut-3-en-1-yl)phenyl)acrylate (3f)^[37]

¹H NMR (400 MHz, DMSO-*d*₆, δ_H) 7.56 (d, *J* = 8.1 Hz, 2H), 7.32 (d, *J* = 8.1 Hz, 2H), 6.99 (d, *J* = 12.7 Hz, 1H), 5.98 (d, *J* = 12.7 Hz, 1H), 5.82 – 5.71 (m, 1H), 5.31 (d, *J* = 4.5 Hz, 1H), 5.03 – 4.95 (m, 2H), 4.60 (q, *J* = 6.0 Hz, 1H), 3.65 (s, 3H), 2.40 – 2.33 (m, 2H).

¹³C NMR (101 MHz, DMSO-*d*₆, δ_C) 166.3 (C_q), 146.8 (C_q), 142.4 (+), 135.4 (+), 132.9 (C_q), 129.5 (+), 125.6 (+), 118.6 (+), 116.8 (–), 71.9 (+), 51.2 (+), 43.5 (–).

HRMS (ESI) (*m/z*): [MH⁺] (C₁₉H₂₀ClO₄⁺) calc.: 233.1172, found: 233.1175.

Yield: 19%

3-(4-(1-hydroxybut-3-en-1-yl)phenyl)propanal (3g)

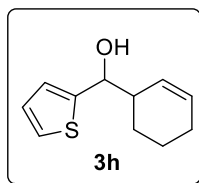
¹H NMR (400 MHz, CDCl₃, δ_H) 9.81 (t, *J* = 1.4 Hz, 1H), 7.32 – 7.24 (m, 2H), 7.21 – 7.14 (m, 2H), 5.87 – 5.73 (m, 1H), 5.19 – 5.11 (m, 2H), 4.70 (dd, *J* = 7.5, 5.4 Hz, 1H), 2.99 – 2.90 (m, 2H), 2.82 – 2.69 (m, 2H), 2.53 – 2.42 (m, 2H), 2.09 (s, 1H).

¹³C NMR (101 MHz, CDCl₃, δ_C) 201.7 (+), 142.1 (C_q), 139.7 (C_q), 134.6 (+), 128.5 (+), 126.2 (+), 118.5 (–), 73.2 (+), 45.3 (–), 43.9 (–), 27.9 (–).

HRMS (APCI) (*m/z*): [MNH₄⁺] (C₁₃H₂₀NO₂⁺) calc.: 222.1489, found: 222.1493.

Yield: 30%

Cyclohex-2-enylthiophen-2-ylmethanol (**3h**)^[38]



anti-product (R,S / S,R)

¹H NMR (400 MHz, CDCl₃, δ_H) 7.29 – 7.26 (m, 1H), 7.03 – 6.94 (m, 2H), 5.88 – 5.80 (m, 1H), 5.51 – 5.43 (m, 1H), 4.83 (d, *J* = 6.9 Hz, 1H), 2.61 – 2.53 (m, 1H), 2.06 – 1.96 (m, 3H), 1.90 – 1.73 (m, 2H), 1.59 – 1.50 (m, 2H).

¹³C NMR (101 MHz, CDCl₃, δ_C) 146.9 (C_q), 130.7 (+), 127.5 (+), 126.6 (+), 124.8 (+), 124.6 (+), 73.9 (+), 43.6 (+), 25.4 (–), 24.6 (–), 21.2 (–).

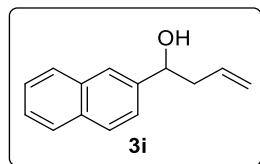
syn-product (R,R / S,S)

¹H NMR (400 MHz, CDCl₃, δ_H) 7.26 – 7.24 (m, 1H), 7.00 – 6.95 (m, 2H), 5.94 – 5.86 (m, 1H), 5.86 – 5.80 (m, 1H), 4.74 (d, *J* = 6.6 Hz, 1H), 2.61 – 2.50 (m, 1H), 2.04 – 1.98 (m, 2H), 1.79 – 1.69 (m, 1H), 1.66 – 1.48 (m, 3H), 1.42 – 1.32 (m, 1H).

¹³C NMR (101 MHz, CDCl₃, δ_C) 147.9 (C_q), 130.7 (+), 126.7 (+), 126.6 (+), 124.6 (+), 124.1 (+), 74.3 (+), 43.5 (+), 26.2 (–), 25.4 (–), 21.5 (–).

Yield: 32 % (mixture syn/anti 1:1)

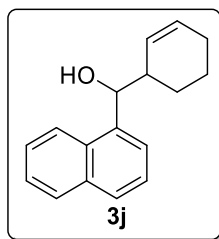
1-(2-Naphthyl)-3buten-1-ol (**3i**)^[39]



¹H NMR (400 MHz, CDCl₃, δ_H) 7.88 – 7.79 (m, 4H), 7.53 – 7.44 (m, 3H), 5.91 – 5.78 (m, 1H), 5.24 – 5.12 (m, 2H), 4.91 (dd, *J* = 7.6, 5.3 Hz, 1H), 2.69 – 2.53 (m, 2H), 2.20 (s, 1H).

¹³C NMR (101 MHz, CDCl₃, δ_C) 141.4 (C_q), 134.5 (+), 133.4 (C_q), 133.1 (C_q), 128.3 (+), 128.1 (+), 127.8 (+), 126.3 (+), 125.9 (+), 124.6 (+), 124.1 (+), 118.7 (–), 73.5 (+), 43.9 (–).

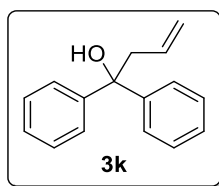
Yield: 48%

Cyclohex-2-enyl(1-naphthyl)methanol (3j)^[40]

¹H NMR (400 MHz, DMSO-*d*₆, δ_H) 8.28 – 8.22 (m, 1H), 8.22 – 8.15 (m, 1H), 7.96 – 7.88 (m, 2H), 7.81 (d, *J* = 8.2 Hz, 2H), 7.65 – 7.59 (m, 2H), 7.56 – 7.43 (m, 6H), 5.90 (dq, *J* = 10.3, 2.2 Hz, 1H), 5.77 – 5.67 (m, 1H), 5.66 – 5.56 (m, 1H), 5.42 (d, *J* = 4.3 Hz, 1H), 5.33 (d, *J* = 4.3 Hz, 1H), 5.29 (dq, *J* = 10.2, 2.3 Hz, 1H), 5.20 (dd, *J* = 6.7, 4.3 Hz, 1H), 5.03 (dd, *J* = 7.0, 4.3 Hz, 1H), 2.62 – 2.51 (m, 2H), 1.99 – 1.83 (m, 4H), 1.76 – 1.57 (m, 4H), 1.44 – 1.27 (m, 4H).

¹³C NMR (101 MHz, DMSO-*d*₆, δ_C) 140.4 (C_q), 140.3 (C_q), 133.4 (C_q), 133.3 (C_q), 130.5 (+), 129.5 (+), 128.7 (+), 128.6 (+), 128.5 (+), 127.9 (+), 127.4 (+), 127.1 (+), 127.0 (+), 125.6 (+), 125.6 (+), 125.3 (+), 125.2 (+), 125.2 (+), 125.2 (+), 124.3 (+), 124.3 (+), 123.9 (+), 123.8 (+), 73.4 (+), 72.3 (+), 42.2 (+), 42.2 (+), 26.4 (–), 24.8 (–), 24.8 (–), 24.2 (–), 21.5 (–), 20.9 (–).

Yield: 48% (mixture syn/anti 1:1)

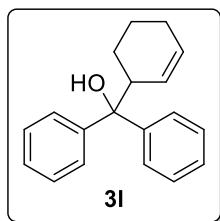
1,1-Diphenylbut-3-en-1-ol (3k)^[8]

¹H NMR (300 MHz, CDCl₃, δ_H) 7.54 – 7.46 (m, 4H), 7.38 – 7.32 (m, 4H), 7.29 – 7.22 (m, 2H), 5.80 – 5.62 (m, 1H), 5.34 – 5.17 (m, 2H), 3.13 (dt, *J* = 7.2, 1.2 Hz, 2H), 2.64 (s, 1H).

¹³C NMR (75 MHz, CDCl₃, δ_C) 146.6 (C_q), 133.5 (+), 128.3 (+), 126.9 (+), 126.1 (+), 120.6 (–), 77.0 (C_q), 46.8 (–).

Yield: 75 %

Cyclohex-2-en-1-ylidiphenylmethanol (3l)^[41]

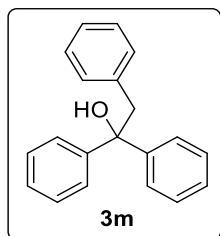


¹H NMR (300 MHz, CDCl₃, δ_H) 7.71 – 7.61 (m, 2H), 7.58 – 7.50 (m, 2H), 7.42 – 7.28 (m, 4H), 7.28 – 7.16 (m, 2H), 6.06 – 5.96 (m, 1H), 5.60 – 5.51 (m, 1H), 3.60 – 3.43 (m, 1H), 2.30 (s, 1H), 2.12 – 2.00 (m, 2H), 1.88 – 1.77 (m, 1H), 1.64 – 1.47 (m, 3H).

¹³C NMR (75 MHz, CDCl₃, δ_C) 146.9 (C_q), 145.6 (C_q), 133.8 (+), 128.4 (+), 128.1 (+), 126.6 (+), 126.5 (+), 126.3 (+), 126.1 (+), 125.5 (+), 79.4 (C_q), 43.8 (+), 25.4 (–), 23.9 (–), 22.1 (–).

Yield: 76 %

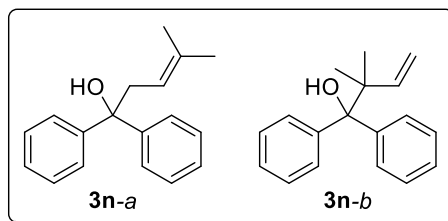
1,1,2-Triphenylethan-1-ol (3m)^[42]



¹H NMR (300 MHz, CDCl₃, δ_H) 7.49 – 7.42 (m, 4H), 7.36 – 7.29 (m, 4H), 7.29 – 7.22 (m, 2H), 7.22 – 7.14 (m, 3H), 6.97 – 6.87 (m, 2H), 3.68 (s, 2H), 2.34 (s, 1H).

¹³C NMR (75 MHz, CDCl₃, δ_C) 146.7 (C_q), 135.9 (C_q), 131.0 (+), 128.2 (+), 128.2 (+), 127.0 (+), 126.9 (+), 126.3 (+), 78.0 (C_q), 48.1 (–).

Yield: 33 %

4-Methyl-1,1-diphenylpent-3-en-1-ol & 2,2-dimethyl-1,1-diphenylbut-3-en-1-ol (3n)^[8, 43]

3n-a:

¹H NMR (400 MHz, CDCl₃, δ_H) 7.51 – 7.46 (m, 4H), 7.37 – 7.30 (m, 4H), 7.26 – 7.21 (m, 2H), 5.12 – 5.04 (m, 1H), 3.05 (d, *J* = 7.4 Hz, 2H), 2.59 (s, 1H), 1.71 (s, 6H).

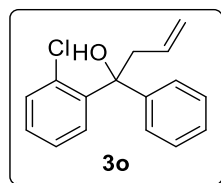
¹³C NMR (101 MHz, CDCl₃, δ_C) 147.1 (C_q), 138.1 (C_q), 128.2 (+), 126.8 (+), 126.1 (+), 118.5 (+), 77.8 (C_q), 40.9 (–), 26.3 (+), 18.4. (+)

3 n-b:

¹H NMR (400 MHz, CDCl₃, δ_H) 7.58 – 7.52 (m, 4H), 7.29 – 7.20 (m, 6H), 6.19 (dd, *J* = 17.6, 10.9 Hz, 1H), 5.26 – 5.10 (m, 2H), 2.46 (s, 1H), 1.19 (s, 6H).

¹³C NMR (101 MHz, CDCl₃, δ_C) 146.5 (+), 145.7 (C_q), 128.6 (+), 127.4 (+), 126.8 (+), 112.8 (–), 81.8 (C_q), 45.6 (C_q), 24.4 (+).

Yield: 77 % (3n-a / 3n-b = 2.6:1)

1-(2-Chlorophenyl)-1-phenylbut-3-en-1-ol (3o)


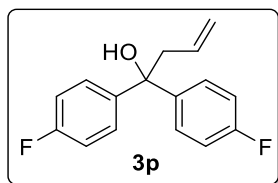
¹H NMR (400 MHz, CDCl₃, δ_H) 7.80 (dd, *J* = 7.9, 1.6 Hz, 1H), 7.33 – 7.17 (m, 8H), 5.74 – 5.61 (m, 1H), 5.16 – 5.03 (m, 2H), 3.41 (ddt, *J* = 14.1, 6.7, 1.3 Hz, 1H), 3.13 (s, 1H), 3.01 (ddt, *J* = 14.1, 7.2, 1.3 Hz, 1H).

¹³C NMR (101 MHz, CDCl₃, δ_C) 145.7 (C_q), 142.7 (C_q), 133.7 (+), 132.5 (C_q), 131.5 (+), 128.9 (+), 128.8 (+), 128.1 (+), 127.2 (+), 126.6 (+), 126.3 (+), 119.1 (–), 77.7 (C_q), 44.7 (–).

HRMS (APCI) (*m/z*): [M + NH₄]⁺ (C₁₆H₁₉ClNO⁺) calc.: 276.1150, found: 276.1150.

Yield: 41 %

1,1-Bis(4-fluorophenyl)but-3-en-1-ol (3p)^[8]



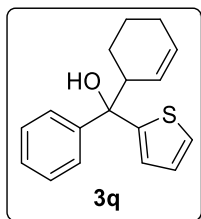
¹H NMR (400 MHz, CDCl₃, δ_H) 7.43 – 7.37 (m, 4H), 7.06 – 6.96 (m, 4H), 5.71 – 5.59 (m, 1H), 5.28 – 5.19 (m, 2H), 3.04 (dt, *J* = 7.2, 1.1 Hz, 2H), 2.59 (s, 1H).

¹³C NMR (101 MHz, CDCl₃, δ_C) 163.1 (C_q), 160.7 (C_q), 142.3 (C_q), 142.3 (C_q), 133.0 (+), 127.9 (+), 127.8 (+), 121.1 (–), 115.2 (+), 115.0 (+), 76.4 (C_q), 47.0 (–).

¹⁹F NMR (376 MHz, CDCl₃, δ_F) -116.4 (s).

Yield: 66 %

Cyclohex-2-en-1-yl(phenyl)(thiophen-2-yl)methanol (3q)

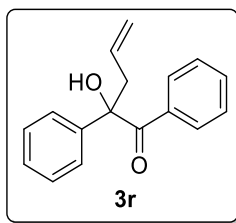


¹H NMR (400 MHz, CDCl₃, δ_H) 7.68 – 7.62 (m, 2H), 7.58 – 7.53 (m, 2H), 7.35 (ddd, *J* = 17.6, 8.4, 7.0 Hz, 4H), 7.29 – 7.15 (m, 4H), 7.12 (dd, *J* = 3.6, 1.2 Hz, 1H), 6.99 (dd, *J* = 5.1, 3.6 Hz, 1H), 6.96 – 6.90 (m, 2H), 6.09 – 6.00 (m, 1H), 5.97 – 5.89 (m, 1H), 5.67 (dq, *J* = 10.3, 2.3 Hz, 1H), 5.44 – 5.35 (m, 1H), 3.41 – 3.32 (m, 1H), 3.32 – 3.23 (m, 1H), 2.65 (s, 1H), 2.44 (s, 1H), 2.06 – 1.97 (m, 4H), 1.88 – 1.68 (m, 3H), 1.63 – 1.46 (m, 3H), 1.44 – 1.36 (m, 2H).

¹³C NMR (101 MHz, CDCl₃, δ_C) 153.3 (C_q), 151.2 (C_q), 146.0 (C_q), 144.7 (C_q), 134.4 (+), 133.3 (+), 128.3 (+), 128.1 (+), 127.0 (+), 126.9 (+), 126.7 (+), 126.3 (+), 126.1 (+), 125.7 (+), 125.3 (+), 124.5 (+), 124.0 (+), 123.3 (+), 123.0 (+), 79.4 (C_q), 79.1 (C_q), 46.4 (+), 46.4 (+), 25.3 (–), 25.3 (–), 24.1 (–), 24.0 (–), 22.0 (–), 21.9 (–).

HRMS (APCI) (*m/z*): [MH⁺ - H₂O] (C₁₇H₁₇S⁺) calc.: 253.1045, found: 253.1045.

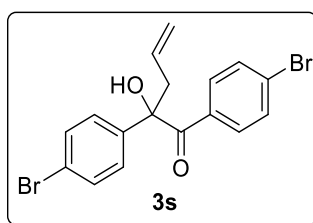
Yield: 57 % (mixture syn/anti 1:1)

2-Hydroxy-1,2-diphenylpent-4-en-1-one (3r)^[44]

¹H NMR (400 MHz, DMSO-*d*₆, δ_H) 7.96 – 7.89 (m, 2H), 7.50 – 7.41 (m, 3H), 7.34 (q, *J* = 7.4 Hz, 4H), 7.26 – 7.18 (m, 1H), 6.47 (s, 1H), 5.70 – 5.56 (m, 1H), 4.94 (d, *J* = 1.3 Hz, 1H), 4.93 – 4.88 (m, 1H), 2.93 – 2.77 (m, 2H).

¹³C NMR (101 MHz, DMSO-*d*₆, δ_C) 200.1 (C_q), 142.1 (C_q), 135.0 (C_q), 133.5 (+), 132.3 (+), 130.2 (+), 128.3 (+), 127.8 (+), 127.0 (+), 124.8 (+), 118.1 (–), 82.0 (C_q), 45.0 (–).

Yield: 65 %

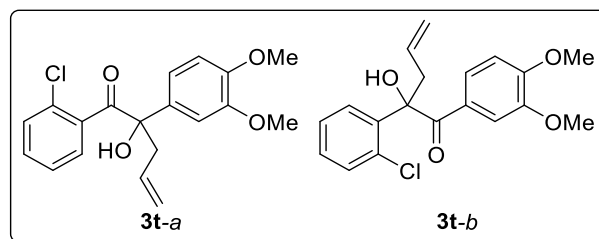
1,2-Bis(4-bromophenyl)-2-hydroxypent-4-en-1-one (3s)^[45]

¹H NMR (300 MHz, CDCl₃, δ_H) 7.71 – 7.63 (m, 2H), 7.54 – 7.42 (m, 4H), 7.39 – 7.32 (m, 2H), 5.81 – 5.59 (m, 1H), 5.23 – 5.02 (m, 2H), 3.84 (s, 1H), 3.10 (ddt, *J* = 13.7, 7.3, 1.0 Hz, 1H), 2.82 (ddt, *J* = 13.7, 7.1, 1.2 Hz, 1H).

¹³C NMR (75 MHz, CDCl₃, δ_C) 199.0 (C_q), 140.7 (C_q), 133.1 (C_q), 132.2 (+), 132.0 (+), 131.9 (+), 131.6 (+), 128.4 (C_q), 127.2 (+), 122.4 (C_q), 121.5 (–), 81.3 (C_q), 44.7 (–).

Yield: 28 %

1-(2-Chlorophenyl)-2-(3,4-dimethoxyphenyl)-2-hydroxypent-4-en-1-one (3t-a) and 2-(2-chlorophenyl)-1-(3,4-dimethoxyphenyl)-2-hydroxypent-4-en-1-one (3t-b)



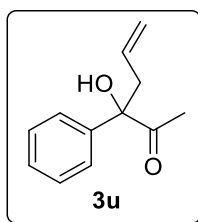
¹H NMR (400 MHz, CDCl₃, δ_H) 7.88 (dd, *J* = 7.9, 1.4 Hz, 1H), 7.40 – 7.31 (m, 3H), 7.30 – 7.23 (m, 4H), 7.06 (td, *J* = 7.6, 1.2 Hz, 1H), 7.03 – 6.97 (m, 3H), 6.86 – 6.80 (m, 1H), 6.68 – 6.62 (m, 2H), 5.87 – 5.66 (m, 2H), 5.24 – 5.17 (m, 3H), 5.10 – 5.04 (m, 1H), 5.00 – 4.91 (m, 1H), 4.76 (s, 1H), 3.87 (s, 4H), 3.83 (s, 3H), 3.81 (s, 4H), 3.69 (s, 3H), 3.56 (s, 1H), 3.21 – 3.10 (m, 2H), 3.08 – 2.98 (m, 1H), 2.89 – 2.81 (m, 1H).

¹³C NMR (101 MHz, CDCl₃, δ_C) 204.6 (C_q), 197.4 (C_q), 153.3 (C_q), 149.0 (C_q), 148.8 (C_q), 148.5 (C_q), 140.7 (C_q), 137.5 (C_q), 133.9 (C_q), 132.3 (+), 131.9 (+), 131.5 (+), 131.1 (C_q), 130.8 (+), 129.9 (+), 129.5 (+), 128.1 (+), 127.4 (+), 127.0 (+), 126.6 (C_q), 125.9 (+), 124.3 (+), 120.8 (–), 119.7 (–), 118.6 (+), 112.1 (+), 111.0 (+), 110.0 (+), 109.3 (+), 82.4 (–), 79.8 (–), 56.0 (+), 55.9 (+), 55.9 (+), 55.8 (+), 43.9 (–), 43.2 (–).

HRMS (ESI) (*m/z*): [MH⁺] (C₁₉H₂₀ClO₄⁺) calc.: 347.1045, found: 347.1052.

Yield: 57 % (3t-a/3t-b = 1:1.3)

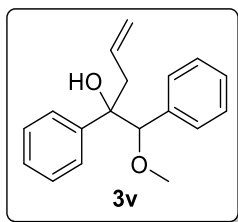
3-Hydroxy-3-phenylhex-5-en-2-one (3u)^[46]



¹H NMR (400 MHz, CDCl₃, δ_H) 7.51 – 7.45 (m, 2H), 7.41 – 7.34 (m, 2H), 7.34 – 7.28 (m, 1H), 5.82 – 5.69 (m, 1H), 5.26 – 5.14 (m, 2H), 4.24 (s, 1H), 3.04 – 2.88 (m, 2H), 2.09 (s, 3H).

¹³C NMR (101 MHz, CDCl₃, δ_C) 208.9 (C_q), 140.6 (C_q), 132.3 (+), 128.8 (+), 128.2 (+), 126.1 (+), 119.8 (–), 82.3 (C_q), 41.6 (–), 24.2 (+).

Yield: 12 %

1-Methoxy-1,2-diphenylpent-4-en-2-ol (3v)

¹H NMR (400 MHz, CDCl₃, δ_H) 7.30 – 7.21 (m, 3H), 7.20 – 7.10 (m, 5H), 7.03 – 6.94 (m, 2H), 5.70 – 5.50 (m, 1H), 5.15 – 4.95 (m, 2H), 4.30 – 4.28 (2 x s, 1H), 3.26 – 3.22 (2 x s, 3H), 2.92 – 2.82 (m, 2H), 2.73 – 2.51 (m, 1H).

¹³C NMR (101 MHz, CDCl₃, δ_C) 142.7 (C_q), 142.2 (C_q), 136.9 (C_q), 136.8 (C_q), 133.9 (+), 133.7 (+), 128.8 (+), 128.7 (+), 128.0 (+), 127.7 (+), 127.7 (+), 127.5 (+), 127.5 (+), 127.0 (+), 126.9 (+), 126.7 (+), 126.6 (+), 118.7 (–), 118.6 (–), 90.6 (+), 89.8 (+), 78.3 (C_q), 78.3 (C_q), 57.6 (+), 57.6 (+), 42.9 (–), 41.1 (–).

Yield: 36 % (mixture syn/anti 1:1)

3.4.3 Detailed optimization of the reaction conditions**Screening of different photocatalysts**

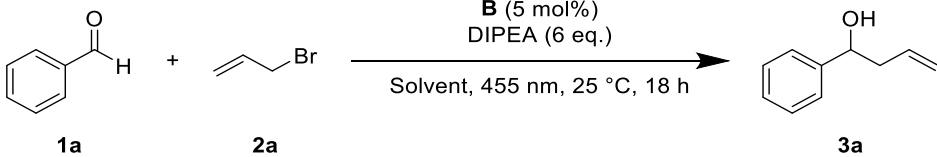
Table 3-3 – Optimization of the reaction conditions: screening of different photocatalysts ^[a]

Entry	Photocatalyst (mol%, hv [nm])	Yield ^[b] [%]
1	4CzIPN (5, 455)	22
2 ^[c]	(Ir[dF(CF ₃)ppy] ₂ (dtbpy))PF ₆ (2, 455)	21
3	D (5, 400)	48
4	Eosin Y (5, 535)	0
5	Fluorescein (5, 535)	0
6	[Ru(bpy) ₃]Cl ₂ (5, 455)	0
7	Rhodamine 6G	0

[a] The reactions were performed using 1 eq. of **1a** and 2 eq. of **2a**. [b] Determined by GC analysis with 1-Naphthol as an internal standard. [c] DMA was used as a solvent instead of DMF.

Screening of different solvents

Table 3-4 – Optimization of the reaction conditions: screening of different solvents^[a]

		
Entry	Solvent	Yield ^[b] [%]
1	DMF (dry)	38
2	MeCN (dry)	24
3	EtOH	24
4	DCE (dry)	19
5	Toluene (dry)	0
6	DMSO	34
7	THF	7
8	DMA	54

[a] The reactions were performed using 1 eq. of **1a** and 1 eq of **2a**. in 2 mL of degassed solvent under nitrogen. [b] Determined by GC analysis with 1-Naphthol as an internal standard.

Screening of different additives

Table 3-5 – Optimization of the reaction conditions: screening of different additives.^[a]

c1ccccc1C=O (1a) + C=CCBr (2a) $\xrightarrow[\text{DMA, 455 nm, 25 } ^\circ\text{C, 18 h}]{\text{B (5 mol\%), e}^-\text{-donor, additive}}$ c1ccccc1C(O)CC=C (3a)

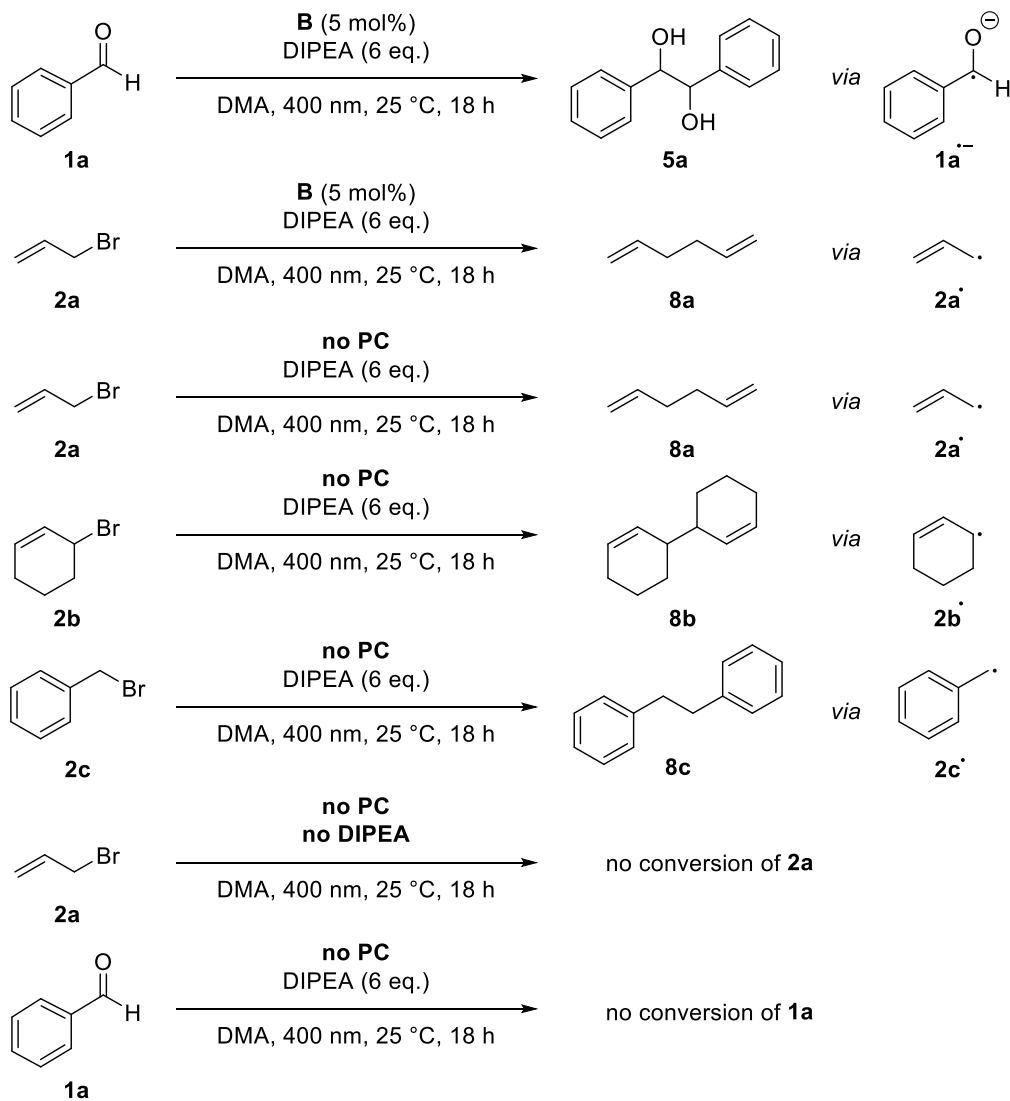
Entry	Electron donor (eq.)	Additive (eq.)	Yield ^[b] [%]
1	DIPEA (6)	—	38
2	TEA (6)	—	0
3	TBA (2)	—	16
4	Hantzsch ester (2)	K ₂ CO ₃ (1)	25
5	DIPEA (6)	LiBF ₄ (1)	43
6 ^[c, d]	DIPEA (6)	LiBF ₄ (1.5)	64
7 ^[c, d]	DIPEA (6)	Li ₂ CO ₃ (1)	56
8 ^[c, d]	DIPEA (6)	LiCl (1.5)	0
9 ^[c, d]	DIPEA (6)	Thiophenol (1)	51
10 ^[c, d]	DIPEA (6)	LiBF ₄ (0.5)	43
11 ^[c, d]	DIPEA (3)	LiBF ₄ (1.5)	39
12 ^[c, d]	DIPEA (6)	La(OTf) ₃ (1)	0
13 ^[c, d]	DIPEA (6)	B ₂ pin ₂ (1)	0

[a] The reactions were performed using 1 eq. of **1a** and 1 eq. of **2a** in 2 mL of degassed solvent under nitrogen, [b] Determined by GC analysis with 1-Naphthol as an internal standard, [c] DMA was used as a solvent instead of DMF, [d] reaction performed at 400 nm.

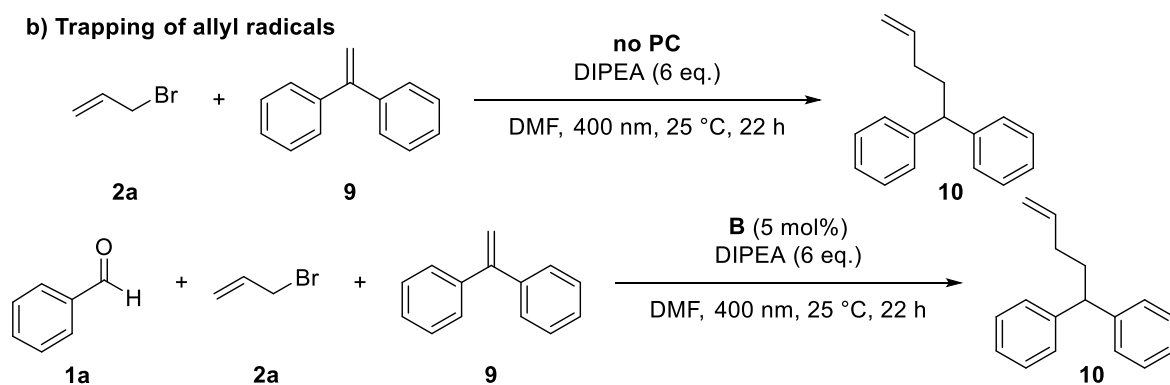
3.4.4 Mechanistic investigations

Control reactions

a) Formation of homocoupling products

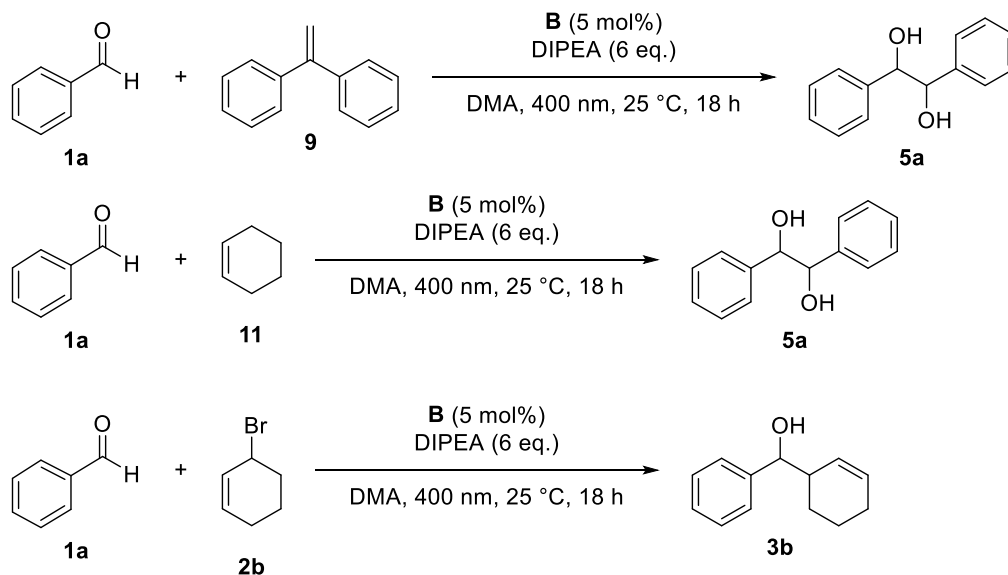


b) Trapping of allyl radicals

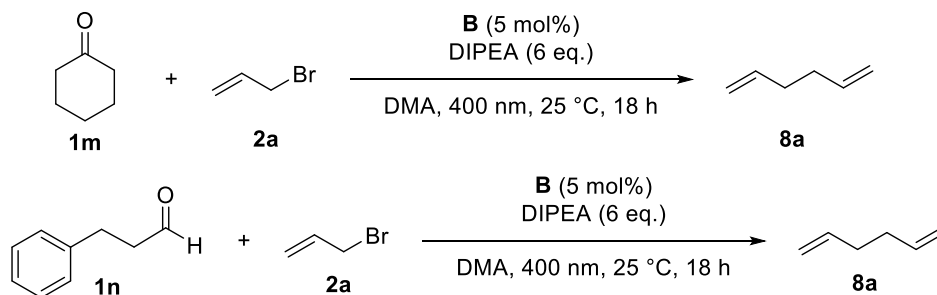


Scheme 3-4 – Control reactions for the formation of ketyl- and allyl-/benzyl radicals.

a) Control reactions for the trapping of ketyl radicals with alkenes



b) Control reactions for the trapping of allyl radicals with carbonyls



Scheme 3-5 – Control experiments for radical-radical cross-coupling

All control experiments were performed with 1 eq. of **1** (0.2 mmol), 2 eq. of **2** (0.4 mmol), 5 mol% photocatalyst **B**, 6 eq. DIPEA (1.2 mmol) in 2 mL degassed solvent (DMA or DMF) under nitrogen. In radical trapping experiments, 10 eq. of 1,1-diphenylethylene **9** were added. The reactions were irradiated with 400 nm at 25 °C. The reaction mixtures were analyzed with GC and GC-MS.

3.4.4.1 Fluorescence quenching experiments

For fluorescence quenching experiments, a 30 μM solution of the photocatalyst **D** in degassed DMF was prepared under nitrogen atmosphere in a gas-tight 10 mm quartz cuvette. The photocatalyst was irradiated with 390 nm and the change of the fluorescence emission upon addition of different potential quenchers was recorded.

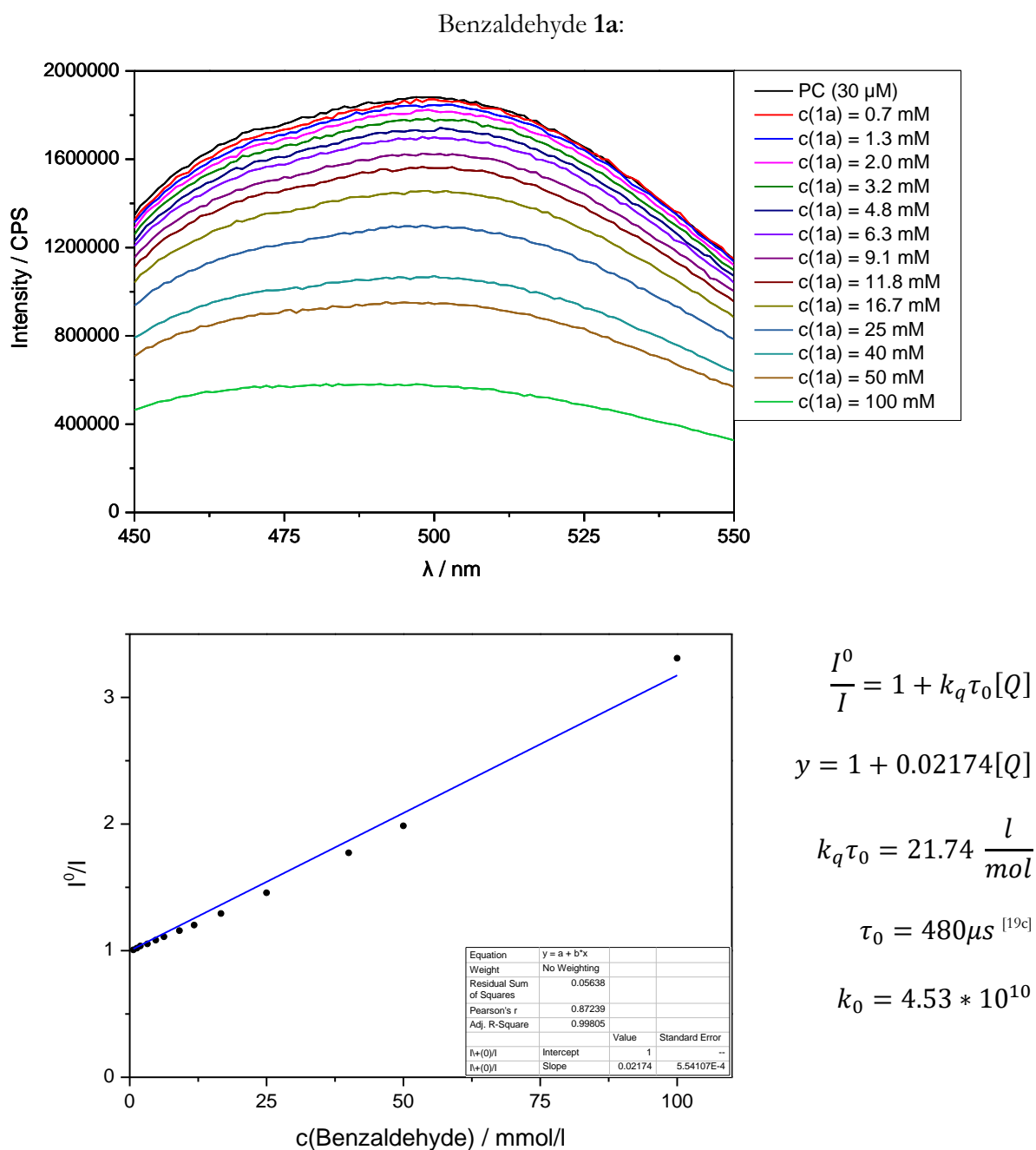


Figure 3-4 – Top: fluorescence quenching of **D** (30 μM in DMF) upon titration with **1a**, bottom: corresponding Stern-Volmer plot.

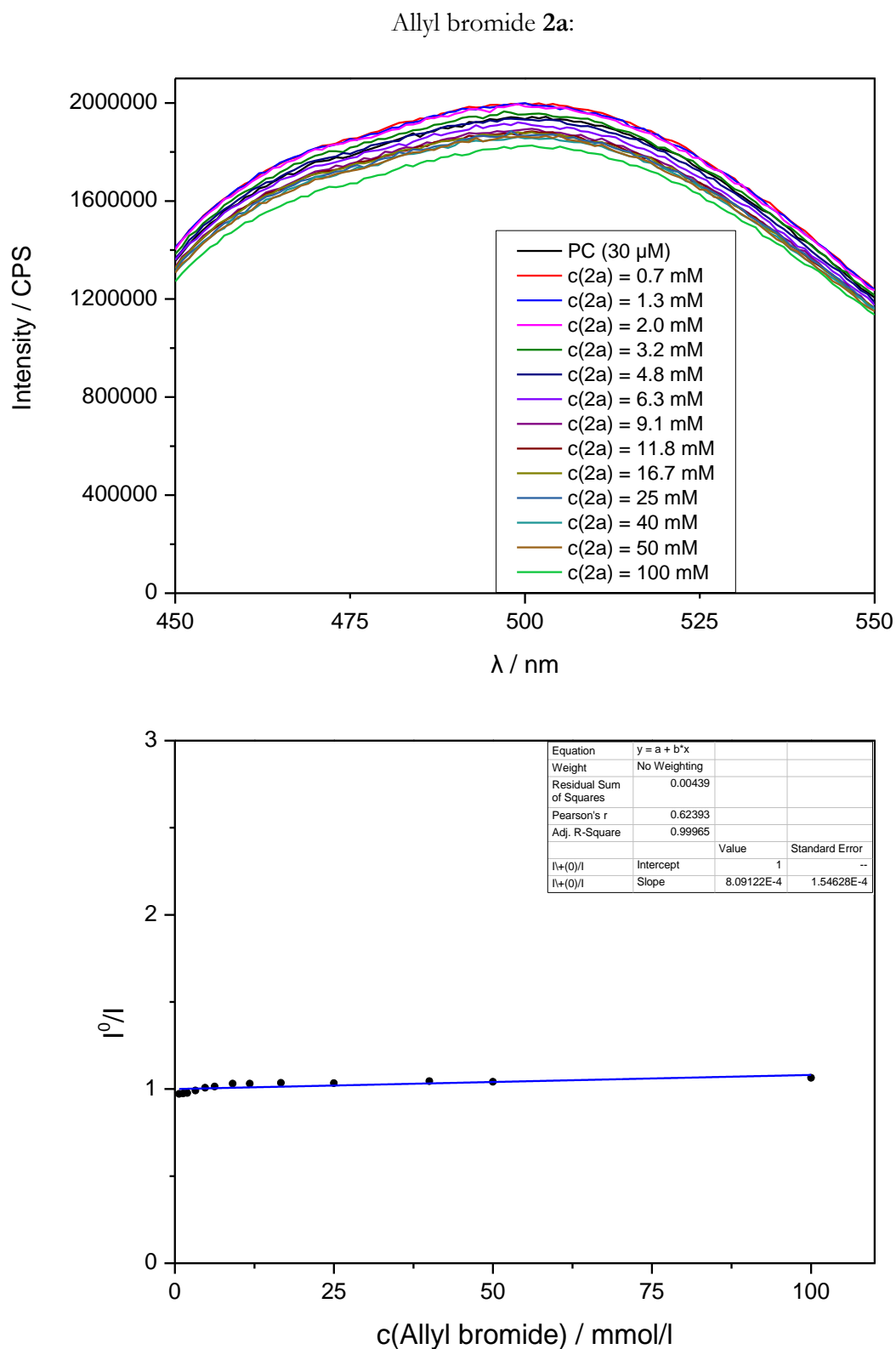


Figure 3-5 – Top: fluorescence quenching of **D** (30 μ M in DMF) upon titration with **2a**, bottom: corresponding Stern-Volmer plot.

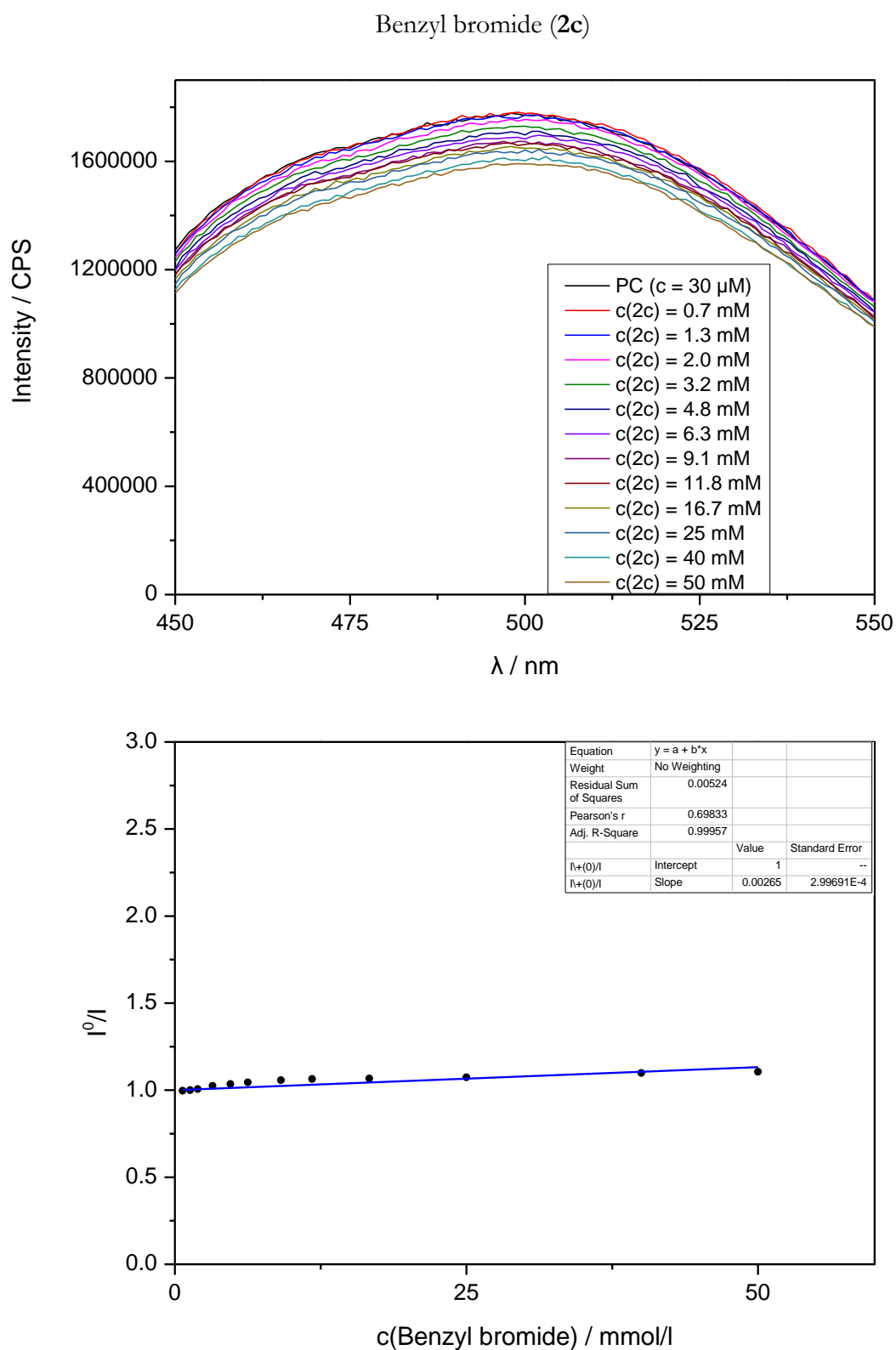


Figure 3-6 – Top: fluorescence quenching of **D** (30 μM in DMF) upon titration with **2c**, bottom: corresponding Stern-Volmer plot.

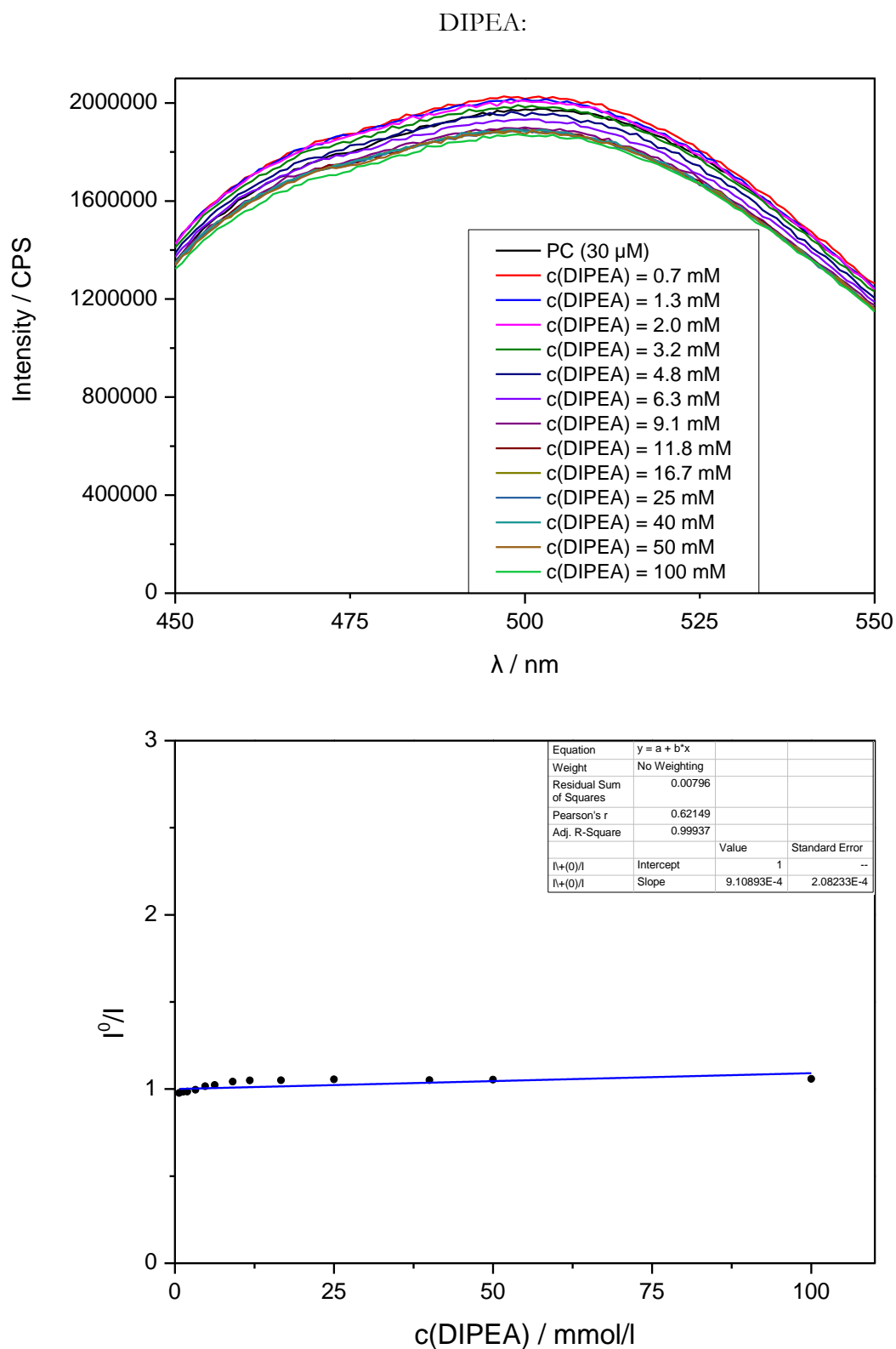


Figure 3-7 – Top: fluorescence quenching of **D** ($30\ \mu\text{M}$ in DMF) upon titration with DIPEA, bottom: corresponding Stern-Volmer plot.

The fluorescence titration experiments show an effective quenching of the emission of photocatalyst **D** after the addition of benzaldehyde (**1a**) (Figure 3-4). This indicates that an electron transfer from the excited state of the photocatalyst to **1a** takes place upon irradiation which leads to the formation of the ketyl radical anion $\mathbf{1a}^{\bullet-}$ and the oxidized form of the photocatalyst $\text{PC}^{\bullet+}$. Allyl bromide (**2a**), benzyl bromide (**2c**) and DIPEA did not quench the emission of the **D**, so there seems to be no interaction between the excited state of the photocatalyst and **2a**, **2c** or DIPEA (Figure 3-5 – 3-7).

3.4.4.2 Cyclic voltammetry measurements

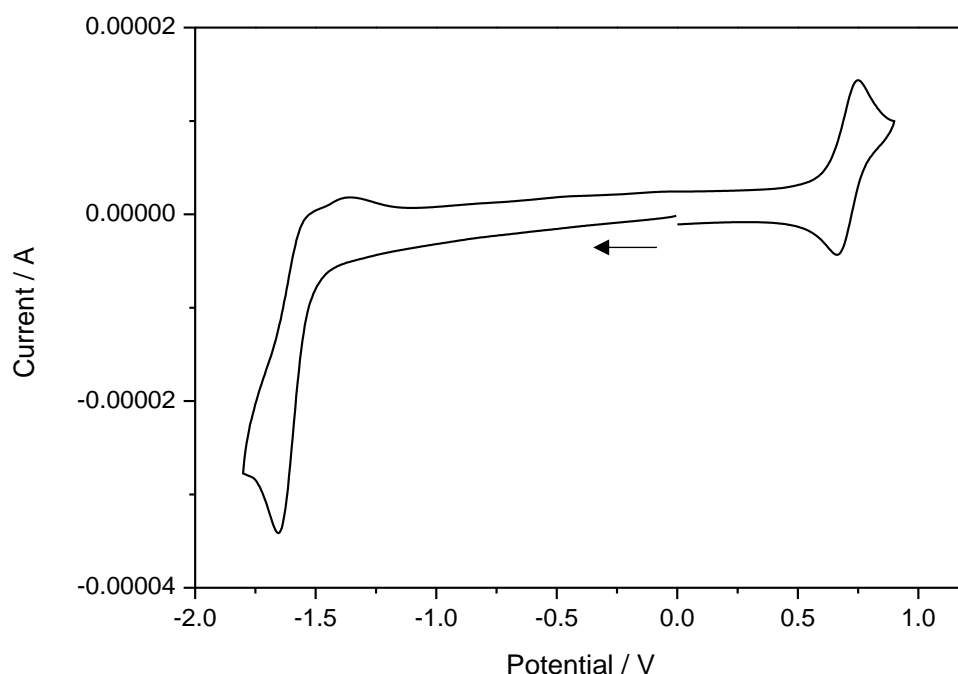


Figure 3-8 – Cyclic voltammogram of benzaldehyde (**1a**) in DMF under argon (scan direction indicated by black arrow). The peak at -1.65 V shows the reduction of **1a** and corresponds to a potential of -2.0 V *vs* SCE; the reversible peaks at 0.66 and 0.75 V correspond to ferrocene, which was used as an internal standard. The measurement was performed with a scan rate of 50 mV/s and with TBATFB (0.1 M) as supporting electrolyte.

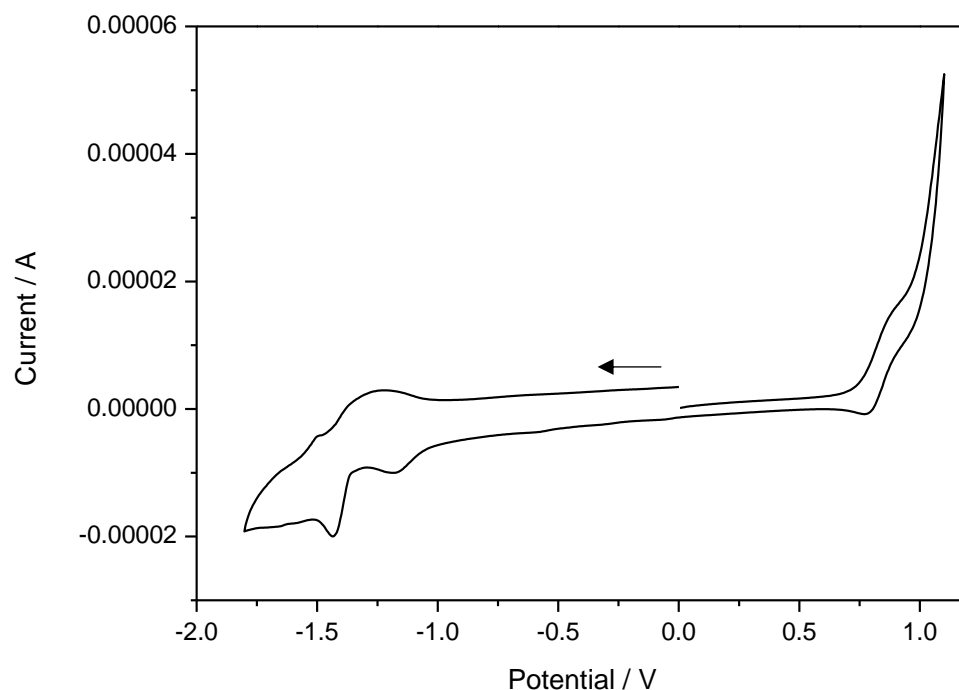


Figure 3-9 – Cyclic voltammogram of a mixture of benzaldehyde (**1a**, 1 eq.), DIPEA (6 eq.) and LiBF_4 (1.5 eq.) in DMF under argon (scan direction indicated by black arrow). The peak at -1.43 V shows the reduction of **1a** and corresponds to a potential of -1.88 V *vs* SCE; the reversible peaks at 0.79 and 0.87 V correspond to ferrocene, which was used as an internal standard. The measurement was performed with a scan rate of 50 mV/s and with TBATFB (0.1 M) as supporting electrolyte.

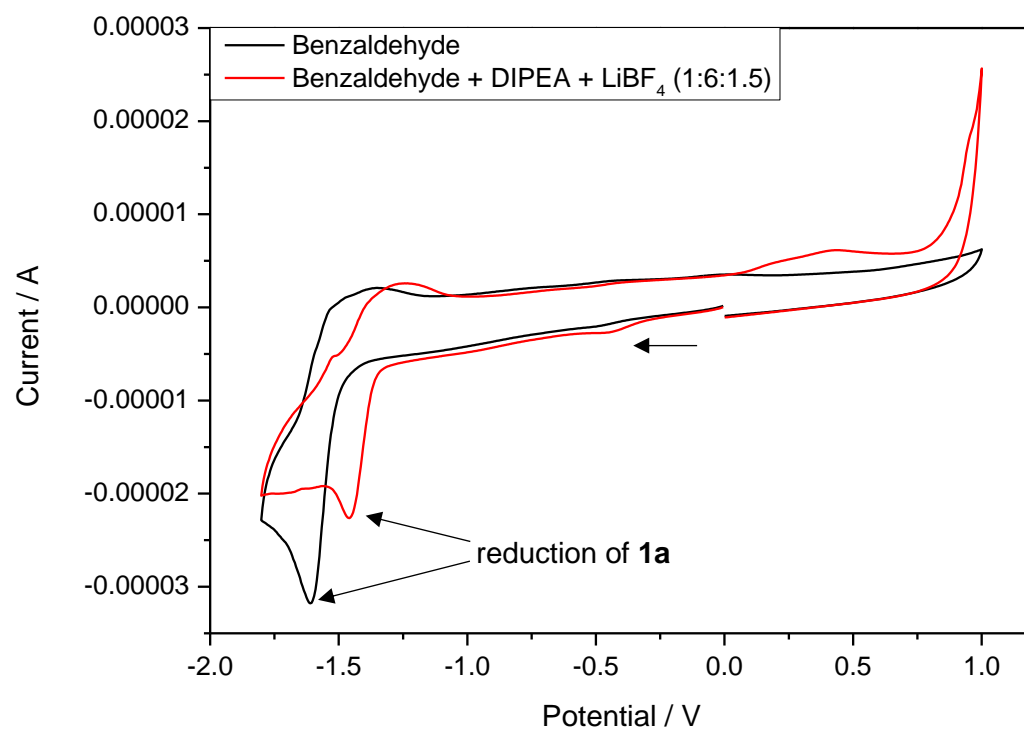


Figure 3-10 – Cyclic voltammograms of benzaldehyde (**1a**, black) and mixture of **1a** (1 eq.), DIPEA (6 eq.) and LiBF_4 (1.5 eq.) (red) under argon (scan direction indicated by black arrow). The peak that corresponds to the reduction of **1a** is shifted to lower potentials upon addition of DIPEA and LiBF_4 . The measurement was performed with a scan rate of 50 mV/s and with TBATFB (0.1 M) as supporting electrolyte.

3.4.4.3 UV/Vis measurements

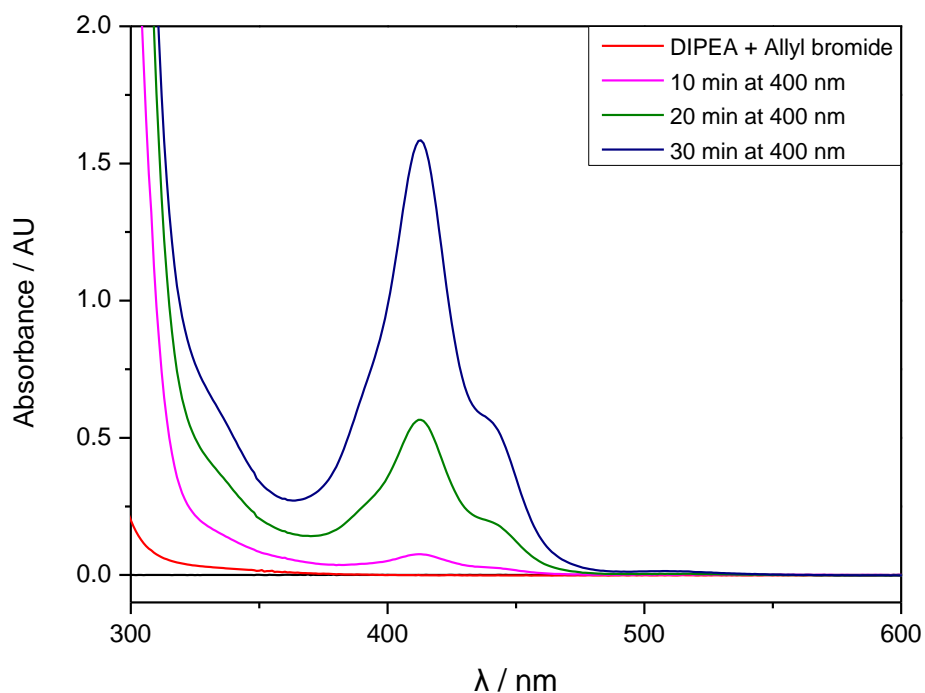


Figure 3-11 – UV/Vis absorption spectra of allyl bromide (**2a**, 1 eq., 0.4 mmol) and DIPEA (3 eq., 1.2 mmol) in DMA before irradiation and after 10, 20 and 30 minutes of 400 nm irradiation.

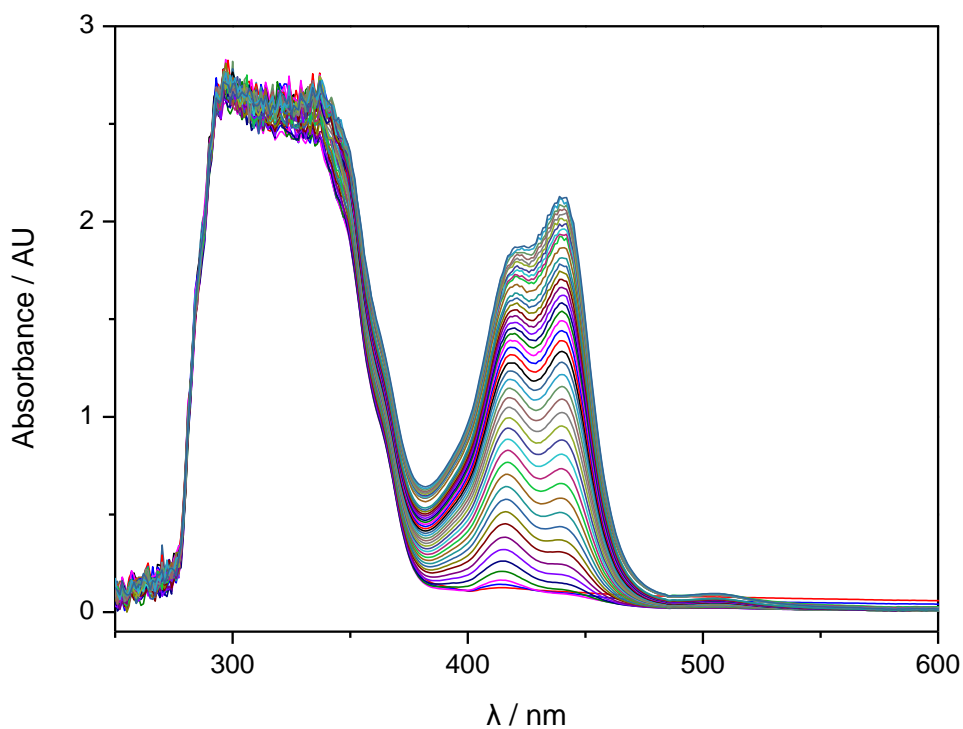


Figure 3-12 – On-line UV/Vis measurements of a mixture of benzaldehyde (**1a**, 1 eq., 0.2 mmol), allyl bromide (**2a**, 2 eq., 0.4 mmol), DIPEA (6 eq., 1.2 mmol) and LiBF₄ (1.5 eq., 0.3 mmol) in DMA (2 mL). The reaction mixture was irradiated for 22 h with 400 nm light, a UV/Vis spectrum was recorded every 30 minutes.

3.4.4.4 Quantum yield determination

The quantum yield was measured using a quantum yield determination setup determined by our group and the group of Riedle:^[47] Thorlabs DT 25/M or DT S25M translation stages (horizontal and vertical), photographic lens with $f = 50$ mm, magnetic stirrer (Faulhaber motor 1524B024S R with 14:1 gear), PS19Q power sensor from Coherent, adjustable power supply (Basetech BT-153-0-15 V/DC 0-3 A 45 W), PowerMax software.

A reaction mixture of **1a** (20.33 μ l, 0.2 mmol, 1 eq.), **2a** (34.62 μ l, 0.2 mmol, 2 eq.), DIPEA (0.2 ml, 1.2 mmol, 6 eq.) and LiBF₄ (28.1 mg, 0.3 mmol, 1.5 eq.) and photocatalyst **B** (6.1 mg, 5 mol%) in 2 ml DMA was degassed with three cycles freeze pump thaw and transferred into a gas tight 10 mm Hellma[®] quartz fluorescence cuvette with a stirring bar under nitrogen atmosphere. A cuvette with solvent (DMA, 2 ml) and a stirring bar was placed in the beam of a 400 nm LED and the transmitted power ($P_{ref} = 72$ mW) was determined by a calibrated photodiode horizontal to the cuvette. The cuvette containing the reaction mixture was placed in the beam of the LED and the transmitted power P_{sample} was measured analogously. The sample was irradiated and the transmitted power as well as the yield of the photocatalytic reaction were recorded after different times (Table 4). These values enabled the determination of the quantum yield according to the following equation **E1**:

$$\Phi = \frac{N_{product}}{N_{ph}} = \frac{N_A * n_{product}}{\frac{E_{light}}{E_{ph}}} = \frac{N_A * n_{product}}{\frac{E_{absorbed} * t}{\frac{h * c}{\lambda}}} = \frac{h * c * N_A * n_{product}}{\lambda * (P_{ref} - P_{sample}) * t} \quad (\text{E1})$$

where Φ is the quantum yield, $N_{product}$ is the number of product molecules generated during the reaction, N_{ph} is the number of absorbed photons, N_A is Avogadro's constant, $n_{product}$ is the amount of product generated in mol, E_{light} is the energy of absorbed light in Joules, E_{ph} is the energy of a single photon, $P_{absorbed}$ is the radiant power absorbed in Watts, t is the irradiation time in seconds, h is the Planck's constant in J*s, c is the speed of light in m s^{-1} , λ is the wavelength of the irradiation source (400 nm), P_{ref} is the radiant power transmitted by a blank sample containing only the solvent and P_{sample} is the radiant power transmitted by the cuvette containing the reaction mixture.

After one hour of irradiation, the yield of the reaction was 34 %, and P_{sample} was 50 μ W, which corresponds to a quantum yield of $\Phi = 7.6\%$

3.4.4.5 NMR-experiments

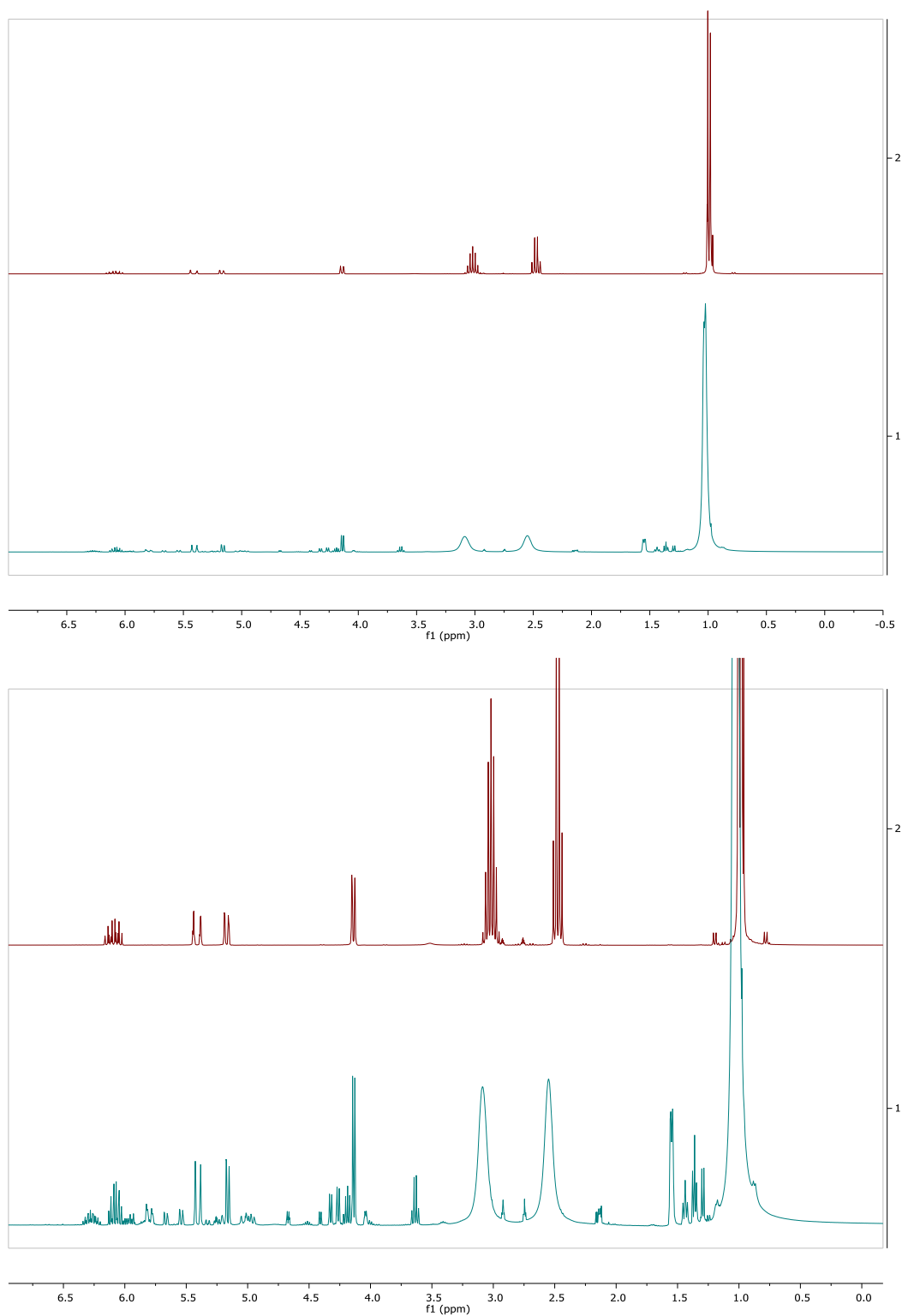
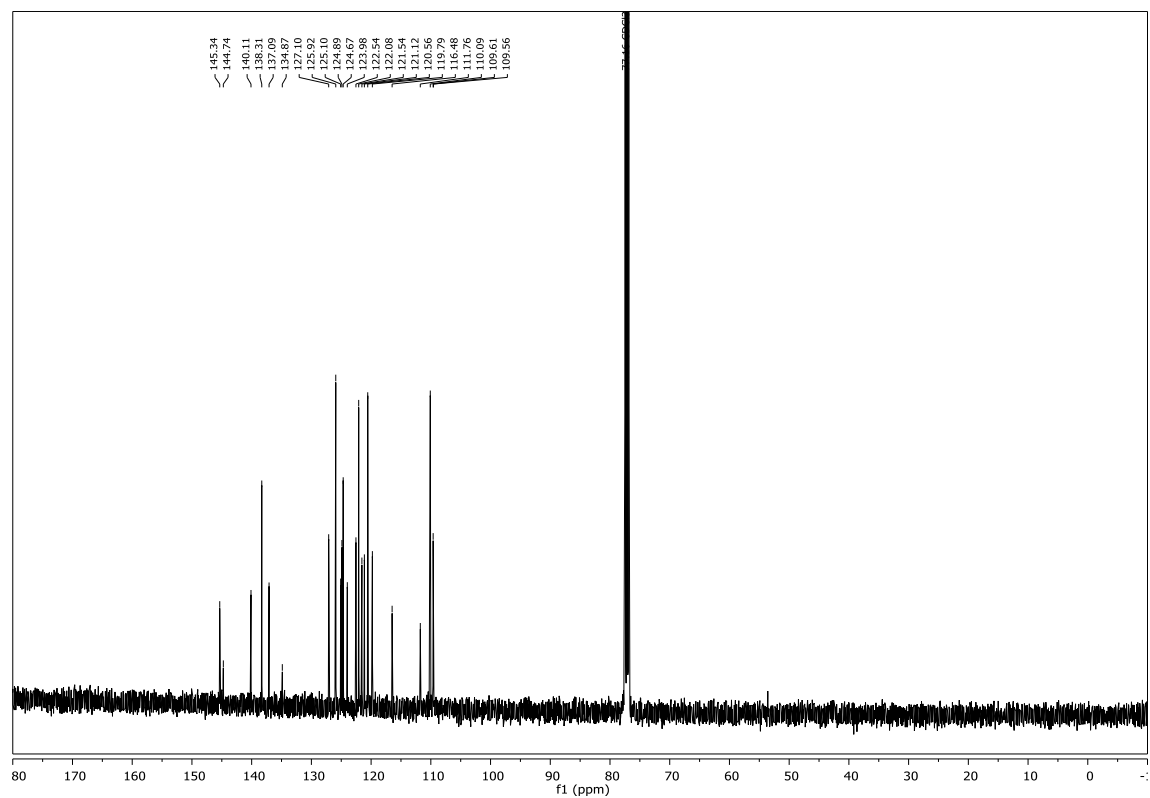
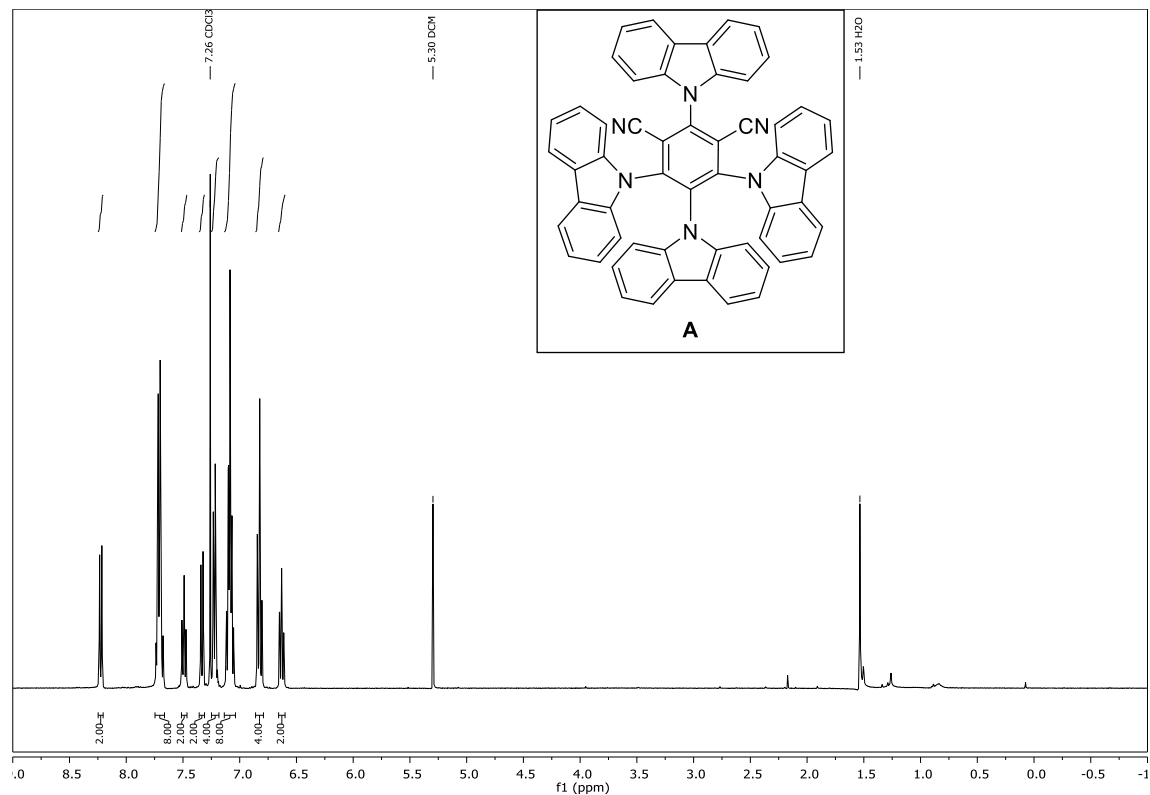


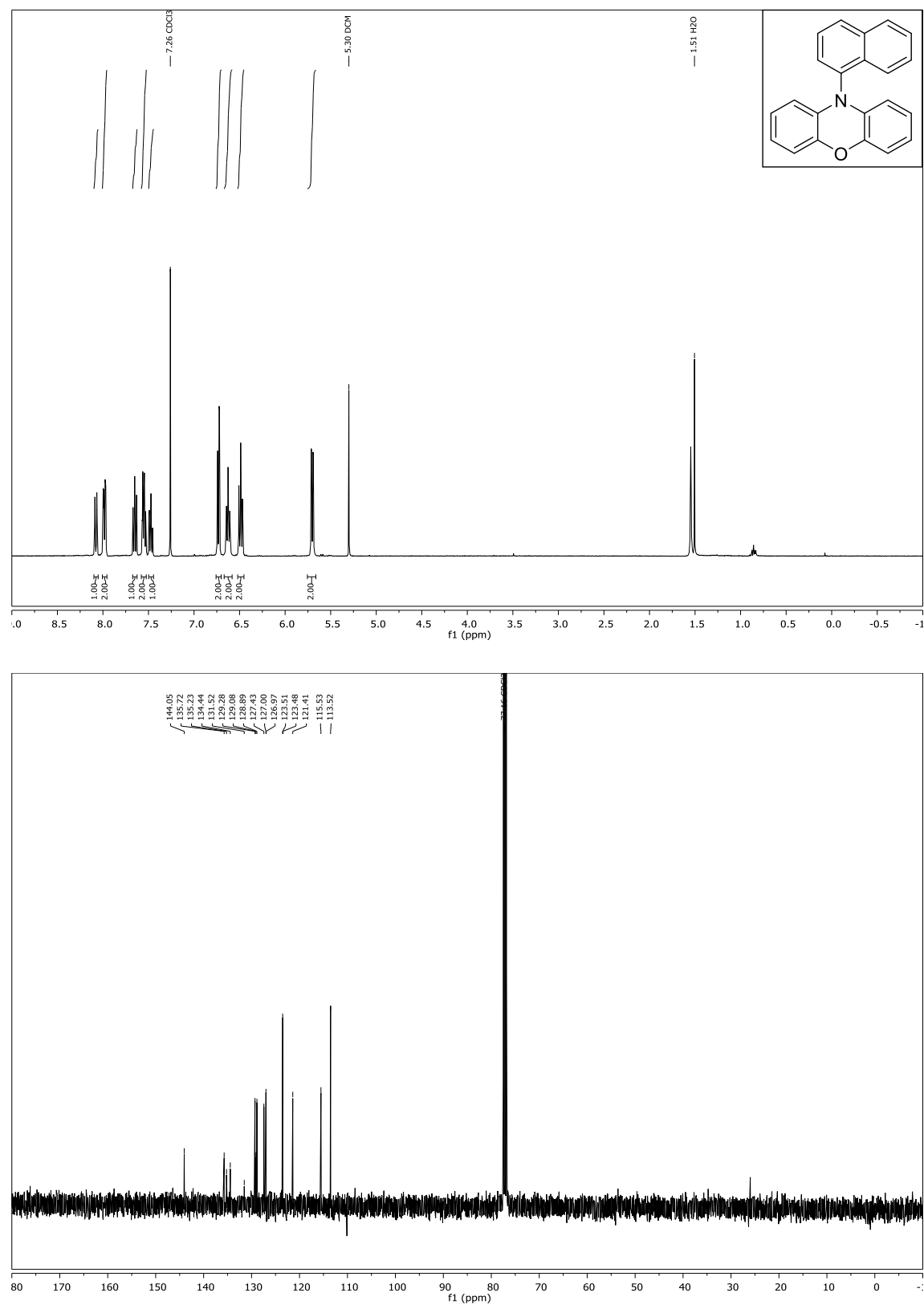
Figure 3-13 – ^1H -NMR-spectra of allyl bromide (**2a**, 1 eq.) and DIPEA (3 eq.) in $\text{DMF-}d_7$ before (red) and after (blue) 22 h of 400 nm irradiation. While the allyl bromide signals remain unchanged, the signals of DIPEA (1.03, 2.55 and 3.09 ppm) show a broadening, which indicates the formation of radicals or ionic species in the reaction mixture upon irradiation.

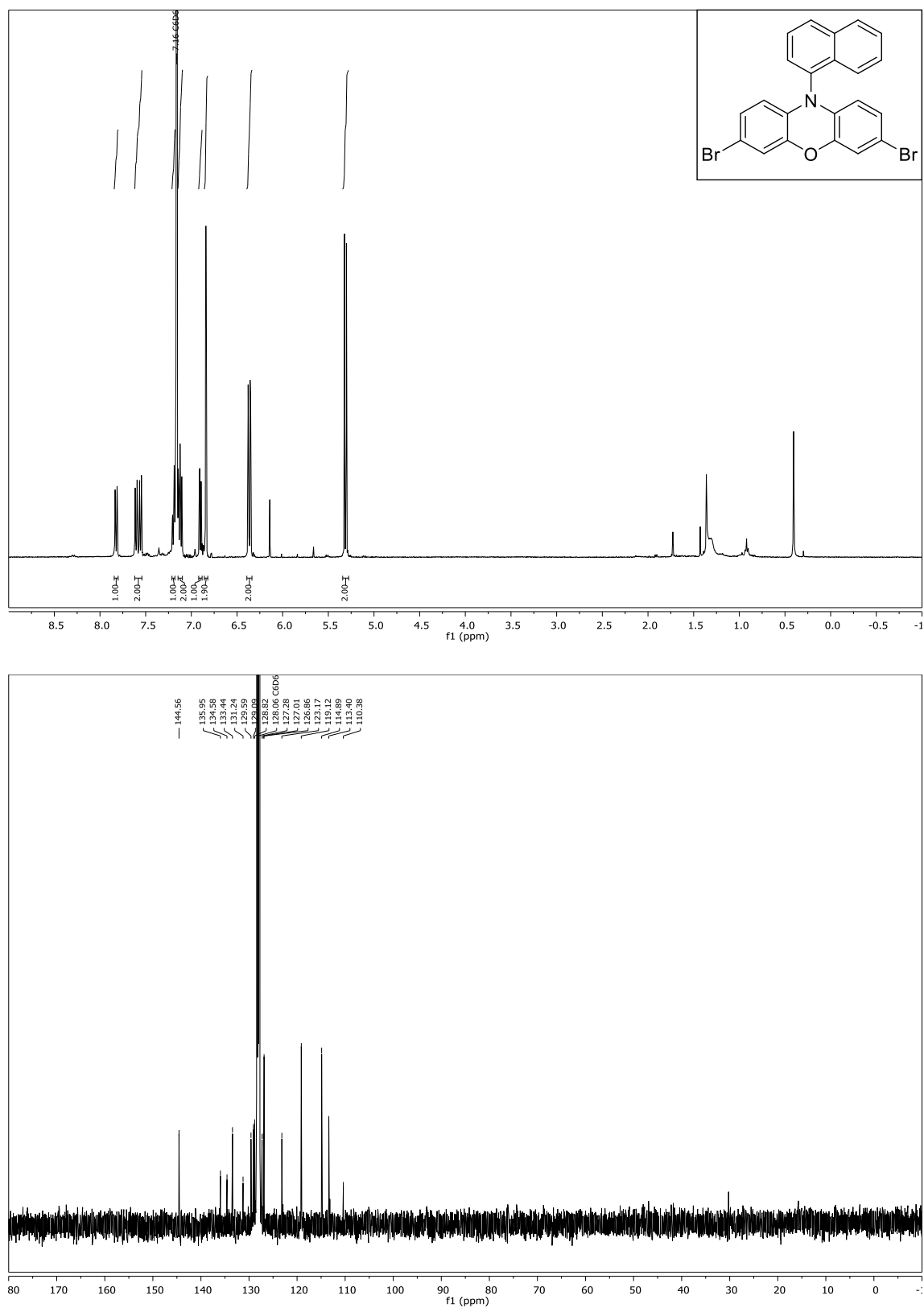
3.5 NMR-spectra

Compound **A** (4CzIPN), ^1H - and ^{13}C -NMR (CDCl_3)

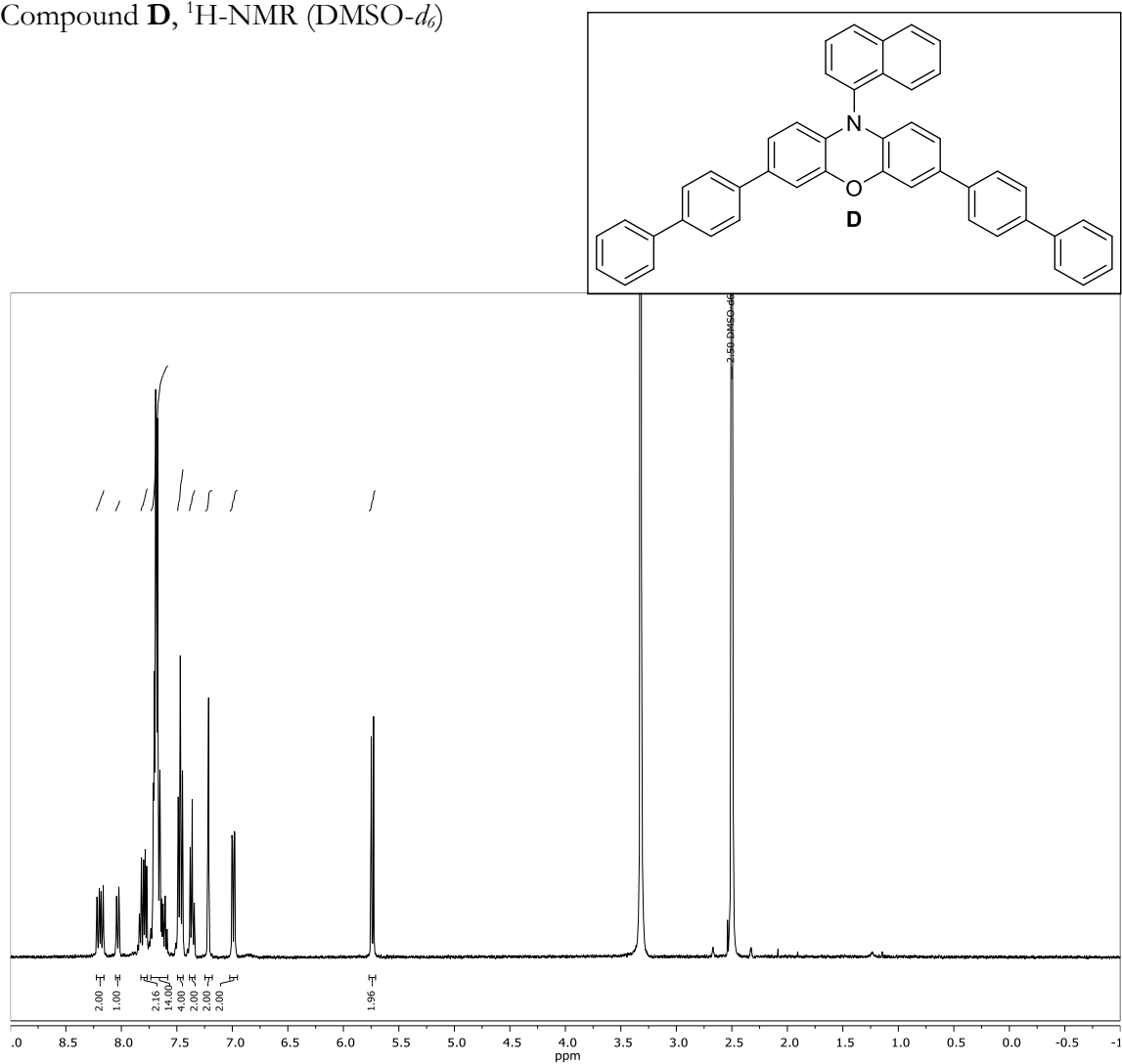


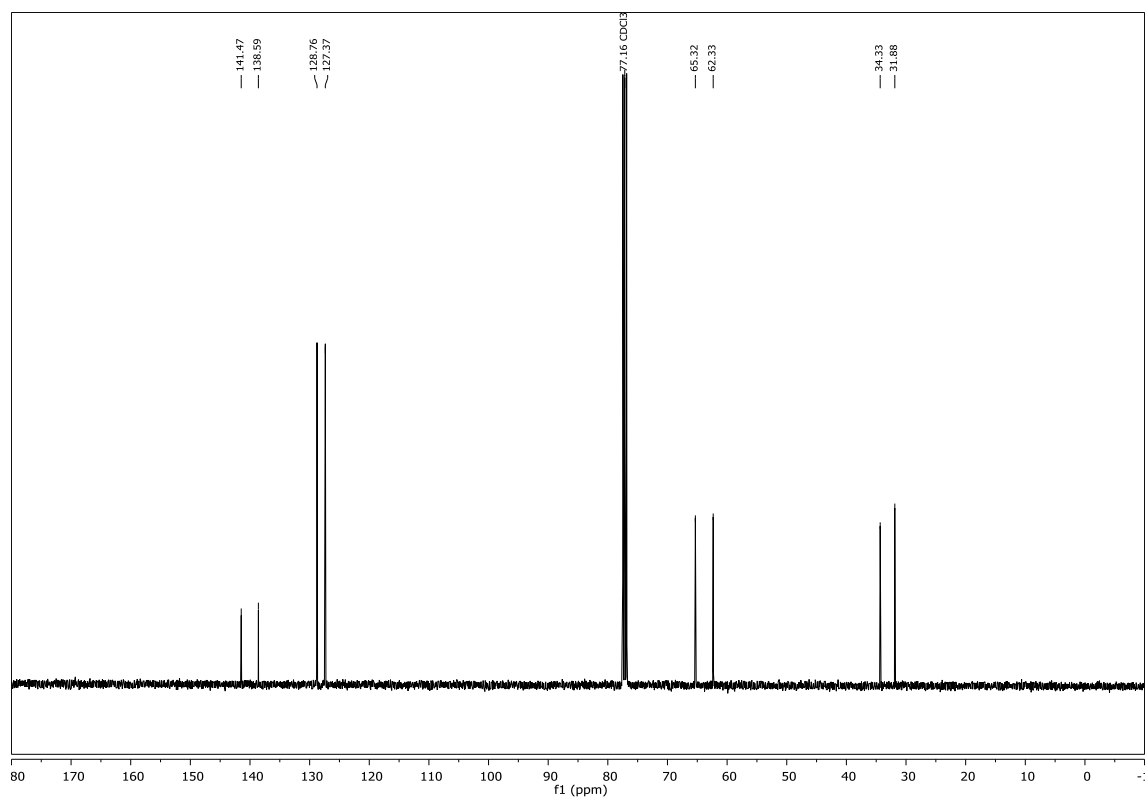
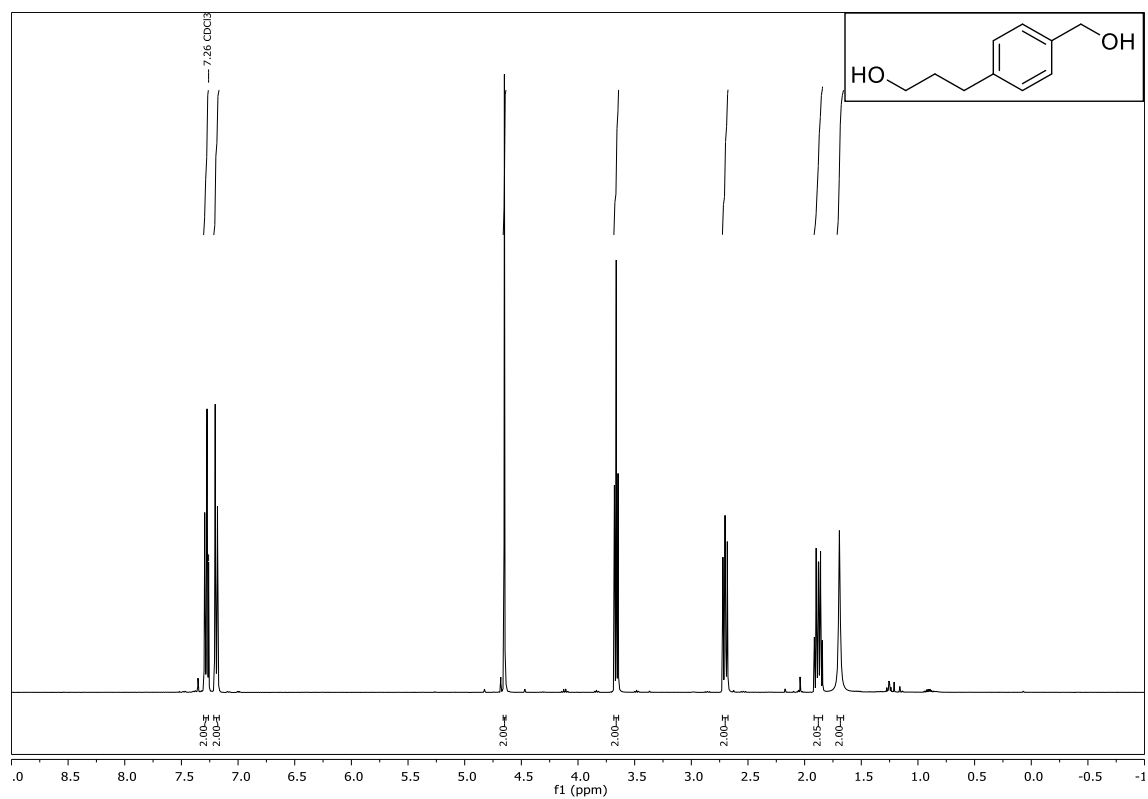
1-Naphthalene-10-phenoxazine, ^1H - and ^{13}C -NMR (CDCl_3)



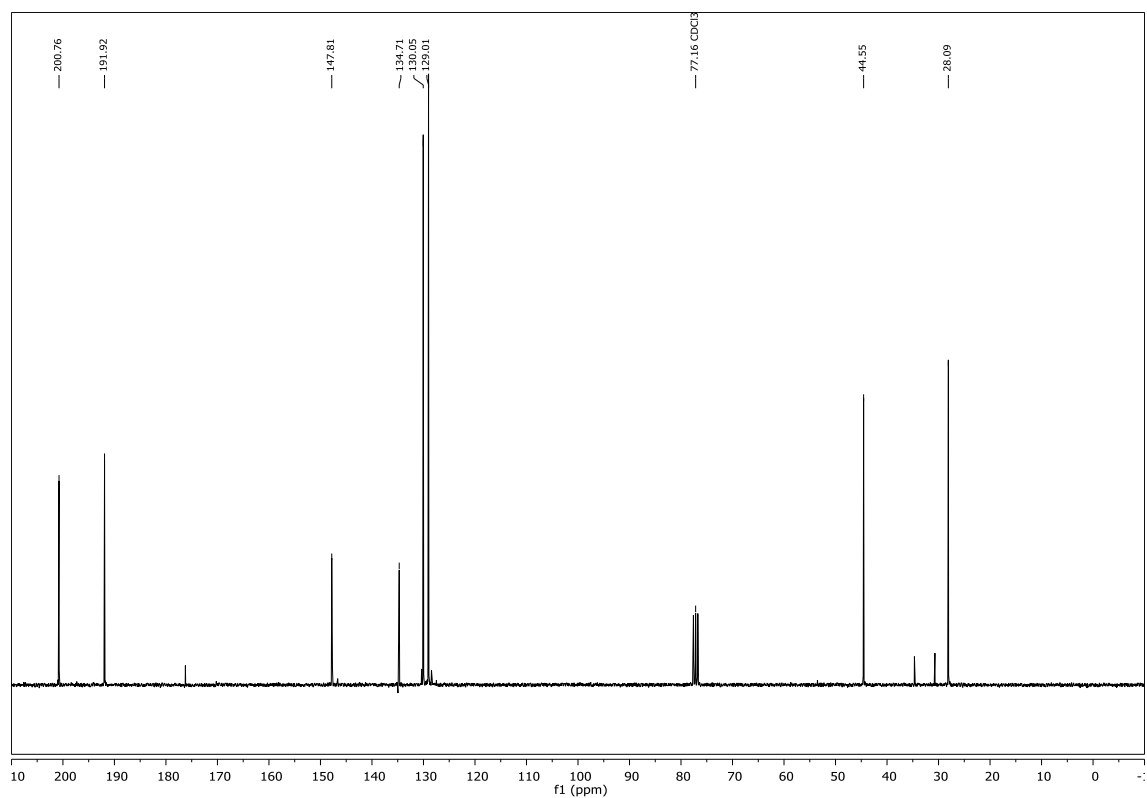
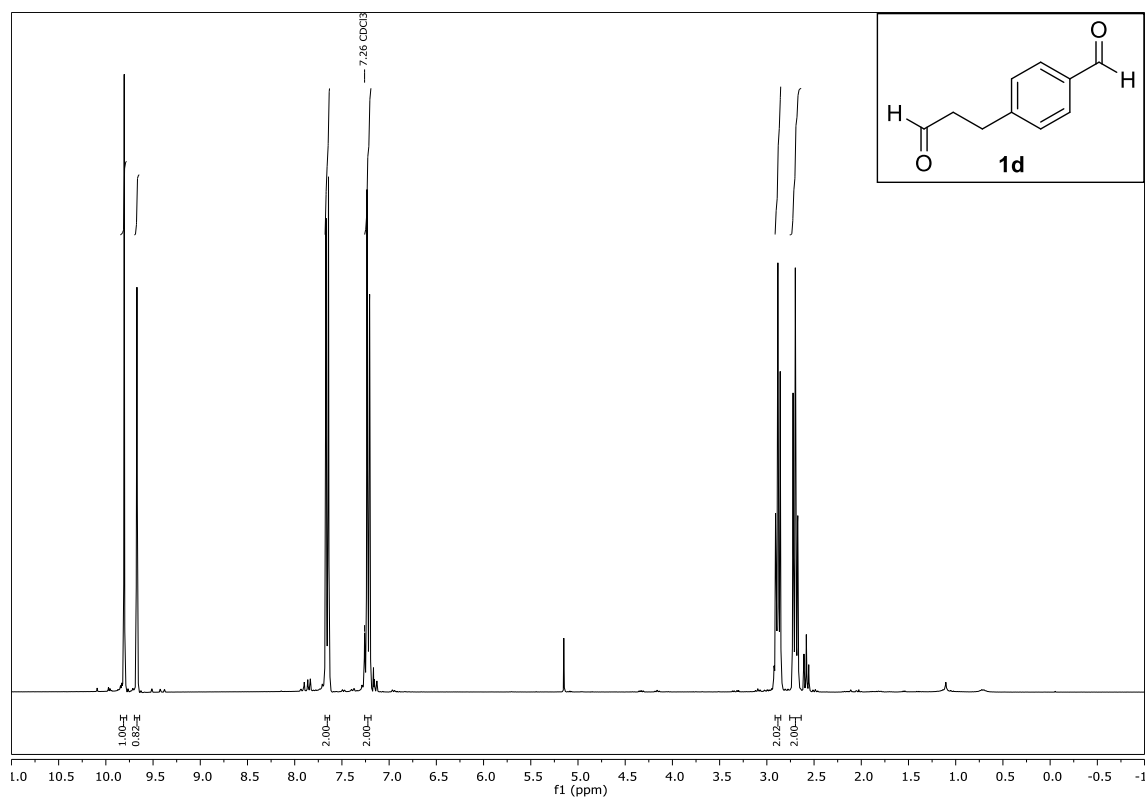
3,7-Dibromo 1-naphthalene-10-phenoxazine, ^1H - and ^{13}C -NMR (C_6D_6)

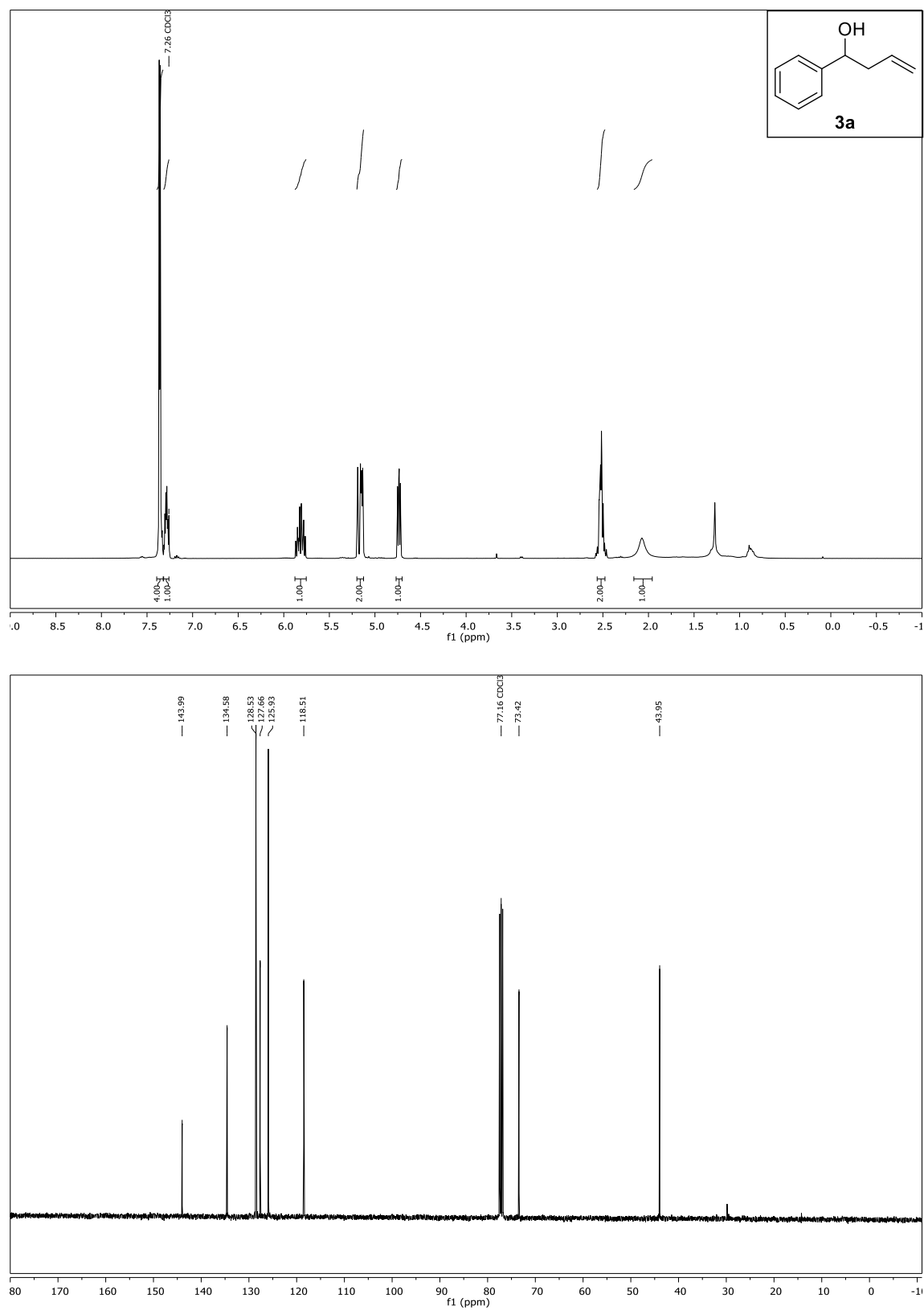
Compound **D**, $^1\text{H-NMR}$ ($\text{DMSO-}d_6$)



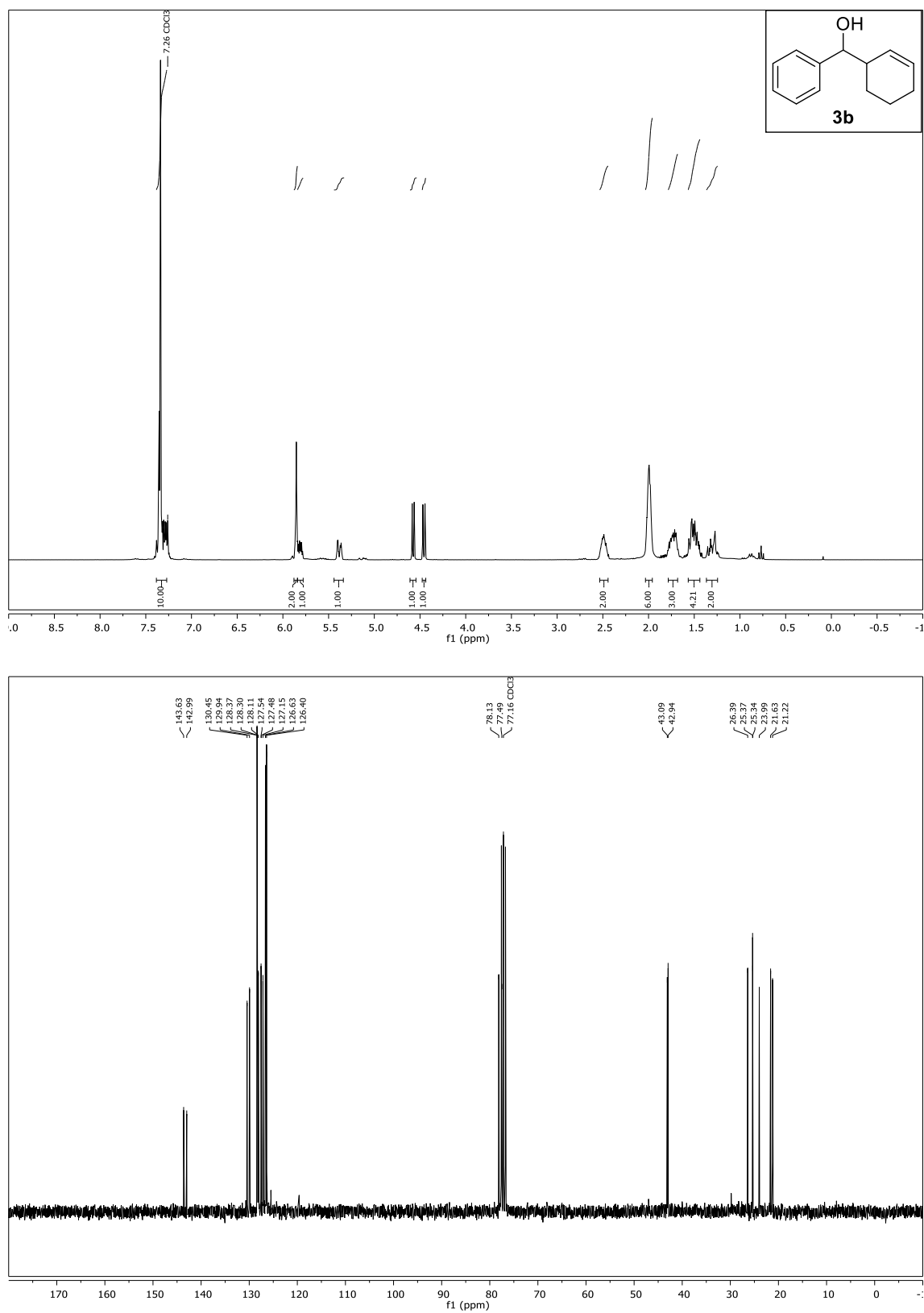
3-(4-(Hydroxymethyl)phenyl)propan-1-ol, ^1H - and ^{13}C -NMR (CDCl_3)

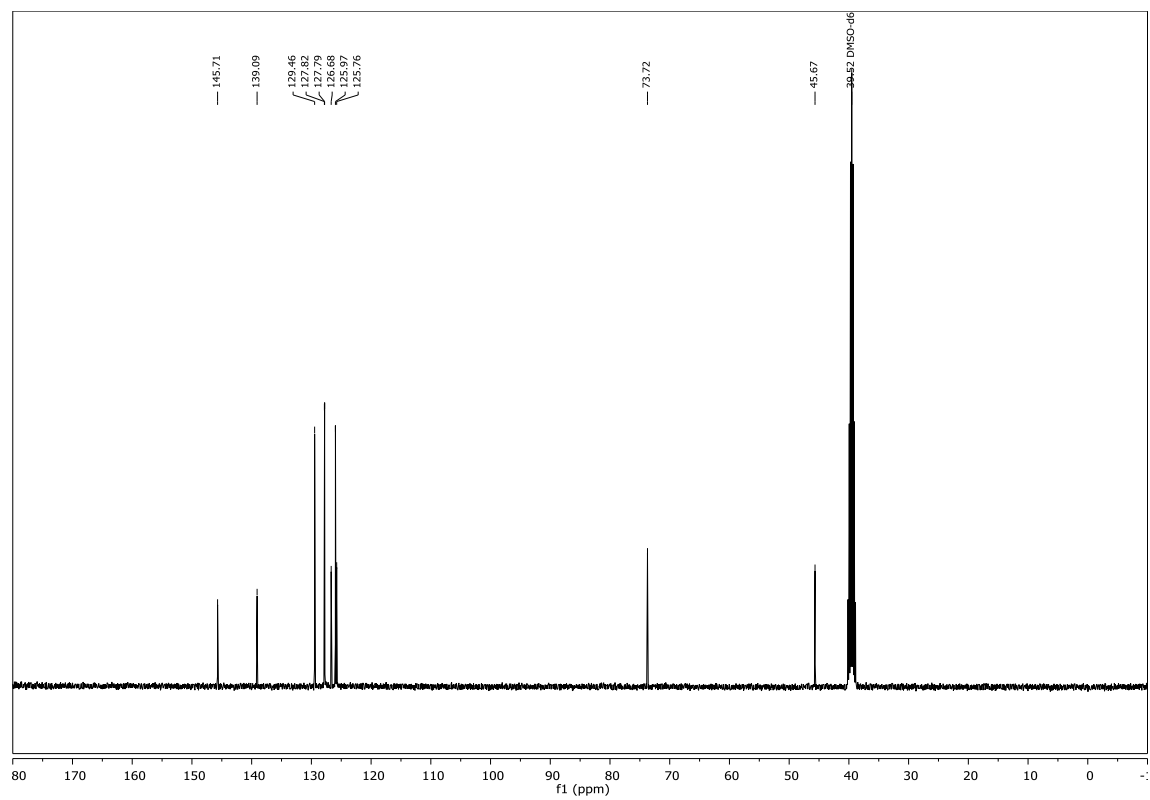
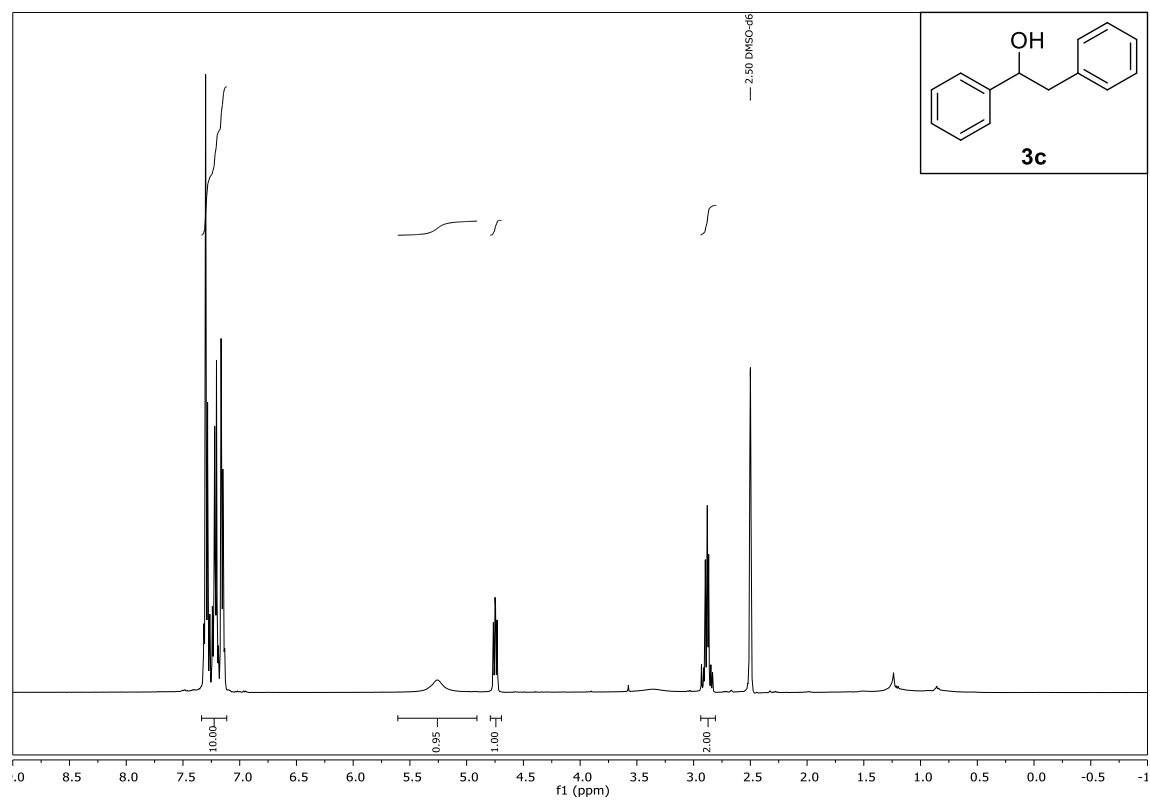
Compound **1d**, ^1H - and ^{13}C -NMR (CDCl_3)



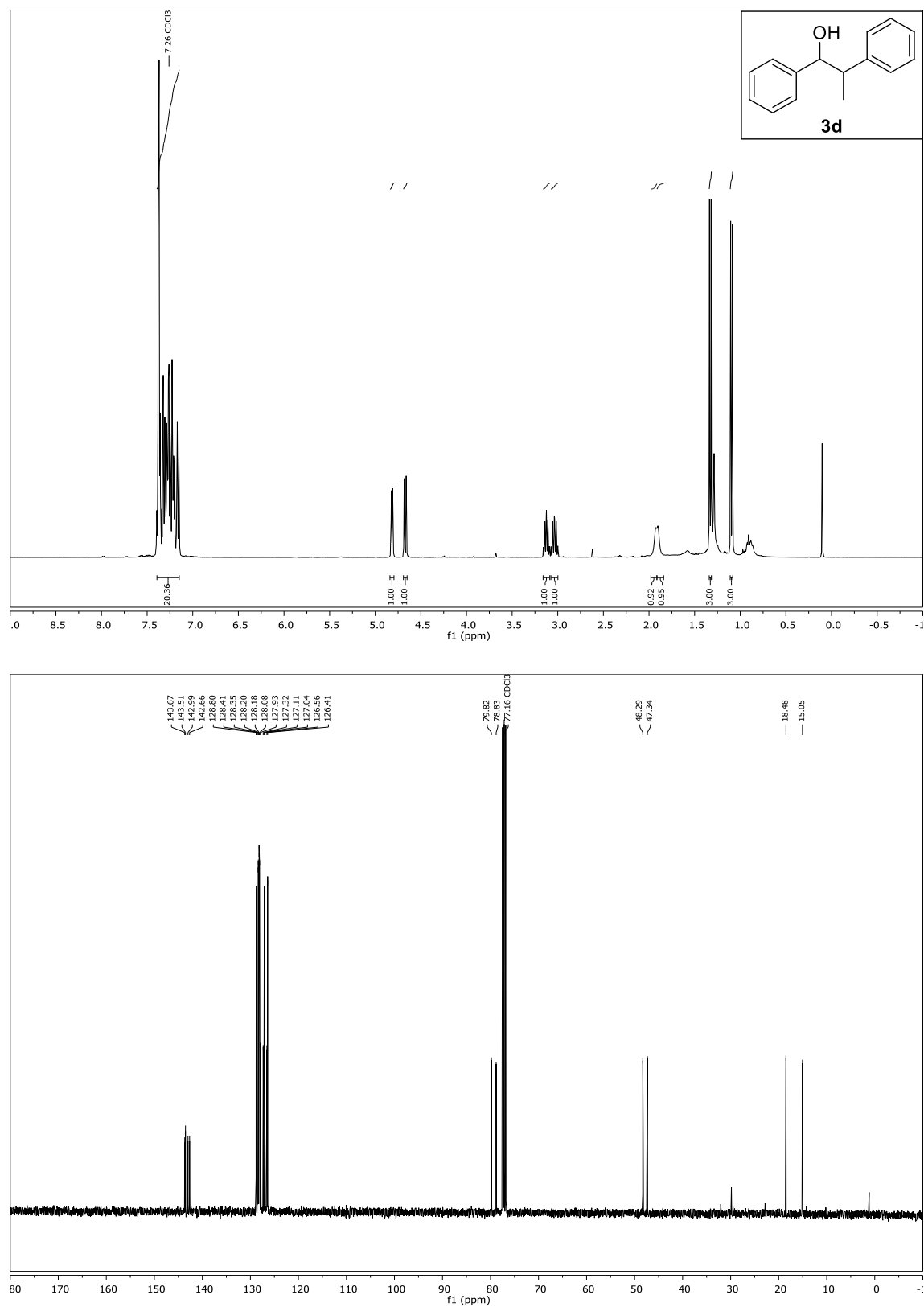
Compound **3a**, ^1H - and ^{13}C -NMR (CDCl_3)

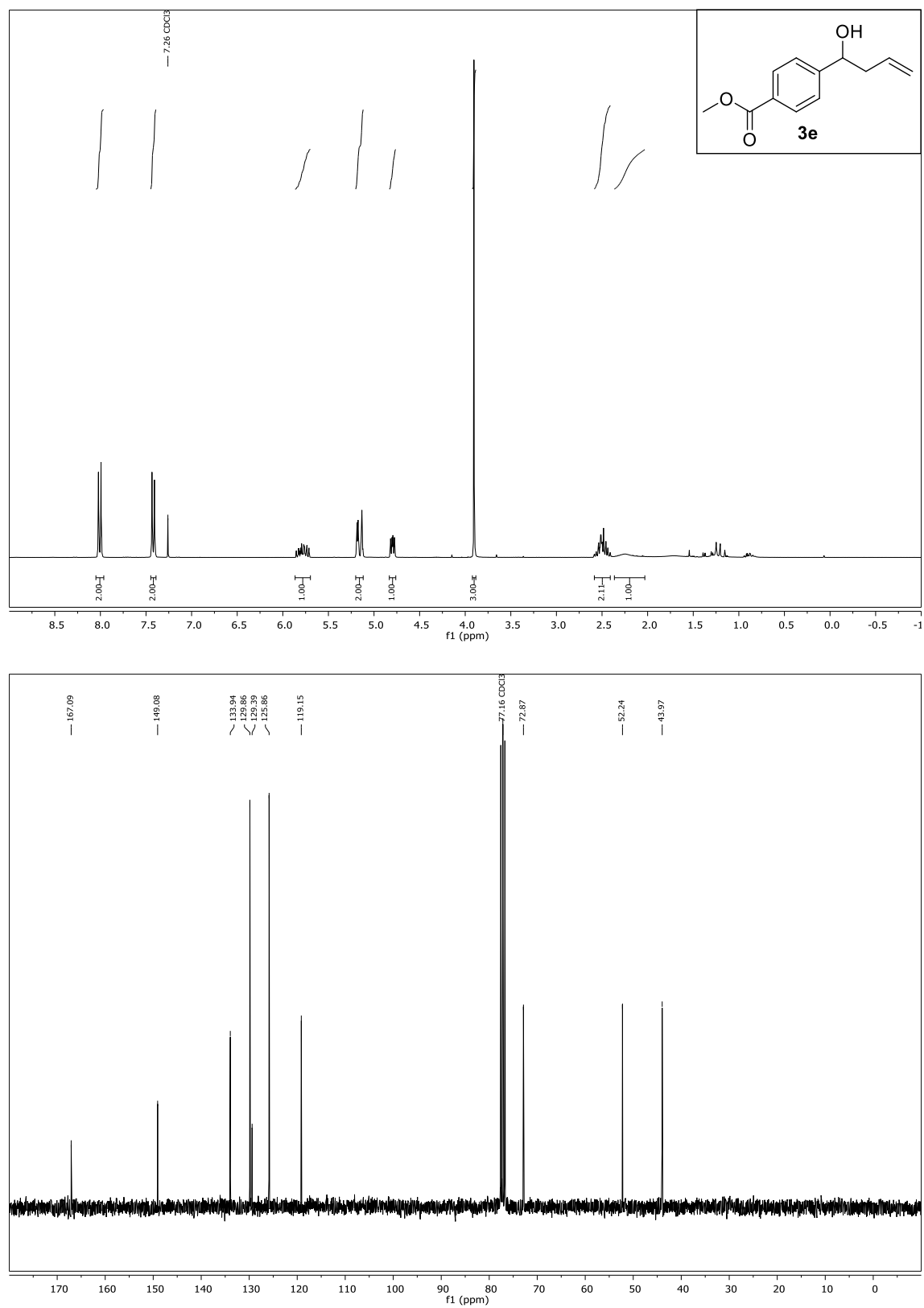
Compound **3b**, ^1H - and ^{13}C -NMR (CDCl_3)



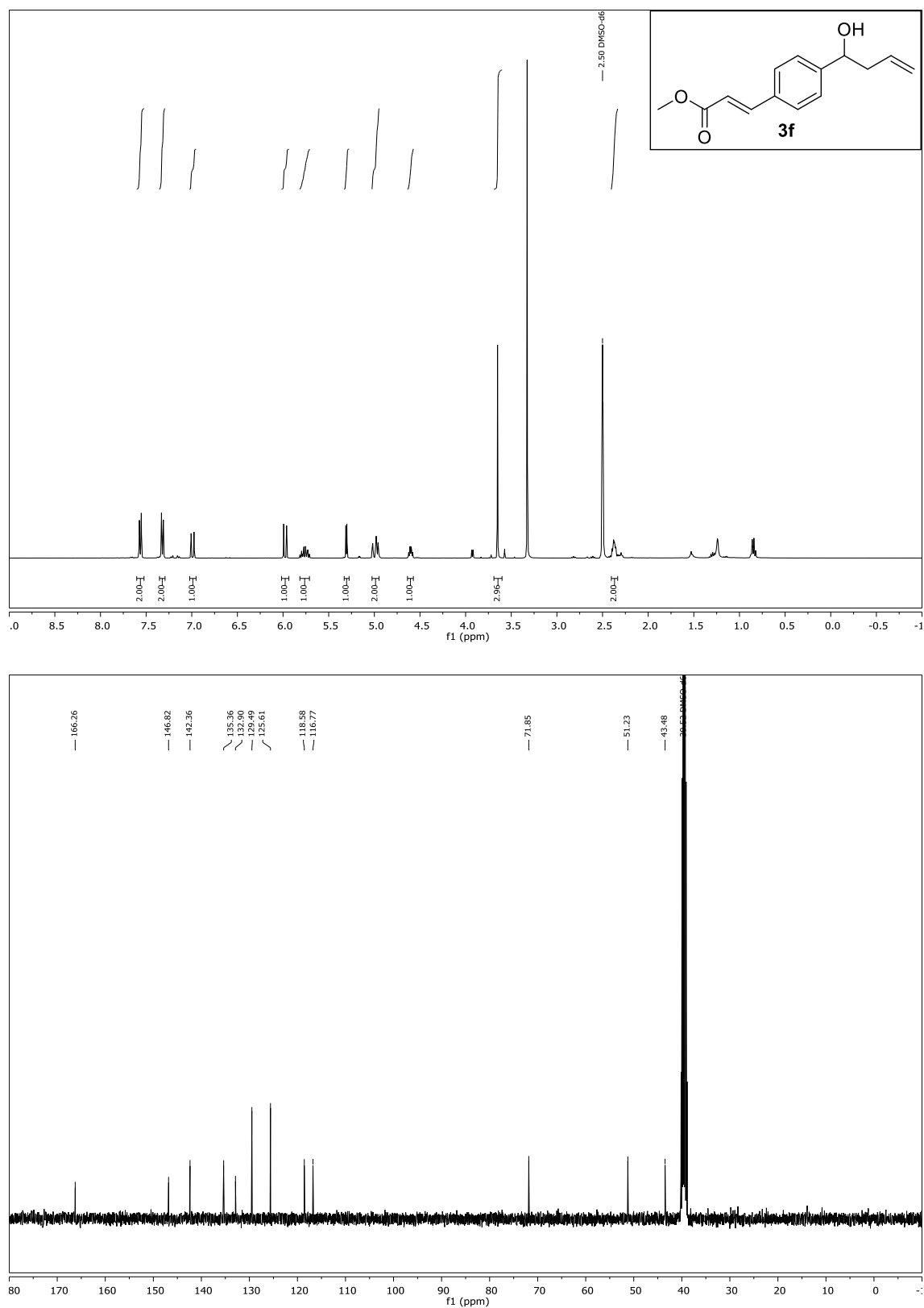
Compound **3c**, ^1H - and ^{13}C -NMR ($\text{DMSO}-d_6$)

Compound **3d**, ^1H - and ^{13}C -NMR (CDCl_3)

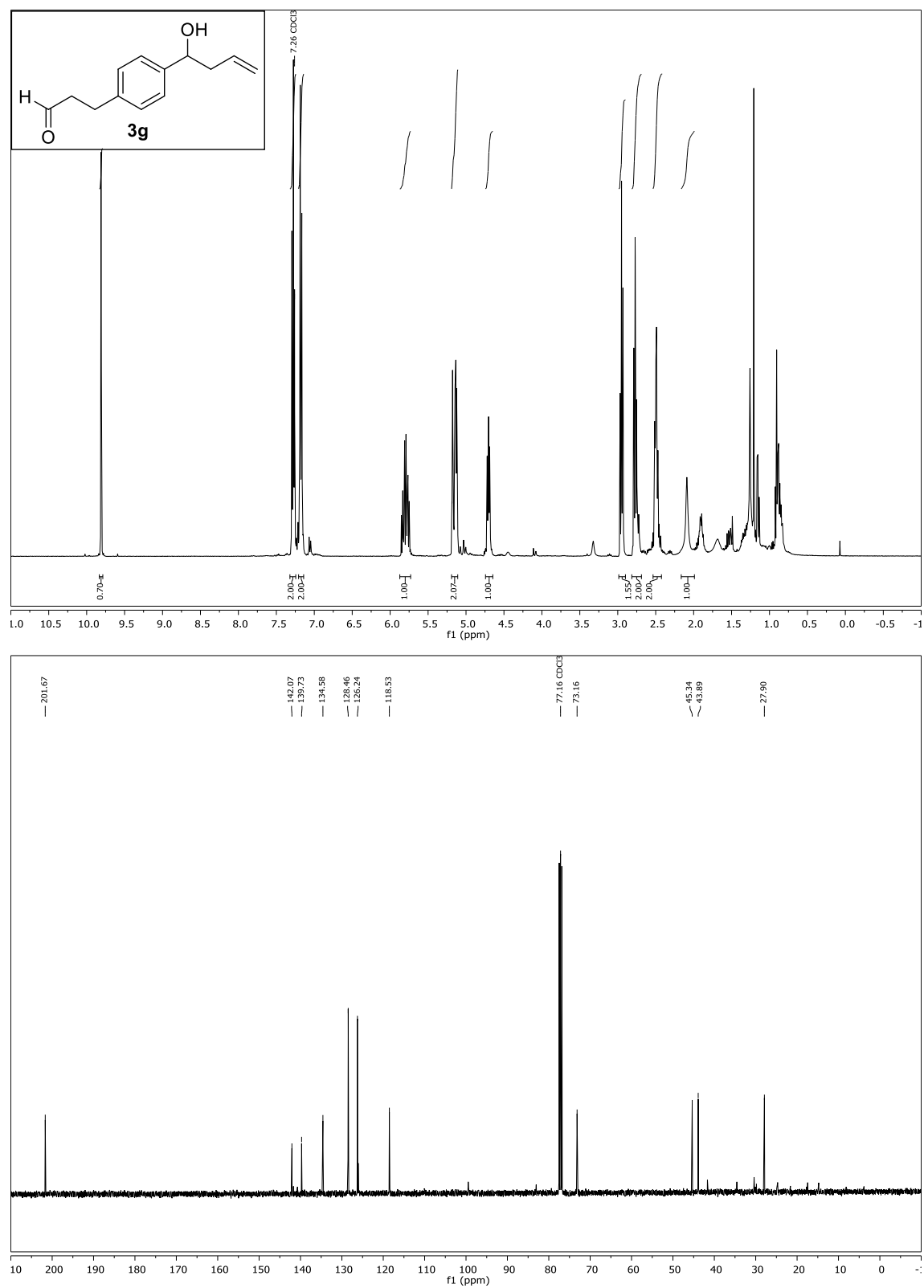


Compound **3e**, ^1H - and ^{13}C -NMR (CDCl_3)

Compound **3f**, ^1H - and ^{13}C -NMR ($\text{DMSO}-d_6$)

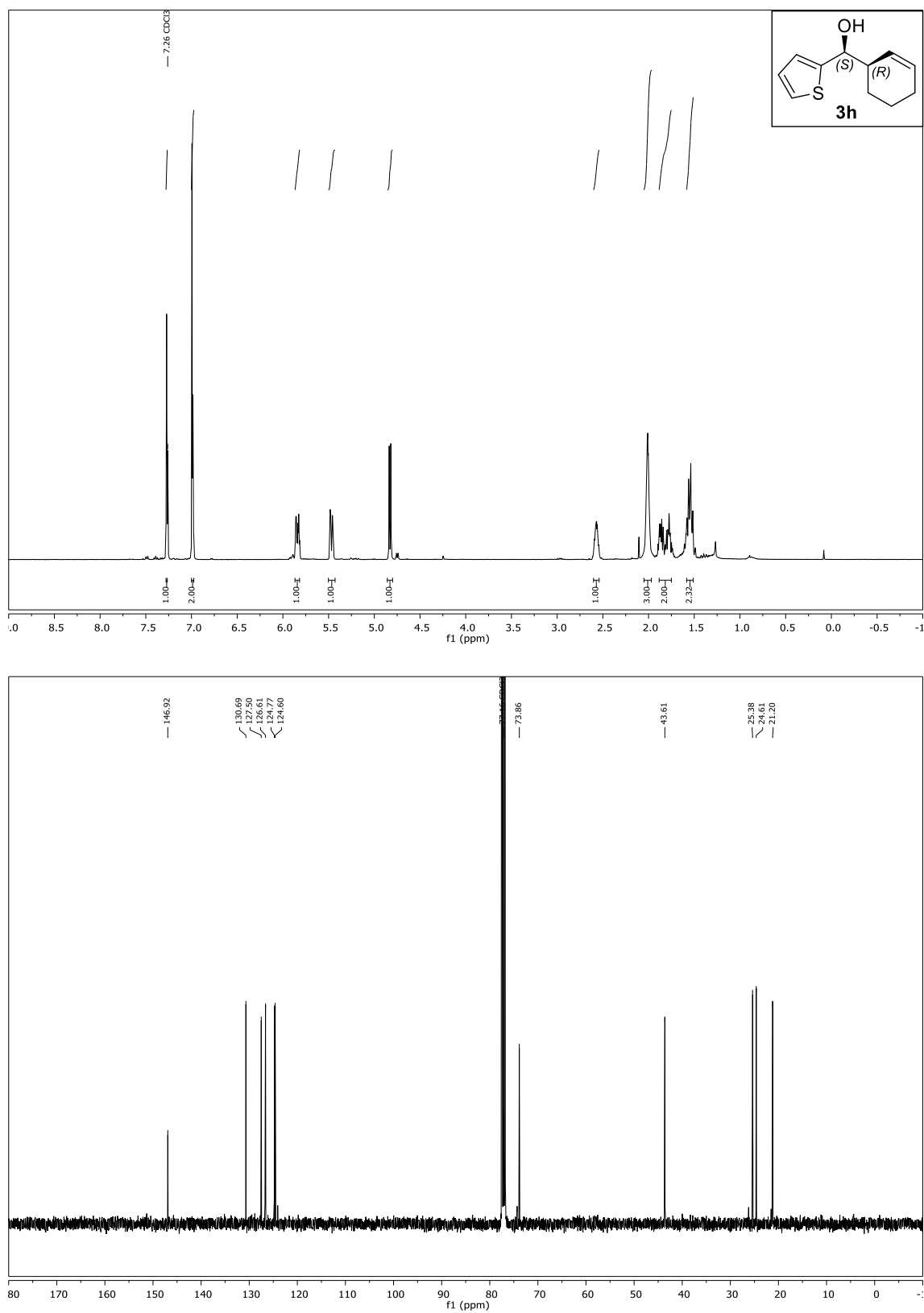


Compound **3g**, ^1H - and ^{13}C -NMR (CDCl_3)*

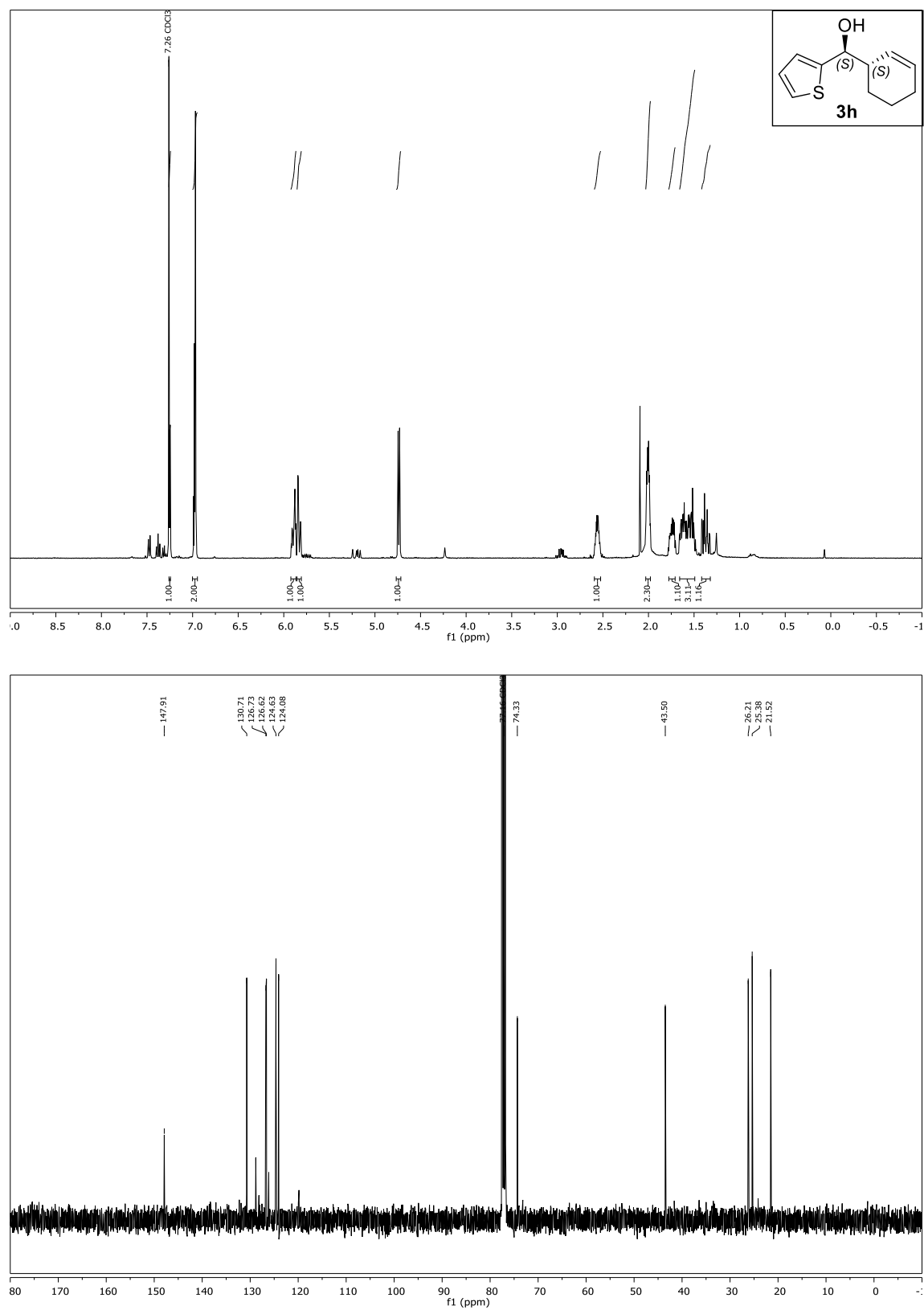


* NMR-studies revealed, that the product is degrading during purification. Hence, no clean NMR of the product could be obtained. The additional signals between 0.5 and 2.2 ppm correspond to degradation products.

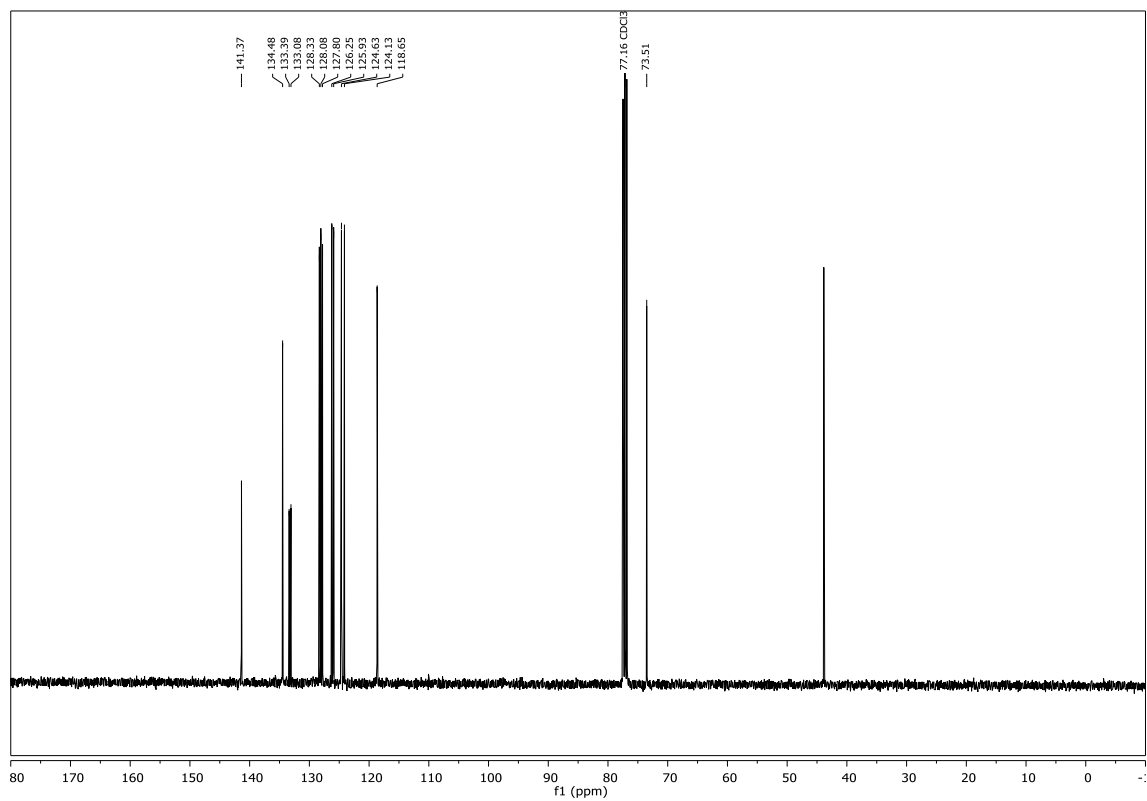
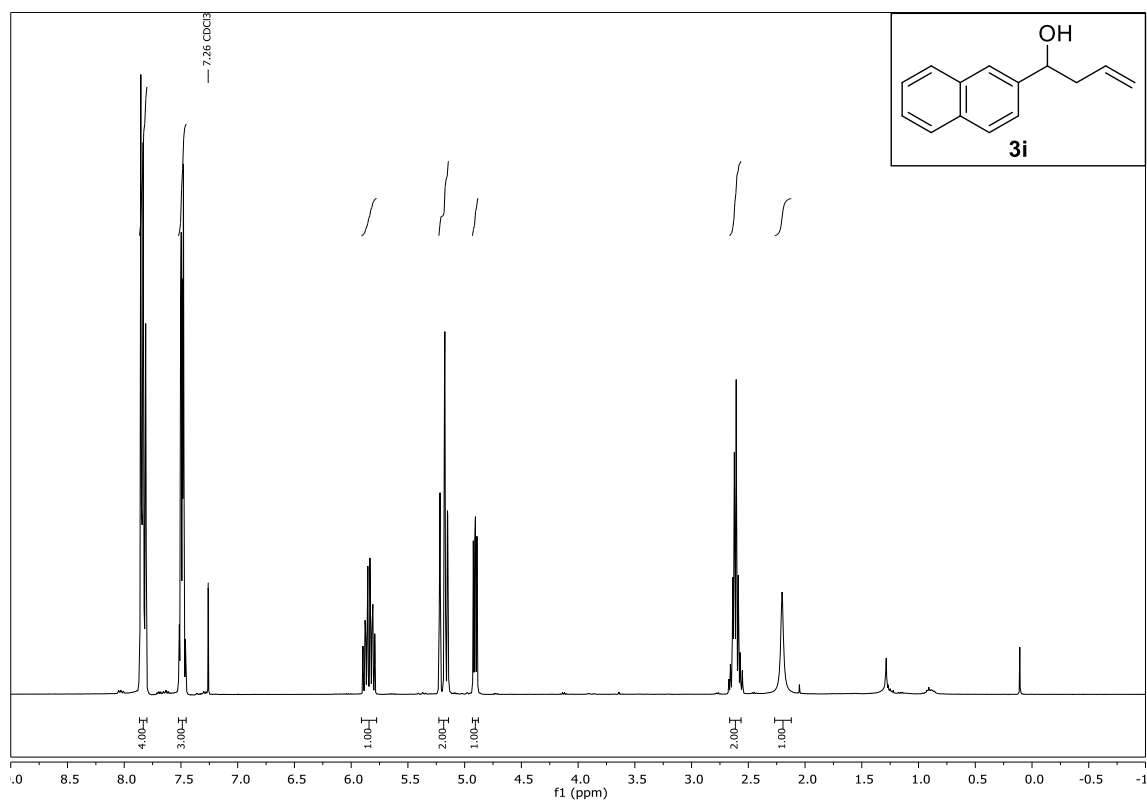
Compound **3h** anti, ^1H - and ^{13}C -NMR (CDCl_3)

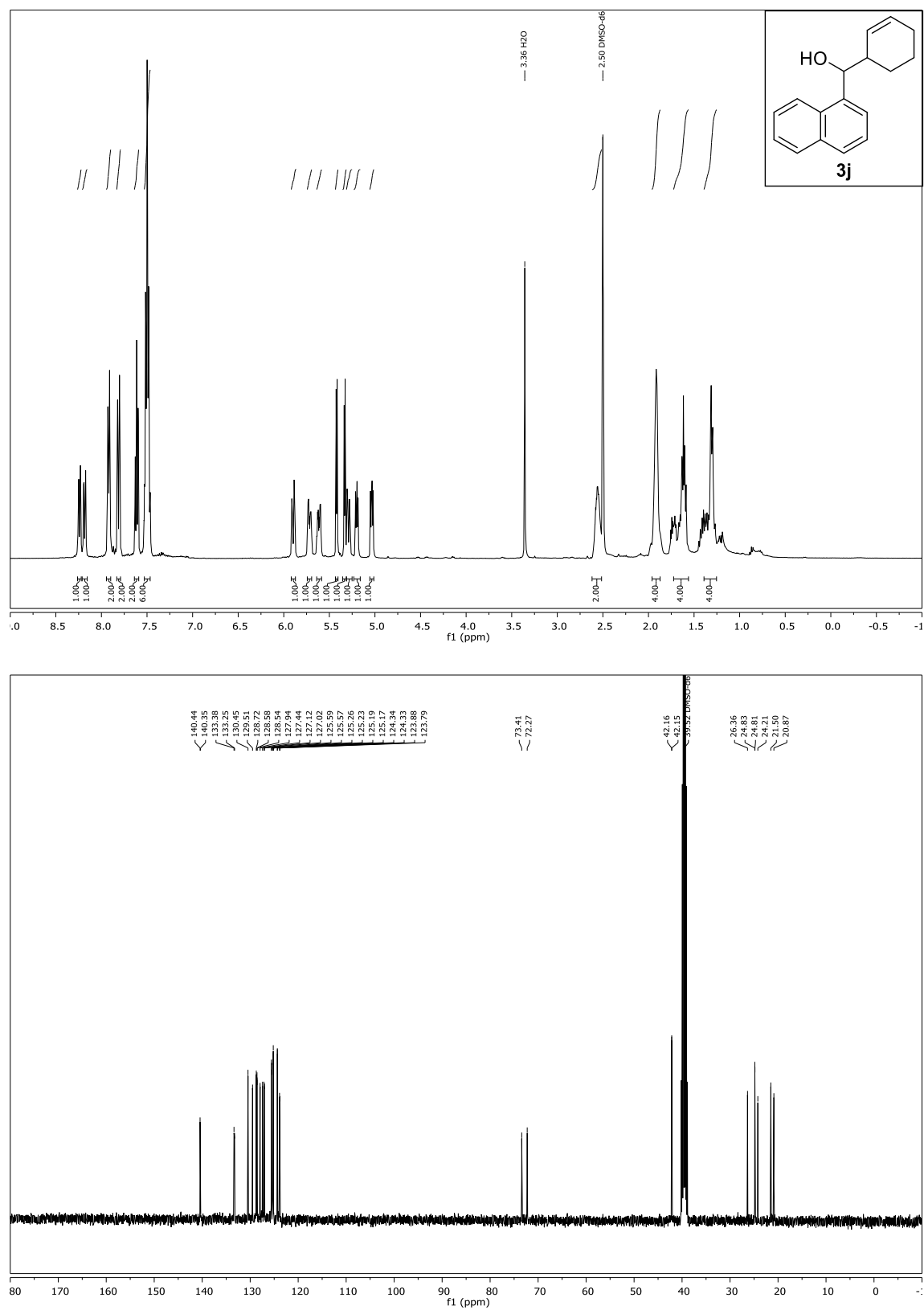


Compound **3h** syn, ^1H - and ^{13}C -NMR (CDCl_3)

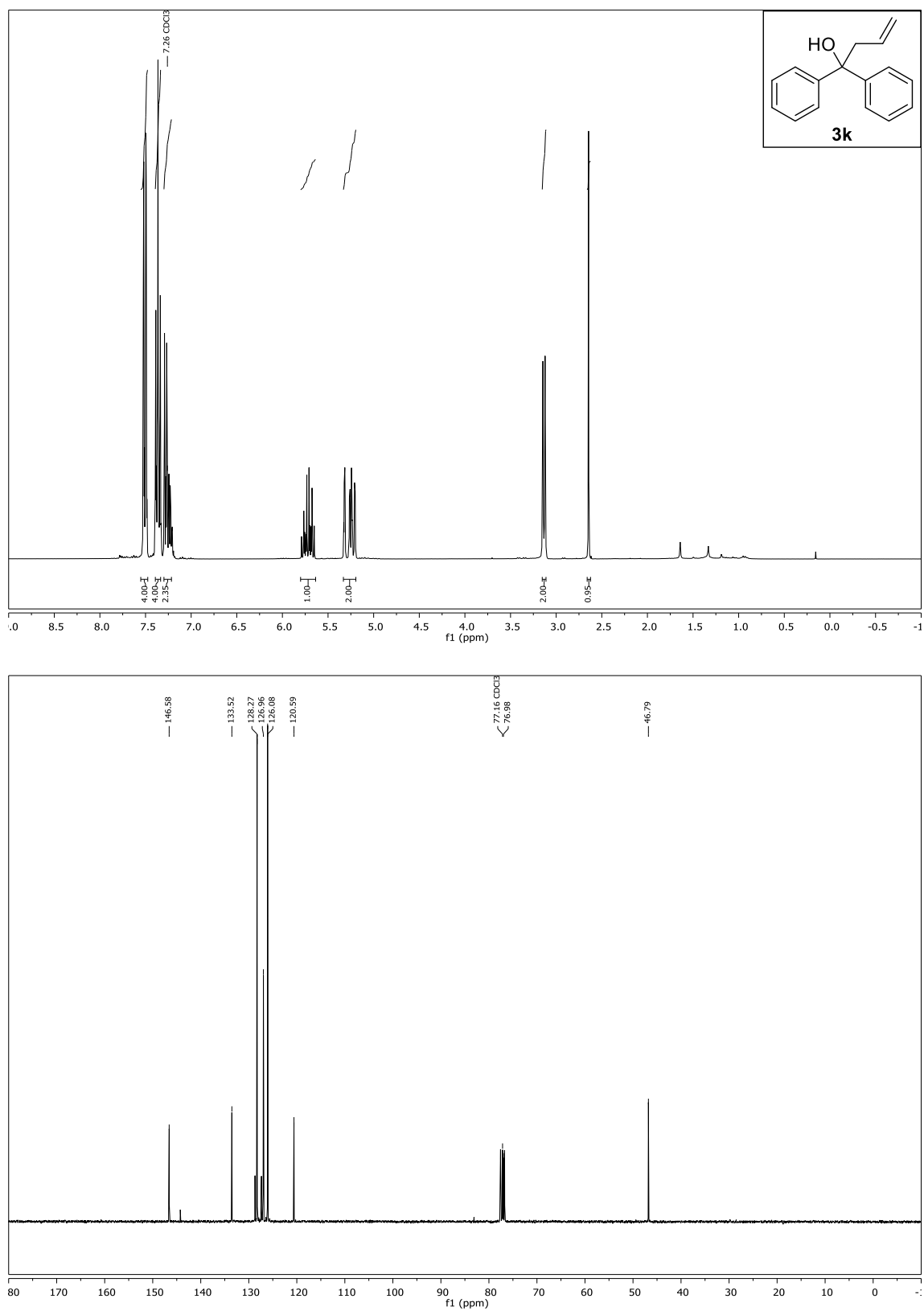


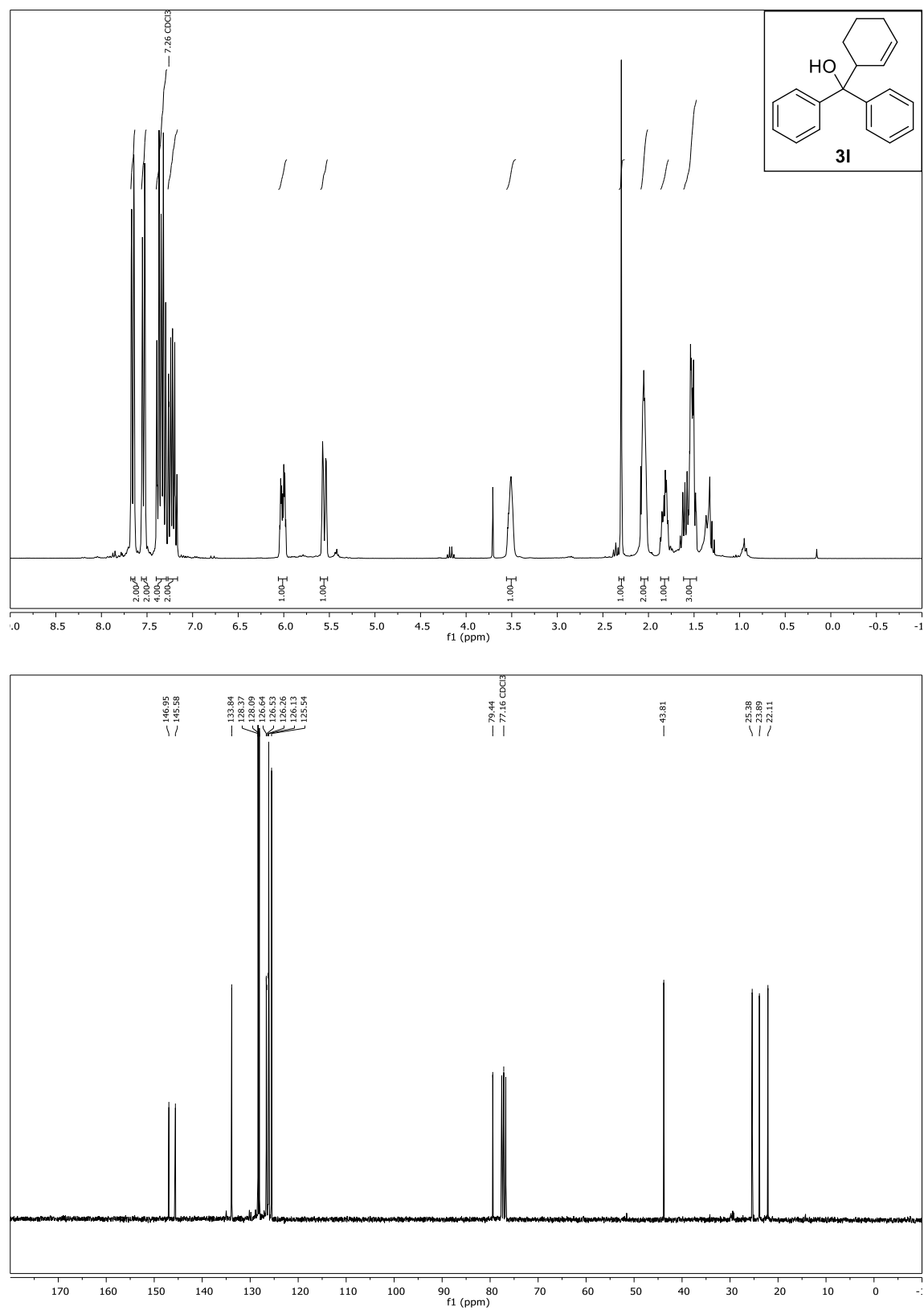
Compound **3i**, ^1H - and ^{13}C -NMR (CDCl_3)



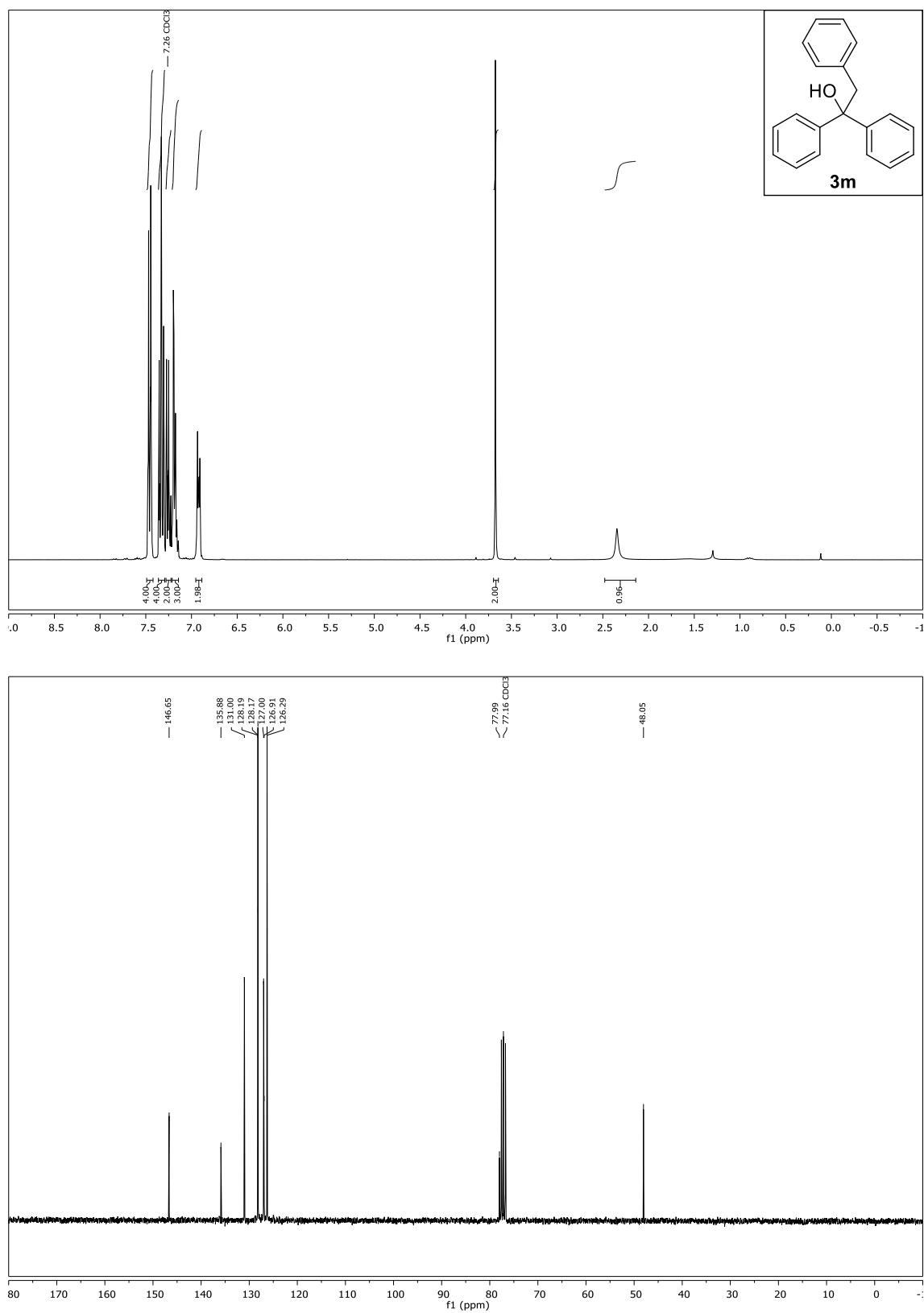
Compound **3j**, ^1H - and ^{13}C -NMR ($\text{DMSO}-d_6$)

Compound **3k**, ^1H - and ^{13}C -NMR (CDCl_3)

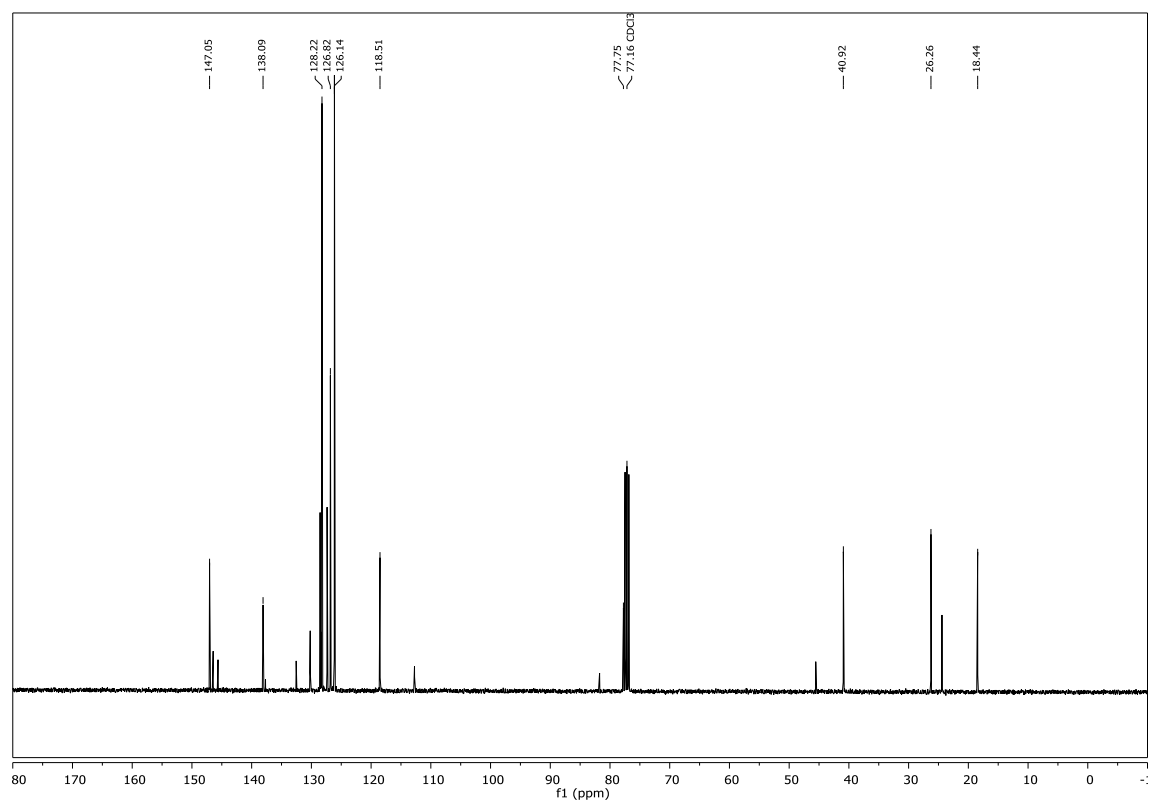
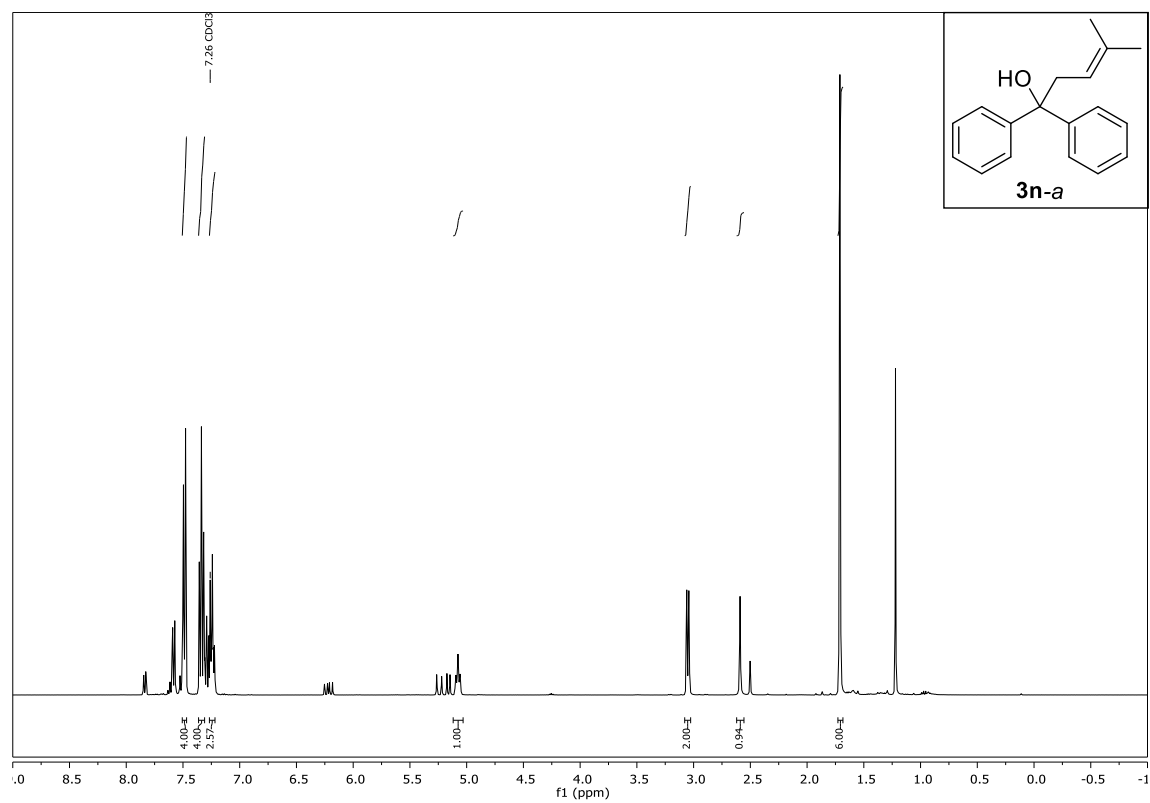


Compound **3I**, ^1H - and ^{13}C -NMR (CDCl_3)

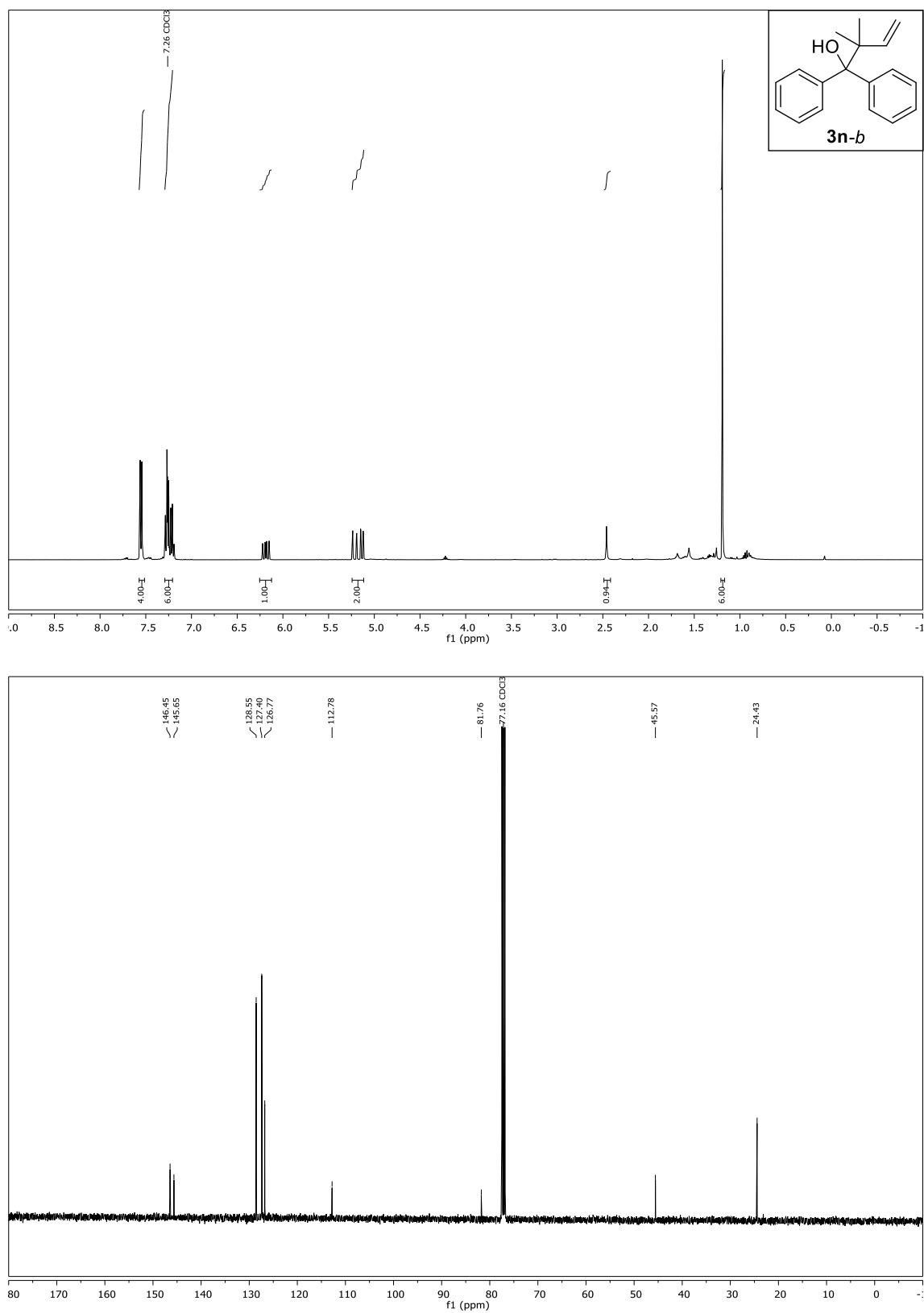
Compound **3m**, ^1H - and ^{13}C -NMR (CDCl_3)



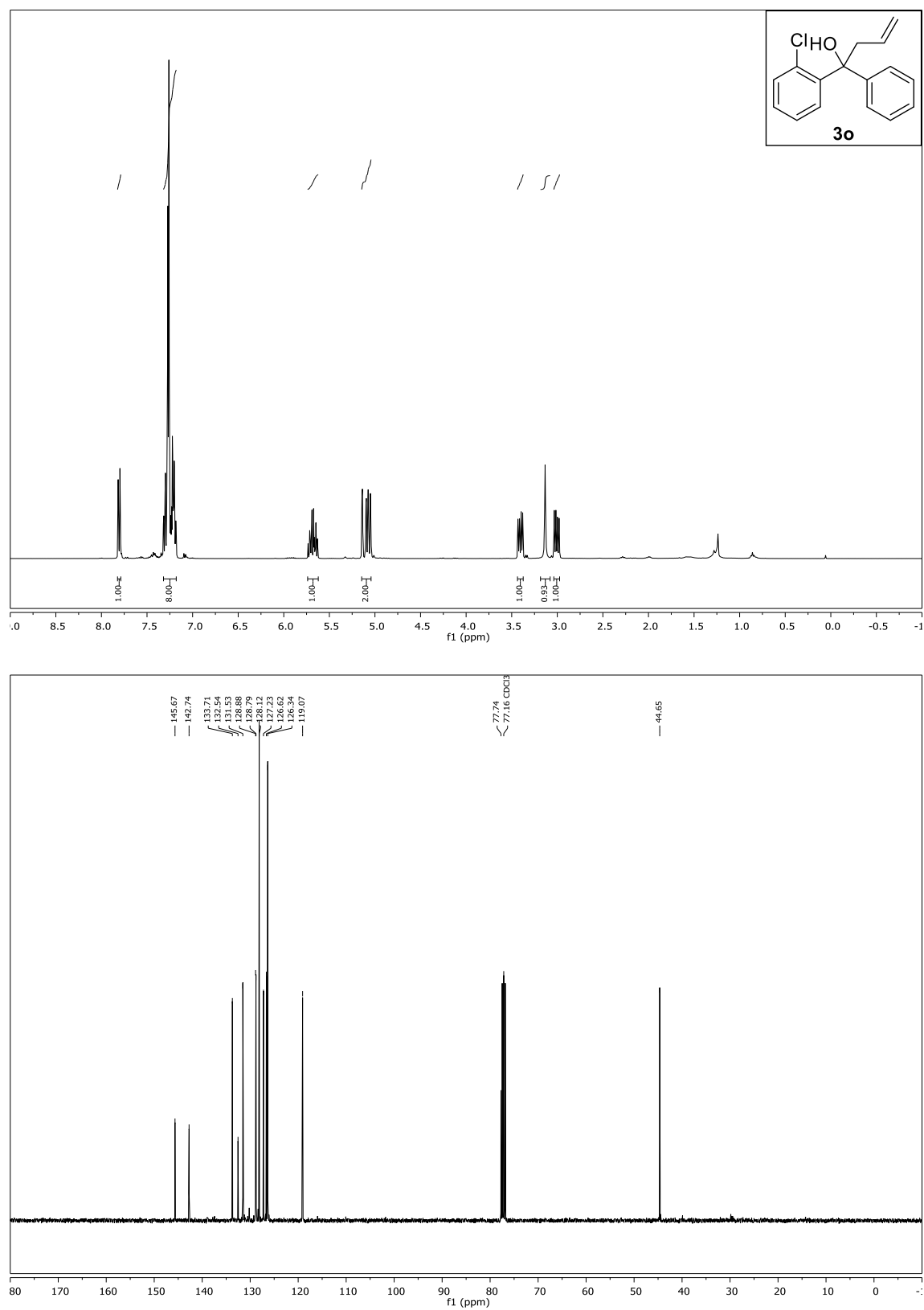
Compound **3n-a**, ^1H - and ^{13}C -NMR (CDCl_3)



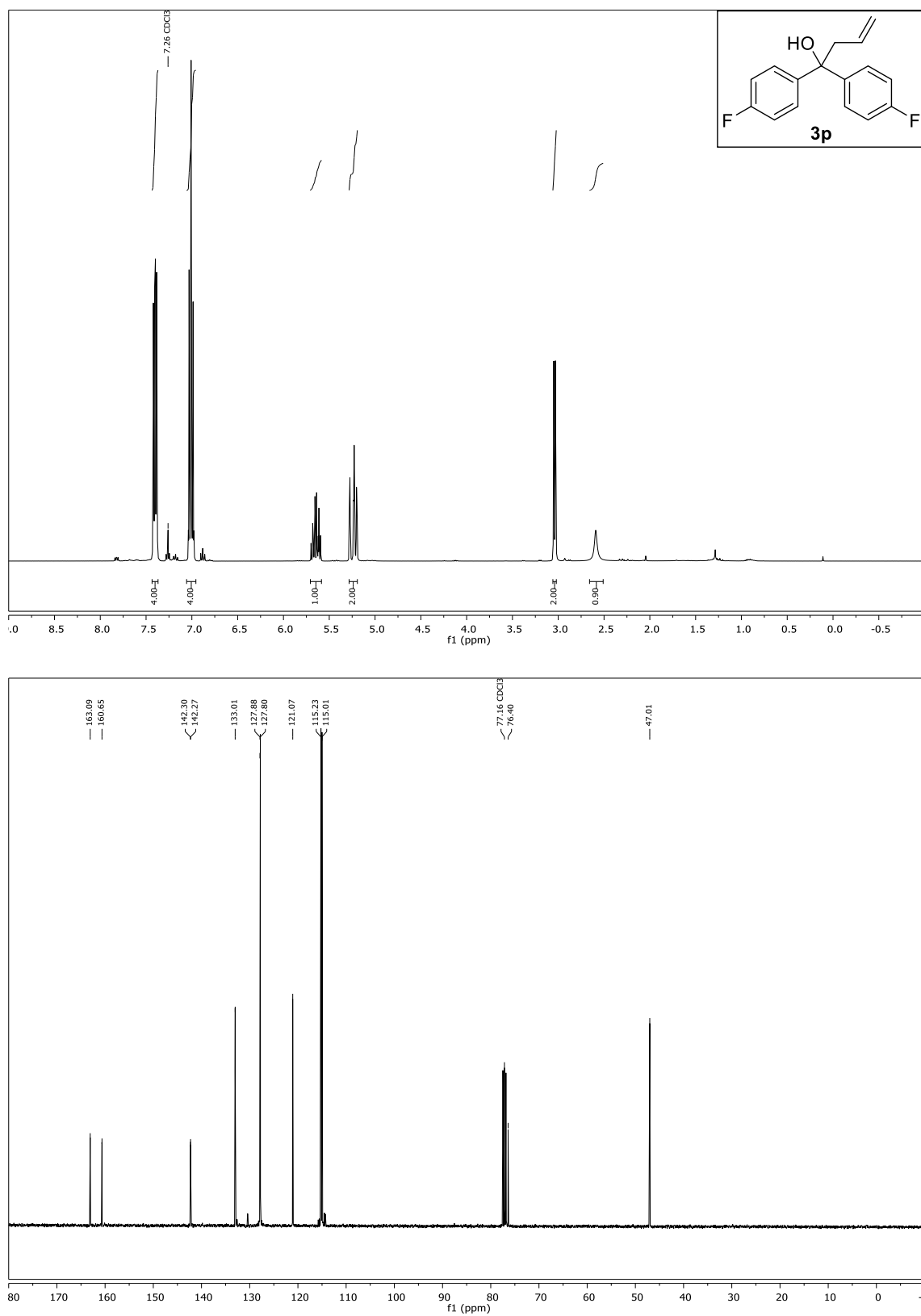
Compound **3n-b**, ^1H - and ^{13}C -NMR (CDCl_3)

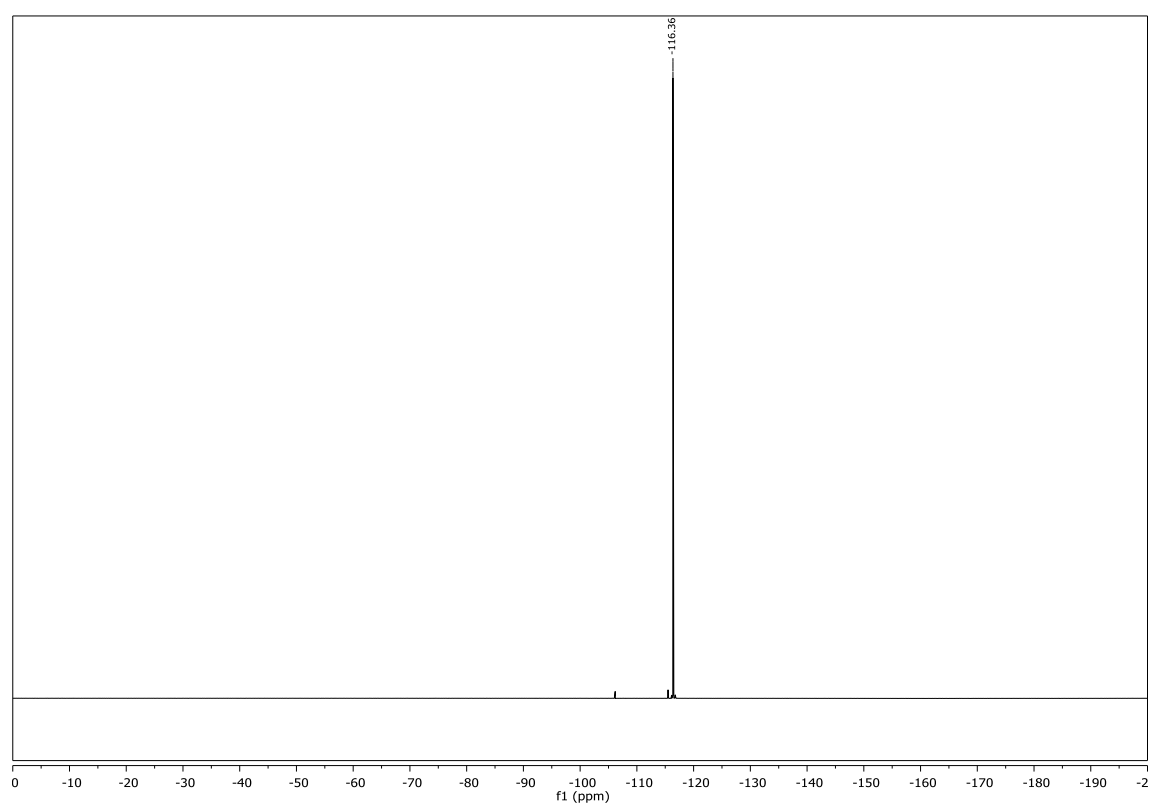


Compound **3o**, ^1H - and ^{13}C -NMR (CDCl_3)

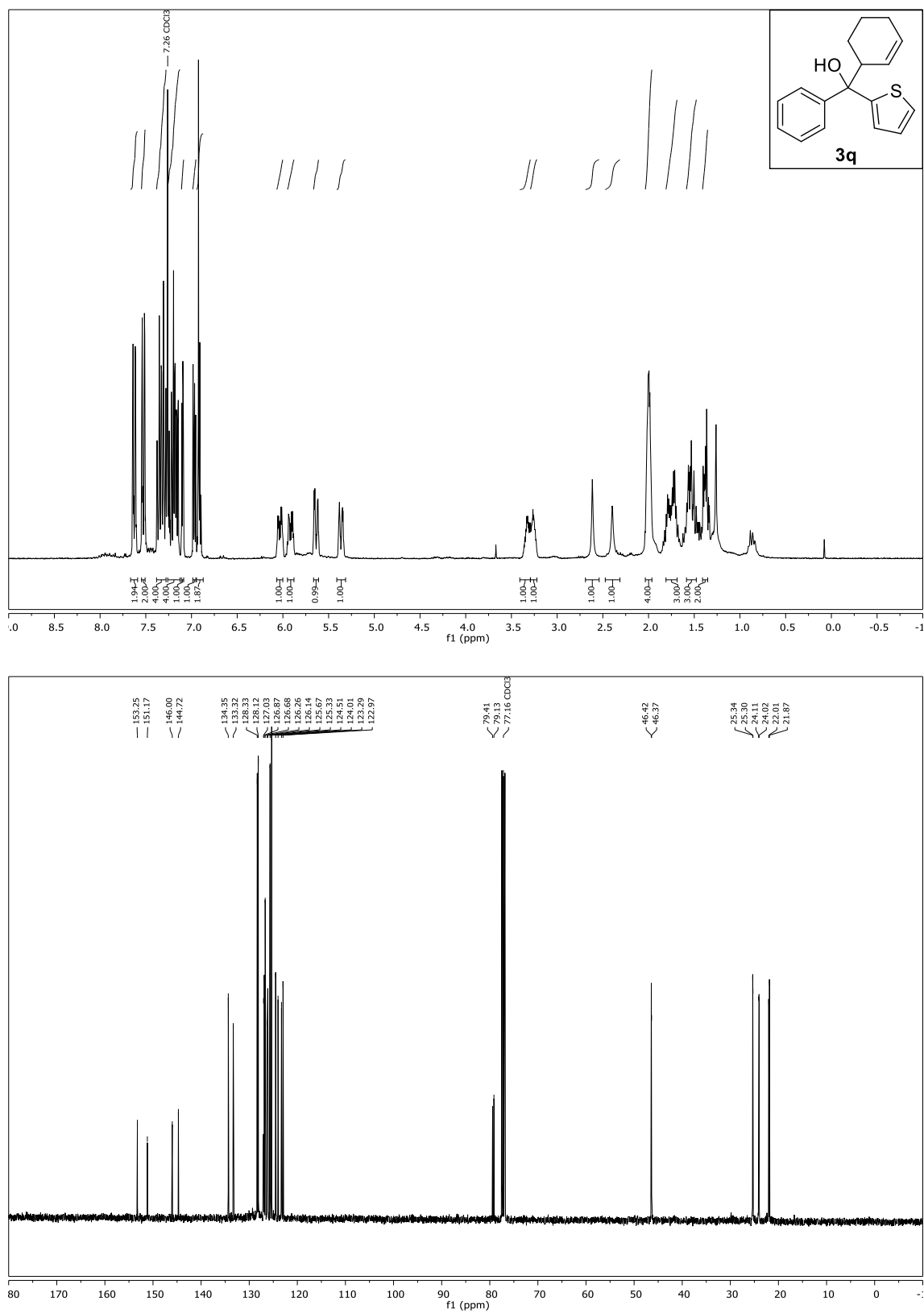


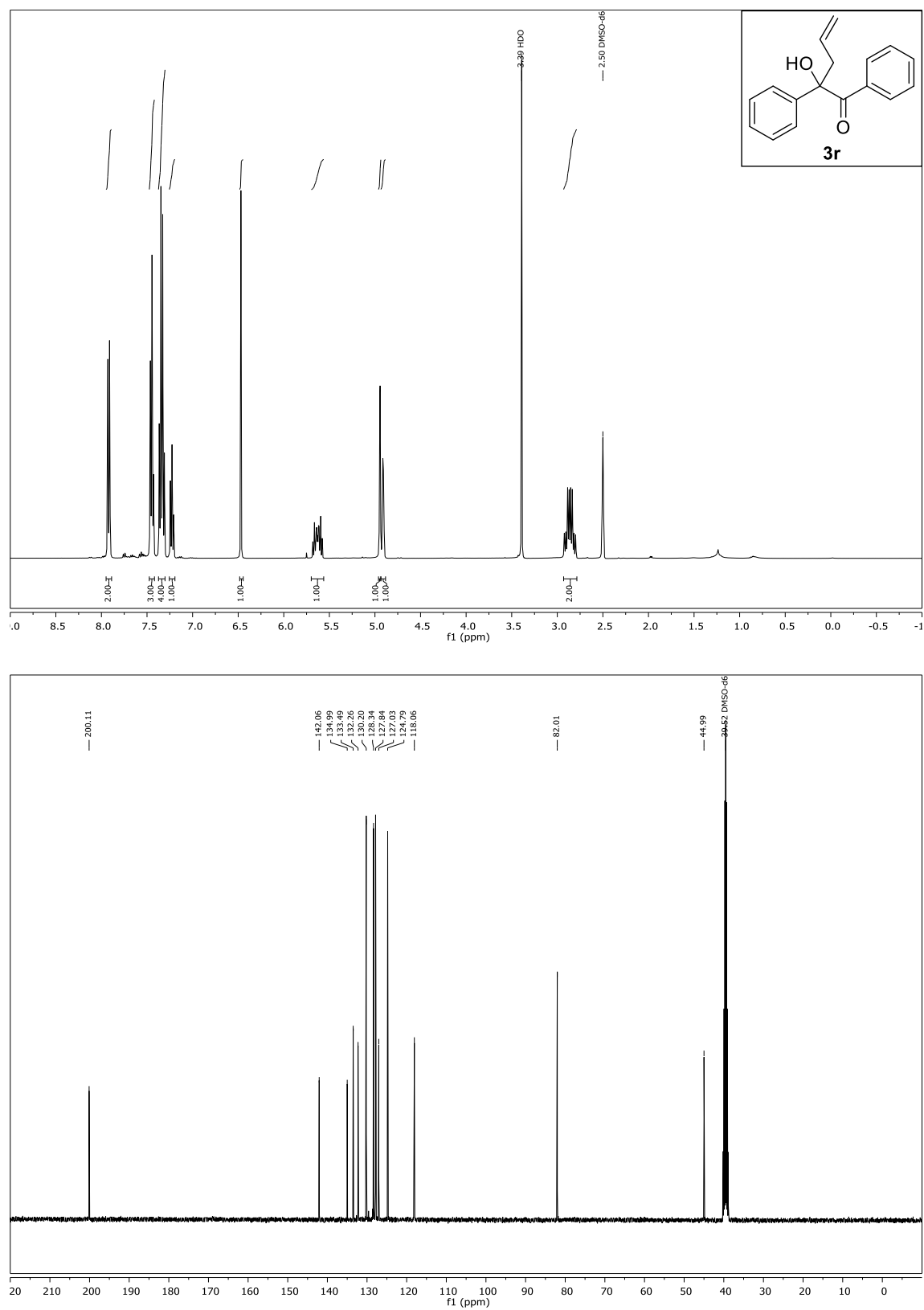
Compound **3p**, ^1H -, ^{13}C and ^{19}F -NMR (CDCl_3)



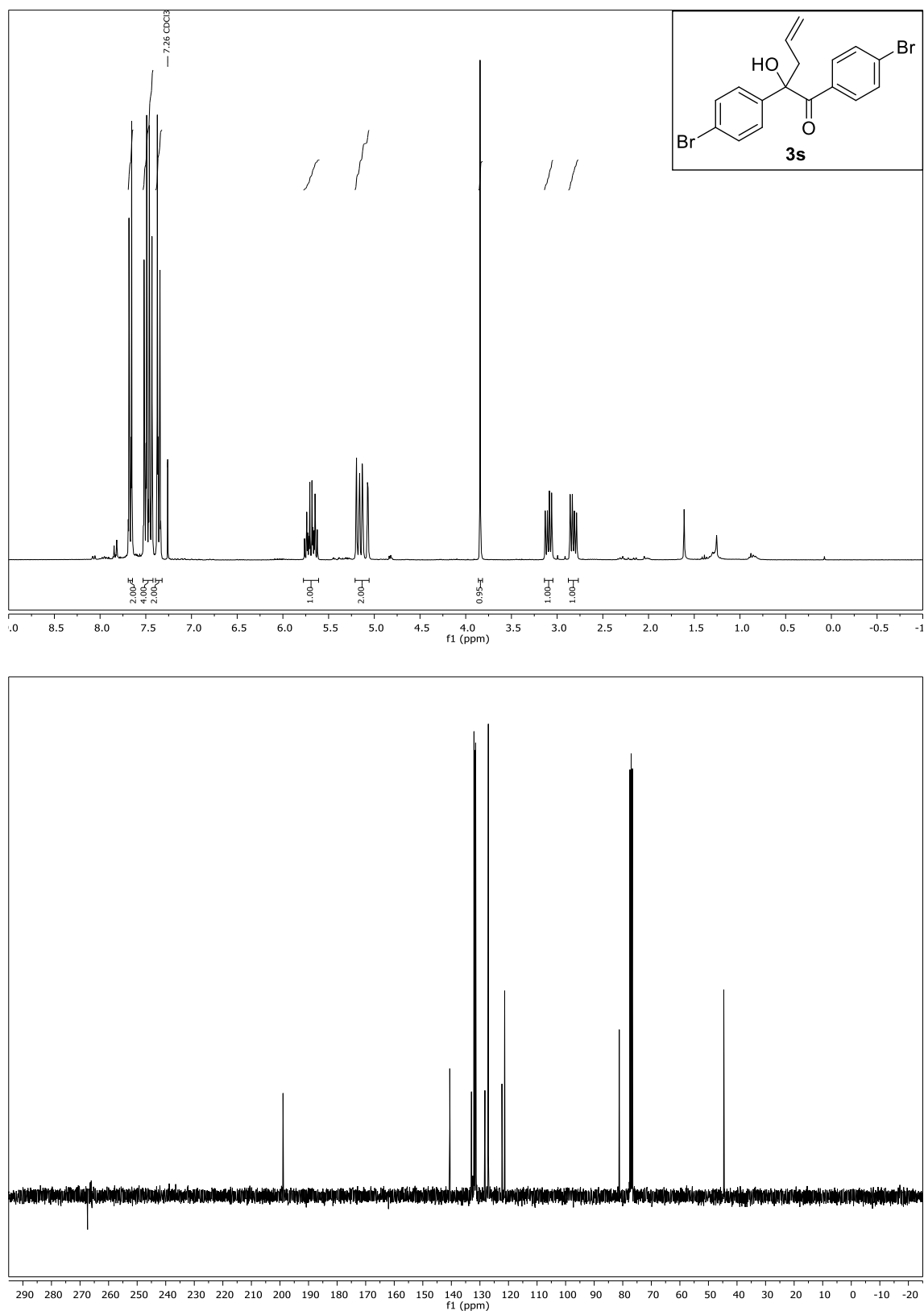


Compound **3q**, ^1H - and ^{13}C -NMR (CDCl_3)

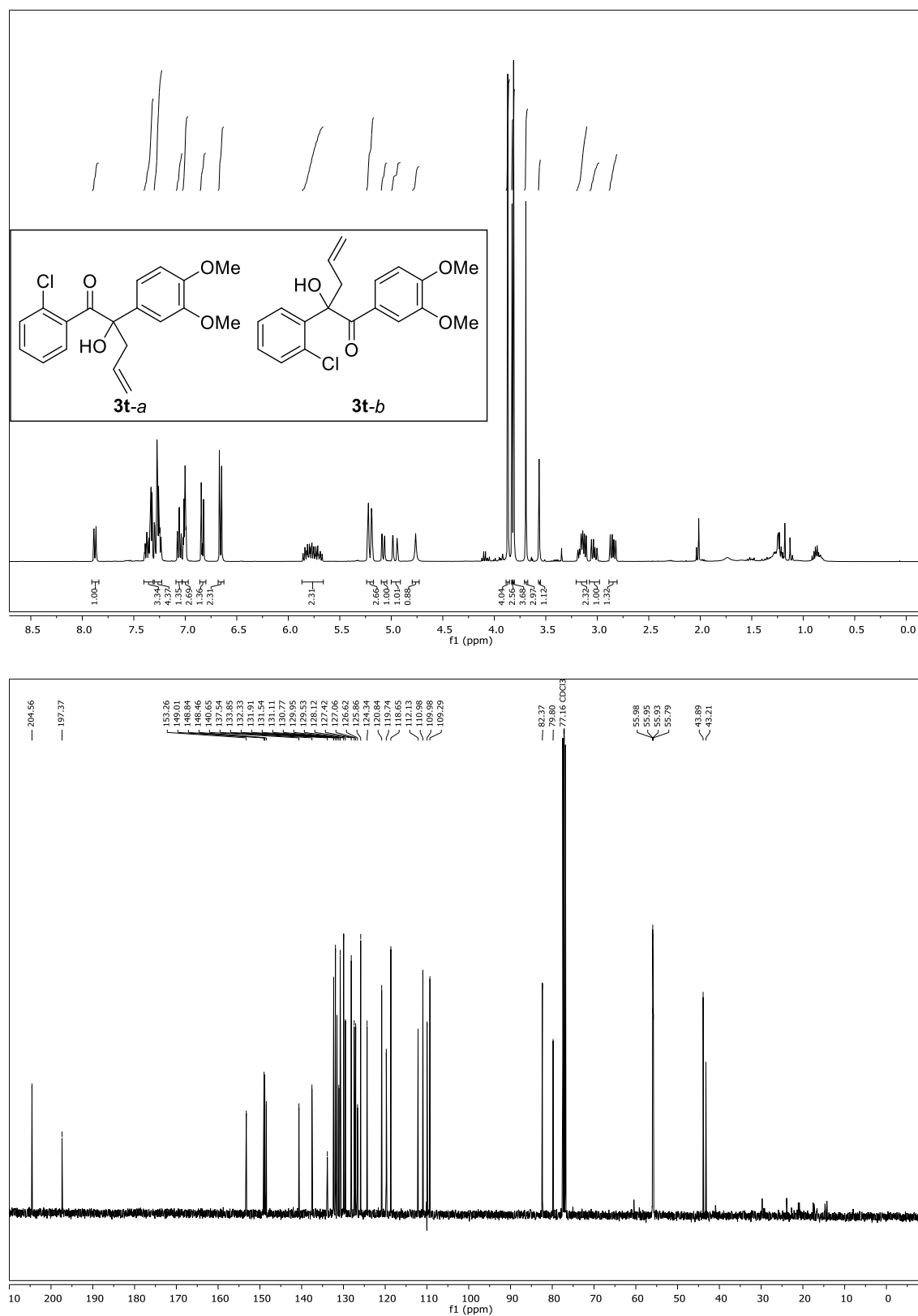


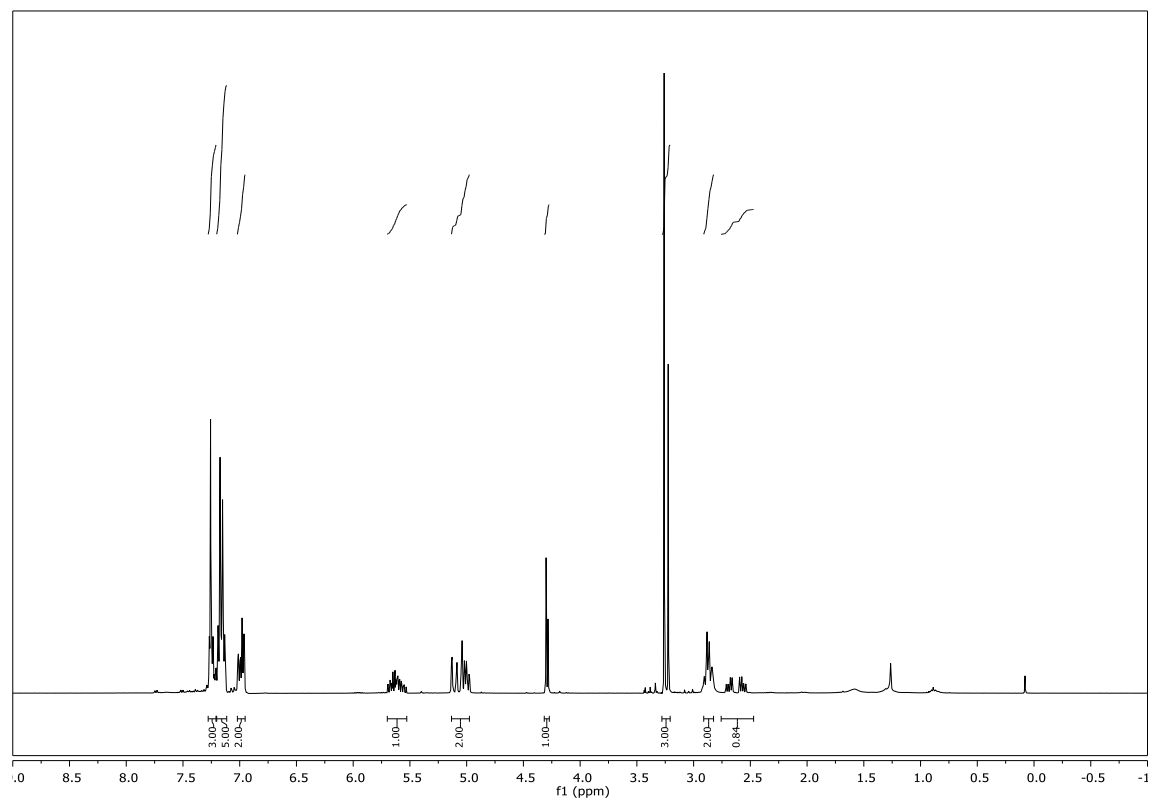
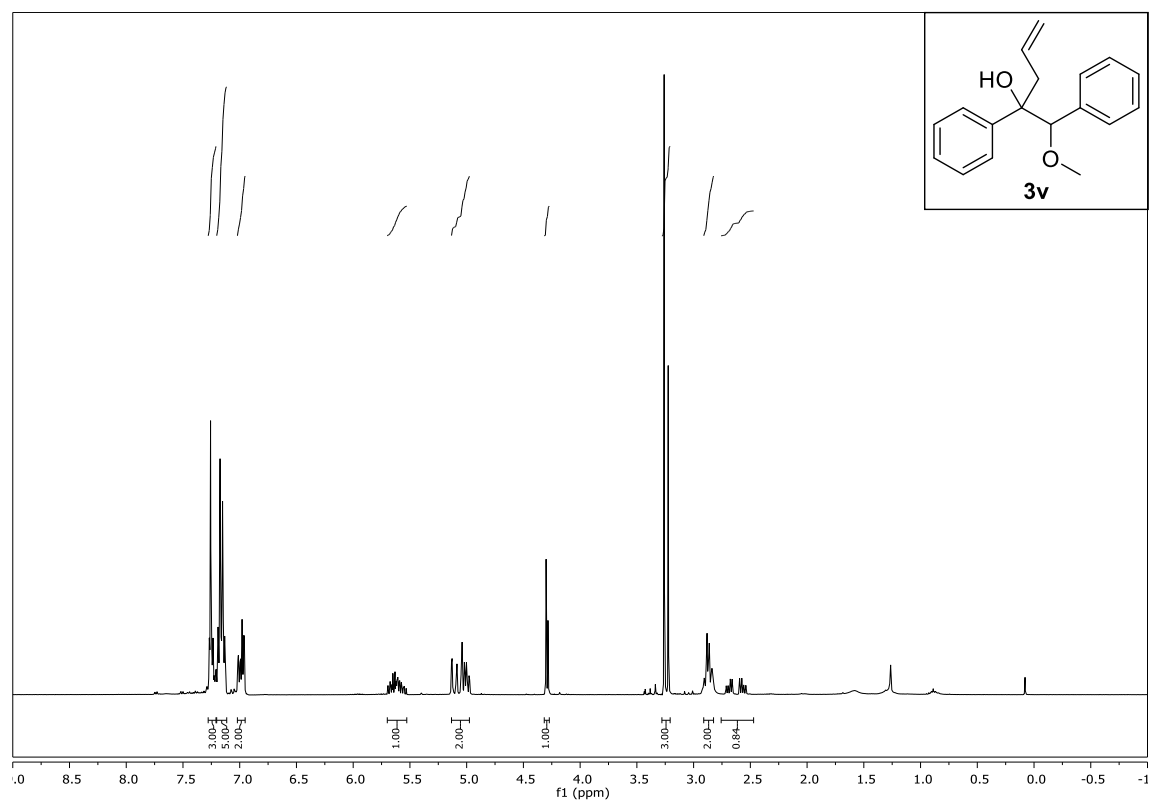
Compound **3r**, ^1H - and ^{13}C -NMR ($\text{DMSO}-d_6$)

Compound **3s**, ^1H - and ^{13}C -NMR (CDCl_3)



Compound **3t-a** and compound **3t-b**, ^1H - and ^{13}C -NMR (CDCl_3)



Compound **3v**, ^1H - and ^{13}C -NMR (CDCl_3)

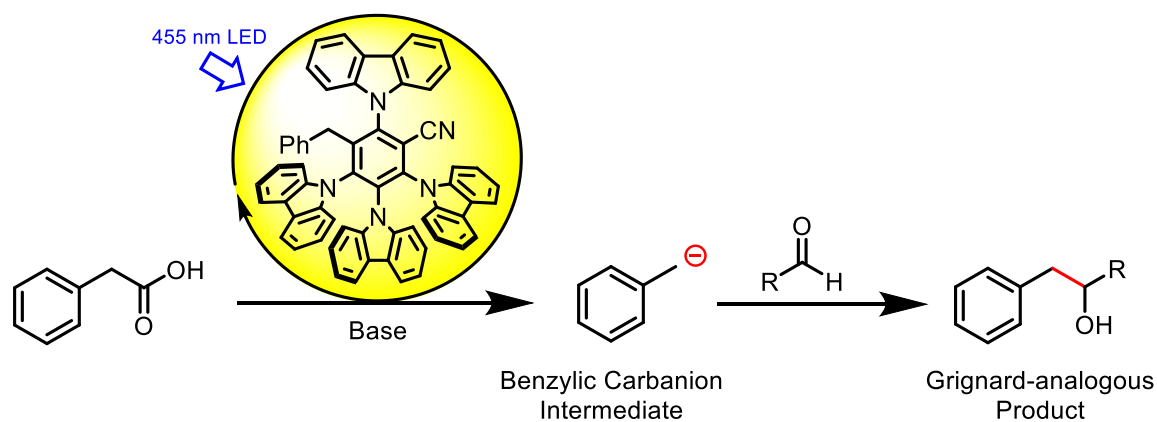
3.6 References

- [1] P. Barbier, *C. R. Acad. Sci.* **1899**, *128*, 110-111.
- [2] a) T. A. Killinger, N. A. Boughton, T. A. Runge, J. Wolinsky, *J. Organomet. Chem.* **1977**, *124*, 131-134; b) C. Petrier, J. L. Luche, *J. Org. Chem.* **1985**, *50*, 910-912; c) F. Zhou, C. J. Li, *Nat. Commun.* **2014**, *5*, 4254; d) L. Keinicke, P. Fristrup, P. O. Norrby, R. Madsen, *J. Am. Chem. Soc.* **2005**, *127*, 15756-15761.
- [3] a) C.-J. Li, W.-C. Zhang, *J. Am. Chem. Soc.* **1998**, *120*, 9102-9103; b) S. Li, J.-X. Wang, X. Wen, X. Ma, *Tetrahedron* **2011**, *67*, 849-855.
- [4] Y. Yamamoto, N. Asao, *Chem. Rev.* **1993**, *93*, 2207-2293.
- [5] a) A. Rizzo, D. Trauner, *Org. Lett.* **2018**, *20*, 1841-1844; b) B. M. Trost, A. B. Pinkerton, *Tetrahedron Lett.* **2000**, *41*, 9627-9631.
- [6] J. Nokami, J. Otera, T. Sudo, R. Okawara, *Organometallics* **1983**, *2*, 191-193.
- [7] a) K. Frimpong, J. Wzorek, C. Lawlor, K. Spencer, T. Mitzel, *J. Org. Chem.* **2009**, *74*, 5861-5870; b) T.-H. Chan, M.-C. Lee, *J. Org. Chem.* **1995**, *60*, 4228-4232.
- [8] S. Wu, Y. Li, S. Zhang, *J. Org. Chem.* **2016**, *81*, 8070-8076.
- [9] C.-J. Li, Y. Meng, X.-H. Yi, J. Ma, T.-H. Chan, *J. Org. Chem.* **1997**, *62*, 8632-8633.
- [10] a) K. Zeitler, *Angew. Chem. Int. Ed.* **2009**, *48*, 9785-9789; b) J. Xuan, W. J. Xiao, *Angew. Chem. Int. Ed.* **2012**, *51*, 6828-6838; c) N. A. Romero, D. A. Nicewicz, *Chem. Rev.* **2016**, *116*, 10075-10166; d) D. Ravelli, S. Protti, M. Fagnoni, *Chem. Rev.* **2016**, *116*, 9850-9913; e) J. P. Goddard, C. Ollivier, L. Fensterbank, *Acc. Chem. Res.* **2016**, *49*, 1924-1936.
- [11] a) K. Hironaka, S. Fukuzumi, T. Tanaka, *J. Chem. Soc., Perkin Trans. 2* **1984**, 1705; b) Y. Zhang, R. Qian, X. Zheng, Y. Zeng, J. Sun, Y. Chen, A. Ding, H. Guo, *Chem. Commun.* **2015**, *51*, 54-57.
- [12] M. Chen, X. Zhao, C. Yang, W. Xia, *Org. Lett.* **2017**, *19*, 3807-3810.
- [13] a) O. Ishitani, C. Pac, H. Sakurai, *J. Org. Chem.* **1983**, *48*, 2941-2942; b) O. Ishitani, S. Yanagida, S. Takamuku, C. Pac, *J. Org. Chem.* **1987**, *52*, 2790-2796; c) T. Ghosh, T. Slanina, B. König, *Chem. Sci.* **2015**, *6*, 2027-2034.
- [14] T. Shibata, A. Kabumoto, T. Shiragami, O. Ishitani, C. Pac, S. Yanagida, *J. Phys. Chem.* **1990**, *94*, 2068-2076.
- [15] a) F. R. Petronijevic, M. Nappi, D. W. MacMillan, *J. Am. Chem. Soc.* **2013**, *135*, 18323-18326; b) M. Nakajima, E. Fava, S. Loescher, Z. Jiang, M. Rueping, *Angew. Chem. Int. Ed.* **2015**, *54*, 8828-8832; c) E. Fava, A. Millet, M. Nakajima, S. Loescher, M. Rueping, *Angew. Chem. Int. Ed.* **2016**, *55*, 6776-6779; d) W. Ding, L. Q. Lu, J. Liu, D. Liu, H. T. Song, W. J. Xiao, *J. Org. Chem.* **2016**, *81*, 7237-7243; e) C. Wang, J. Qin, X. Shen, R. Riedel, K. Harms, E. Meggers, *Angew. Chem. Int. Ed.* **2016**, *55*, 685-688.
- [16] a) G. Pandey, S. Hajra, M. K. Ghorai, K. R. Kumar, *J. Org. Chem.* **1997**, *62*, 5966-5973; b) M. A. Ischay, M. E. Anzovino, J. Du, T. P. Yoon, *J. Am. Chem. Soc.* **2008**, *130*, 12886-12887; c) J. Du, T. P. Yoon, *J. Am. Chem. Soc.* **2009**, *131*, 14604-14605; d) K. T. Tarantino, P. Liu, R. R. Knowles, *J. Am. Chem. Soc.* **2013**, *135*, 10022-10025; e) L. J. Rono, H. G. Yayla, D. Y. Wang, M. F. Armstrong, R. R. Knowles, *J. Am. Chem. Soc.* **2013**, *135*, 17735-17738; f) E. Fava, M. Nakajima, A. L. Nguyen, M. Rueping, *J. Org. Chem.* **2016**, *81*, 6959-6964; g) W. Li, Y. Duan, M. Zhang, J. Cheng, C. Zhu, *Chem. Commun.* **2016**, *52*, 7596-7599.
- [17] a) L. Qi, Y. Chen, *Angew. Chem. Int. Ed.* **2016**, *55*, 13312-13315; b) K. N. Lee, Z. Lei, M. Y. Ngai, *J. Am. Chem. Soc.* **2017**, *139*, 5003-5006.
- [18] Y. Nishigaichi, T. Orimi, A. Takuwa, *J. Organomet. Chem.* **2009**, *694*, 3837-3839.

- [19] a) J. C. Theriot, C. H. Lim, H. Yang, M. D. Ryan, C. B. Musgrave, G. M. Miyake, *Science* **2016**, *352*, 1082-1086; b) R. M. Pearson, C. H. Lim, B. G. McCarthy, C. B. Musgrave, G. M. Miyake, *J. Am. Chem. Soc.* **2016**, *138*, 11399-11407; c) Y. Du, R. M. Pearson, C. H. Lim, S. M. Sartor, M. D. Ryan, H. Yang, N. H. Damrauer, G. M. Miyake, *Chem. Eur. J.* **2017**, *23*, 10962-10968; d) B. G. McCarthy, R. M. Pearson, C. H. Lim, S. M. Sartor, N. H. Damrauer, G. M. Miyake, *J. Am. Chem. Soc.* **2018**, *140*, 5088-5101.
- [20] P. J. Wagner, R. J. Truman, A. E. Puchalski, R. Wake, *J. Am. Chem. Soc.* **1986**, *108*, 7727-7738.
- [21] J. L. Jeffrey, F. R. Petronijevic, D. W. MacMillan, *J. Am. Chem. Soc.* **2015**, *137*, 8404-8407.
- [22] D. Griller, K. U. Ingold, *Acc. Chem. Res.* **1976**, *9*, 13-19.
- [23] a) A. Studer, *Chem. Eur. J.* **2001**, *7*, 1159-1164; b) J. D. Cuthbertson, D. W. MacMillan, *Nature* **2015**, *519*, 74-77.
- [24] S. Hünig, P. Kreitmeier, G. Märkl, J. Sauer, *Verlag Lehmanns* **2006**.
- [25] R. K. Harris, E. D. Becker, S. M. Cabral de Menezes, R. Goodfellow, P. Granger, *Magn. Reson. Chem.* **2002**, *40*, 489-505.
- [26] G. R. Fulmer, A. J. M. Miller, N. H. Sherden, H. E. Gottlieb, A. Nudelman, B. M. Stoltz, J. E. Bercaw, K. I. Goldberg, *Organometallics* **2010**, *29*, 2176-2179.
- [27] V. V. Pavlishchuk, A. W. Addison, *Inorg. Chim. Acta* **2000**, *298*, 97-102.
- [28] J. Luo, J. Zhang, *ACS Catal.* **2016**, *6*, 873-877.
- [29] S. Kuwano, S. Harada, R. Oriez, K. Yamada, *Chem. Commun.* **2012**, *48*, 145-147.
- [30] A. Samanta, B. J. Ravoo, *Chemistry* **2014**, *20*, 4966-4973.
- [31] S. Imai, H. Togo, *Tetrahedron* **2016**, *72*, 6948-6954.
- [32] J.-H. Kim, M. E. El-Khouly, Y. Araki, O. Ito, K.-Y. Kay, *Chem. Lett.* **2008**, *37*, 544-545.
- [33] S. Kobayashi, K. Nishio, *J. Org. Chem.* **1994**, *59*, 6620-6628.
- [34] G. P. Howell, A. J. Minnaard, B. L. Feringa, *Org. Biomol. Chem.* **2006**, *4*, 1278.
- [35] Y. Corre, V. Rysak, X. Trivelli, F. Agbossou-Niedercorn, C. Michon, *Eur. J. Org. Chem.* **2017**, *2017*, 4820-4826.
- [36] L. M. Fleury, A. D. Kosal, J. T. Masters, B. L. Ashfeld, *J. Org. Chem.* **2013**, *78*, 253-269.
- [37] K. Koide, J. M. Finkelstein, Z. Ball, G. L. Verdine, *J. Am. Chem. Soc.* **2001**, *123*, 398-408.
- [38] J. F. Bower, R. L. Patman, M. J. Krische, *Org. Lett.* **2008**, *10*, 1033-1035.
- [39] G.-l. Li, G. Zhao, *Org. Lett.* **2006**, *8*, 633-636.
- [40] W. Wang, T. Zhang, M. Shi, *Organometallics* **2009**, *28*, 2640-2642.
- [41] J. J. Eisch, J. H. Merkley, J. E. Galle, *J. Org. Chem.* **1979**, *44*, 587-593.
- [42] H. Wang, X. J. Dai, C. J. Li, *Nat. Chem.* **2017**, *9*, 374-378.
- [43] A. R. Katritzky, H. Wu, L. Xie, *J. Org. Chem.* **1996**, *61*, 4035-4039.
- [44] D. Goswami, A. Chattopadhyay, A. Sharma, S. Chattopadhyay, *J. Org. Chem.* **2012**, *77*, 11064-11070.
- [45] J. He, S. Tang, S. Tang, J. Liu, Y. Sun, X. Pan, X. She, *Tetrahedron Lett.* **2009**, *50*, 430-433.
- [46] E. J. Enholm, K. M. Moran, P. E. Whitley, M. A. Battiste, *J. Am. Chem. Soc.* **1998**, *120*, 3807-3808.
- [47] U. Megerle, R. Lechner, B. König, E. Riedle, *Photochem. Photobiol. Sci.* **2010**, *9*, 1400-1406.

CHAPTER 4

4 Photocatalytic carbanion generation - benzylation of aliphatic aldehydes to secondary alcohols



This chapter has been published in: K. Donabauer, M. Maity, A. L. Berger, G. S. Huff, S. Crespi, B. König, *Chem Sci.* **2019**, *10*, 5162-5166.

K. Donabauer carried out the reactions in Table 1, a part of the reactions in Table 2, performed the mechanistic investigations and wrote the manuscript. M. Maity carried out a part of the reactions in Table 2. A. L. Berger carried out a part of the reactions in Table 2. G. S. Huff performed *in situ* IR-measurements. G. S. Huff and S. Crespi performed DFT calculations. B. König supervised the project and is corresponding author.

4.1 Introduction

Photocatalysis is a fast growing field in chemistry, enabling novel transformations previously unattainable under thermal conditions.^[1] The formation of carbon–carbon bonds is at the core of organic synthesis^[2] and many photocatalytic methods have been reported over the last two decades, the majority of which involve the generation of one or more radical species as key intermediates.^[3] In contrast, photocatalytic C–C bond formations involving anionic species as key intermediates are rare,^[4] although the reaction between a carbanion and a carbon electrophile, *e.g.* the Grignard reaction,^[5] is the most typical C–C bond forming reaction. Thus, photocatalytic methods to generate and utilize carbanion intermediates are desired in order to expand the limits of photocatalytic transformations from open shell to closed shell reactivity.

Commonly used photocatalysts, however, are only known to transfer a single electron to a substrate at once (SET), forming the corresponding radical and are not able to transfer two electrons in one step to generate the corresponding carbanion.^[3] Thus, the most intuitive way to photocatalytic carbanion generation is by two subsequent SETs, *i.e.* a consecutive two-fold reduction.^[6] There are a few literature examples illustrating the synthetic applicability of this strategy.^[4a, 4b] These include the carbanion formation from 1,2-dibromomalonates giving cyclopropanes after addition to electron poor alkenes^[4a] and the carbanion formation from tetraalkyl ammonium salts followed by their addition to aromatic aldehydes (Scheme 4-1a).^[4b] The latter transformation reported by Yu *et al.* is especially interesting, as it is similar to the commonly used Grignard reaction. However, this method seems to be limited to aromatic aldehydes.

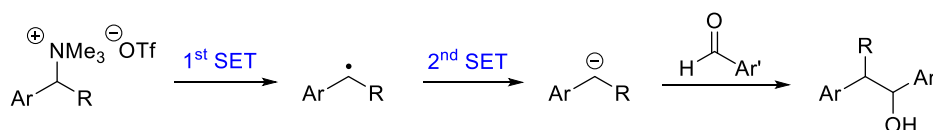
Beside the generation of a carbanion *via* a consecutive two-fold reduction, redox-neutral carbanion formations are proposed in several reports as well, typically by the reduction of a radical intermediate during the regeneration of the photocatalyst. However, this carbanion is in most cases simply protonated^[7] and examples where it is synthetically used are scarce.^[4c-i, 8] These include the formation of a C–S bond with benzenesulfonothioates as electrophiles^[4c] and intramolecular ring closures *via* an S_N2 reaction (Scheme 4-1b).^[4f-i]

To the best of our knowledge, there is so far no report for a redox-neutral photocatalytic carbanion generation followed by its intermolecular reaction with an aliphatic aldehyde or ketone as electrophile (Scheme 4-1c). As mentioned above, aldehydes and ketones are in this regard especially interesting electrophiles, as the corresponding transformation is analogous to

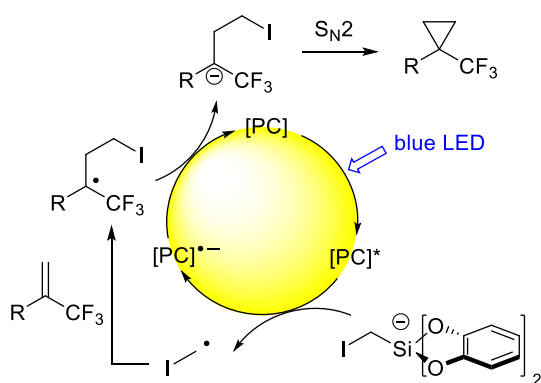
the widespread Grignard reaction. Additionally, substituted carbonyl compounds are poor radical traps for an intermolecular radical addition and forming the desired product using established photocatalytic protocols for radical addition to double bonds is generally not successful.^[9] An exception to this is the photocatalytic radical addition enabled by *in situ* Brønsted acid activation yielding 3-alkoxy alcohols as reaction products reported by Glorius *et al.*^[10] Mainly aromatic carbonyl compounds could be used as radical traps.

Inspired by the above mentioned reports, we envisioned a photocatalytic cycle, in which a carbanion is formed from readily available carboxylic acids. Here, the *in situ* formed carboxylate is oxidized to the corresponding radical. This intermediate is prone to CO₂ exclusion, forming the carbon centered radical, which may be converted to the corresponding carbanion by SET from the reduced photocatalyst. The desired product is then formed by addition of the carbanion to an aldehyde as electrophile (Scheme 4-1c). Herein we describe our efforts to realize this catalytic cycle.

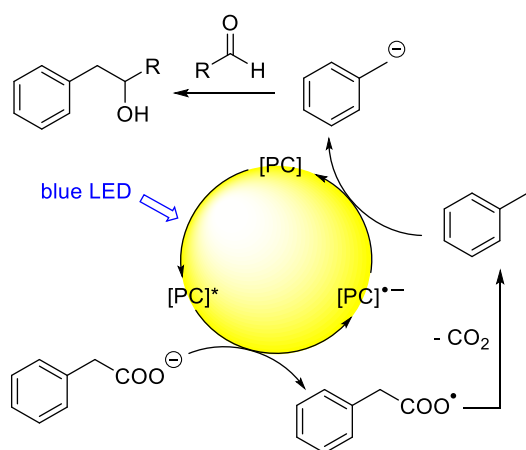
a) Yu *et al.* 2018: Reductive photocatalytic carbanion formation via two consecutive SETs



b) Molander *et al.* 2018: Redox-neutral photocatalytic carbanion formation



c) Envisioned catalytic cycle



Scheme 4-1 - (a) Photocatalytic carbanion generation *via* two consecutive SETs. (b) Redox-neutral carbanion generation followed by intramolecular S_N2 reaction. (c) Envisioned catalytic cycle.

4.2 Results and discussion

With the envisioned photocatalytic cycle in mind, the coupling between phenylacetic acid (**1a**) and *n*-pentanal (**2a**) was chosen as model reaction. Compound **1a** was selected as carbanion precursor, since the corresponding benzylic radical as well as the desired carbanion intermediate are stabilized by the aromatic moiety. As the photocatalyst is supposed to engage in a single electron oxidation as well as reduction, employing a catalyst with both a strong oxidation as well as reduction power is crucial. 4CzIPN is an in this regard very attractive organic photocatalyst, exhibiting an excited state redox potential of $E_{1/2}(P^*/P^{\bullet}) = +1.35$ V *vs* SCE and a ground state reduction potential of $E_{1/2}^{\text{red}}(P/P^{\bullet}) = -1.21$ V *vs* SCE in MeCN.^[11] With 4CzIPN as catalyst and Cs₂CO₃ as base, the reaction proceeded smoothly yielding the desired addition product **3a** in 73% GC- yield after 16 h (Table 4-1). Toluene (**4a**) was observed as a second product in 15% yield resulting from the reaction with protons as electrophile. To increase the reaction yield, several parameters were optimized (Table 4-1, for the full optimization process see experimental part).

Table 4-1 – Optimization of the reaction conditions.^[a]

Entry	Solvent	Additive (eq.)	Yield 3a ^[b] [%]	Yield 4a ^[b] [%]
1	Dry DMF	—	73	15
2	Dry DMA	—	75	11
3	DMA	—	75 (63) ^[c]	12
4	DMA	H ₂ O (3 eq.)	34	55
5 ^[d]	DMA	—	not detected (n.d.)	n.d.
6 ^[e]	DMA	—	n.d.	n.d.
7 ^[f]	DMA	—	n.d.	n.d.
8 ^[g]	DMA	—	64 (48) ^[c]	12

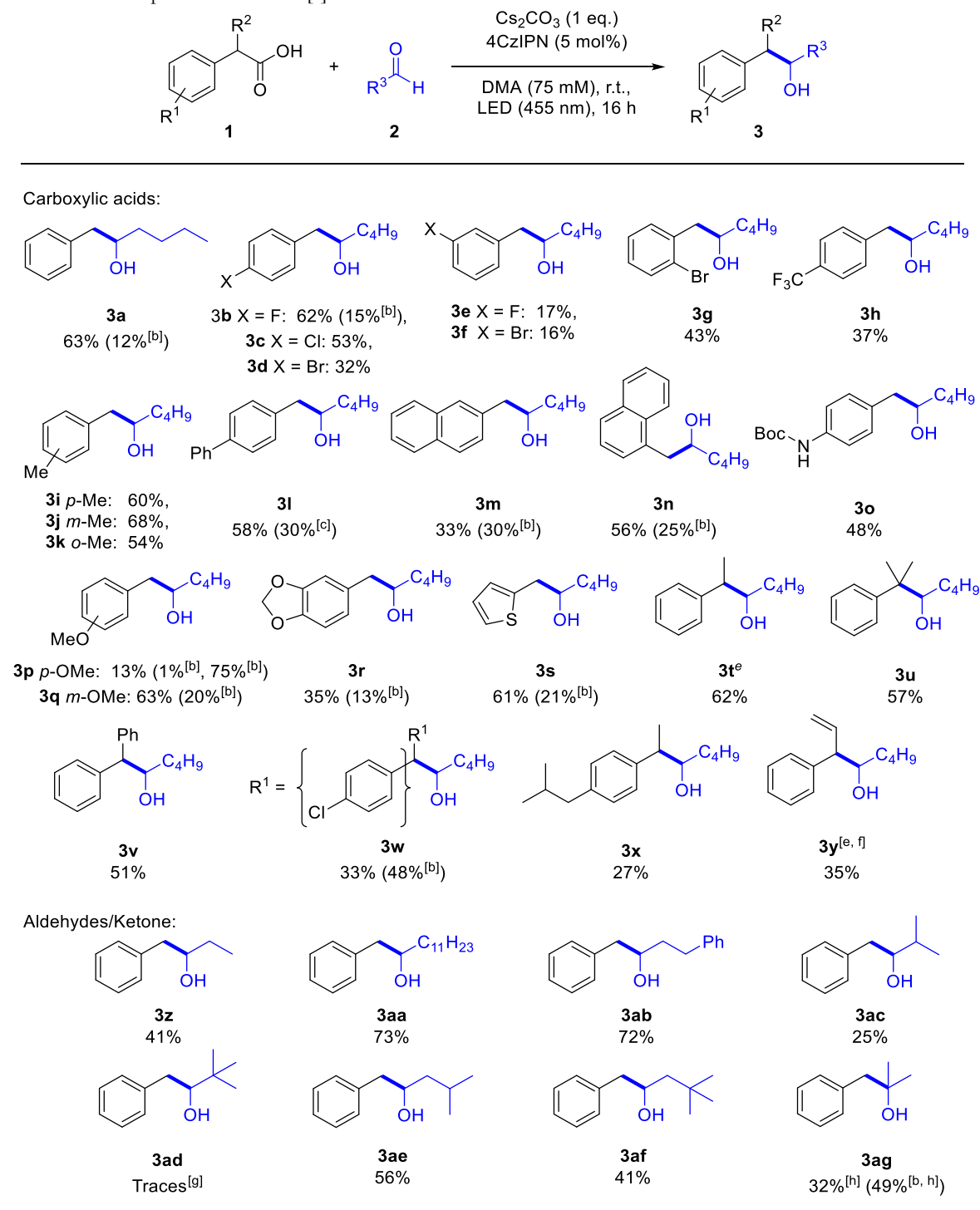
[a] Reactions were performed with **1a** (150 μmol, 1 eq.), **2a** (3 eq.) and Cs₂CO₃ (1 eq.) in degassed solvent (2 mL) under a nitrogen atmosphere. [b] GC-Yield determined with *n*-decane as internal standard. [c] Isolated yield in parentheses. [d] Reaction performed in absence of 4CzIPN. [e] Reaction performed in the dark. [f] Reaction performed without base. [g] The preformed NBu₄⁺ carboxylate salt (NBu₄PA, **5**) was used instead of **1a** in absence of Cs₂CO₃.

A slight improvement could be realized by using DMA as solvent. Interestingly, prior drying of the solvent over 4 Å molecular sieve did not improve the yield significantly (entries 2 and 3), whereas the addition of H₂O gave more toluene (**4a**) (entry 4). Control experiments confirmed that photocatalyst, light and base (entries 5-7) are necessary for the reaction conversion. However, the reaction can be performed in absence of base when using the preformed NBu₄⁺ carboxylate salt (**5**) (entry 8), suggesting that the base merely serves to generate the carboxylate.

The reaction proceeds with various carboxylic acids (Table 4-2) as carbanion precursors in moderate to good yields. Halogen or -CF₃ substituted phenyl acetic acid derivatives give the desired products (**3b-h**). The presence of an additional methyl or phenyl group on the aromatic ring (**3i-l**), extended aromatic systems (**3m-n**), a Boc-protected amine (**3o**) and methoxy (**3p-r**) functional groups or additional substituents on the benzylic carbon (**3t-v**) are tolerated.

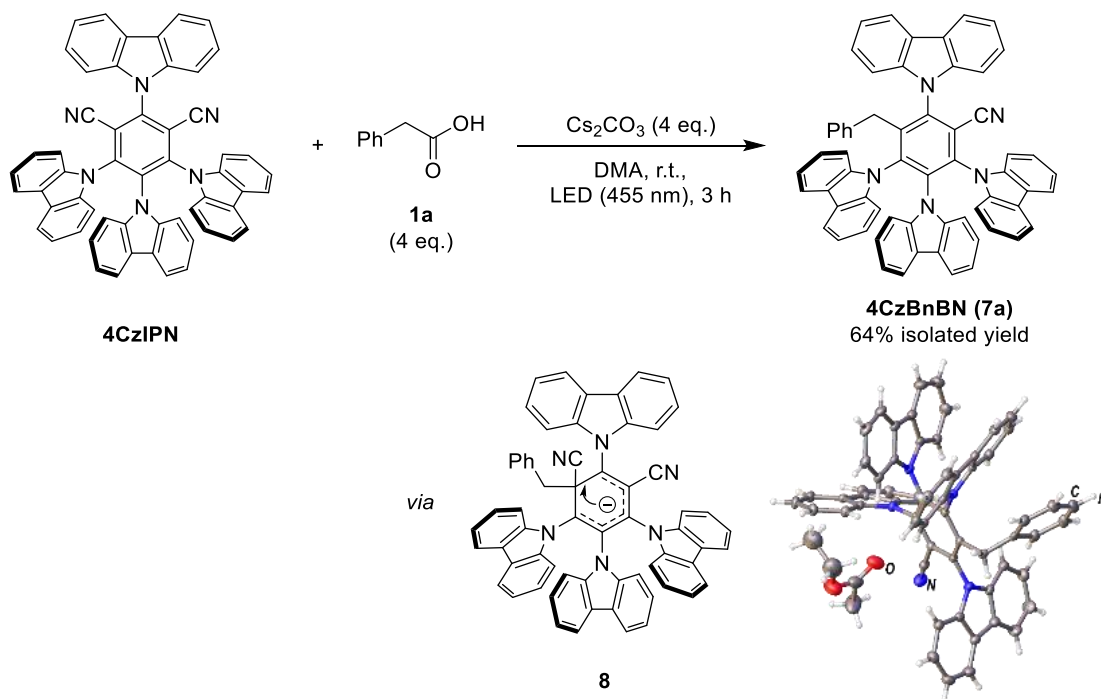
The presence of a stabilizing aromatic moiety is necessary. Aliphatic and allylic carboxylic acids yield only traces of the desired product or none at all. Aliphatic aldehydes bearing short or long chains (**3z-ab**) react well as electrophiles. The presence of an additional methyl group at the α -carbon decreased the yield to 25% (**3ac**) and only traces of the product could be observed when pivalaldehyde was employed (**3ad**). Substituents in the β -position (**3ae**) are tolerated and even adding a second methyl group showed only a minor effect (**3af**). Aromatic aldehydes, *e.g.* benzaldehyde (**2i**), gave the corresponding product as well, but a radical-radical cross coupling of the benzyl radical and the ketyl radical similar to our previous report^[12] instead of a carbanion generation cannot be excluded (Experimental part, section 4.4.7.10).

The formation of byproducts was investigated for selected examples (**3a-b**, **3l-n**, **3p-s**, **3w**) and an almost complete mass balance could be obtained in most cases when combining the yield of the desired (**3**) and the decarboxylated (**4**) product (Table 4-2). If this was not the case, *e.g.* for **3p**, an incomplete conversion of **1** was observed. Ketones, *e.g.* acetone (**6**), yield only small amounts of the tertiary alcohol (Experimental part, Table 4-11). Using acetone (**6**) as co-solvent (1:1 mixture of DMA and acetone) increased the yield and **3ag** could be isolated in 32% (Table 4-2). Further, several electrophiles for an intermolecular S_N2 reaction were tested (Experimental part, Table 4-13), however an efficient system could not be found and only product traces were detected in some cases.

Table 4-2 – Scope of the reaction.[a]

[a] Reactions were performed with **1** (150 μ mol, 1 eq.) and **2** (3 eq.) in degassed DMA (2 mL) under a nitrogen atmosphere. If not noted otherwise, the numbers indicate isolated yields. [b] GC-yield of the corresponding decarboxylated side-product **4** determined by GC-FID analysis with *n*-decane as internal standard. [c] Isolated yield of the corresponding decarboxylated side-product **4**. [d] Recovered starting material **1** after complete reaction time. [e] Mixture of syn- and anti-product was obtained. [f] *trans*-styrylacetic acid rather than α -vinylphenylacetic acid was used as starting material. [g] Observed by GC-MS, not isolated. [h] Acetone/DMA (1:1) was used as solvent.

Starting the mechanistic investigation, a photo-conversion of 4CzIPN was observed during the course of the reaction (Experimental part, Figure 4-2). The degradation product could be isolated and identified as 4CzBnBN (**7a**) by X-ray crystal structure analysis (Scheme 4-2). Compound **7a** is likely formed by radical addition of the benzyl radical to the radical anion of 4CzIPN, followed by cyanide elimination similar to reactions reported by different groups.^[13] 4CzBnBN seems to be significantly more photo-stable and the product resulting from a second cyanide elimination could only be detected in traces. Performing the benzylation reaction with 4CzBnBN as catalyst gave the desired product as well (Experimental part, Scheme 4-7), showing that 4CzBnBN is contributing and likely the main active catalyst for the carbanion formation. Ground state potentials of $E_{1/2}^{\text{ox}}(\text{P}^{\bullet+}/\text{P}) = +1.48 \text{ V vs SCE}$ and $E_{1/2}^{\text{red}}(\text{P}/\text{P}^{\bullet-}) = -1.72 \text{ V vs SCE}$ in DMF were measured by CV.



Scheme 4-2 – Isolation of 4CzIPN photo-conversion product 4CzBnBN (**7a**). The reaction was performed with 4CzIPN (30 μmol , 1 eq.) and **1a** (4 eq.) in degassed DMA (2 mL) under a nitrogen atmosphere.

The first step in our mechanistic hypothesis is the oxidation of the carboxylate followed by the extrusion of CO_2 to generate a benzyl radical. There are several reports describing this process with various photoredox catalysts.^[14] Accordingly, the emission of 4CzBnBN could be quenched upon addition of NBu_4PA (**5**) resulting in a linear Stern-Volmer plot (Experimental part, Figure 4-8), confirming the interaction between the excited photocatalyst and the

substrate. The following CO₂ elimination could be monitored by *in situ* IR spectroscopy (Figure 4-1) together with the depletion of the aldehyde in course of the reaction.

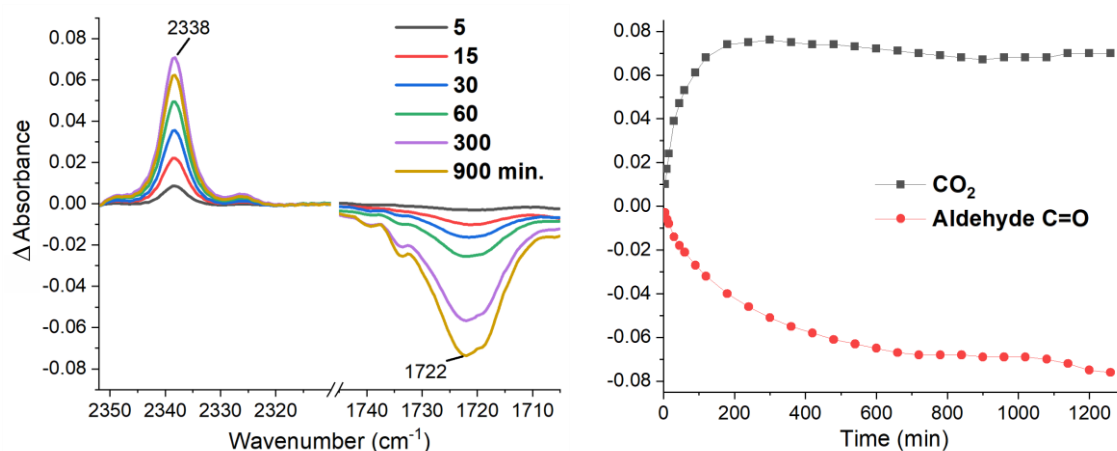
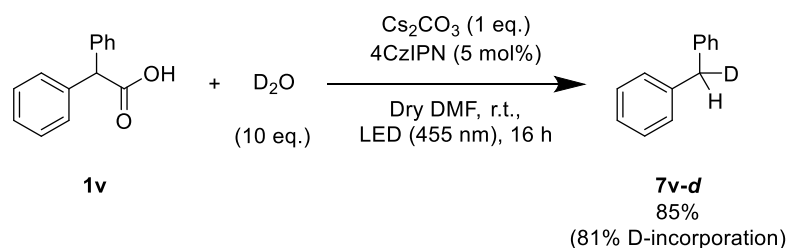


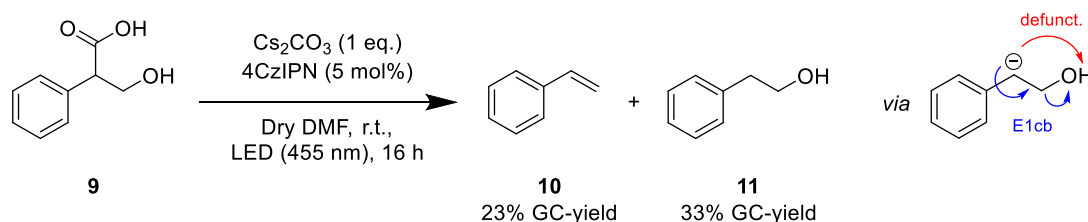
Figure 4-1 – *In situ* FT-IR studies. Irradiation of a solution containing NBu₄PA (**5**) (75 mM), **2a** (75 mM) and 4CzBnBN (3.75 mM) in dry DMA lead to the formation of CO₂ (2338 cm⁻¹) and the depletion of **2a** (1722 cm⁻¹).

Next, deuterium labeling experiments were conducted to support the formation of an anionic intermediate during the later course of the reaction (Scheme 4-3a). With D₂O as electrophile, the corresponding deuterated decarboxylated starting material was isolated (**4v-d**). As a control experiment, the non-deuterated product (**4v**) was obtained when the reaction was performed in deuterated DMF in absence of D₂O. Addition of D₂O to a reaction mixture after completed irradiation did not yield any **4v-d** from **4v** *via* base-induced (Cs₂CO₃) H/D-exchange (Experimental part, Scheme 4-8).

a) Deuterium labeling



b) E1cb elimination

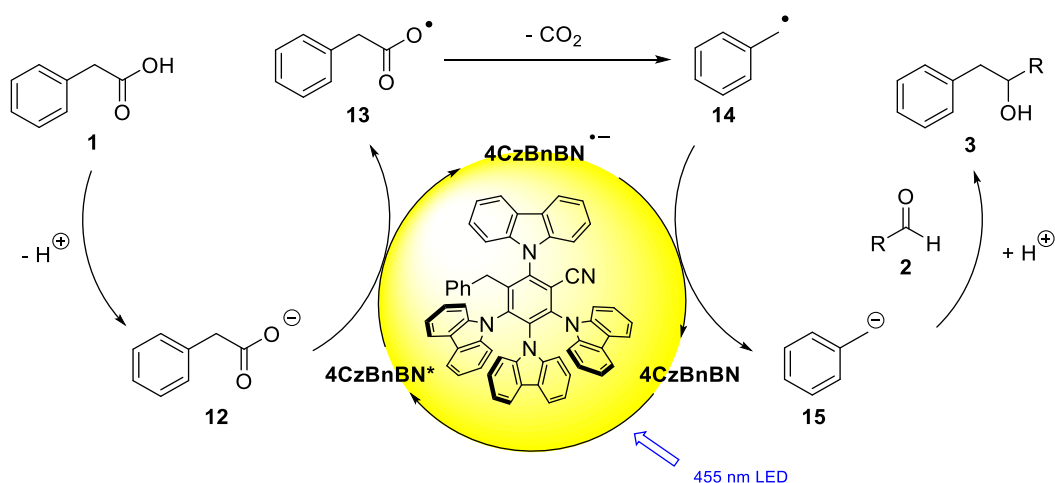


Scheme 4-3 – Experiments supporting the formation of a reactive anionic intermediate.

In addition to the incorporation of deuterium, a carbanion intermediate is expected to engage in an E1cb elimination if an appropriate leaving group is present in the homobenzylic position. Hence, tropic acid (**9**) was subjected to the reaction conditions (Scheme 4-3b). Indeed, styrene (**10**) together with the decarboxylated byproduct (**11**) was detected. To exclude styrene formation from **11** by a simple E2 elimination induced by Cs₂CO₃, **11** was directly subjected to the applied reaction conditions, yielding no styrene (Experimental part, Scheme 4-9).

In order to thoroughly study the feasibility and selectivity of the addition of the benzyl anion (**15**) to the electrophile, a computational analysis was performed. The C=O addition and the acid-base reaction of **15** and the C α -H was proven at the SMD(DMF)- ω B97X-D/TZVP level of theory (Experimental part, Section 4.4.7.9). Indeed, the reaction of the benzyl anion with the aldehydes results to be exothermal ($\Delta G = -6.9$ kcal/mol) and slightly kinetically favored ($\Delta G^* = +6.2$ kcal/mol) compared to the abstraction of the acidic proton in the α position ($\Delta G^* = +6.8$ kcal/mol). Ketones were found to be less selective towards the C=O addition of the benzyl anion compared to the aldehydes (see compound **3ag**). As a parallelism, the reaction of the benzyl anion with the ketonic C=O is almost thermoneutral ($\Delta G = +1.5$ kcal/mol). The competing acid-base reaction is exothermal ($\Delta G = -12.1$ kcal/mol), with comparable barriers (ΔG^* ca. 10 kcal/mol). The barriers for the reactions of **15** with DMA are higher compared to the ones of aldehydes and ketones.

Considering the experimental observations, computational results and cited literature reports, the following mechanism is proposed (Scheme 4-4): Carboxylic acid **1a** is deprotonated by the base (Cs₂CO₃) to give carboxylate **12**. The carboxylate ($E_{1/2}^{ox}$ (NBu₄PA **5**) = +1.27 *vs* SCE^[14a]) can be oxidized by the excited photocatalyst 4CzBnBN ($E_{1/2}^{ox}(P^*/P^{\bullet-}) = +1.21$ V *vs* SCE) and the generated radical species **13** is transformed to the benzylic radical **14** by elimination of CO₂. The radical anion of 4CzBnBN is with a reduction potential of $E_{1/2}^{red}(P/P^{\bullet-}) = -1.72$ V *vs* SCE not able to reduce aliphatic aldehydes ($E_{1/2}^{red}$ (3-methylbutanal **2g**) = -2.24 V *vs* SCE^[15]) and hence transfers an electron to the more easily reducible benzyl radical ($E_{1/2}^{red} = -1.43$ V *vs* SCE^[16]) to form carbanion **15**. This species is capable of adding to aldehydes (**2**) forming the desired product **3** after protonation of the alcoholate.



4.3 Conclusion

In summary, a redox-neutral procedure to benzylate aliphatic aldehydes *via* the photocatalytic generation of a carbanion intermediate is presented, rendering the desired Grignard analogous products in moderate to good yields. The proposed mechanism is supported by emission quenching, *in situ* UV/VIS and *in situ* IR studies, while the presence of the reactive anionic intermediate is shown by deuterium labeling, E1cb Elimination and DFT calculation.

4.4 Experimental part

4.4.1 General information

Starting materials and reagents were purchased from commercial suppliers (Sigma Aldrich, Alfa Aesar, Acros, Fluka, TCI or VWR) and used without further purification. Solvents were used as p.a. grade or dried and distilled according to literature known procedures.^[17] For automated flash column chromatography industrial grade of solvents was used. All reactions with oxygen- or moisture-sensitive reagents were carried out in glassware, which was dried before use by heating under vacuum. Dry nitrogen was used as inert gas atmosphere. Liquids were added *via* syringe, needle and septum techniques unless otherwise stated.

All NMR spectra were measured at room temperature using a Bruker Avance 300 (300 MHz for ¹H, 75 MHz for ¹³C, 282 MHz for ¹⁹F) or a Bruker Avance 400 (400 MHz for ¹H, 101 MHz for ¹³C, 376 MHz for ¹⁹F)^[18] NMR spectrometer. All chemical shifts are reported in δ -scale as parts per million [ppm] (multiplicity, coupling constant *J*, number of protons) relative to the solvent residual peaks as the internal standard.^[19] Coupling constants *J* are given in Hertz [Hz]. Abbreviations used for signal multiplicity: ¹H-NMR: b = broad, s = singlet, d = doublet, t = triplet, q = quartet, hept = heptet dd = doublet of doublets, dt = doublet of triplets, dq = doublet of quartets, and m = multiplet; ¹³C-NMR: (+) = primary/tertiary, (–) = secondary, (C_q) = quaternary carbon.

HRMS (high resolution mass spectra) and LRMS (low resolution mass spectra) were measured at the Central Analytical Laboratory of the University of Regensburg. These mass spectra were recorded on a Finnigan MAT 95, ThermoQuest Finnigan TSQ 7000, Finnigan MAT SSQ 710 A or an Agilent Q-TOF 6540 UHD instrument.

GC measurements were performed on a GC 7890 from Agilent Technologies. Data acquisition and evaluation was done with Agilent ChemStation Rev.C.01.04. GC/MS measurements were performed on a 7890A GC system from Agilent Technologies with an Agilent 5975 MSD Detector. Data acquisition and evaluation was done with MSD ChemStation E.02.02.1431. A capillary column HP-5MS/30 m x 0.25 mm/0.25 μ M film and helium as carrier gas (flow rate of 1 mL/min) were used. The injector temperature (split injection: 40:1 split) was 280 °C, detection temperature 300 °C (FID). GC measurements were made and investigated *via* integration of the signal obtained. The GC oven temperature program was adjusted as follows: initial temperature 40 °C was kept for 3 minutes, the temperature was increased at a rate of 15 °C/min over a period of 16 minutes until 280 °C was reached and kept for 5 minutes, the

temperature was again increased at a rate of 25 °C/min over a period of 48 seconds until the final temperature (300 °C) was reached and kept for 5 minutes. *n*-Decane was used as an internal standard.

Analytical TLC was performed on silica gel coated alumina plates (MN TLC sheets ALUGRAM® Xtra SIL G/UV₂₅₄). Visualization was done by UV light (254 or 366 nm). If necessary, potassium permanganate or ceric ammonium molybdate was used for chemical staining.

Purification by column chromatography was performed with silica gel 60 M (40-63 µm, 230-440 mesh, Merck) or with a pre-packed Biotage® Snap Ultra HP-Sphere™ 25 µm column on a Biotage® Isolera™ Spektra One device.

For irradiation with blue light OSRAM Oslon SSL 80 LDCQ7P-1U3U (blue, $\lambda_{\text{max}} = 455$ nm, $I_{\text{max}} = 1000$ mA, 1.12 W) was used. For irradiation with green light Cree XPEGRN L1 G4 Q4 (green, $\lambda_{\text{max}} = 535$ nm, $I_{\text{max}} = 1000$ mA, 1.12 W), and for irradiation with 400 nm Edison EDEV-SLC1-03 ($\lambda_{\text{max}} = 400$ nm, $I_{\text{max}} = 700$ mA, 400 mW) was used.

Fluorescence spectra were measured on a HORIBA FluoroMax®-4 Spectrofluorometer at room temperature. Gas tight 10 mm Hellma® quartz fluorescence cuvettes with a screw cap with PTFE-coated silicon septum were used. FluorEssence Version 3.5.1.20 was used as a software for measurement and analysis.

UV-Vis absorption spectroscopy was performed at 25 °C on a Varian Cary 100 Spectrometer with a 10 mm quartz cuvette.

Oxidation and reduction potentials given in the text are cited from literature reports. All potentials therein were determined in acetonitrile.

CCDC 1884950 contains the supplementary crystallographic data for this paper. These data are provided free of charge by The Cambridge Crystallographic Data Centre.

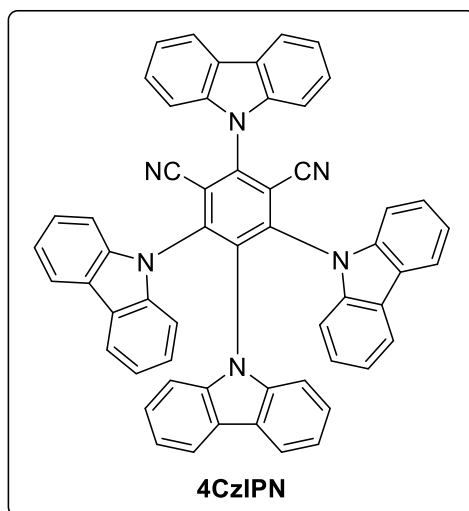
4.4.2 Synthetic procedures

4.4.2.1 Synthesis of photocatalysts

2,4,5,6-Tetrakis(carbazol-9-yl)-4,6-dicyanobenzene (4CzIPN)^[11]

The photocatalyst was synthesized using an adapted literature procedure.^[11]

NaH (60% in paraffin oil, 800 mg, 20 mmol, 10 eq.) was added portionwise to a stirred solution of carbazole (1.67 g, 10 mmol, 5 eq.) in dry THF (40 mL). The reaction mixture was heated to 35 °C and stirred for 1 h before adding tetrafluoroisophthalonitrile (400 mg, 2 mmol, 1 eq.). The reaction mixture was stirred at 35 °C overnight for approx. 16 h, afterwards quenched by H₂O (2 mL) and concentrated *in vacuo*. The solid residue was washed with H₂O and EtOH to yield the crude product, which was purified by recrystallization from hexane/DCM to give 2,4,5,6-tetrakis(carbazol-9-yl)-4,6-dicyano-benzene (4CzIPN) as bright yellow powder (840 mg, 1.06 mmol, 53%).

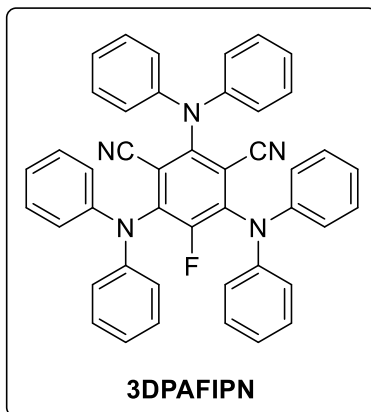


¹H-NMR (400 MHz, CDCl₃, δ_H): 8.22 (d, J = 7.7 Hz, 2H), 7.75 – 7.67 (m, 8H), 7.52 – 7.47 (m, 2H), 7.33 (d, J = 7.8 Hz, 2H), 7.25 – 7.19 (m, 4H), 7.12 – 7.05 (m, 8H), 6.82 (t, J = 8.2 Hz, 4H), 6.63 (td, J = 7.6, 1.2 Hz, 2H).

¹³C-NMR (101 MHz, CDCl₃, δ_C): 145.3, 144.7, 140.1, 138.3, 137.1, 134.9, 127.1, 125.9, 125.1, 124.9, 124.7, 124.0, 122.5, 122.1, 121.5, 121.1, 120.6, 119.8, 116.5, 111.8, 110.1, 109.6, 109.6.

2,4,6-Tris(diphenylamino)-5-fluoroisophthalonitrile (3DPAFIPN)^[20]

The photocatalyst was synthesized analogous to 4CzIPN with diphenylamine (1.69 g, 10 mmol, 5 eq.) instead of carbazole. 2,4,6-Tris(diphenylamino)-5-fluoroisophthalonitrile (3DPAFIPN) (900 mg, 1.39 mmol, 70%) was obtained as bright yellow powder.



¹H-NMR (300 MHz, CDCl₃, δ_H): 7.29 – 7.24 (m, 16H), 7.12-7.04 (m, 8H), 7.02 – 6.98 (m, 16H).

¹³C-NMR (75 MHz, CDCl₃, δ_C): 145.7, 145.4, 143.3, 143.1, 129.6, 129.5, 124.7, 124.2, 122.9, 122.8, 112.7, 109.0.

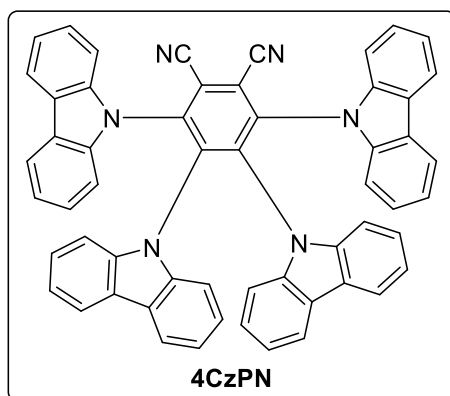
¹⁹F-NMR (282 MHz, CDCl₃, δ_F): -121.81 (s).

Field desorption mass spectra (**FD-MS**) (m/z): [M⁺] (C₄₄H₃₀FN₅⁺) calc. 647.25; observed 647.1977.

FD-MS revealed, that 4DPAFIPN^[11] is present in smaller amount as well (m/z): [M⁺] (C₅₆H₄₀N₆⁺) calc. 796.33; observed 796.2684. It may be the impurity visible in the NMR.

3,4,5,6-Tetra(carbazol-9-yl)phthalonitrile (4CzPN)^[11]

The photocatalyst was synthesized using the adapted literature procedure analogous to 4CzIPN with tetrafluorophthalonitrile (400 mg, 2 mmol, 1 eq.) instead of tetrafluoroisophthalonitrile. 3,4,5,6-Tet-ra(carbazol-9-yl)phthalonitrile (4CzPN) (584 mg, 0.74 mmol, 37%) was obtained as bright orange powder.



¹H-NMR (400 MHz, CDCl₃, δ_H): 7.89 – 7.86 (m, 4H), 7.72 – 7.68 (m, 4H), 7.38 (t, *J* = 7.4 Hz, 8H), 7.16 – 7.09 (m, 8H), 6.73 (t, *J* = 7.5 Hz, 4H), 6.59 (t, *J* = 8.2 Hz, 4H).

[Ir(dF-CF₃-ppy)₂(dtbpy)](PF₆)

The photocatalyst was synthesized according to a literature procedure.^[21]

3,7-Di(4-biphenyl) 1-naphthalene-10-phenoxazine

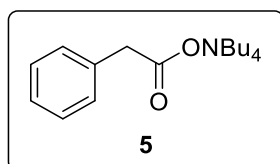
The photocatalyst was synthesized according to a literature procedure.^[22]

4.4.2.2 Synthesis of starting materials

Tetrabutylammonium phenylacetate (NBu₄PA) (**5**) solution

Tetrabutylammonium phenylacetate (**5**) was obtained using an adapted literature procedure.^[7g] An NBu₄OH in H₂O solution (40 wt%, 1.3 mL, 2 mmol, 1 eq.) and H₂O (2 mL) were added to phenylacetic acid (**1a**) (286 mg, 2.1 mmol, 1.05 eq.). The mixture was stirred for 2 h during which it became a clear solution. Subsequently, the water was removed by freeze drying for 2 d yielding the hygroscopic Tertbutylammonium phenylacetate salt (**5**). (A small amount for the NMR-analysis was taken at this point).

4 Å Molecular sieve was added to the residue followed by either dry DMF (27 mL) or dry DMA (27 mL) to obtain a 75 mM solution of **5**. The solution was allowed to stand for at least 1 d before further use.



¹H-NMR (300 MHz, d₇-DMF, δ_H): 7.34 – 7.29 (m, 2H), 7.21 – 7.14 (m, 2H), 7.09 – 7.03 (m, 1H), 3.45 – 3.37 (m, 8H), 3.30 (s, 2H), 1.81 – 1.68 (m, 8H), 1.45 – 1.32 (m, 8H), 0.96 (t, *J* = 7.3 Hz, 12H).

¹³C-NMR (75 MHz, d₇-DMF, δ_C): 174.1 (C_q), 142.4 (C_q), 130.4 (+), 128.3 (+), 125.5 (+), 59.2 (–), 48.2 (–), 24.6 (–), 20.6 (–), 14.2 (+).

4.4.3 Photocatalytic benzylation of aldehydes

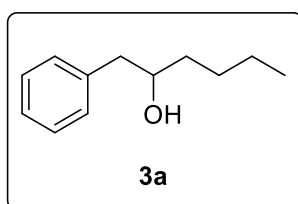
General procedure for the photocatalytic benzylation of aldehydes (general procedure A)

A 5 mL crimp cap vial equipped with a magnetic stirring bar was loaded with 4CzIPN (5.9 mg, 7.5 μ mol, 5 mol%), Cs₂CO₃ (48.9 mg, 150 μ mol, 1 eq.), the corresponding carboxylic acid (150 μ mol, 1 eq.), the corresponding aldehyde (450 μ mol, 3 eq.) and DMA (2 mL). In doing so, all solid compounds were added before capping the vial, whereas all liquid compounds were added *via* syringe after setting the capped vial under inert conditions. The reaction mixture was degassed by four cycles of freeze-pump-thaw and subsequently stirred under light irradiation using a 455 nm (\pm 25 nm) LED for 16 h at 25 °C.

Two reaction batches were combined and diluted with brine (15 mL), water (5 mL) and ethyl acetate (15 mL). The phases were separated and the water phase was extracted with ethyl acetate (3 x 8 mL). The combined organic phases were washed with H₂O/brine (1:1) (15 mL) and dried over Na₂SO₄. The solvent was removed under reduced pressure and the crude product was purified by automated flash column chromatography (PE/EtOAc, 0-20% EtOAc). If necessary, the product was further purified by another automated flash column chromatography (DCM/MeOH, 1% MeOH), yielding the corresponding product.

If specified in the table, the corresponding decarboxylated side-product was isolated along the desired coupling product in the purification process or was quantified in a separate reaction batch by GC-FID analysis directly after the reaction with *n*-decane as internal standard.

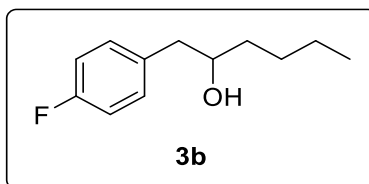
1-Phenylhexan-2-ol (3a)^[23]



¹H-NMR (300 MHz, CDCl₃, δ_H): 7.36 – 7.20 (m, 5H), 3.86 – 3.77 (m, 1H), 2.84 (dd, *J* = 13.5, 4.2 Hz, 1H), 2.65 (dd, *J* = 13.5, 8.4 Hz, 1H), 1.67-1.27 (m, 7H), 0.92 (t, *J* = 7.1 Hz, 2H).

¹³C-NMR (75 MHz, CDCl₃, δ_C): 138.8 (C_q), 129.5 (+), 128.7 (+), 126.5 (+), 72.8 (+), 44.2 (–), 36.7 (–), 28.1 (–), 22.9 (–), 14.2 (+).

Yield: 63% (colorless liquid)

1-(4-Fluorophenyl)hexan-2-ol (3b)

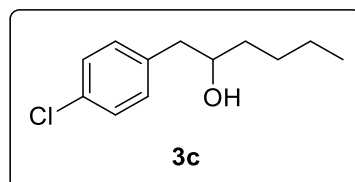
$^1\text{H-NMR}$ (300 MHz, CDCl_3 , δ_{H}): 7.20 – 7.13 (m, 2H), 7.03 – 6.95 (m, 2H), 3.80 – 3.72 (m, 2H), 2.78 (dd, $J = 13.7, 4.3$ Hz, 1H), 2.61 (dd, $J = 13.7, 8.2$ Hz, 1H), 1.66 (s, 1H), 1.53–1.28 (m, 6H), 0.91 (t, $J = 7.1$ Hz, 3H).

$^{13}\text{C-NMR}$ (75 MHz, CDCl_3 , δ_{C}): 161.7 (d, $^1J_{\text{CF}} = 244.2$ Hz, C_q), 134.5 (d, $^4J_{\text{CF}} = 3.3$ Hz, C_q), 130.9 (d, $^3J_{\text{CF}} = 7.8$ Hz, +), 115.3 (d, $^2J_{\text{CF}} = 21.1$ Hz, +), 72.8 (d, $J_{\text{CF}} = 0.9$ Hz, +), 43.2 (–), 36.6 (–), 28.0 (–), 22.8 (–), 14.2 (+).

$^{19}\text{F-NMR}$ (282 MHz, CDCl_3 , δ_{F}): -117.40 (s).

HRMS (EI) (m/z): $[\text{M}^+]$ ($\text{C}_{12}\text{H}_{17}\text{FO}^+$) calc. 196.12579; observed 196.12558.

Yield: 62% (colorless, highly viscous oil)

1-(4-Chlorophenyl)hexan-2-ol (3c)

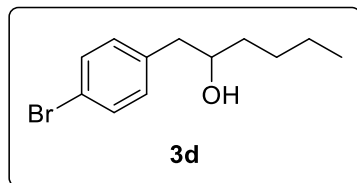
$^1\text{H-NMR}$ (300 MHz, CDCl_3 , δ_{H}): 7.30 – 7.25 (m, 2H), 7.18 – 7.11 (m, 2H), 3.82–3.73 (m, 1H), 2.79 (dd, $J = 13.7, 4.3$ Hz, 1H), 2.62 (dd, $J = 13.6, 8.3$ Hz, 1H), 1.54 (s, 1H), 1.51 – 1.27 (m, 6H), 0.91 (t, $J = 7.1$ Hz, 3H).

$^{13}\text{C-NMR}$ (75 MHz, CDCl_3 , δ_{C}): 137.3 (C_q), 132.3 (C_q), 130.9 (+), 128.7 (+), 72.7 (+), 43.4 (–), 36.7 (–), 28.0 (–), 22.8 (–), 14.2 (+).

HRMS (APCI) (m/z): $[\text{MNH}_4^+]$ ($\text{C}_{12}\text{H}_{21}\text{ClNO}^+$) calc.: 230.1306, found: 230.1325.

Yield: 53% (white solid)

1-(4-Bromophenyl)hexan-2-ol (**3d**)



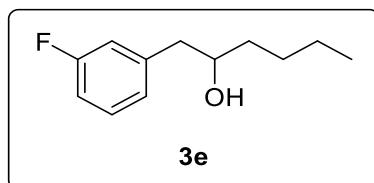
$^1\text{H-NMR}$ (300 MHz, CDCl_3 , δ_{H}): 7.46 – 7.40 (m, 2H), 7.12 – 7.07 (m, 2H), 3.82 – 3.74 (m, 1H), 2.77 (dd, $J = 13.6, 4.3$ Hz, 1H), 2.61 (dd, $J = 13.7, 8.3$ Hz, 1H), 1.56 – 1.27 (m, 7H), 0.91 (t, $J = 7.1$ Hz, 2H).

$^{13}\text{C-NMR}$ (75 MHz, CDCl_3 , δ_{C}): 137.8 (C_q), 131.7 (+), 131.3 (+), 120.4 (C_q), 72.7 (+), 43.5 (–), 36.7 (–), 28.0 (–), 22.8 (–), 14.2 (+).

HRMS (APCI) (m/z): $[\text{MNH}_4^+]$ ($\text{C}_{12}\text{H}_{21}\text{ClNO}^+$) calc.: 274.0801, found: 274.0805.

Yield: 32% (white solid)

1-(3-Fluorophenyl)hexan-2-ol (**3e**)



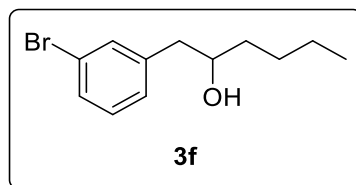
$^1\text{H-NMR}$ (300 MHz, CDCl_3 , δ_{H}): 7.31 – 7.23 (m, 2H), 7.02 – 6.89 (m, 3H), 3.86 – 3.77 (m, 1H), 2.82 (dd, $J = 13.6, 4.2$ Hz, 1H), 2.65 (dd, $J = 13.6, 8.3$ Hz, 1H), 1.58 – 1.30 (m, 7H), 0.91 (t, $J = 7.1$ Hz, 3H).

$^{13}\text{C-NMR}$ (75 MHz, CDCl_3 , δ_{C}): 163.0 (d, $^1J_{\text{CF}} = 245.8$ Hz, C_q), 141.5 (d, $^3J_{\text{CF}} = 7.3$ Hz, C_q), 130.0 (d, $^3J_{\text{CF}} = 8.4$ Hz, +), 125.2 (d, $^4J_{\text{CF}} = 2.7$ Hz, +), 116.4 (d, $^2J_{\text{CF}} = 20.9$ Hz, +), 113.4 (d, $^2J_{\text{CF}} = 21.0$ Hz, +), 72.6 (+), 43.9 (–), 36.7 (–), 28.0 (–), 22.8 (–), 14.2 (+).

$^{19}\text{F-NMR}$ (282 MHz, CDCl_3 , δ_{F}): -113.93 (s).

HRMS (APCI) (m/z): $[\text{MNH}_4^+]$ ($\text{C}_{12}\text{H}_{21}\text{FNO}^+$) calc.: 214.1602, found: 214.1599.

Yield: 17% (colorless liquid)

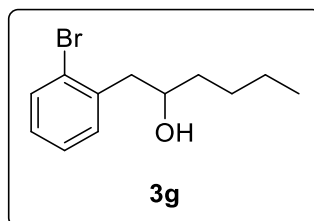
1-(3-Bromophenyl)hexan-2-ol (3f)

$^1\text{H-NMR}$ (400 MHz, CDCl_3 , δ_{H}): 7.40 – 7.34 (m, 2H), 7.20 – 7.13 (m, 2H), 3.84 – 3.77 (m, 1H), 2.79 (dd, $J = 13.7, 4.1$ Hz, 1H), 2.62 (dd, $J = 13.7, 8.4$ Hz, 1H), 1.53 – 1.31 (m, 7H), 0.92 (t, $J = 7.1$ Hz, 3H).

$^{13}\text{C-NMR}$ (101 MHz, CDCl_3 , δ_{C}): 141.3 (C_q), 132.5 (+), 130.2 (+), 129.7 (+), 128.2 (+), 122.7 (C_q), 72.6 (+), 43.8 (–), 36.8 (–), 28.0 (–), 22.8 (–), 14.2 (+).

HRMS (APCI) (m/z): $[\text{MNH}_4^+]$ ($\text{C}_{12}\text{H}_{21}\text{BrNO}^+$) calc.: 274.0801, found: 274.0804.

Yield: 16% (colorless, highly viscous oil)

1-(2-Bromophenyl)hexan-2-ol (3g)

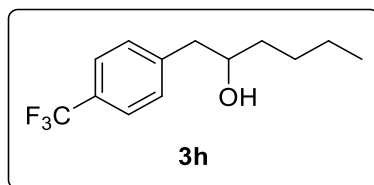
$^1\text{H-NMR}$ (300 MHz, CDCl_3 , δ_{H}): 7.58 – 7.53 (m, 1H), 7.29 – 7.22 (m, 2H), 7.14 – 7.05 (m, 1H), 3.97 – 3.87 (m, 1H), 3.03 (dd, $J = 13.6, 3.9$ Hz, 1H), 2.74 (dd, $J = 13.6, 8.7$ Hz, 1H), 1.61 – 1.30 (m, 7H), 0.92 (t, $J = 7.1$ Hz, 2H).

$^{13}\text{C-NMR}$ (75 MHz, CDCl_3 , δ_{C}): 138.5 (C_q), 133.1 (+), 131.9 (+), 128.3 (+), 127.5 (+), 125.0 (C_q), 71.3 (+), 44.2 (–), 37.0 (–), 28.0 (–), 22.9 (–), 14.2 (+).

HRMS (EI) (m/z): $[\text{M}^+]$ ($\text{C}_{12}\text{H}_{17}\text{BrO}^+$) calc.: 256.04573, found: 256.04613.

Yield: 43% (colorless, highly viscous oil)

1-(4-(Trifluoromethyl)phenyl)hexan-2-ol (3h)



¹H-NMR (300 MHz, CDCl₃, δ_H): 7.56 (d, *J* = 8.0 Hz, 2H), 7.34 (d, *J* = 8.0 Hz, 2H), 3.89 – 3.79 (m, 1H), 2.87 (dd, *J* = 13.6, 4.2 Hz, 1H), 2.72 (dd, *J* = 13.6, 8.3 Hz, 1H), 1.55 – 1.30 (m, 7H), 0.92 (t, *J* = 7.2 Hz, 3H).

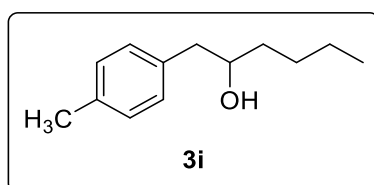
¹³C-NMR (75 MHz, CDCl₃, δ_C): 143.1 (d, ⁵*J*_{CF} = 1.5 Hz, C_q), 129.9 (+), 128.8 (d, ²*J*_{CF} = 32.2 Hz, C_q), 125.5 (q, ³*J*_{CF} = 3.7 Hz, +), 124.4 (d, ¹*J*_{CF} = 272.0 Hz, C_q), 72.6 (+), 43.9 (–), 36.9 (–), 28.0 (–), 22.8 (–), 14.2 (+).

¹⁹F-NMR (282 MHz, CDCl₃, δ_F): -62.9 (s).

HRMS (APCI) (*m/z*): [MNH₄⁺] (C₁₃H₂₁F₃NO⁺) calc.: 264.1570, found: 264.1575.

Yield: 37% (white solid)

1-(*p*-Tolyl)hexan-2-ol (3i)

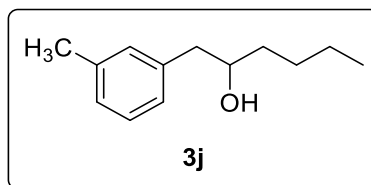


¹H-NMR (300 MHz, CDCl₃, δ_H): 7.16 – 7.09 (m, 4 H), 3.83 – 3.75 (m, 1H), 2.81 (dd, *J* = 13.6, 4.2 Hz, 1H), 2.60 (dd, *J* = 13.6, 8.4 Hz, 1H), 2.34 (s, 3H), 1.59 – 1.30 (m, 7H), 0.92 (t, *J* = 7.1 Hz, 3H).

¹³C-NMR (75 MHz, CDCl₃, δ_C): 136.1 (C_q), 135.6 (C_q), 129.4 (+), 129.4 (+), 72.8 (+), 43.7 (–), 36.6 (–), 28.1 (–), 22.9 (–), 21.2 (+), 14.2 (+).

HRMS (EI) (*m/z*): [M⁺] (C₁₃H₂₀O⁺) calc.: 192.15087, found: 192.15122.

Yield: 60% (colorless liquid)

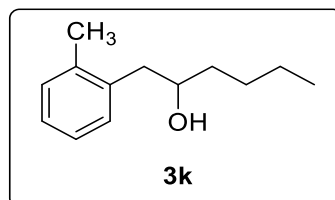
1-(*m*-Tolyl)hexan-2-ol (3j)

¹H-NMR (300 MHz, CDCl₃, δ_H): 7.25 – 7.18 (m, 1H), 7.08 – 7.00 (m, 3H), 3.85 – 3.76 (m, 1H), 2.81 (dd, *J* = 13.5, 4.1 Hz, 1H), 2.60 (dd, *J* = 13.5, 8.5 Hz, 1H), 2.35 (s, 3H), 1.59 (s, 1H), 1.55 – 1.30 (m, 6H), 0.93 (t, *J* = 7.1 Hz, 2H).

¹³C-NMR (75 MHz, CDCl₃, δ_C): 138.7 (C_q), 138.3 (C_q), 130.3 (+), 128.6 (+), 127.3 (+), 126.5 (+), 72.8 (+), 44.1 (–), 36.7 (–), 28.1 (–), 22.9 (–), 21.5 (+), 14.2 (+).

HRMS (EI) (*m/z*): [*M*⁺] (C₁₃H₂₀O⁺) calc.: 192.15087, found: 192.15049.

Yield: 68% (colorless liquid)

1-(*o*-Tolyl)hexan-2-ol (3k)

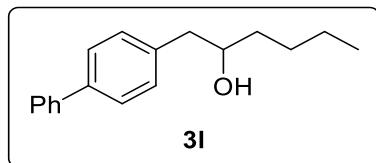
¹H-NMR (300 MHz, CDCl₃, δ_H): 7.20 – 7.13 (m, 4H), 3.85–3.77 (m, 1H), 2.86 (dd, *J* = 13.7, 4.2 Hz, 1H), 2.67 (dd, *J* = 13.7, 8.8 Hz, 1H), 2.35 (s, 3H), 1.64 (s, 1H), 1.59 – 1.32 (m, 6H), 0.94 (t, *J* = 7.1 Hz, 3H).

¹³C-NMR (75 MHz, CDCl₃, δ_C): 137.1 (C_q), 136.7 (C_q), 130.6 (+), 130.3 (+), 126.6 (+), 126.1 (+), 71.8 (+), 41.4 (–), 37.0 (–), 28.1 (–), 22.9 (–), 19.8 (+), 14.2 (+).

HRMS (EI) (*m/z*): [*M*⁺] (C₁₃H₂₀O⁺) calc.: 192.15087, found: 192.15057.

Yield: 54% (colorless liquid)

1-([1,1'-Biphenyl]-4-yl)hexan-2-ol (3l)^[24]



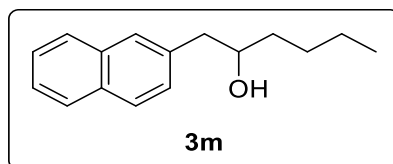
¹H-NMR (300 MHz, CDCl₃, δ_H): 7.63 – 7.55 (m, 4H), 7.49 – 7.43 (m, 2H), 7.39 – 7.29 (m, 3H), 3.91 – 3.83 (m, 1H), 2.90 (dd, *J* = 13.6, 4.2 Hz, 1H), 2.71 (dd, *J* = 13.6, 8.4 Hz, 1H), 1.68 (s, 1H), 1.61 – 1.35 (m, 6H), 0.96 (t, *J* = 7.1 Hz, 3H).

¹³C-NMR (75 MHz, CDCl₃, δ_C): 141.0 (C_q), 139.4 (C_q), 137.9 (C_q), 130.0 (+), 128.9 (+), 127.3 (+), 127.2 (+), 127.1 (+), 72.8 (+), 43.8 (–), 36.7 (–), 28.1 (–), 22.9 (–), 14.2 (+).

HRMS (EI) (*m/z*): [*M*⁺] (C₁₃H₂₀O⁺) calc.: 254.16652, found: 254.16588.

Yield: 58% (white solid)

1-(Naphthalen-2-yl)hexan-2-ol (3m)

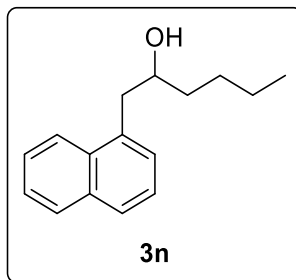


¹H-NMR (300 MHz, CDCl₃, δ_H): 7.87 – 7.78 (m, 3H), 7.68 (s, 1H), 7.52 – 7.42 (m, 2H), 7.37 (dd, *J* = 8.4, 1.7 Hz, 1H), 3.96 – 3.87 (m, 1H), 3.01 (dd, *J* = 13.5, 4.2 Hz, 1H), 2.82 (dd, *J* = 13.5, 8.4 Hz, 1H), 1.65 – 1.29 (m, 7H), 0.94 (t, *J* = 7.1 Hz, 3H).

¹³C-NMR (75 MHz, CDCl₃, δ_C): 136.3 (C_q), 133.7 (C_q), 132.4 (C_q), 128.3 (+), 128.0 (+), 127.9 (+), 127.8 (+), 127.6 (+), 126.2 (+), 125.6 (+), 72.7 (+), 44.3 (–), 36.7 (–), 28.1 (–), 22.9 (–), 14.3 (+).

HRMS (EI) (*m/z*): [*M*⁺] (C₁₆H₂₀O⁺) calc.: 228.15087, found: 228.15084.

Yield: 33% (colorless liquid)

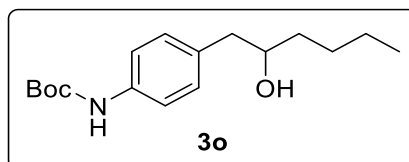
1-(Naphthalen-1-yl)hexan-2-ol (3n)

$^1\text{H-NMR}$ (300 MHz, CDCl_3 , δ_{H}): 8.07 – 8.03 (m, 1H), 7.90 – 7.87 (m, 1H), 7.79 – 7.75 (m, 1H), 7.57 – 7.36 (m, 4H), 4.03 – 3.93 (m, 1H), 3.37 (dd, $J = 13.8, 3.9$ Hz, 1H), 3.05 (dd, $J = 13.8, 8.7$ Hz, 1H), 1.69 – 1.31 (m, 7H), 0.95 (t, $J = 7.1$ Hz, 3H).

$^{13}\text{C-NMR}$ (75 MHz, CDCl_3 , δ_{C}): 134.9 (C_q), 134.1 (C_q), 132.3 (C_q), 129.0 (+), 127.8 (+), 127.5 (+), 126.1 (+), 125.8 (+), 125.6 (+), 124.0 (+), 72.1 (+), 41.4 (–), 37.1 (–), 28.1 (–), 22.9 (–), 14.3 (+).

HRMS (EI) (m/z): $[\text{M}^+]$ ($\text{C}_{16}\text{H}_{20}\text{O}^+$) calc.: 228.15087, found: 228.15109.

Yield: 56% (colorless liquid)

***tert*-Butyl (4-(2-hydroxyhexyl)phenyl)carbamate (3o)**

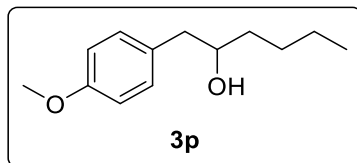
$^1\text{H-NMR}$ (300 MHz, CDCl_3 , δ_{H}): 7.27 – 7.21 (m, 2H), 7.10 – 7.05 (m, 2H), 6.53 (s, 1H), 3.75 – 3.66 (m, 1H), 2.72 (dd, $J = 13.6, 4.3$ Hz, 1H), 2.53 (dd, $J = 13.6, 8.3$ Hz, 1H), 1.59 (s, 1H), 1.46 (s, 9H), 1.45 – 1.20 (m, 6H), 0.85 (t, $J = 7.1$ Hz, 3H).

$^{13}\text{C-NMR}$ (75 MHz, CDCl_3 , δ_{C}): 153.0 (C_q), 136.9 (C_q), 133.3 (C_q), 130.0 (+), 119.0 (+), 80.6 (C_q), 72.8 (+), 43.4 (–), 36.5 (–), 28.5 (+), 28.1 (–), 22.8 (–), 14.2 (+).

HRMS (ESI) (m/z): $[\text{MNH}_4^+]$ ($\text{C}_{17}\text{H}_{31}\text{N}_2\text{O}_3^+$) calc.: 311.2329, found: 311.2331.

Yield: 48% (white solid)

1-(4-Methoxyphenyl)hexan-2-ol (3p)



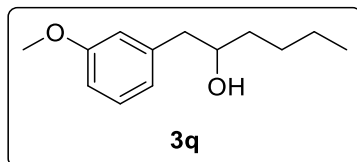
$^1\text{H-NMR}$ (300 MHz, CDCl_3 , δ_{H}): 7.16 – 7.10 (m, 2H), 6.88 – 6.83 (m, 2H), 3.82 – 3.71 (m, 4H), 2.78 (dd, $J = 13.7, 4.2$ Hz, 1H), 2.58 (dd, $J = 13.7, 8.4$ Hz, 1H), 1.58 (s, 1H), 1.52 – 1.43 (m, 3H), 1.41 – 1.28 (m, 3H), 0.91 (t, $J = 7.1$ Hz, 3H).

$^{13}\text{C-NMR}$ (75 MHz, CDCl_3 , δ_{C}): 158.4 (C_q), 130.7 (C_q), 130.5 (+), 114.1 (+), 72.9 (+), 55.4 (+), 43.2 (–), 36.6 (–), 28.1 (–), 22.9 (–), 14.2 (+).

HRMS (APCI) (m/z): $[\text{MNH}_4^+]$ ($\text{C}_{13}\text{H}_{24}\text{NO}_2^+$) calc.: 266.1802, found: 266.1804.

Yield: 13% (colorless liquid)

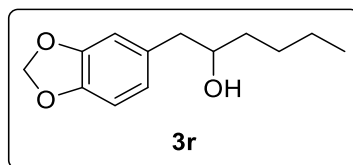
1-(3-Methoxyphenyl)hexan-2-ol (3q)^[25]



$^1\text{H-NMR}$ (300 MHz, CDCl_3 , δ_{H}): 7.26 – 7.19 (m, 1H), 6.83 – 6.75 (m, 3H), 3.87 – 3.73 (m, 4H), 2.81 (dd, $J = 13.5, 4.2$ Hz, 1H), 2.62 (dd, $J = 13.5, 8.4$ Hz, 1H), 1.69 (d, $J = 3.5$ Hz, 1H), 1.55 – 1.30 (m, 6H), 0.92 (t, $J = 7.1$ Hz, 3H).

$^{13}\text{C-NMR}$ (75 MHz, CDCl_3 , δ_{C}): 159.8 (C_q), 140.4 (C_q), 129.6 (+), 121.8 (+), 115.2 (+), 111.8 (+), 72.7 (+), 55.2 (+), 44.2 (–), 36.6 (–), 28.0 (–), 22.8 (–), 14.2 (+).

Yield: 63% (colorless liquid)

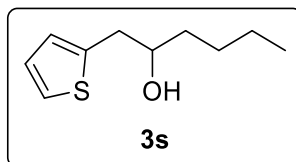
1-(Benzo[d][1,3]dioxol-5-yl)hexan-2-ol (3r)

$^1\text{H-NMR}$ (300 MHz, CDCl_3 , δ_{H}): 6.77 – 6.63 (m, 3H), 5.93 (s, 2H), 3.79 – 3.69 (m, 1H), 2.74 (dd, $J = 13.7, 4.2$ Hz, 1H), 2.54 (dd, $J = 13.7, 8.4$ Hz, 1H), 1.57 (s, 1H), 1.51 – 1.29 (m, 6H), 0.91 (t, $J = 7.1$ Hz, 3H).

$^{13}\text{C-NMR}$ (75 MHz, CDCl_3 , δ_{C}): 147.9 (C_q), 146.3 (C_q), 132.5 (C_q), 122.4 (+), 109.8 (+), 108.4 (+), 101.0 (–), 72.8 (+), 43.8 (–), 36.6 (–), 28.1 (–), 22.9 (–), 14.2 (+).

HRMS (EI) (m/z): [M^+] ($\text{C}_{13}\text{H}_{18}\text{O}_3^+$) calc.: 222.12505, found: 222.12541.

Yield: 35% (colorless liquid)

1-(Thiophen-2-yl)hexan-2-ol (3s)

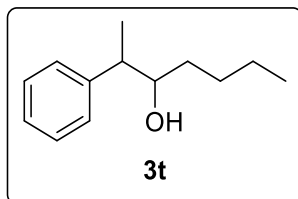
$^1\text{H-NMR}$ (300 MHz, CDCl_3 , δ_{H}): 7.18 (dd, $J = 5.1, 1.2$ Hz, 1H), 6.99 – 6.93 (m, 1H), 6.88 – 6.85 (m, 1H), 3.84 – 3.76 (m, 1H), 3.04 (ddd, $J = 14.7, 4.0, 0.8$ Hz, 1H), 2.88 (dd, $J = 14.8, 8.0$ Hz, 1H), 1.76 (s, 1H), 1.57 – 1.29 (m, 6H), 0.92 (t, $J = 7.1$ Hz, 3H).

$^{13}\text{C-NMR}$ (75 MHz, CDCl_3 , δ_{C}): 140.8 (C_q), 127.1 (+), 126.1 (+), 124.3 (+), 72.5 (+), 38.1 (–), 36.4 (–), 28.0 (–), 22.8 (–), 14.2 (+).

HRMS (EI) (m/z): [M^+] ($\text{C}_{10}\text{H}_{16}\text{OS}^+$) calc.: 184.09164, found: 184.09188.

Yield: 61% (colorless liquid)

2-Phenylheptan-3-ol (*syn/anti* diastereomeric mixture) (3t)^[26]

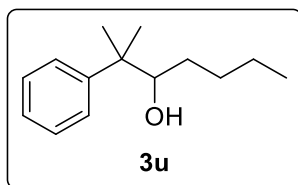


¹H-NMR (diastereomeric mixture) (300 MHz, CDCl₃, δ_H): 7.36 – 7.19 (m, 5H), 3.70 – 3.62 (m, 1H), 2.83 – 2.71 (m, 1H), 1.59 – 1.24 (m, 10H), 0.95 – 0.84 (m, 3H).

¹³C-NMR (diastereomeric mixture) (75 MHz, CDCl₃, δ_C): 144.8 (C_q), 143.7 (C_q), 128.7 (+), 128.6 (+), 128.3 (+), 127.9 (+), 126.8 (+), 126.5 (+), 76.3 (+), 76.2 (+), 46.2 (+), 45.7 (+), 34.5 (–), 34.3 (–), 28.4 (–), 28.0 (–), 22.9 (–), 22.8 (–), 18.1 (+), 15.5 (+), 14.3 (+), 14.2 (+).

Yield: 62% (colorless liquid)

2-Methyl-2-phenylheptan-3-ol (3u)

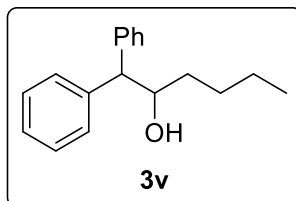


¹H-NMR (300 MHz, CDCl₃, δ_H): 7.41 – 7.30 (m, 4H), 7.25 – 7.19 (m, 1H), 3.63 – 3.57 (m, 1H), 1.51 – 1.18 (m, 13H), 0.87 (t, *J* = 7.0 Hz, 3H).

¹³C-NMR (75 MHz, CDCl₃, δ_C): 147.4 (C_q), 128.4 (+), 126.6 (+), 126. (+), 79.8 (+), 42.8 (C_q), 31.3 (–), 29.4 (–), 24.4 (+), 23.7 (+), 22.8 (–), 14.2 (+).

HRMS (APCI) (*m/z*): [MH⁺–H₂O] (C₁₄H₂₁⁺) calc.: 189.1638, found: 189.1642.

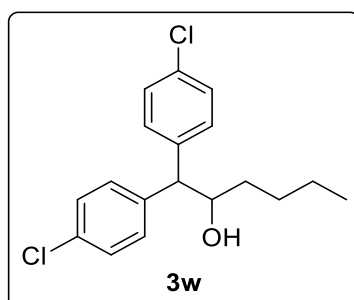
Yield: 57% (colorless liquid)

1,1-diphenylhexan-2-ol (3v)^[24]

¹H-NMR (400 MHz, CDCl₃, δ_H): 7.41 – 7.17 (m, 10H), 4.38 – 4.32 (m, 1H), 3.90 (d, *J* = 8.3 Hz, 1H), 1.58 (s, 1H), 1.54 – 1.22 (m, 6H), 0.87 (t, *J* = 7.2 Hz, 3H).

¹³C-NMR (101 MHz, CDCl₃, δ_C): 142.7 (C_q), 141.7 (C_q), 129.0 (+), 128.9 (+), 128.7 (+), 128.4 (+), 127.0 (+), 126.6 (+), 73.9 (+), 58.9 (+), 34.9 (–), 28.2 (–), 22.8 (–), 14.2 (+).

Yield: 51% (colorless liquid)

1,1-Bis(4-chlorophenyl)hexan-2-ol (3w)

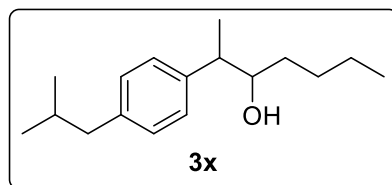
¹H-NMR (300 MHz, CDCl₃): δ 7.30 – 7.18 (m, 8H), 4.29 – 4.22 (m, 1H), 3.86 (d, *J* = 7.5 Hz, 1H), 1.53 (s, 1H), 1.49 – 1.22 (m, 6H), 0.87 (t, *J* = 7.2 Hz, 3H).

¹³C-NMR (75 MHz, CDCl₃): δ 140.8 (C_q), 139.6 (C_q), 132.9 (C_q), 132.6 (C_q), 130.4 (+), 129.7 (+), 129.0 (+), 129.0 (+), 73.7 (+), 57.1 (+), 35.1 (–), 28.1 (–), 22.7 (–), 14.2 (+).

HRMS (APCI) (*m/z*): [MNH₄⁺] (C₁₈H₂₄OCl₂N) calc.: 340.1229, found: 340.1230.

Yield: 33% (colorless liquid)

2-(4-isobutylphenyl)heptan-3-ol (**3x**)



¹H-NMR (300 MHz, CDCl₃, δ_H): 7.14 – 7.06 (m, 4H), 3.69 – 3.61 (m, 1H), 2.81 – 2.72 (m, 1H), 2.45 (d, *J* = 7.2 Hz, 2H), 1.85 (hept, *J* = 6.8 Hz, 1H), 1.46 – 1.36 (m, 3H), 1.32 – 1.24 (m, 6H), 0.92 – 0.86 (m, 9H).

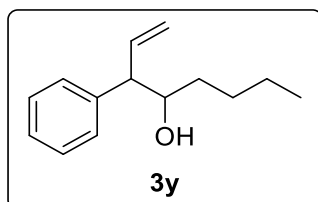
¹³C-NMR (75 MHz, CDCl₃, δ_C): 141.9 (C_q), 139.8 (C_q), 129.3 (+), 127.6 (+), 76.4 (+), 45.2 (+), 45.2

(–), 34.4 (–), 30.4 (+), 28.4 (–), 22.8 (–), 22.6 (+), 15.2 (+), 14.2 (+).

HRMS (APCI) (*m/z*): [MH⁺ - H₂O] (C₁₇H₂₇⁺) calc.: 231.2107, found: 231.2119.

Yield: 27% (colorless oil)

3-Phenyloct-1-en-4-ol (*syn/anti* diastereomeric mixture) (**3y**)^[27]



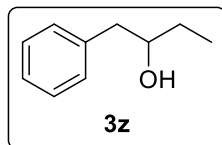
Starting materials: (*E*)-4-phenylbut-3-enoic acid (*trans*-styrylacetic acid) and *n*-pentanal (**2a**).

¹H-NMR (300 MHz, CDCl₃, δ_H): 7.38 – 7.18 (m, 5H), 6.19 – 6.00 (m, 1H), 5.26 – 5.09 (m, 2H), 3.90 – 3.75 (m, 1H), 3.35 – 3.22 (m, 1H), 1.85 – 1.81 [1.66 – 1.63] (m, 1H), 1.53 – 1.21 (m, 6H), 0.94 – 0.82 (m, 3H).

¹³C-NMR (75 MHz, CDCl₃, δ_C): 141.8 (C_q), 141.1 (C_q), 138.8 (+), 138.5 (+), 128.9 (+), 128.8 (+), 128.6 (+), 128.1 (+), 127.0 (+), 126.7 (+), 118.0 (–), 116.8 (–), 74.4 (+), 74.1 (+), 57.5 (+), 57.5 (+), 34.3 (–), 34.2 (–), 28.1 (–), 28.0 (–), 22.9 (–), 22.8 (–), 14.2 (+), 14.2 (+).

HRMS (APCI) (*m/z*): [MNH₄⁺] (C₁₄H₂₄ON⁺) calc.: 222.1853, found: 222.1852.

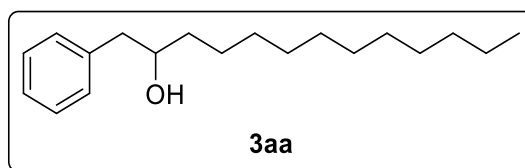
Yield: 35% (colorless liquid)

1-Phenylbutan-2-ol (3z)^[28]

¹H-NMR (400 MHz, CDCl₃, δ_H): 7.35 – 7.29 (m, 2H), 7.26 – 7.20 (m, 3H), 3.79 – 3.72 (m, 1H), 2.84 (dd, *J* = 13.6, 4.3 Hz, 1H), 2.65 (dd, *J* = 13.6, 8.4 Hz, 1H), 1.62 – 1.49 (m, 3H), 1.00 (t, *J* = 7.4 Hz, 3H).

¹³C-NMR (101 MHz, CDCl₃, δ_C): 138.8 (C_q), 129.6 (+), 128.7 (+), 126.6 (+), 74.2 (+), 43.7 (–), 29.7 (–), 10.2 (+).

Yield: 41% (colorless liquid)

1-Phenyltridecan-2-ol (3aa)

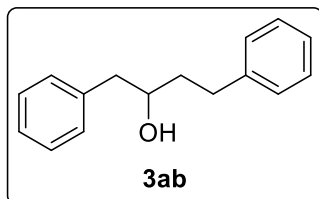
¹H-NMR (400 MHz, CDCl₃, δ_H) 7.35 – 7.29 (m, 2H), 7.26 – 7.21 (m, 3H), 3.85 – 3.78 (m, 1H), 2.84 (dd, *J* = 13.5, 4.3 Hz, 1H), 2.65 (dd, *J* = 13.5, 8.4 Hz, 1H), 1.75 – 1.61 (m, 1H), 1.54 – 1.49 (m, 2H), 1.34 – 1.26 (m, 18H), 0.90 (t, *J* = 6.8 Hz, 3H).

¹³C-NMR (101 MHz, CDCl₃, δ_C) 138.8 (C_q), 129.5 (+), 128.6 (+), 126.5 (+), 72.8 (+), 44.2 (–), 37.0 (–), 32.1 (–), 29.8 (–), 29.8 (–), 29.8 (–), 29.5 (–), 25.9 (–), 22.8 (–), 14.3 (+).

HRMS (APCI) (*m/z*): [MNH₄⁺] (C₁₉H₃₆NO⁺) calc.: 294.2791, found: 294.2794.

Yield: 73% (brown solid)

1,4-Diphenylbutan-2-ol (3ab)^[29]

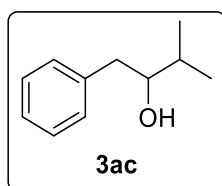


¹H-NMR (300 MHz, CDCl₃, δ_H) 7.38 – 7.21 (m, 10H), 3.91 – 3.82 (m, 1H), 2.94 – 2.83 (m, 2H), 2.80 – 2.67 (m, 2H), 1.92 – 1.82 (m, 2H), 1.66 (s, 1H).

¹³C-NMR (75 MHz, CDCl₃, δ_C) 142.1 (C_q), 138.5 (C_q), 129.6 (+), 128.7 (+), 128.6 (+), 128.5 (+), 126.6 (+), 125.9 (+), 72.0 (+), 44.2 (–), 38.5 (–), 32.2 (–).

Yield: 72% (yellow solid)

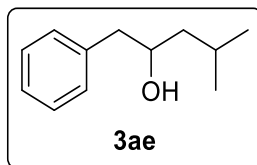
3-Methyl-1-phenylbutan-2-ol (3ac)^[28a, 30]



¹H-NMR (400 MHz, CDCl₃, δ_H): 7.35 – 7.29 (m, 2H), 7.26 – 7.21 (m, 3H), 3.63 – 3.56 (m, 1H), 2.86 (dd, *J* = 13.6, 3.5 Hz, 1H), 2.61 (dd, *J* = 13.6, 9.4 Hz, 1H), 1.81 – 1.72 (m, 1H), 1.46 (s, 1H), 1.01 (d, *J* = 6.8 Hz, 6H).

¹³C-NMR (101 MHz, CDCl₃, δ_C): 139.3 (C_q), 129.5 (+), 128.7 (+), 126.5(+), 77.6 (+), 40.9 (–), 33.3 (+), 19.1 (+), 17.6 (+).

Yield: 25% (colorless liquid)

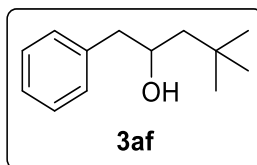
4-Methyl-1-phenylpentan-2-ol (3ae)^[31]

¹H-NMR (400 MHz, CDCl₃, δ_H): 7.35 – 7.30 (m, 2H), 7.26 – 7.21 (m, 3H), 3.90 (hept, *J* = 4.1 Hz, 1H), 2.82 (dd, *J* = 13.6, 4.1 Hz, 1H), 2.64 (dd, *J* = 13.5, 8.4 Hz, 1H), 1.89 – 1.79 (m, 1H), 1.57 (s, 1H), 1.51 – 1.44 (m, 1H), 1.35 – 1.28 (m, 1H), 0.94 (dd, *J* = 12.3, 6.6 Hz, 6H).

¹³C-NMR (101 MHz, CDCl₃, δ_C): 138.8 (C_q), 129.6 (+), 128.7 (+), 126.6 (+), 70.8 (+), 46.2 (–), 44.7 (–), 24.8 (+), 23.6 (+), 22.2 (+).

HRMS (APCI) (*m/z*): [MNH₄⁺] (C₁₂H₂₂NO⁺) calc.: 196.1696, found: 196.1695.

Yield: 56% (colorless liquid)

4,4-Dimethyl-1-phenylpentan-2-ol (3af)^[32]

¹H-NMR (300 MHz, CDCl₃, δ_H) 7.36 – 7.29 (m, 2H), 7.27 – 7.20 (m, 3H), 4.01 – 3.92 (m, 1H), 2.78 (dd, *J* = 13.4, 4.5 Hz, 1H), 2.67 (dd, *J* = 13.4, 8.4 Hz, 1H), 1.50 – 1.43 (m, 3H), 0.97 (s, 9H).

¹³C-NMR (75 MHz, CDCl₃, δ_C) 138.8 (C_q), 129.6 (+), 128.7 (+), 126.6 (+), 70.5 (+), 50.5 (–), 46.2 (–), 30.5 (C_q), 30.3 (+).

HRMS (APCI) (*m/z*): [MNH₄⁺] (C₁₃H₂₄NO⁺) calc.: 210.1852, found: 210.1850.

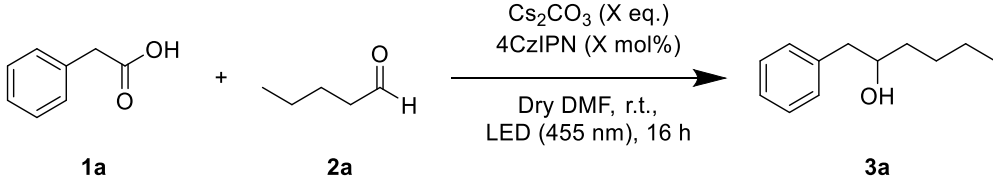
Yield: 41% (colorless liquid)

4.4.4 Detailed reaction optimization process

General procedure for the reaction optimization process (General Procedure B)

A 5 mL crimp cap vial equipped with a magnetic stirring bar was loaded with photocatalyst, base, phenylacetic acid (**1a**), *n*-pentanal (**2a**), solvent and if noted an additive in the amounts given in the corresponding tables. In doing so, all solid compounds were added before capping the vial, whereas all liquid compounds were added *via* syringe after setting the capped vial under inert conditions. The reaction mixture was degassed by four cycles of freeze-pump-thaw and subsequently stirred under light irradiation for the given time at 25 °C. Subsequently, an aliquot of the reaction mixture was submitted to GC-FID analysis to determine the product yield with *n*-decane as internal standard.

Table 4-3 – Control experiments in absence of either photocatalyst, light or base.^[a]

				
Entry	Catalyst loading [mol%]	Pentanal [eq.]	Cs ₂ CO ₃ [eq.]	Yield 3a ^[b] [%]
1	2	3	1	70
2	-	10	1	n.d.
3 ^[c]	2	10	1	n.d.
4	2	10	-	n.d.

[a] Reactions were performed with phenylacetic acid (**1a**) (150 μmol, 1 eq.) in dry DMF (2 mL). [b] Determined by GC-FID analysis with *n*-decane as internal standard. [c] Reaction performed in absence of light.

Table 4-4 – Optimization of reaction time, catalyst- and base loading.^[a]

Entry	Catalyst loading [mol%]	Cs ₂ CO ₃ [eq.]	Time [h]	Yield ^[b] 3a [%]	Yield ^[b] 4a [%]
1	2	1	6	51	9
2	2	1	16	70	15
3	2	1	24	73	16
4	5	1	6	67	13
5	5	1	16	73	15
6	5	1	24	73	17
7	5	1.5	16	39	12
8	5	0.5	16	50	5

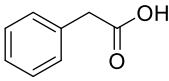
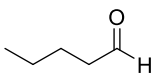
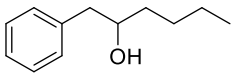
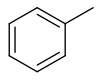
[a] Reactions were performed with phenylacetic acid (**1a**) (150 μmol, 1 eq.) and *n*-pentanal (**2a**) (450 μmol, 3 eq.) in dry DMF (2 mL). [b] Determined by GC-FID analysis with *n*-decane as internal standard.

Table 4-5 – Solvent screening.^[a]

Entry	Solvent	Yield ^[b] 3a [%]	Yield ^[b] 4a [%]
1	Dry DMF	73	15
2	Dry DMA	75	11
3	Dry DCM	n.d.	n.d.
4	Dry EtOAc	n.d.	n.d.
5	Dry MeCN	20	20
6	Dry THF	Traces	n.d.
7	DMA	75	12
8	1,4-Dioxane	Traces	n.d.
9 ^[c]	DMA	42	13

[a] Reactions were performed with phenylacetic acid (**1a**) (150 μmol, 1 eq.) and *n*-pentanal (**2a**) (450 μmol, 3 eq.) in 2 mL solvent. [b] Determined by GC-FID analysis with *n*-decane as internal standard. [c] Without prior freeze-pump-thaw degassing of reaction mixture before irradiation.

Table 4-6 – Base screening.^[a]

<div style="display: flex; align-items: center; justify-content: center;"> <div style="text-align: center;">  <p>1a</p> </div> <div style="margin: 0 10px;">+</div> <div style="text-align: center;">  <p>2a</p> </div> <div style="margin: 0 10px;">→</div> <div style="text-align: center;">  <p>3a</p> </div> <div style="margin: 0 10px;">+</div> <div style="text-align: center;">  <p>4a</p> </div> </div>			
Base (X eq.) 4CzIPN (5 mol%) DMA, r.t., LED (455 nm), 16 h			
Entry	Base (eq.)	Yield 3a ^[b] [%]	Yield 4a ^[b] [%]
1	Cs ₂ CO ₃ (1)	75	12
2	K ₂ CO ₃ (1)	68	18
3	Na ₂ CO ₃ (1)	60	23
4	CsF (1)	65	16
5	CsF (1.5)	69	16
6	KOAc (1)	72	16
7	KOAc (1.5)	72	18
8	CF ₃ COOK (1.5)	7	Traces
9	CsOAc (1)	49	11
10	CsOAc (1.5)	46	11
11	NBu ₄ OAc (1.5)	61	12
12	DBU (1.5)	Traces	n.d.
13	Lutidin (1.5)	Traces	n.d.
14	Tetramethylguanidine (1.5)	7	3
15	2,2,6,6-Tetramethyl- piperidine (1.5)	Traces	n.d.

[a] Reactions were performed with phenylacetic acid (**1a**) (150 μmol, 1 eq.) and *n*-pentanal (**2a**) (450 μmol, 3 eq.) in DMA (2 mL). [b] Determined by GC-FID analysis with *n*-decane as internal standard.

Table 4-7 – Photocatalyst screening.^[a]

Entry	Photocatalyst (Irradiation wavelength [nm], loading [mol%])	Yield ^[b] 3a [%]	Yield ^[b] 4a [%]
1	4CzIPN (455, 5)	75	12
2	4CzPN (455, 5)	55	10
3	3DPAFIPN (455, 5)	6	Traces
4	[Ir(dF-CF ₃ -ppy) ₂ (dtbpy)](PF ₆) (455, 2)	4	5
5	3,7-Di(4-biphenyl) 1-naphthalene-10-phenoxazine (400, 5)	Traces	n.d.
6	Rhodamin-6G (455, 5)	n.d.	n.d.
7	Dicyanoanthracene (400, 5)	6	Traces
8	[Acr ⁺ -Mes](ClO ₄) (455, 5)	n.d.	n.d.
9	2,4,6-Triphenylpyrylium (455, 5)	n.d.	n.d.
10	Eosin Y (535, 5)	n.d.	n.d.

[a] Reactions were performed with phenylacetic acid (**1a**) (150 μ mol, 1 eq.) and *n*-pentanal (**2a**) (450 μ mol, 3 eq.) in DMA (2 mL). [b] Determined by GC-FID analysis with *n*-decane as internal standard.

Table 4-8 – Variation of the electrophile amount.^[a]

Entry	2a (eq.)	Yield ^[b] 3a [%]	Yield ^[b] 4a [%]
1	1	50	31
2	2	67	17
3	3	75	12
4	5	78	7
5	10	79	3

[a] Reactions were performed with phenylacetic acid (**1a**) (150 μ mol, 1 eq.) in DMA (2 mL). [b] Determined by GC-FID analysis with *n*-decane as internal standard.

Table 4-9 – Additive screening.^[a]

$ \text{C}_6\text{H}_5\text{CH}_2\text{COOH} \quad (1\text{a}) + \text{CH}_3(\text{CH}_2)_3\text{CHO} \quad (2\text{a}) \xrightarrow[\text{DMA, r.t., LED (455 nm), 16 h}]{\text{Cs}_2\text{CO}_3 (1 \text{ eq.}), 4\text{CzIPN (5 mol\%)} \text{ Additive (X eq.)}} \text{C}_6\text{H}_5\text{CH}_2\text{CH(OH)CH}_2\text{CH}_2\text{CH}_3 \quad (3\text{a}) + \text{C}_6\text{H}_5\text{CH}_3 \quad (4\text{a}) $				
Entry	Additive (eq.)	Yield ^[b] 3a [%]	Yield ^[b] 4a [%]	
1	H ₂ O (3)	34	55	
2	LiBF ₄ (1)	35	18	
3	B ₂ pin ₂ (1)	n.d.	n.d.	
4	Sc(OTf) ₃ (0.5)	Traces	Traces	

[a] Reactions were performed with phenylacetic acid (**1a**) (150 μmol, 1 eq.) and *n*-pentanal (**2a**) (450 μmol, 3 eq.) in DMA (2 mL). [b] Determined by GC-FID analysis with *n*-decane as internal standard.

Table 4-10 – Repetition of control experiments with optimized conditions.^[a]

$ \text{C}_6\text{H}_5\text{CH}_2\text{COOH} \quad (1\text{a}) + \text{CH}_3(\text{CH}_2)_3\text{CHO} \quad (2\text{a}) \xrightarrow[\text{DMA, r.t., LED (455 nm), 16 h}]{\text{Cs}_2\text{CO}_3 (1 \text{ eq.}), 4\text{CzIPN (5 mol\%)}} \text{C}_6\text{H}_5\text{CH}_2\text{CH(OH)CH}_2\text{CH}_2\text{CH}_3 \quad (3\text{a}) + \text{C}_6\text{H}_5\text{CH}_3 \quad (4\text{a}) $				
Entry	Catalyst loading [mol%]	Cs ₂ CO ₃ [eq.]	Yield ^[b] 3a [%]	Yield ^[b] 4a [%]
1	5	1	75	12
2	-	1	n.d.	n.d.
3 ^[c]	5	1	n.d.	n.d.
4	5	-	n.d.	n.d.

[a] Reactions were performed with phenylacetic acid (**1a**) (150 μmol, 1 eq.) and *n*-pentanal (**2a**) (150 μmol, 3 eq.) in DMA (2 mL). [b] Determined by GC-FID analysis with *n*-decane as internal standard. [c] Reaction performed in absence of light.

4.4.5 Photocatalytic benzylation of acetone and use of potassium benzyltrifluoroborate as a carbanion precursor

Photocatalytic benzylation of acetone (**6**) with phenylacetic acid (**1a**) – GC-Yields

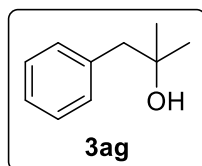
The GC-Yields of the photocatalytic benzylation of acetone (**6**) with phenylacetic acid (**1a**) were determined according to General Procedure B with acetone (**6**) instead of *n*-pentanal (**2a**)

Table 4-11 – Benzylation of acetone (**6**) with phenylacetic acid (**1a**).^[a]

Entry	Acetone equivalents	Yield ^[b] 3ag [%]	Yield ^[b] 4a [%]
1	3	4	77
2	10	13	70
3 ^[c]	Approx. 91 (1 mL)	39	49

[a] Reactions were performed with phenylacetic acid (**1a**) (150 μ mol, 1 eq.) in DMA (2 mL). [b] Determined by GC-FID analysis with *n*-decane as internal standard. [c] Acetone/DMA (1:1) (2 mL) was used as solvent.

2-Methyl-1-phenylpropan-2-ol (**3ag**)^[33]



2-Methyl-1-phenylpropan-2-ol (**3ag**) was synthesized according to General Procedure A with an acetone/DMA (1:1) (2 mL) mixture as solvent.

¹H-NMR (400 MHz, CDCl₃, δ_{H}): 7.35 – 7.19 (m, 5H), 2.77 (s, 2H), 1.23 (s, 6H).

¹³C-NMR (101 MHz, CDCl₃, δ_{C}): 137.9 (C_q), 130.6 (+), 128.3 (+), 126.6 (+), 70.9 (C_q), 49.9 (–), 29.3 (+).

Yield: 32% (colorless liquid)

Photocatalytic benzylation of *n*-pentanal (**2a**) with potassium benzyltrifluoroborate (**16**)

According to the proposed mechanism, every compound that bears a functional group in a benzylic position that can be oxidized by the excited photocatalyst leading to the formation of a benzyl radical should be a viable carbanion precursor. Hence, it was attempted to use benzyltrifluoroborate (**16**) as starting material. Furthermore, **16** does not hold a protic hydrogen and it was tested if the yield can thus be increased.

Indeed, benzylation product **3a** using *n*-pentanal (**2a**) and potassium benzyltrifluoroborate (**16**) as carbanion precursor could be isolated according to General Procedure A in absence of Cs₂CO₃ and with **16** instead of a carboxylic acid. Only a very small increase of yield in **3a** accompanied by a small decrease in toluene (**4a**) side product compared to carboxylic acids as starting material could be observed.



Scheme 4-4 – Benzylation of *n*-pentanal (**2a**) with potassium benzyltrifluoroborate (**16**) as carbanion precursor.

Photocatalytic benzylation of acetone (**6**) with potassium benzyltrifluoroborate (**16**) – GC-Yields

The GC-Yields of the photocatalytic benzylation of acetone (**6**) with potassium benzyltrifluoroborate (**16**) were determined according to General Procedure B with **16** instead of phenylacetic acid (**1a**) and acetone (**6**) instead of *n*-pentanal (**2a**) in absence of Cs₂CO₃.

Table 4-12 – Benzylation of acetone (**6**) with potassium benzyltrifluoroborate (**16**).^[a]

Entry	Acetone equivalents	Yield ^[b] 3ag [%]	Yield ^[b] 4a [%]
1	3	6	67
2	10	13	56
3 ^[c]	Approx. 91 (1 mL)	43	43

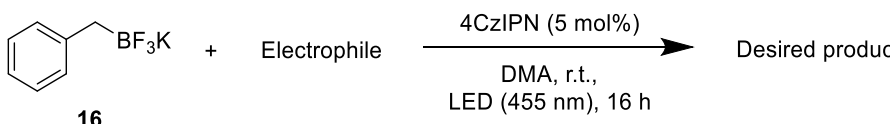
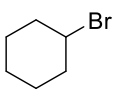
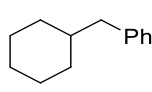
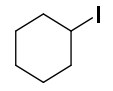
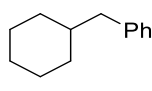
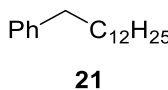
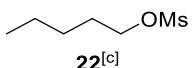
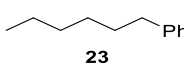
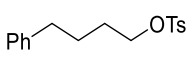
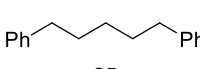
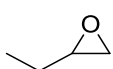
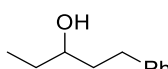
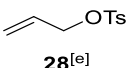
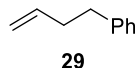
[a] Reactions were performed with potassium benzyltrifluoroborate (**16**) (150 μmol, 1 eq.) in DMA (2 mL). [b] Determined by GC-FID analysis with *n*-decane as internal standard. [c] Acetone/DMA (1:1) (2 mL) was used as solvent.

4.4.6 Attempted S_N2 reactions with potassium benzyltrifluoroborate as a carbanion precursor

Attempted S_N2 reactions with potassium benzyltrifluoroborate (**16**) as carbanion precursor were performed according to General Procedure B in absence of Cs₂CO₃, with **16** instead of phenyl acetic acid (**1a**) and with the electrophile according to Table S11 instead of *n*-pentanal (**2a**). After the given reaction time, the mixture was submitted to GC-MS analysis.

16 was used instead of **1a** to avoid an esterification reaction with the carboxylate as direct electrophile.

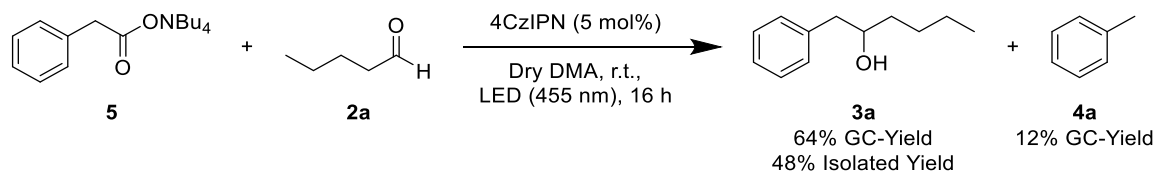
Table 4-13 – Attempted S_N2 reactions with potassium benzyltrifluoroborate (**16**) as carbanion precursor.^[a]

<div style="text-align: center;">  </div>			
Entry	Electrophile	Desired product	Product Formation ^[b]
1	 17	 18	n.d.
2	 19	 18	Traces detected
3	C ₁₂ H ₂₅ –I 20	 21	Traces detected
4	 22 ^[c]	 23	n.d.
5	 24 ^[d]	 25	n.d.
6	 26	 27	n.d.
7	 28 ^[e]	 29	Traces detected

[a] Reactions were performed with potassium benzyltrifluoroborate (**16**) (150 μmol, 1 eq.) and the corresponding electrophile (450 μmol, 3 eq.) in DMA (2 mL). [b] Determined by GC-MS analysis. [c] Starting material synthesized according to a literature procure.^[34] [d] Starting material synthesized according to a literature procure.^[35] [e] Starting material synthesized according to a literature procure.^[36]

4.4.7 Mechanistic investigations

4.4.7.1 Photocatalytic benzylation with NBu₄PA (5) as carbanion precursor



Scheme 4-5 – Benzylation of *n*-pentanal (**2a**) with NBu₄PA (**5**).

A 5 mL crimp cap vial equipped with a magnetic stirring bar was loaded with 4CzIPN (5.9 mg, 7.5 μ mol, 5 mol%) and set under inert conditions. Subsequently, a solution of tetrabutylammonium phenylacetate (**5**) in dry DMA (75 mM, 2 mL, 150 μ mol, 1 eq.) followed by *n*-pentanal (**2a**) (48 μ L, 450 μ mol, 3 eq.) were added *via* syringe. The reaction mixture was degassed by four cycles of freeze-pump-thaw and subsequently stirred under light irradiation using a 455 nm (\pm 25 nm) LED for 16 h at 25 $^{\circ}$ C.

One reaction batch was submitted to GC-FID analysis to determine the product GC-yield with *n*-decane as internal standard, while the desired product was isolated from two other batches.

For the isolation, the two combined reaction mixtures were diluted with brine (15 mL), water (5 mL) and ethyl acetate (15 mL). The phases were separated and the water phase was extracted with ethyl acetate (3 x 8 mL). The combined organic phases were washed with H₂O/brine (1:1) (15 mL) and dried over Na₂SO₄. The solvent was removed under reduced pressure and the crude product was purified by automated flash column chromatography (PE/EtOAc, 0-15% EtOAc). 1-Phenylhexan-2-ol (**3a**) was obtained as colorless oil (25.8 mg, 145 μ mol, 48%).

4.4.7.2 Photo-degradation of 4CzIPN

Online UV-VIS

During the course of the reaction, 4CzIPN is photo-degraded. This process was monitored by a UV-VIS online measurement. For this purpose, a sample containing 4CzIPN (37.5 μM) and NBu₄PA (**5**) (750 μM) in degassed dry DMA (100-fold dilution in respect to the reaction concentration) in a gas-tight fluorescence cuvette was irradiated using a 455 nm (\pm 25 nm) LED for 10 min at 25 °C, while recording UV-VIS spectra at defined times after start of the irradiation (Figure S1, right). As reference, the same measurement was repeated in absence of NBu₄PA (**5**) using an analogous sample containing only 4CzIPN (37.5 μM) (Figure S1, left). The data shows, that the photo-degradation of 4CzIPN is highly accelerated in the presence of NBu₄PA (**5**), indicating a photoreaction between 4CzIPN and the carboxylate.

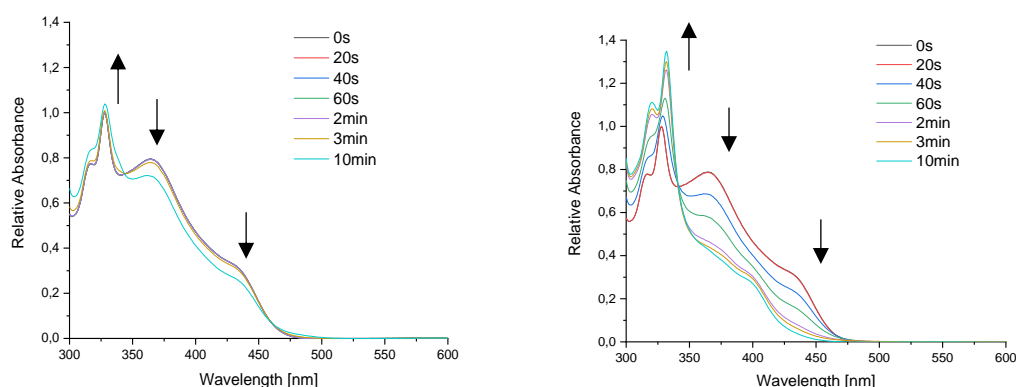
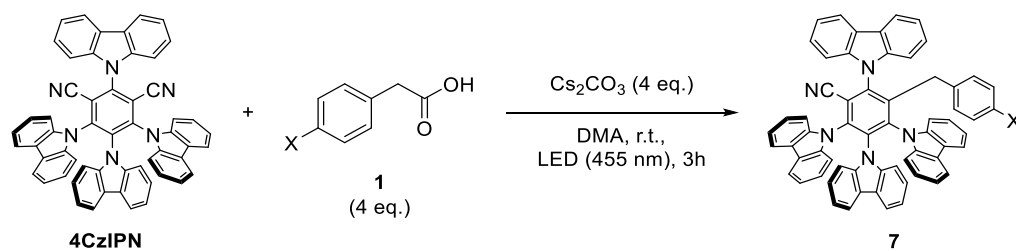


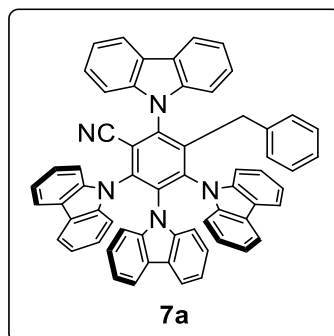
Figure 4-2 – Left: UV-VIS online measurement of a sample containing 4CzIPN (37.5 μM) in degassed dry DMA. Right: UV-VIS online measurement of a sample containing 4CzIPN (37.5 μM) and NBu₄PA (**5**) (750 μM) in degassed dry DMA. Both spectra are normalized to the absorbance maxima of 4CzIPN at 328 nm before irradiation.

Procedure for 4CzIPN photo-conversion to 4CzBnBN



Scheme 4-6 – Photo-conversion of 4CzIPN to 4CzBnBN.

A 5 mL crimp cap vial equipped with a magnetic stirring bar was loaded with 4CzIPN (23.7 mg, 30 μ mol, 1 eq.), Cs_2CO_3 (39.1 mg, 120 μ mol, 4 eq.), the carboxylic acid (120 μ mol, 4 eq.) and DMA (2 mL). In doing so, all solid compounds were added before capping the vial, whereas all liquid compounds were added *via* syringe after setting the capped vial under inert conditions. The reaction mixture was degassed by three cycles of freeze-pump-thaw and subsequently stirred under light irradiation using a 455 nm (\pm 25 nm) LED for 3 h at 25 $^\circ\text{C}$. Two reaction batches were combined and diluted with brine (15 mL), water (5 mL) and ethyl acetate (15 mL). The phases were separated and the water phase was extracted with ethyl acetate (10 mL). The combined organic phases were washed with brine/ H_2O (1:1) (4x10 mL) and dried over MgSO_4 . The solvent was removed under reduced pressure and the crude product was purified by automated flash column chromatography (PE/EtOAc, 10-20% EtOAc).

(2*r*,4*r*,5*r*,6*r*)-3-benzyl-2,4,5,6-tetra(9*H*-carbazol-9-yl)benzonitrile (4CzBnBN) (7a)

Phenylacetic acid was used as carboxylic aid. The product was obtained as light yellow solid. Clear colorless/light yellow plate-shaped crystals could be obtained by recrystallization from PE/EA (8:2).

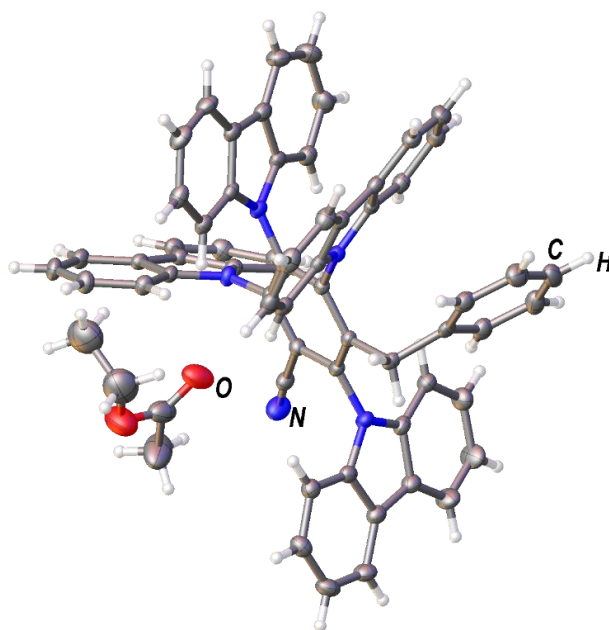
¹H-NMR (400 MHz, d₇-DMF, δ_H): 8.30 (d, *J* = 7.7 Hz, 2H), 8.10 (d, *J* = 8.2 Hz, 1H), 7.92 (d, *J* = 8.2 Hz, 2H), 7.88–7.75 (m, 8H), 7.64 (t, *J* = 8.1 Hz, 2H), 7.45–7.36 (m, 4H), 7.21–7.12 (m, 4H), 7.10–6.99 (m, 4H), 6.84–6.74 (m, 4H), 6.48 (t, *J* = 7.3 Hz, 1H), 6.41 (t, *J* = 7.3 Hz, 2H), 6.13 (d, *J* = 7.2 Hz, 2H), 3.72 (s, 2H).

¹³C-NMR (101 MHz, d₇-DMF, δ_C): 146.6, 144.4, 142.9, 141.9, 141.6, 140.9, 140.4, 140.0, 139.2, 137.5, 128.4, 128.3, 127.8, 126.6, 126.5, 126.3, 125.3, 124.8, 124.6, 124.3, 124.1, 122.0, 121.8, 121.7, 121.4, 121.0, 120.9, 120.2, 119.5, 114.2, 113.0, 112.6, 112.4, 111.6

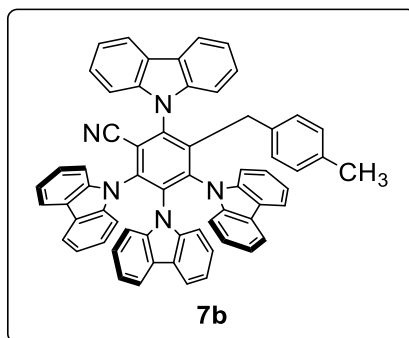
LRMS (FD-MS) (*m/z*): [*M*⁺] (C₆₂H₃₉N₅⁺) calc.: 853.32, found: 853.36.

Yield: 64%.

Crystal structure (CCDC 1884950):



(2*r*,3*r*,4*r*,6*r*)-2,3,4,6-tetra(9*H*-carbazol-9-yl)-5-(4-methylbenzyl)benzonitrile (**7b**)



4-methylphenylacetic acid was used as carboxylic acid. The product was obtained as light yellow solid.

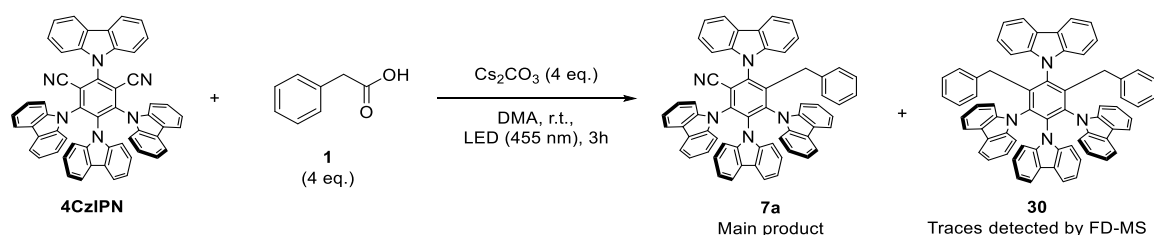
¹H-NMR (300 MHz, d₇-DMF, δ_H): 8.30 (d, *J* = 7.7 Hz, 2H), 8.07 (d, *J* = 8.2 Hz, 1H), 7.94–7.75 (m, 10H), 7.64 (t, *J* = 8.2 Hz, 2H), 7.46–7.36 (m, 4H), 7.21–6.99 (m, 8H), 6.83–6.73 (m, 4H), 6.19 (d, *J* = 7.8 Hz, 2H), 5.95 (d, *J* = 8.0 Hz, 2H), 3.62 (s, 2H), 1.78 (s, 3H).

¹³C-NMR (75 MHz, d₇-DMF, δ_C): 146.9, 144.3, 142.8, 141.8, 141.6, 140.9, 140.4, 140.1, 139.2, 136.0, 134.4, 129.1, 128.2, 127.7, 126.5, 126.2, 125.3, 124.8, 124.6, 124.4, 124.1, 122.0, 121.7, 121.3, 121.0, 120.9, 120.2, 119.4, 114.2, 113.0, 112.6, 112.4, 111.6, 20.9.

LRMS (FD-MS) (*m/z*): [*M*⁺] (C₆₃H₄₁N₅⁺) calc.: 867.34, found: 867.29.

Yield: 47%.

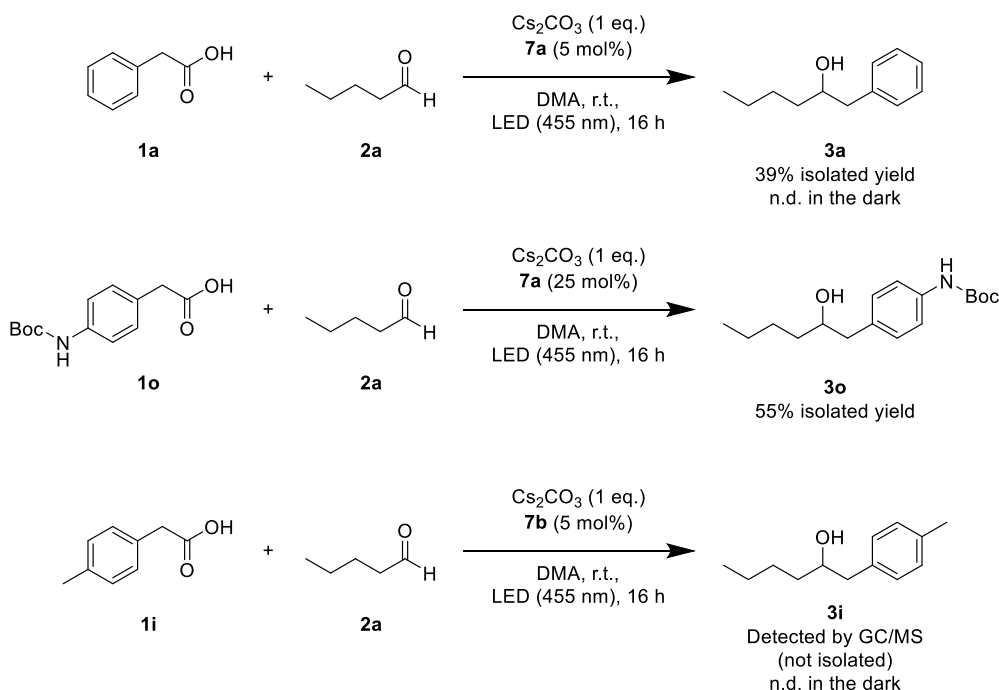
During the synthesis of **7a**, FD-MS analysis of the solid residue prior to column chromatography showed, that **7a** is the main product, while the degradation product from a two-fold cyanide elimination (**30**) is only generated in traces (Scheme 4-7).



Scheme 4-7 – Cyanide elimination products of 4CzIPN with phenylacetic acid (**1a**).

4CzBnBN as photocatalyst

Compounds **7a** and **7b** could both be used as catalyst for the benzylation of aliphatic aldehydes, following general procedure A (Scheme 4-8). In accordance, the use of 4CzIPN derivatives with one cyano group and five electron donating groups was recently reported.^[20]



Scheme 4-8 – Benzylation of *n*-pentanal (**2a**) using **7a** (upper and middle) and **7b** (lower) as catalyst.

7a and **7b** are light yellow powders. The UV/VIS-spectra were measured. They show a weak absorption within the range of the employed LED at the reaction concentration (Figure 4-3).

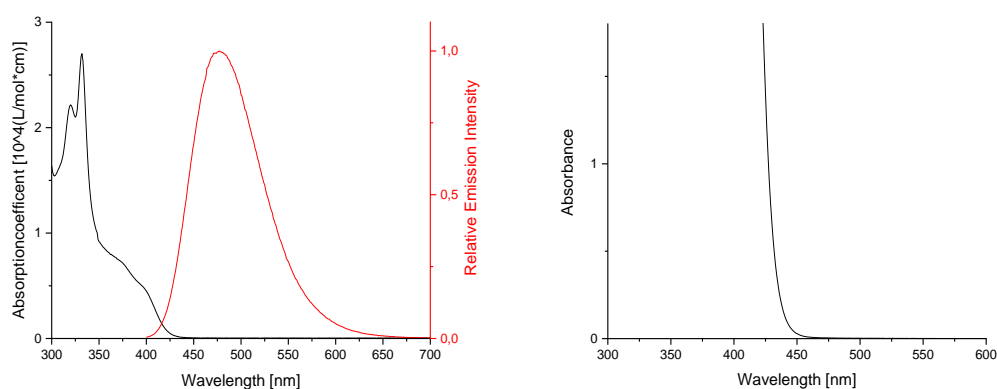


Figure 4-3 – Left: UV/VIS absorption (black) and emission (red) spectrum of **7a** in dry DMA (37.5 μM). Right: UV/VIS absorption spectrum of **7a** in dry DMA at reaction concentration (3.75 mM).

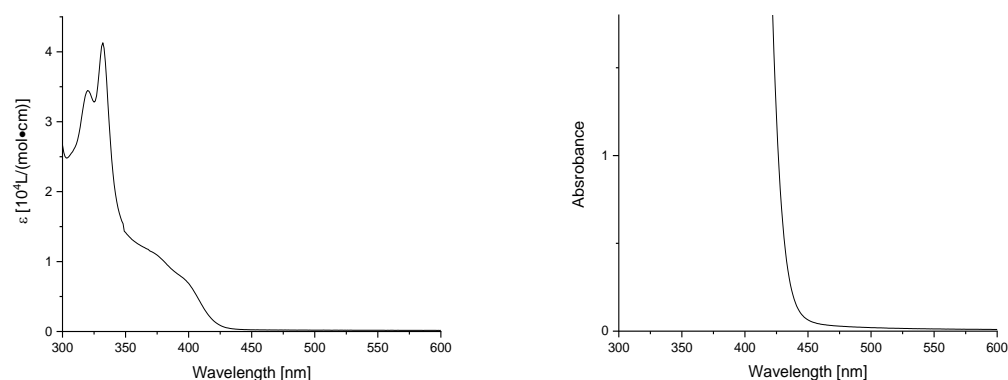


Figure 4-4 – Left: UV/VIS absorption spectrum of **7b** in dry DMA (37.5 μ M). Right: UV/VIS absorption spectrum of **7b** in dry DMA at reaction concentration (3.75 mM).

4.4.7.3 Cyclic voltammetry measurement

The CV measurement was performed with the three-electrode potentiostat galvanostat PGSTAT302N from Metrohm Autolab using a glassy carbon working electrode, a platinum wire counter electrode, a silver wire as a reference electrode and Tetrabutylammonium tetrafluoroborate (TBATFB) (0.1 M) as supporting electrolyte. The potentials were achieved relative to the Fc/Fc⁺ redox couple with ferrocene as internal standard.^[37] The control of the measurement instrument, the acquisition and processing of the cyclic voltammetric data were performed with the software Metrohm Autolab NOVA 1.10.4. The measurement was carried out as follows: a 0.1 M solution of TBATFB in DMF was added to the measuring cell and the solution was degassed by argon purge for 5 min. After recording the baseline a solution of 4CzBnBN in DMF (0.01 M) was added and the solution was again degassed by a stream of argon for 5 min. The cyclic voltammogram was recorded with two scans. Afterwards ferrocene (2.20 mg, 12.0 μ mol) was added to the solution which was again degassed by argon purge for 5 min and the final measurement was performed with three scans.

A ground state oxidation potential of $E_{1/2}(4\text{CzBnBN}^+/4\text{CzBnBN}) = +1.48 \text{ V vs SCE}$ and ground state reduction potential of $E_{1/2}(4\text{CzBnBN}/4\text{CzBnBN}^-) = -1.72 \text{ V vs SCE}$ in DMF could be determined. The emission maximum was measured to be 477 nm (in dry DMA). The excited state potentials were estimated from the crossing point of the normalized absorption and emission spectra (Figure S2). $E_{1/2}(4\text{CzBnBN}^+/4\text{CzBnBN}^*) = +1.21 \text{ V vs SCE}$ and $E_{1/2}(4\text{CzBnBN}^*/4\text{CzBnBN}^-) = -1.45 \text{ V vs SCE}$.

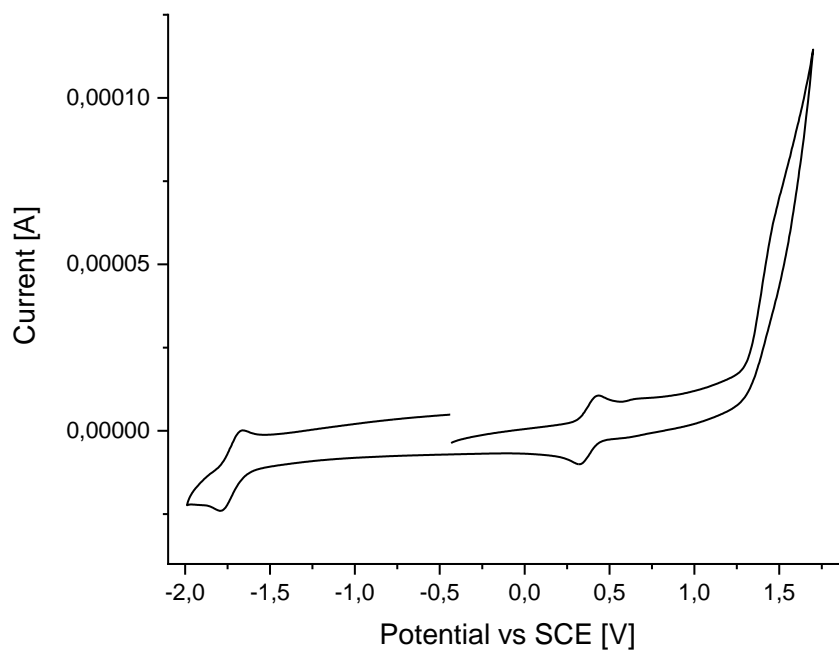


Figure 4-5 – CV of 4CzBnBN (**7a**) in DMF. The reversible peak at 0.380 V refers to the added internal standard ferrocene. The measurement was conducted with TBATFB (0.1 M) as supporting electrolyte and a scan rate of 50 mV/s.

4.4.7.4 Fluorescence quenching studies

Emission quenching of 4CzIPN with NBu₄PA (5)

For the emission quenching experiment of 4CzIPN with NBu₄PA, a 15 μ M solution of 4CzIPN in degassed dry DMF was prepared under nitrogen atmosphere in a gas-tight 10 mm quartz cuvette. The photocatalyst was irradiated at 435 nm and the change of the fluorescence emission upon addition of different amounts of quencher solution was measured (Figure 4-6). The quencher solution contained NBu₄PA (c = 67.5 mM, dry DMF) as quencher, as well as 4CzIPN (c = 15 μ M) to exclude an emission decrease due to dilution.

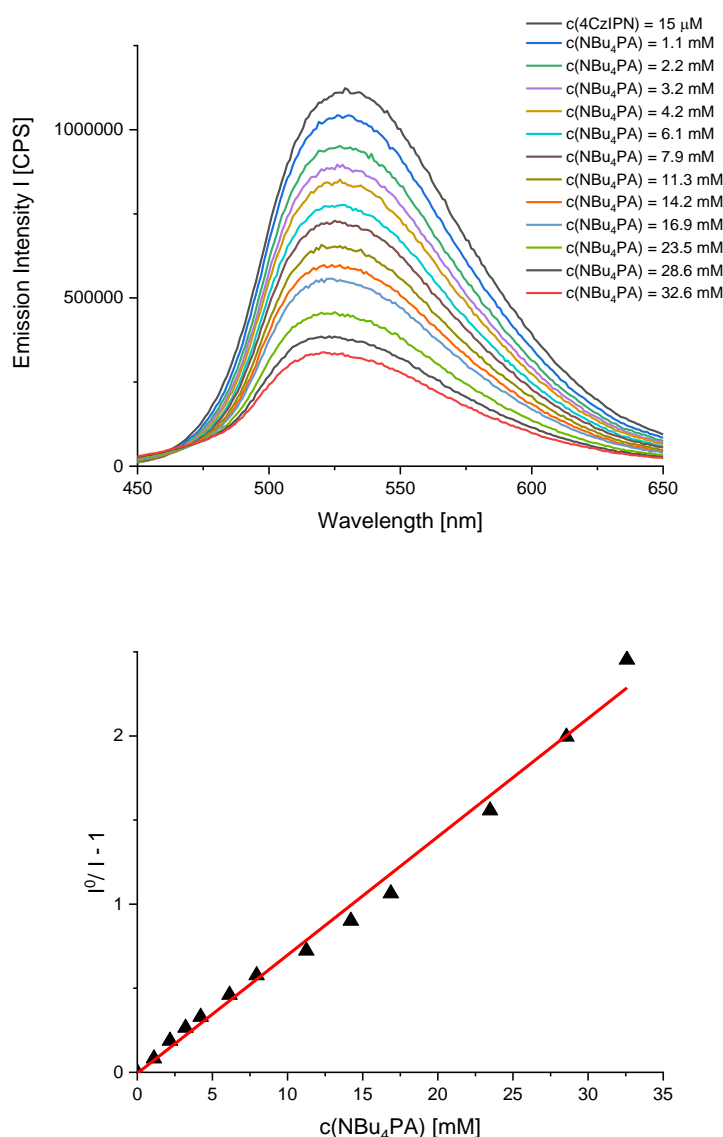


Figure 4-6 – Upper: Emission quenching of 4CzIPN (15 μ M in dry DMF) upon titration with NBu₄PA (5). Lower: Corresponding Stern-Volmer plot with a Stern-Volmer constant of $K_{SV} = 70.3 \mu\text{M}^{-1}$.

An efficient quenching of 4CzIPN upon the addition of NBu₄PA (**5**) could be observed (Figure S5). By plotting $I^0/I-1$ versus the quencher concentration, a Stern-Volmer constant of $K_{SV} = 70.3 \mu\text{M}^{-1}$ was determined from the slope of the linear fit.

$$\frac{I^0}{I} - 1 = K_{SV} \cdot [Q]$$

(With I^0 being the fluorescence intensity at 535 nm in absence of the quencher, I the fluorescence intensity at 535 nm in presence of the quencher and $[Q]$ the quencher concentration)

Emission quenching of 4CzIPN with *n*-pentanal (**2a**)

An 80 μM solution of 4CzIPN in DMA was prepared in a 10 mm quartz cuvette. The photocatalyst was irradiated with 435 nm and the change of the fluorescence emission upon addition of different amounts of quencher solution was measured. The quencher solution contained *n*-pentanal (**2a**) ($c = 18.7 \text{ mM}$, DMA) as well as 4CzIPN ($c = 80 \mu\text{M}$). The Quenching experiment showed, that *n*-pentanal (**2a**) does not efficiently quench the excited state of 4CzIPN (Figure 4-7).

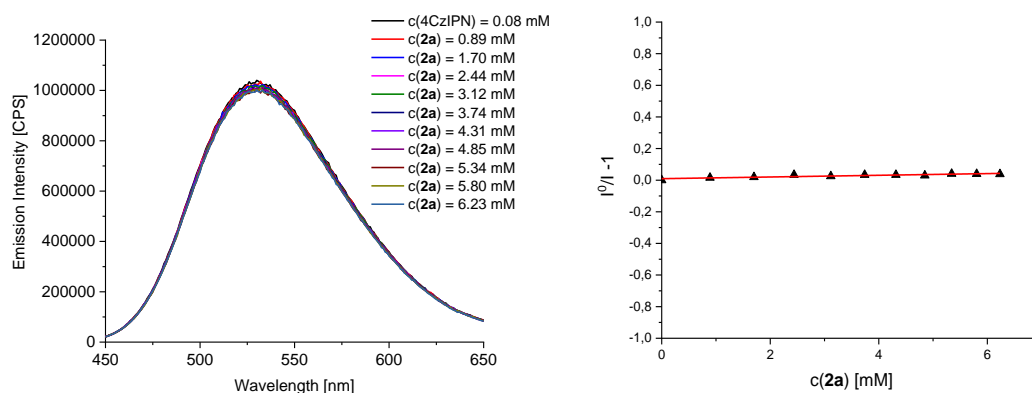


Figure 4-7 – Left: Emission quenching of 4CzIPN (80 μM in DMA) upon titration with *n*-pentanal (**2a**). Right: Corresponding Stern-Volmer plot.

Fluorescence quenching of 4CzBnBN (7a) with NBu₄PA (5)

For the emission quenching experiment of 4CzBnBN with NBu₄PA (5), a 37.5 μ M solution of 4CzBnBN in degassed dry DMA was prepared under nitrogen atmosphere in a gas-tight 10 mm quartz cuvette. The photocatalyst was irradiated at 390 nm and the change of the fluorescence emission upon addition of different amounts of quencher solution was measured (Figure 4-8). The quencher solution contained NBu₄PA (c = 67.5 mM, dry DMA) as quencher, as well as 4CzBnBN (c = 37.5 μ M) to exclude an emission decrease due to dilution. An efficient quenching of 4CzBnBN upon the addition of NBu₄PA (5) could be observed.

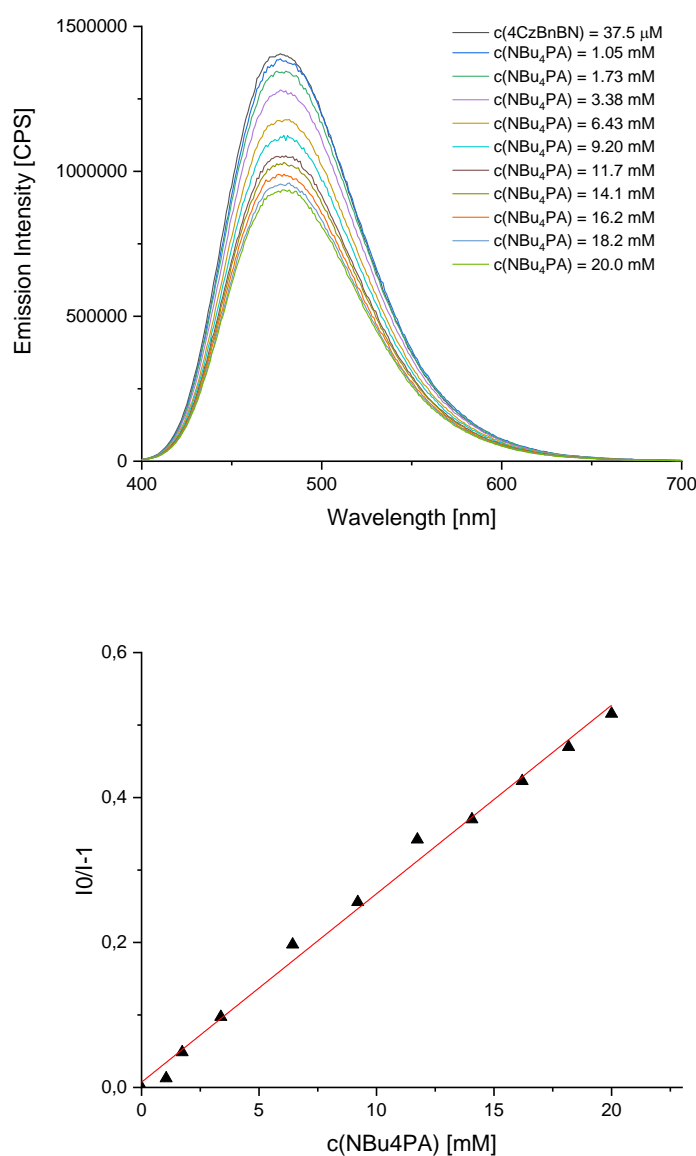


Figure 4-8 – Upper: Emission quenching of 4CzBnBN (37.5 μ M in dry DMA) upon titration with NBu₄PA (5). Lower: Corresponding Stern-Volmer plot with a Stern-Volmer constant of $K_{SV} = 26.0 \mu\text{M}^{-1}$.

4.4.7.5 *In situ* FT-IR measurements

FT-IR spectra were recorded on Varian Excalibur 3100 spectrometer using 1 cm^{-1} resolution. A solution of NBu₄PA (**5**) (75 mM), *n*-pentanal (75 mM) and 4CzBnBN (3.75 mM) in dry DMA (6 mL) was prepared and degassed by three cycles of freeze-pump-thaw. The sample was held in a septum-capped vial connected to a Harrick Scientific (Pleasantville, New York) DLC-S25 flow cell with a $56\text{ }\mu\text{m}$ path length and CaF₂ windows. The vial was irradiated from the bottom with a 455 nm ($\pm 25\text{ nm}$) LED and circulated to the flow cell with a peristaltic pump at a flow rate of 3 mL/min . Spectra were recorded at 5-minute intervals using the starting reaction mixture as a blank so that difference spectra were produced (Figure 4-9). The main features are the appearance of a dissolved CO₂ band at 2338 cm^{-1} and a negative aldehyde C=O stretch at 1722 cm^{-1} . Kinetic plots show saturation of the solution with CO₂ after about 3 hours. Complete loss of the aldehyde is apparent after about 10 hours.

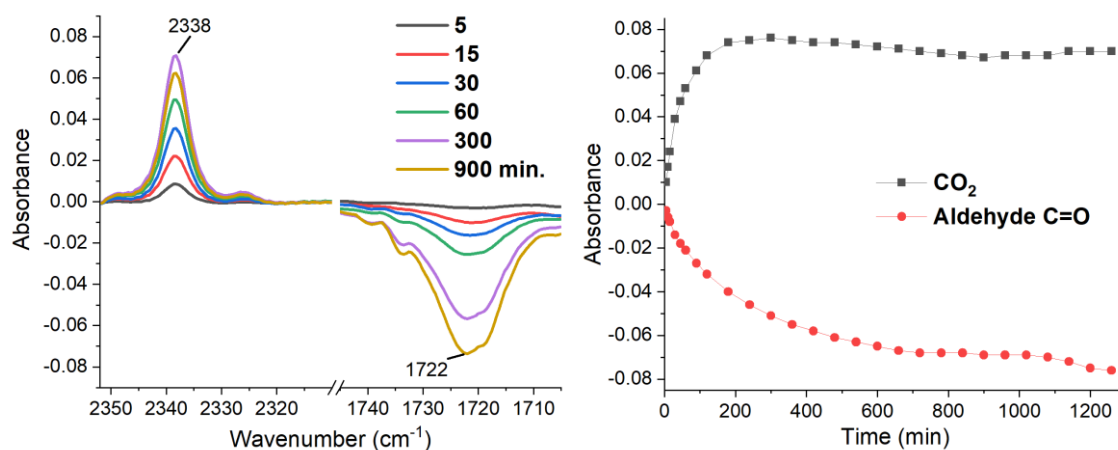
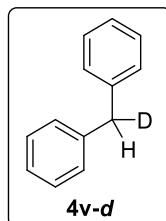


Figure 4-9 – Left : FT-IR difference spectra of a solution containing NBu₄PA (**5**) (75 mM), *n*-pentanal (75 mM) and 4CzBnBN (3.75 mM) in degassed dry DMA (6 mL) irradiated using a 455 nm ($\pm 25\text{ nm}$) LED at defined periods of time after irradiation start. Right: corresponding kinetic plot of the CO₂ band at 2338 cm^{-1} and aldehyde C=O stretch at 1722 cm^{-1} .

4.4.7.6 Deuterium labeling studies

Employing D₂O instead of an aldehyde as electrophile leads to the formation of the corresponding deuterated product.

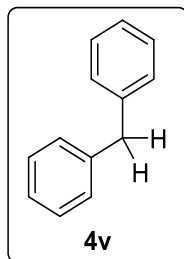
Diphenylmethane-d₁ (**4v-d**)^[38]



A 5 mL crimp cap vial equipped with a magnetic stirring bar was loaded with 4CzIPN (5.9 mg, 7.5 μ mol, 5 mol%), Cs₂CO₃ (48.9 mg, 150 μ mol, 1 eq.) and diphenylacetic acid (**1v**) (31.8 mg, 150 μ mol, 1 eq.). The vial was set under inert conditions and dry DMF (2 mL) followed by D₂O (30 μ L, 1.50 mmol, 10 eq.) were added *via* syringe. The reaction mixture was degassed by four cycles of freeze-pump-thaw and subsequently stirred under light irradiation using a 455 nm (\pm 25 nm) LED for 16 h at 25 °C.

The reaction mixture was diluted with brine (10 mL), water (5 mL) and ethyl acetate (10 mL). The phases were separated and the water phase was extracted with ethyl acetate (3 x 6 mL). The combined organic phases were washed with H₂O/brine (1:1) (3 x 10 mL) and dried over Na₂SO₄. The solvent was removed under reduced pressure and the crude product was purified by automated flash column chromatography (PE). Diphenylmethane-*d*₁ (**4v-d**) (21.6 mg, 128 μ mol, 85%, 81% deuterium incorporation) was obtained as colorless oil.

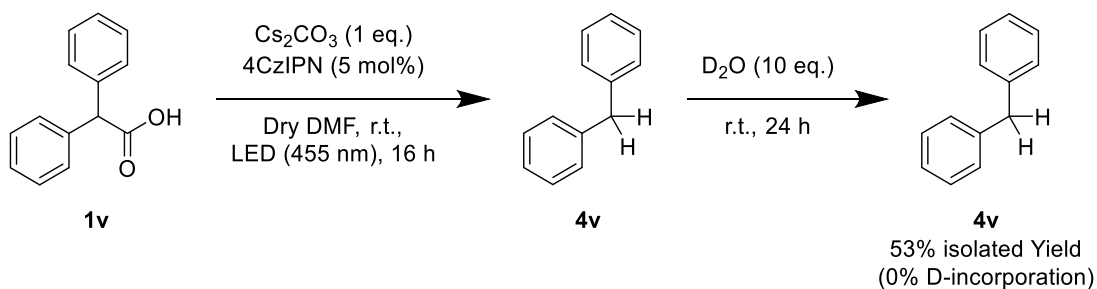
¹H-NMR (400 MHz, CDCl₃, δ_{H}): 7.35 – 7.17 (m, 10H), 4.00-3.96 (m, 1H).

Diphenylmethane (4v)^[39]

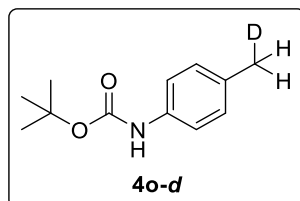
Following the same experimental procedure in absence of D₂O with d₇-DMF instead of dry DMF as solvent, diphenylmethane (**4v**) was obtained in 75% isolated yield with no deuterium incorporation.

¹H-NMR (400 MHz, CDCl₃, δ_H): 7.35 – 7.17 (m, 10H), 3.99 (s, 2H).

To exclude that **4v-d** is formed by an H/D-exchange between **4v** and D₂O in the presence of Cs₂CO₃, the reactive intermediate was generated in absence of D₂O to form **4v**. Subsequently, D₂O was added to the reaction mixture and it was stirred for further 24 h. **4v** was not deuterated (Scheme 4-9).



Scheme 4-9 – Control experiment for the exclusion of an H/D exchange between **4v** and D₂O in presence of Cs₂CO₃.

4-Methylphenyl)carbamic acid *tert*-butyl ester-*d*₁ (4o-*d*)

A 5 mL crimp cap vial equipped with a magnetic stirring bar was loaded with 4CzIPN (5.9 mg, 7.5 μ mol, 5 mol%), Cs₂CO₃ (48.9 mg, 150 μ mol, 1 eq.) and 4-(*t*-Butyloxycarbonylamino)phenylacetic acid (**1o**) (37.7 mg, 150 μ mol, 1 eq.). The vial was set under inert conditions and dry DMA (2 mL) followed by D₂O (30 μ L, 1.50 mmol, 10 eq.) were added *via* syringe. The reaction mixture was degassed by four cycles of freeze-pump-thaw and subsequently stirred under light irradiation using a 455 nm (\pm 25 nm) LED for 16 h at 25 °C. Two reaction batches were combined and diluted with brine (10 mL), water (5 mL) and ethyl acetate (10 mL). The phases were separated and the water phase was extracted with ethyl acetate (3 x 6 mL). The combined organic phases were washed with H₂O/brine (1:1) (3 x 10 mL) and dried over Na₂SO₄. The solvent was removed under reduced pressure and the crude product was purified by automated flash column chromatography (PE/EtOAc 0-20%). (4-Methylphenyl)carbamic acid *tert*-butyl ester-*d*₁ (**4o-*d***) (41.6 mg, 200 μ mol, 67%, 84% deuterium incorporation) was obtained as white solid.

¹H-NMR (300 MHz, CDCl₃, δ_{H}): 7.24 (d, J = 8.4 Hz, 2H), 7.09 (d, J = 8.5 Hz, 2H), 6.46 (s, 1H), 2.30-2.27 (m, 2H), 1.52 (s, 9H).

¹³C-NMR (75 MHz, CDCl₃, δ_{C}): 153.0 (C_q), 135.8 (C_q), 132.6 (C_q), 129.6 (+), 118.8 (+), 80.4 (C_q), 28.5 (+), 20.8 (+, non-deuterated), 20.6 (t, J = 19.5 Hz, -).

HRMS (ESI) (m/z): [MH⁺] (C₁₂H₁₆DNO₂⁺) calc.: 209.1395, found: 209.1391.

4.4.7.7 NMR *in-situ* irradiation studies

A benzyl anion (**15**) is expected to show a highly upfield-shifted NMR-signal. It was attempted to detect its potential presence by measuring NMR-spectra while *in-situ* irradiating the reaction mixture in absence of electrophiles like aldehydes or water. Therefore, potassium benzyltrifluoroborate (**16**) (14.9 mg, 75 μmol , 1 eq.) and 4CzIPN (3 mg, 3.8 μmol , 5 mol%) were dissolved in 0.5 mL dry d_7 -DMF and the solution was irradiated using a 455 nm LED while simultaneously measuring NMR-spectra at defined periods of time.

No new upfield-shifted peak after irradiation could be detected. However, the depletion of residual H_2O was observed, indicating the generation of a reactive anionic species.^[40] Additionally, the generation of toluene and formation of 4CzBnBN could be detected (Figure 4-10).

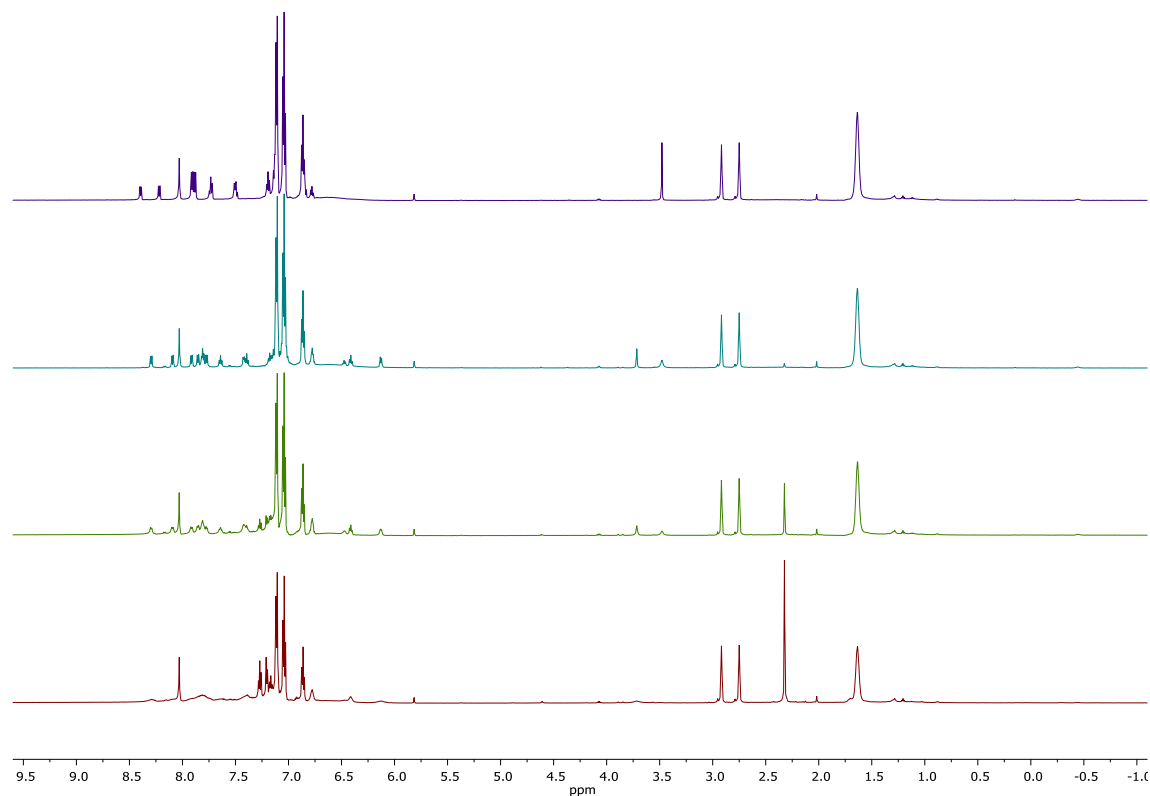


Figure 4-10 – Measurement of NMR-spectra during irradiation of a mixture containing potassium benzyltrifluoroborate (**16**) (75 μmol , 1 eq.) and 4CzIPN (3.8 μmol , 5 mol%) in dry d_7 -DMF (0.5 mL).

4.4.7.8 E1cb-elimination reactions

The proposed carbanion intermediate is expected to undergo an E1cb elimination in case a suitable leaving group is present. Thus, the styrene (**10**) formation of two benzylic carboxylic acids bearing different leaving groups in the homobenzylic position was monitored. Dry DMF instead of DMA was chosen as solvent, as the DMA peak covers the potential styrene peak in the GC-FID analysis. The formation of styrene (**10**) was confirmed by GC-FID retention time, GC-MS analysis and crude NMR.

Photocatalytic E1cb-elimination of benzylic carboxylic acids bearing leaving groups in the homobenzylic position (General procedure C)

A 5 mL crimp cap vial equipped with a magnetic stirring bar was loaded with 4CzIPN (5.9 mg, 7.5 μ mol, 5 mol%), Cs₂CO₃ (48.9 mg, 150 μ mol, 1 eq.) and the carboxylic acid (150 μ mol, 1 eq.). The vial was set under inert conditions and dry DMF (2 mL) was added *via* syringe. The reaction mixture was degassed by four cycles of freeze-pump-thaw and subsequently stirred under light irradiation using a 455 nm (\pm 25 nm) LED for 16 h at 25 °C. An aliquot of the reaction mixture was submitted to GC-FID analysis to quantify the product yields with *n*-decane as internal standard.

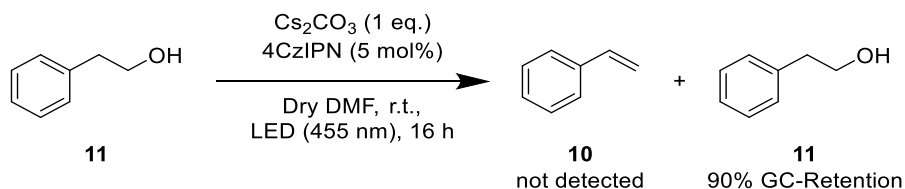
Table 4-14 – E1cb-elimination of tropic acid (**9**).^[a]

Entry	Photocatalyst	Base	Yield ^[b] 10 [%]	Yield ^[b] 11 [%]
1	Yes	Yes	23	33
2	No	Yes	n.d.	n.d.
3 ^[c]	Yes	Yes	n.d.	n.d.
4	Yes	No	n.d.	n.d.

[a] Reactions were performed with tropic acid (**9**) (150 μ mol, 1 eq.) in dry DMF (2 mL). [b] Determined by GC-FID analysis with *n*-decane as internal standard. [c] Reaction performed in absence of light.

Control experiment 2-phenylethanol (**11**) under reaction conditions

2-Phenylethanol (**11**) instead of tropic acid (**9**) was subjected to General Procedure C, to exclude a styrene (**10**) formation by a decarboxylation of **9** to **11** followed by an E2-elimination with Cs_2CO_3 (Scheme S4-10).

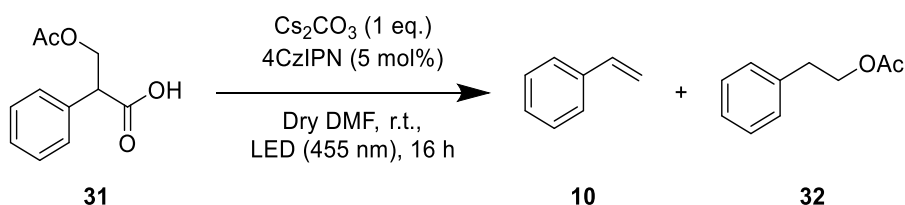


Scheme 4-10 – Control experiment excluding the formation of styrene (**10**) by an E2-elimination of **11** in presence of Cs_2CO_3 .

E1cb-elimination of acetyltropic acid (**31**)

Acetyltropic acid (**31**) was subjected to General procedure C.

Table 4-15 – E1cb-elimination of acetyltropic acid (**31**).^[a]

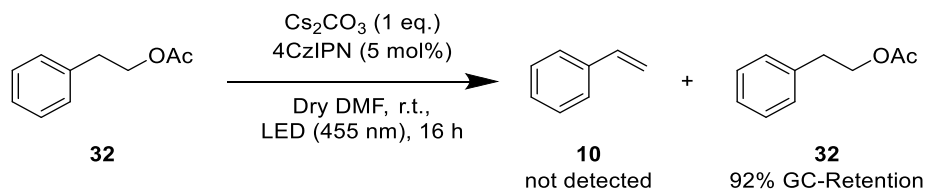


Entry	Photocatalyst	Base	Yield ^[b] 10 [%]	Yield ^[b] 32 [%]
1	Yes	Yes	72	n.d.
2	No	Yes	18	n.d.
3 ^[c]	Yes	Yes	13	n.d.
4	Yes	No	9	n.d.

[a] Reactions were performed with tropic acid (**31**) (150 μmol , 1 eq.) in dry DMF (2 mL). [b] Determined by GC-FID analysis with *n*-decane as internal standard. [c] Reaction performed in absence of light.

Control experiment 2-phenylacetate (**32**) under reaction conditions

2-Phenylacetate (**32**) instead of acetyltropic acid (**31**) was subjected to General Procedure C, to exclude a styrene (**10**) formation by a decarboxylation of **31** to **32** followed by an E2-elimination with Cs_2CO_3 (Scheme 4-11).



Scheme 4-11 – Control experiment excluding the formation of styrene (**10**) by an E2-elimination of **30** in presence of Cs_2CO_3 .

Crude NMR of the E1cb-elimination of acetyltropic acid (**31**)

To verify the formation of styrene beyond GC-FID and GC-MS analysis, acetyltropic acid (**31**) was subjected to General Procedure C in d_7 -DMF and the reaction solution was irradiated within the NMR tube. NMR-spectra before and after the irradiation were measured. The characteristic peaks of styrene can be observed in the ^1H -NMR of the reaction mixture after completed reaction (Figure 4-11).

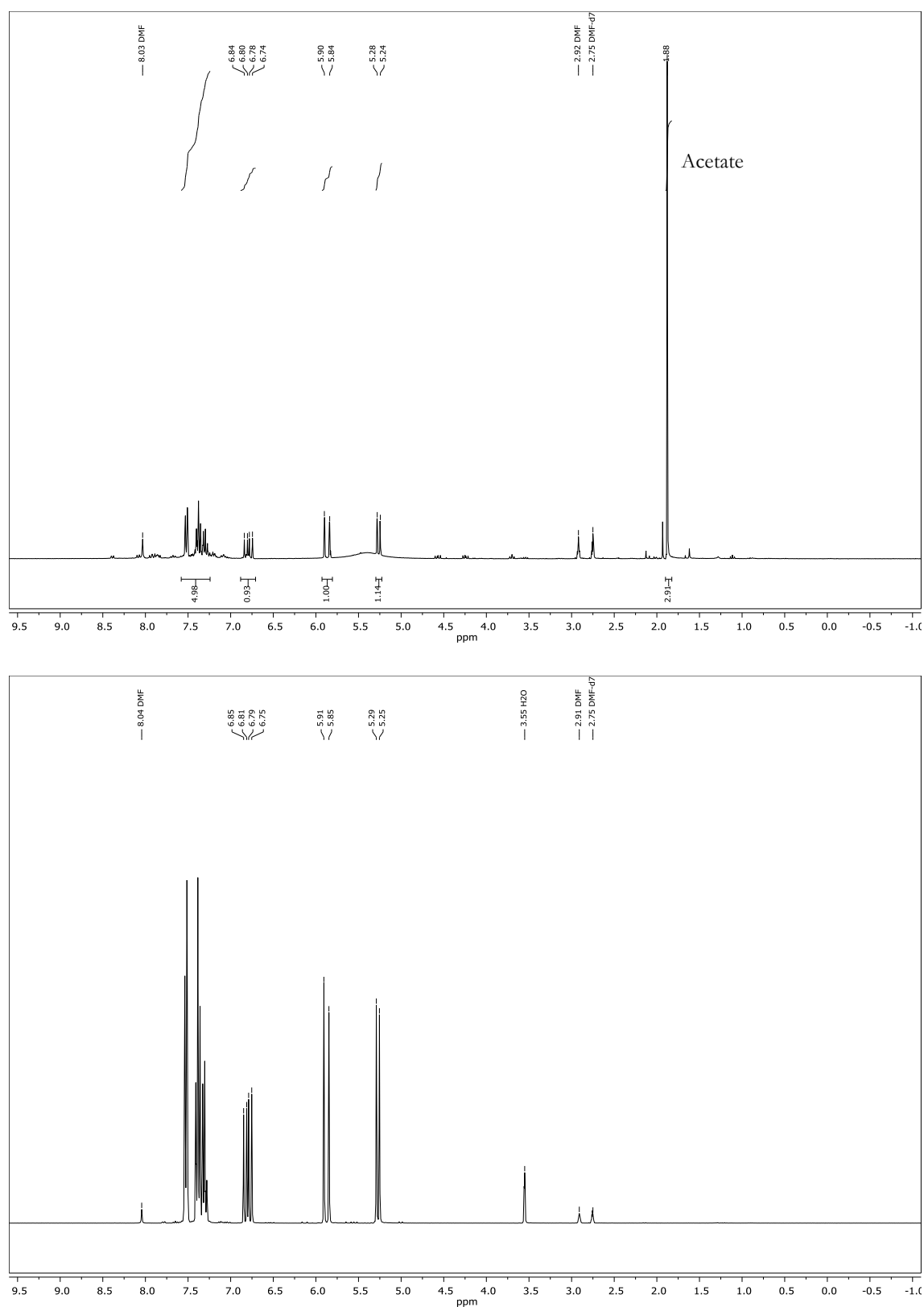


Figure 4-11 – ^1H -NMR of crude reaction mixture of photocatalytic E1cb elimination of acetyltropic acid (**31**) to styrene (**10**) (upper) compared to ^1H -NMR of styrene (**10**) in $\text{DMF-}d_7$ (lower).

4.4.7.9 DFT-calculations

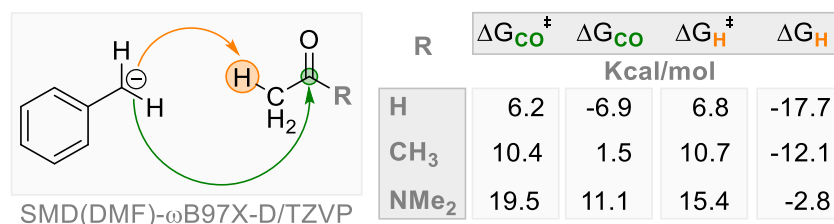


Figure 4-12 – Calculated energy values for possible reaction pathways with 4CzIPN as photocatalyst.

DFT calculations were performed using Gaussian 09 Revision E.01.^[41] All structures were optimized using the ω B97X-D functional with the TZVP basis set. The SMD solvation model^[42] for DMF was included in all the optimizations. DMF was used instead of DMA due to the similar dielectric constant. Frequency calculations confirmed that the optimized structures were local minima or transition states and were used to calculate Gibbs free energies. The saddle points were connected to the reagents and products *via* the Intrinsic Reaction Coordinate method.

The competition between the abstraction of the proton in a of the carbonyl and the C=O attack of the benzyl anion **15** was tested for aldehydes, ketones and the solvent (DMA). For the calculations, acetaldehyde was chosen as the prototypical member of the aldehyde class while acetone was selected for the ketones. The results of the analysis are reported in Figure 4-12.

Interestingly, all the kinetic barriers are extremely low. Even the barrier of the acid-base reaction between **15** and DMA are compatible with a reaction extremely feasible at room temperature. Hence we can state that the reduction product (toluene) can confidently come both from the reaction of the benzyl anion with the H in a to the carbonyl of the solvent and of the one of the aldehyde/ketone. The acid-base reaction with the DMA is kinetically less favored, but it is equally feasible due to the higher concentration of the species.

The energies and cartesian coordinates of the species analyzed are herein reported.

15 + acetaldehyde (H^+ abstraction): reagent

C	0.0371434505	2.0396221661	1.5674770206
H	-0.4788084362	1.8872708996	2.5101288245
H	0.0547957072	3.0440309903	1.1568191851
C	0.650995074	0.9819951888	0.9059473867
C	1.332047693	1.1357427676	-0.3527885488
C	0.6412002781	-0.3679248519	1.4044608695
C	1.9428516698	0.0812132877	-0.9982581799
H	1.3672362649	2.1250551122	-0.8010809675
C	1.2620780297	-1.4067060285	0.7421901973
H	0.133859765	-0.5677287626	2.3444368812
C	1.926446064	-1.216563459	-0.4743271734
H	2.4437495189	0.2692950846	-1.9441950486
H	1.2220726803	-2.4014956894	1.1777791601
H	2.4113957851	-2.038413275	-0.9864500689
C	-1.7770808914	-0.742053442	-1.1126856041
O	-2.5190921275	-1.66493574	-0.863037017
C	-2.2065579229	0.6789308765	-1.2430087672
H	-1.7755401081	1.2467389698	-0.408243494
H	-1.7903018301	1.1027638218	-2.1607570777
H	-3.292406704	0.7730505337	-1.2333748698
H	-0.6964009604	-0.9252594503	-1.2567807078

Energy= -424.86724

Zero-point correction= 0.170443 (Hartree/Particle)

Thermal correction to Gibbs Free Energy= 0.132256

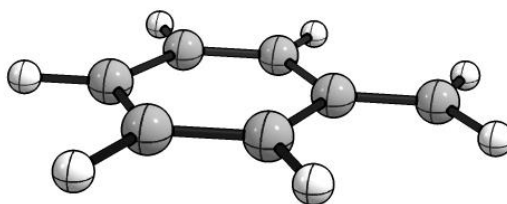
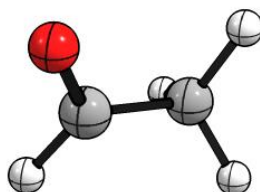
Sum of electronic and zero-point Energies= -424.696797

Sum of electronic and thermal Energies= -424.685413

Sum of electronic and thermal Enthalpies= -424.684469

Sum of electronic and thermal Free Energies= -424.734984

G + ZVPE = -424.564541



15 + acetaldehyde (H^+ abstraction): product

C	-0.1598240874	1.9221698929	0.5879016987
H	-0.7512183768	1.6671130112	1.4697765429
H	0.2805404222	2.908312311	0.7428828466
C	0.8968899017	0.8845104056	0.32706662
C	2.2164840724	1.247890884	0.0684542125
C	0.5665251486	-0.4727387461	0.3261153552
C	3.1869886137	0.2852649064	-0.185588766
H	2.4901651459	2.2978345224	0.0669669298
C	1.5348337762	-1.4346214697	0.0722484978
H	-0.4607171479	-0.7717871019	0.529175425
C	2.8493120856	-1.0609960685	-0.1848580639
H	4.2091556959	0.5888945896	-0.3810503091
H	1.2621204824	-2.4842092778	0.0773063635
H	3.6042941629	-1.8134547615	-0.3809037239
C	-2.965515025	-0.7819052011	-0.4682580711
O	-2.7035267626	-1.1593319155	0.7113309881
C	-3.456185647	0.4228656626	-0.9115060511
H	-0.8539325186	1.9882143899	-0.2546896166
H	-3.6294476383	0.5889306327	-1.970001751
H	-3.6894397865	1.226926767	-0.2168014382
H	-2.7723415174	-1.5162804333	-1.2884176893

Energy= -424.8972188

Zero-point correction= 0.172281 (Hartree/Particle)

Thermal correction to Gibbs Free Energy= 0.132143

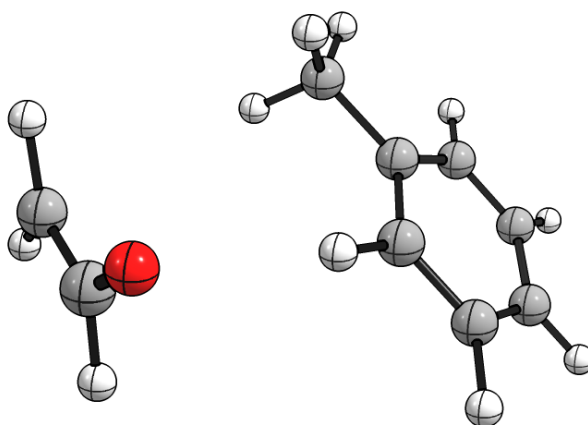
Sum of electronic and zero-point Energies= -424.724937

Sum of electronic and thermal Energies= -424.713522

Sum of electronic and thermal Enthalpies= -424.712578

Sum of electronic and thermal Free Energies= -424.765075

G + ZVPE = -424.592794



15 + acetaldehyde (H^+ abstraction): TS

C	-0.6039184283	2.4481481751	-0.4577577892
H	-0.2326765965	2.7045958318	-1.4502395933
H	-0.9989122122	3.3053671742	0.0877038944
C	-1.3528824303	1.2294764874	-0.3577869144
C	-2.2773777125	0.9904228069	0.6888675314
C	-1.0792852098	0.1260877504	-1.2015468709
C	-2.8918309393	-0.2376537855	0.8569791722
H	-2.5154669418	1.8017833068	1.3704246448
C	-1.7020666269	-1.1013635792	-1.0292076749
H	-0.3698235177	0.2533193009	-2.0132140982
C	-2.6153847868	-1.3035571409	0.0002131001
H	-3.5987971217	-0.3701620448	1.6698968353
H	-1.4640398156	-1.9153310531	-1.7067448529
H	-3.0998391232	-2.2634096581	0.1332961774
C	2.1493849698	0.3252760261	-0.1418938736
O	2.8280247766	0.4060392613	-1.1686519951
C	1.788299013	1.4076872913	0.7243909639
H	0.6925248919	1.9384661173	0.2048160734
H	1.4888738812	1.0988833812	1.726574977
H	2.4875615711	2.2456899419	0.7182985303
H	1.7001661689	-0.6576086211	0.1194772023

Energy= -424.8512799

Zero-point correction= 0.167382 (Hartree/Particle)

Thermal correction to Gibbs Free Energy= 0.130227

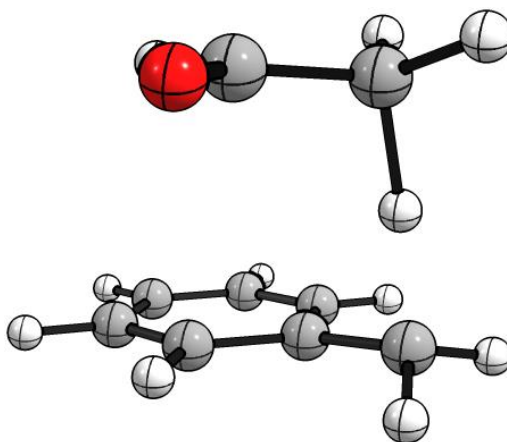
Sum of electronic and zero-point Energies= -424.683898

Sum of electronic and thermal Energies= -424.673899

Sum of electronic and thermal Enthalpies= -424.672955

Sum of electronic and thermal Free Energies= -424.721053

G + ZVPE = -424.553671



15 + acetaldehyde (C=O attack): reagent

C	-0.1886612606	0.4276492021	2.2426191649
H	-0.6523566777	-0.4079876983	2.7569666133
H	-0.3270212908	1.4195473228	2.6607163425
C	0.621611911	0.2243564516	1.1307608541
C	1.2747147212	1.2981312245	0.4304796962
C	0.8528663385	-1.0759355776	0.5598031023
C	2.0191845777	1.091640837	-0.7122094335
H	1.1535804648	2.3093402978	0.8093687516
C	1.6006381832	-1.257480708	-0.5850574212
H	0.4049634909	-1.9393049631	1.0441459929
C	2.1967171495	-0.184787899	-1.2573768926
H	2.4749660343	1.9490060003	-1.2001676031
H	1.7276079134	-2.2655767643	-0.9706423501
H	2.7817082411	-0.3378360427	-2.1559373924
C	-2.5441675875	-0.2695377174	-0.4434530868
O	-3.7183288067	-0.0998951778	-0.2070647531
H	-1.9721379985	-1.0357466556	0.1123299664
C	-1.7660085456	0.4817329553	-1.4693299755
H	-0.9413846362	1.0073261829	-0.9775824719
H	-1.3096957229	-0.229493747	-2.1643305244
H	-2.3969764992	1.1872894765	-2.0093695795

Energy= -424.867137

Zero-point correction= 0.170380 (Hartree/Particle)

Thermal correction to Gibbs Free Energy= 0.131174

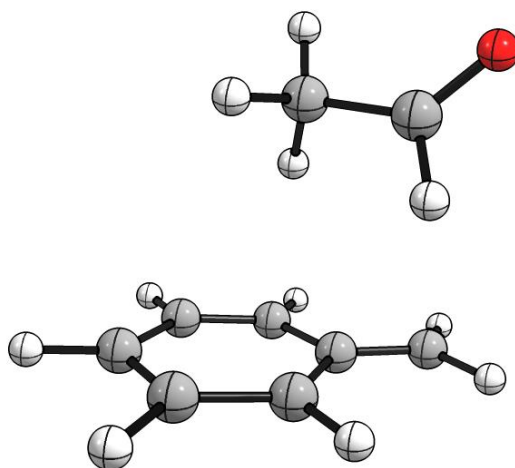
Sum of electronic and zero-point Energies= -424.696757

Sum of electronic and thermal Energies= -424.685245

Sum of electronic and thermal Enthalpies= -424.684301

Sum of electronic and thermal Free Energies= -424.735962

G + ZVPE = -424.565582



15 + acetaldehyde (C=O attack): product

C	-0.9698015879	0.2241330894	1.1041002958
H	-1.0780256088	-0.4439016272	1.9630670152
H	-1.1062026051	1.2499781857	1.4619233631
C	0.3889412581	0.0595209953	0.4930769536
C	1.1159567486	1.1533089014	0.0185400563
C	0.9405500882	-1.2123872995	0.3185162089
C	2.3448013717	0.9864157646	-0.6061170139
H	0.7093265734	2.1518441355	0.1412063747
C	2.1677913904	-1.386558609	-0.3083906256
H	0.3997800921	-2.0784886354	0.686001461
C	2.8759012731	-0.2865113622	-0.7759202163
H	2.8892375193	1.8535709067	-0.9628548432
H	2.5728353161	-2.3849357489	-0.4301362542
H	3.8344232238	-0.4189076411	-1.2640680419
C	-2.1904276406	-0.0984197761	0.1619697066
O	-3.3531720573	-0.0267497736	0.8138460055
H	-1.952168515	-1.1309713818	-0.2359001094
C	-2.1295217158	0.8235345001	-1.0786453263
H	-1.2132403774	0.7115269573	-1.6702881066
H	-2.9818635228	0.599497533	-1.7266981004
H	-2.2138642239	1.8712988858	-0.7656978027

Energy= -424.8947076

Zero-point correction= 0.176442 (Hartree/Particle)

Thermal correction to Gibbs Free Energy= 0.141750

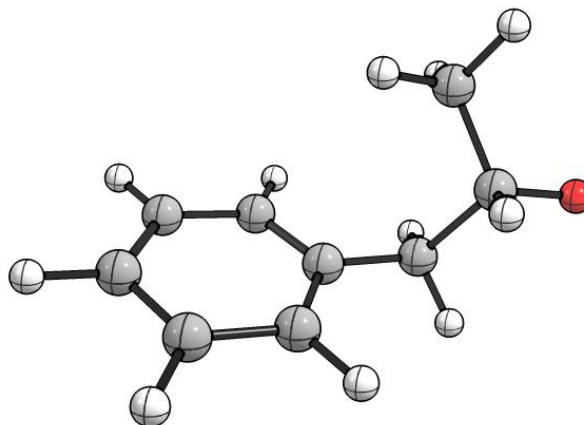
Sum of electronic and zero-point Energies= -424.718265

Sum of electronic and thermal Energies= -424.709192

Sum of electronic and thermal Enthalpies= -424.708247

Sum of electronic and thermal Free Energies= -424.752958

G + ZVPE = -424.576516



15 + acetaldehyde (C=O attack): TS

C	-1.2712815871	0.5606559034	1.5557947492
H	-1.6551094836	-0.2255368155	2.1964268242
H	-1.5837852967	1.5732324269	1.7925940643
C	-0.0802857286	0.3514532893	0.8425327701
C	0.6100191298	1.4059950581	0.1690408968
C	0.4686256133	-0.9519131856	0.6376726364
C	1.7344588252	1.1777266066	-0.6003467604
H	0.2401185051	2.4211769514	0.2805590521
C	1.5953915557	-1.1634179314	-0.1358309835
H	-0.011775661	-1.7985053336	1.1199361975
C	2.252762239	-0.108434693	-0.7707450773
H	2.2232087458	2.0205013892	-1.0804499259
H	1.9726848258	-2.1757170471	-0.248600206
H	3.1374599808	-0.2804942694	-1.3716344544
C	-3.0136040396	0.0305456589	-0.0221655472
O	-4.0704234753	-0.0835324994	0.5982035979
H	-2.3789345442	-0.855456346	-0.205217795
C	-2.7627895408	1.1822787786	-0.9610143213
H	-1.7026502704	1.2967808301	-1.1902976403
H	-3.2943080962	0.9789277247	-1.8986510325
H	-3.1558257871	2.1115297137	-0.5442264447

Energy= -424.8632841

Zero-point correction= 0.171791 (Hartree/Particle)

Thermal correction to Gibbs Free Energy= 0.135747

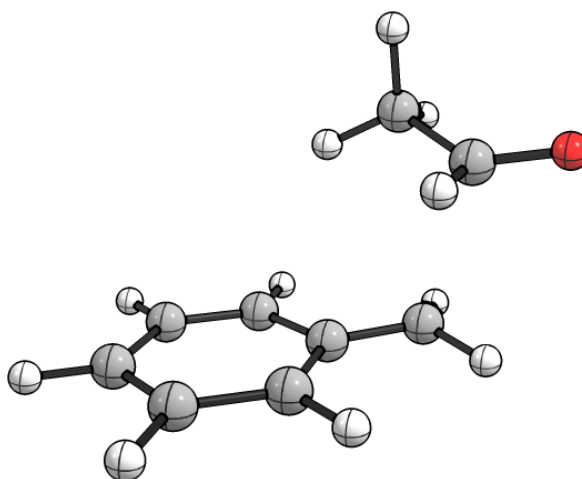
Sum of electronic and zero-point Energies= -424.691493

Sum of electronic and thermal Energies= -424.681635

Sum of electronic and thermal Enthalpies= -424.680691

Sum of electronic and thermal Free Energies= -424.727537

G + ZVPE = -424.555746



15 + acetone (H^+ abstraction): product

C	-0.0752531939	2.1395549532	0.8801034935
H	0.1836486033	2.5783818718	1.8462771802
H	-0.0548667175	2.927652181	0.1257456747
C	0.8586971529	1.0186412129	0.5227919569
C	1.2840703209	0.8253693421	-0.7900937941
C	1.2752495678	0.1048624205	1.4909716365
C	2.0947879551	-0.2502965009	-1.129804212
H	0.969139005	1.5233910364	-1.5581750729
C	2.0871298469	-0.9707081905	1.1576301798
H	0.9548073061	0.2380741497	2.519093074
C	2.4977892512	-1.1555081955	-0.1569716446
H	2.4103253262	-0.3825241729	-2.1584620537
H	2.3971538992	-1.6691520072	1.9265696979
H	3.1300021847	-1.9954947923	-0.4197840742
C	-2.2951468386	-0.2048130873	-0.5629666884
O	-2.7160383566	-0.0158561899	0.6191612936
C	-2.4435738985	0.6567248792	-1.6320562894
H	-1.0978161966	1.7512399352	0.9446493049
H	-2.0398160408	0.4232977623	-2.6113434943
H	-2.9642122061	1.6029685232	-1.5068422198
C	-1.5395733055	-1.5129931594	-0.8053535468
H	-2.1914456517	-2.3604577647	-0.5718780255
H	-1.1758636302	-1.6247476182	-1.8295758461
H	-0.6854773833	-1.5662315885	-0.1233775304

Energy= -464.2200049

Zero-point correction= 0.200937 (Hartree/Particle)

Thermal correction to Gibbs Free Energy= 0.161576

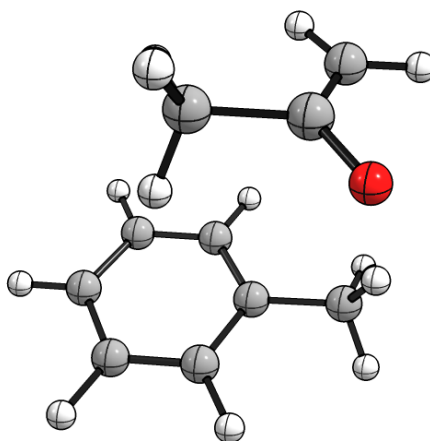
Sum of electronic and zero-point Energies= -464.019068

Sum of electronic and thermal Energies= -464.006793

Sum of electronic and thermal Enthalpies= -464.005849

Sum of electronic and thermal Free Energies= -464.058429

G + ZVPE = -463.857492



15 + acetone (H^+ abstraction): reagent

C	0.5951962749	2.6493868771	0.1976203463
H	-0.0609646863	2.9986422518	0.9883309335
H	0.8902397533	3.3605436108	-0.5673399387
C	1.0907989631	1.3495823339	0.1988381153
C	1.9861909057	0.8498420773	-0.811374022
C	0.7409456034	0.380297577	1.2032111935
C	2.4599420298	-0.4453893016	-0.8054653391
H	2.2944527379	1.523377139	-1.6065807356
C	1.2283677693	-0.9101252877	1.188145671
H	0.0636703468	0.6815974943	1.9977638163
C	2.0961105895	-1.3612314128	0.1882468954
H	3.1321596583	-0.7580878148	-1.6001786754
H	0.9192801963	-1.5924400848	1.9754801728
H	2.4734581274	-2.3764516791	0.1851111245
C	-2.1858368128	-0.9298520566	-0.2841539879
O	-2.5797431511	-1.7773131508	0.4909224113
C	-2.6072290685	0.5089544802	-0.1735311596
H	-1.7244285567	1.1473338974	-0.0629346573
H	-3.1060794076	0.8165318821	-1.0969092559
H	-3.2785782612	0.6518286228	0.6721035661
C	-1.2730304631	-1.2660314566	-1.4322098196
H	-1.8389067318	-1.1894686873	-2.365808942
H	-0.4526990551	-0.5471984223	-1.4917426544
H	-0.8802207615	-2.2765328892	-1.3312300586

Energy= -464.1958901

Zero-point correction= 0.198781 (Hartree/Particle)

Thermal correction to Gibbs Free Energy= 0.158955

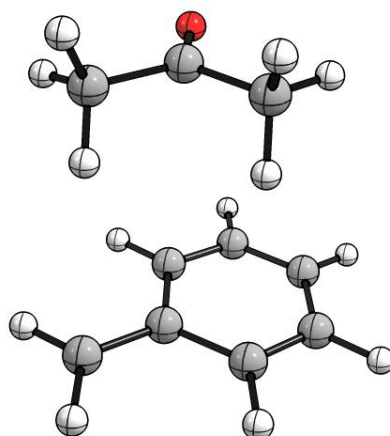
Sum of electronic and zero-point Energies= -463.997109

Sum of electronic and thermal Energies= -463.984427

Sum of electronic and thermal Enthalpies= -463.983483

Sum of electronic and thermal Free Energies= -464.036935

G + ZVPE = -463.838154



15 + acetone (H^+ abstraction): TS

C	-0.065038	2.208279	0.459612
H	-0.343235	2.474136	1.480392
H	0.115416	3.080203	-0.170695
C	0.881059	1.132606	0.328849
C	1.589752	0.908617	-0.874844
C	1.011826	0.130764	1.318433
C	2.353576	-0.22906	-1.07368
H	1.521828	1.649489	-1.665892
C	1.779349	-1.003739	1.115595
H	0.484283	0.254808	2.2595
C	2.455433	-1.205866	-0.085363
H	2.874509	-0.360906	-2.016654
H	1.844738	-1.748326	1.90251
H	3.050176	-2.097345	-0.244323
C	-2.294851	-0.473329	-0.155707
O	-2.938908	-0.734124	0.869131
C	-2.254623	0.829261	-0.765146
H	-1.254693	1.507412	-0.154495
H	-1.962193	0.842432	-1.815909
H	-3.131443	1.443865	-0.556783
C	-1.445714	-1.566526	-0.78754
H	-2.073531	-2.146471	-1.472279
H	-0.606881	-1.165165	-1.358518
H	-1.072331	-2.247182	-0.021149

Energy= -464.1759247

Zero-point correction= 0.196069 (Hartree/Particle)

Thermal correction to Gibbs Free Energy= 0.158756

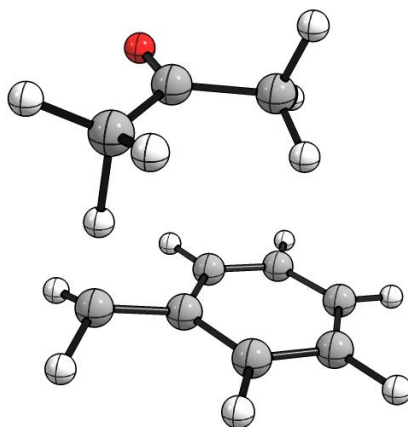
Sum of electronic and zero-point Energies= -463.979856

Sum of electronic and thermal Energies= -463.968778

Sum of electronic and thermal Enthalpies= -463.967834

Sum of electronic and thermal Free Energies= -464.017169

G + ZVPE = -463.821100



15 + acetone (C=O attack): product

C	-0.8928609531	0.6993394903	0.7955854668
H	-1.2696108829	0.314336109	1.7484007636
H	-0.8681179722	1.7925235552	0.8648966407
C	0.495047031	0.1914688395	0.5624288278
C	1.4926418087	1.0183824007	0.0429624217
C	0.8203389558	-1.1437027712	0.8143417068
C	2.7696137684	0.5350298191	-0.2161778425
H	1.2624108845	2.0587210358	-0.1637746561
C	2.0943333019	-1.632584535	0.5573183165
H	0.0477896983	-1.798390555	1.1965700567
C	3.0768411324	-0.794898198	0.0410897983
H	3.5256343941	1.200282382	-0.6183757027
H	2.3246954289	-2.672173022	0.7633227185
H	4.0723877921	-1.1756335042	-0.1562957006
C	-1.9461292048	0.2401593393	-0.2990522904
O	-2.0945759289	-1.0918183036	-0.3447354235
C	-3.267897549	0.9577943786	0.0916179346
H	-3.185453456	2.051379727	0.1334612867
H	-4.0443045492	0.701215462	-0.6364232114
H	-3.6003102201	0.6007907109	1.0718866705
C	-1.4958803826	0.8243922949	-1.665290565
H	-2.2594223769	0.59866068	-2.4169416619
H	-1.3391415379	1.9106388196	-1.6534947833
H	-0.5655171823	0.347714845	-1.9864917719

Energy= -464.2124778

Zero-point correction= 0.204793 (Hartree/Particle)

Thermal correction to Gibbs Free Energy= 0.169361

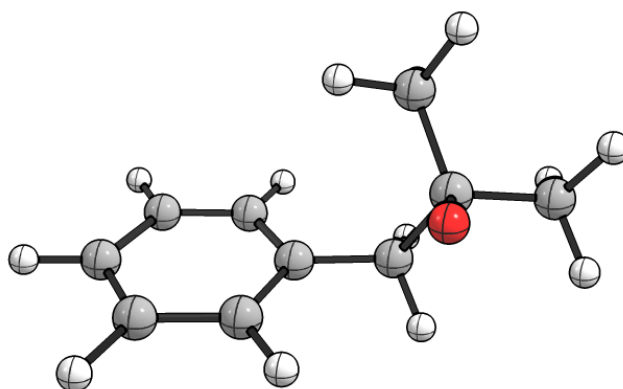
Sum of electronic and zero-point Energies= -464.007685

Sum of electronic and thermal Energies= -463.997445

Sum of electronic and thermal Enthalpies= -463.996501

Sum of electronic and thermal Free Energies= -464.043117

G + ZVPE = -463.838324



15 + acetone (C=O attack): reagent

C	-0.1856228449	1.8273236502	2.1148049162
H	-0.9377122286	1.4080890354	2.7754055052
H	-0.0332059981	2.9019774569	2.1356024693
C	0.5868209881	1.0088475103	1.2965625969
C	1.6022115311	1.5168748279	0.4121568722
C	0.429183085	-0.4205029285	1.2483803081
C	2.3513317768	0.6956351967	-0.4043110181
H	1.7781322478	2.5891287398	0.3906272714
C	1.1899934214	-1.2215504292	0.4223587214
H	-0.3255038488	-0.8785377424	1.8819763793
C	2.167520212	-0.6916863931	-0.4260484034
H	3.1015559184	1.1459565417	-1.0489051089
H	1.0140890077	-2.2938617476	0.4315340491
H	2.7574009552	-1.3281285265	-1.0741832049
C	-2.0708402181	-0.6788036084	-1.2200869489
O	-2.2364871988	-1.8687894214	-1.393368878
C	-2.8206433159	0.0796362081	-0.1586808477
H	-2.1550737994	0.7531162614	0.3885615632
H	-3.5742189352	0.7045013749	-0.6485247948
H	-3.3170336555	-0.6053802257	0.5277406648
C	-1.1347491369	0.1283495093	-2.0774007966
H	-1.7000319821	0.9080639275	-2.5958155158
H	-0.4005301203	0.6317229805	-1.4427274085
H	-0.6277458609	-0.5052691978	-2.8035323913

Energy= -464.195812

Zero-point correction= 0.197791 (Hartree/Particle)

Thermal correction to Gibbs Free Energy= 0.157330

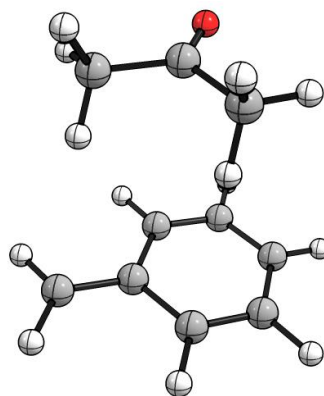
Sum of electronic and zero-point Energies= -463.998021

Sum of electronic and thermal Energies= -463.985662

Sum of electronic and thermal Enthalpies= -463.984718

Sum of electronic and thermal Free Energies= -464.038482

G + ZVPE = -463.840691



15 + acetone (C=O attack): TS

C	-1.0947611727	1.064241857	0.9323372038
H	-1.698845713	0.5686161772	1.6856662254
H	-1.2022120695	2.1447768034	0.8822074614
C	0.1493935055	0.4979817885	0.5912467424
C	1.1383653397	1.2096238567	-0.1499596887
C	0.4629785491	-0.8649944983	0.8637219004
C	2.3178087657	0.6179928955	-0.5620316945
H	0.9541446579	2.2527159468	-0.3910141409
C	1.646485856	-1.4451673253	0.4441866992
H	-0.2526178407	-1.4591048882	1.4225225426
C	2.5972253426	-0.7195334098	-0.2749521573
H	3.0382164874	1.2099815524	-1.118969118
H	1.8372323282	-2.4873161444	0.6835583418
H	3.5248855771	-1.1781850678	-0.595668212
C	-2.518685014	0.2990474596	-0.7956782181
O	-2.4334332099	-0.9364285052	-0.8146143195
C	-3.7417809106	0.9494996023	-0.1699578432
H	-3.5906687308	2.0029809949	0.0657018669
H	-4.5673331179	0.8769820456	-0.8904648557
H	-4.0381451724	0.4131227998	0.7320148334
C	-1.8494497395	1.1044838802	-1.8911631596
H	-2.4177240646	0.9573465775	-2.8183466901
H	-1.8212323139	2.1727080812	-1.6729544637
H	-0.8331975495	0.7444055402	-2.0592730561

Energy= -464.18536

Zero-point correction= 0.199509 (Hartree/Particle)

Thermal correction to Gibbs Free Energy= 0.161701

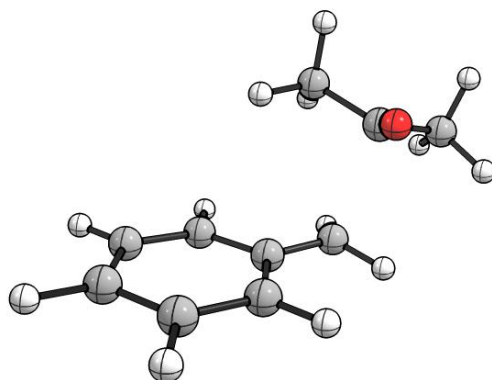
Sum of electronic and zero-point Energies= -463.985851

Sum of electronic and thermal Energies= -463.974495

Sum of electronic and thermal Enthalpies= -463.973551

Sum of electronic and thermal Free Energies= -464.023659

G + ZVPE = -463.824150



15 + DMA (H⁺ abstraction): product

C	-0.3086030857	2.1796188253	-0.7551228408
H	-0.3164794032	2.311419668	-1.8384929435
H	-0.5440886097	3.1407628275	-0.2920020268
C	-1.2859068166	1.1203125111	-0.3305247308
C	-1.6023915125	0.9484509348	1.01751095
C	-1.8737662837	0.263926373	-1.2583785264
C	-2.4738094697	-0.0510748231	1.4253182062
H	-1.1507736121	1.6017780741	1.7562180318
C	-2.7466665675	-0.7403709371	-0.8553947761
H	-1.6433403843	0.3812806527	-2.3117885499
C	-3.0496487752	-0.9024518535	0.4890118417
H	-2.702772573	-0.1673221085	2.4784011031
H	-3.190004008	-1.3959776545	-1.5961569949
H	-3.7304163338	-1.683468265	0.8066015383
C	2.3626395381	0.0993008783	0.5372929061
O	3.0161041353	1.0035275538	-0.0557204201
C	2.0755612866	0.0929585886	1.9020231629
H	0.7102192174	1.910492365	-0.4575694974
H	1.4577569652	-0.6476497744	2.3895918824
H	2.4559799449	0.9130515572	2.5003159849
N	1.9250842199	-0.9985465785	-0.2604159375
C	1.7812039216	-0.7699066999	-1.6818909839
H	1.9127521967	-1.7096867124	-2.2258522056
H	0.7934603117	-0.3633533825	-1.9472217305
H	2.5392593567	-0.0620702137	-2.0062744597
C	0.9761963606	-1.9452471389	0.2793911028
H	0.8360940799	-2.7577394585	-0.4367833977
H	1.3479397282	-2.3863353113	1.2056997612
H	-0.0099398278	-1.5012948979	0.4833095501

Energy= -558.8841059

Zero-point correction= 0.246235 (Hartree/Particle)

Thermal correction to Gibbs Free Energy= 0.204161

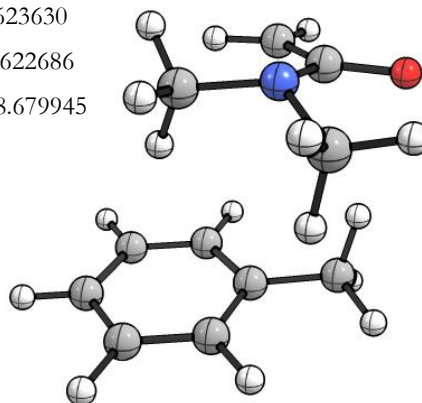
Sum of electronic and zero-point Energies= -558.637871

Sum of electronic and thermal Energies= -558.623630

Sum of electronic and thermal Enthalpies= -558.622686

Sum of electronic and thermal Free Energies= -558.679945

G + ZVPE = -558.433710



15 + DMA (H⁺ abstraction): reagent

C	1.4107461985	2.8895062522	0.4454555983
H	0.7428976009	3.3065012375	1.1924150402
H	1.9040937851	3.57744978	-0.2337537653
C	1.6739407607	1.5239426717	0.4016669159
C	2.5701833896	0.9273200933	-0.553657173
C	1.0604701743	0.5801155125	1.2980353903
C	2.8023112822	-0.431534329	-0.6023005715
H	3.0745074855	1.5775628086	-1.2635294653
C	1.3074078609	-0.7746500615	1.2289884239
H	0.3653317542	0.9541514733	2.0447869422
C	2.1791582195	-1.3205677477	0.2803671228
H	3.4879538293	-0.81653096	-1.3525867471
H	0.7978731469	-1.4330231239	1.9275672095
H	2.3663302086	-2.3863475342	0.2336542055
C	-2.2699727489	-0.1965995934	0.1591906711
O	-2.916289695	-0.5469297202	1.1454803921
C	-2.156575431	1.2594953183	-0.222966436
H	-1.1224976538	1.6055754151	-0.1412295524
H	-2.4810526401	1.4313718036	-1.251184087
H	-2.7789266611	1.8432246598	0.4515521607
N	-1.627205571	-1.079342765	-0.6409660959
C	-1.6776859132	-2.4993398769	-0.3596326081
H	-2.1030167975	-3.0419400477	-1.2082321202
H	-0.6736546019	-2.8867021684	-0.165866519
H	-2.2977461719	-2.6664767391	0.5168247226
C	-0.8314162209	-0.6608651056	-1.7833798689
H	-0.2781674732	-1.5233804062	-2.1504002499
H	-1.4554380215	-0.2837009249	-2.5981261876
H	-0.106379095	0.1063660777	-1.5064333481

Energy= -558.8759995

Zero-point correction= 0.245515 (Hartree/Particle)

Thermal correction to Gibbs Free Energy= 0.201265

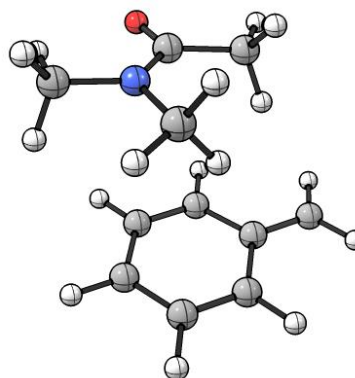
Sum of electronic and zero-point Energies= -558.630485

Sum of electronic and thermal Energies= -558.615162

Sum of electronic and thermal Enthalpies= -558.614217

Sum of electronic and thermal Free Energies= -558.674735

G + ZVPE = -558.429220



15 + DMA (H⁺ abstraction): TS

C	0.5253599404	2.3289031967	0.6902301388
H	0.1732721752	2.496484489	1.7100694196
H	0.9212245551	3.2412896364	0.2399319794
C	1.3463173869	1.1538843582	0.517307484
C	2.2415716748	1.0165034976	-0.5680130505
C	1.1828312868	0.0107710751	1.332691086
C	2.9246766172	-0.1650815653	-0.8092762672
H	2.3968723238	1.8648015146	-1.2280272661
C	1.8660284047	-1.1682749088	1.0862253624
H	0.4932711007	0.0607045692	2.1700124336
C	2.7475995535	-1.2747685227	0.0127012962
H	3.605459211	-0.2218793129	-1.6526659172
H	1.7094177384	-2.019197352	1.7413846784
H	3.2809940955	-2.1982131047	-0.1782278444
C	-2.2511700321	0.3602588078	-0.0561735933
O	-2.8913628783	0.3413997419	1.0117287684
C	-1.8665729052	1.5984455474	-0.7027334093
H	-0.6911349974	1.9835654321	-0.042434172
H	-1.6245848573	1.560472526	-1.7623740402
H	-2.5607497028	2.4047248663	-0.4676822304
N	-1.8116908079	-0.8365576814	-0.6045412945
C	-1.8274947856	-2.0240657882	0.2216611312
H	-2.0117804288	-2.9065793882	-0.3951064569
H	-0.8716202982	-2.1651143714	0.7460610244
H	-2.6162676377	-1.9352252765	0.9637455561
C	-0.8913306537	-0.8694076222	-1.7236180945
H	-0.7422043542	-1.907408914	-2.0213401429
H	-1.2938403351	-0.3358762693	-2.5858697111
H	0.0878826104	-0.4407421805	-1.4769428682

Energy= -558.8487253

Zero-point correction= 0.242210 (Hartree/Particle)

Thermal correction to Gibbs Free Energy= 0.201884

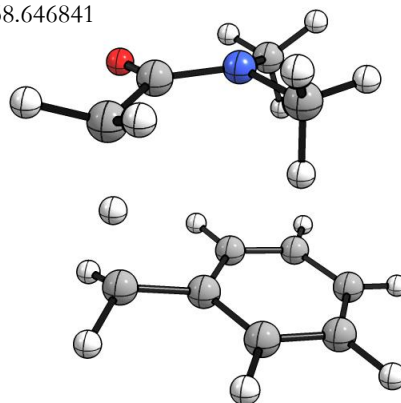
Sum of electronic and zero-point Energies= -558.606515

Sum of electronic and thermal Energies= -558.592889

Sum of electronic and thermal Enthalpies= -558.591945

Sum of electronic and thermal Free Energies= -558.646841

G + ZVPE = -558.404631



15 + DMA (C=O attack): product

C	0.4239863919	-0.0612798545	-0.7779996533
H	0.6779334926	-0.9863804838	-1.3026345364
H	0.6674435543	0.7743616174	-1.4399696138
C	-1.0446677822	-0.0363038099	-0.4940694942
C	-1.797518633	1.1256665108	-0.6733110775
C	-1.7018918006	-1.1703037014	-0.0092680679
C	-3.1556166707	1.1598999786	-0.3790459942
H	-1.3092288027	2.0193635997	-1.0488955947
C	-3.0577480064	-1.1422451068	0.285900692
H	-1.1227610094	-2.070072688	0.1548644552
C	-3.7933007943	0.0238738306	0.1017492778
H	-3.7160880751	2.0759224709	-0.5297543423
H	-3.5463583471	-2.0353597355	0.6599080713
H	-4.8532926234	0.0436901947	0.3274204333
C	1.3294938748	-0.0325971128	0.5287220009
O	1.0892202445	-1.0561643771	1.3264379851
C	1.1116748504	1.3235264947	1.2466811177
H	1.8444447536	1.4113762034	2.0536415142
H	1.1889781334	2.2089425865	0.6076169608
H	0.1146012367	1.3199529307	1.6919970705
N	2.7957252513	-0.038169687	0.062754618
C	3.2003690841	0.9614845796	-0.902918266
H	2.8671665121	1.9566105595	-0.6077714002
H	4.2939215605	0.9917383673	-0.9689111953
H	2.8267993605	0.7717711294	-1.9259566886
C	3.2304174159	-1.3467199186	-0.3689678525
H	2.897919661	-1.6076507233	-1.3926980369
H	4.3249763385	-1.4038593322	-0.3655593823
H	2.8266518287	-2.0861675227	0.3211289989

Energy= -558.8701278

Zero-point correction= 0.249650 (Hartree/Particle)

Thermal correction to Gibbs Free Energy= 0.210494

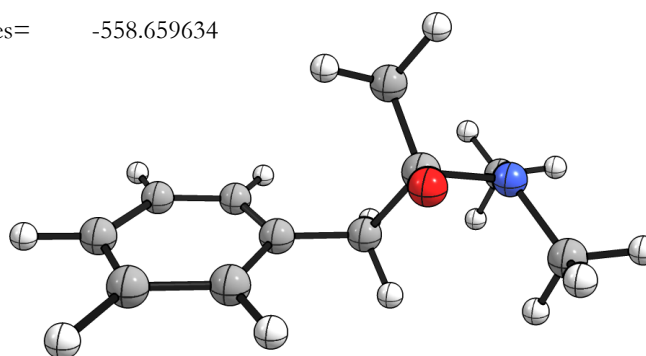
Sum of electronic and zero-point Energies= -558.620478

Sum of electronic and thermal Energies= -558.607577

Sum of electronic and thermal Enthalpies= -558.606633

Sum of electronic and thermal Free Energies= -558.659634

G + ZVPE = -558.409984



15 + DMA (C=O attack): reagent

C	-0.1214481693	-0.8688868804	-2.4224190948
H	0.1449926484	-1.9209512598	-2.4248790479
H	0.3445235923	-0.2275299186	-3.1635998773
C	-0.9697886491	-0.3458078976	-1.4534546471
C	-1.315888404	1.0502258525	-1.3809257768
C	-1.5841730865	-1.152298148	-0.4303425518
C	-2.1814891831	1.5506770702	-0.4299465353
H	-0.8806440948	1.7284740815	-2.1098947737
C	-2.4456548611	-0.6291392582	0.5096789133
H	-1.3560375117	-2.2145657837	-0.407196368
C	-2.7727466963	0.731826333	0.5380736767
H	-2.4032017188	2.6147322532	-0.4357768966
H	-2.875345232	-1.2976516839	1.2510174558
H	-3.4493264578	1.1349454431	1.2815361041
C	1.6201293638	-0.4138432545	1.3042475586
O	1.7362749373	-1.5508149862	1.7579410969
C	0.6894314866	0.5819700073	1.9569193504
H	1.2372912464	1.4479981055	2.3340200581
H	-0.0705699413	0.9359473561	1.2580586189
H	0.1976586577	0.0855046353	2.7902638262
N	2.3205808911	0.0008517993	0.2206654228
C	2.2318867714	1.317974517	-0.3752953009
H	1.5687598106	1.9707137049	0.1823682814
H	3.2239250398	1.7781821517	-0.4044893835
H	1.8591170751	1.2385579541	-1.4008083013
C	3.2126161521	-0.9102506692	-0.4659079125
H	2.9158631833	-1.0009976055	-1.5148031904
H	4.2415107196	-0.5401600915	-0.4248867219
H	3.1645164302	-1.8877348274	0.0049040161

Energy= -558.8760453

Zero-point correction= 0.245525 (Hartree/Particle)

Thermal correction to Gibbs Free Energy= 0.202843

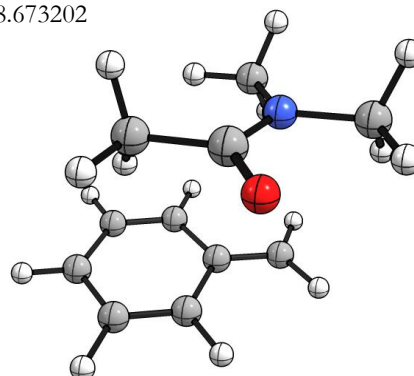
Sum of electronic and zero-point Energies= -558.630521

Sum of electronic and thermal Energies= -558.615447

Sum of electronic and thermal Enthalpies= -558.614503

Sum of electronic and thermal Free Energies= -558.673202

G + ZVPE = -558.427677



15 + DMA (C=O attack):TS

C	0.7962351019	-0.26007225	1.1788690135
H	1.2586529886	0.5697170474	1.7097659296
H	0.993607132	-1.2294843299	1.6323930798
C	-0.5302527819	-0.0419723075	0.7119281901
C	-1.4051348605	-1.1100213856	0.3813697372
C	-1.022817296	1.2591139927	0.4354860679
C	-2.6551402384	-0.8924969656	-0.1715439714
H	-1.0786288566	-2.1279514053	0.5735202167
C	-2.2765590679	1.4689255913	-0.1124433823
H	-0.3926203295	2.111735711	0.6659236741
C	-3.1136466187	0.3993191293	-0.4285460002
H	-3.2866831414	-1.7444343504	-0.4046975225
H	-2.6106188133	2.4850655561	-0.2995774892
H	-4.0939606912	0.5677647821	-0.8583478468
C	2.0471228495	-0.2094680354	-0.629497034
O	1.6161014559	0.7216283928	-1.3432738697
C	1.7439463201	-1.6320884263	-1.079710983
H	2.3434614396	-1.8515685019	-1.9713645668
H	1.9339843643	-2.4034668538	-0.3360788699
H	0.6922307538	-1.6784941772	-1.3599369506
N	3.3456488796	-0.0388970727	-0.0424503384
C	3.804270834	-0.9611820717	0.9740545402
H	3.6323736201	-1.995180956	0.6823140648
H	4.8811303835	-0.8348354576	1.1112513724
H	3.3205891161	-0.7939123433	1.9473135608
C	3.6886284755	1.3290406448	0.2778224086
H	3.1720899447	1.6904098383	1.1824469281
H	4.764365695	1.4022643656	0.4543637199
H	3.4164546112	1.980049669	-0.5493394987

Energy= -558.8501053

Zero-point correction= 0.246688 (Hartree/Particle)

Thermal correction to Gibbs Free Energy= 0.206845

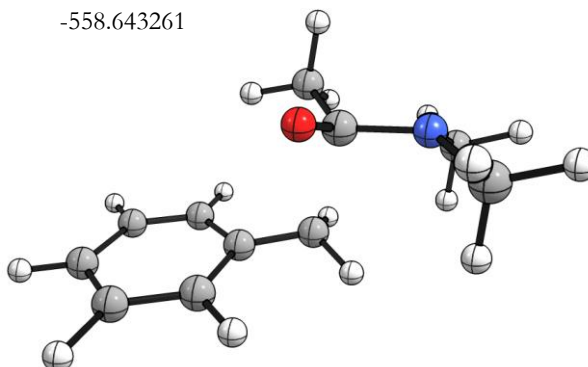
Sum of electronic and zero-point Energies= -558.603418

Sum of electronic and thermal Energies= -558.590146

Sum of electronic and thermal Enthalpies= -558.589202

Sum of electronic and thermal Free Energies= -558.643261

G + ZVPE = -558.396573

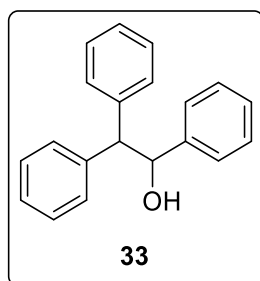


4.4.7.10 Photocatalytic benzylation of aromatic aldehydes

General procedure for the photocatalytic benzylation of aromatic aldehydes (General Procedure D)

A 5 mL crimp cap vial equipped with a magnetic stirring bar was loaded with 4CzIPN (2 mg, 2.5 μmol , 2.5 mol%), Cs_2CO_3 (48.9 mg, 150 μmol , 1.5 eq.) and the corresponding carboxylic acid (150 μmol , 1.5 eq.). The vial was set under inert conditions and dry DMF (2 mL) and the corresponding aldehyde or ketone (100 μmol , 1 eq.) were added *via* syringe. The reaction mixture was degassed by four cycles of freeze-pump-thaw and subsequently stirred under light irradiation using a 455 nm (\pm 25 nm) LED for 16 h at 25 $^\circ\text{C}$.

Four reaction batches were combined and diluted with H_2O (10 mL) and EtOAc (10 mL). The phases were separated and the aqueous phase was extracted with EtOAc (3 x 10 mL). The combined organic phases were washed with 2 M HCl (15 mL) and subsequently dried over Na_2SO_4 . The crude product was purified by automated flash column chromatography (PE/EtOAc, 0-20% EtOAc). If noted, the GC-yield was determined by GC-FID analysis using 1-naphthol as internal standard.

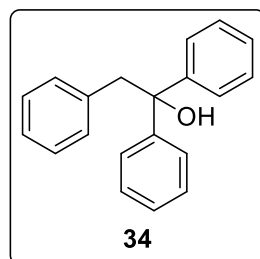
1,2,2-Triphenylethan-1-ol (33)^[24]

$^1\text{H-NMR}$ (300 MHz, CDCl_3 , δ_{H}): 7.45 – 7.05 (m, 15H), 5.41 (d, J = 8.8 Hz, 1H), 4.26 (d, J = 8.8, 1H).

$^{13}\text{C-NMR}$ (75 MHz, CDCl_3 , δ_{C}): 142.3, 141.6, 141.0, 129.1, 128.9, 128.7, 128.4, 128.2, 127.7, 127.1, 127.0, 126.5, 77.0, 60.5.

Yield: 71%

1,1,2-Triphenylethan-1-ol (**34**)^[43]

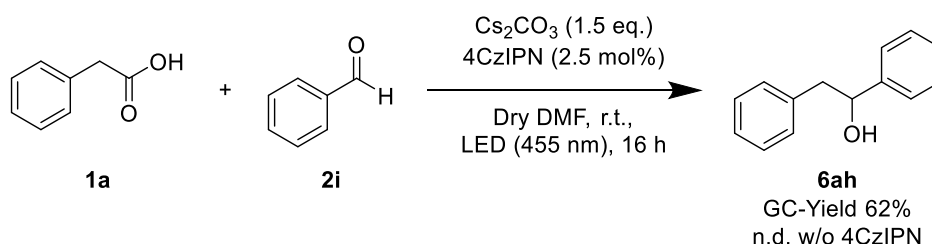


¹H-NMR (300 MHz, CDCl₃, δ_H): 7.48 – 7.12 (m, 13H), 6.95 – 6.88 (m, 2H), 3.67 (s, 2H), 2.34 (s, 1H).

¹³C-NMR (75 MHz, CDCl₃, δ_C): 146.7, 135.9, 131.0, 128.2, 128.2, 127.0, 126.9, 126.3, 78.0, 48.1.

Yield: 27%

1,2-Diphenylethan-1-ol (**6ah**) could be formed as well. Only the GC-yield was determined in this case (Scheme 4-12).

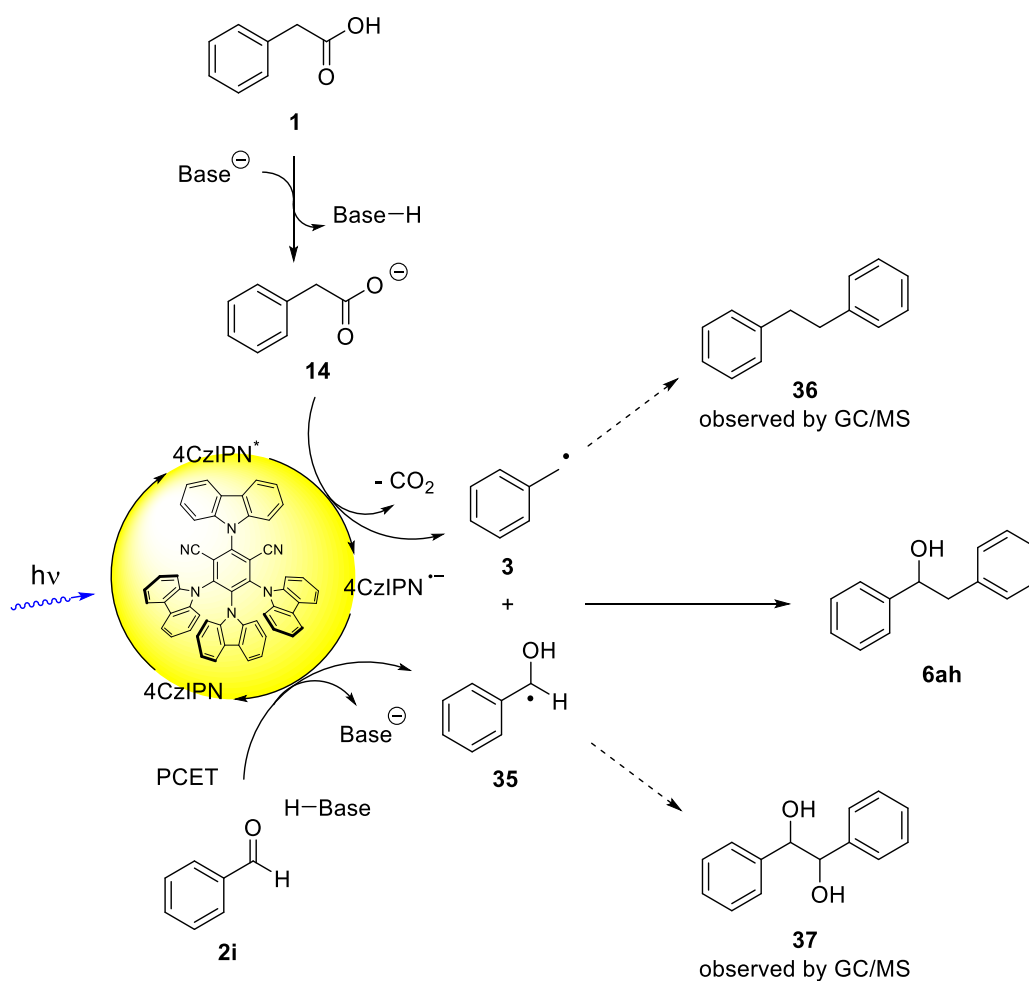


Scheme 4-12 – Benzylation of benzaldehyde (**2i**) with phenylacetic acid (**1a**).

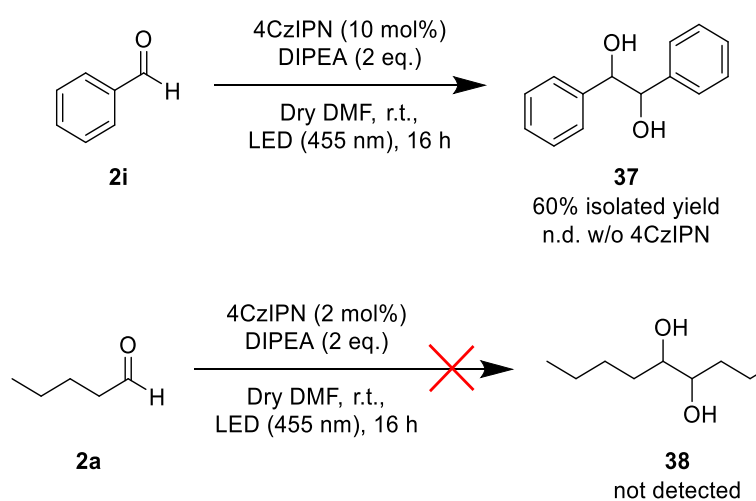
Proposed mechanism for the photocatalytic benzylation of aromatic aldehydes

When employing aromatic instead of aliphatic aldehydes, the corresponding coupling product can be formed as well, yet a radical-radical cross-coupling similar to our previously reported procedure^[12] is the likely pathway (Scheme 4-13). Observations supporting a radical-radical cross coupling mechanism are the formation of the corresponding homocoupling products **36** and **37** detected by GC/FID and GC/MS in several reactions in the brief optimization process. Furthermore, 4CzIPN is a viable photocatalyst for the pinacol homocoupling of benzaldehyde (**2i**) ($E_{1/2}^{\text{red}} = -1.93 \text{ V vs SCE}^{[15]}$) with DIPEA as electron donor (Scheme 4-14, upper).^[44] An analogous reaction is not possible with *n*-pentanal (**2a**) ($E_{1/2}^{\text{red}}(\text{3-methylbutanal } \mathbf{2g}) = -2.24 \text{ V vs SCE}^{[15]}$) (Scheme 4-14, lower).

Thus aromatic aldehydes (or ketones) were not included in the substrate scope, although the corresponding products can be formed under the same conditions.



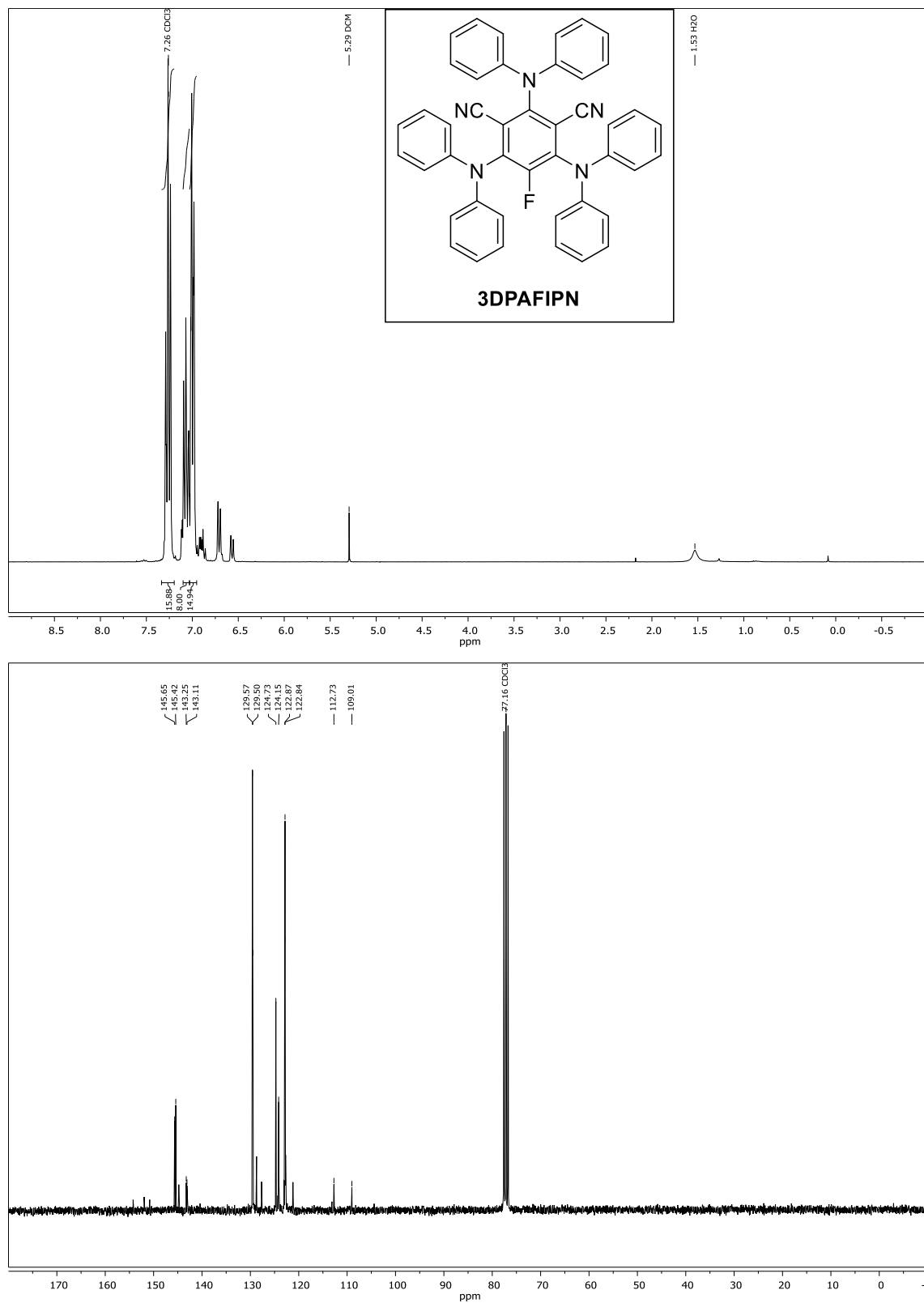
Scheme 4-13 – Proposed mechanism for the benzylation of aromatic aldehydes.

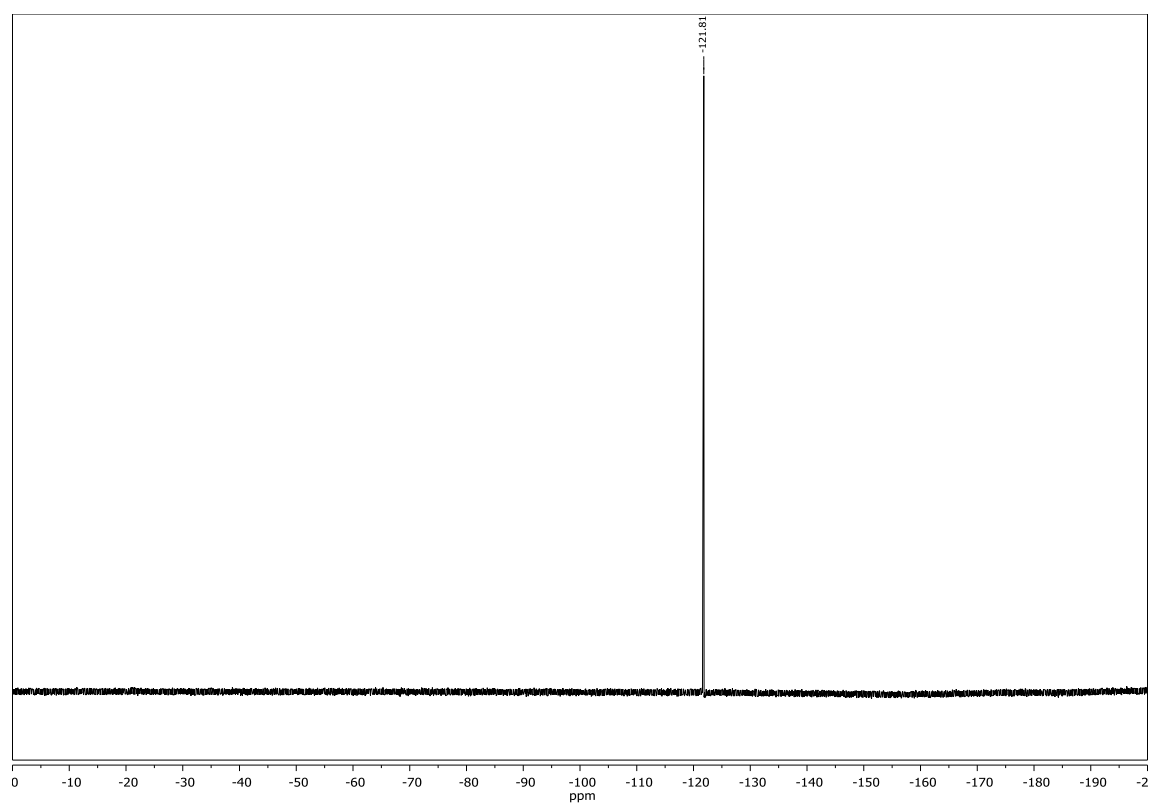


Scheme 4-14 – Photocatalytic pinacol reaction of benzaldehyde (**2i**) (upper) and *n*-pentanal (**2a**) (lower) with 4CzIPN as catalyst.

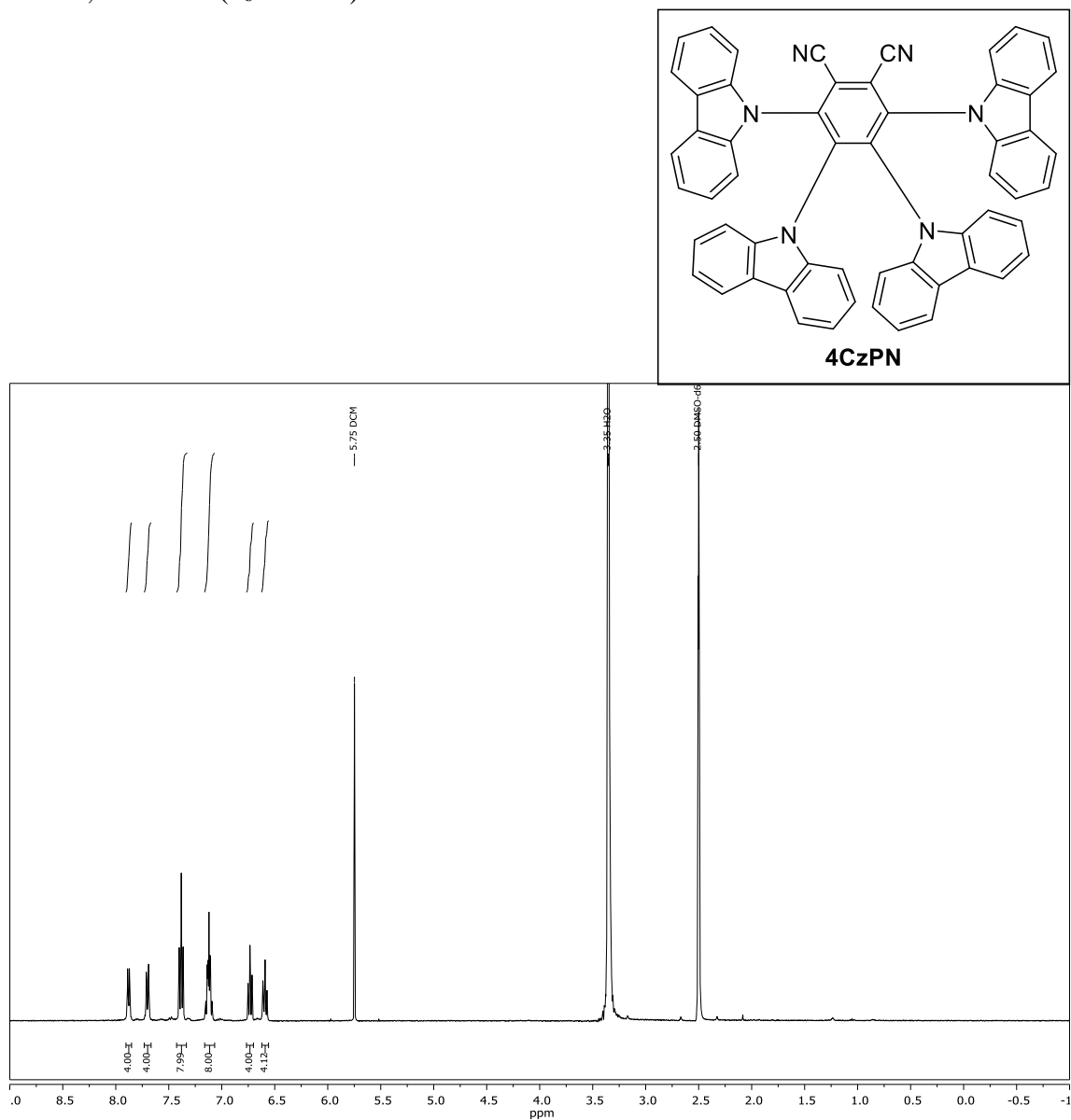
4.5 NMR-spectra

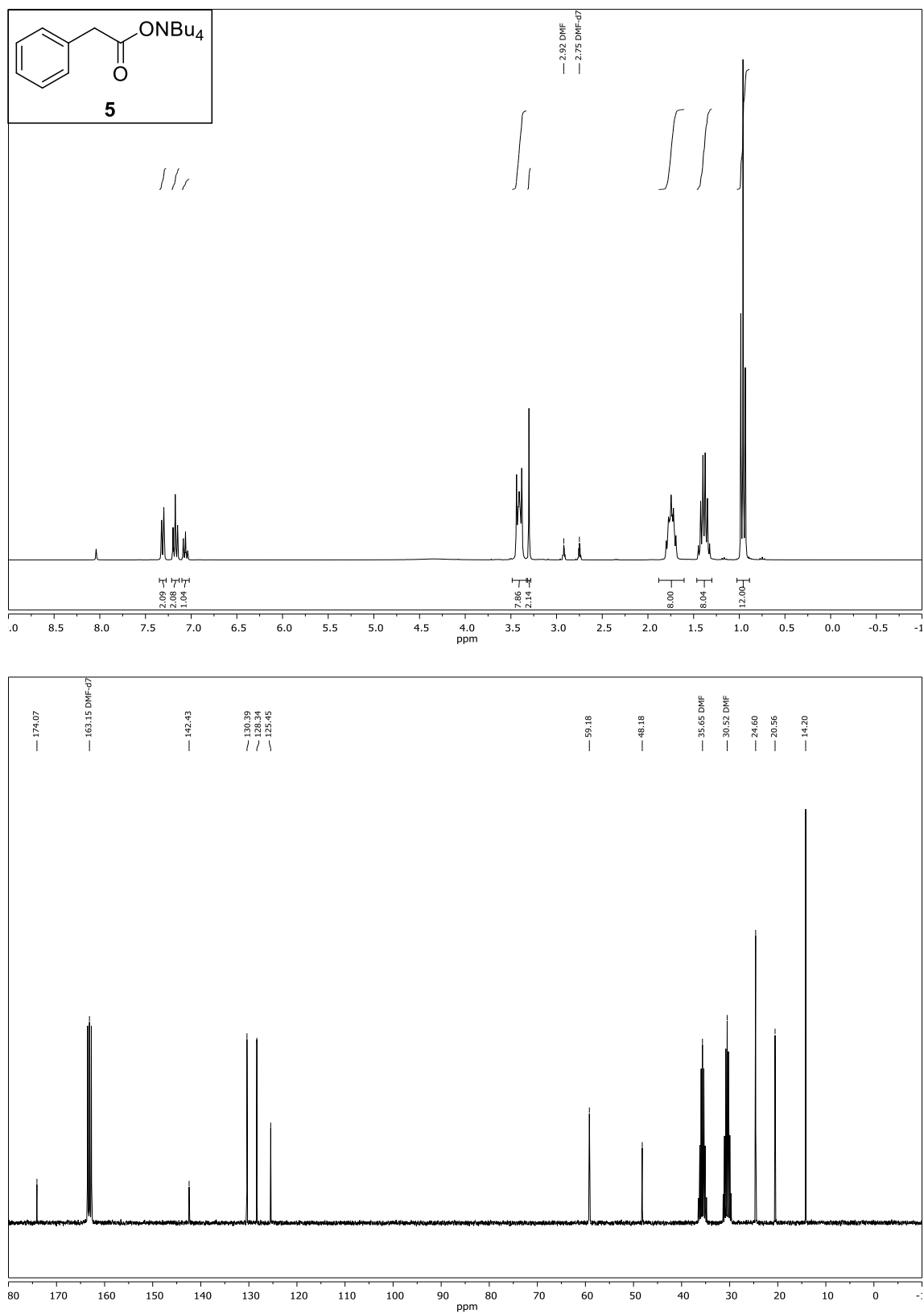
3DPAFIPN, ^1H -, ^{13}C -NMR and ^{19}F -NMR (CDCl_3)



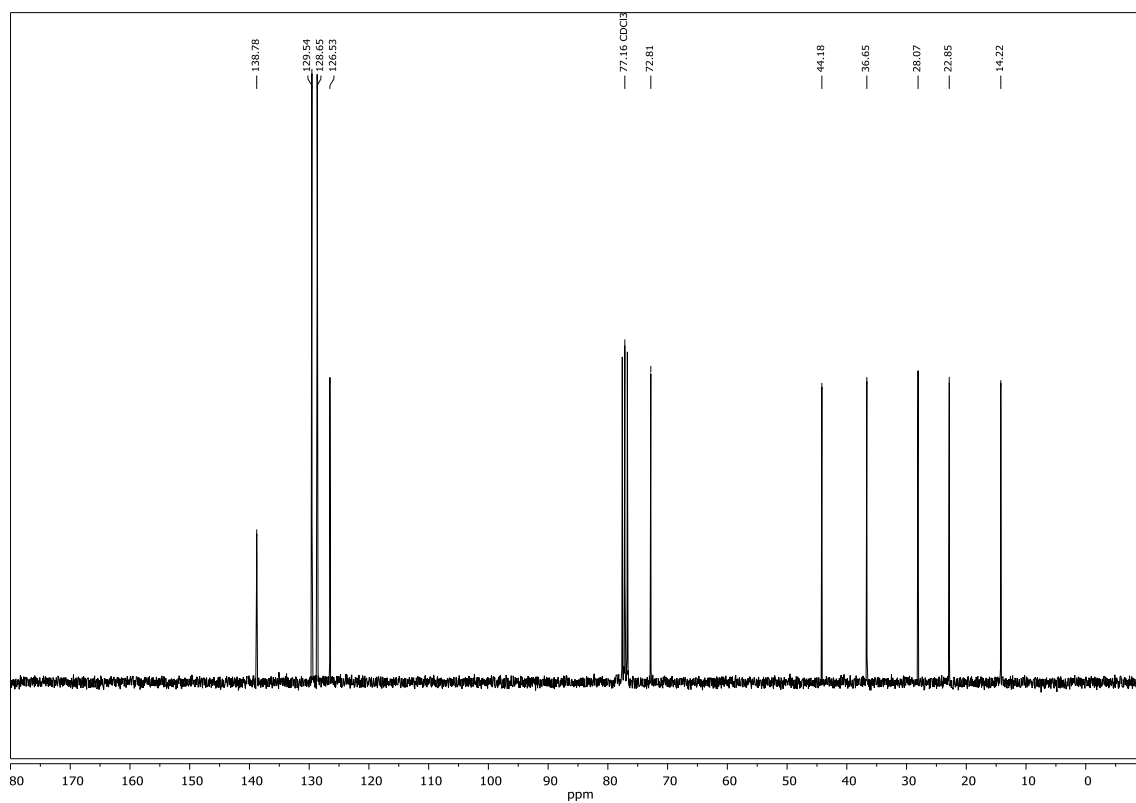
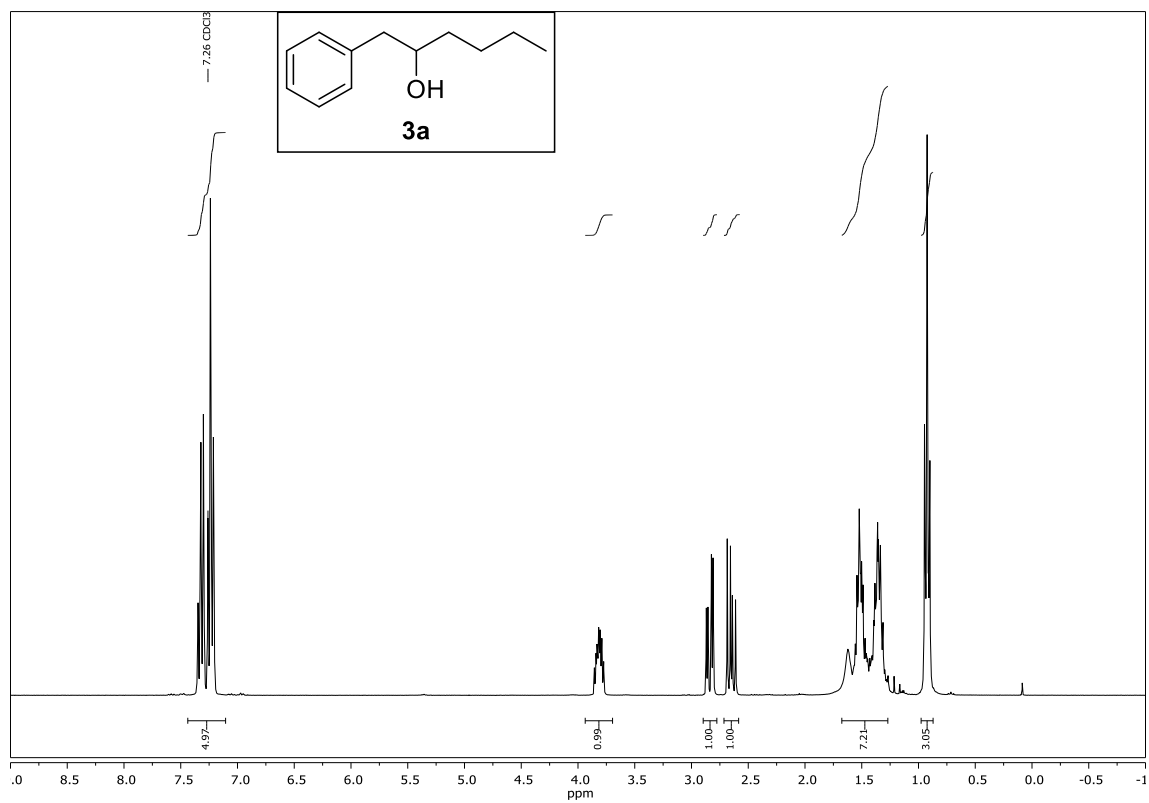


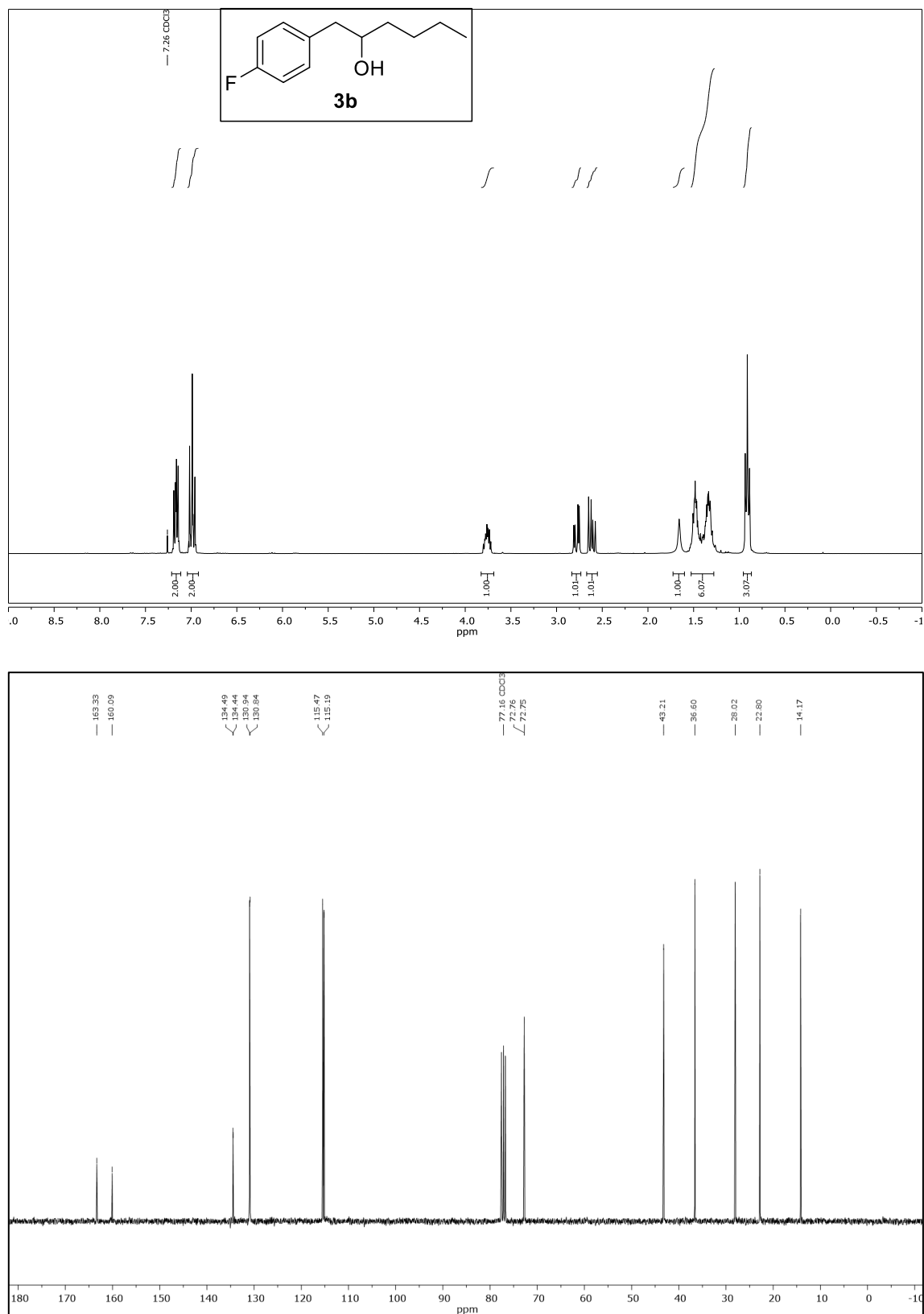
4CzPN, ^1H -NMR (d_6 -DMSO)

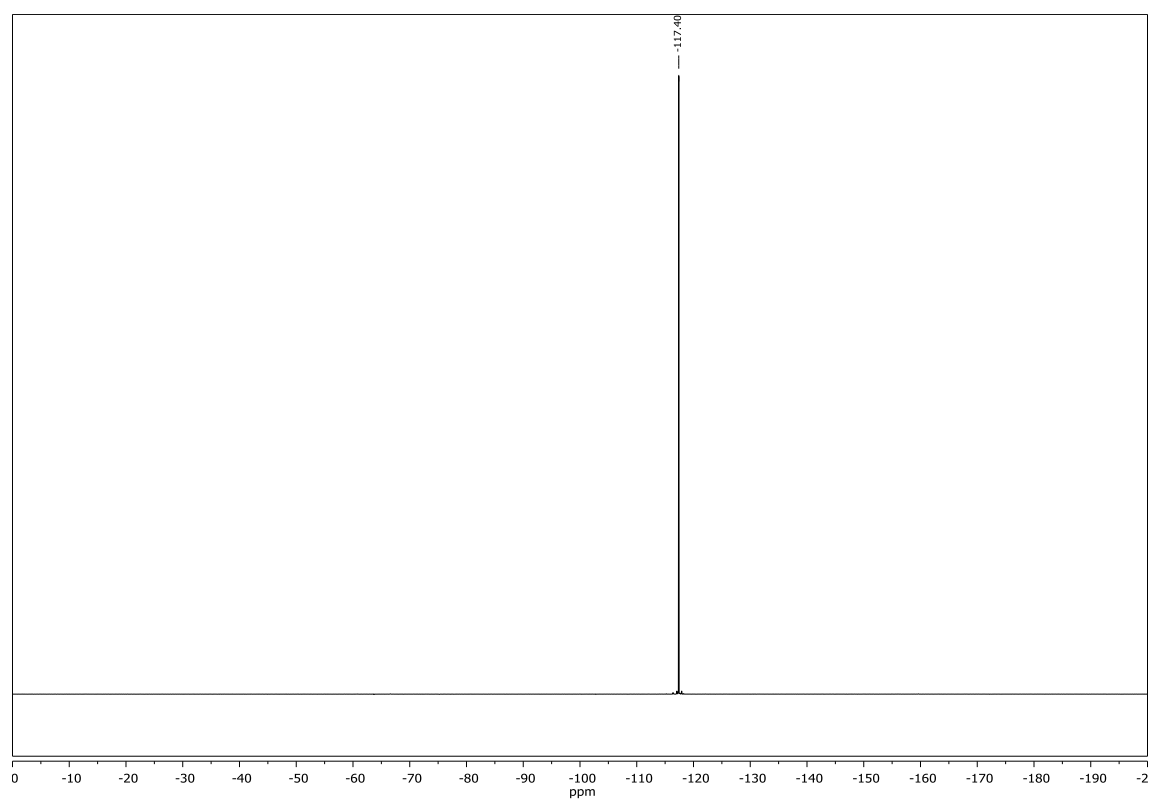


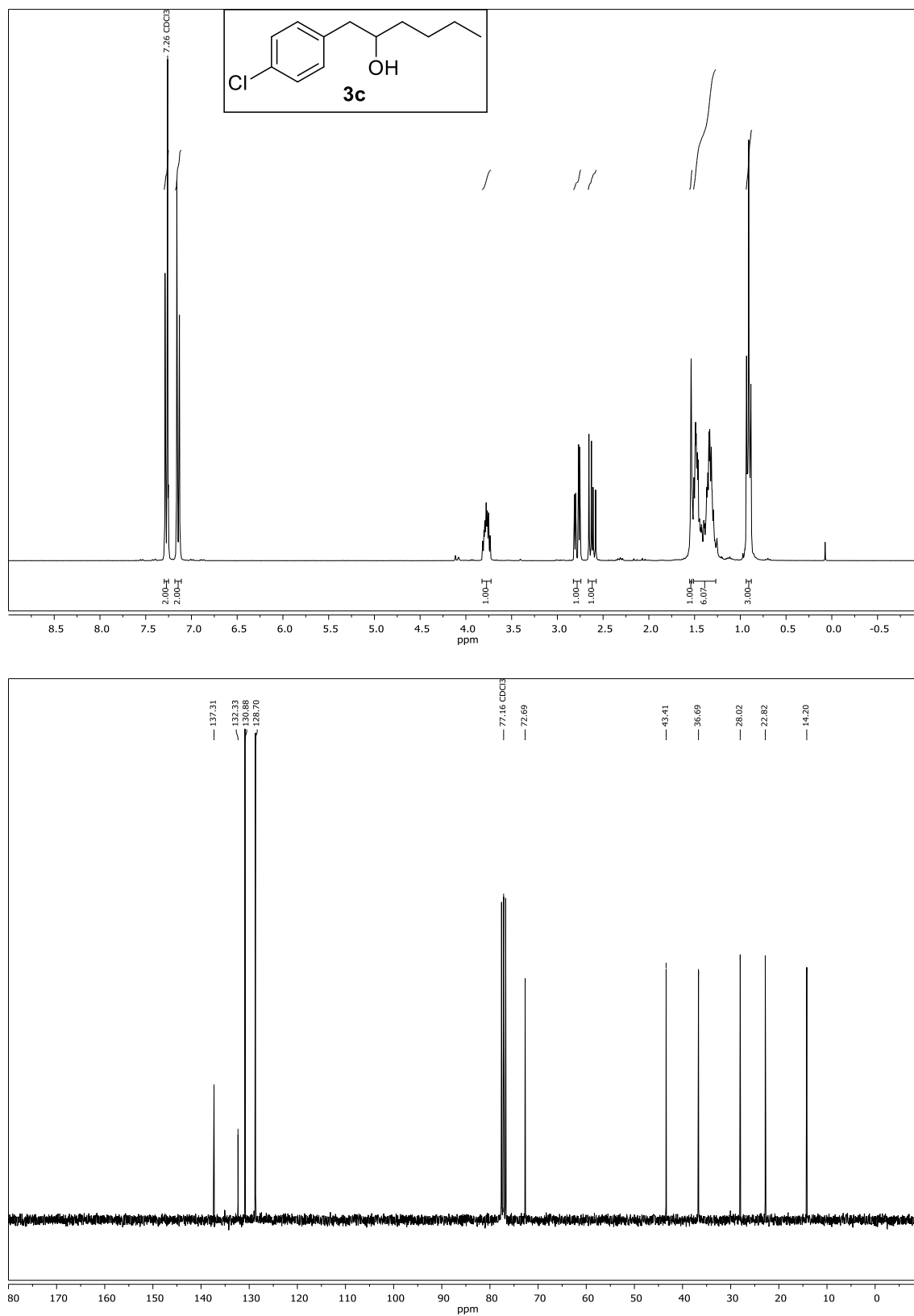
Compound **5**, ^1H - and ^{13}C -NMR (CDCl_3)

Compound **3a**, ^1H - and ^{13}C -NMR (CDCl_3)

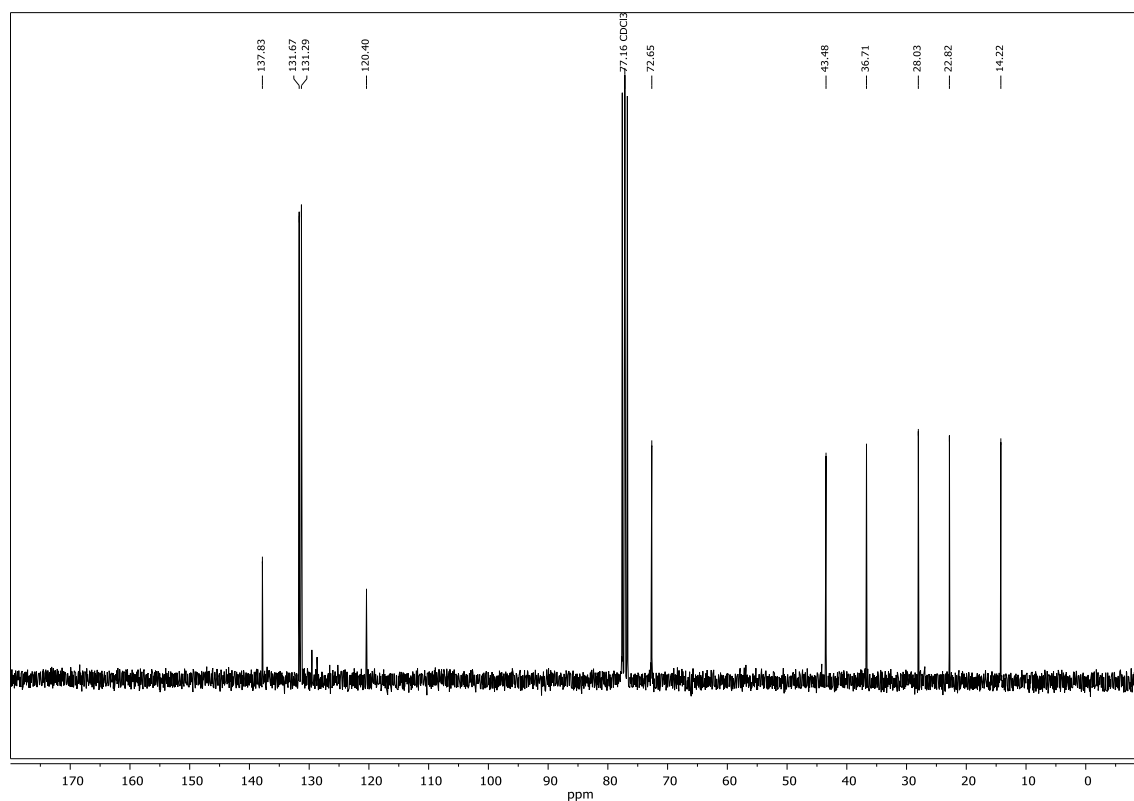
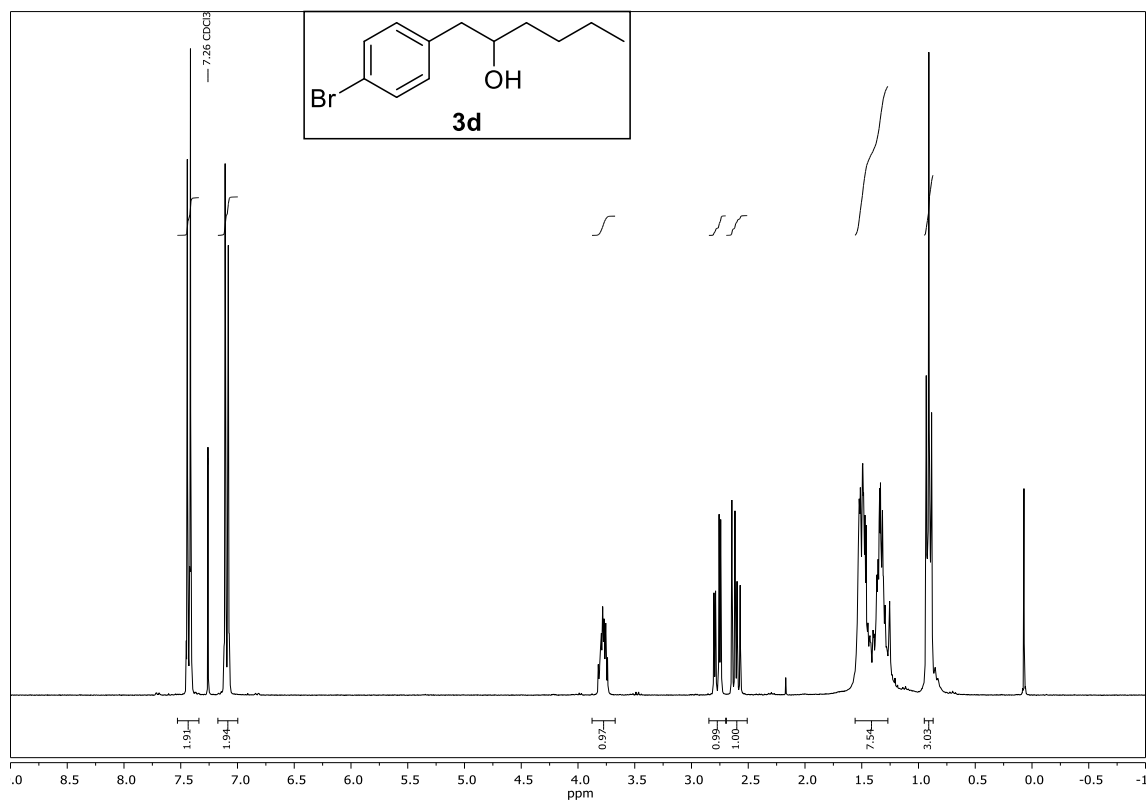


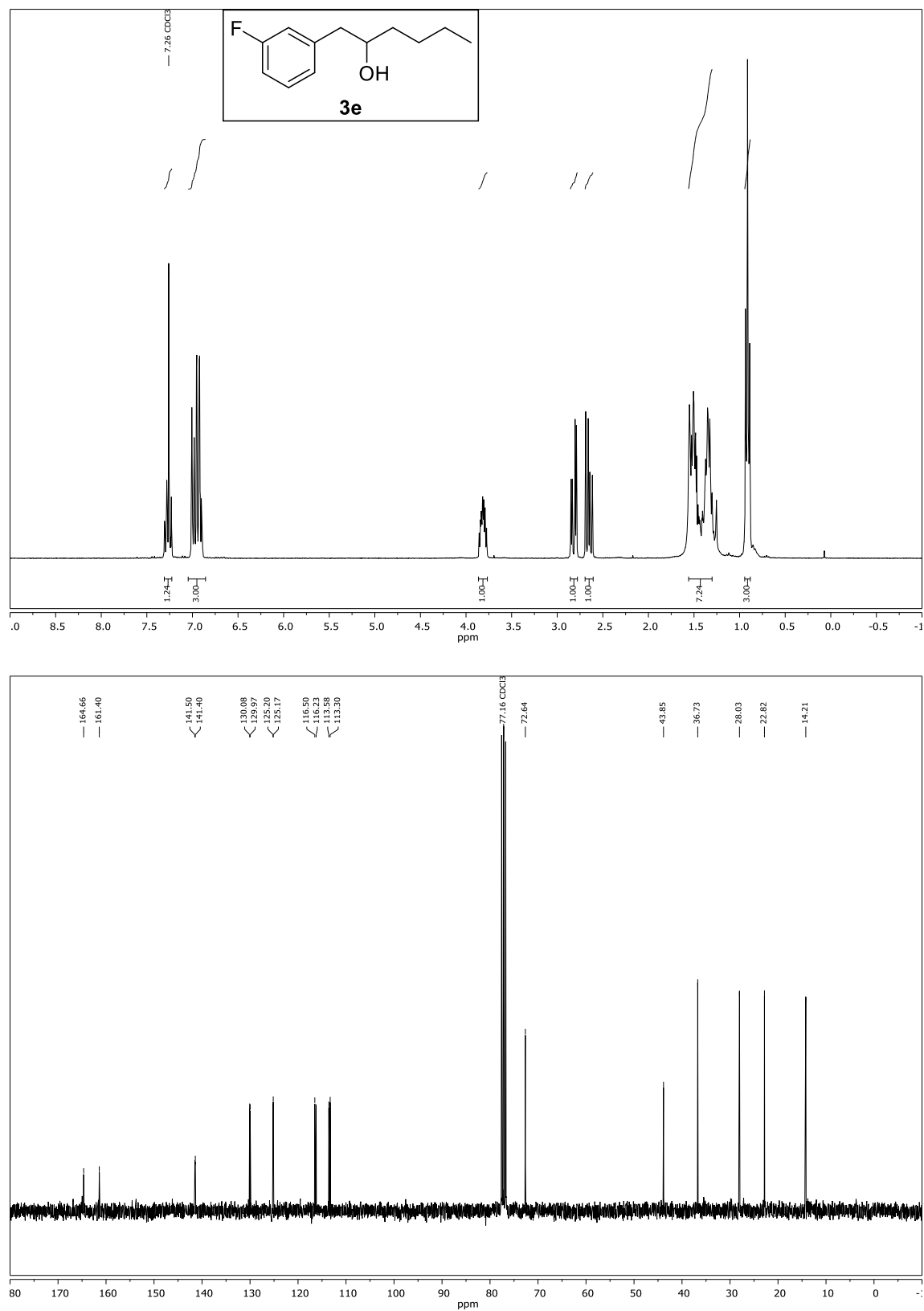
Compound **3b**, ^1H -, ^{13}C -NMR and ^{19}F -NMR (CDCl_3)

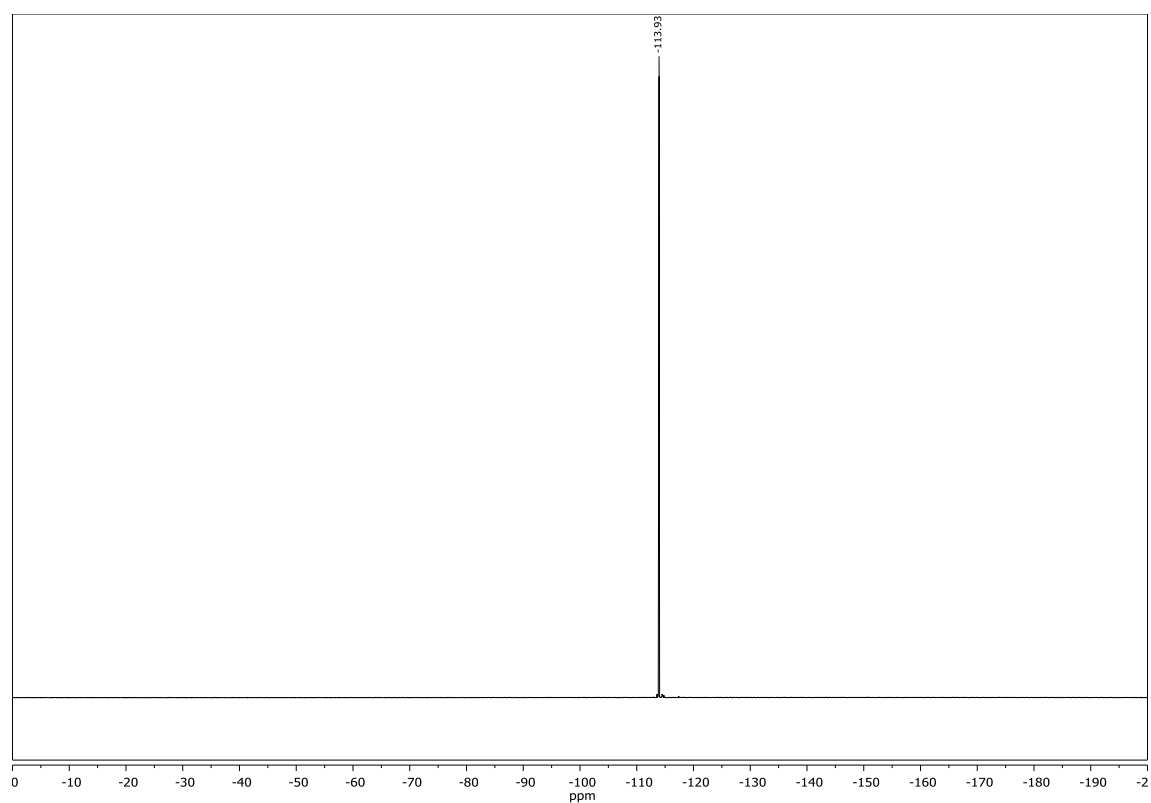


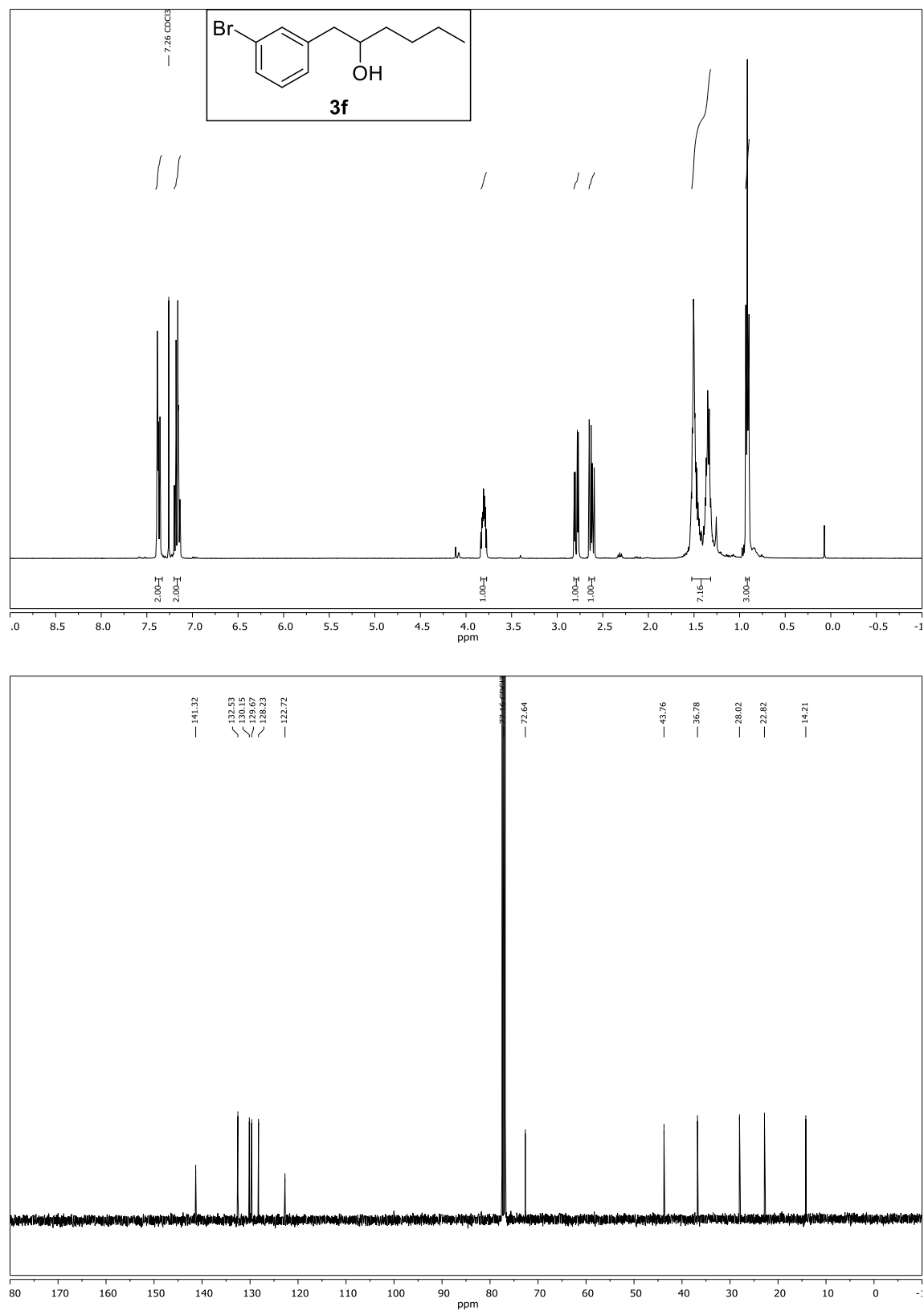
Compound **3c**, ^1H - and ^{13}C -NMR (CDCl_3)

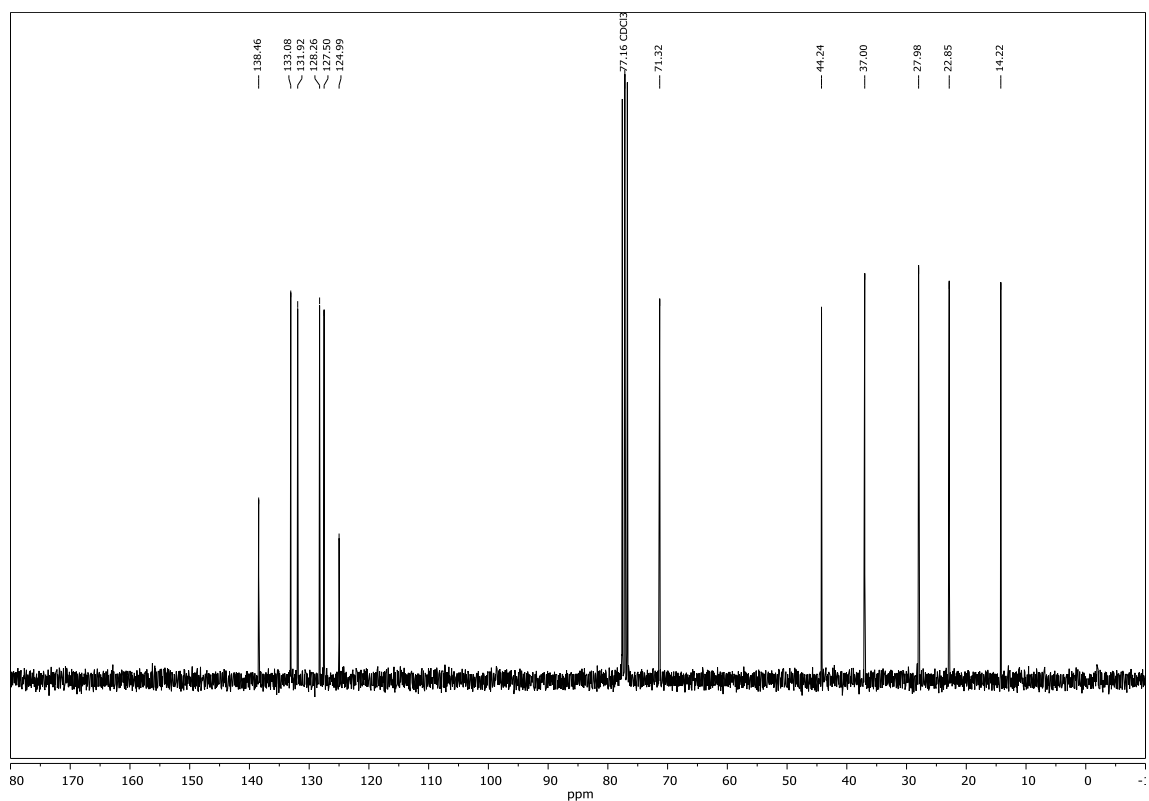
Compound **3d**, ^1H - and ^{13}C -NMR (CDCl_3)

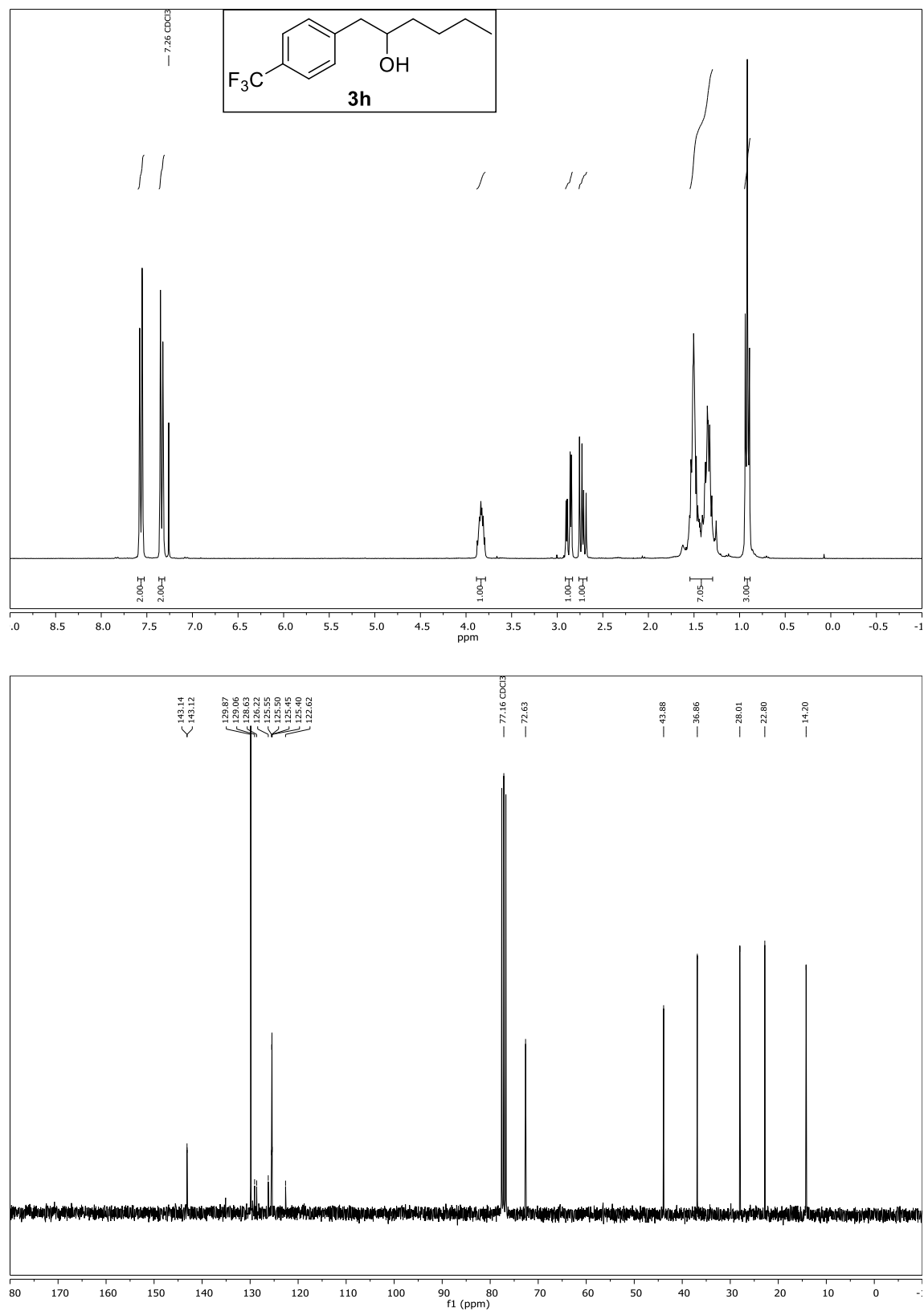


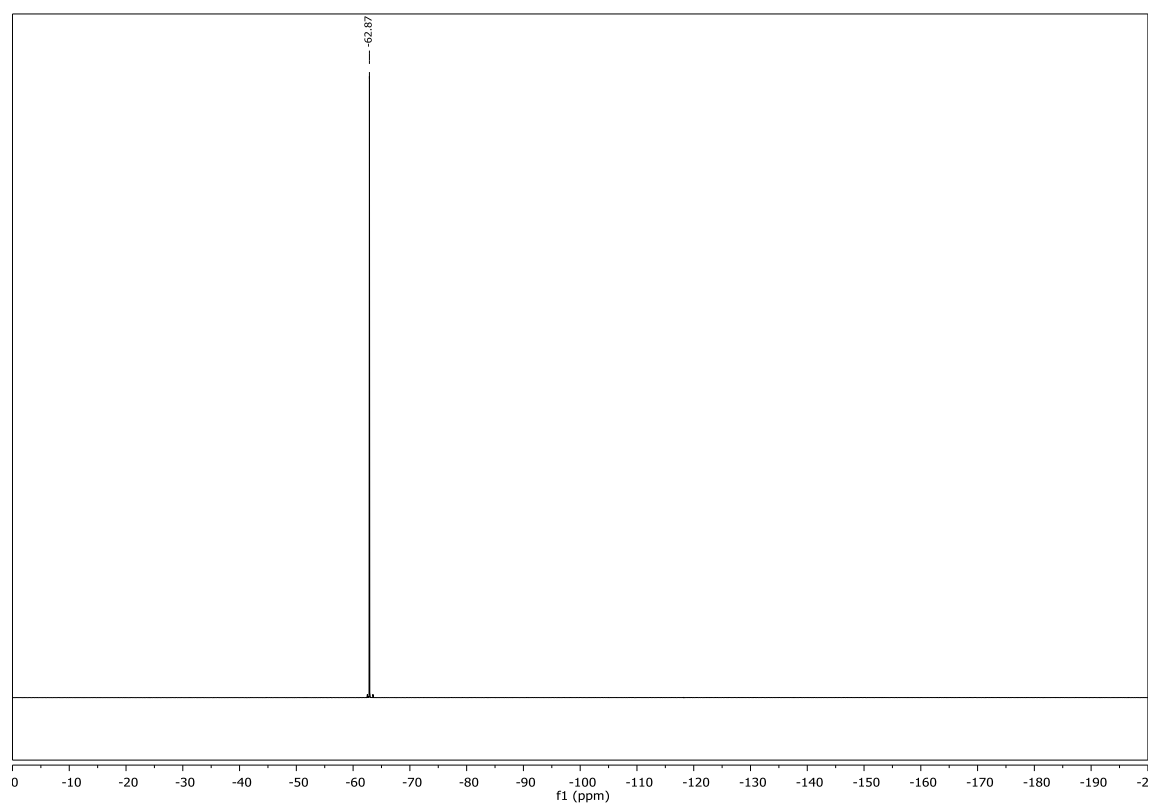
Compound **3e**, ^1H -, ^{13}C -NMR and ^{19}F -NMR (CDCl_3)

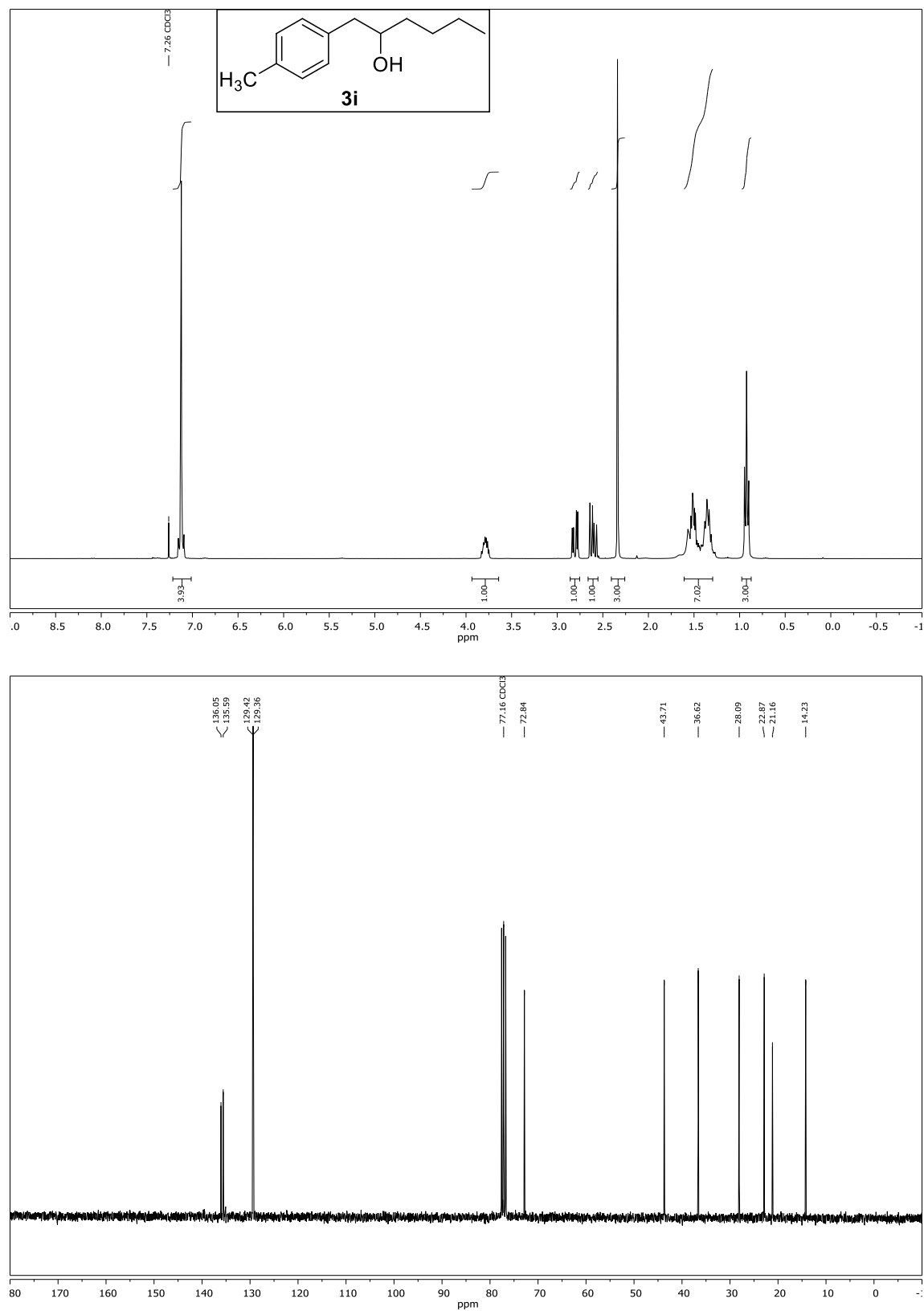


Compound **3f**, ^1H - and ^{13}C -NMR (CDCl_3)

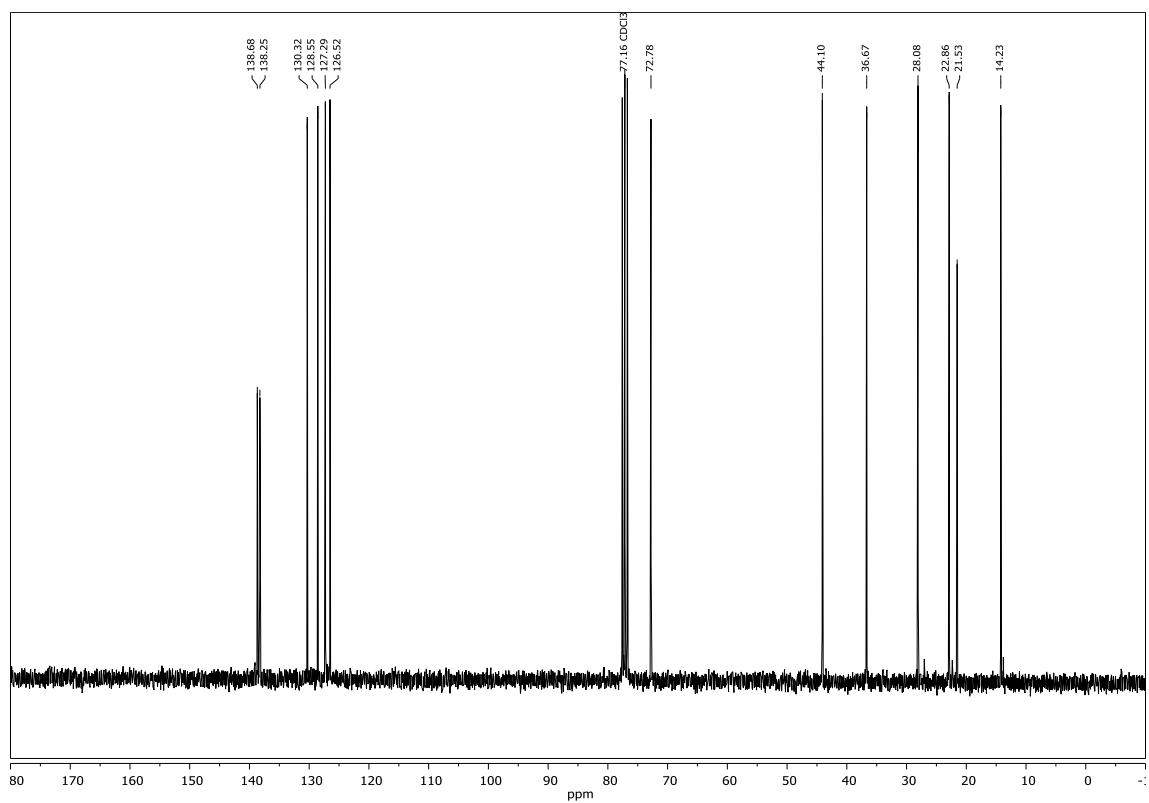
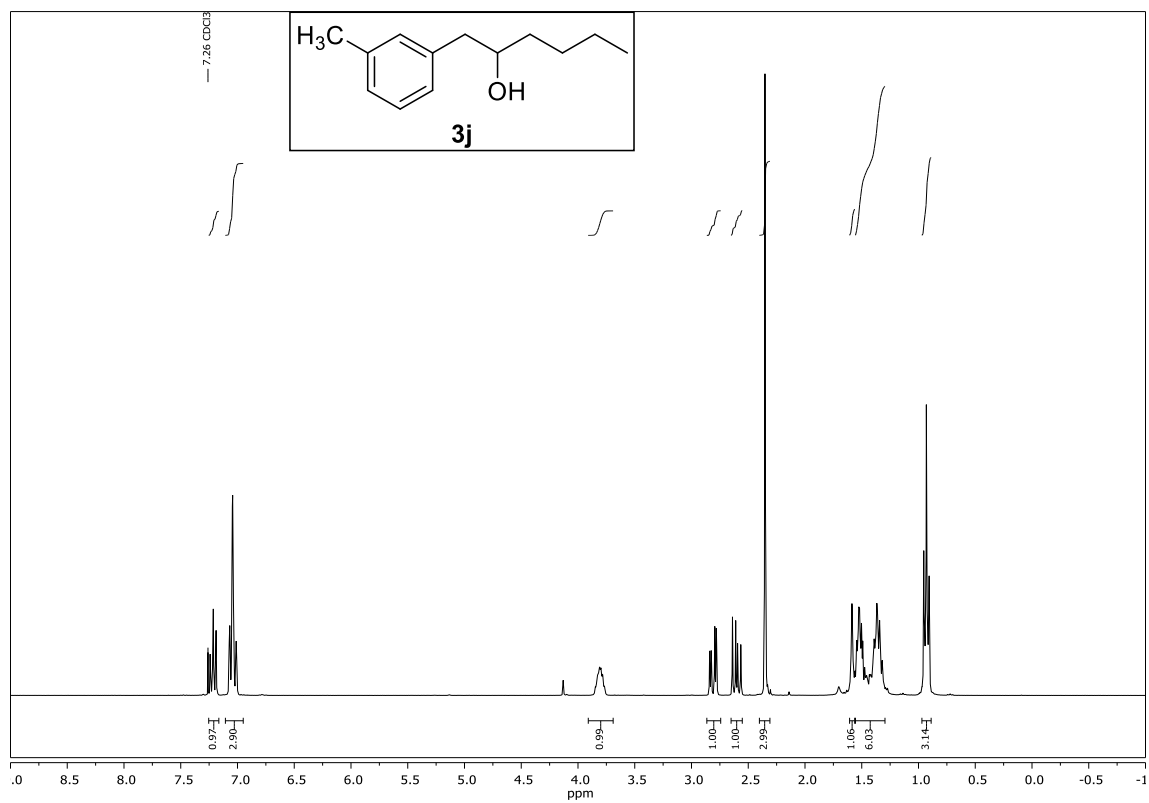


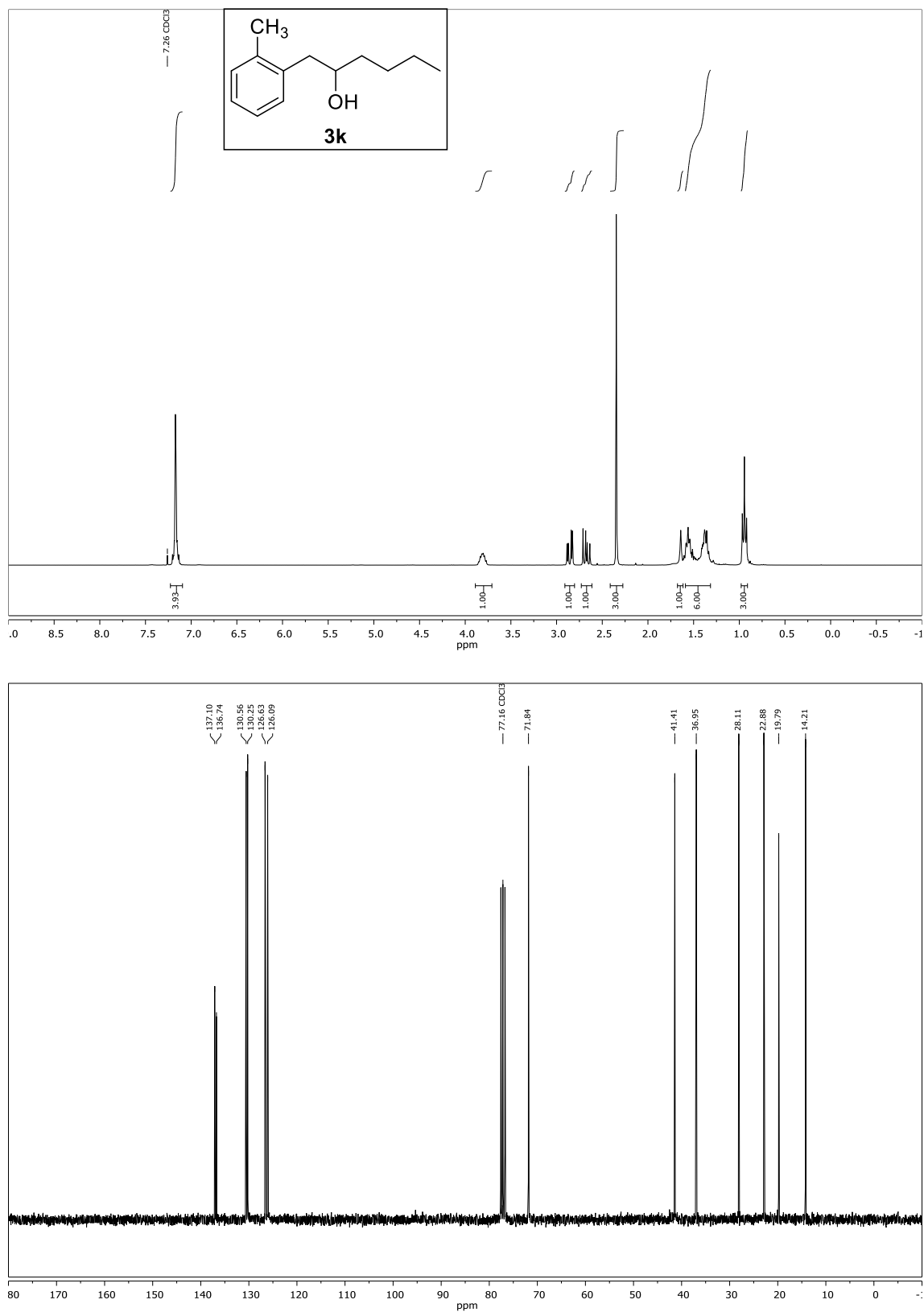
Compound **3h**, ^1H -, ^{13}C -NMR and ^{19}F -NMR (CDCl_3)



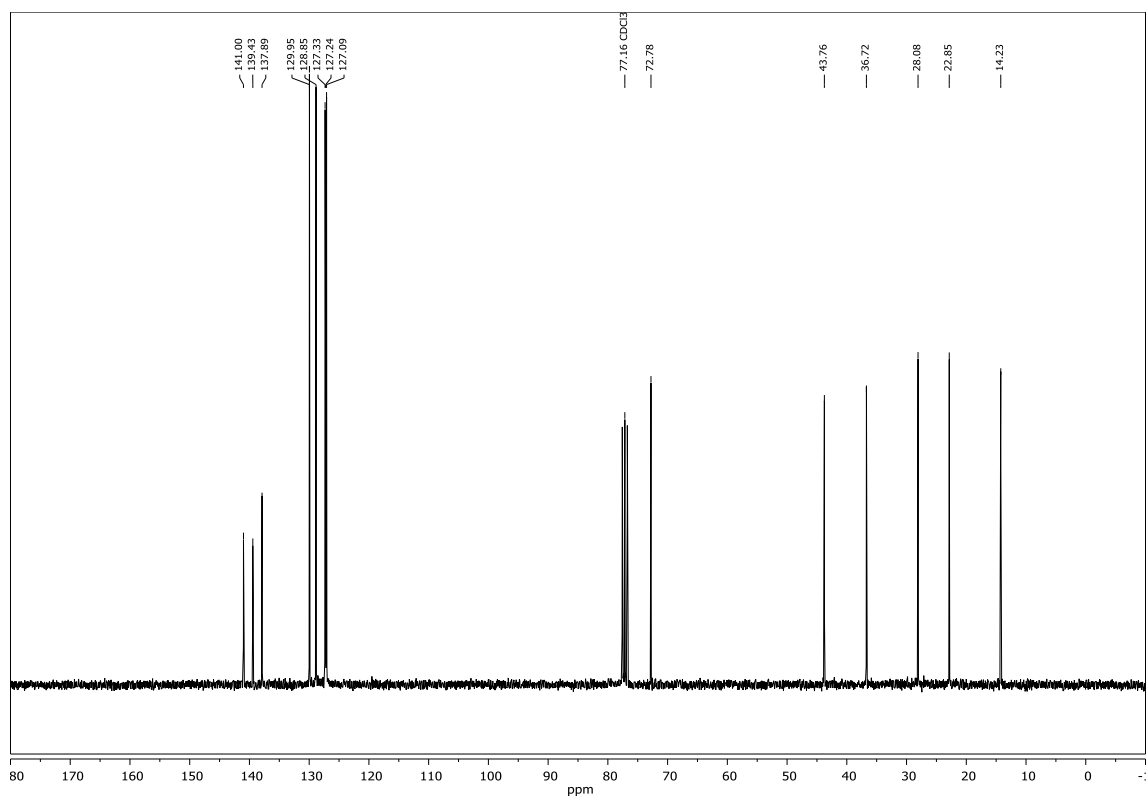
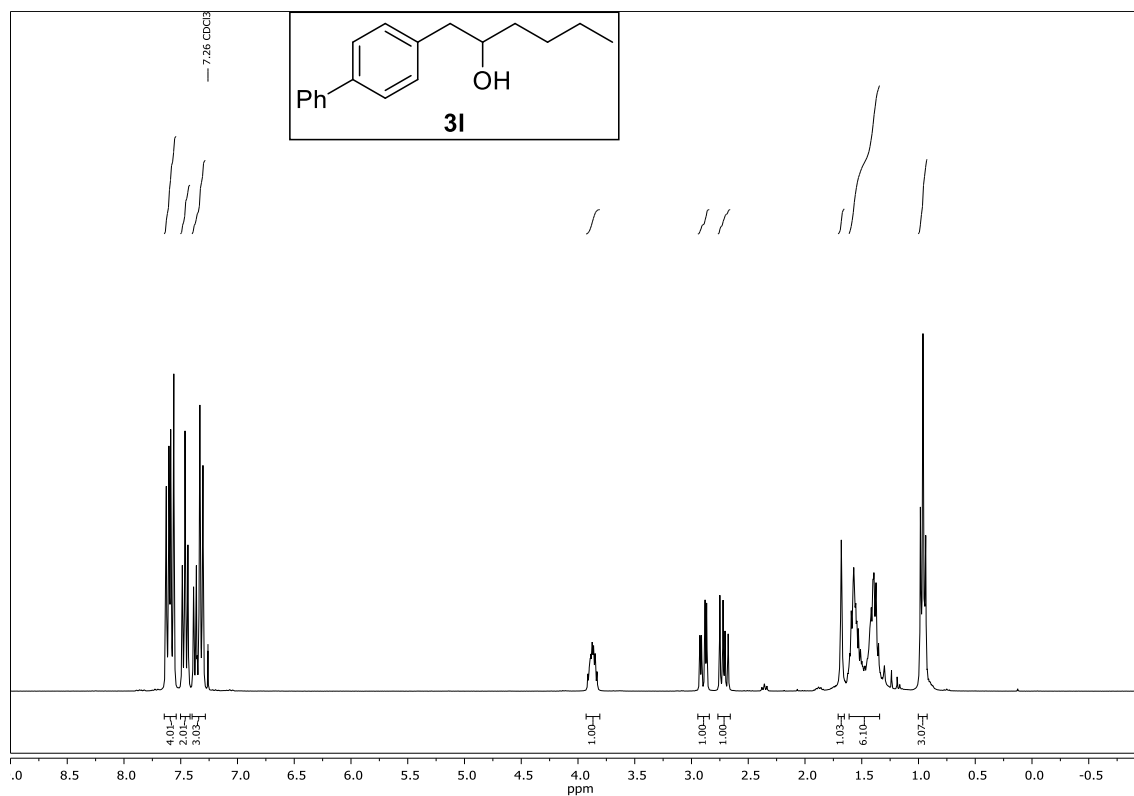
Compound **3i**, ^1H - and ^{13}C -NMR (CDCl_3)

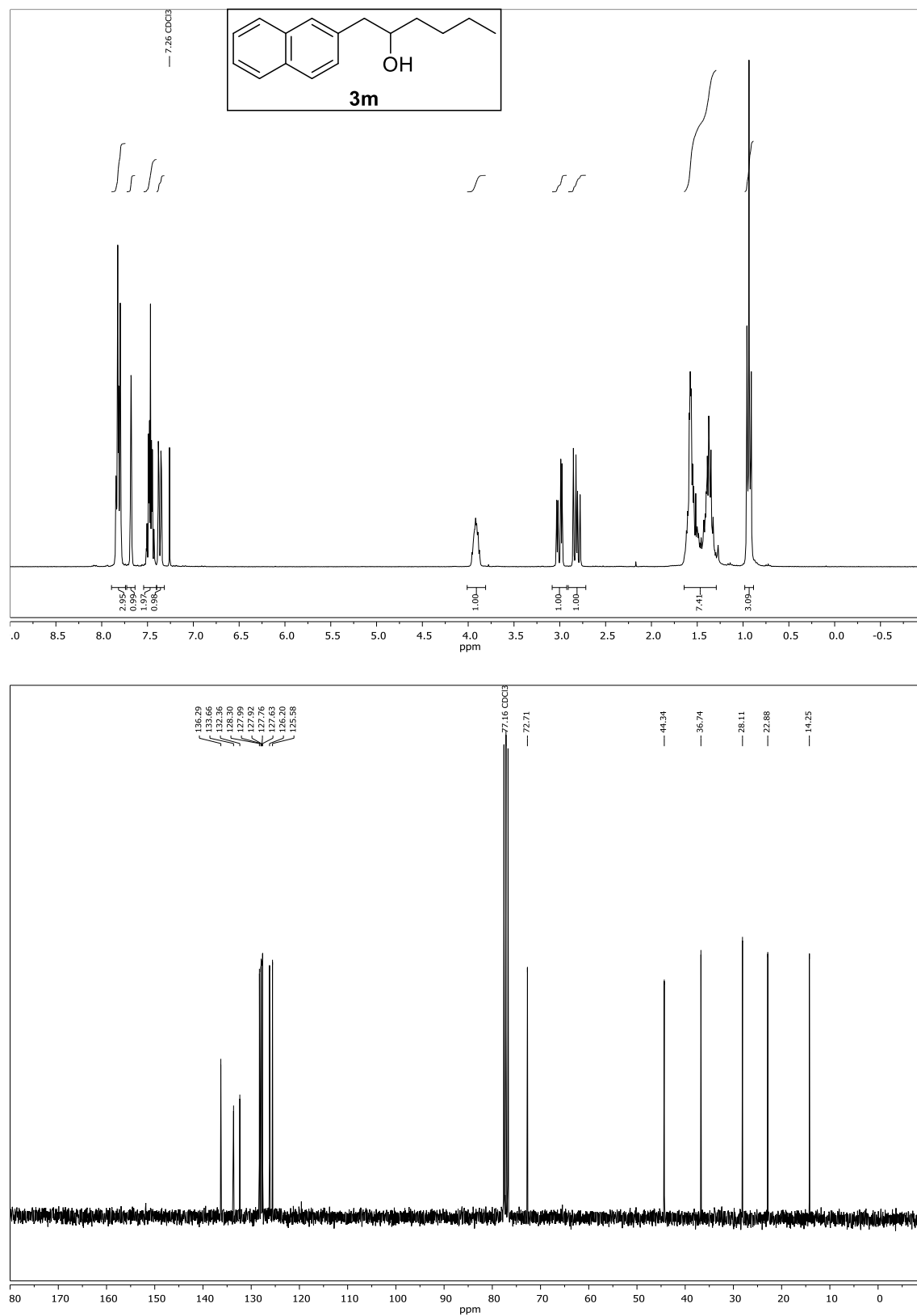
Compound **3j**, ^1H - and ^{13}C -NMR (CDCl_3)



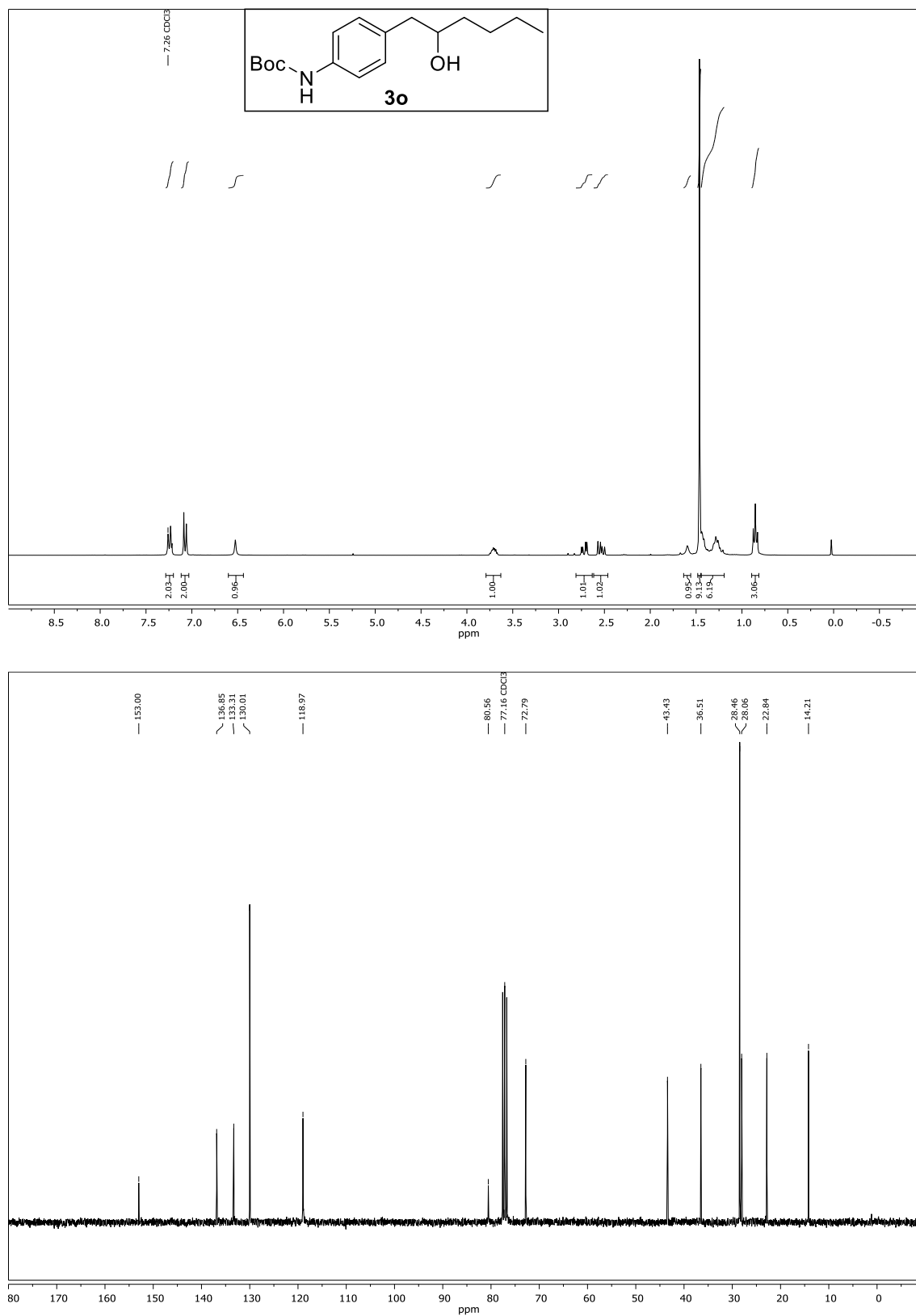
Compound **3k**, ^1H - and ^{13}C -NMR (CDCl_3)

Compound **3l**, ^1H - and ^{13}C -NMR (CDCl_3)

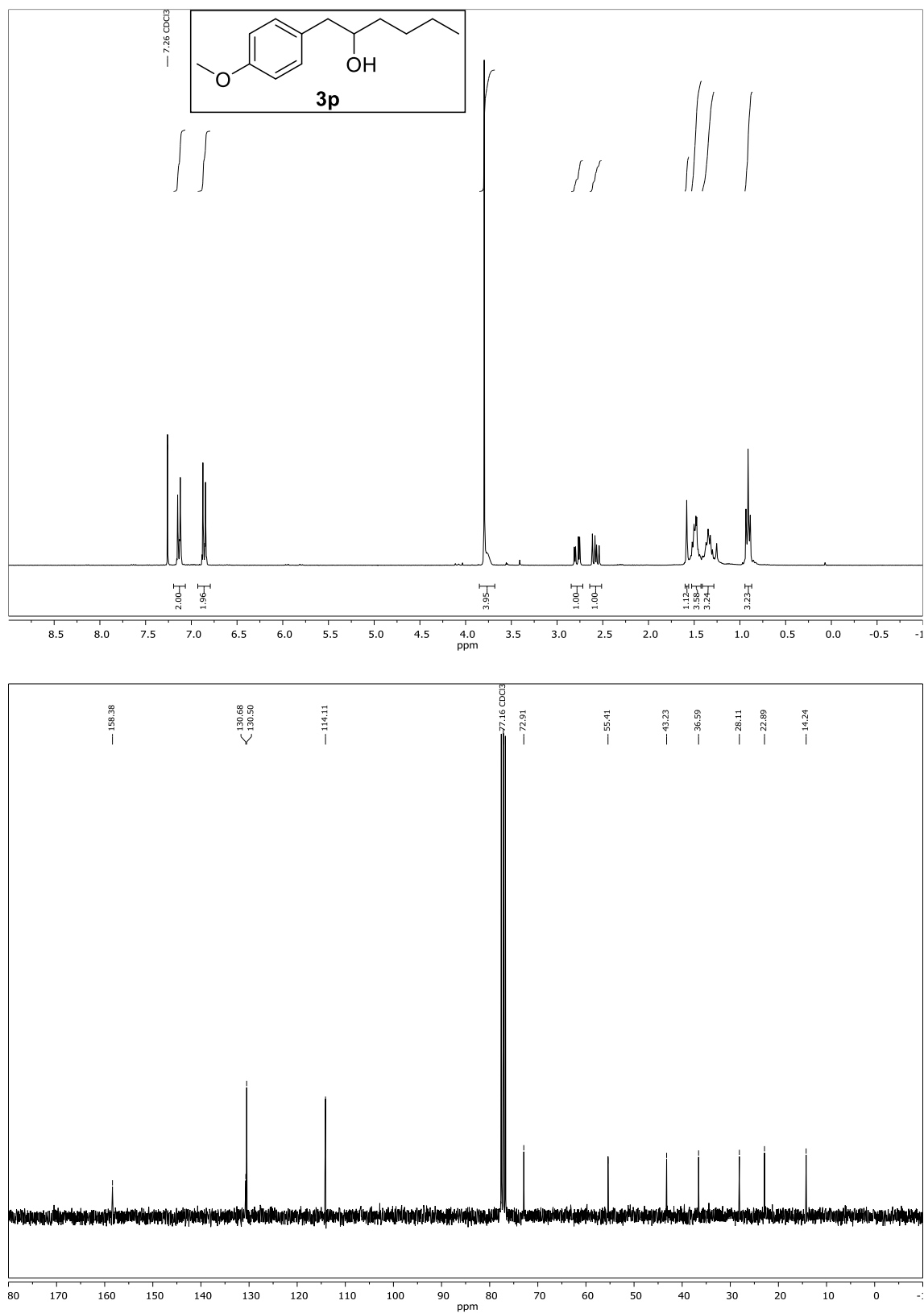


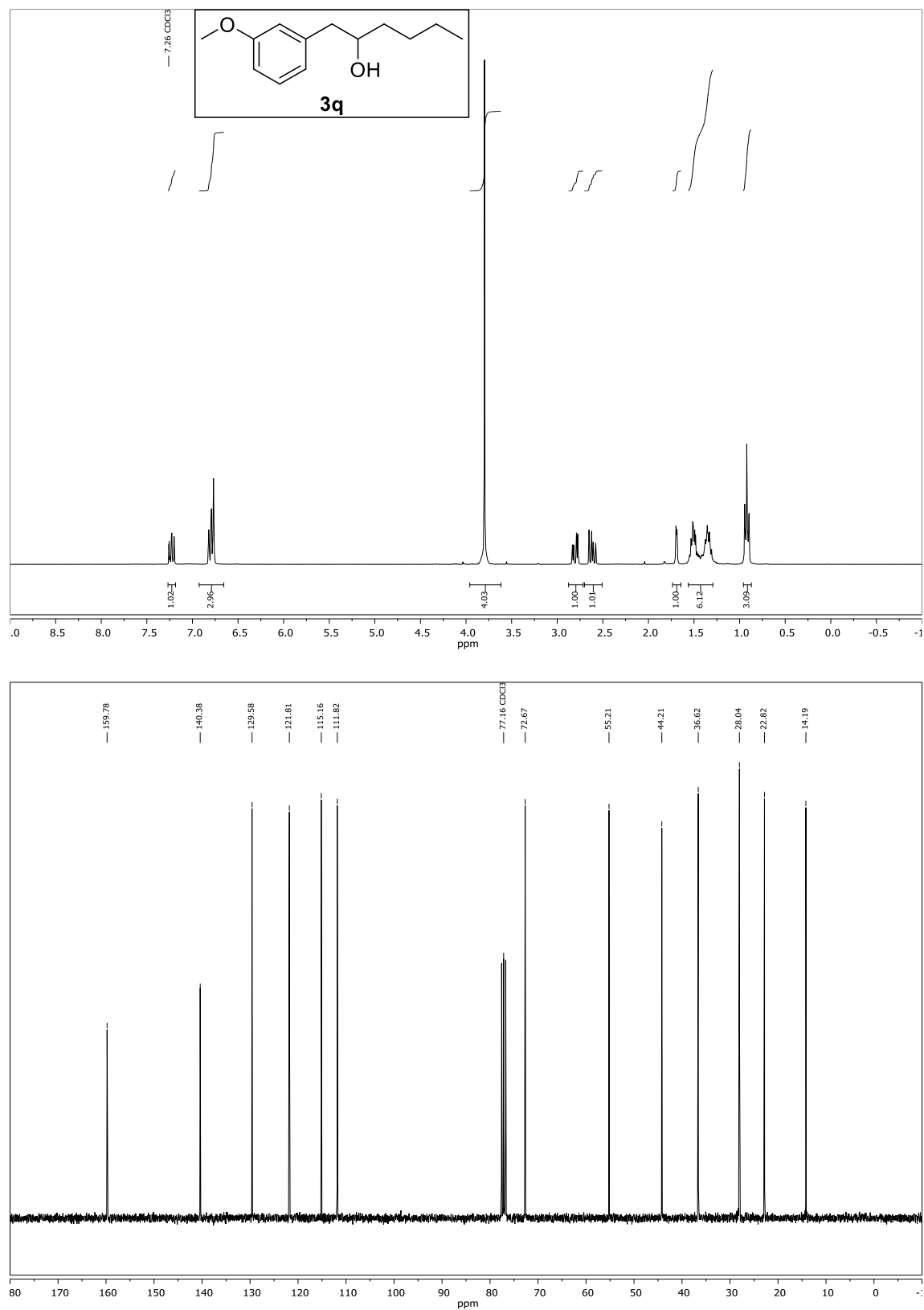
Compound **3m**, ^1H - and ^{13}C -NMR (CDCl_3)



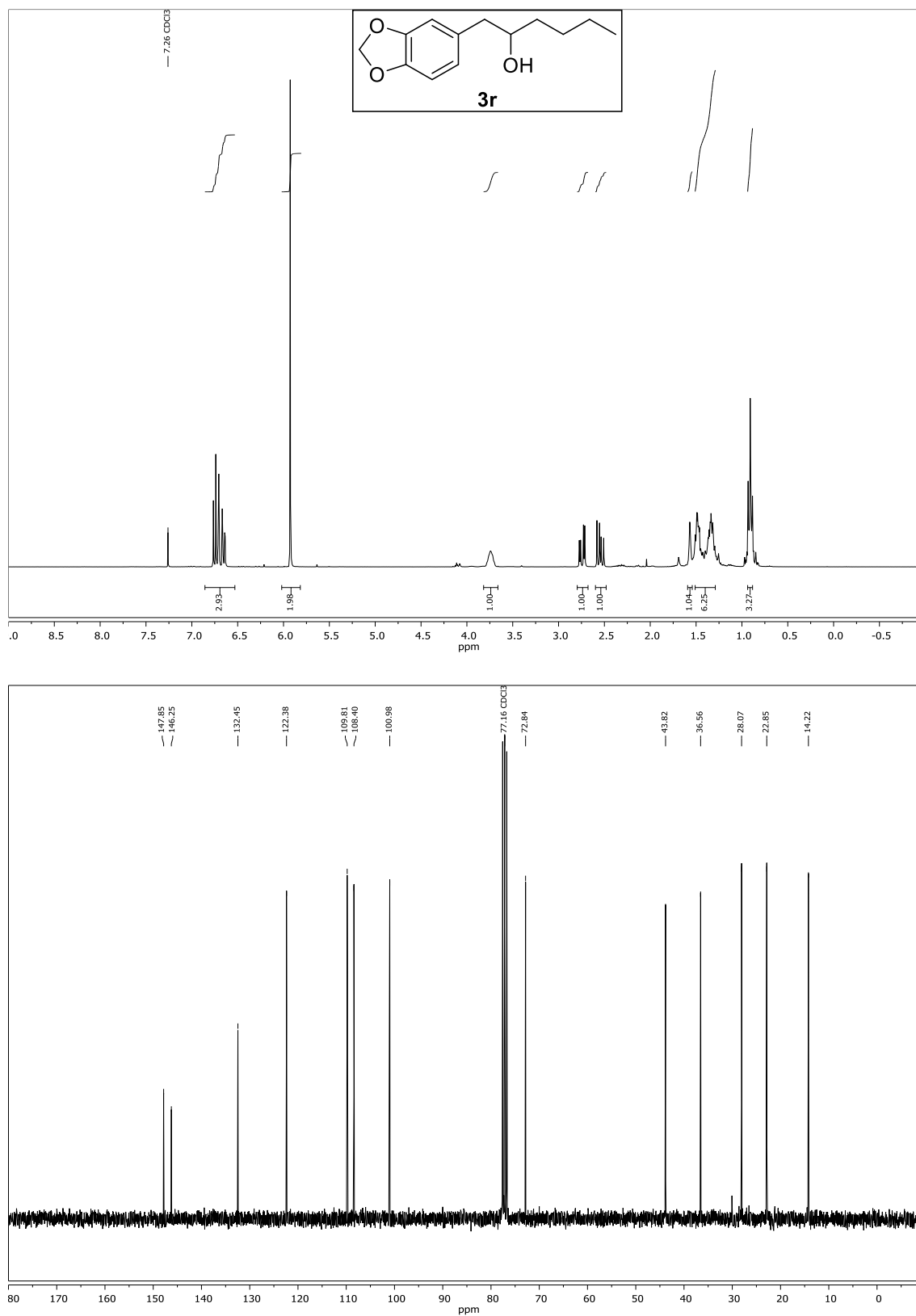
Compound **3o**, ^1H - and ^{13}C -NMR (CDCl_3)

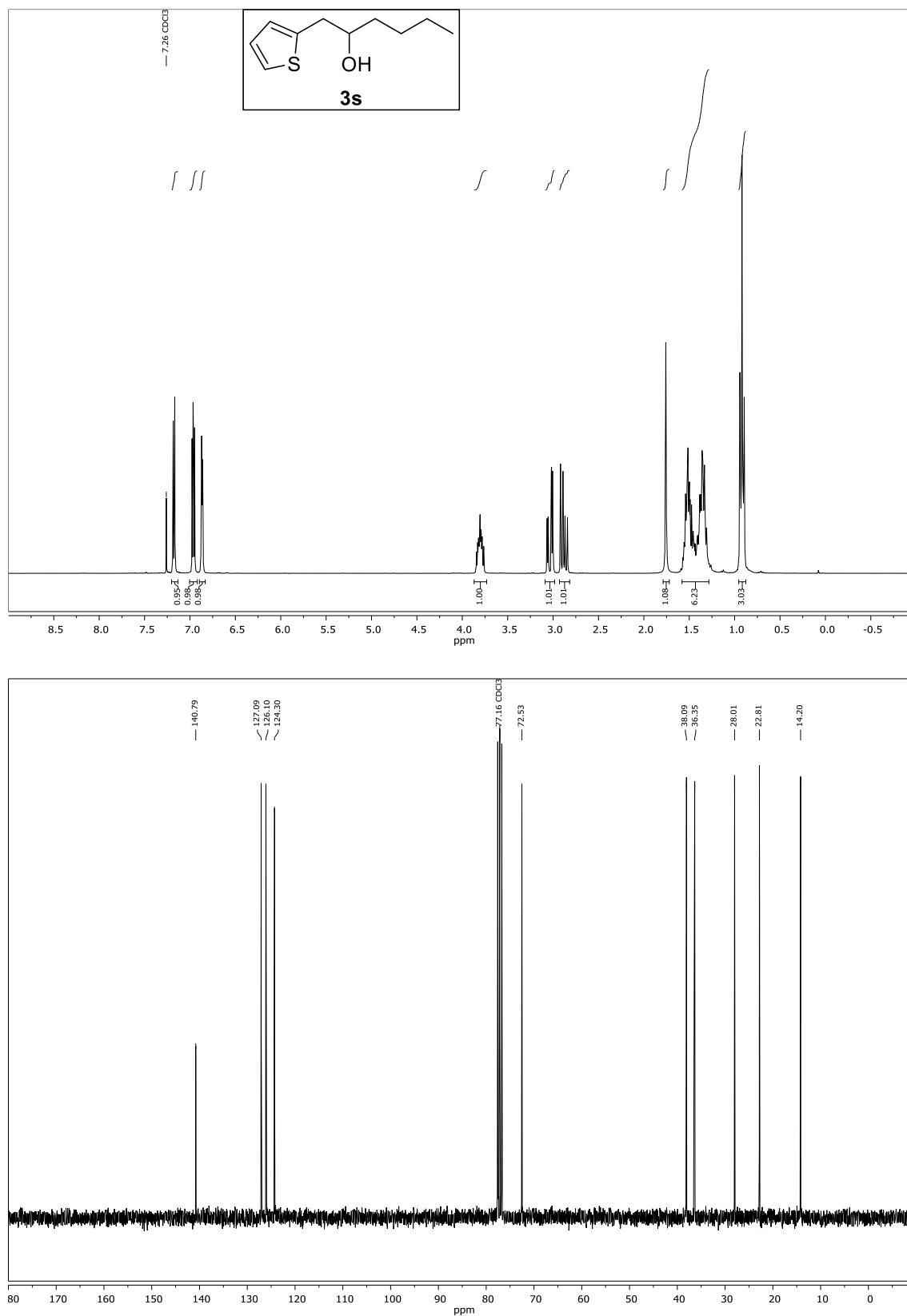
Compound **3p**, ^1H - and ^{13}C -NMR (CDCl_3)



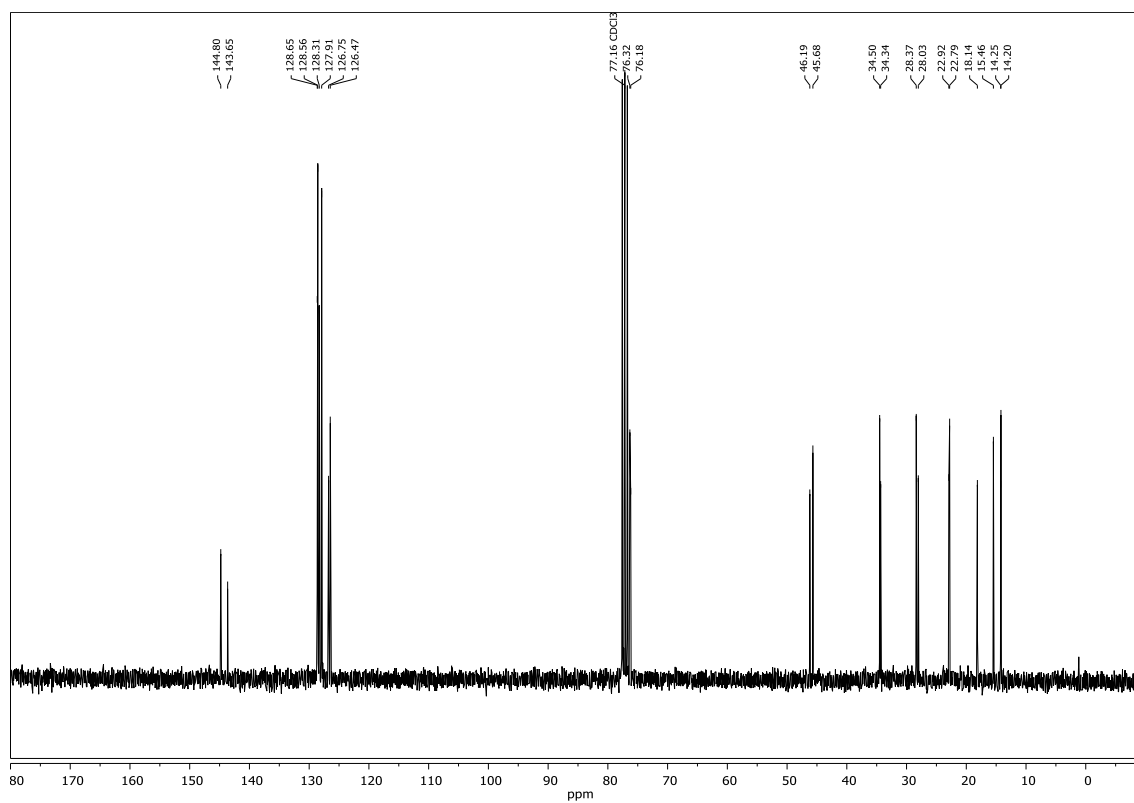
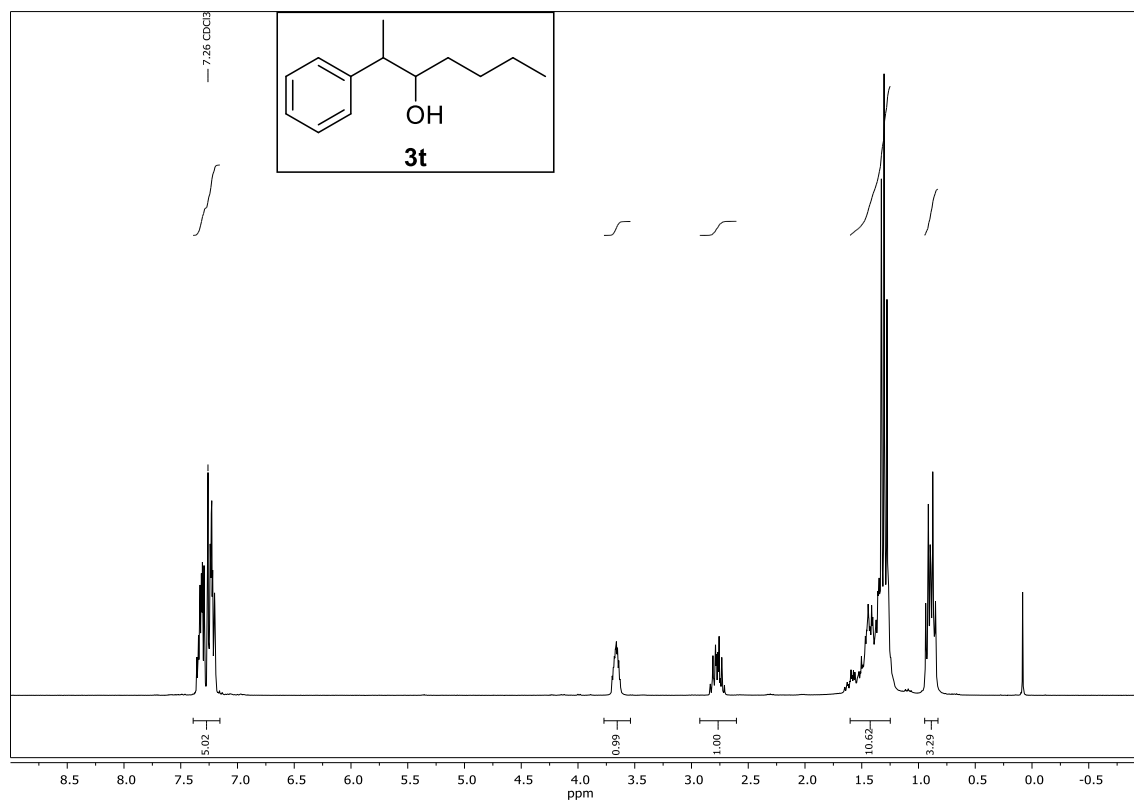
Compound **3q**, ^1H - and ^{13}C -NMR (CDCl_3)

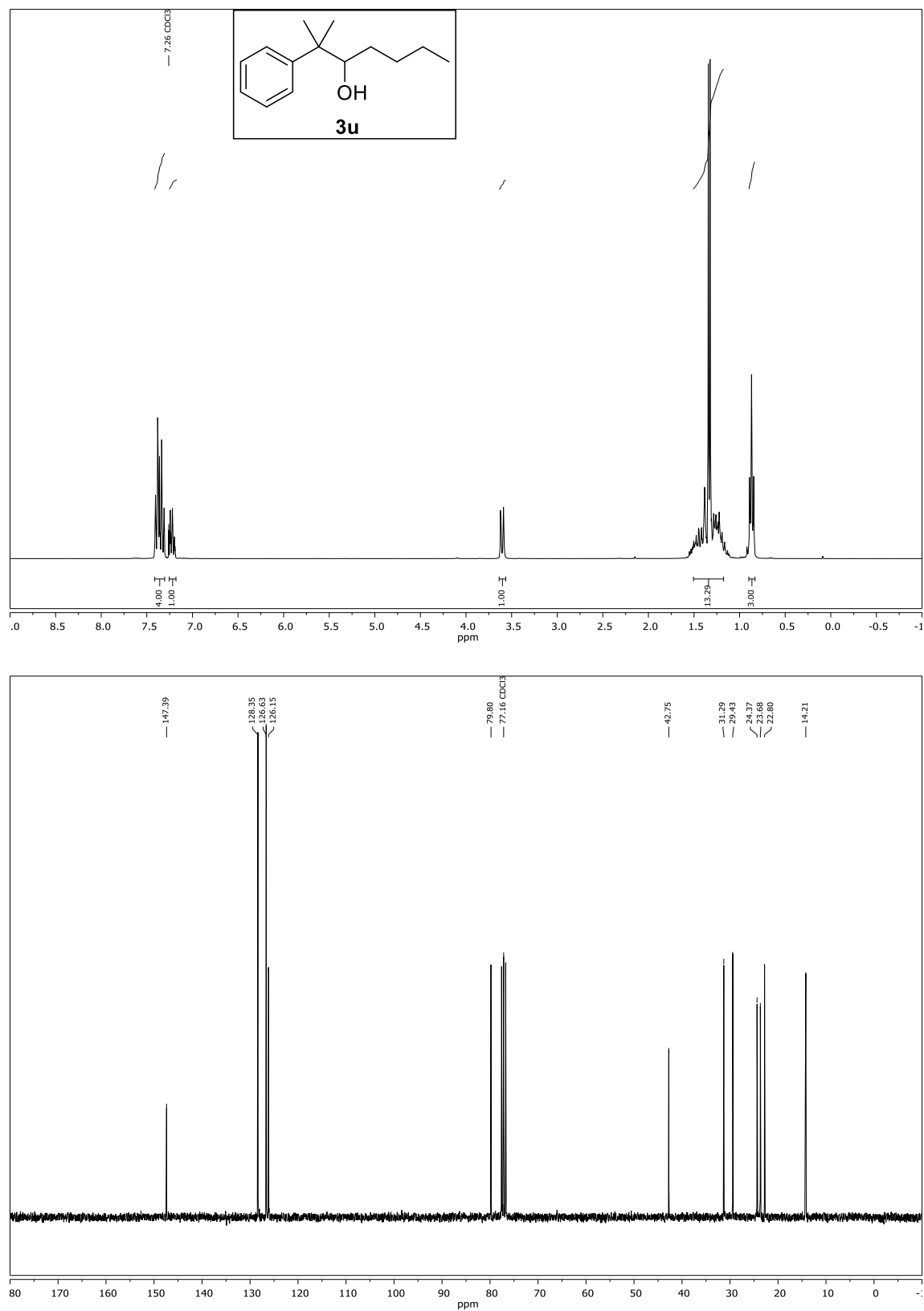
Compound **3r**, ^1H - and ^{13}C -NMR (CDCl_3)



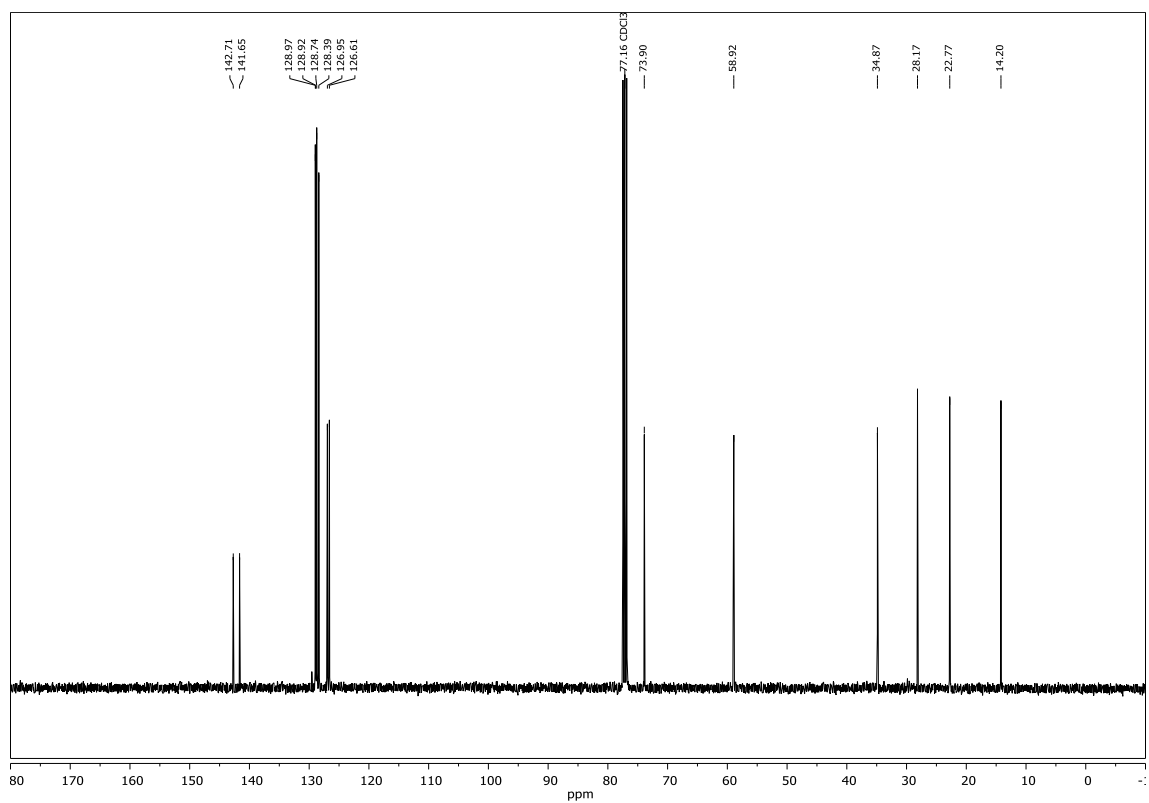
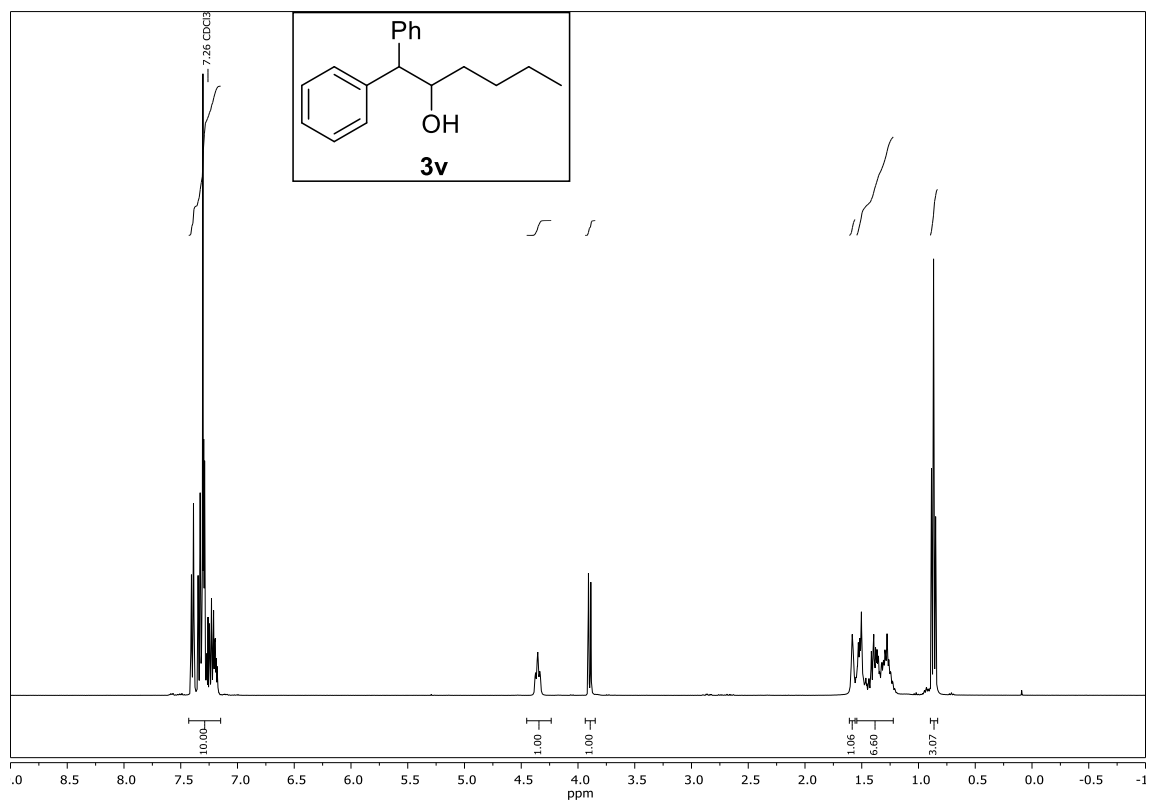
Compound **3s**, ^1H - and ^{13}C -NMR (CDCl_3)

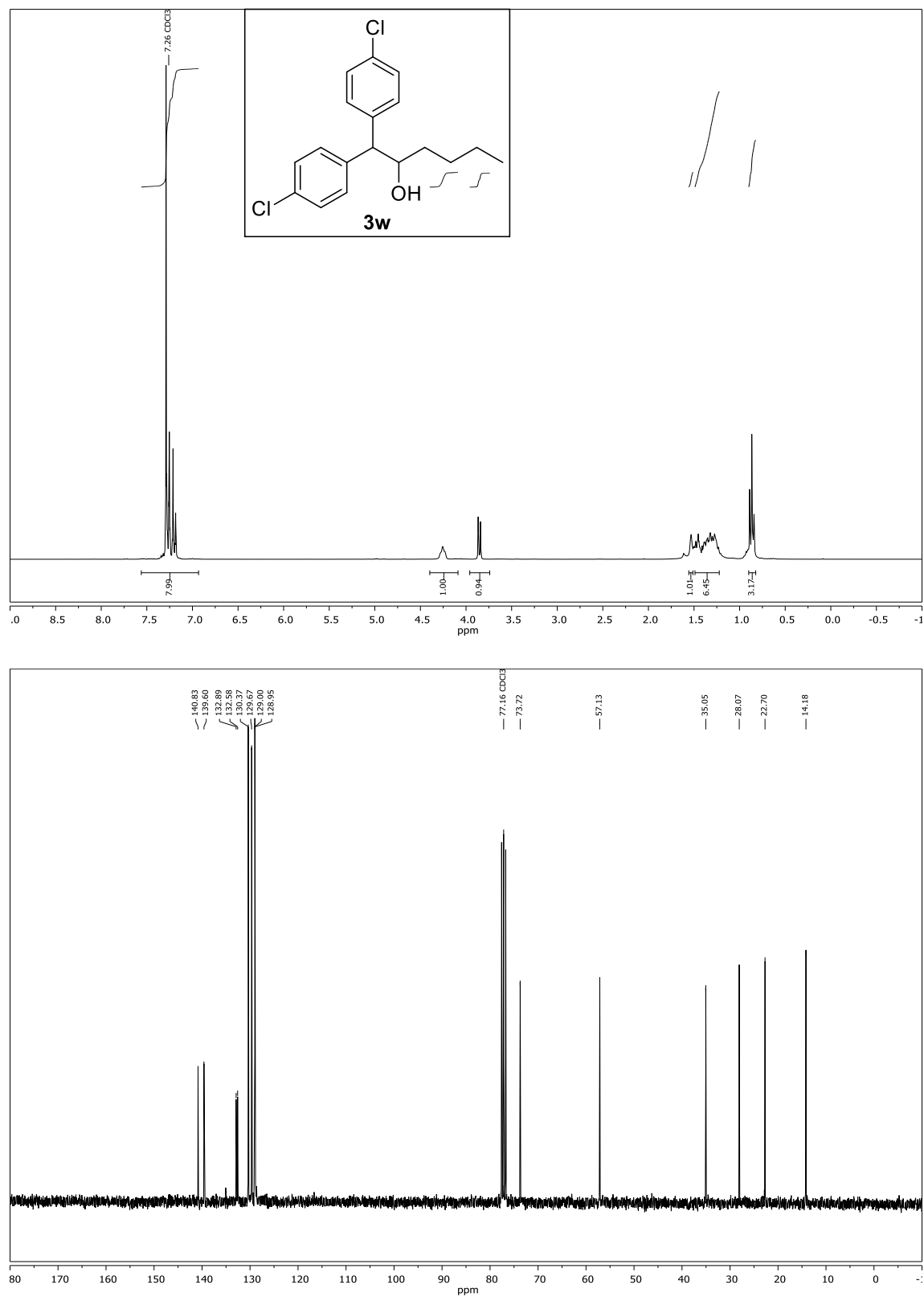
Compound **3t**, ^1H - and ^{13}C -NMR (CDCl_3)



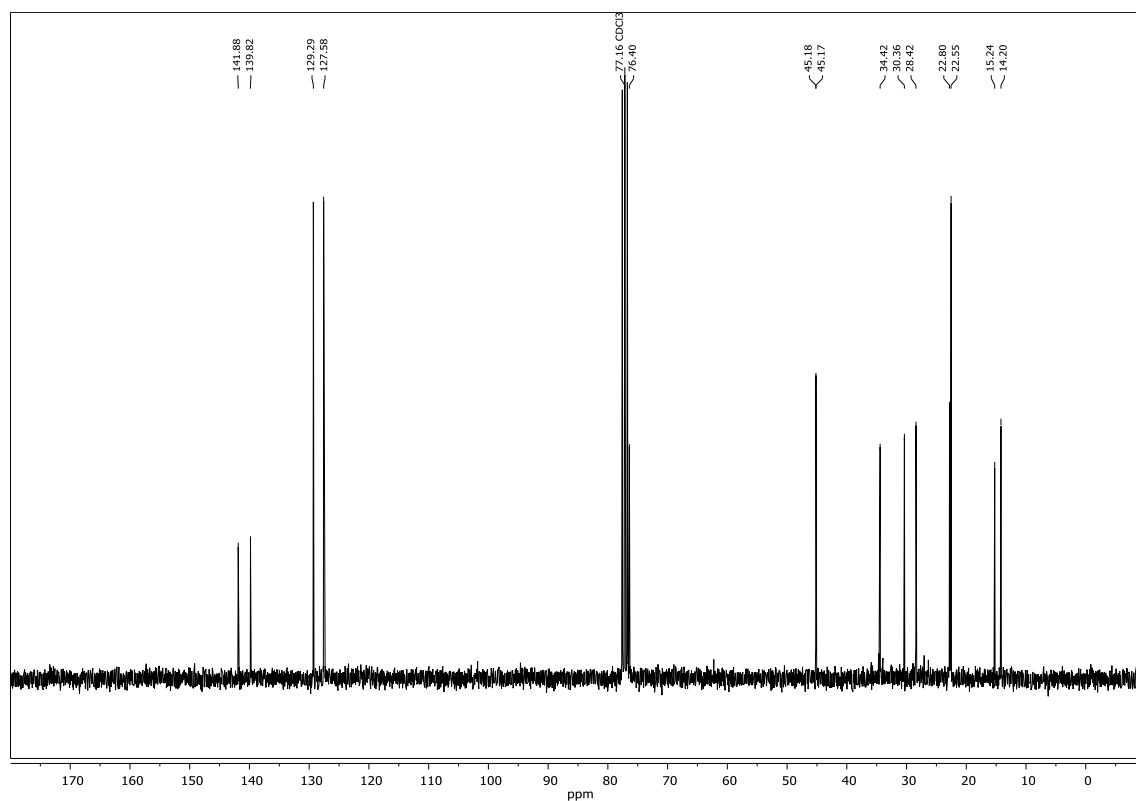
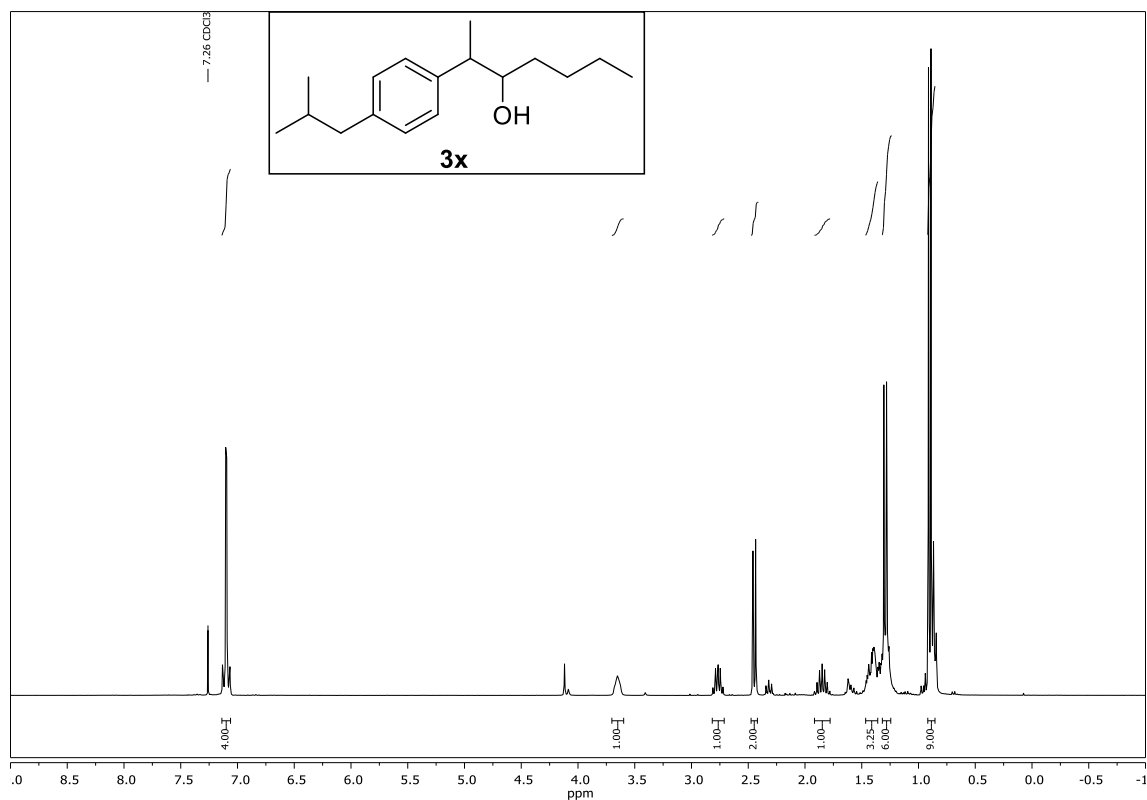
Compound **3u**, ^1H - and ^{13}C -NMR (CDCl_3)

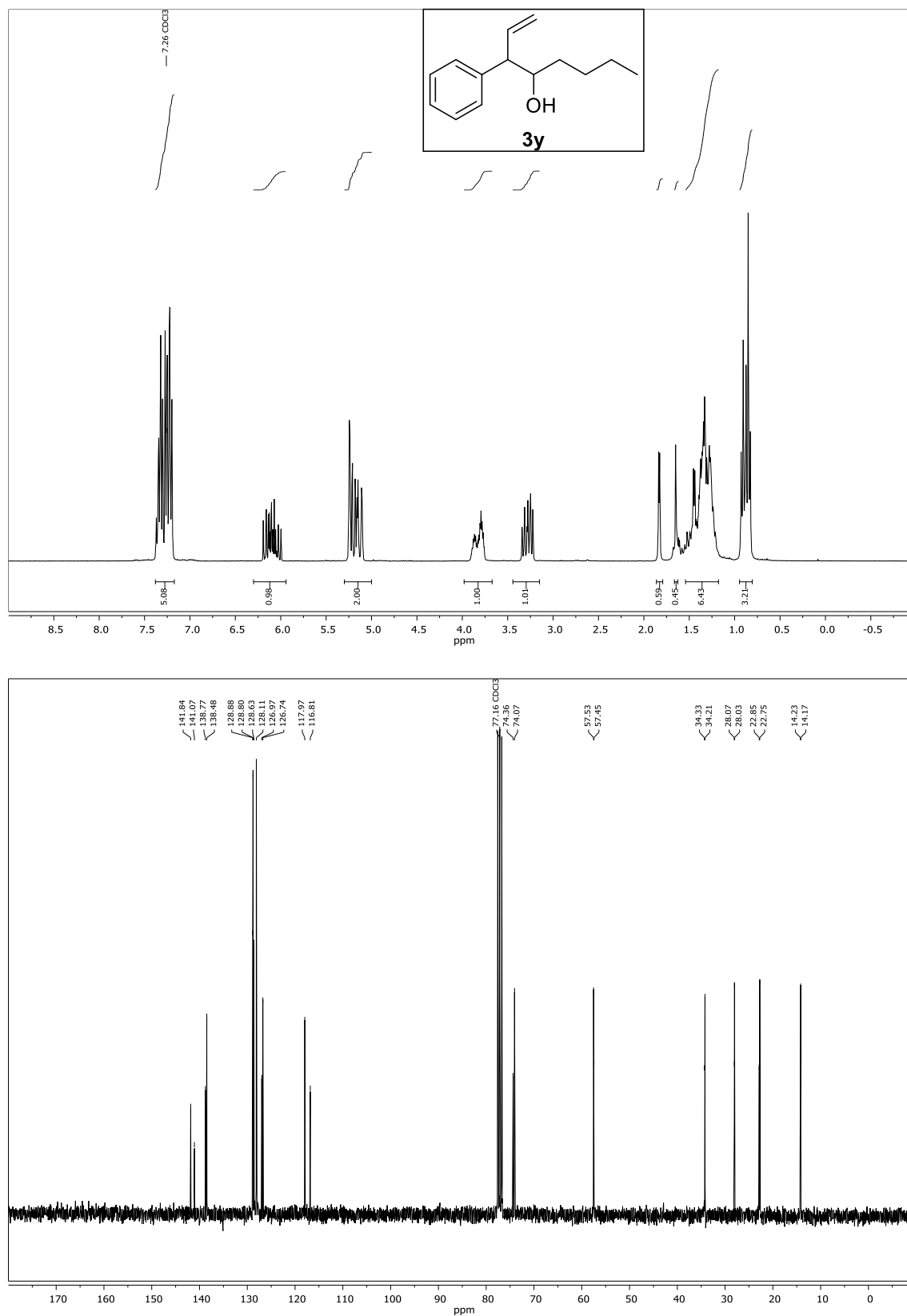
Compound **3v**, ^1H - and ^{13}C -NMR (CDCl_3)



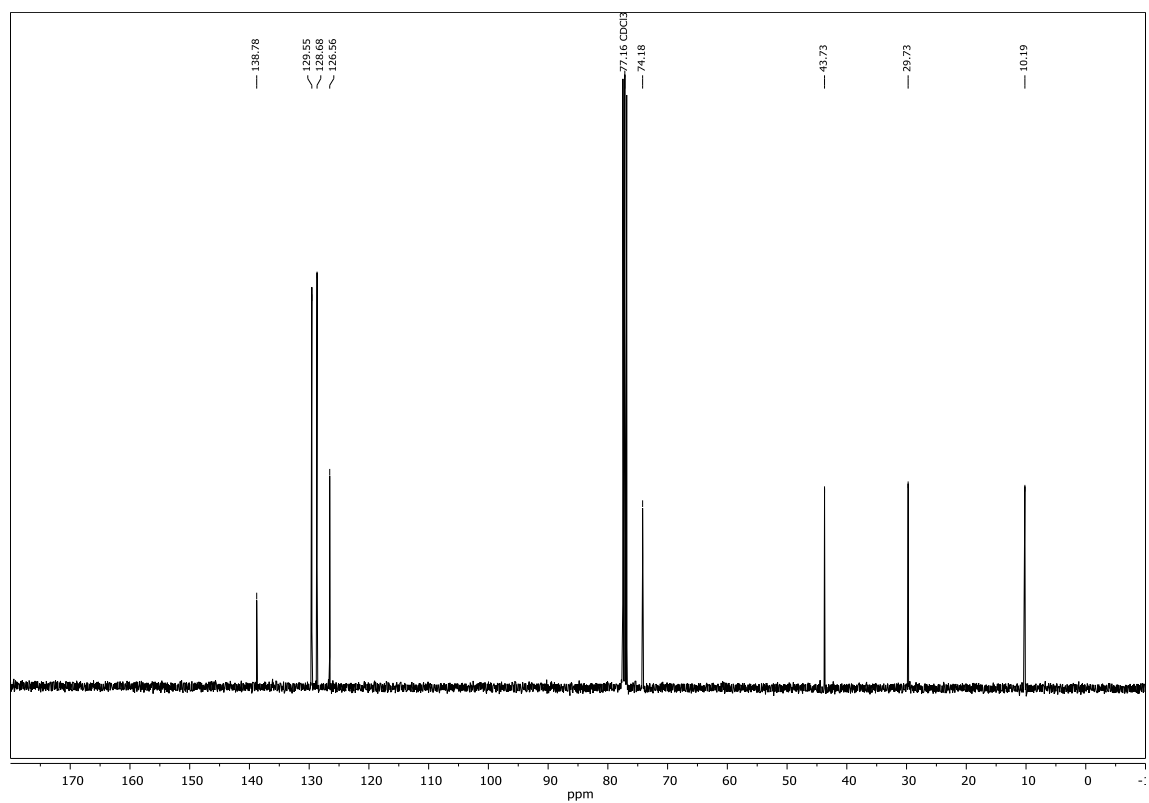
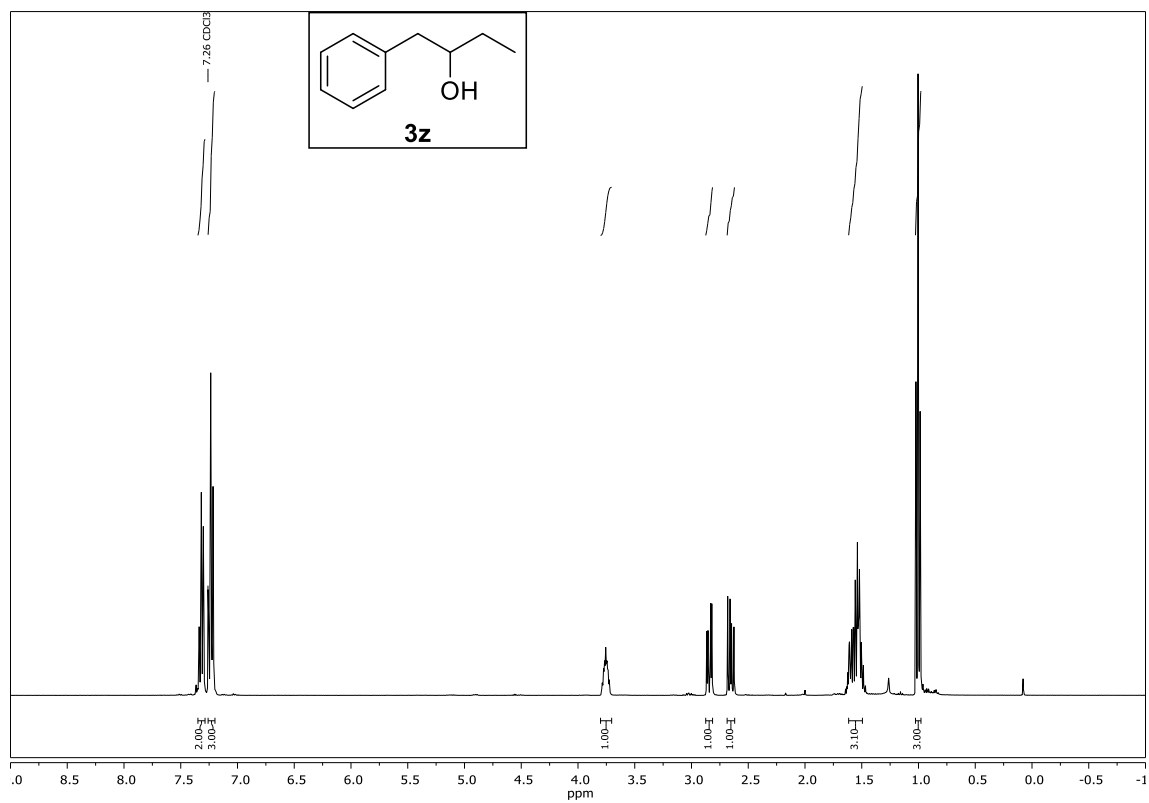
Compound **3w**, ^1H - and ^{13}C -NMR (CDCl_3)

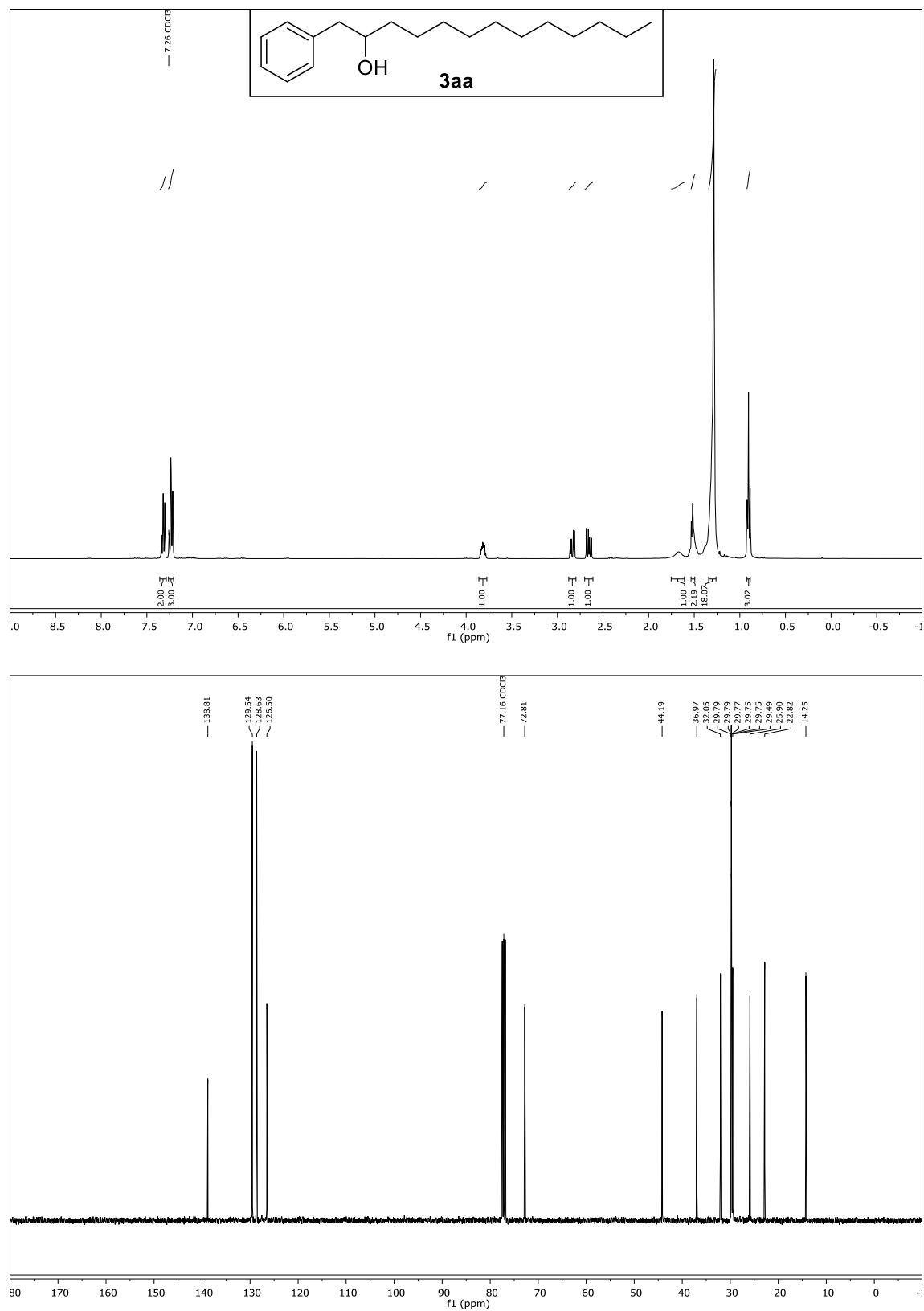
Compound **3x**, ^1H - and ^{13}C -NMR (CDCl_3)



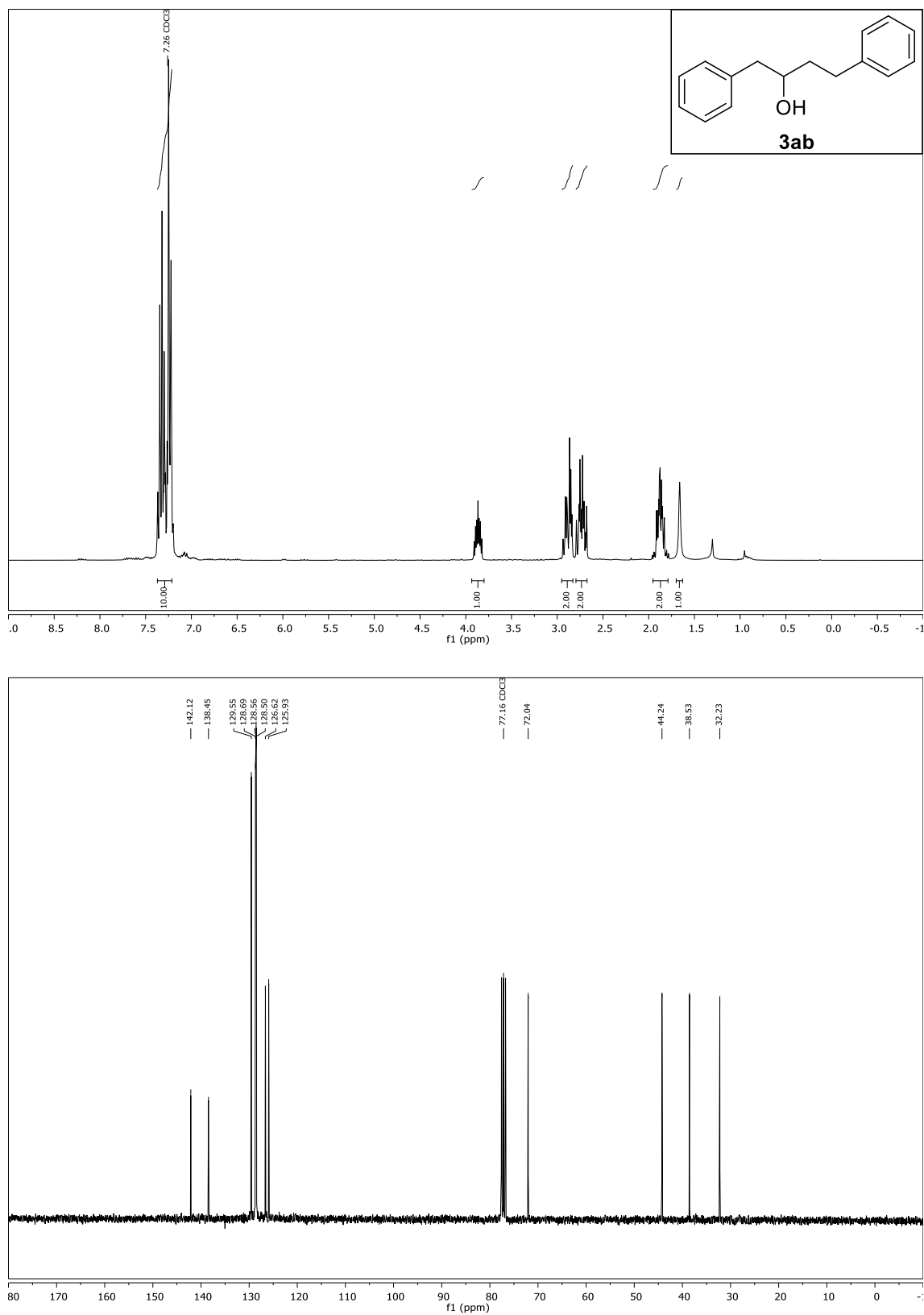
Compound **3y**, ^1H - and ^{13}C -NMR (CDCl_3)

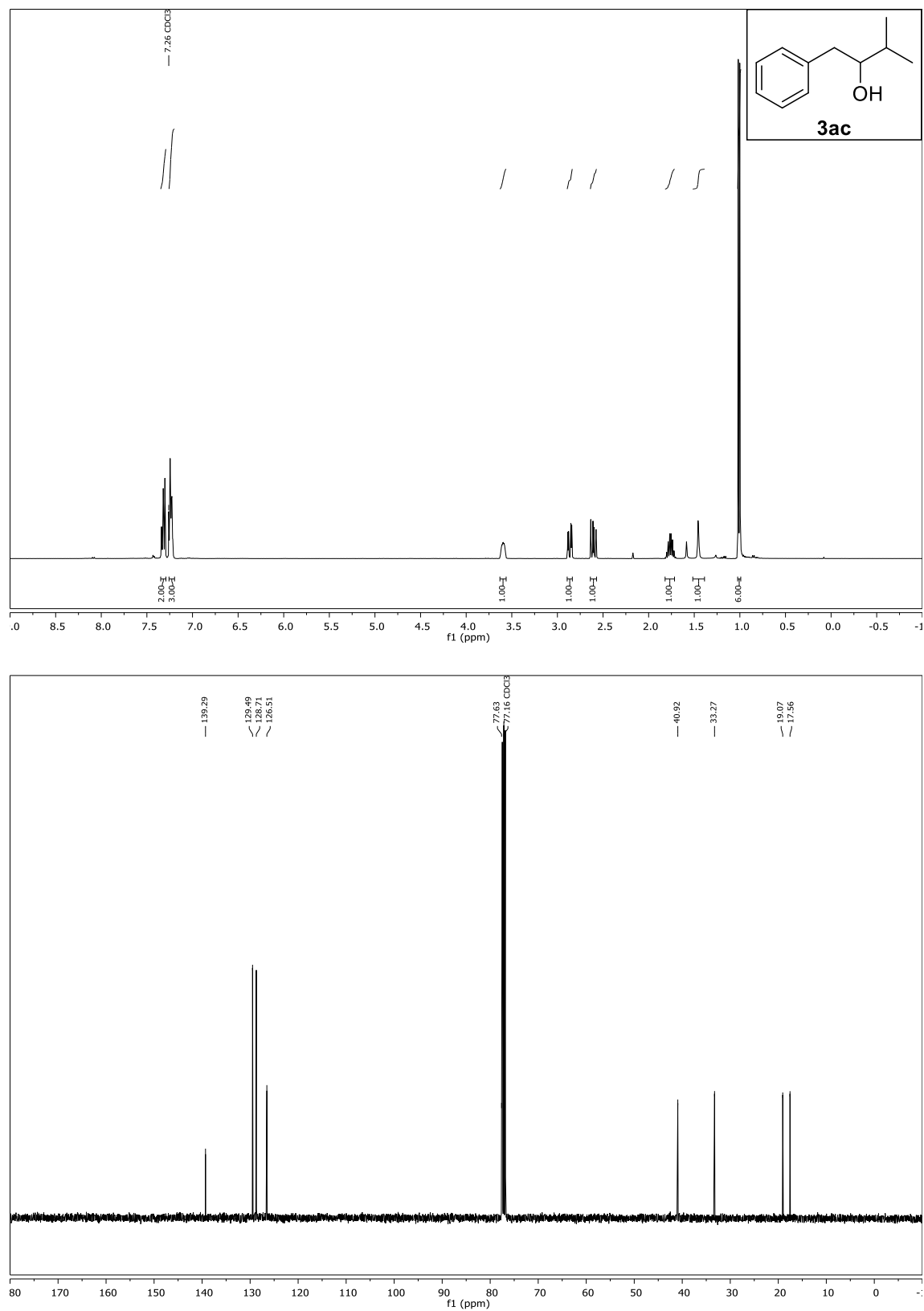
Compound **3z**, ^1H - and ^{13}C -NMR (CDCl_3)



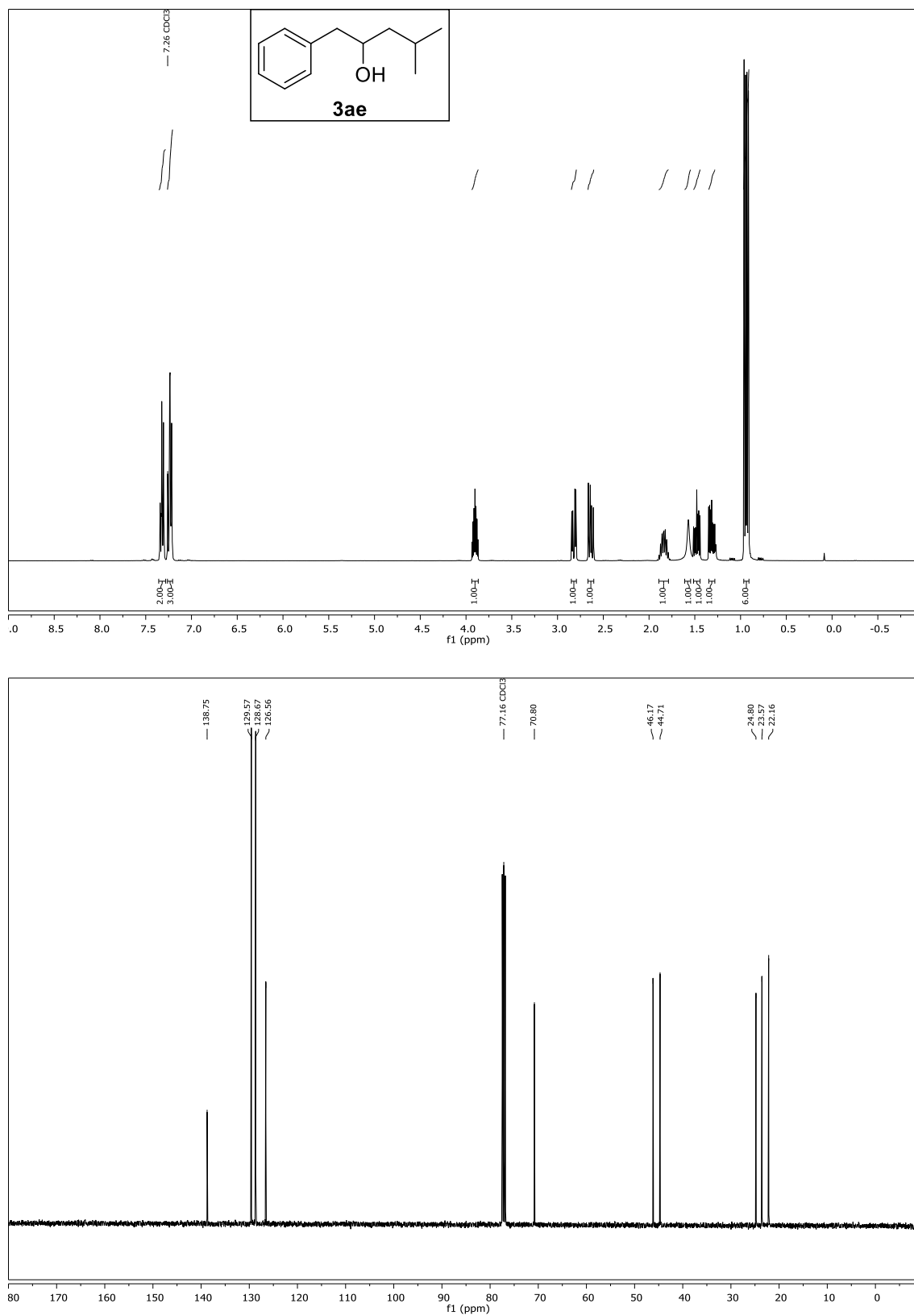
Compound **3aa**, ^1H - and ^{13}C -NMR (CDCl_3)

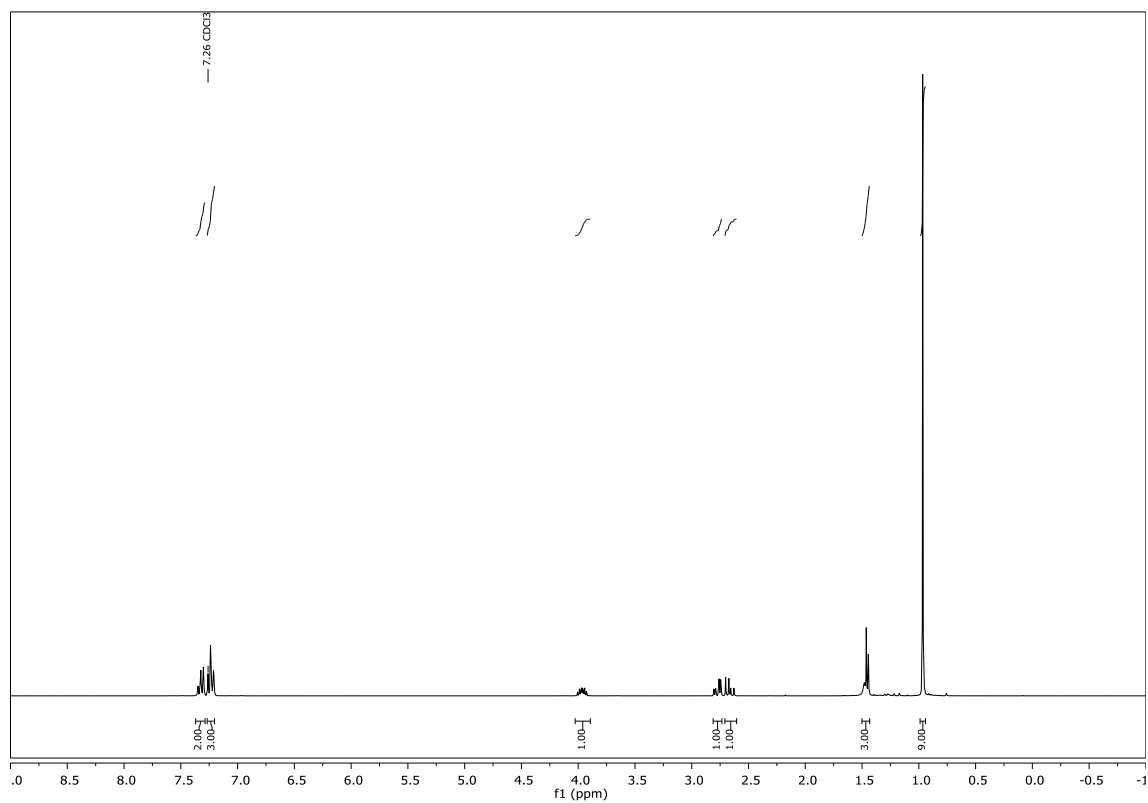
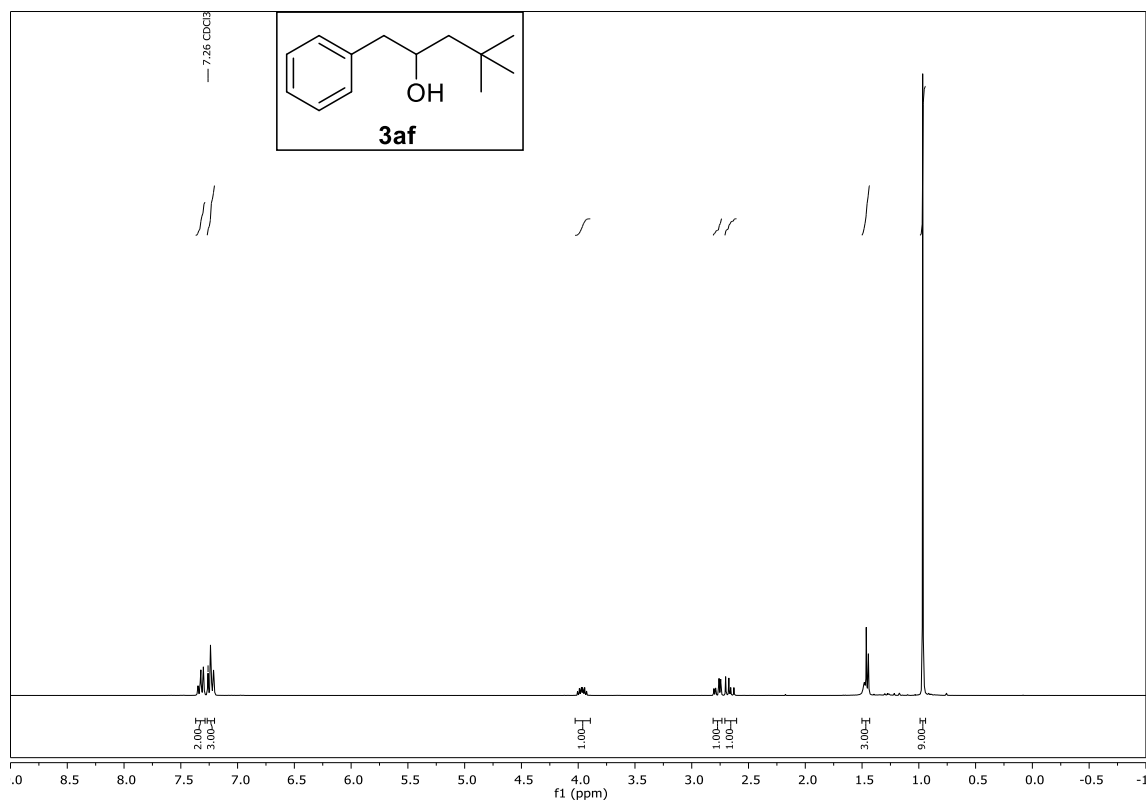
Compound **3ab**, ^1H - and ^{13}C -NMR (CDCl_3)



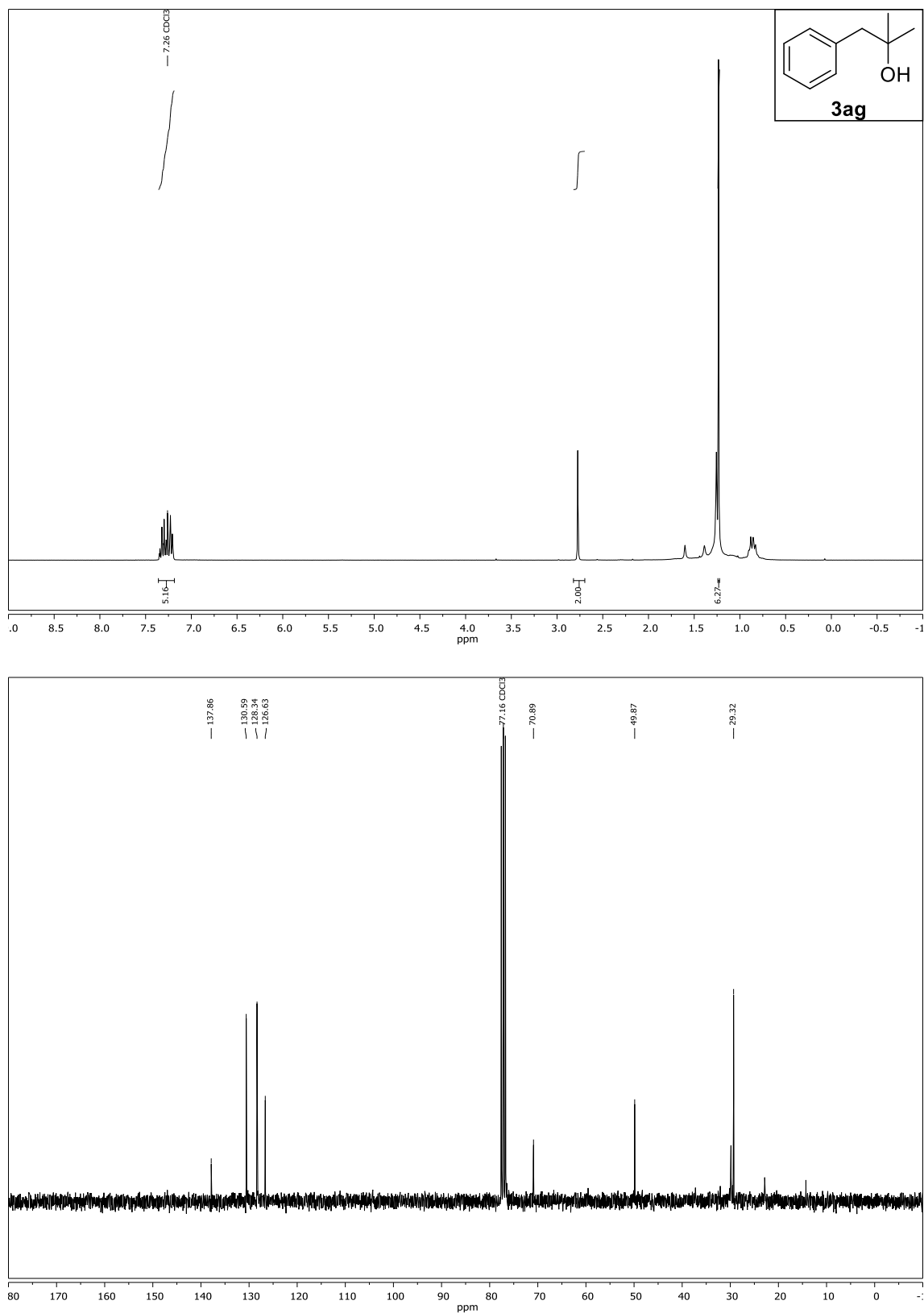
Compound **3ac**, ^1H - and ^{13}C -NMR (CDCl_3)

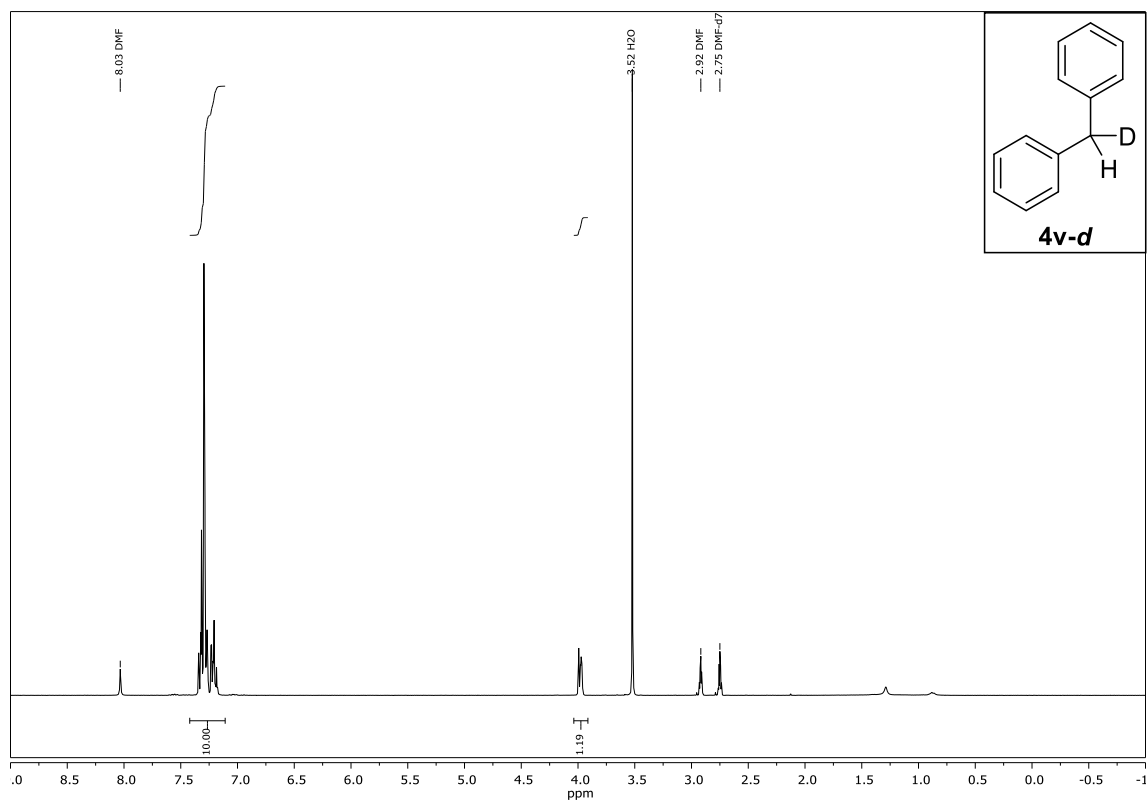
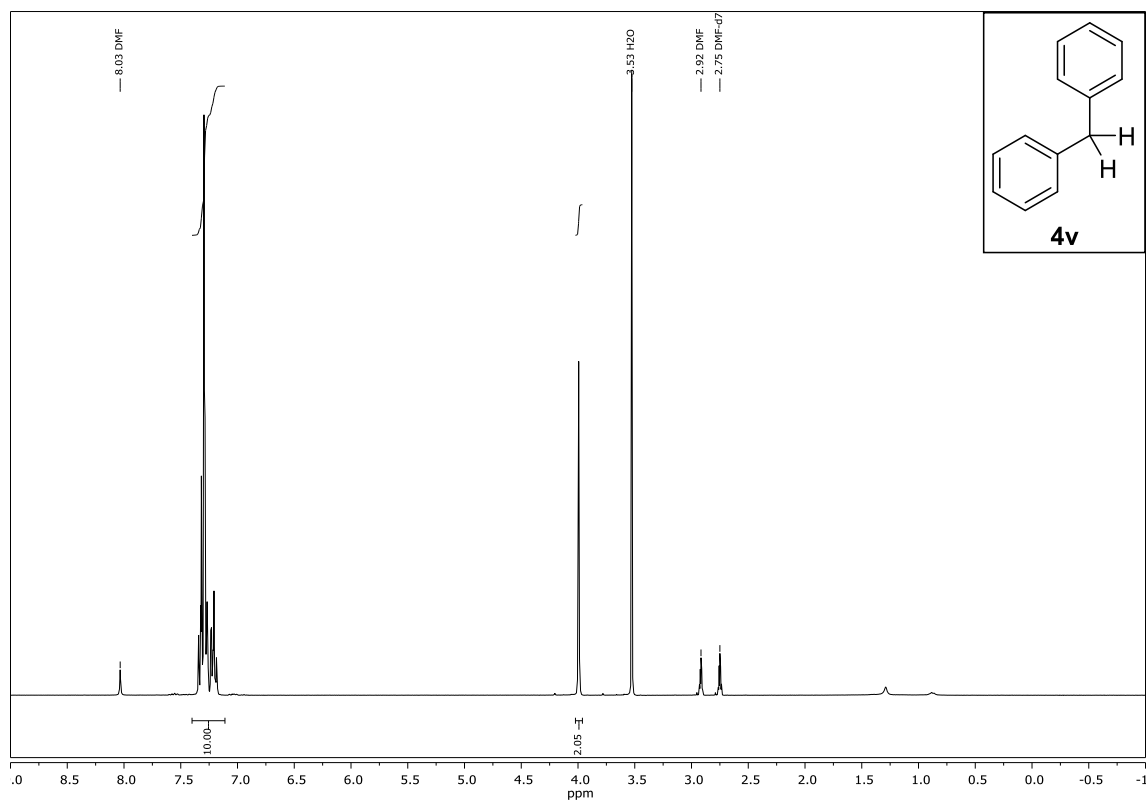
Compound **3ae**, ^1H - and ^{13}C -NMR (CDCl_3)



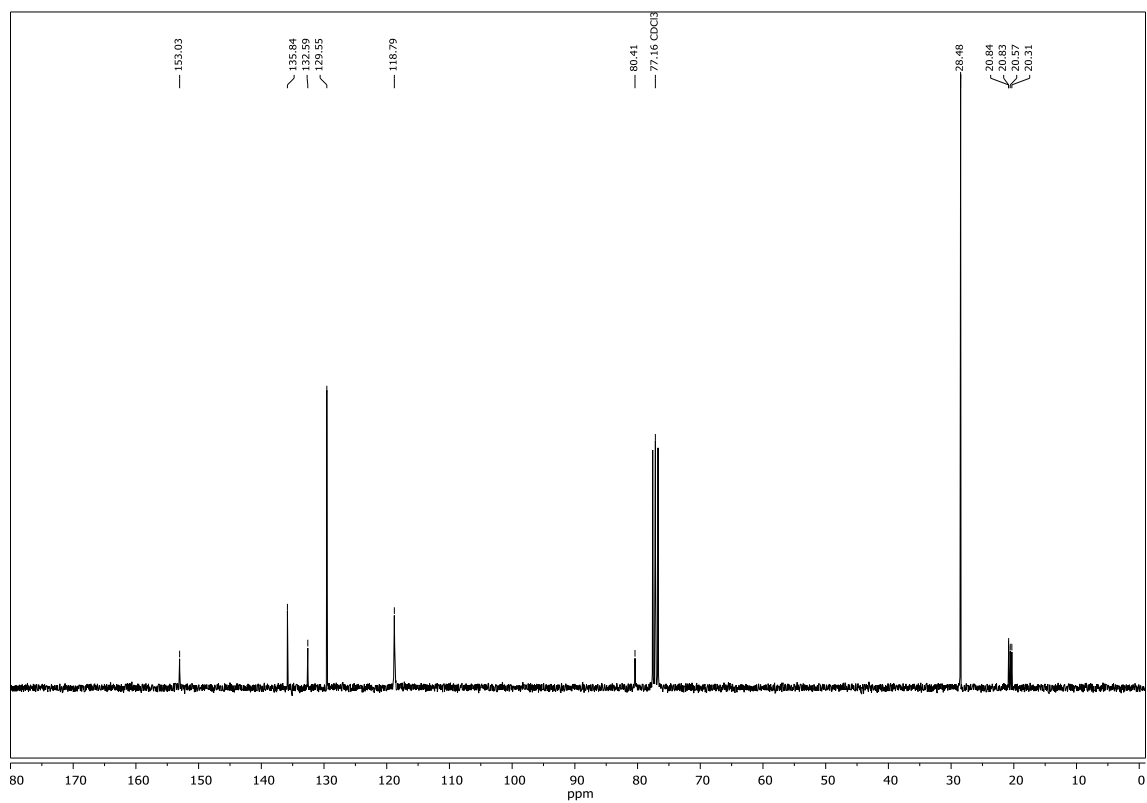
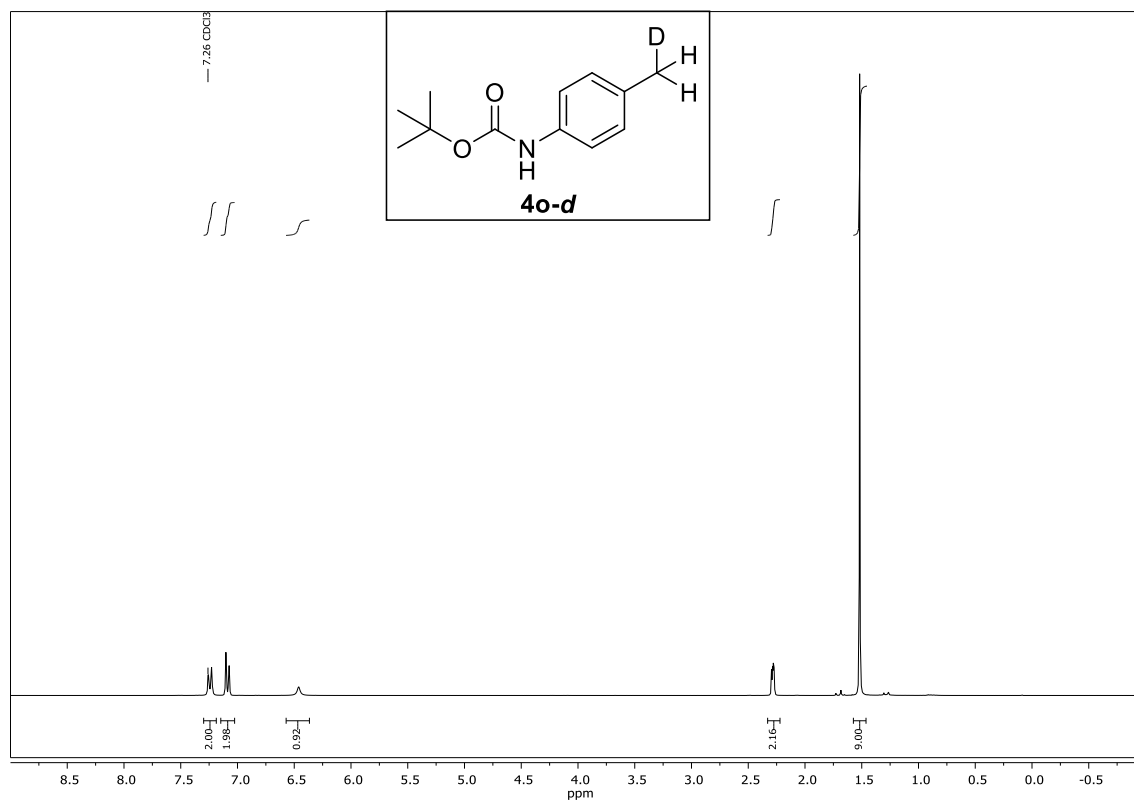
Compound **3af**, ^1H - and ^{13}C -NMR (CDCl_3)

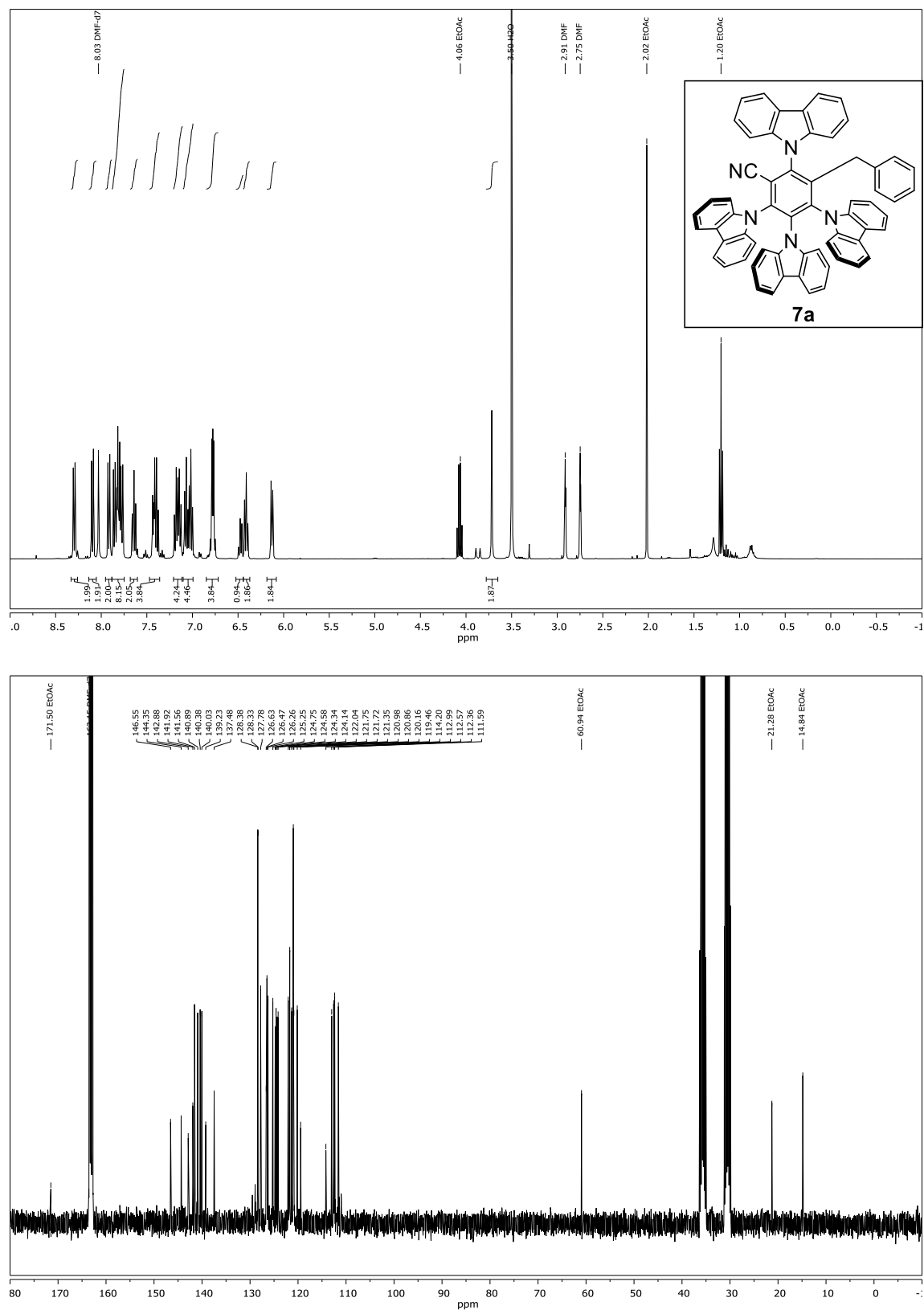
Compound **3ag**, ^1H - and ^{13}C -NMR (CDCl_3)



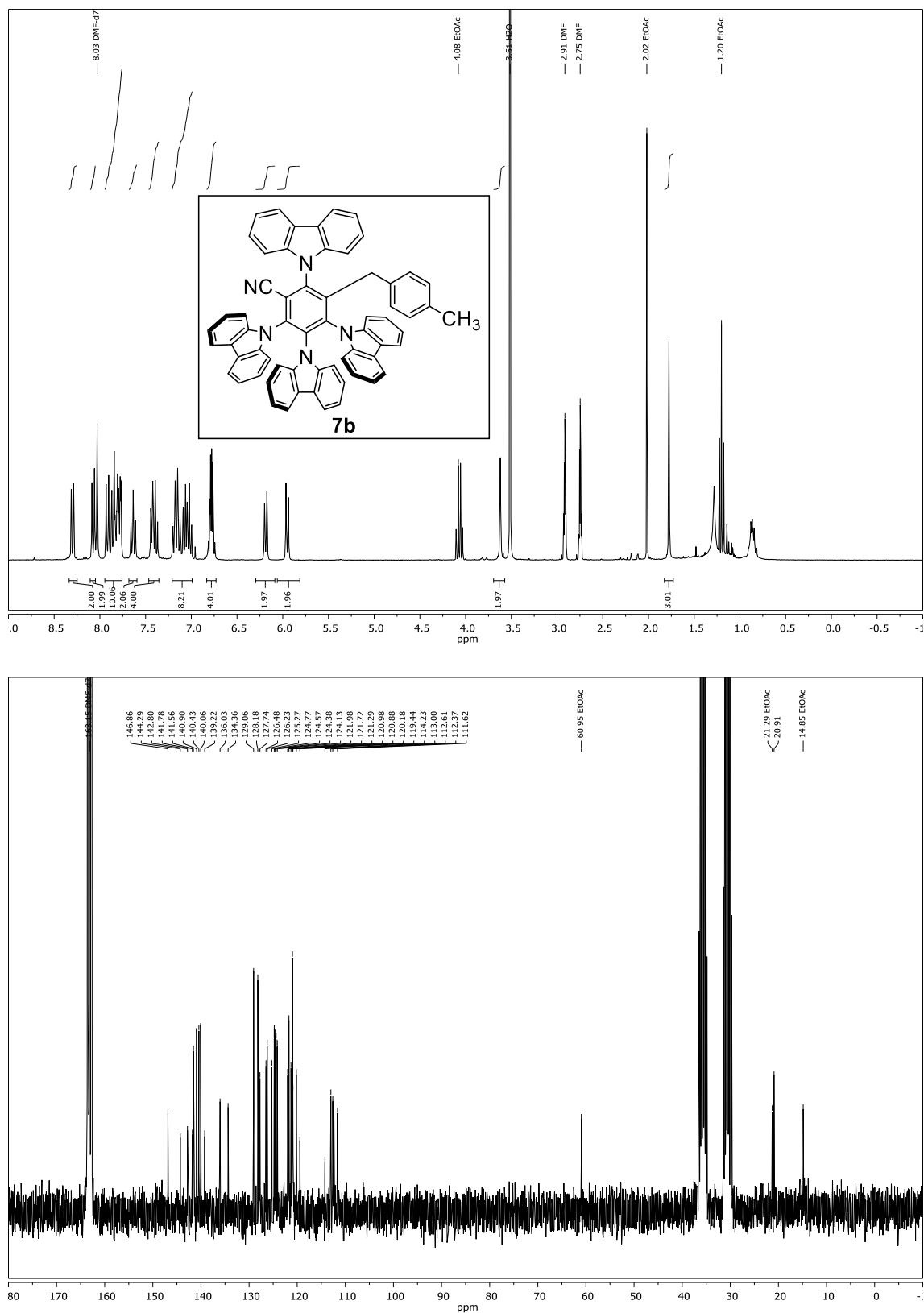
Compound **4v-d**, ^1H -NMR (d_7 -DMF)Compound **4v**, ^1H -NMR (d_7 -DMF)

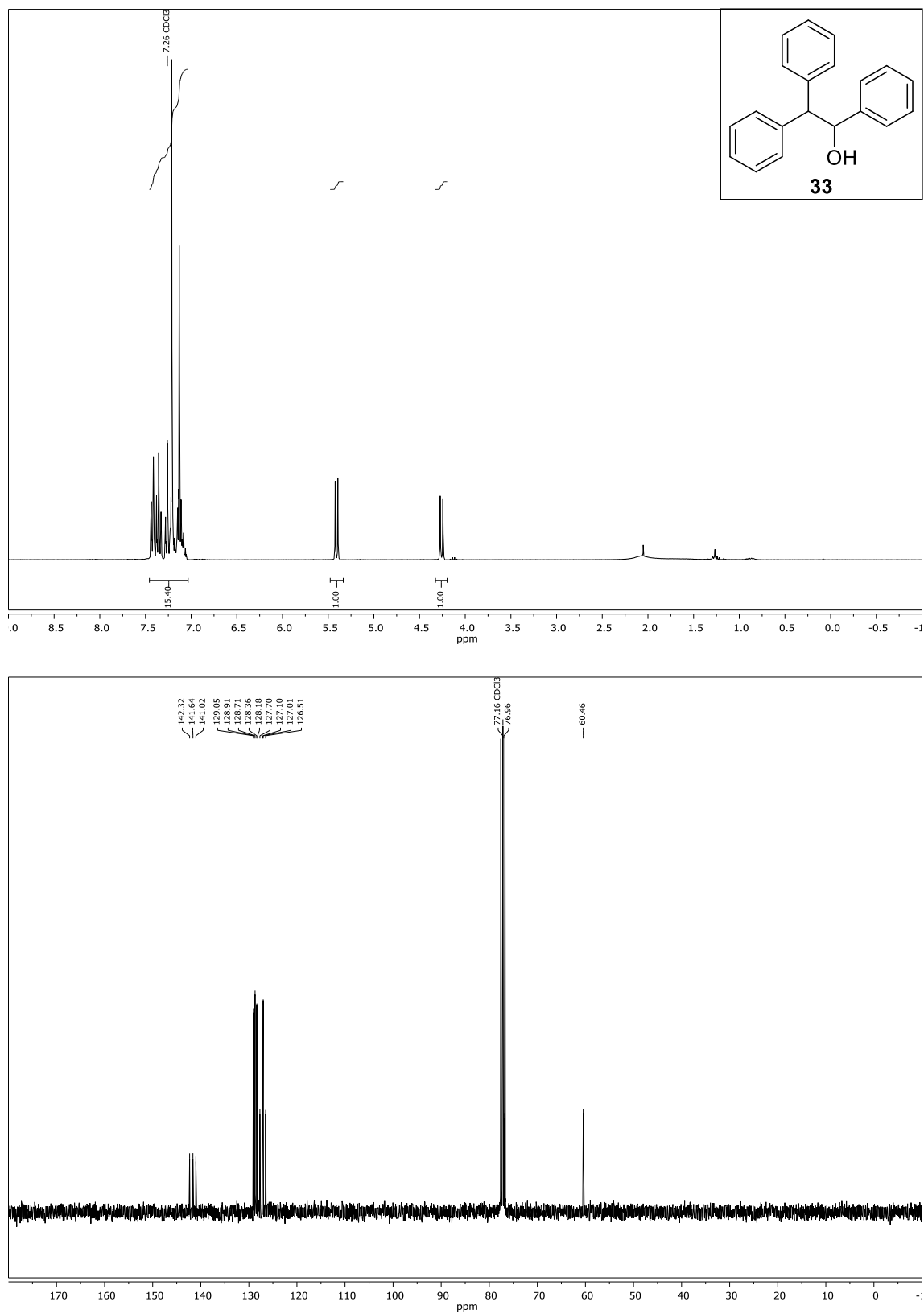
Compound **4o-d**, ^1H - and ^{13}C -NMR (CDCl_3)



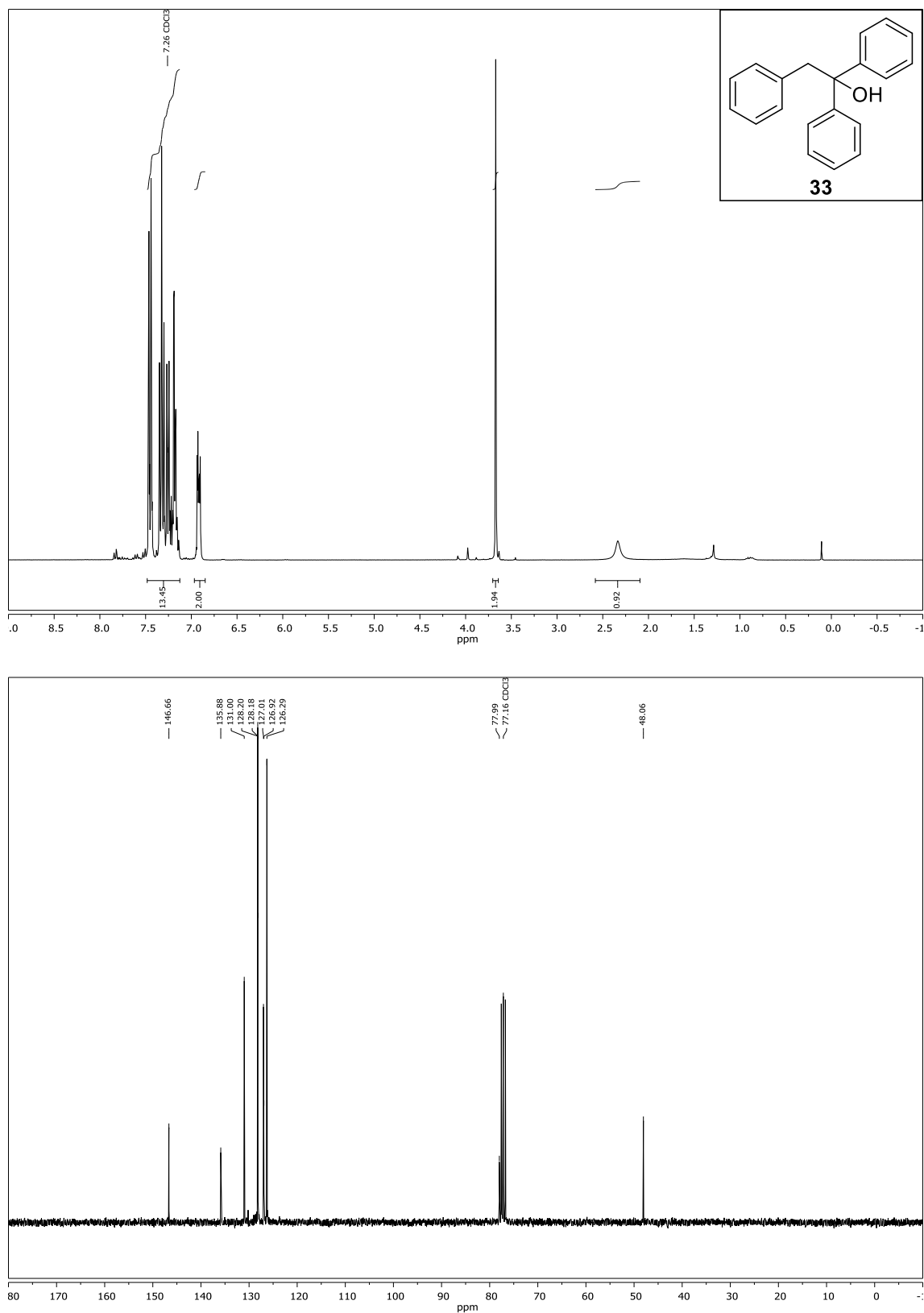
Compound **7a**, ^1H - and ^{13}C -NMR ($\text{d}_7\text{-DMF}$)

Compound **7b**, ^1H - and ^{13}C -NMR ($\text{d}_7\text{-DMF}$)



Compound **33**, ^1H - and ^{13}C -NMR (CDCl_3)

Compound **34**, ^1H - and ^{13}C -NMR (CDCl_3)



4.6 References

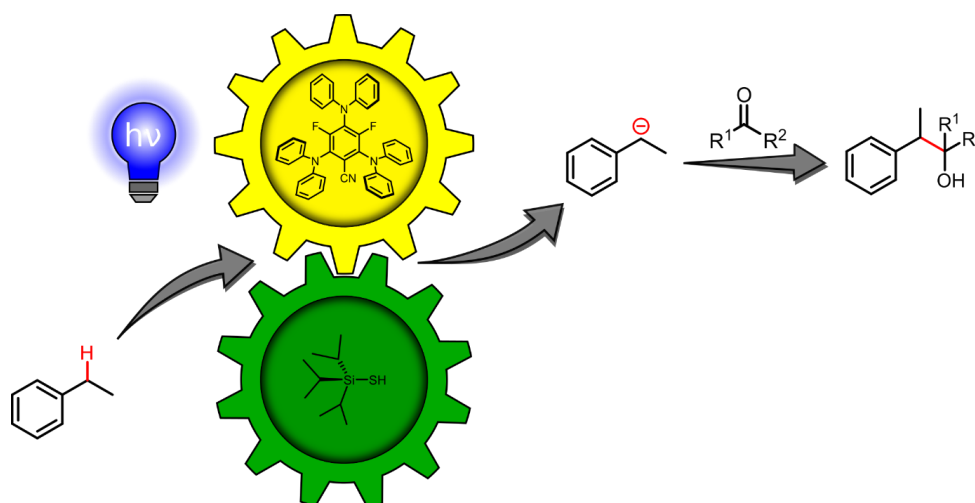
- [1] M. H. Shaw, J. Twilton, D. W. MacMillan, *J. Org. Chem.* **2016**, *81*, 6898-6926.
- [2] G. Brahmachari, *RSC Advances* **2016**, *6*, 64676-64725.
- [3] a) D. Ravelli, S. Protti, M. Fagnoni, *Chem. Rev.* **2016**, *116*, 9850-9913; b) J. Twilton, C. Le, P. Zhang, M. H. Shaw, R. W. Evans, D. W. C. MacMillan, *Nat. Rev. Chem.* **2017**, *1*; c) C. K. Prier, D. A. Rankic, D. W. MacMillan, *Chem. Rev.* **2013**, *113*, 5322-5363; d) N. A. Romero, D. A. Nicewicz, *Chem. Rev.* **2016**, *116*, 10075-10166; e) L. Marzo, S. K. Pagire, O. Reiser, B. König, *Angew. Chem. Int. Ed.* **2018**, *57*, 10034-10072; f) I. Ghosh, L. Marzo, A. Das, R. Shaikh, B. König, *Acc. Chem. Res.* **2016**, *49*, 1566-1577.
- [4] a) Y. Zhang, R. Qian, X. Zheng, Y. Zeng, J. Sun, Y. Chen, A. Ding, H. Guo, *Chem. Commun.* **2015**, *51*, 54-57; b) L. L. Liao, G. M. Cao, J. H. Ye, G. Q. Sun, W. J. Zhou, Y. Y. Gui, S. S. Yan, G. Shen, D. G. Yu, *J. Am. Chem. Soc.* **2018**, *140*, 17338-17342; c) Y. Kumagai, T. Naoe, K. Nishikawa, K. Osaka, T. Morita, Y. Yoshimi, *Aust. J. Chem.* **2015**, *68*, 1668; d) V. R. Yatham, Y. Shen, R. Martin, *Angew. Chem. Int. Ed.* **2017**, *56*, 10915-10919; e) W. Kong, H. An, Q. Song, *Chem. Commun.* **2017**, *53*, 8968-8971; f) J. P. Phelan, S. B. Lang, J. S. Compton, C. B. Kelly, R. Dykstra, O. Gutierrez, G. A. Molander, *J. Am. Chem. Soc.* **2018**, *140*, 8037-8047; g) J. A. Milligan, J. P. Phelan, V. C. Polites, C. B. Kelly, G. A. Molander, *Org. Lett.* **2018**, *20*, 6840-6844; h) C. Shu, R. S. Mega, B. J. Andreassen, A. Noble, V. K. Aggarwal, *Angew. Chem. Int. Ed.* **2018**, *57*, 15430-15434; i) C. Shu, A. Noble, V. K. Aggarwal, *Angew. Chem. Int. Ed.* **2019**, *58*, 3870-3874.
- [5] a) V. Grignard, *C. R. Acad. Sci.* **1900**, *130*, 1322-1325; b) G. S. Silverman, P. E. Rakita, *Handbook of Grignard Reagents*, Taylor & Francis, **1996**.
- [6] a) K. Hironaka, S. Fukuzumi, T. Tanaka, *J. Chem. Soc., Perkin Trans. 2* **1984**, 1705; b) J.-M. Kern, J.-P. Sauvage, *J. Chem. Soc., Chem. Commun.* **1987**, 546-548; c) D. Li, C.-M. Che, H.-L. Kwong, V. W.-W. Yam, *J. Chem. Soc., Dalton Trans.* **1992**, 3325-3329.
- [7] a) H. Yokoi, T. Nakano, W. Fujita, K. Ishiguro, Y. Sawaki, *J. Am. Chem. Soc.* **1998**, *120*, 12453-12458; b) H. Huang, C. Yu, Y. Zhang, Y. Zhang, P. S. Mariano, W. Wang, *J. Am. Chem. Soc.* **2017**, *139*, 9799-9802; c) Y. Yasu, T. Koike, M. Akita, *Adv. Synth. Catal.* **2012**, *354*, 3414-3420; d) A. J. Musacchio, L. Q. Nguyen, G. H. Beard, R. R. Knowles, *J. Am. Chem. Soc.* **2014**, *136*, 12217-12220; e) R. Zhou, H. Liu, H. Tao, X. Yu, J. Wu, *Chem. Sci.* **2017**, *8*, 4654-4659; f) A. Gualandi, D. Mazzearella, A. Ortega-Martínez, L. Mengozzi, F. Calcinelli, E. Matteucci, F. Monti, N. Armaroli, L. Sambri, P. G. Cozzi, *ACS Catal.* **2017**, *7*, 5357-5362; g) X. Dong, P. Hu, W. Shen, Z. Li, R. Liu, X. Liu, *Polymers* **2017**, *9*; h) A. Noble, R. S. Mega, D. Pflasterer, E. L. Myers, V. K. Aggarwal, *Angew. Chem. Int. Ed.* **2018**, *57*, 2155-2159.
- [8] S. B. Lang, R. J. Wiles, C. B. Kelly, G. A. Molander, *Angew. Chem. Int. Ed.* **2017**, *56*, 15073-15077.
- [9] a) A. Clerici, O. Porta, P. Zago, *Tetrahedron* **1986**, *42*, 561-572; b) A. Clerici, O. Porta, *J. Org. Chem.* **1989**, *54*, 3872-3878; c) S. Wilsey, P. Dowd, K. N. Houk, *J. Org. Chem.* **1999**, *64*, 8801-8811; d) C. Che, Z. Qian, M. Wu, Y. Zhao, G. Zhu, *J. Org. Chem.* **2018**, *83*, 5665-5673.
- [10] L. Pitzer, F. Sandfort, F. Strieth-Kalthoff, F. Glorius, *J. Am. Chem. Soc.* **2017**, *139*, 13652-13655.
- [11] J. Luo, J. Zhang, *ACS Catal.* **2016**, *6*, 873-877.
- [12] A. L. Berger, K. Donabauer, B. König, *Chem. Sci.* **2018**, *9*, 7230-7235.

- [13] a) T. Itou, Y. Yoshimi, T. Morita, Y. Tokunaga, M. Hatanaka, *Tetrahedron* **2009**, *65*, 263-269; b) M. T. Pirnot, D. A. Rankic, D. B. Martin, D. W. MacMillan, *Science* **2013**, *339*, 1593-1596.
- [14] a) L. Capaldo, L. Buzzetti, D. Merli, M. Fagnoni, D. Ravelli, *J. Org. Chem.* **2016**, *81*, 7102-7109; b) T. Patra, D. Maiti, *Chemistry* **2017**, *23*, 7382-7401; c) J. Schwarz, B. König, *Green Chem.* **2018**, *20*, 323-361; d) H. Huang, X. Li, C. Yu, Y. Zhang, P. S. Mariano, W. Wang, *Angew. Chem. Int. Ed.* **2017**, *56*, 1500-1505.
- [15] D. Nicewicz, H. Roth, N. Romero, *Synlett* **2015**, *27*, 714-723.
- [16] a) D. D. M. Wayner, D. J. McPhee, D. Griller, *J. Am. Chem. Soc.* **1988**, *110*, 132-137; b) B. A. Sim, D. Griller, D. D. M. Wayner, *J. Am. Chem. Soc.* **1989**, *111*, 754-755.
- [17] S. Hünig, P. Kreitmeier, G. Märkl, J. Sauer, *Verlag Lehmanns* **2006**.
- [18] R. K. Harris, E. D. Becker, S. M. Cabral de Menezes, R. Goodfellow, P. Granger, *Magn. Reson. Chem.* **2002**, *40*, 489-505.
- [19] G. R. Fulmer, A. J. M. Miller, N. H. Sherden, H. E. Gottlieb, A. Nudelman, B. M. Stoltz, J. E. Bercaw, K. I. Goldberg, *Organometallics* **2010**, *29*, 2176-2179.
- [20] E. Speckmeier, T. G. Fischer, K. Zeitler, *J. Am. Chem. Soc.* **2018**, *140*, 15353-15365.
- [21] M. S. Lowry, J. I. Goldsmith, J. D. Slinker, R. Rohl, R. A. Pascal, G. G. Malliaras, S. Bernhard, *Chem. Mater.* **2005**, *17*, 5712-5719.
- [22] R. M. Pearson, C. H. Lim, B. G. McCarthy, C. B. Musgrave, G. M. Miyake, *J. Am. Chem. Soc.* **2016**, *138*, 11399-11407.
- [23] P. R. Blakemore, S. P. Marsden, H. D. Vater, *Org. Lett.* **2006**, *8*, 773-776.
- [24] A. R. Katritzky, Y. Fang, *Heterocycles* **2000**, *53*, 1783.
- [25] M. Das, D. F. O'Shea, *Tetrahedron* **2013**, *69*, 6448-6460.
- [26] a) M. T. Reetz, S. Stanchev, H. Haning, *Tetrahedron* **1992**, *48*, 6813-6820; b) S.-i. Fukuzawa, K. Mutoh, T. Tsuchimoto, T. Hiyama, *J. Org. Chem.* **1996**, *61*, 5400-5405.
- [27] D. Basavaiah, P. Dharma Rao, *Tetrahedron: Asymmetry* **1995**, *6*, 789-800.
- [28] a) S. Zushi, Y. Kodama, Y. Fukuda, K. Nishihata, M. Nishio, M. Hirota, J. Uzawa, *Bull. Chem. Soc. Jpn.* **1981**, *54*, 2113-2119; b) R. D. Rieke, R. M. Wehmeyer, T.-C. Wu, G. W. Ebert, *Tetrahedron* **1989**, *45*, 443-454.
- [29] M. Chierchia, C. Law, J. P. Morken, *Angew. Chem. Int. Ed.* **2017**, *56*, 11870-11874.
- [30] A. Rioz-Martinez, G. de Gonzalo, D. E. Torres Pazmino, M. W. Fraaije, V. Gotor, *J. Org. Chem.* **2010**, *75*, 2073-2076.
- [31] B. Bennetau, J. Dunogues, *Tetrahedron Lett.* **1983**, *24*, 4217-4218.
- [32] G. Zweifel, R. Fisher, A. Horng, *Synthesis* **2002**, *1973*, 37-38.
- [33] A. Fernandez-Mateos, S. Encinas Madrazo, P. Herrero Teijon, R. Rubio Gonzalez, *J. Org. Chem.* **2009**, *74*, 3913-3918.
- [34] M. Blesic, M. Swadzba-Kwasny, T. Belhocine, H. Q. Gunaratne, J. N. Lopes, M. F. Gomes, A. A. Padua, K. R. Seddon, L. P. Rebelo, *Phys. Chem. Chem. Phys.* **2009**, *11*, 8939-8948.
- [35] Y. Liu, J. Cornella, R. Martin, *J. Am. Chem. Soc.* **2014**, *136*, 11212-11215.
- [36] W. Xu, T. Li, G. Li, Y. Wu, T. Miyashita, *J. of Photochem. and Photobiol. A* **2011**, *219*, 50-57.
- [37] V. V. Pavlishchuk, A. W. Addison, *Inorg. Chim. Acta* **2000**, *298*, 97-102.
- [38] T. Kurita, F. Aoki, T. Mizumoto, T. Maejima, H. Esaki, T. Maegawa, Y. Monguchi, H. Sajiki, *Chemistry* **2008**, *14*, 3371-3379.
- [39] M. Pena-Lopez, M. Ayan-Varela, L. A. Sarandeses, J. Perez Sestelo, *Chemistry* **2010**, *16*, 9905-9909.
- [40] K. Takahashi, M. Takaki, R. Asami, *Org. Magn. Reson.* **1971**, *3*, 539-543.

-
- [41] M. J. Frisch, G. W. Trucks, H. B. Schlegel, G. E. Scuseria, M. A. Robb, J. R. Cheeseman, G. Scalmani, V. Barone, B. Mennucci, G. A. Petersson, H. Nakatsuji, M. Caricato, X. Li, H. P. Hratchian, A. F. Izmaylov, J. Bloino, Z. G., J. L. Sonnenberg, M. Hada, M. Ehara, K. Toyota, R. Fukuda, J. Hasegawa, M. Ishida, T. Nakajima, Y. Honda, O. Kitao, H. Nakai, T. Vreven, J. A. Montgomery Jr., J. E. Peralta, F. Ogliaro, M. Bearpark, J. J. Heyd, E. Brothers, K. N. Kudin, V. N. Staroverov, T. Keith, R. Kobayashi, J. Normand, K. Raghavachari, A. Rendell, J. C. Burant, S. S. Iyengar, J. Tomasi, M. Cossi, N. Rega, J. M. Millam, M. Klene, J. E. Knox, J. B. Cross, V. Bakken, C. Adamo, J. Jaramillo, R. Gomperts, R. E. Stratmann, O. Yazyev, A. J. Austin, R. Cammi, C. Pomelli, J. W. Ochterski, R. L. Martin, K. Morokuma, V. G. Zakrzewski, G. A. Voth, P. Salvador, J. J. Dannenberg, S. Dapprich, A. D. Daniels, O. Farkas, J. B. Foresman, J. V. Ortiz, J. Cioslowski, D. J. Fox, *Gaussian, Inc., Wallingford CT* **2013**.
- [42] A. V. Marenich, C. J. Cramer, D. G. Truhlar, *J. Phys. Chem. B* **2009**, *113*, 6378-6396.
- [43] T. Taniguchi, H. Zaimoku, H. Ishibashi, *Chemistry* **2011**, *17*, 4307-4312.
- [44] M. Nakajima, E. Fava, S. Loescher, Z. Jiang, M. Rueping, *Angew. Chem. Int. Ed.* **2015**, *54*, 8828-8832.

CHAPTER 5

5 Photocatalytic carbanion generation from C–H bonds - reductant free Barbier/Grignard-type reactions



This chapter has been published in: A. L. Berger, K. Donabauer, B. König, *Chem. Sci.* **2019**, *10*, 10991-10996.

A. L. Berger and K. Donabauer contributed equally to this project. A. L. Berger and K. Donabauer developed the project, A. L. Berger carried out the reactions in Table 5-1, Table 5-2 and a part of the reactions in Table 5-3. K. Donabauer carried out a part of the reactions in Table 5-3. A. L. Berger and K. Donabauer wrote the manuscript. B. König supervised the project and is corresponding author.

5.1 Introduction

Novel catalytic methods generally aim to produce a desired chemical compound from ever-simpler starting materials, maximizing the atom and step economy.^[1] Hence, the functionalization of C–H bonds has received great attention, as it illustrates the most straightforward retrosynthetic path for the synthesis of a targeted product.^[2] There are several methods for C–H functionalizations summarized in comprehensive reviews.^[3] A prominent example is the C–H activation by metal insertion,^[3c-f] comprising cases of very high and catalyst controlled regioselectivity.^[4] Another prevalent method is hydrogen atom transfer,^[3g] which is used to generate carbon centred radicals for subsequent functionalization from unreactive C–H bonds by the abstraction of a hydrogen atom.

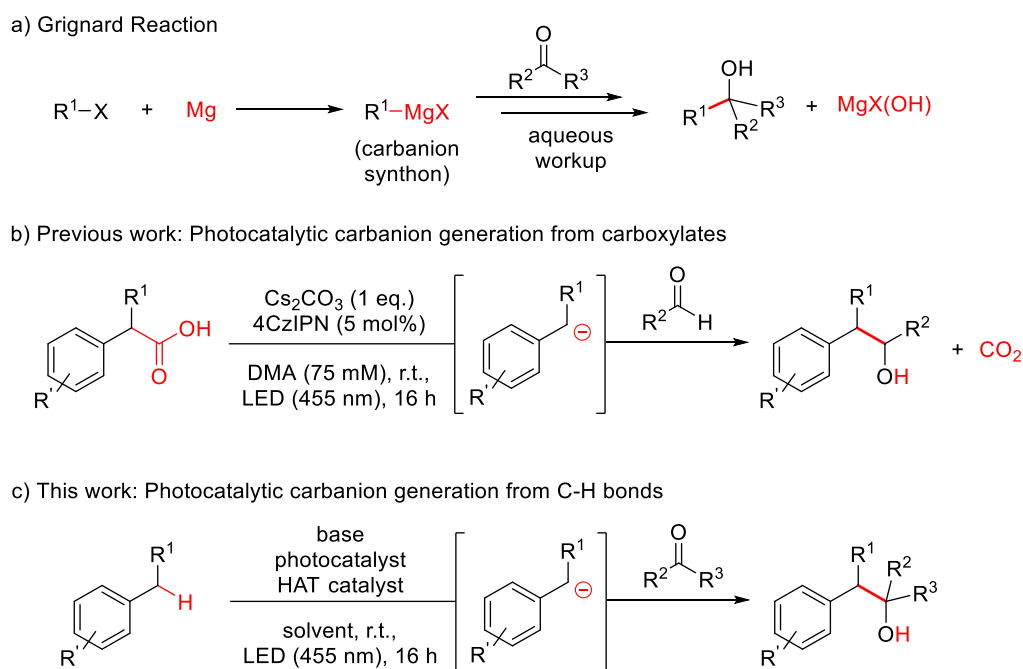
Recently, the combination of hydrogen atom transfer (HAT) and photocatalysis has evolved into a powerful method yielding carbon radicals under mild conditions often without the need of a sacrificial oxidant or reductant.^[5] With this approach, several impressive examples for C–C and C–X bond formations were reported, utilizing C–H bonds in order to arrive at the desired product in high or even full atom economy.^[6] While photocatalysis, especially in combination with HAT catalysis, mainly revolves around the generation and subsequent reaction of radical species,^[7] some groups have recently proposed the generation of carbanions as crucial intermediates in photocatalytic transformations.^[7a, 8] The formation of carbanionic intermediates is of particular interest as they are the reactive intermediates in the widely used Grignard and Barbier reactions (Scheme 5-1a).^[9] However, these reactions produce stoichiometric amounts of metal salt waste^[9c] and require organohalide starting materials which often have to be prepared.^[10]

In our previous report we aimed to overcome those drawbacks by using carboxylates to generate carbanionic intermediates in a photocatalytic reaction (Scheme 5-1b).^[8g] Though, only aldehydes were efficient electrophiles and CO₂ was released as a stoichiometric by-product. Developing this method further, we wondered if C–H bonds could directly be activated to form the desired Grignard analogous products, maximizing the atom economy.

The most straight-forward C–H activation giving potential access to carbanion intermediates from unfunctionalized starting materials is the deprotonation of the respective C–H bond. However, with a pK_a value of approximately 43 (in DMSO),^[11] even benzylic C–H bonds would require the use of highly active bases like *n*Bu–Li (pK_a approx. 50) exceeding *e.g.* LDA (pK_a = 35 in DMSO)^[12] in reactivity, which limits the functional group tolerance and gives

rises to potential side reactions. Additionally, many of these strong bases can directly add to carbonyl compounds or be quenched by the deprotonation of the more acidic proton in α position of the carbonyl (pK_a of acetone = 26 in DMSO),^[13] which may also be the case for the desired benzyl anion. Additionally, waste products resulting from the use of metal bases again diminish the atom economy. Considering this, the generation of carbanions by the combination of HAT- and photocatalysis could overcome these issues and illustrates a valuable method for a redox-neutral, waste-free synthesis of Grignard-type products without the use of metals or strong bases (Scheme 5-1c).

In a recent report, our group could show the applicability of this concept for the photocarboxylation of benzylic C–H bonds via carbanionic intermediates.^[14] In this work, we aim to extend this method to the synthesis of secondary and tertiary benzylic alcohols from unfunctionalized starting materials and aldehydes or ketones in a photocatalytic two-step deprotonation reaction.



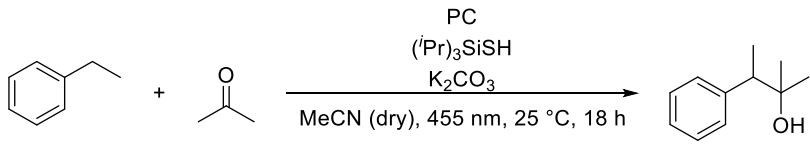
Scheme 5-1 – a) Grignard Reaction. (b) Photocatalytic carbanion generation from carboxylates and addition to aldehydes. (c) Envisioned photocatalytic carbanion generation from C–H bonds for Grignard-type reactions in full atom economy.

5.2 Results and discussion

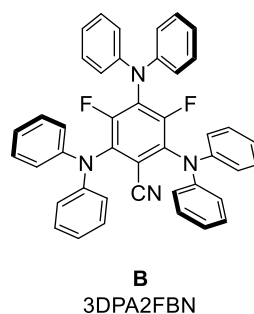
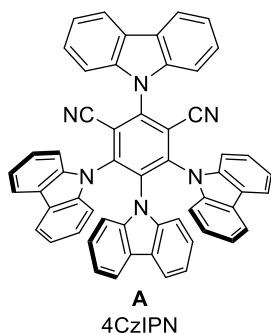
With our aim in mind, we chose ethylbenzene (**1a**) as model substrate, because its benzylic C–H bonds have a low bond dissociation energy (BDE = 85.4 kcal/mol^[15]) and benzylic radicals can be converted into the corresponding carbanion by single electron transfer (SET) using a reduced photocatalyst.^[8g] Acetone (**2a**) was chosen as electrophile, as ketones do not bear a carbonyl hydrogen, which has shown to be prone to C–H abstraction by electrophilic radicals.^[16]

The first product formation was observed using the combination of 4CzIPN (**A**) as photocatalyst and (iPr)₃SiSH as HAT catalyst. With K₂CO₃ as base and dry MeCN as solvent, the coupling product (**3a**) between **1a** and **2a** was detected in traces (Table 5-1, entry 1). A higher yield of 21% was obtained by adding grinded 4 Å molecular sieves to the reaction (Table 5-1, entry 2). Increasing the amount of **2a** by using it as a co-solvent in a 1:1 mixture with dry acetonitrile gave a yield of 49% (Table 5-1, entry 3). Reducing the amount of (iPr)₃SiSH and molecular sieves gave a slightly enhanced yield (Table 5-1, entry 4). Using 3DPA2FBN (**B**) as a photocatalyst increased the yield to 50% when 10 eq. **2a** were used and 86% when acetone was used as a co-solvent (Table 5-1, entries 5 and 6). The reaction improved slightly by reducing the loading of photocatalyst **B** to 3 mol% and the amount of K₂CO₃ to 10 mol% (Table 5-1, entry 7). Control experiments showed, that the yield is significantly lower when the reaction is performed without base (Table 5-1, entry 8) and no product was detected in absence of light, photocatalyst or HAT catalyst (Table 5-1, entries 9-11).

Table 5-1 – Optimization of the reaction conditions for the photocatalytic HAT-reaction of ethylbenzene (**1a**) with acetone (**2a**) as an electrophile



Entry	Amount of 2a	Photocatalyst (mol%)	Amount of (<i>i</i> Pr) ₃ SiSH	Amount of base	Additive	Yield [%] ^[b]
1	10 eq.	4CzIPN (5)	20 mol%	20 mol%	–	3
2	10 eq.	4CzIPN (5)	20 mol%	20 mol%	4 Å MS (100 mg)	21
3	co-solvent (1:1)	4CzIPN (5)	20 mol%	20 mol%	4 Å MS (100 mg)	49
4	10 eq.	4CzIPN (5)	10 mol%	20 mol%	4 Å MS (50 mg)	30
5	10 eq.	3DPA2FBN (5)	10 mol%	20 mol%	4 Å MS (50 mg)	50
6	co-solvent (1:1)	3DPA2FBN (5)	10 mol%	20 mol%	4 Å MS (50 mg)	86
7	10 eq.	3DPA2FBN (3)	10 mol%	10 mol%	4 Å MS (50 mg)	59
8	10 eq.	3DPA2FBN (5)	10 mol%	–	4 Å MS (50 mg)	27
9	10	–	10 mol%	20 mol%	4 Å MS (100 mg)	0
10 ^[c]	10	4CzIPN (5)	10 mol%	20 mol%	4 Å MS (100 mg)	0
11	10	4CzIPN (5)	–	20 mol%	4 Å MS (100 mg)	0



[a] The reaction was performed using 1 eq. (0.2 mmol) **1a** in 2 mL degassed solvent, b] yields were determined with GC-FID analysis using *n*-decane as an internal standard, [c] reaction was performed in the dark.

The kinetic profile of the reaction shows a quite fast linear increase of product formation in the first hours. However, after 5 hours, the conversion of starting material stops at a product yield of 50 to 55%, which increased only slightly by prolonging the reaction time (Figure 5-1).

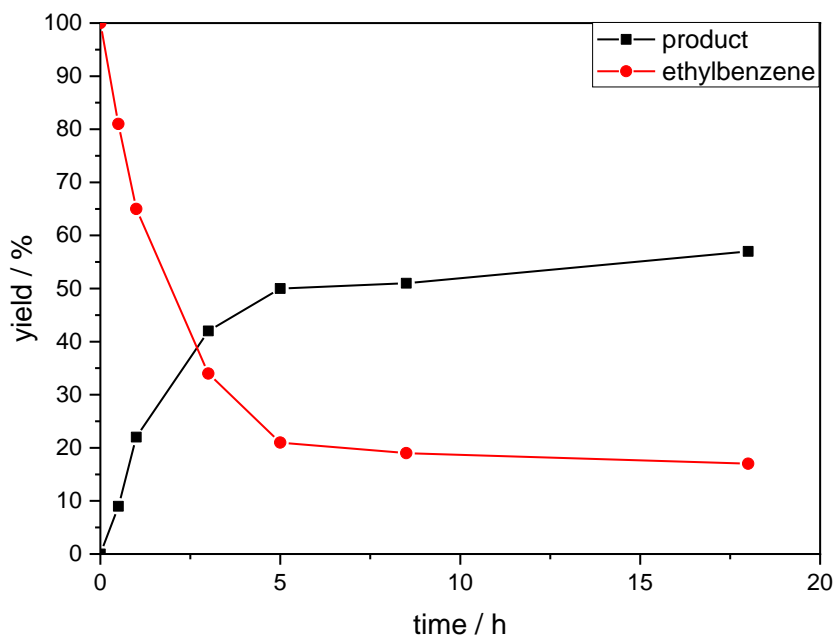
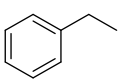
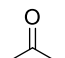
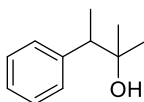
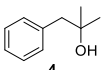
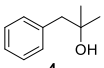


Figure 5-1 – Product formation and consumption of starting material during the reaction.

To exclude the possibility, that the termination of the reaction is caused by the decomposition of either the photocatalyst or the hydrogen atom transfer catalyst, both compounds were added to the reaction separately or in combination after several hours (Table 5-2, entries 1-3). However, the yield of the desired product **3a** could not be increased for any of the combinations. To test if the reaction was inhibited by the formation of the product, 2-methyl-1-phenyl-2-propanol **4** was added due to its structural similarity to product **3a**. Indeed, the yield decreased to 39% when 0.5 eq. **4** was added and to 11% with 1 eq. **4** (Table 5-2, entries 4 and 5). The addition of 1 eq. 1-heptanol also decreased the yield to 21% (Table 5-2, entry 6), indicating that the presence of alcohols causes the reaction to stop, presumably due to the protic hydroxy groups quenching the carbanion.

Table 5-2 – Investigations of product inhibition of the reaction.

<div style="display: flex; align-items: center; justify-content: center;"> <div style="text-align: center; margin-right: 10px;">  1a </div> <div style="margin: 0 10px;">+</div> <div style="text-align: center; margin-right: 10px;">  2a </div> <div style="text-align: center; margin-right: 10px;"> $\xrightarrow[\text{4 Å MS}]{\begin{array}{l} \text{3DPA2FBN (5 mol\%)} \\ (\text{tPr})_3\text{SiSH (10 mol\%)} \\ \text{K}_2\text{CO}_3 \text{ (10 mol\%)} \end{array}}$ </div> <div style="text-align: center; margin-left: 10px;">  3a </div> </div>		
Entry	Additive	Yield [%] ^[b]
1 ^[c]	3DPA2FBN (5 mol%)	41
2 ^[c]	(<i>t</i> Pr) ₃ SiSH (10 mol%)	50
3 ^[c]	3DPA2FBN (3 mol%) (<i>t</i> Pr) ₃ SiSH (10 mol%)	60
4	 (0.5 eq.)	39
5	 (1 eq.)	11
6	1-Heptanol (1 eq.)	21

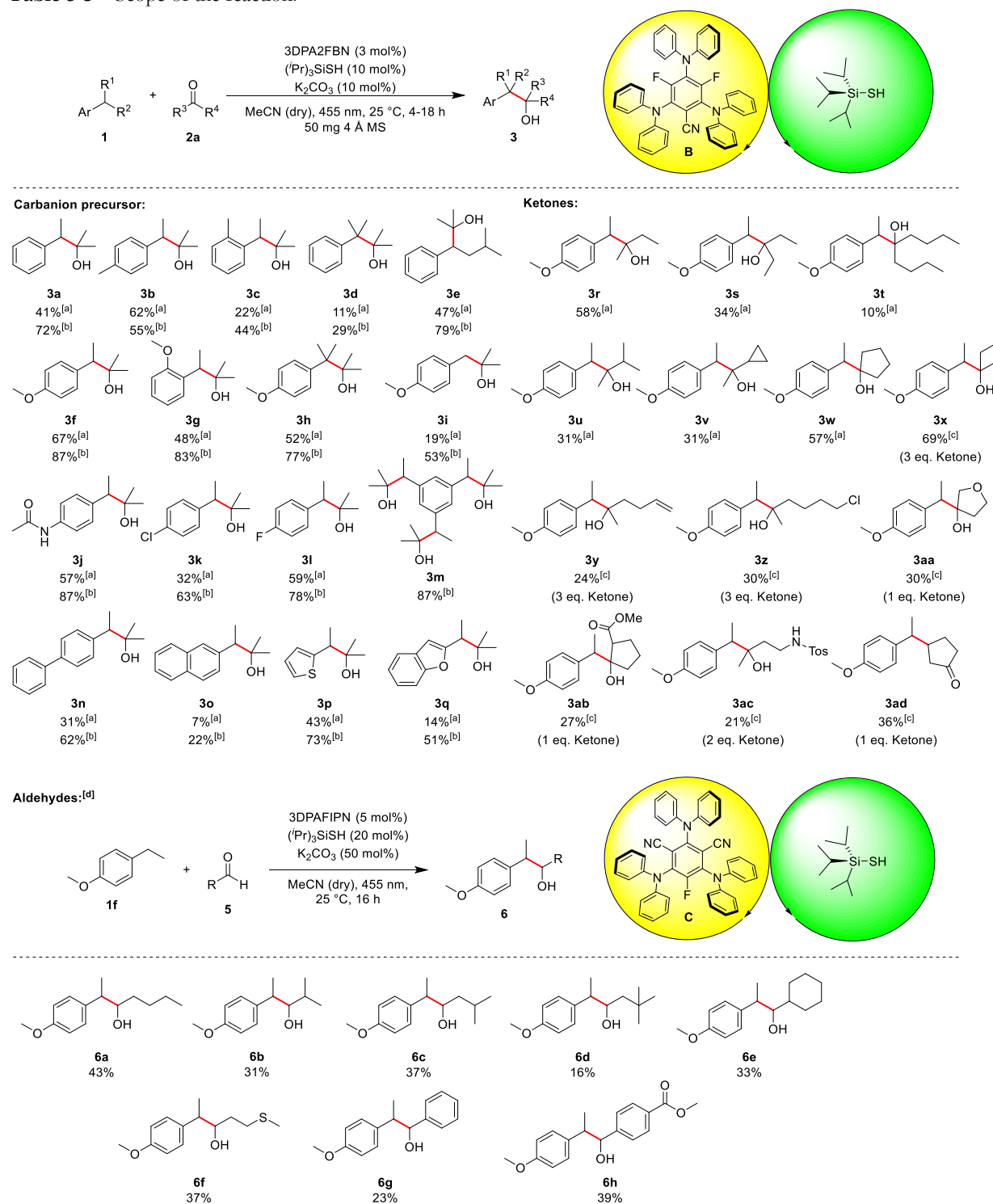
[a] The reaction was performed using 1 eq. (0.2 mmol) **1a** and 10 eq. **2a** in 2 mL degassed solvent, [b] yields were determined with GC-FID analysis using *n*-decane as an internal standard, [c] additional catalyst was added after 14 h.

The scope of the reaction was investigated for various ethylbenzene derivatives, ketones and aldehydes (Table 5-3). In most cases, good yields were obtained when the electrophile acetone was used as a co-solvent in a 1:1 mixture with acetonitrile, while using 10 eq. of electrophile led to moderate yields. Besides ethylbenzene **1a** (41%/72%, **3a**), 4- or 2-ethyltoluene were also viable substrates for the reaction (**3b** and **3c**). Notably, 4-ethyltoluene **1b** was the only substrate where using less electrophile seemed to be beneficial for the reaction, as a yield of 62% was obtained for 10 eq. **2a**, while using acetone as a co-solvent only lead to 55% of the desired product **3b**. Using cumene **1d** decreased the yield to 29% (11% with 10 eq. **2a**), presumably due to enhanced steric hindrance in the benzylic position (**3d**). The reaction proceeded well with isopentylbenzene **1e**, yielding the corresponding product **3e** in 47% and 79%, respectively. Ethylbenzene derivatives containing electron donating substituents, such as methoxy- (**3f** – **3i**) or amide-groups (**3j**) led to significantly increased yields of up to 87% (**3f** and **3j**). In contrast, no product was obtained with electron deficient substrates such as 4-ethylbenzonitrile or 1-ethyl-4-(trifluoromethyl)benzene, presumably due to the lower reactivity of the corresponding carbanion intermediate. While unsubstituted toluene did not

lead to any product formation due to the bond dissociation energy of the benzylic C–H bond exceeding the capability of the hydrogen atom transfer catalyst (toluene: BDE = 89 kcal/mol, (Pr)₃SiSH: BDE = 87 kcal/mol),^[17] 4-methoxytoluene **1i** gave the corresponding product **3i** in 19% and 53%, respectively. Chlorine and fluorine substituents at the aromatic ring were also well tolerated in the reaction (**3k** and **3l**) and using triethylbenzene **1m** led to 87% of the triple substituted product **3m** when acetone was used as a co-solvent. For this substrate, no product could be isolated when only 10 eq. **2a** was used, as an inseparable mixture of single, double and triple substituted product was obtained. *p*-Phenyl substituted ethylbenzene could also be used in the reaction, yielding 62% of product **3n** (31% with 10 eq. **2a**). In contrast, 2-ethylnaphthalene **1o** gave only low yields of 7% and 22%, respectively (**3o**). Heteroaromatic substrates were also viable substrates for the reaction as moderate to good yields were obtained when 2-ethylthiophene **1p** or -benzofurane **1q** were used (**3p** and **3q**).

Moving to ketones, the effect of steric hindrance was investigated first. A good yield can still be obtained when the carbon chain is extended at one side (**3r**), whereas the yield is notably affected when both sides bear longer chains (**3s** and **3t**) or an additional group is present in α -position (**3u** and **3v**). No ring opening products were observed when a cyclopropane ring was present in α -position, indicating that no radical processes are involved in the addition to the electrophile. The reaction proceeds well with cyclic ketones (**3w** and **3x**), especially with cyclobutanone (**3x**), altogether displaying the significant influence of steric hindrance. In terms of functional group tolerance, alkenes (**3y**), alkyl chlorides (**3z**), ethers (**3aa**), esters (**3ab**) and protected amines (**3ac**) are viable substrates. However, the amount of electrophile has to be reduced in these cases, causing a decrease in yield. Notably, if an α,β -unsaturated system is used, the 1,4-addition product (**3ad**) is obtained, while the 1,2-addition product was not observed. As noted above, aldehydes are prone to C–H abstraction from the carbonyl position,^[16] seemingly leading to deleterious side reactions. Hence, the reaction conditions were adapted, mainly by using an excess of the ethyl benzene instead of the electrophile (see SI for all optimization parameters). Under the modified reaction conditions, aldehydes are feasible substrates, but yields are generally only low to moderate (up to 43% for **6a**). As with ketones, steric hindrance has a significant effect (**6a–6e**). Thioethers are tolerated (**6f**) despite the presence of C–H bonds in α -position to the heteroatom. Further, employing aromatic aldehydes gave the desired products as well (**6g** and **6h**), and the yield increased with an additional electron withdrawing ester group (**6h**).

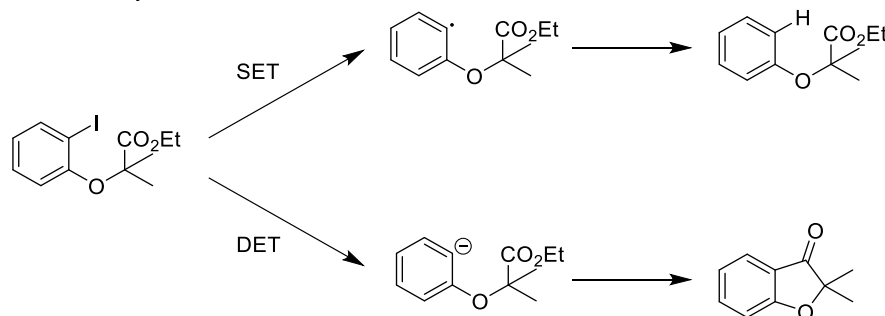
Table 5-3 – Scope of the reaction.



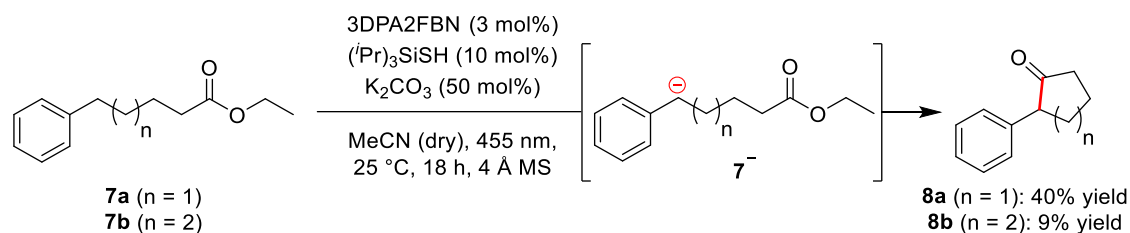
[a] The reaction was performed using 1 eq. (0.2 mmol) **1** and 10 eq. of the respective ketone in 2 mL dry, degassed MeCN, [b] the reaction was performed using 1 eq. (0.2 mmol) **1** and **2a** as co-solvent in a 1:1 mixture with dry MeCN in 2 mL degassed solvent mixture, [c] the reaction was performed using 1 eq. (0.2 mmol) **1** and the respective ketone in the amount given in the table in 2 mL dry, degassed MeCN, [d] the reaction was performed using 1 eq. (0.15 mmol) **5** and 3 eq. **1f** in 2 mL dry, degassed MeCN.

To investigate the mechanism of the reaction, a carbanion test system based on a molecule used by Murphy *et al.* to confirm the generation of aryl anions (Scheme 5-2a) was used.^[18] According to Murphy, radicals are not capable of adding to esters. Therefore, ethyl-5-phenylpentanoate **7a** was subjected to the standard reaction conditions. The formation of the cyclic ketone **8a** indicates the presence of the anionic intermediate **7a⁻** (Scheme 5-2b).

a) Murphy carbanion test system



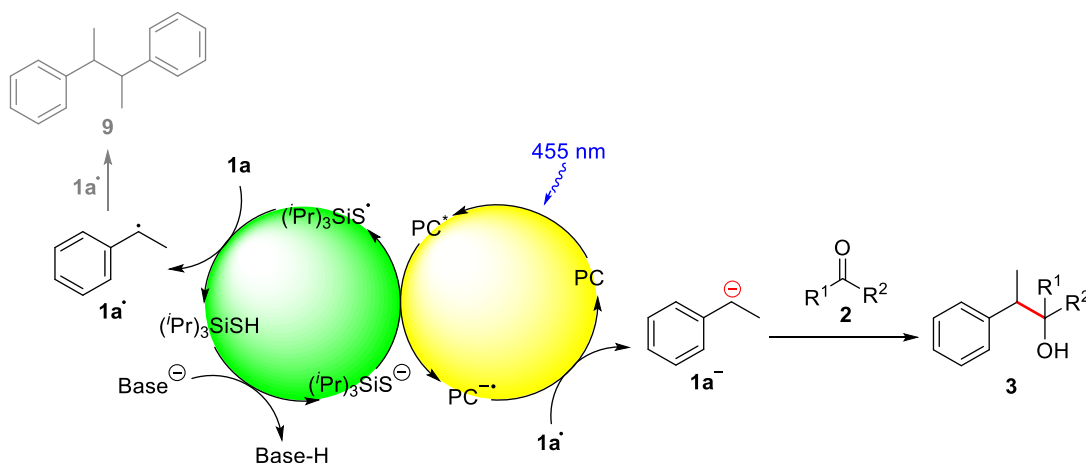
b) Carbanion test system for this reaction



Scheme 5-2 – Carbanion test system a) developed by Murphy *et al.* for the detection of aryl anions and b) test system used for this reaction.

In addition to this, fluorescence quenching studies were performed to confirm the interaction of the excited state of the photocatalyst with the deprotonated HAT catalyst $(i\text{Pr})_3\text{SiS}^-$. Efficient fluorescence quenching was observed for the photocatalysts **B** and **C** upon addition of $(i\text{Pr})_3\text{SiS}^-$, indicating the oxidation of the deprotonated hydrogen atom transfer catalyst by the excited state of the photocatalyst (experimental part, Figure 5-4 and 5-5). To further confirm this, cyclic voltammetry measurements were performed (Supporting Information, Figure S5). Indeed, a potential of 0.67 V *vs.* SCE in MeCN was obtained for a 1:2 mixture of $(i\text{Pr})_3\text{SiSH}$ and K_2CO_3 which is well in the range of photocatalyst **B** and **C** ($E_{1/2}(\text{3DPA2FBN}^*/\text{3DPA2FBN}^{\cdot-}) = 0.92 \text{ V vs. SCE}$, $E_{1/2}(\text{3DPAFIPN}^*/\text{3DPAFIPN}^{\cdot-}) = 1.09 \text{ V vs. SCE}$).^[19] Lastly, the formation of benzylic radicals (**1[•]**) during the reaction is indicated by the presence of small amounts of the homocoupling product **9** in the reaction mixture (experimental part, Figure 5-7).

Based on these mechanistic investigations, the reaction mechanism depicted in Scheme 5-3 is proposed. The photocatalyst is excited upon irradiation with blue light and after deprotonation with K_2CO_3 , $(i\text{Pr})_3\text{SiS}^-$ can be oxidized to $(i\text{Pr})_3\text{SiS}^\bullet$ by a SET to the excited photocatalyst PC^* . The generated sulfur radical is capable of abstracting a hydrogen atom from ethylbenzene **1a**, generating the benzylic radical **1a** $^\bullet$ (**1a**: BDE = 85.4 kcal/mol,^[15] $(i\text{Pr})_3\text{SiSH}$: BDE = 87 kcal/mol^[17]). Compound **1a** $^\bullet$ ($E_{1/2}(\text{1a}^\bullet/\text{1a}^-) = 1.60 \text{ V vs. SCE}$)^[20] can be reduced by the radical anion of the photocatalyst $\text{PC}^{\bullet-}$ ($E_{1/2}(\text{3DPA2FBN}/\text{3DPA2FBN}^-) = -1.92 \text{ V vs. SCE}$, $E_{1/2}(\text{3DPAFIPN}/\text{3DPAFIPN}^-) = -1.59 \text{ V vs. SCE}$),^[19] thus closing the photocatalytic cycle. The resulting benzylic anion **1a** $^-$ reacts with electrophiles like aldehydes or ketones, leading to the desired product **3**.



Scheme 5-3 – Proposed reaction mechanism.

5.3 Conclusion

In summary, we have developed a method for the photocatalytic generation of carbanions from benzylic C–H bonds, which react with electrophiles, such as aldehydes or ketones, to generate homobenzylic alcohols as products. The reaction represents a formal two-step deprotonation of the non-acidic benzylic C–H bond and could be a mechanistic alternative to classic C–C bond forming reactions such as the Grignard or Barbier reaction, giving the same products. However, instead of using stoichiometric amounts of a zero-valent metal and halogenated precursor, an organic photocatalyst, catalytic amounts of a hydrogen atom transfer reagent and visible light are used to generate carbanionic intermediates directly from C–H bonds, yielding the desired product in a redox neutral reaction with full atom economy.

5.4 Experimental part

5.4.1 General information

Starting materials and reagents were purchased from commercial suppliers (Sigma Aldrich, Alfa Aesar, Acros, Fluka, TCI or VWR) and used without further purification. Solvents were used as p.a. grade or dried and distilled according to literature known procedures.^[21] For automated flash column chromatography distilled solvents was used. All reactions with oxygen- or moisture-sensitive reagents were carried out in glassware, which was dried before use by heating under vacuum. Dry nitrogen was used as inert gas atmosphere. Liquids were added via syringe, needle and septum techniques unless otherwise stated.

All NMR spectra were measured at room temperature using a Bruker Avance 300 (300 MHz for ^1H , 75 MHz for ^{13}C , 282 MHz for ^{19}F) or a Bruker Avance 400 (400 MHz for ^1H , 101 MHz for ^{13}C , 376 MHz for ^{19}F)^[22] NMR spectrometer. All chemical shifts are reported in δ -scale as parts per million [ppm] (multiplicity, coupling constant J , number of protons) relative to the solvent residual peaks as the internal standard.^[23]

Coupling constants J are given in Hertz [Hz]. Abbreviations used for signal multiplicity: ^1H -NMR: b = broad, s = singlet, d = doublet, t = triplet, q = quartet, hept = heptet dd = doublet of doublets, dt = doublet of triplets, dq = doublet of quartets, and m = multiplet; ^{13}C -NMR: (+) = primary/tertiary, (–) = secondary, (C_q) = quaternary carbon).

The mass spectrometrical measurements were performed at the Central Analytical Laboratory of the University of Regensburg. All mass spectra were recorded on a Finnigan MAT 95, ThermoQuest Finnigan TSQ 7000, Finnigan MAT SSQ 710 A or an Agilent Q-TOF 6540 UHD instrument.

For the optimization using aldehydes following GC method was used: GC measurements were performed on a GC 6890 from Agilent Technologies. Data acquisition and evaluation was done with Agilent ChemStation Rev.C.01.04. A capillary column DB-WAX UI/30 m x 0.25 mm/0.25 μm film and helium as carrier gas (flow rate of 1 mL/min) were used. The injector temperature (split injection: 30:1 split) was 280 °C, detection temperature 310 °C (FID). GC measurements were made and investigated *via* integration of the signal obtained. The GC oven temperature program was adjusted as follows: initial temperature 40 °C was kept for 3 minutes, the temperature was increased at a rate of 15 °C/min over a period of 12 minutes until 220 °C was reached and kept for 5 minutes, the temperature was again increased

at a rate of 25 °C/min over a period of 48 seconds until the final temperature (240 °C) was reached and kept for 5 minutes. 1-Heptanol was used as an internal standard.

For every other use following GC method was used: GC measurements were performed on a GC 7890 from Agilent Technologies. Data acquisition and evaluation was done with Agilent ChemStation Rev.C.01.04. GC/MS measurements were performed on a 7890A GC system from Agilent Technologies with an Agilent 5975 MSD Detector. Data acquisition and evaluation was done with MSD ChemStation E.02.02.1431.A capillary column HP-5MS/30 m x 0.25 mm/0.25 µM film and helium as carrier gas (flow rate of 1 mL/min) were used. The injector temperature (split injection: 40:1 split) was 280 °C, detection temperature 300 °C (FID). GC measurements were made and investigated via integration of the signal obtained. The GC oven temperature program was adjusted as follows: initial temperature 40 °C was kept for 3 minutes, the temperature was increased at a rate of 15 °C/min over a period of 16 minutes until 280 °C was reached and kept for 5 minutes, the temperature was again increased at a rate of 25 °C/min over a period of 48 seconds until the final temperature (300 °C) was reached and kept for 5 minutes. If noted, *n*-decane was used as an internal standard.

Analytical TLC was performed on silica gel coated alumina plates (MN TLC sheets ALUGRAM® Xtra SIL G/UV₂₅₄). Visualization was done by UV light (254 or 366 nm). If necessary, potassium permanganate, vanillin or ceric ammonium molybdate was used for chemical staining.

Purification by column chromatography was performed with silica gel 60 M (40-63 µm, 230-440 mesh, Merck) on a Biotage® Isolera™ Spektra One device.

For irradiation with blue light OSRAM Oslon SSL 80 LDCQ7P-1U3U (blue, λ_{max} = 455 nm, I_{max} = 1000 mA, 1.12 W) was used. For irradiation with green light Cree XPEGRN L1 G4 Q4 (green, λ_{max} = 535 nm, I_{max} = 1000 mA, 1.12 W) was used.

CV measurements were performed with the three-electrode potentiostat galvanostat PGSTAT302N from Metrohm Autolab using a glassy carbon working electrode, a platinum wire counter electrode, a silver wire as a reference electrode and TBATFB 0.1 M as supporting electrolyte. The potentials were achieved relative to the Fc/Fc⁺ redox couple with ferrocene as internal standard.^[24] The control of the measurement instrument, the acquisition and processing of the cyclic voltammetric data were performed with the software Metrohm Autolab NOVA 1.10.4. The measurements were carried out as follows: a 0.1 M solution of TBATFB in acetonitrile was added to the measuring cell and the solution was degassed by

argon purge for 5 min. After recording the baseline the electroactive compound was added (0.01 M) and the solution was again degassed a stream of argon for 5 min. The cyclic voltammogram was recorded with one to three scans. Afterwards ferrocene (2.20 mg, 12.0 μmol) was added to the solution which was again degassed by argon purge for 5 min and the final measurement was performed with three scans.

Fluorescence spectra were measured on a HORIBA FluoroMax[®]-4 Spectrofluorometer at room temperature. Gas tight 10 mm Hellma[®] quartz fluorescence cuvettes with a screw cap with PTFE -coated silicon septum were used. FluorEssence Version 3.5.1.20 was used as a software for measurement and analysis.

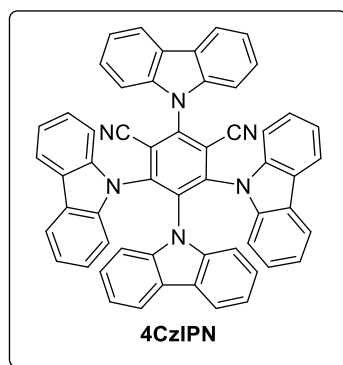
5.4.2 General procedures

5.4.2.1 Synthesis of photocatalysts

2,4,5,6-Tetrakis(carbazole-9-yl)-4,6-dicyanobenzene (4CzIPN)

The photocatalyst was synthesized according to a literature procedure.^[25]

NaH (60% in paraffin oil, 800 mg, 20 mmol, 10 eq.) was slowly added to a stirred solution of carbazole (1.67 g, 10 mmol, 5 eq.) in dry THF (40 mL). The reaction mixture was heated to 35 °C and stirred for 1 h before adding tetrafluoroisophthalonitrile (400 mg, 2 mmol, 1 eq.). The reaction mixture was stirred at 35 °C for 16 h, afterwards quenched by H₂O (2 mL) and concentrated *in vacuo*. The solid residue was washed with H₂O and EtOH to yield the crude product, which was purified by recrystallization from hexane/DCM to give 2,4,5,6-tetrakis(carbazol-9-yl)-4,6-dicyano-benzene (4CzIPN) as bright yellow powder (840 mg, 1.06 mmol, 53%).



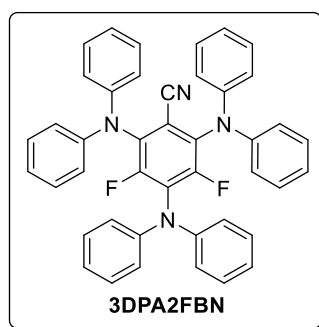
¹H-NMR (400 MHz, CDCl₃, δ_H): 8.22 (d, *J* = 7.7 Hz, 2H), 7.75 – 7.67 (m, 8H), 7.52 – 7.47 (m, 2H), 7.33 (d, *J* = 7.8 Hz, 2H), 7.25 – 7.19 (m, 4H), 7.12 – 7.05 (m, 8H), 6.82 (t, *J* = 8.2 Hz, 4H), 6.63 (td, *J* = 7.6, 1.2 Hz, 2H).

¹³C-NMR (101 MHz, CDCl₃, δ_C): 145.3, 144.7, 140.1, 138.3, 137.1, 134.9, 127.1, 125.9, 125.1, 124.9, 124.7, 124.0, 122.5, 122.1, 121.5, 121.1, 120.6, 119.8, 116.5, 111.8, 110.1, 109.6, 109.6.

2,4,6-Tris(diphenylamino)-3,5-difluorobenzonitrile (3DPA2FBN)

The photocatalyst was synthesized according to a literature procedure.^[19]

Under nitrogen atmosphere, diphenylamine (1.27 g, 7.5 mmol, 1.25 eq.) was dissolved in dry THF (40 ml) in a flame dried Schlenk flask. Sodium hydride (60% in paraffin oil, 0.45 g, 11.3 mmol, 5.6 eq.) was slowly added and the reaction mixture was stirred at 50 °C for 30 minutes. Pentafluorobenzonitrile (255 µl, 0.39 g, 2 mmol, 1 eq.) was added and the reaction was stirred at room temperature for 24 h. The reaction mixture was quenched with water (2 ml) and concentrated under vacuum. The residue was dissolved in DCM and washed with brine. The organic phase was dried over Na₂SO₄ and the solvent was removed under reduced pressure. Purification of the crude product was performed by flash column chromatography on silica gel (PE/DCM, DCM 20 – 80%) yielding the desired product.



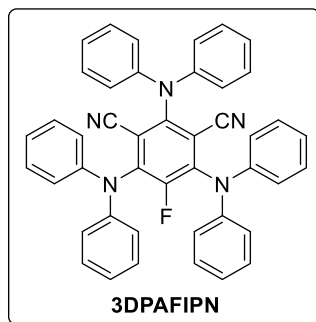
¹H NMR (300 MHz, CDCl₃, δ_H) 7.26 – 7.20 (m, 12H), 7.07 – 7.00 (m, 6H), 6.99 – 6.95 (m, 12H).

¹⁹F NMR (282 MHz, CDCl₃, δ_F) -120.72 (s).

HRMS (EI+) (*m/z*): [*M*⁺] (C₄₃H₃₀F₂N₄⁺) calc.: 640.2433, found: 640.2430.

2,4,6-Tris(diphenylamino)-5-fluoroisophthalonitrile (3DPAFIPN)

The photocatalyst was synthesized according to a literature procedure,^[19] and analogous to 4CzIPN with 2,3,5,6-tetrafluorobenzonitrile (350 mg, 2 mmol, 1 eq.) instead of carbazole. The crude product was purified by automated flash column chromatography (PE/DCM 20-80%). 2,4,6-Tris(diphenylamino)-5-fluoroisophthalonitrile (3DPAFIPN) (910 mg, 1.40 mmol, 70%) was obtained as bright yellow powder.



¹H-NMR (400 MHz, CDCl₃, δ_H): 7.30 – 7.23 (m, 12H), 7.11-7.02 (m, 6H), 7.02 – 6.96 (m, 12H).

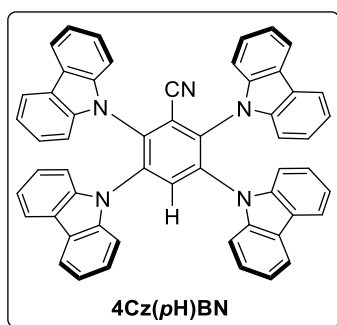
¹⁹F-NMR (377 MHz, CDCl₃, δ_F): -121.83 (s).

HRMS (FD-MS) (m/z): [M⁺] (C₄₄H₃₀FN₅⁺) calc. 647.2485; observed 647.1977.

FD-MS revealed, that 4DPAFIPN^[25] is present in small amount as well (m/z): [M⁺] (C₅₆H₄₀N₆⁺) calc. 796.3314; observed 796.2684. It may be the impurity visible in the NMR.

2,3,5,6-Tetrakis(carbazol-9-yl)benzonitrile (4Cz(pH)BN)

The photocatalyst was synthesized analogous to 4CzIPN with diphenylamine (1.69 g, 10 mmol, 5 eq.) instead of tetrafluoroisophthalonitrile. The crude product was purified by automated flash column chromatography (PE/DCM 20-80%). 2,3,5,6-Tetrakis(carbazol-9-yl)benzonitrile (4Cz(pH)BN) (1.00 g, 1.31 mmol, 66%) was obtained as pale yellow powder.



¹H-NMR (300 MHz, CDCl₃, δ_H): 8.44 (s, 1H), 7.82-7.74 (m, 8H), 7.39-7.280 (m, 8H), 7.23-7.08 (m, 16H).

¹³C-NMR (75 MHz, CDCl₃, δ_C): 139.3, 139.0, 137.9, 136.7, 125.9, 124.4, 124.0, 121.4, 121.1, 120.5, 120.4, 110.0, 109.4.

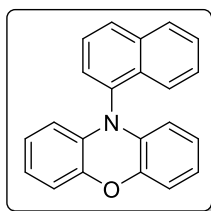
HRMS (FD-MS) (m/z): [M⁺] (C₅₅H₃₃N₅⁺) calc. 763.2731; observed 763.2712.

3,7-Di(4-biphenyl) 1-naphthalene-10-phenoxazine

The photocatalysts was synthesized according to a literature procedure.^[26]

1-Naphthalene-10-phenoxazine

A flame dried Schlenk flask was equipped with phenoxazine (2.0 g, 10.9 mmol, 1 eq.), NaO^tBu (2.1 g, 21.8 mmol, 2 eq.), RuPhos (131.2 mg, 0.32 mmol, 3 mol%), RuPhos precatalyst (229.5 mg, 0.32 mmol, 3 mol%), 1-bromonaphthalene (3.1 ml, 21.8 mmol, 2 eq.) and 12 ml dry dioxane. The reaction mixture was stirred at 130 °C for 48 h. After cooling to room temperature DCM (20 ml) was added and the solution was washed with water (3 x 20 ml), brine (1 x 20 ml) and dried over MgSO₄. After removing the solvents under reduced pressure, the crude product was obtained. It was purified by recrystallization from DCM. After recrystallization, the solution was layered with hexane at –25 °C and the product was obtained as a light yellow powder.



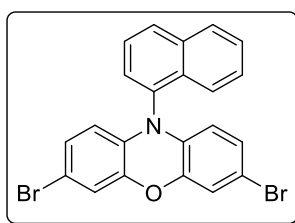
¹H NMR (400 MHz, CDCl₃, δ_H) 8.08 (d, *J* = 8.4 Hz, 1H), 8.02 – 7.94 (m, 2H), 7.68 – 7.60 (m, 1H), 7.59 – 7.52 (m, 2H), 7.51 – 7.44 (m, 1H), 6.78 – 6.69 (m, 2H), 6.63 (t, *J* = 7.6 Hz, 2H), 6.49 (dt, *J* = 7.7, 1.5 Hz, 2H), 5.70 (dd, *J* = 8.0, 1.5 Hz, 2H).

¹³C NMR (101 MHz, CDCl₃, δ_C) 144.1 (C_q), 135.7 (C_q), 135.2 (C_q), 134.4 (C_q), 131.5 (C_q), 129.3 (+), 129.1 (+), 128.9 (+), 127.4 (+), 127.0 (+), 126.9 (+), 123.5 (+), 123.5 (+), 121.4 (+), 115.5 (+), 113.5 (+).

Yield: 78%

3,7-Dibromo 1-naphthalene-10-phenoxazine

In a flask which was covered in aluminum foil to block out light, 1-naphthalene-10-phenoxazine (1.6 g, 5.2 mmol, 1 eq.) was dissolved in 160 ml chloroform. 160 ml of glacial acetic acid was added to the solution. *N*-Bromosuccinimide (1.9 mg, 10.6 mmol, 2.1 eq.) was added to the stirred reaction mixture in small portions in the dark. After stirring at room temperature for 2 h, the solvents were removed under reduced pressure. The solid residue was dissolved in chloroform, washed with water (3 x 20 ml), brine (1 x 20 ml) and dried with MgSO_4 and the product was collected as a brown powder.



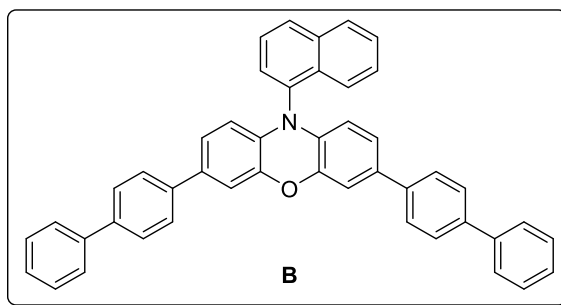
^1H NMR (400 MHz, Benzene- d_6 , δ_{H}) δ 7.82 (d, $J = 8.3$ Hz, 1H), 7.57 (dd, $J = 18.9, 8.1$ Hz, 2H), 7.21 – 7.18 (m, 1H), 7.15 – 7.10 (m, 2H), 6.90 (dd, $J = 7.3, 1.2$ Hz, 1H), 6.84 (d, $J = 2.2$ Hz, 2H), 6.36 (dd, $J = 8.5, 2.2$ Hz, 2H), 5.31 (d, $J = 8.5$ Hz, 2H).

^{13}C NMR (101 MHz, Benzene- d_6 , δ_{C}) 144.6 (C_q), 135.9 (C_q), 134.6 (C_q), 133.4 (C_q), 131.2 (C_q), 129.6 (+), 129.1 (+), 128.8 (+), 127.3 (+), 127.0 (+), 126.9 (+), 123.2 (+), 119.1 (+), 114.(+), 113.4 (+), 110.4 (C_q).

Yield: 77%

3,7-Di(4-biphenyl) 1-naphthalene-10-phenoxazine (Miyake catalyst)

In a flame dried Schlenk flask 3,7-dibromo 1-naphthalene-10-phenoxazine (1.1 g, 2.2 mmol, 1 eq.) and 4-biphenylboronic acid (1.9 g, 9.7 mmol, 4 eq.) were dissolved in 90 ml THF. 27 ml of a 2 M solution of K_2CO_3 in water was added to the solution and the reaction mixture was stirred at 80 °C for 20 minutes. After that, a solution of palladium tetrakis(triphenylphosphine) (420 mg, 0.4 mmol, 15 mol%) in 90 ml THF was added and the mixture was refluxed at 100 °C for 24 h. After cooling to room temperature, the solvents were removed under reduced pressure. The solid residue was dissolved in DCM, washed with water (2 x 20 ml), brine (1 x 20 ml) and dried with $MgSO_4$. The crude product was purified by recrystallization in DCM/Methanol and the product was obtained as a light tan powder.



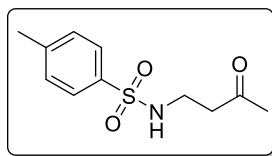
1H NMR (400 MHz, $DMSO-d_6$, δ_H) 8.18 (dd, $J = 14.5, 8.0$ Hz, 2H), 8.02 (d, $J = 8.2$ Hz, 1H), 7.81 – 7.76 (m, 2H), 7.72 – 7.7 (m, 14H), 7.46 (t, $J = 7.8$ Hz, 4H), 7.38 – 7.33 (m, 2H), 7.21 (d, $J = 2.1$ Hz, 2H), 6.98 (dd, $J = 8.4, 2.1$ Hz, 2H), 5.73 (d, $J = 8.3$ Hz, 2H).

Yield: 80%

5.4.2.2 Synthesis of starting materials

N-(3-Oxobutyl)-*p*-toluenesulfonamide

The substrate was synthesized according to a literature procedure.^[27]

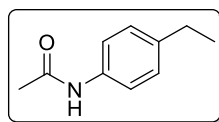


To a solution of *p*-toluenesulfonamide (1.71 g, 10.0 mmol, 1 eq.) dissolved in CHCl_3 (40 mL) were added Al_2O_3 (2 g, neutral) and methyl vinyl ketone (1.01 mL, 12.0 mmol, 1.2 eq.). The mixture was stirred at 45 °C in a stoppered flask for 6 days. Afterwards, the solution was filtered and the Al_2CO_3 was washed with EtOAc (30 mL). The solvent was evaporated and the crude product was purified by Automated flash column chromatography (DCM/MeOH, 2% MeOH) to afford *N*-(3-Oxobutyl)-*p*-toluenesulfonamide as white solid (600 mg, 25% yield).

¹H NMR (400 MHz, CDCl_3 , δ_{H}) 7.63 (d, J = 8.3 Hz, 2H), 7.25 (d, J = 8.0 Hz, 2H), 5.37 (t, J = 6.4 Hz, 1H), 3.07 (q, J = 6.1 Hz, 2H), 2.62 (t, J = 6.0 Hz, 2H), 2.36 (s, 3H), 2.04 (s, 3H).

N-(4-Ethylphenyl)acetamide

The substrate was synthesized according to a literature procedure.^[28]



4-ethylaniline (1.21 g, 10 mmol, 1 eq) was added to a round-bottom flask. Then the flask was purged with argon and dry DCM (40 mL) was added. Acetic anhydride (1.14 mL, 12 mmol, 1.2 eq) was added and the reaction was stirred at room temperature and monitored by TLC. Upon completion, the reaction mixture was washed with a saturated solution of sodium carbonate, the organic layers dried with MgSO_4 and the solvent removed under reduced pressure. Purification by column chromatography (ethyl acetate/petroleum ether) afforded the product as a white solid (1.52 g, 93% yield).

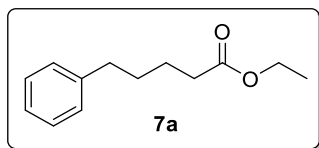
¹H NMR (300 MHz, CDCl_3 , δ_{H}) 7.53 (s, 1H), 7.43 – 7.35 (m, 2H), 7.17 – 7.08 (m, 2H), 2.60 (q, J = 7.7 Hz, 2H), 2.15 (s, 3H), 1.20 (t, J = 7.6 Hz, 3H).

¹³C NMR (75 MHz, CDCl_3 , δ_{C}) 168.5, 140.5, 135.6, 128.4, 120.3, 28.4, 24.6, 15.8.

HRMS (EI) (m/z): [M^+] $\text{C}_{10}\text{H}_{13}\text{NO}^+$: calc.: 163.0992, found: 163.0993.

Ethyl-5-phenylpentanoate (7a)^[29]

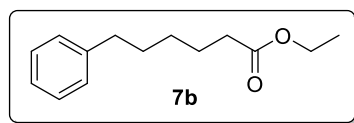
The substrate was synthesized according to modified literature procedure.^[30]



Sulfuric acid (533 μ L, 10.0 mmol, 1 eq.) was added to a solution of 5-phenylpentanoic acid (1.78 g, 10.0 mmol, 1 eq.) in ethanol (30 mL) cooled to 0 °C. The reaction mixture was warmed to room temperature and subsequently refluxed for 16 h. After cooling to room temperature, the solvent was evaporated. The residue was diluted with EtOAc (50 mL) and washed with NH_4Cl (aq., sat.) (3x20 mL). The organic phase was washed with brine (20 mL) and dried over MgSO_4 . The solvent was evaporated and the crude product was purified by automated flash column chromatography (Petroleum ether/Ethyl acetate 0-20%). Ethyl-5-phenylpentanoate (1.79 g, 8.68 mmol, 87%) was obtained as colorless liquid.

^1H NMR (300 MHz, CDCl_3 , δ_{H}) 7.31-7.24 (m, 2H), 7.21-7.14 (m, 3H), 4.12 (q, J = 7.1 Hz, 2H), 2.67-2.59 (m, 2H), 2.36-2.29 (m, 2H), 1.74-1.59 (m, 4H), 1.25 (t, J = 7.1 Hz, 3H).

^{13}C NMR (75 MHz, CDCl_3 , δ_{C}) 173.8, 142.3, 128.5, 128.5, 125.9, 60.4, 35.7, 34.4, 31.1, 24.8, 14.4.

Ethyl-6-phenylhexanoate^[31]

The substrate was synthesized analogous to ethyl-5-phenylpentanoate (**7a**) with 6-phenylhexanoic acid (470 mg, 2.5 mmol, 1 eq.) instead of 5-phenylpentanoic acid (1.78 g, 10.0 mmol, 1 eq.) using the solvents in half of the amount noted above.

Yield: 70% (387 mg, 1.75 mmol), colorless liquid.

^1H NMR (300 MHz, CDCl_3 , δ_{H}) 7.31-7.14 (m, 5H), 4.12 (q, J = 7.1 Hz, 2H), 2.65-2.57 (m, 2H), 2.29 (t, J = 7.5 Hz, 2H), 1.72-1.55 (m, 4H), 1.42-1.30 (m, 2H), 1.25 (t, J = 7.1 Hz, 3H).

^{13}C NMR (75 MHz, CDCl_3 , δ_{C}) 173.9, 142.7, 128.5, 128.4, 125.8, 60.3, 35.9, 34.4, 31.3, 28.9, 25.0, 14.4.

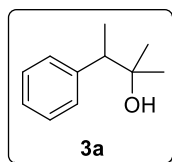
5.4.2.3 General procedure for the photocatalytic generation of carbanions from benzylic C–H bonds

General procedure for the photocatalytic benzylation of ketones (general procedure A)

A 5 mL crimp cap vial was equipped with the photocatalyst 3DPA2FBN (3.8 mg, 6.0 μmol , 3 mol%), K_2CO_3 (2.8 mg, 20.0 μmol , 10 mol%), grinded molecular sieves (50 mg) and a stirring bar. The vessel was capped and dry acetonitrile (2 mL), the ethylbenzene derivative **1** (0.2 mmol, 1 eq.), triisopropylsilanethiol (4.3 μL , 20.0 μmol , 10 mol%) and the corresponding ketone **2** (2.0 mmol, 10 eq., unless noted otherwise) were added via syringe under a nitrogen atmosphere. The reaction mixture was degassed by three cycles of freeze pump thaw and stirred and irradiated using a blue LED (455 nm \pm 15 nm) for 16 h at 25 $^\circ\text{C}$. The progress could be monitored by TLC, GC analysis and GC-MS analysis.

For isolation, the reaction mixture was diluted with water (10 mL), extracted with ethyl acetate (3 x 20 mL), washed with brine (1 x 20 mL) and dried over Na_2SO_4 . The crude product was obtained by removing the solvents under reduced pressure. Purification was performed by automated flash column chromatography (DCM/MeOH 0-10% MeOH if not noted otherwise) yielding the corresponding product **3**.

2-Methyl-3-phenylbutan-2-ol (**3a**)^[32]



^1H NMR (300 MHz, CDCl_3 , δ_{H}) 7.37 – 7.18 (m, 5H), 2.81 (q, $J = 7.2$ Hz, 1H), 1.37 (s, 1H), 1.35 (d, $J = 7.2$ Hz, 3H), 1.19 (s, 6H).

^{13}C NMR (75 MHz, CDCl_3 , δ_{C}) 143.4 (C_q), 129.1 (+), 128.2 (+), 126.6 (+), 72.8 (C_q), 50.5 (+), 28.2 (+), 27.0 (+), 15.9 (+).

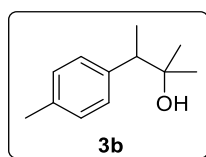
HRMS (APCI) (m/z): $[\text{MNH}_4]^+$ ($\text{C}_{11}\text{H}_{20}\text{NO}^+$) calc.: 182.1539, found: 182.1538.

Yield: with 10 eq. acetone: 41%

with acetone as co-solvent: 72%

slightly yellow liquid

2-Methyl-3-(p-tolyl)butan-2-ol (**3b**)



¹H NMR (400 MHz, CDCl₃, δ_H) 7.19 – 7.08 (m, 4H), 2.78 (q, *J* = 7.2 Hz, 1H), 2.34 (s, 3H), 1.33 (d, *J* = 7.2 Hz, 3H), 1.19 (s, 3H), 1.18 (s, 3H).

¹³C NMR (101 MHz, CDCl₃, δ_C) 140.3(C_q), 136.2 (C_q), 129.0 (+), 128.9 (+), 72.8 (C_q), 50.1 (+), 28.2 (+), 26.9 (+), 21.1 (+), 16.0 (+).

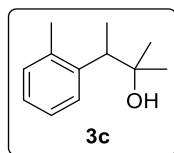
HRMS (APCI) (*m/z*): [MNH₄⁺] (C₁₂H₂₂NO⁺) calc.: 196.1696, found: 196.1697.

Yield: with 10 eq. acetone: 62%

with acetone as co-solvent: 55%

slightly yellow liquid

2-Methyl-3-(o-tolyl)butan-2-ol (**3c**)



¹H NMR (300 MHz, CDCl₃, δ_H) 7.38 – 7.31 (m, 1H), 7.22 – 7.09 (m, 3H), 3.17 (q, *J* = 7.1 Hz, 1H), 2.38 (s, 3H), 1.41 (s, 1H), 1.30 (d, *J* = 7.2 Hz, 3H), 1.26 (s, 3H), 1.19 (s, 3H).

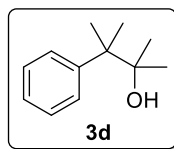
¹³C NMR (75 MHz, CDCl₃, δ_C) 142.3 (C_q), 136.9 (C_q), 130.5 (+), 127.5 (+), 126.2 (+), 126.0 (+), 73.6 (C_q), 43.9 (+), 28.5 (+), 27.3 (+), 20.8 (+), 16.6 (+).

HRMS (APCI) (*m/z*): [MNH₄⁺] (C₁₂H₂₂NO⁺) calc.: 196.1696, found: 196.1699.

Yield: with 10 eq. acetone: 22%

with acetone as co-solvent: 44%

slightly yellow liquid

2,3-Dimethyl-3-phenylbutan-2-ol (3d)^[33]

¹H NMR (400 MHz, CDCl₃, δ_H) 7.48 – 7.44 (m, 2H), 7.35 – 7.29 (m, 2H), 7.25 – 7.19 (m, 1H), 1.43 (s, 6H), 1.34 (s, 1H), 1.15 (s, 6H).

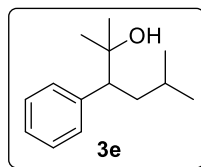
¹³C NMR (101 MHz, CDCl₃, δ_C) 146.4 (C_q), 128.2 (+), 127.8 (+), 126.1 (+), 74.6 (C_q), 45.2 (C_q), 25.8 (+), 24.5 (+).

HRMS (APCI) (m/z): [MNH₄⁺] (C₁₂H₂₂NO⁺) calc.: 196.1696, found: 196.1696.

Yield: with 10 eq. acetone: 11%

with acetone as co-solvent: 29%

slightly yellow liquid

2,5-Dimethyl-3-phenylhexan-2-ol (3e)^[34]

¹H NMR (400 MHz, CDCl₃, δ_H) 7.35 – 7.26 (m, 2H), 7.26 – 7.20 (m, 3H), 2.69 (dd, *J* = 12.3, 3.2 Hz, 1H), 1.85 (ddd, *J* = 13.4, 12.4, 3.4 Hz, 1H), 1.49 (ddd, *J* = 13.6, 10.5, 3.2 Hz, 1H), 1.35 (s, 1H), 1.27 – 1.20 (m, 1H), 1.18 (d, *J* = 1.9 Hz, 6H), 0.85 (d, *J* = 6.7 Hz, 3H), 0.81 (d, *J* = 6.5 Hz, 3H).

¹³C NMR (101 MHz, CDCl₃, δ_C) 141.4 (C_q), 129.7 (+), 128.2 (+), 126.6 (+), 72.8 (C_q), 54.9 (+), 38.7 (–), 28.3 (+), 27.8 (+), 25.8 (+), 24.4 (+), 21.1 (+).

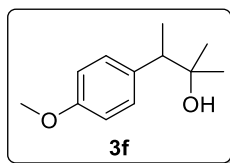
HRMS (APCI) (m/z): [MNH₄⁺] (C₁₄H₂₆NO⁺) calc.: 224.2009, found: 224.2009.

Yield: with 10 eq. acetone: 47%

with acetone as co-solvent: 79%

slightly yellow liquid

3-(4-Methoxyphenyl)-2-methylbutan-2-ol (3f)



¹H NMR (300 MHz, CDCl₃, δ_H) 7.20 – 7.13 (m, 2H), 6.88 – 6.81 (m, 2H), 3.79 (s, 3H), 2.76 (q, *J* = 7.2 Hz, 1H), 1.69 (s, 1H), 1.31 (d, *J* = 7.2 Hz, 3H), 1.17 (s, 3H), 1.16 (s, 3H).

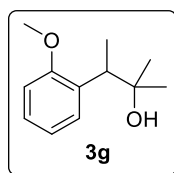
¹³C NMR (75 MHz, CDCl₃, δ_C) 158.3 (C_q), 135.4 (C_q), 129.9 (+), 113.5 (+), 72.8 (C_q), 55.3 (+), 49.6 (+), 28.0 (+), 26.9 (+), 16.0 (+).

HRMS (APCI) (*m/z*): [MNH₄⁺] (C₁₂H₂₂NO₂⁺) calc.: 212.1645, found: 212.1648.

Yield: with 10 eq. acetone: 67%
with acetone as co-solvent: 87%

slightly yellow liquid

3-(2-Methoxyphenyl)-2-methylbutan-2-ol (3g)



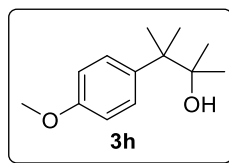
¹H NMR (300 MHz, CDCl₃, δ_H) 7.26 – 7.18 (m, 2H), 6.99 – 6.86 (m, 2H), 3.83 (s, 3H), 3.37 (q, *J* = 7.3 Hz, 1H), 2.46 (s, 1H), 1.30 (d, *J* = 7.3 Hz, 3H), 1.19 (s, 3H), 1.17 (s, 3H).

¹³C NMR (75 MHz, CDCl₃, δ_C) 157.1 (C_q), 132.3 (C_q), 129.3 (+), 127.3 (+), 120.8 (+), 110.7 (+), 73.4 (C_q), 55.5 (+), 29.2 (+), 26.4 (+), 15.6 (+).

HRMS (APCI) (*m/z*): [MNH₄⁺] (C₁₂H₂₂NO₂⁺) calc.: 212.1645, found: 212.1641.

Yield: with 10 eq. acetone: 48%
with acetone as co-solvent: 83%

yellow liquid

3-(4-Methoxyphenyl)-2,3-dimethylbutan-2-ol (3h)^[35]

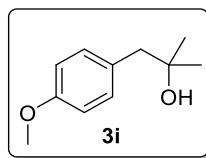
¹H NMR (400 MHz, CDCl₃, δ_H) 7.39 – 7.34 (m, 2H), 6.88 – 6.83 (m, 2H), 3.80 (s, 3H), 1.40 (s, 6H), 1.27 (s, 1H), 1.14 (s, 6H).

¹³C NMR (101 MHz, CDCl₃, δ_C) 157.8 (C_q), 138.4 (C_q), 129.2 (+), 113.1 (+), 74.7 (C_q), 55.3 (+), 44.6 (C_q), 25.8 (+), 24.6 (+).

HRMS (APCI) (m/z): [MNH₄⁺] (C₁₃H₂₄NO₂⁺) calc.: 226.1802, found: 226.1804.

Yield: with 10 eq. acetone: 52%
with acetone as co-solvent: 77%

slightly yellow liquid

1-(4-Methoxyphenyl)-2-methylpropan-2-ol (3i)^[36]

¹H NMR (300 MHz, CDCl₃, δ_H) 7.16 – 7.10 (m, 2H), 6.89 – 6.82 (m, 2H), 3.80 (s, 3H), 2.71 (s, 2H), 1.44 (s, 1H), 1.21 (s, 6H).

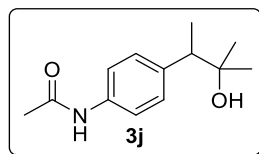
¹³C NMR (75 MHz, CDCl₃, δ_C) 158.5 (C_q), 131.5 (+), 129.9 (C_q), 113.8 (+), 70.9 (C_q), 55.4 (+), 48.9 (–), 29.2 (+).

HRMS (EI+) (m/z): [M⁺] (C₁₁H₁₆O₂⁺) calc.: 180.1145, found: 180.1154.

Yield: with 10 eq. acetone: 19%
with acetone as co-solvent: 53%

slightly yellow liquid

***N*-(4-(3-Hydroxy-3-methylbutan-2-yl)phenyl)acetamide (3j)**



¹H NMR (300 MHz, CDCl₃, δ_H) 8.24 (s, 1H), 7.44 – 7.38 (m, 2H), 7.17 – 7.09 (m, 2H), 2.73 (q, *J* = 7.2 Hz, 1H), 2.11 (s, 3H), 2.00 (s, 1H), 1.27 (d, *J* = 7.2 Hz, 3H), 1.13 (s, 6H).

¹³C NMR (75 MHz, CDCl₃, δ_C) 169.1 (C_q), 139.4 (C_q), 136.5 (C_q), 129.4 (+), 119.9 (+), 72.8 (C_q), 49.9 (+), 28.1 (+), 26.9 (+), 24.4 (+), 15.9 (+).

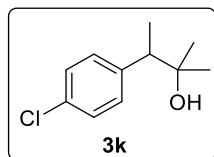
HRMS (APCI) (*m/z*): [MNH₄⁺] (C₁₃H₂₃N₂O₂⁺) calc.: 239.1754, found: 239.1756.

Yield: with 10 eq. acetone: 57%

with acetone as co-solvent: 87%

white solid

3-(4-Chlorophenyl)-2-methylbutan-2-ol (3k)



¹H NMR (300 MHz, CDCl₃, δ_H) 7.31 – 7.15 (m, 4H), 2.77 (q, *J* = 7.2 Hz, 1H), 1.35 (s, 1H), 1.31 (d, *J* = 7.2 Hz, 3H), 1.18 (s, 3H), 1.16 (s, 3H).

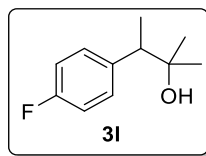
¹³C NMR (75 MHz, CDCl₃, δ_C) 142.1 (C_q), 132.3 (C_q), 130.4 (+), 128.2 (+), 72.7 (C_q), 49.9 (+), 28.2 (+), 27.2 (+), 15.9 (+).

HRMS (APCI) (*m/z*): [MNH₄⁺] (C₁₁H₁₉ClNO⁺) calc.: 216.1150, found: 216.1150.

Yield: with 10 eq. acetone: 32%

with acetone as co-solvent: 53%

slightly yellow liquid

3-(4-Fluorophenyl)-2-methylbutan-2-ol (3l)

^1H NMR (300 MHz, CDCl_3 , δ_{H}) 7.25 – 7.17 (m, 2H), 7.04 – 6.93 (m, 2H), 2.78 (q, $J = 7.2$ Hz, 1H), 1.31 (d, $J = 7.3$ Hz, 3H), 1.17 (s, 3H), 1.16 (s, 3H).

^{13}C NMR (75 MHz, CDCl_3 , δ_{C}) 161.7 (d, $^1J_{\text{CF}} = 244.3$ Hz, C_q), 139.2 (d, $^4J_{\text{CF}} = 3.3$ Hz, C_q), 130.4 (d, $^3J_{\text{CF}} = 7.7$ Hz, +), 114.9 (d, $^2J_{\text{CF}} = 20.9$ Hz, +), 72.7 (C_q), 49.7 (+), 28.2 (+), 27.1 (+), 16.1 (+).

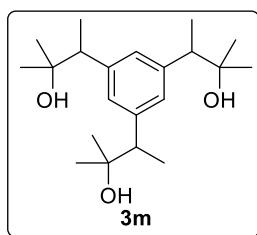
^{19}F NMR (282 MHz, CDCl_3 , δ_{F}) -117.4.

HRMS (APCI) (m/z): $[\text{MNH}_4^+]$ ($\text{C}_{11}\text{H}_{19}\text{FNO}^+$) calc.: 200.1445, found: 200.1444.

Yield: with 10 eq. acetone: 59%

with acetone as co-solvent: 78%

slightly yellow liquid

3,3',3''-(Benzene-1,3,5-triyl)tris(2-methylbutan-2-ol) (3m)

^1H NMR (300 MHz, CDCl_3 , δ_{H}) 6.97 (s, 3H), 2.80 – 2.71 (m, 3H), 1.93 (s, 3H), 1.31 (d, $J = 7.2$ Hz, 9H), 1.16 – 1.10 (m, 18H).

^{13}C NMR (75 MHz, CDCl_3 , δ_{C}) 142.4 (C_q), 142.4 (C_q), 128.2 (+), 128.1 (+), 127.8 (+), 72.9 (C_q), 50.4 (+), 50.4 (+), 28.4 (+), 26.7 (+), 15.9 (+).

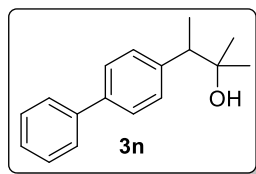
HRMS (APCI) (m/z): $[\text{MNH}_4^+]$ ($\text{C}_{21}\text{H}_{40}\text{NO}_3^+$) calc.: 354.3003, found: 354.3003.

Yield: with 10 eq. acetone:

with acetone as co-solvent: 87%

yellow liquid

3-([1,1'-Biphenyl]-4-yl)-2-methylbutan-2-ol (**3n**)



¹H NMR (400 MHz, CDCl₃, δ_H) 7.65 – 7.59 (m, 2H), 7.59 – 7.54 (m, 2H), 7.49 – 7.42 (m, 2H), 7.38 – 7.32 (m, 3H), 2.88 (q, *J* = 7.2 Hz, 1H), 1.50 (s, 1H), 1.40 (d, *J* = 7.2 Hz, 3H), 1.24 (s, 6H).

¹³C NMR (101 MHz, CDCl₃, δ_C) 142.6 (C_q), 141.0 (C_q), 139.5 (C_q), 129.5 (+), 128.9 (+), 127.2 (+), 127.1 (+), 126.8 (+), 72.8 (C_q), 50.2 (+), 28.3 (+), 27.1 (+), 15.9 (+).

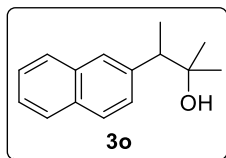
HRMS (EI+) (*m/z*): [*M*⁺] (C₁₇H₂₀O⁺) calc.: 240.1509, found: 240.1517.

Yield: with 10 eq. acetone: 31%

with acetone as co-solvent: 62%

yellowish solid

2-Methyl-3-(naphthalen-2-yl)butan-2-ol (**3o**)^[37]



¹H NMR (400 MHz, CDCl₃, δ_H) 7.85 – 7.77 (m, 3H), 7.70 (s, 1H), 7.50 – 7.40 (m, 3H), 2.99 (q, *J* = 7.2 Hz, 1H), 1.45 (d, *J* = 7.3 Hz, 3H), 1.27 (s, 1H), 1.24 (s, 3H), 1.23 (s, 3H).

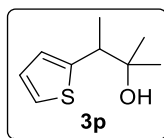
¹³C NMR (101 MHz, CDCl₃, δ_C) 141.1 (C_q), 133.4 (C_q), 132.5 (C_q), 127.9 (+), 127.7 (+), 127.7 (+), 127.6 (+), 127.5 (+), 126.1 (+), 125.6 (+), 73.0 (C_q), 50.6 (+), 28.4 (+), 27.2 (+), 16.1 (+).

HRMS (APCI) (*m/z*): [*MNH*₄⁺] (C₁₅H₂₂NO⁺) calc.: 232.1696, found: 232.1697.

Yield: with 10 eq. acetone: 7%

with acetone as co-solvent: 34%

slightly yellow liquid

2-Methyl-3-(thiophen-2-yl)butan-2-ol (3p)

^1H NMR (400 MHz, CDCl_3 , δ_{H}) 7.20 – 7.15 (m, 1H), 6.99 – 6.94 (m, 1H), 6.89 – 6.87 (m, 1H), 3.12 (q, $J = 7.2$ Hz, 1H), 1.59 (s, 1H), 1.38 (d, $J = 7.2$ Hz, 3H), 1.24 (s, 3H), 1.21 (s, 3H).

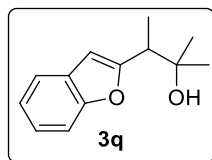
^{13}C NMR (101 MHz, CDCl_3 , δ_{C}) 146.6 (C_q), 126.5 (+), 125.4 (+), 123.7 (+), 72.3 (C_q), 46.6 (+), 28.1 (+), 26.5 (+), 17.8/ (+).

HRMS (APCI) (m/z): [$\text{M}+\text{H}^+$] ($\text{C}_9\text{H}_{15}\text{OS}^+$) calc.: 171.0838, found: 171.0836.

Yield: with 10 eq. acetone: 43%

with acetone as co-solvent: 73%

slightly yellow liquid

3-(Benzofuran-2-yl)-2-methylbutan-2-ol (3q)

^1H NMR (400 MHz, CDCl_3 , δ_{H}) 7.55 – 7.43 (m, 2H), 7.27 – 7.19 (m, 2H), 6.50 (s, 1H), 3.04 (q, $J = 7.2$ Hz, 1H), 2.01 (s, 1H), 1.40 (d, $J = 7.2$ Hz, 3H), 1.28 (s, 3H), 1.24 (s, 3H).

^{13}C NMR (101 MHz, CDCl_3 , δ_{C}) 160.9 (C_q), 154.6 (C_q), 128.5 (C_q), 123.6 (+), 122.8 (+), 120.6 (+), 111.1 (+), 103.6 (+), 72.8 (C_q), 45.0 (+), 28.0 (+), 26.9 (+), 14.3 (+).

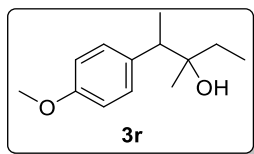
HRMS (EI+) (m/z): [M^+] ($\text{C}_{13}\text{H}_{16}\text{O}_2^+$) calc.: 204.1145, found: 204.1147.

Yield: with 10 eq. acetone: 14%

with acetone as co-solvent: 51%

colorless liquid

2-(4-Methoxyphenyl)-3-methylpentan-3-ol (3r)



Column chromatography: First column: DCM/MeOH 0-5%. Second column: *n*-pentane/EtOAc 0-35%.

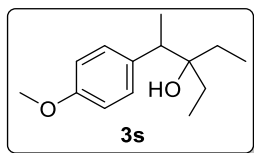
¹H-NMR (diastereomeric mixture) (300 MHz, CDCl₃, δ_H): 7.21-7.14 (m, 2H), 6.88-6.82 (m, 2H), 3.79 (s, 3H), 2.86-2.74 (m, 1H), 1.61-1.38 (m, 2H), 1.30 [1.28] (d, *J* = 3.3 Hz, 3H), 1.20 (s, 1H), 1.10 [1.04] (s, 3H), 0.94 [0.92] (t, *J* = 7.4 Hz, 3H).

¹³C-NMR (diastereomeric mixture) (75 MHz, CDCl₃, δ_C): 158.3 (C_q), 158.2 (C_q), 135.6 (C_q), 135.2 (C_q), 130.1 (+), 130.0 (+), 113.5 (+), 113.5 (+), 74.6 (C_q), 74.4 (C_q), 55.3 (+), 47.8 (+), 47.1 (+), 33.0 (–), 31.8 (–), 24.5 (+), 23.3 (+), 16.0 (+), 15.6 (+), 8.3 (+), 8.1 (+).

HRMS (APCI) (*m/z*): [MNH₄⁺] (C₁₃H₂₄NO₂⁺) calc.: 226.1802, found: 226.1805.

Yield: 58% (slightly yellow liquid).

3-Ethyl-2-(4-methoxyphenyl)pentan-3-ol (3s)



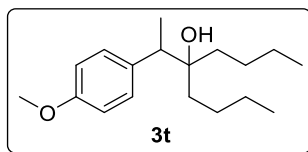
Column chromatography: *n*-Pentane/EtOAc 0-20%.

¹H-NMR (300 MHz, CDCl₃, δ_H): 7.20-7.15 (m, 2H), 6.87-6.82 (m, 2H), 3.80 (s, 3H), 2.83 (q, *J* = 7.2 Hz, 1H), 1.56 (q, *J* = 7.5 MHz, 2H), 1.42-1.19 (m, 5H), 1.01 (bs, 1H), 0.91-0.80 (m, 6H).

¹³C-NMR (75 MHz, CDCl₃, δ_C): 158.2 (C_q), 135.7 (C_q), 130.1 (+), 113.6 (+), 76.1 (C_q), 55.4 (+), 44.7 (+), 29.2 (–), 27.4 (–), 15.6 (+), 8.1 (+), 7.8 (+).

HRMS (APCI) (*m/z*): [MNH₄⁺] (C₁₄H₂₆NO₂⁺) calc.: 240.1958, found: 240.1961.

Yield: 34% (slightly yellow liquid).

5-(1-(4-Methoxyphenyl)ethyl)nonan-5-ol (3t)

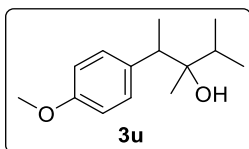
Column chromatography: *n*-Pentane/EtOAc 0-20%.

¹H-NMR (300 MHz, CDCl₃, δ_H): 7.19-7.13 (m, 2H), 6.87-6.82 (m, 2H), 3.80 (s, 3H), 2.81 (q, *J* = 7.2 Hz, 1H), 1.59-1.01 (m, 16H), 0.96-0.82 (m, 6H).

¹³C-NMR (75 MHz, CDCl₃, δ_C): 158.2 (C_q), 135.7 (C_q), 130.2 (+), 113.6 (+), 75.8 (C_q), 55.4 (+), 45.4 (+), 37.3 (-), 35.4 (-), 26.0 (-), 25.8 (-), 23.6 (-), 23.4 (-), 15.6 (+), 14.3 (+), 14.3 (+).

HRMS (APCI) (*m/z*): [MNH₄⁺] (C₁₈H₃₄NO₂⁺) calc.: 296.2584, found: 296.2586.

Yield: 10% (colorless liquid).

2-(4-Methoxyphenyl)-3,4-dimethylpentan-3-ol (3u)

Column chromatography: *n*-Pentane/EtOAc 0-20%.

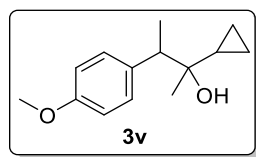
¹H-NMR (diastereomeric mixture) (300 MHz, CDCl₃, δ_H): 7.23-7.14 (m, 2H), 6.87-6.82 (m, 2H), 3.80 (s, 3H), 2.97 [2.85] (q, *J* = 7.2 Hz, 1H), 2.02-1.92 [1.62-1.53] (m, 1H), 1.27 [1.26] (d, *J* = 7.2 Hz, 3H), 1.12 (s, 1H), 1.06 [0.83] (s, 3H), 1.01-0.90 (m, 6H).

¹³C-NMR (diastereomeric mixture) (75 MHz, CDCl₃, δ_C): 158.2 (C_q), 158.2 (C_q), 136.5 (C_q), 135.7 (C_q), 130.1 (+), 113.6 (+), 113.5 (+), 76.2 (C_q), 76.1 (C_q), 55.3 (+), 45.3 (+), 44.5 (+), 34.6 (+), 33.7 (+), 20.4 (+), 19.4 (+), 18.2 (+), 18.0 (+), 17.3 (+), 16.8 (+), 16.3 (+), 15.0 (+).

HRMS (APCI) (*m/z*): [MNH₄⁺] (C₁₄H₂₆NO₂⁺) calc.: 240.1958, found: 240.1960.

Yield: 31% (colorless liquid).

2-Cyclopropyl-3-(4-methoxyphenyl)butan-2-ol (3v)



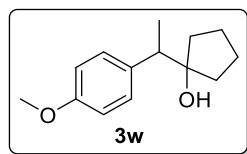
Column chromatography: DCM (for 1.5 CV) followed by *n*-hexane/EtOAc 0-20% gradient.

¹H-NMR (diastereomeric mixture) (300 MHz, CDCl₃, δ_H): 7.25 – 7.15 (m, 2H), 6.88 – 6.78 (m, 2H), 3.80 (s, 3H), 2.93 – 2.77 (m, 1H), 1.38 [1,37] (d, *J* = 7.3 Hz, 2H), 1.06 [1.01] (s, 3H), 0.94 – 0.79 (m, 1H), 0.41 – 0.17 (m, 4H).

¹³C-NMR (diastereomeric mixture) (75 MHz, CDCl₃ δ_C): 158.3 (C_q), 135.5 (C_q), 130.2 (+), 113.4 (+), 72.9 (C_q), 72.7 (C_q), 55.3 (+), 50.1 (+), 49.8 (+), 24.9 (+), 23.1 (+), 19.9 (+), 19.0 (+), 16.0 (+), 1.4 (–), 1.3 (–), 0.9 (–), 0.6 (–).

Yield: 31% (slightly yellow liquid).

1-(1-(4-Methoxyphenyl)ethyl)cyclopentan-1-ol (**3w**)



Column chromatography: DCM (for 1.5 CV) followed by *n*-hexane/EtOAc 0-25%.

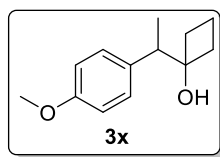
¹H-NMR (400 MHz, CDCl₃, δ_H): 7.22-7.18 (m, 2H), 6.87-6.83 (m, 2H), 3.80 (s, 3H), 2.78 (q, *J* = 7.1 Hz, 1H), 1.89-1.55 (m, 7H), 1.34 (d, *J* = 7.1 Hz, 3H), 1.27-1.21 (m, 1H), 1.05 (bs, 1H).

¹³C-NMR (101 MHz, CDCl₃, δ_C): 158.3 (C_q), 136.3 (C_q), 129.5 (+), 113.7 (+), 84.8 (C_q), 55.4 (+), 48.0 (+), 39.7 (–), 37.9 (–), 23.9 (–), 23.7 (–), 16.4 (+).

HRMS (EI) (*m/z*): [*M*⁺] (C₁₄H₂₀O₂⁺) calc.: 220.1458, found: 220.1448.

Yield: 57% (slightly yellow liquid).

1-(1-(4-Methoxyphenyl)ethyl)cyclobutan-1-ol (**3x**)



Ketone equivalents: 3 eq. cyclobutanone were used for the reaction.

Column chromatography: DCM (for 1.5 CV) followed by *n*-Pentane/EtOAc 0-20%.

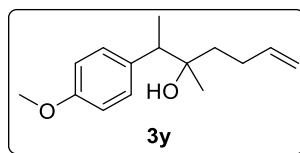
¹H-NMR (400 MHz, CDCl₃, δ_H): 7.24-7.19 (m, 2H), 6.88-6.83 (m, 2H), 3.80 (s, 3H), 2.88 (q, *J* = 7.1 Hz, 1H), 2.27-2.09 (m, 2H), 2.05-1.96 (m, 1H), 1.91-1.71 (m, 2H), 1.63-1.53 (m, 2H), 1.29 (d, *J* = 7.1 Hz, 3H).

¹³C-NMR (101 MHz, CDCl₃, δ_C): 158.4 (C_q), 134.7 (C_q), 129.6 (+), 113.8 (+), 78.2 (C_q), 55.4 (+), 46.4 (+), 34.6 (-), 34.2 (-), 14.6 (+), 12.6 (-).

HRMS (EI) (*m/z*): [M⁺] (C₁₃H₁₈O₂⁺) calc.: 206.1301, found: 206.1299.

Yield: 69% (colorless liquid).

2-(4-Methoxyphenyl)-3-methylhept-6-en-3-ol (3y)



Ketone equivalents: 3 eq. 5-hexen-2-one were used for the reaction.

Column chromatography: DCM (for 1.5 CV) followed by *n*-pentane/EtOAc 0-20%.

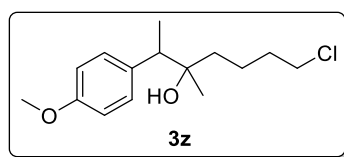
¹H-NMR (diastereomeric mixture) (400 MHz, CDCl₃, δ_H): 7.20-7.14 (m, 2H), 6.88-6.82 (m, 2H), 5.88-5.77 (m, 1H), 5.06-4.91 (m, 2H), 3.80 (s, 3H), 2.86-2.74 (m, 1H), 2.23-2.04 (m, 2H), 1.62-1.46 (m, 2H), 1.31 [1.29] (d, *J* = 7.2 Hz, 3H), 1.27-1.21 (m, 1H), 1.12 [1.10] (s, 3H).

¹³C-NMR (diastereomeric mixture) (101 MHz, CDCl₃, δ_C): 158.4 (C_q), 158.4 (C_q), 139.3 (+), 139.2 (+), 135.3 (C_q), 134.9 (C_q), 130.2 (+), 130.1 (+), 114.5 (-), 114.4 (-), 113.6 (+), 113.6 (+), 74.4 (C_q), 74.3 (C_q), 55.4 (+), 48.7 (+), 47.8 (+), 39.6 (-), 38.4 (-), 28.4 (-), 28.3 (-), 24.9 (+), 23.7 (+), 16.0 (+), 15.7 (+).

HRMS (APCI) (*m/z*): [MNH₄⁺] (C₁₅H₂₆NO₂⁺) calc.: 252.1958, found: 252.1958.

Yield: 24% (colorless liquid).

7-Chloro-2-(4-methoxyphenyl)-3-methylheptan-3-ol (3z)



Ketone equivalents: 3 eq. 6-chloro-2-hexanone were used for the reaction.

Column chromatography: DCM (for 1.5 CV) followed by *n*-pentane/EtOAc 0-20%.

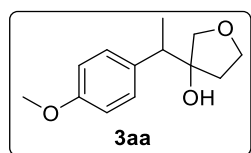
¹H-NMR (diastereomeric mixture) (300 MHz, CDCl₃, δ_H): 7.20-7.13 (m, 2H), 6.88-6.82 (m, 2H), 3.80 [3.80] (s, 3H), 3.54 [3.53] (t, *J* = 6.6 Hz, 2H), 2.86-2.74 (m, 1H), 1.82-1.37 (m, 6H), 1.29 [1.28] (d, *J* = 7.2 Hz, 3H), 1.20 (s, 1H), 1.11 [1.08] (s, 3H).

¹³C-NMR (diastereomeric mixture) (75 MHz, CDCl₃, δ_C): 158.4 (C_q), 158.3 (C_q), 135.3 (C_q), 134.8 (C_q), 130.2 (+), 130.0 (+), 113.6 (+), 113.6 (+), 74.3 (C_q), 74.2 (C_q), 55.4 (+), 48.3 (+), 47.5 (+), 45.2 (–), 45.2 (–), 39.8 (–), 38.5 (–), 33.3 (–), 33.2 (–), 25.1 (+), 23.7 (+), 21.4 (–), 21.2 (–), 16.0 (+), 15.6 (+).

HRMS (APCI) (m/z): [MNH₄⁺] (C₁₅H₂₇ClNO₂⁺) calc.: 288.1725, found: 288.1728.

Yield: 30% (colorless liquid).

3-(1-(4-Methoxyphenyl)ethyl)tetrahydrofuran-3-ol (**3aa**)



Ketone equivalents: 1 eq. tetrahydrofuran-3-one was used for the reaction.

Column chromatography: First column: DCM/MeOH (98:2). Second column: *n*-hexane/EtOAc 35-50%.

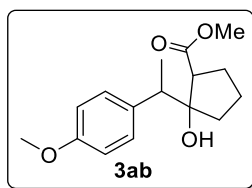
¹H-NMR (diastereomeric mixture) (300 MHz, CDCl₃, δ_H): 7.24-7.17 (m, 2H), 6.89-6.82 (m, 2H), 4.08-3.85 (m, 2H), 3.79 [3.79] (s, 3H), 3.77-3.65 + 3.30-3.25 (m, 2H), 2.87 [2.87] (q, *J* = 7.1 Hz, 1H), 2.05-1.91 + 1.53-1.44 (m, 2H), 1.73 [1.68] (bs, 1H), 1.38 [1.33] (d, *J* = 7.2 Hz, 3H).

¹³C-NMR (diastereomeric mixture) (101 MHz, CDCl₃, δ_C): 158.6 (C_q), 158.6 (C_q), 135.1 (C_q), 135.1 (C_q), 129.4 (+), 129.1 (+), 113.9 (+), 113.9 (+), 83.6 (C_q), 79.0 (–), 78.0 (–), 68.1 (–), 67.8 (–), 55.4 (+), 55.4 (+), 45.8 (+), 45.6 (+), 40.0 (–), 38.7 (–), 16.5 (+), 16.4 (+).

HRMS (APCI) (m/z): [MHN₄⁺] (C₁₃H₂₂NO₃) calc.: 240.1594, found: 240.1596.

Yield: 30% (slightly yellow solid).

Methyl 2-hydroxy-2-(1-(4-methoxyphenyl)ethyl)cyclopentane-1-carboxylate (**3ab**)



Ketone equivalents: 1 eq. methyl 2-oxocyclopentanecarboxylate was used for the reaction.

Column chromatography: First column: DCM (for 1.5 CV) followed by *n*-pentane/EtOAc 0-20% gradient. Second column: DCM/EtOAc 10%.

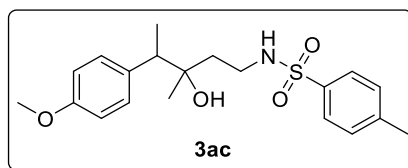
¹H-NMR (diastereomeric mixture) (300 MHz, CDCl₃, δ_H): 7.19-7.12 (m, 2H), 6.84-6.77 (m, 2H), 4.17 [3.88] (s, 1H), 3.78 [3.78] (s, 3H), 3.72 [3.27] (s, 3H), 2.95 [2.71] (q, *J* = 7.2 Hz, 1H), 2.61-2.43 (m, 1H), 2.06-1.56 (m, 6H), 1.34 [1.33] (q, *J* = 7.1 Hz, 3H).

¹³C-NMR (diastereomeric mixture) (75 MHz, CDCl₃, δ_C): 177.2 (C_q), 177.0 (C_q), 158.4 (C_q), 158.3 (C_q), 135.8 (C_q), 135.5 (C_q), 129.8 (+), 129.6 (+), 113.5 (+), 113.4 (+), 85.3 (C_q), 85.1 (C_q), 55.4 (+), 55.3 (+), 51.9 (+), 51.5(+), 50.6 (+), 49.6 (+), 48.5 (+), 47.1 (+), 38.7 (−), 35.4 (−), 30.2 (−), 29.1 (−), 22.0 (−), 21.6 (−), 16.8 (+), 16.4 (+).

HRMS (APCI) (*m/z*): [MNH₄⁺] (C₁₆H₂₆NO₄) calc.: 296.1856, found: 296.1857.

Yield: 27% (colorless liquid).

***N*-(3-hydroxy-4-(4-methoxyphenyl)-3-methylpentyl)-4-methylbenzenesulfonamide (3ac)**



Ketone equivalents: 2 eq. *N*-(3-oxobutyl)-*p*-toluenesulfonamide were used for the reaction.

Column chromatography: DCM/MeOH (98:2).

¹H-NMR (diastereomeric mixture) (300 MHz, CDCl₃, δ_H): 7.76-7.70 (m, 2H), 7.32-7.26 (m, 2H), 7.09-7.02 (m, 2H), 6.86-6.79 (m, 2H), 5.63-5.40 (m, 1H), 3.79 [3.78] (s, 3H), 3.20-2.97 (m, 2H), 2.74-2.62 (m, 1H), 2.41 (s, 3H), 1.74-1.44 (m, 3H), 1.23 [1.19] (d, *J* = 7.2 Hz, 3H), 1.00 [0.97] (s, 3H).

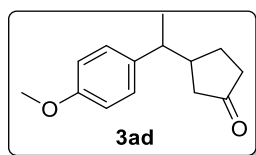
¹³C-NMR (diastereomeric mixture) (75 MHz, CDCl₃, δ_C): 158.7 (C_q), 158.6 (C_q), 143.3 (C_q), 143.3 (C_q), 137.0 (C_q), 137.0 (C_q), 134.2 (C_q), 133.4 (C_q), 130.2 (+), 129.9 (+), 129.7 (+), 129.7

(+), 127.2 (+), 127.2 (+), 113.8 (+), 113.8 (+), 75.3 (C_q), 75.1 (C_q), 55.4 (+), 49.6 (+), 48.5 (+), 39.6 (–), 39.6 (–), 37.5 (–), 36.5 (–), 23.9 (+), 23.0 (+), 21.6 (+), 15.8 (+), 15.4 (+).

HRMS (ESI) (m/z): [MH⁺] (C₂₀H₂₈NO₄S⁺) calc.: 378.1734, found: 378.1735.

Yield: 21% (yellow solid).

3-(1-(4-Methoxyphenyl)ethyl)cyclopentan-1-one (3ad)



Ketone equivalents: 1 eq. 2-cyclopentene-1-one was used for the reaction.

Column chromatography: First column: DCM/MeOH 0-5%. Second column: *n*-pentane/EtOAc 0-40%.

¹H-NMR (diastereomeric mixture) (400 MHz, CDCl₃, δ_H): 7.12-7.05 (m, 2H), 6.88-6.81 (m, 2H), 3.80 [3.78] (s, 3H), 2.59-1.88 (m, 6H), 1.81-1.70 (m, 1H), 1.64-1.33 (m, 1H), 1.30 [1.27] (d, *J* = 6.9 Hz, 3H).

¹³C-NMR (diastereomeric mixture) (101 MHz, CDCl₃, δ_C): 219.5 (C_q), 219.2 (C_q), 158.2 (C_q), 158.2 (C_q), 138.0 (C_q), 137.6 (C_q), 128.2 (+), 128.1 (+), 114.0 (+), 113.9 (+), 55.4 (+), 45.1 (+), 44.9 (+), 44.7 (+), 44.5 (+), 44.4 (–), 44.4 (–), 39.1 (–), 39.0 (–), 28.5 (–), 28.4 (–), 21.2 (+), 20.2 (+).

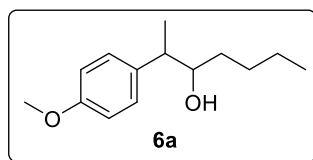
HRMS (EI) (m/z): [M⁺] (C₁₄H₁₈O₂⁺) calc.: 218.1301, found: 218.1305.

Yield: 36% (colorless liquid).

General procedure for the photocatalytic benzylation of aldehydes (general procedure B)

A 5 mL crimp cap vial equipped with a magnetic stirring bar was loaded with 3DPAFIPN (4.9 mg, 7.50 μmol , 3 mol%), K_2CO_3 (10.4 mg, 75.0 μmol , 50 mol%), $(\text{Pr})_3\text{SiSH}$ (4.3 μL , 20 μmol , 10 mol%), the corresponding ethyl benzene derivative (450 μmol , 3 eq.), the corresponding aldehyde (150 μmol , 1 eq.) and dry MeCN. In doing so, all solid compounds were added before capping the vial, whereas all liquid compounds were added *via* syringe after setting the capped vial under inert conditions. The reaction mixture was degassed by three cycles of freeze-pump-thaw and subsequently stirred under light irradiation using a 455 nm (± 15 nm) LED for 16 h at 25 $^\circ\text{C}$. Two reaction batches were combined and diluted with brine (10 mL), water (10 mL) and ethyl acetate (15 mL). The phases were separated, and the water phase was extracted with ethyl acetate (3 x 7 mL). The combined organic phases were washed with brine (10 mL) and dried over Na_2SO_4 . The solvent was removed under reduced pressure and the crude product was purified by automated flash column chromatography (*n*-pentane/ethyl acetate, 0-20% if not noticed otherwise).

2-(4-Methoxyphenyl)heptan-3-ol (6a)



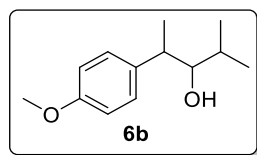
$^1\text{H-NMR}$ (diastereomeric mixture) (400 MHz, CDCl_3 , δ_{H}): 7.18-7.11 (m, 2H), 6.89-6.84 (m, 2H), 3.80 (s, 3H), 3.64-3.58 (m, 1H), 2.78-2.67 (m, 1H), 1.60-1.23 (m, 10H), 0.91 [0.87] (t, $J = 7.1$ Hz, 3H).

$^{13}\text{C-NMR}$ (diastereomeric mixture) (101 MHz, CDCl_3 , δ_{C}): 158.4 (C_q), 158.2 (C_q), 136.8 (C_q), 135.5 (C_q), 129.2 (+), 128.8 (+), 114.1 (+), 114.0 (+), 76.5 (+), 76.3 (+), 55.4 (+), 45.3 (+), 44.8 (+), 34.4 (−), 34.4 (−), 28.4 (−), 28.1 (−), 22.9 (−), 22.8 (−), 18.3 (+), 15.6 (+), 14.2 (+), 14.2 (+).

HRMS (APCI) (m/z): $[\text{MNH}_4^+]$ ($\text{C}_{14}\text{H}_{26}\text{NO}_2^+$) calc.: 240.1958, found: 240.1961.

Yield: 43% (slightly yellow liquid).

2-(4-Methoxyphenyl)-4-methylpentan-3-ol (6b)



Column chromatography: *n*-Pentane/EtOAc 0-25%.

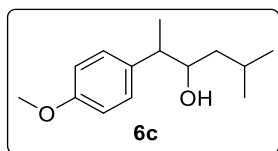
¹H-NMR (diastereomeric mixture) (400 MHz, CDCl₃, δ_H): 7.21-7.11 (m, 2H), 6.89-6.83 (m, 2H), 3.80 [3.79] (s, 3H), 3.40-3.34 (m, 1H), 2.89-2.77 (m, 1H), 1.81-1.55 (m, 1H), 1.43 (bs, 1H), 1.28 [1.23] (d, *J* = 7.0 Hz, 3H), 1.04-0.88 (m, 6H).

¹³C-NMR (diastereomeric mixture) (101 MHz, CDCl₃, δ_C): 158.4 (C_q), 158.2 (C_q), 137.3 (C_q), 136.1 (C_q), 129.2 (+), 128.6 (+), 114.1 (+), 114.0 (+), 81.5 (+), 80.7 (+), 55.4 (+), 42.6 (+), 42.0 (+), 30.3 (+), 30.1 (+), 20.6 (+), 20.1 (+), 18.9 (+), 16.9 (+), 15.9 (+), 15.6 (+).

HRMS (APCI) (*m/z*): [MNH₄⁺] (C₁₃H₂₄NO₂⁺) calc.: 226.1802, found: 226.1802.

Yield: 31% (slightly yellow liquid).

2-(4-Methoxyphenyl)-5-methylhexan-3-ol (6c)



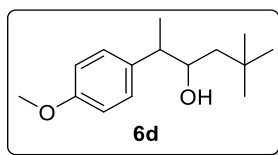
¹H-NMR (diastereomeric mixture) (400 MHz, CDCl₃, δ_H): 7.18-7.11 (m, 2H), 6.89-6.84 (m, 2H), 3.80 (s, 3H), 3.74-3.64 (m, 1H), 2.76-2.62 (m, 1H), 1.87-1.71 (m, 1H), 1.43 (bs, 1H), 1.34-1.13 (m, 5H), 0.94-0.84 (m, 6H).

¹³C-NMR (diastereomeric mixture) (101 MHz, CDCl₃, δ_C): 158.4 (C_q), 158.2 (C_q), 136.8 (C_q), 135.5 (C_q), 129.3 (+), 128.8 (+), 114.1 (+), 114.0 (+), 74.3 (+), 74.2 (+), 55.4 (+), 45.9 (+), 45.2 (+), 44.1 (-), 43.9 (-), 24.9 (+), 24.8 (+), 24.0 (+), 23.8 (+), 21.9 (+), 21.8 (+), 18.3 (+), 15.6 (+).

HRMS (APCI) (*m/z*): [MNH₄⁺] (C₁₄H₂₆NO₂⁺) calc.: 240.1958, found: 240.1962.

Yield: 37% (slightly yellow liquid).

2-(4-Methoxyphenyl)-5,5-dimethylhexan-3-ol (6d)



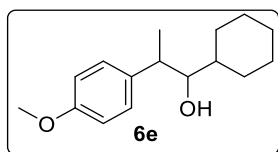
$^1\text{H-NMR}$ (diastereomeric mixture) (300 MHz, CDCl_3 , δ_{H}): 7.19-7.11 (m, 2H), 6.89-6.83 (m, 2H), 3.82-3.70 (m, 4H), 2.74-2.61 (m, 1H), 1.50 [1.37] (dd, $J = 14.6, 1.5$ Hz, 2H), 1.27 [1.25] (d, $J = 7.1$ Hz, 3H), 0.94 [0.90] (s, 9H).

$^{13}\text{C-NMR}$ (diastereomeric mixture) (75 MHz, CDCl_3 , δ_{C}): 158.4 (C_q), 158.2 (C_q), 136.8 (C_q), 135.4 (C_q), 129.3 (+), 128.9 (+), 114.0 (+), 113.9 (+), 74.0 (+), 73.8 (+), 55.4 (+), 48.5 (−), 48.5 (−), 46.6 (+), 46.3 (+), 30.4 (C_q), 30.4 (C_q), 30.3 (+), 30.2 (+), 18.1 (+), 15.3 (+).

HRMS (APCI) (m/z): $[\text{MNH}_4^+]$ ($\text{C}_{15}\text{H}_{28}\text{NO}_2^+$) calc.: 254.2115, found: 254.2114.

Yield: 16% (slightly yellow liquid).

1-Cyclohexyl-2-(4-methoxyphenyl)propan-1-ol (**6e**)



Column chromatography: *n*-Pentane/EtOAc 0-25%.

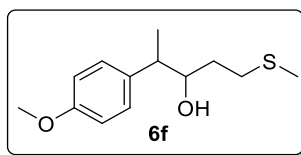
$^1\text{H-NMR}$ (diastereomeric mixture) (400 MHz, CDCl_3 , δ_{H}): 7.20-7.11 (m, 2H), 6.89-6.84 (m, 2H), 3.80 (s, 3H), 3.39-3.33 (m, 1H), 2.95-2.82 (m, 1H), 1.95-1.59 (m, 5H), 1.45-1.19 (m, 10H).

$^{13}\text{C-NMR}$ (diastereomeric mixture) (101 MHz, CDCl_3 , δ_{C}): 158.4 (C_q), 158.1 (C_q), 137.4 (C_q), 136.0 (C_q), 129.2 (+), 128.7 (+), 114.1 (+), 114.0 (+), 80.7 (+), 80.3 (+), 55.4 (+), 41.8 (+), 41.0 (+), 40.2 (+), 40.2 (+), 30.8 (−), 30.1 (−), 27.9 (−), 26.7 (−), 26.7 (−), 26.6 (−), 26.4 (−), 26.4 (−), 26.1 (−), 19.0 (+), 15.0 (+).

HRMS (EI) (m/z): $[\text{M}^+]$ ($\text{C}_{16}\text{H}_{24}\text{O}_2^+$) calc.: 248.1771, found: 248.1767.

Yield: 33% (slightly yellow liquid).

4-(4-Methoxyphenyl)-1-(methylthio)pentan-3-ol (**6f**)



Column chromatography: *n*-Pentane/EtOAc 0-25%.

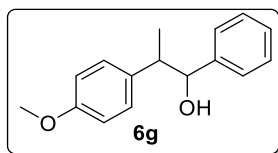
¹H-NMR (diastereomeric mixture) (400 MHz, CDCl₃, δ_H): 7.18-7.10 (m, 2H), 6.89-6.83 (m, 2H), 3.81-3.71 (m, 4H), 2.77-2.52 (m, 3H), 2.09 [2.03] (s, 3H), 1.90-1.53 (m, 3H), 1.30 [1.27] (t, *J* = 7.0 Hz, 3H).

¹³C-NMR (diastereomeric mixture) (101 MHz, CDCl₃, δ_C): 158.5 (C_q), 158.3 (C_q), 136.3 (C_q), 135.1 (C_q), 129.2 (+), 128.8 (+), 114.1 (+), 114.0 (+), 75.6 (+), 75.2 (+), 55.4 (+), 45.4 (+), 45.2 (+), 33.8 (–), 33.5 (–), 31.3 (–), 31.1 (–), 18.1 (+), 16.4 (+), 15.7 (+), 15.5 (+).

HRMS (APCI) (*m/z*): [MNH₄⁺] (C₁₃H₂₄NO₂S⁺) calc.: 258.1522, found: 258.1525.

Yield: 37% (slightly yellow liquid).

2-(4-Methoxyphenyl)-1-phenylpropan-1-ol (6g)^[38]



Column chromatography: *n*-Pentane/EtOAc 0-35%.

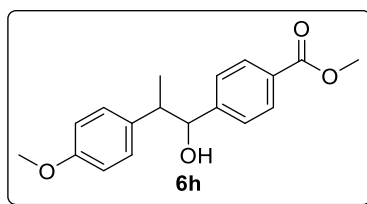
¹H-NMR (diastereomeric mixture) (300 MHz, CDCl₃, δ_H): 7.29-7.09 (m, 5H), 7.00-6.68 (m, 4H), 4.68 [4.51] (d, *J* = 5.7 Hz, [*J* = 8.7 Hz], 1H), 3.73 [3.69] (s, 3H), 3.04-2.83 (m, 1H), 1.84-1.71 (m, 1H), 1.19 [0.96] (d, *J* = 7.1 Hz, 3H).

¹³C-NMR (diastereomeric mixture) (75 MHz, CDCl₃, δ_C): 158.6 (C_q), 158.2 (C_q), 143.0 (C_q), 142.7 (C_q), 135.6 (C_q), 135.3 (C_q), 129.1 (+), 128.4 (+), 128.1 (+), 127.9 (+), 127.3 (+), 127.1 (+), 126.4 (+), 114.2 (+), 113.7 (+), 79.9 (+), 78.9 (+), 55.4 (+), 55.3 (+), 47.5 (+), 46.4 (+), 18.6 (+), 15.2 (+).

HRMS (APCI) (*m/z*): [MNH₄⁺] (C₁₆H₂₂NO₂⁺) calc.: 260.1645, found: 260.1645.

Yield: 23% (slightly yellow liquid).

Methyl 4-(1-hydroxy-2-(4-methoxyphenyl)propyl)benzoate (6h)



Column chromatography: *n*-Pentane/EtOAc 0-25%.

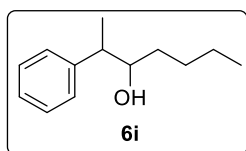
¹H-NMR (diastereomeric mixture) (400 MHz, CDCl₃, δ_H): 8.02-7.90 (m, 2H), 7.40-7.23 (m, 2H), 7.18-7.00 (m, 2H), 6.90-6.76 (m, 2H), 4.79 [4.66] (d, *J* = 5.8 Hz, [*J* = 8.1 Hz], 1H), 3.91 [3.89] (s, 3H), 3.80 [3.76] (s, 3H), 3.10-2.92 (m, 1H), 1.98 (s, 1H), 1.26 [1.08] (d, *J* = 7.1 Hz, 3H).

¹³C-NMR (diastereomeric mixture) (101 MHz, CDCl₃, δ_C): 167.1 (C_q), 167.1 (C_q), 158.7 (C_q), 158.4 (C_q), 148.2 (C_q), 147.9 (C_q), 135.0 (C_q), 134.5 (C_q), 129.6 (+), 129.6 (C_q), 129.4 (+), 129.2 (+), 129.1 (+), 129.0 (C_q), 127.0 (+), 126.4 (+), 114.2 (+), 113.8 (+), 79.3 (+), 78.6 (+), 55.4 (+), 55.3 (+), 52.2 (+), 52.2 (+), 47.4 (+), 46.4 (+), 18.2 (+), 15.2 (+).

HRMS (ESI) (*m/z*): [MNH₄⁺] (C₁₈H₂₄NO₄⁺) calc.: 318.1700, found: 318.1704.

Yield: 39% (slightly yellow liquid).

2-Phenylhetan-3-ol (**6i**)^[39]



Column chromatography: *n*-Pentane/EtOAc 0-30%.

¹H-NMR (diastereomeric mixture) (300 MHz, CDCl₃, δ_H): 7.37-7.17 (m, 5H), 3.70-3.62 (m, 1H), 2.84-2.70 (m, 1H), 1.63-1.22 (m, 10H), 0.91 [0.87] (t, *J* = 7.0 Hz, 3H).

¹³C-NMR (diastereomeric mixture) (75 MHz, CDCl₃, δ_C): 144.8 (C_q), 143.7 (C_q), 128.7 (+), 128.6 (+), 128.3 (+), 127.9 (+), 126.8 (+), 126.5 (+), 76.4 (+), 76.2 (+), 46.2 (+), 45.7 (+), 34.5 (-), 34.4 (-), 28.4 (-), 28.1 (-), 22.9 (-), 22.8 (-), 18.2 (+), 15.5 (+), 14.3 (+), 14.2 (+).

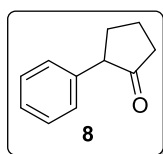
HRMS (APCI) (*m/z*): [MNH₄⁺] (C₁₃H₂₄NO⁺) calc.: 210.1852, found: 210.1853.

Yield: 28% (slightly yellow liquid).

General procedure for the intramolecular ring closure with esters as electrophiles (general procedure C)

A 5 mL crimp cap vial equipped with a magnetic stirring bar was loaded with 3DPA2FBN (3.8 mg, 6.00 μ mol, 3 mol%), K_2CO_3 (13.8 mg, 100 μ mol, 50 mol%), $(Pr)_3SiSH$ (4.3 μ L, 20.0 μ mol, 10 mol%), the corresponding ester (200 μ mol, 1 eq.), 4 \AA molecular sieve (50 mg) and dry MeCN. In doing so, all solid compounds were added before capping the vial, whereas all liquid compounds were added *via* syringe after setting the capped vial under inert conditions. The reaction mixture was degassed by three cycles of freeze-pump-thaw and subsequently stirred under light irradiation using a 455 nm (± 15 nm) LED for 16 h at 25 $^{\circ}C$. Two reaction batches were combined and diluted with brine (10 mL), water (10 mL) and ethyl acetate (15 mL). The phases were separated, and the water phase was extracted with ethyl acetate (3 x 7 mL). The combined organic phases were washed with brine (10 mL) and dried over Na_2SO_4 . The solvent was removed under reduced pressure and the crude product was purified by automated flash column chromatography (*n*-pentane/DCM 50-100%)

2-Phenylcyclopentan-1-one (8a)^[40]



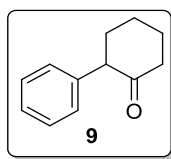
1H -NMR (diastereomeric mixture) (300 MHz, $CDCl_3$, δ_H): 7.38-7.16 (m, 5H), 3.38-3.28 (m, 1H), 2.57-2.43 (m, 2H), 2.37-2.24 (m, 1H), 2.23-2.05 (m, 2H), 2.03-1.87 (m, 1H).

^{13}C -NMR (diastereomeric mixture) (75 MHz, $CDCl_3$, δ_C): 218.2 (C_q), 138.5 (C_q), 128.7 (+), 128.3 (+), 127.0 (+), 55.5 (+), 38.6 (–), 31.9 (–), 21.0 (–).

HRMS (EI) (m/z): [M^+] ($C_{11}H_{12}O^+$) calc.: 160.0883, found: 160.0881.

Yield: 40% (slightly yellow liquid).

2-Phenylcyclohexan-1-one (8b)^[41]



Column chromatography: *n*-Pentane/DCM 50-100%.

¹H-NMR (diastereomeric mixture) (300 MHz, CDCl₃, δ_H): 7.37-7.22 (m, 3H), 7.17-7.11 (m, 2H), 3.63 [3.59] (d, *J* = 5.4 Hz, 1H), 2.58-2.40 (m, 2H), 2.33-2.22 (m, 1H), 2.21-2.09 (m, 1H), 2.09-1.92 (m, 2H), 1.91-1.74 (m, 2H).

¹³C-NMR (diastereomeric mixture) (75 MHz, CDCl₃, δ_C): 210.5 (C_q), 138.9 (C_q), 128.7 (+), 128.5 (+), 127.0 (+), 57.6 (+), 42.4 (−), 35.3 (−), 28.0 (−), 25.5 (−).

HRMS (EI) (*m/z*): [*M*⁺] (C₁₂H₁₄O⁺) calc.: 174.1039, found: 174.1035.

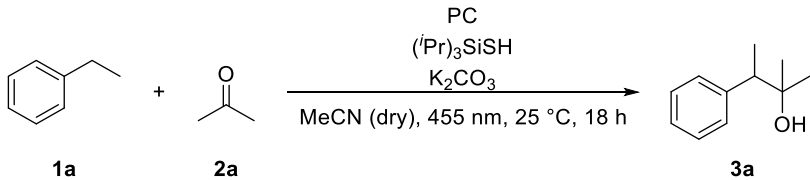
Yield: 9% (white solid).

5.4.3 Detailed optimization of the reaction conditions

5.4.3.1 Optimization process with ketones as electrophiles

When the reaction was performed with ethylbenzene **1a**, 4CzIPN **A** as a photocatalyst, (tPr)₃SiSH as a hydrogen atom transfer catalyst, K₂CO₃ as a base and acetone **2a** as an electrophile, traces of the desired product **3a** could be observed (Table 5-4, entry 1). A higher yield of 21% could be obtained by adding grinded 4 Å molecular sieves to the reaction (Table 5-4, entry 2). Increasing the amount of **2a** by using it as a co-solvent in a 1:1 mixture with dry acetonitrile gave a yield of 49% (Table 5-4 entry 3). A higher loading of hydrogen atom transfer catalyst (30 mol% instead of 20 mol%) or photocatalyst from (10 mol% instead of 5) decreased the yield (Table 5-4, entries 4 and 5) while reducing the amount of (tPr)₃SiSH gave a slightly enhanced yield (Table 5-4, entry 6). Using 3DPA2FBN **B** as a photocatalyst increased the yield to 50% when 10 equivalents **2a** was used and 86% when acetone was used as a co-solvent (Table 5-4, entries 7 and 8). The reaction could be improved slightly by reducing the loading of photocatalyst **B** to 3 mol% and the amount of K₂CO₃ to 10 mol% (Table 5-4, entry 9). Control experiments showed, that the yield is significantly lower when the reaction is performed without the base and no product is formed at all without light, photocatalyst or hydrogen atom transfer catalyst (Table 5-4, entries 10-13).

Table 5-4 – Optimization of the reaction conditions for the photocatalytic HAT-reaction of ethylbenzene with acetone as an electrophile.^[a]

<div style="text-align: center;">  </div>						
Entry	Amount of 2a	Photocatalyst (mol%)	Amount of (iPr) ₃ SiSH	Amount of base	Additive	Yield [%] ^[b]
1	10 eq.	4CzIPN (5)	20 mol%	20 mol%	–	3
2	10 eq.	4CzIPN (5)	20 mol%	20 mol%	4 Å MS (100 mg)	21
3	Co-solvent (1:1)	4CzIPN (5)	20 mol%	20 mol%	4 Å MS (100 mg)	49
4	10 eq.	4CzIPN (5)	30 mol%	30 mol%	4 Å MS (100 mg)	17
5	10 eq.	4CzIPN (10)	10 mol%	20 mol%	4 Å MS (50 mg)	18
6	10 eq.	4CzIPN (5)	10 mol%	20 mol%	4 Å MS (50 mg)	30
7	10 eq.	3DPA2FBN (5)	10 mol%	20 mol%	4 Å MS (50 mg)	50
8	Co-solvent (1:1)	3DPA2FBN (5)	10 mol%	20 mol%	4 Å MS (50 mg)	86
9	10 eq.	3DPA2FBN (3)	10 mol%	10 mol%	4 Å MS (50 mg)	59
10	10 eq.	3DPA2FBN (5)	10 mol%	–	4 Å MS (50 mg)	27
11	10	–	10 mol%	20 mol%	4 Å MS (100 mg)	0
12 ^[c]	10	4CzIPN (5)	10 mol%	20 mol%	4 Å MS (100 mg)	0
13	10	4CzIPN (5)	–	20 mol%	4 Å MS (100 mg)	0

[a] The reaction was performed using 1 eq. (0.2 mmol) **1a** in 2 mL degassed solvent, [b] yields were determined with GC-FID analysis using *n*-decane as an internal standard, [c] reaction was performed in the dark.

Screening of different photocatalysts

Table 5-5 – Optimization of the reaction conditions: screening of different photocatalysts.^[a]

Entry	Photocatalyst (mol%, hv [nm])	Yield ^[b] [%]
1	4CzIPN (5, 455)	30
2	3DPA2FBN (5, 455)	50
3	3DPAFIPN (5, 455)	28
4	Ru(bpy) ₃ Cl ₂ (5, 455)	0
5	Eosin Y (5, 535)	0
6	Fluorescein (5, 535)	0
7	Rhodamine 6G (5, 455)	0
8	<i>fac</i> -Ir(ppy) ₃ (2, 400)	0
9	(Ir[dF(CF ₃)ppy] ₂ (dtbpy))PF ₆ (2, 400)	0
10	Miyake catalyst (5, 400)	0

[a] The reaction was performed using 1 eq. (0.2 mmol) **1a** and 10 eq. (2 mmol) **2a** in 2 mL dry, degassed acetonitrile, [b] yields were determined with GC-FID analysis using *n*-decane as an internal standard.

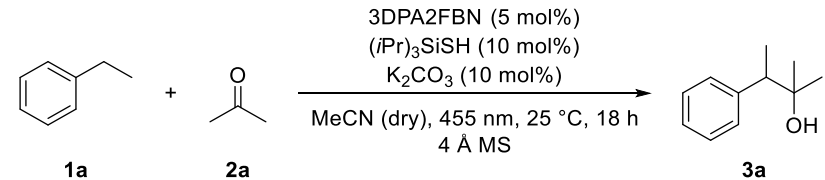
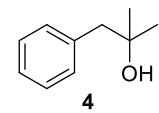
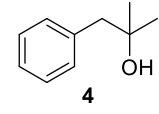
Screening of different hydrogen atom transfer catalysts

Table 5-6 – Optimization of the reaction conditions: screening of different hydrogen atom transfer catalysts.^[a]

<div style="text-align: center;"> </div>		
Entry	HAT-catalyst (mol%)	Yield ^[b] [%]
1	(<i>i</i> -Pr) ₃ SiSH (20)	30
2	Methyl thioglycolate (20)	traces
3	Ethyl 2-mercaptopropionate (20)	traces
4	3-Mercaptopropyltrimethoxysilan (20)	0
5	Quinuclidine (20)	0
6	1,1'-Binaaphthyl-2,2'-diyl hydrogenphosphate (20)	0
7	<i>N</i> -(3,5-bis(trifluoromethyl)phenyl)- 2,4,6- Triisopropylbenzenesulfonamide ^[17] (20 mol%)	0
8	NaBr (20)	0
9	(NH ₄)Br (20)	0

[a] The reaction was performed using 1 eq. (0.2 mmol) **1a** and 10 eq. (2 mmol) **2a** in 2 mL dry, degassed acetonitrile, [b] yields were determined with GC-FID analysis using *n*-decane as an internal standard.

Investigations on product inhibition and *in-situ* protection of alcohols**Table 5-7** – Optimization of the reaction conditions: investigations on product inhibition.^[a]

<div style="text-align: center;">  </div>		
Entry	Additive	Yield [%] ^[b]
1 ^[c]	3DPA2FBN (5 mol%)	41
2 ^[c]	(<i>i</i> Pr) ₃ SiSH (10 mol%)	50
3 ^[c]	3DPA2FBN (3 mol%) (<i>i</i> Pr) ₃ SiSH (10 mol%)	60
4	 (0.5 eq.)	39
5	 (1 eq.)	11
6	1-Heptanol (1 eq.)	21
7	TMS-Cl (1 eq.)	—
8	TMS-DMA (1 eq.)	—
9	BSTFA (1 eq.)	traces
10	Heptamethyldisilazane (1 eq.)	traces

[a] The reaction was performed using 1 eq. (0.2 mmol) **1a** and 10 eq. (2 mmol) **2a** in 2 mL dry, degassed acetonitrile, [b] yields were determined with GC-FID analysis using *n*-decane as an internal standard, [c] additional catalyst was added after 14 h.

5.4.3.2 Optimization process with aldehydes as electrophiles

General procedure for the reaction optimization process with aldehydes as electrophiles (general procedure D)

A 5 mL crimp cap vial equipped with a magnetic stirring bar was loaded with photocatalyst, base, ethylbenzene (**1a**), *n*-pentanal (**5a**), solvent and if noted an additive in the amounts given in the corresponding tables (S5-S15). In doing so, all solid compounds were added before capping the vial, whereas all liquid compounds were added *via* syringe after setting the capped vial under inert conditions. The reaction mixture was degassed by three cycles of freeze-pump-thaw and subsequently stirred under light irradiation for the given time at 25 °C. Subsequently, an aliquot of the reaction mixture was submitted to GC-FID analysis to determine the product yield with 1-heptanol as internal standard.

Table 5-8 – Benzylation of aldehydes: first successful reaction and control experiments.^[a]

Entry	Photocatalyst	HAT catalyst	Base	Product formation
1	4CzIPN (5 mol%)	(<i>i</i> Pr) ₃ SiSH (10 mol%)	K ₂ CO ₃ (50 mol%)	Traces Detected by GC/MS
2	–	(<i>i</i> Pr) ₃ SiSH (10 mol%)	K ₂ CO ₃ (50 mol%)	Not detected (n.d.)
3	4CzIPN (5 mol%)	–	K ₂ CO ₃ (50 mol%)	n.d.
4 ^[b]	4CzIPN (5 mol%)	(<i>i</i> Pr) ₃ SiSH (10 mol%)	K ₂ CO ₃ (50 mol%)	n.d.
5	4CzIPN (5 mol%)	(<i>i</i> Pr) ₃ SiSH (10 mol%)	–	Traces Detected by GC/MS

[a] Reactions were performed with **1a** (150 μmol, 1 eq.) and **5a** (450 μmol, 3 eq.) in degassed dry MeCN (2 mL) under a nitrogen atmosphere and irradiation using a 455 nm (±15 nm) LED. [b] Reaction performed in absence of light.

Table 5-9 – Benzylation of aldehydes: ethylbenzene/aldehyde ratio alteration.^[a]

Entry	Amount of ethylbenzene [eq.]	Amount of <i>n</i> -pentanal [eq.]	Yield ^[b] [%]
1	1	10	Traces
2	1	3	3
3	1	1	10
4	3	1	16
5 ^[c]	3	1	20

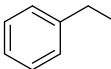
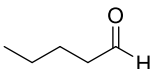
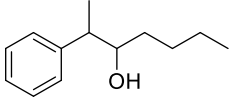
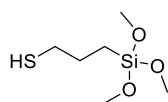
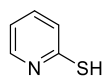
[a] Reactions were performed with 1 eq. being 150 μ mol, 4CzIPN (5 mol% in respect to 1 eq), (*i*Pr)₃SiSH (20 mol%), K₂CO₃ (50 mol%) and molecular sieve (4 Å, 50 mg) in degassed dry MeCN (2 mL) under a nitrogen atmosphere and irradiation using a 455 nm (\pm 15 nm) LED.
 [b] GC-Yield using 1-heptanol as internal standard. [c] No molecular sieve.

Table 5-10 – Benzylation of aldehydes: variation of base and HAT amount.^[a]

Entry	Amount of (<i>i</i> Pr) ₃ SiSH [mol%]	Amount of K ₂ CO ₃ [mol%]	Yield ^[b] [%]
1	10	50	10
2	20	50	20
3	50	50	8
4	20	—	6
5	20	10	20
6	20	100	18

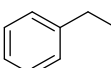
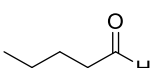
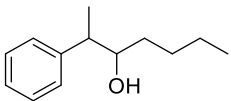
[a] Reactions were performed with **5a** (150 μ mol, 1 eq), **1a** (450 μ mol, 3 eq), 4CzIPN (5 mol%), (*i*Pr)₃SiSH and K₂CO₃ in degassed dry MeCN (2 mL) under a nitrogen atmosphere and irradiation using a 455 nm (\pm 15 nm) LED. [b] GC-Yield using 1-heptanol as internal standard.

Table 5-11 – Benzylation of aldehydes: change of HAT catalyst and solvent.[a]

$ \begin{array}{c} \text{4CzIPN (5 mol\%)} \\ \text{HAT (20 mol\%)} \\ \text{K}_2\text{CO}_3 \text{ (50 mol\%)} \\ \text{dry solvent (2 mL), r.t.,} \\ \text{LED (455 nm), 16 h} \end{array} $			
	+		
1a		5a	6i
Entry	Solvent	HAT catalyst	Yield ^[b] [%]
1	MeCN	(<i>i</i> Pr) ₃ SiSH	20
2	DMF	(<i>i</i> Pr) ₃ SiSH	2
3 ^[c]	DMF	Quinuclidine	n.d.
4	MeCN		2
5	MeCN	HS–C ₉ H ₁₉	3
6	MeCN		Not detected (n.d.)
7	MeCN	NaBr	n.d.

[a] Reactions were performed with **5a** (150 μmol, 1 eq), **1a** (450 μmol, 3 eq), 4CzIPN (5 mol%), HAT catalyst (20 mol%) and K₂CO₃ (50 mol%) in degassed dry MeCN (2 mL) under a nitrogen atmosphere and irradiation using a 455 nm (±15 nm) LED. [b] GC-Yield using 1-heptanol as internal standard. [c] Toluene instead of ethylbenzene was used.

Table 5-12 – Benzylation of aldehydes: photocatalyst screening.[a]

$ \begin{array}{c} \text{Photocatalyst (X mol\%)} \\ (\textit{i}\text{Pr})_3\text{SiSH (20 mol\%)} \\ \text{K}_2\text{CO}_3 \text{ (50 mol\%)} \\ \text{dry MeCN (2 mL), r.t.,} \\ \text{LED (455 nm), 16 h} \end{array} $		
	+	
1a		5a
		
Entry	Photocatalyst	Yield ^[b] [%]
1	4CzIPN (5 mol%)	20
2	3DPA2FBN (5 mol%)	10
3	3DPAFIPN (5 mol%)	32
4 ^[c]	3DPAFIPN (5 mol%)	27
5	4Cz(<i>p</i> H)BN (5 mol%)	20
6	(Ir[dF(CF ₃)ppy] ₂ (dtbpy))PF ₆ (2 mol%)	2
7	Miyake catalyst	n.d.

[a] Reactions were performed with **5a** (150 μmol, 1 eq), **1a** (450 μmol, 3 eq), photocatalyst, (*i*Pr)₃SiSH (20 mol%) and K₂CO₃ (50 mol%) in degassed dry MeCN (2 mL) under a nitrogen atmosphere and irradiation using a 455 nm (±15 nm) LED. [b] GC-Yield using 1-heptanol as internal standard. [c] 20 mol% of K₂CO₃ was used.

Table 5-13 – Benzylation of aldehydes: base and additive screening.^[a]

Entry	Base	Additive	Yield ^[b] [%]
1	K ₂ CO ₃	—	32
2	Li ₂ CO ₃	—	13
3	Na ₂ CO ₃	—	15
4	Cs ₂ CO ₃	—	7
5	Lutidin	—	13
6	K ₂ CO ₃	B ₂ pin ₂ (25 mol%)	33
7	K ₂ CO ₃	 (50 mol%)	15
8	Lutidin	 (50 mol%)	26

[a] Reactions were performed with **5a** (150 μmol, 1 eq), **1a** (450 μmol, 3 eq), 3DPAFIPN (5 mol%), (iPr)₃SiSH (20 mol%), base (50 mol%) and an additive if noted in degassed dry MeCN (2 mL) under a nitrogen atmosphere and irradiation using a 455 nm (±15 nm) LED.

[b] GC-Yield using 1-heptanol as internal standard.

Table 5-14 – Benzylation of aldehydes: reaction time variation.^[a]

Entry	Time [h]	Yield ^[b] [%]	Entry	Time [h]	Yield ^[b] [%]
1	1	27	4	16	32
2	2	31	5 ^[c]	16	32
3	4	33	6 ^[d]	16	22

[a] Reactions were performed with **5a** (150 μmol, 1 eq), **1a** (450 μmol, 3 eq), 3DPAFIPN (5 mol%), (iPr)₃SiSH (20 mol%) and K₂CO₃ (50 mol%) in degassed dry MeCN (2 mL) under a nitrogen atmosphere and irradiation using a 455 nm (±15 nm) LED. [b] GC-Yield using 1-heptanol as internal standard. [c] The reaction was executed as described in [a] in 1.5 mL dry MeCN. After 2 h of irradiation, a dry MeCN solution (0.5 mL) containing additional 3DPAFIPN (7.5 μmol, 5 mol%) was injected *via* syringe and the mixture was irradiated for further 14 h. [d] Reaction was executed as described in [a]. After 2 h of irradiation, a dry MeCN solution (0.5 mL) containing additional 3DPAFIPN (7.5 μmol, 5 mol%) and (iPr)₃SiSH (30 μmol, 20 mol%) was injected *via* syringe and the mixture was irradiated for further 14 h.

Table 5-17 – Benzylation of aldehydes: variation of experimental execution.

1a	5a	6i
Entry	Experimental variation	Yield ^[a] [%]
1 ^[b]	Aldehyde added <i>via</i> syringe pump	19
2 ^[c]	Executed in micro-flow reactor	12 (26) ^[d]
3 ^[e]	Reaction temperature 0 °C	27
4 ^[f]	1 eq set to 200 μmol instead of 150 μmol	23

[a] GC-Yield using 1-heptanol as internal standard. [b] Reaction was performed with **1a** (450 μmol, 3 eq), 3DPAFIPN (5 mol%), (iPr)₃SiSH (20 mol%) and K₂CO₃ (50 mol%) in degassed dry MeCN (1.5 mL) under a nitrogen atmosphere and irradiation using a 455 nm (±15 nm) LED. A solution of **5a** (150 μmol, 1 eq) in dry MeCN (0.5 mL) was added *via* syringe pump in 4 h (0.125 mL/h). After completed addition the mixture was stirred overnight (12 h). [c] Reaction was performed with **5a** (150 μmol, 1 eq), **1a** (450 μmol, 3 eq), 3DPAFIPN (5 mol%), (iPr)₃SiSH (20 mol%), lutidin (50 mol%) and tris(trimethylsilyl)silane (50 mol%) in degassed dry MeCN (2 mL) under a nitrogen atmosphere and irradiation using a 455 nm (±15 nm) LED in a micro-flow reactor (reactor retention time 1.7 h). [d] Reaction was performed as described in [c], yet in batch over 16 h. [e] Reaction was performed with **5a** (150 μmol, 1 eq), **1a** (450 μmol, 3 eq), 3DPAFIPN (5 mol%), (iPr)₃SiSH (20 mol%) and K₂CO₃ (50 mol%) in degassed dry MeCN (2 mL) under a nitrogen atmosphere and irradiation using a 455 nm (±15 nm) LED at 0 °C. [f] Reaction was performed with **1a** (200 μmol, 1 eq), **5a** (600 μmol, 3 eq), 3DPAFIPN (5 mol%), (iPr)₃SiSH (20 mol%) and K₂CO₃ (50 mol%) in degassed dry MeCN (2 mL) under a nitrogen atmosphere and irradiation using a 455 nm (±15 nm) LED.

Table 5-18 – Benzylation of aldehydes, repetition of control experiments with optimized conditions.^[a]

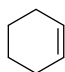
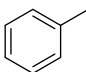
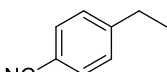
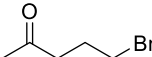
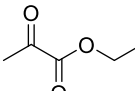
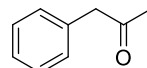
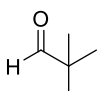
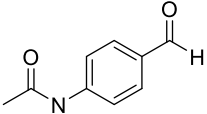
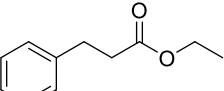
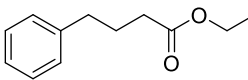
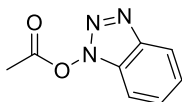
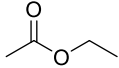
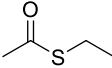
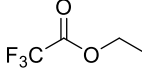
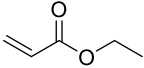
Reaction scheme showing the synthesis of **6i** from **1a** and **5a** using 3DPAFIPN (*X* mol%), (*i*Pr)₃SiSH (*X* mol%), and K₂CO₃ (*X* mol%) in dry MeCN (2 mL), r.t., LED (455 nm), 16 h.

Entry	Photocatalyst	HAT catalyst	Base	Yield ^[b] [%]
1	3DPAFIPN (5 mol%)	(<i>i</i> Pr) ₃ SiSH (20 mol%)	K ₂ CO ₃ (50 mol%)	32 (28) ^[c]
2	—	(<i>i</i> Pr) ₃ SiSH (20 mol%)	K ₂ CO ₃ (50 mol%)	n.d.
3	3DPAFIPN (5 mol%)	—	K ₂ CO ₃ (50 mol%)	n.d.
4	3DPAFIPN (5 mol%)	(<i>i</i> Pr) ₃ SiSH (20 mol%)	—	10
5 ^[d]	3DPAFIPN (5 mol%)	(<i>i</i> Pr) ₃ SiSH (20 mol%)	K ₂ CO ₃ (50 mol%)	n.d.

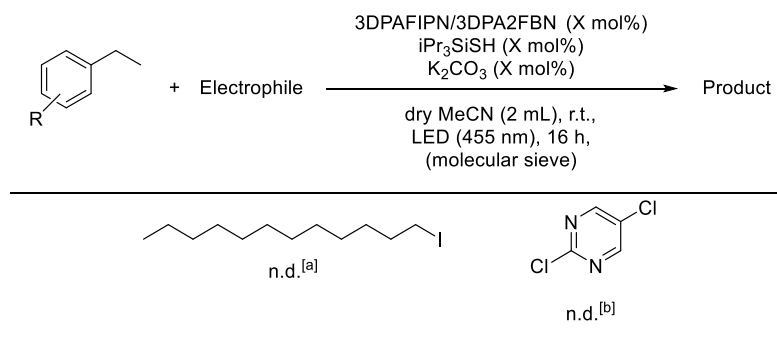
[a] Reactions were performed with **5a** (150 μmol, 1 eq) and **1a** (450 μmol, 3 eq) in degassed dry MeCN (2 mL) under a nitrogen atmosphere. [b] GC-Yield using 1-heptanol as internal standard. [c] Isolated yield in parentheses. [d] Executed in the dark.

5.4.4 Unsuccessful transformations

Table 5-19 – Unsuitable substrates for the photocatalytic C–H to carbanion activation followed by the addition to carbonyl compounds.

<div></div>	
Carbanion precursors	Ketones
<div> n.d.^[a]</div> <div> n.d.^[a]</div> <div> n.d.^[b]</div>	<div> n.d.^[c,d]</div> <div> n.d.^[e]</div> <div> n.d.^[e]</div>
Aldehydes	Esters (Intramolecular)
<div> n.d.^[f]</div> <div> n.d.^[f]</div>	<div> n.d.^[g]</div> <div> n.d.^[g]</div>
Esters (Intermolecular)	
<div> n.d.^[h,i]</div> <div> n.d.^[j]</div> <div> Traces detected by GC/MS^[j]</div> <div> n.d.^[k]</div> <div> Traces detected by GC/MS^[l]</div>	

[a] Reaction performed according to general procedure A with acetone as electrophile. [b] Reaction performed according to General procedure B with n-pentanal as electrophile. [c] Reaction performed according to general procedure A with ethylbenzene as carbanion precursor. [d] Substrate synthesized according to literature procedure.^[42] [e] Reaction performed according to general procedure A with 4-ethylanisole as carbanion precursor. [f] Reaction performed according to general procedure B with 4-ethylanisole as carbanion precursor. [g] Reaction performed according to general procedure C. [h] Reaction performed according to general procedure C with ethylbenzene (200 μmol , 1 eq.) as carbanion precursor and the corresponding electrophile (1 eq.). [i] Substrate synthesized according to an adapted literature procedure.^[43] [j] Reaction performed according to general procedure C with ethylbenzene (200 μmol , 1 eq.) as carbanion precursor and the corresponding electrophile (10 eq.). [k] Reaction performed according to [j] with 3 eq. electrophile. [l] Reaction performed according to [j] with 1 eq. electrophile.

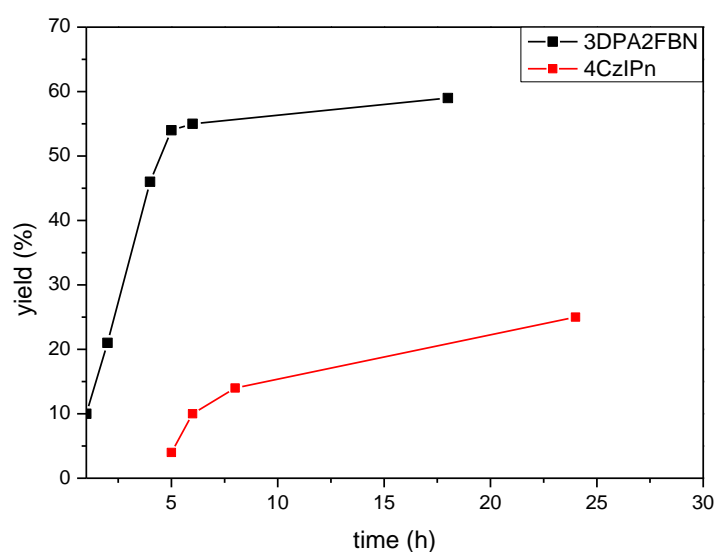
Table 5-20 – Attempted S_N2 reactions.

[a] Reaction performed according to General Procedure B with ethylbenzene as carbanion precursor. [b] Reaction performed according to General Procedure A with ethylbenzene (200 μ mol, 1 eq.) as carbanion precursor and the corresponding electrophile (2 eq.).

5.4.5 Mechanistic investigations

5.4.5.1 Reaction kinetics

The reactions were performed using 1 eq. ethylbenzene **1a** (0.2 mmol), 10 eq. acetone **2a** (2 mmol), 3 mol% photocatalyst, 10 mol% $(i\text{Pr})_3\text{SiSH}$, 10 mol% K_2CO_3 and 50 mg grinded 3 \AA molecular sieves in 2 ml dry, degassed acetonitrile. The reaction was irradiated with blue LEDs (455 nm \pm 15 nm). The yield of the reactions were determined with GC-FID analysis using *n*-decane as an internal standard.

**Figure 5-2** – Kinetic profile of the reaction with 4CzIPN (**A**) and 3DPA2FBN (**B**) as a photocatalyst.

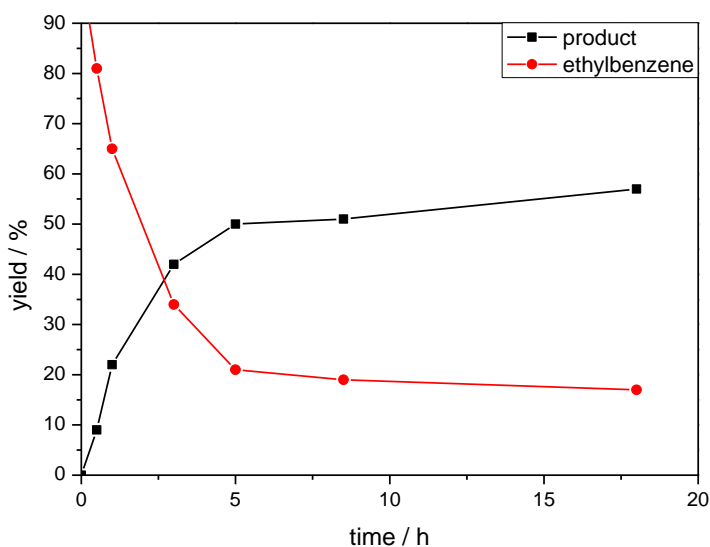


Figure 5-3 – Product formation and consumption of starting material during the reaction.

5.4.5.2 Fluorescence quenching studies

For the emission quenching of 3DPAFIPN with $(\text{Pr})_3\text{SiS}^-$, a 37.5 μM solution of 3DPAFIPN in degassed p.A. MeCN (6.1 mg 3DPAFIPN diluted in 250 mL p.A. MeCN) was given into a gas-tight 10 mm quartz cuvette and set under a nitrogen atmosphere. The photocatalyst was irradiated at 435 nm and the change of the fluorescence emission upon addition of different amounts of quencher solution was measured (Figure 5-4). The quencher solution was prepared by the addition of the above described 37.5 μM 3DPAFIPN solution to K_2CO_3 (11.1 mg, 80 μmol) and $(\text{Pr})_3\text{SiSH}$ (17.1 μL , 80 μmol) in a volumetric flask (2 mL). As K_2CO_3 is not soluble in organic solvents, a solid residue remains, which can be K_2CO_3 or KHCO_3 .

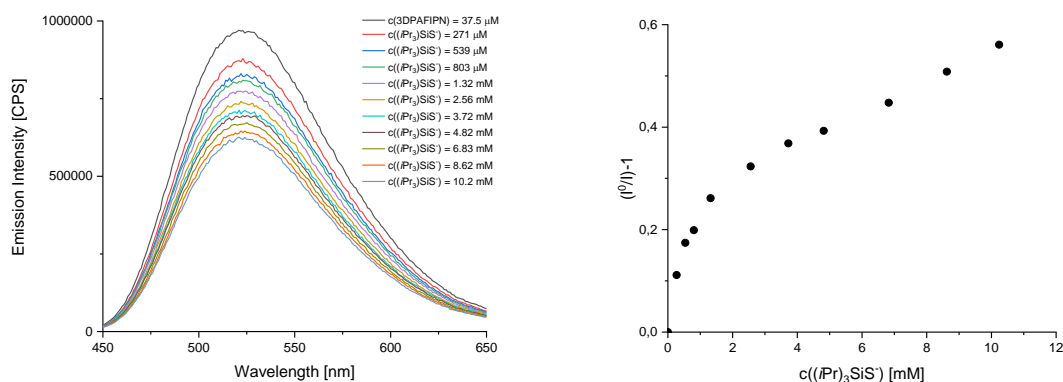


Figure 5-4 – Left: Emission quenching of 3DPAFIPN (37.5 μM in MeCN) upon titration with a quencher solution containing $(\text{Pr})_3\text{SiSH}$ (41 mM in MeCN) and 3DPAFIPN (37.5 μM in dry MeCN) treated with K_2CO_3 . Right: Corresponding Stern-Volmer plot (I_{max} at 526 nm).

An efficient fluorescence quenching of 3DPAFIPN upon addition of $(\text{Pr})_3\text{SiS}^-$ was observed, indicating an interaction between the excited photocatalyst and the deprotonated HAT catalyst. However, a linear Stern-Volmer correlation was not obtained.

The measurement was executed in the same manner using 3DPA2FBN instead of 3DPAFIPN (figure S4) using an excitation wavelength of 400 nm. An efficient fluorescence quenching of 3DPAFIPN upon addition of $(\text{Pr})_3\text{SiS}^-$ was observed, indicating an interaction between the excited photocatalyst and the deprotonated HAT catalyst (Figure S4, left). By plotting $(I^0/I)-1$ versus the quencher concentration, a Stern-Volmer constant of $K_{SV} = 42.1 \text{ M}^{-1}$ was determined from the slope of the linear fit (Figure 5-5, right):

$$\frac{I^0}{I} - 1 = K_{SV} \cdot [Q]$$

(With I^0 being the fluorescence intensity at 490 nm in absence of the quencher, I the fluorescence intensity at 490 nm in presence of the quencher and $[Q]$ the quencher concentration)

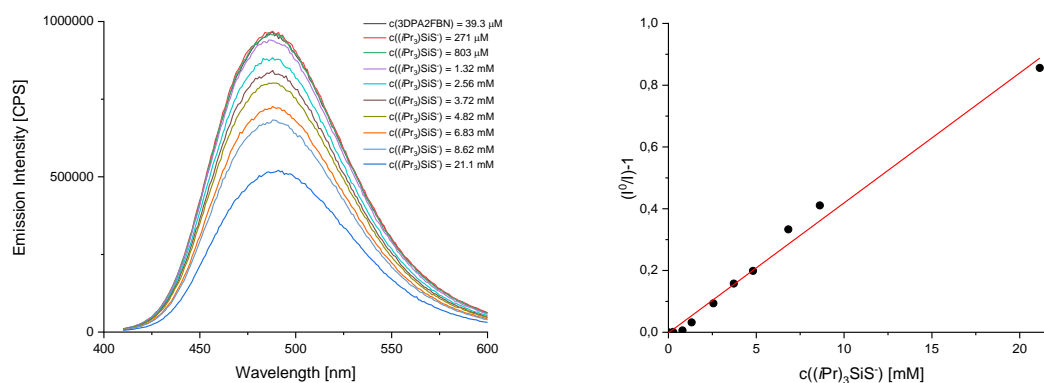


Figure 5-5 – Left: Emission quenching of 3DPA2FBN (39.3 μM in MeCN) upon titration with a quencher solution containing $(\text{Pr})_3\text{SiSH}$ (41 mM in MeCN) and 3DPAFIPN (39.3 μM in dry MeCN) treated with K_2CO_3 . Right: Corresponding Stern-Volmer plot (I_{max} at 490 nm).

5.4.5.3 Cyclic voltammetry measurements

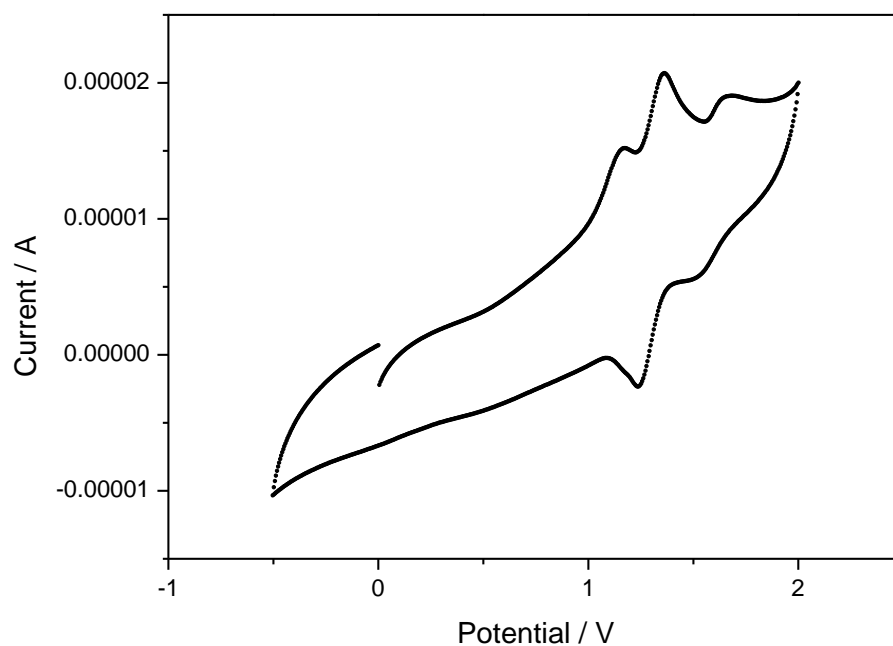
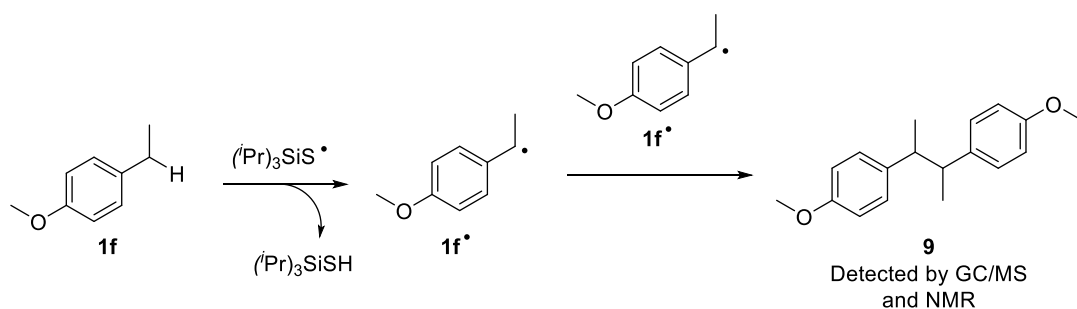


Figure 5-6 – Cyclic voltammogram of $(\text{Pr})_3\text{SiSH}$ and K_2CO_3 (1:2) in MeCN under argon. The reversible peaks at 1.53 and 1.66 V show the oxidation of $(\text{Pr})_3\text{SiS}^-$ and correspond to a potential of 0.67 V *vs* SCE; the reversible peaks at 1.24 and 1.36 V correspond to ferrocene, which was used as an internal standard.

5.4.5.4 Radical-radical homocoupling

After the oxidation of the deprotonated HAT species ($(^i\text{Pr})_3\text{SiS}^-$) by the excited photocatalyst, the activated HAT catalyst ($(^i\text{Pr})_3\text{SiS}^\bullet$) is proposed to abstract a hydrogen atom from the ethyl benzene derivative yielding the corresponding benzyl radical **1f** $^\bullet$. The presence of **1f** $^\bullet$ is supported by the detection of the resulting radical-radical homocoupling product of 4-ethylanisol (**9**) by GC/MS and by NMR during the isolation of product **6c** (Scheme 5-4, Figure 5-7).



Scheme 5-4 – Formation of radical-radical homocoupling product **9**.

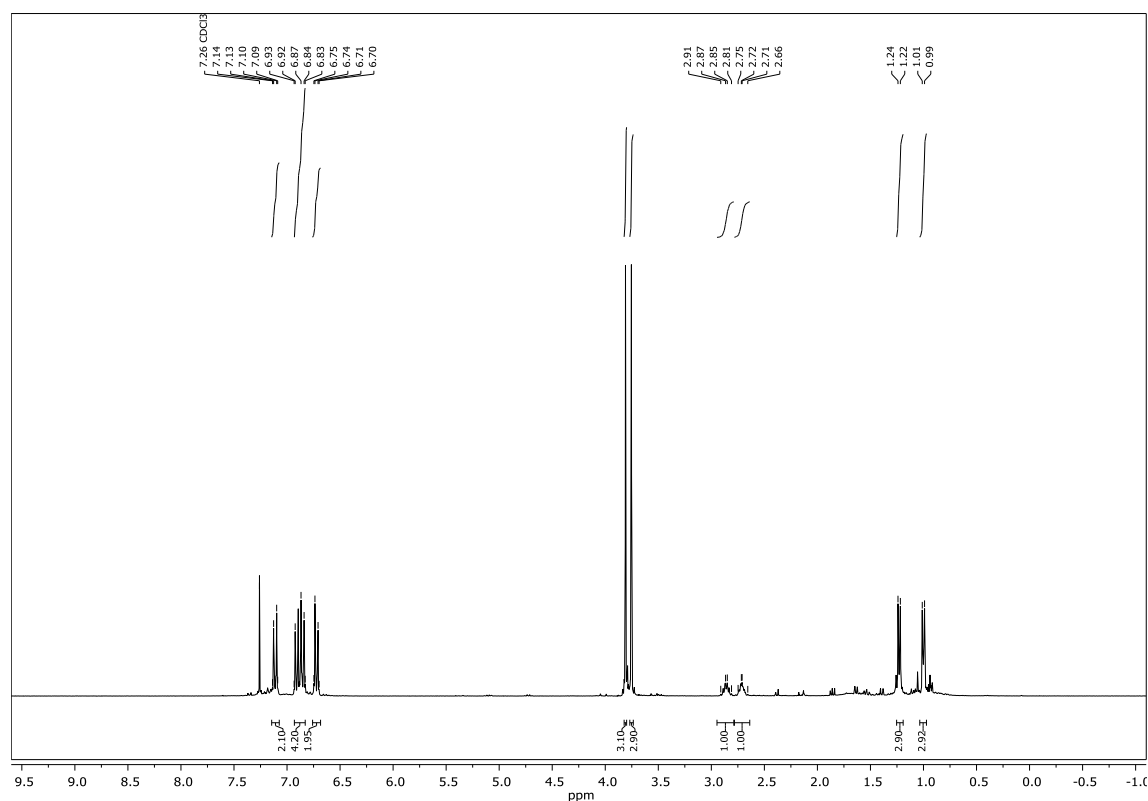


Figure 5-7 – Crude NMR of **9** obtained during the isolation of **6c**.

5.4.5.5 Intramolecular ring closure using an ester as an electrophile

The formation of a reactive carbanion is the key step of the proposed reaction mechanism. The carbanion is proposed to be generated by the SET reduction of carbon radical **1**[•] by the reduced photocatalyst. The generation of the carbanion intermediate is supported by the successful intramolecular ring closure using esters as electrophiles. As described by Murphy *et al.*,^[18] esters are not known to react with radicals, yet are susceptible to an addition by ionic nucleophiles. Hence, Murphy and co-workers designed compound **10** as carbanion testing system, which will give product **11** if a radical intermediate is involved, while product **12** can only be formed if the corresponding carbanion intermediate is generated (Scheme 5-8).

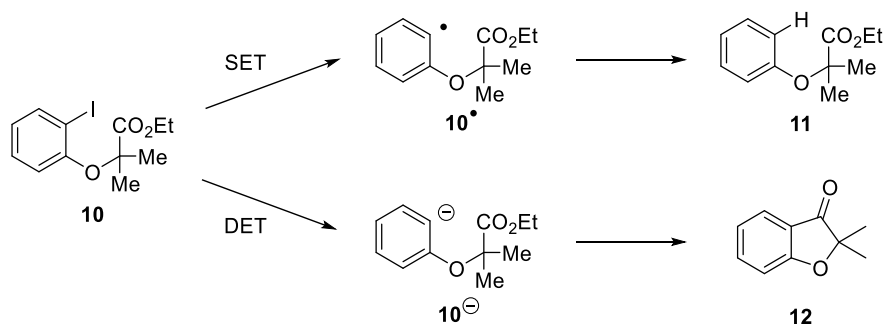


Figure 5-8 – Carbanion test system designed by Murphy *et al.*

Compound **7a** (and **7b**) can be regarded as a similar yet simpler carbanion test system. Thus, the formation of cyclization product **8a** (and **8b**) (Scheme 5-9) supports the proposed carbanion intermediate.

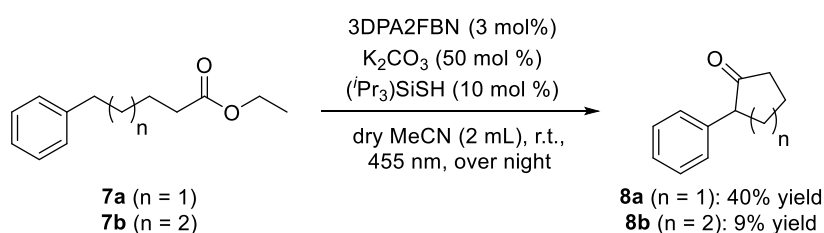
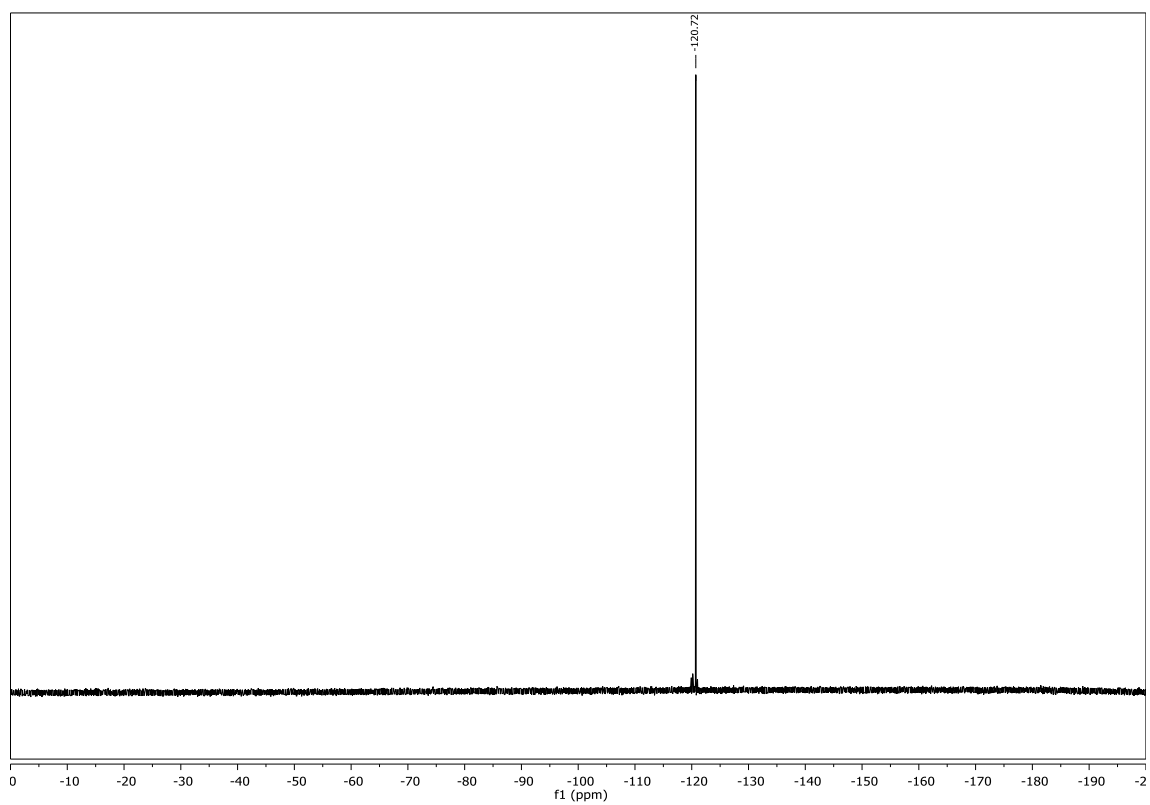
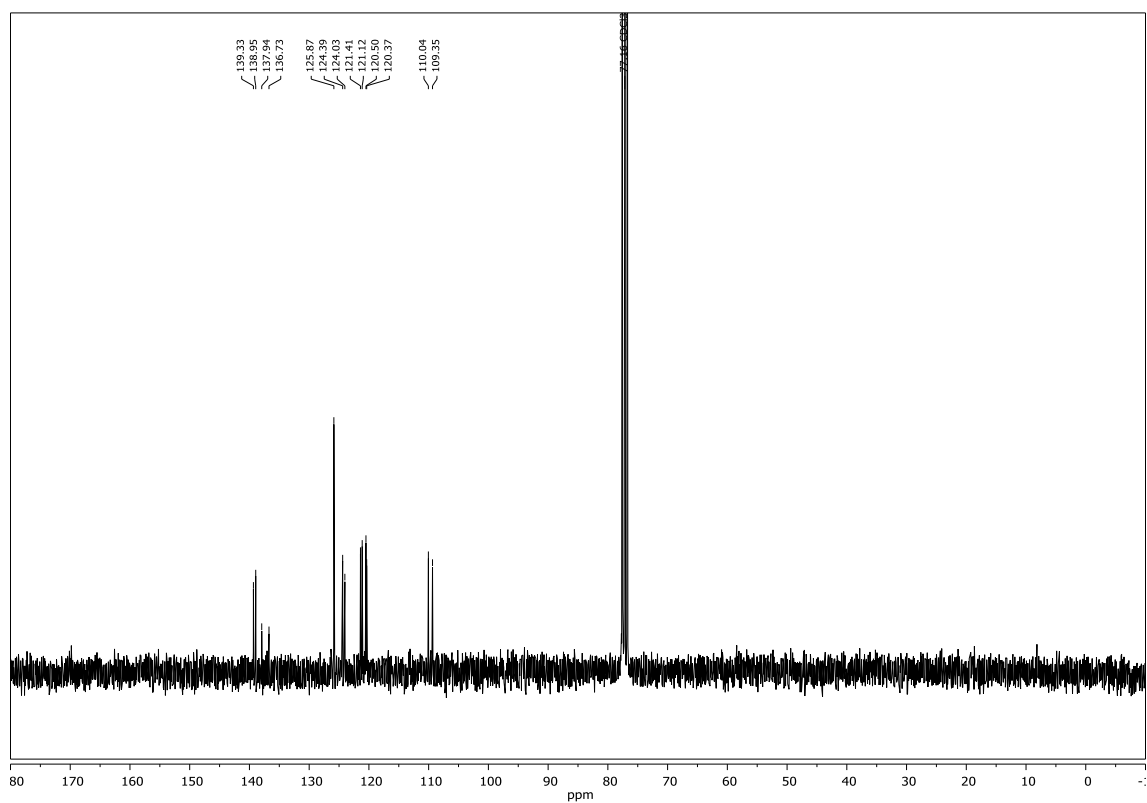
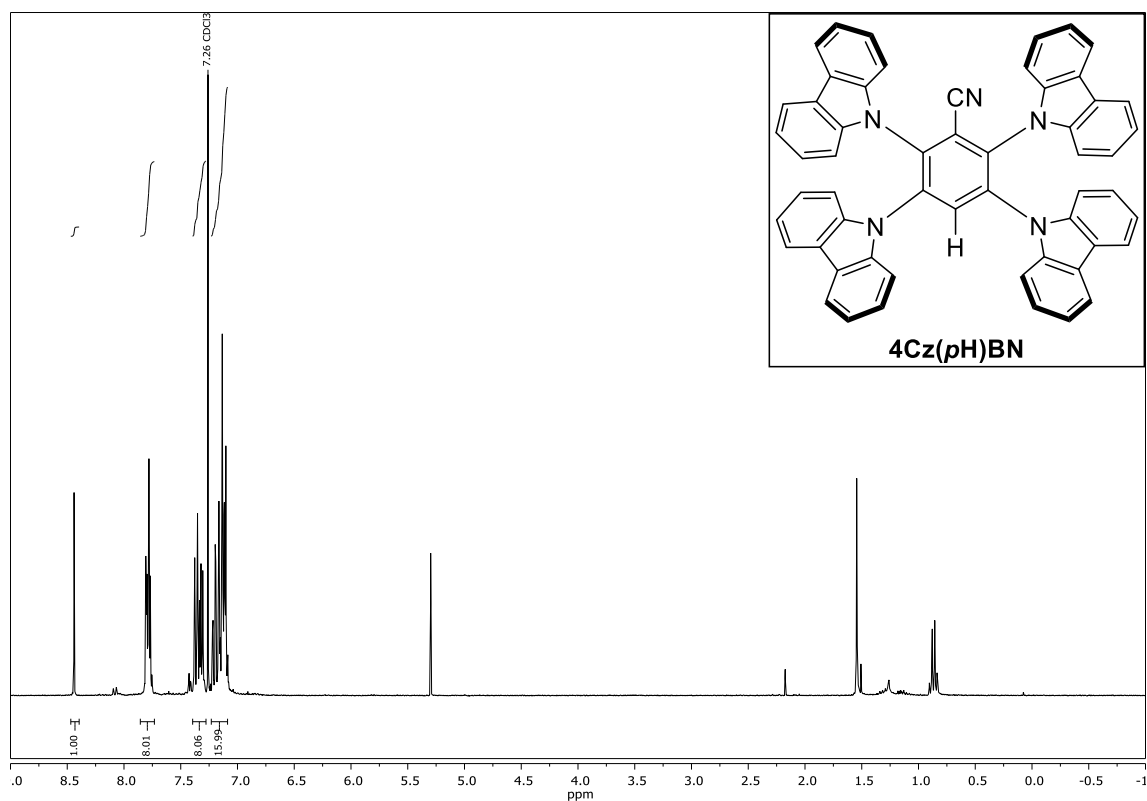


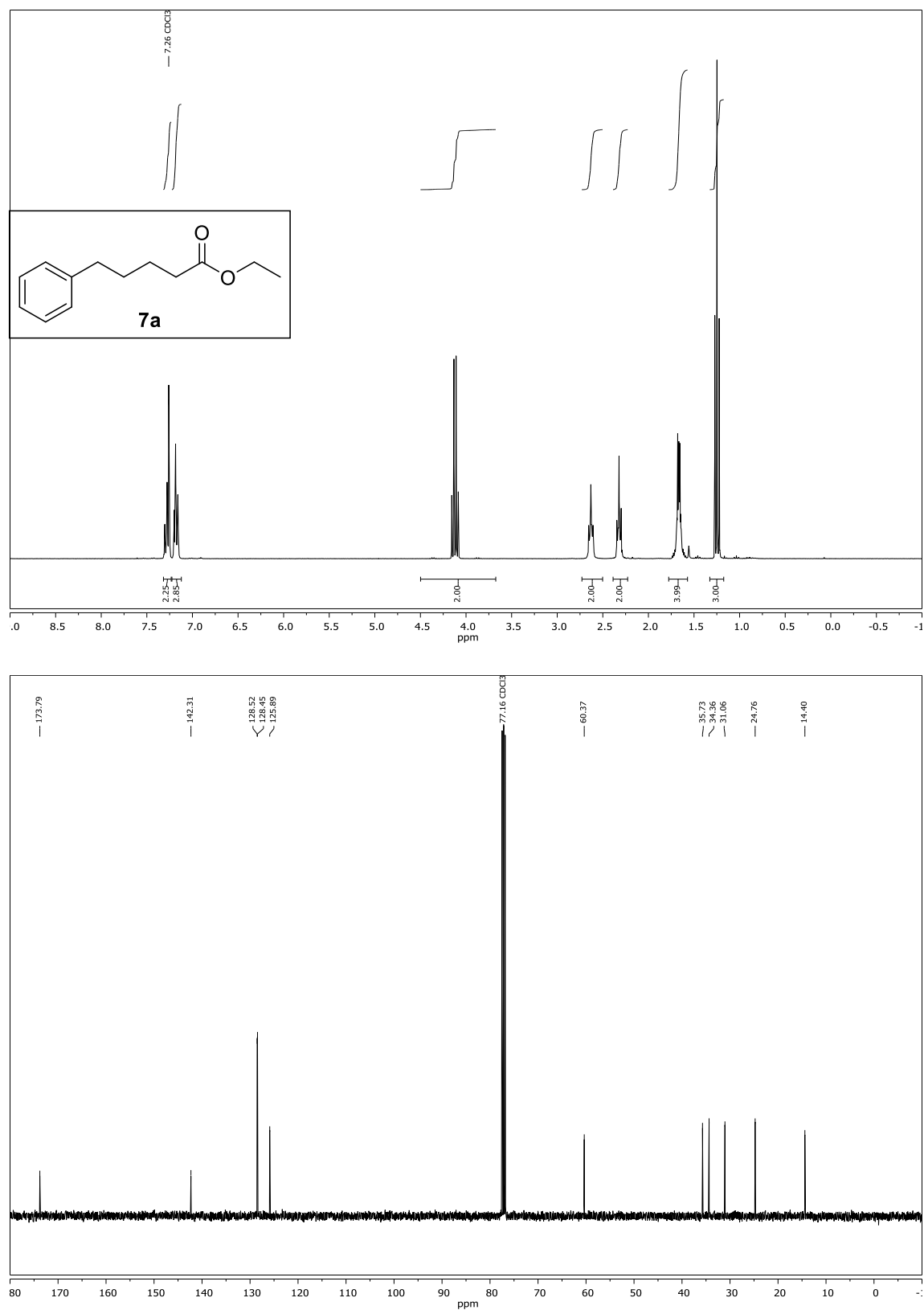
Figure 5-9 – Formation of cyclization product **8a** and **8b**.

Chemical structure of 3DPA2FBN is shown in the top right corner. The structure is a benzene ring substituted with a cyano group (CN), two fluorine atoms (F), and three diphenylamino groups (NPh₂).

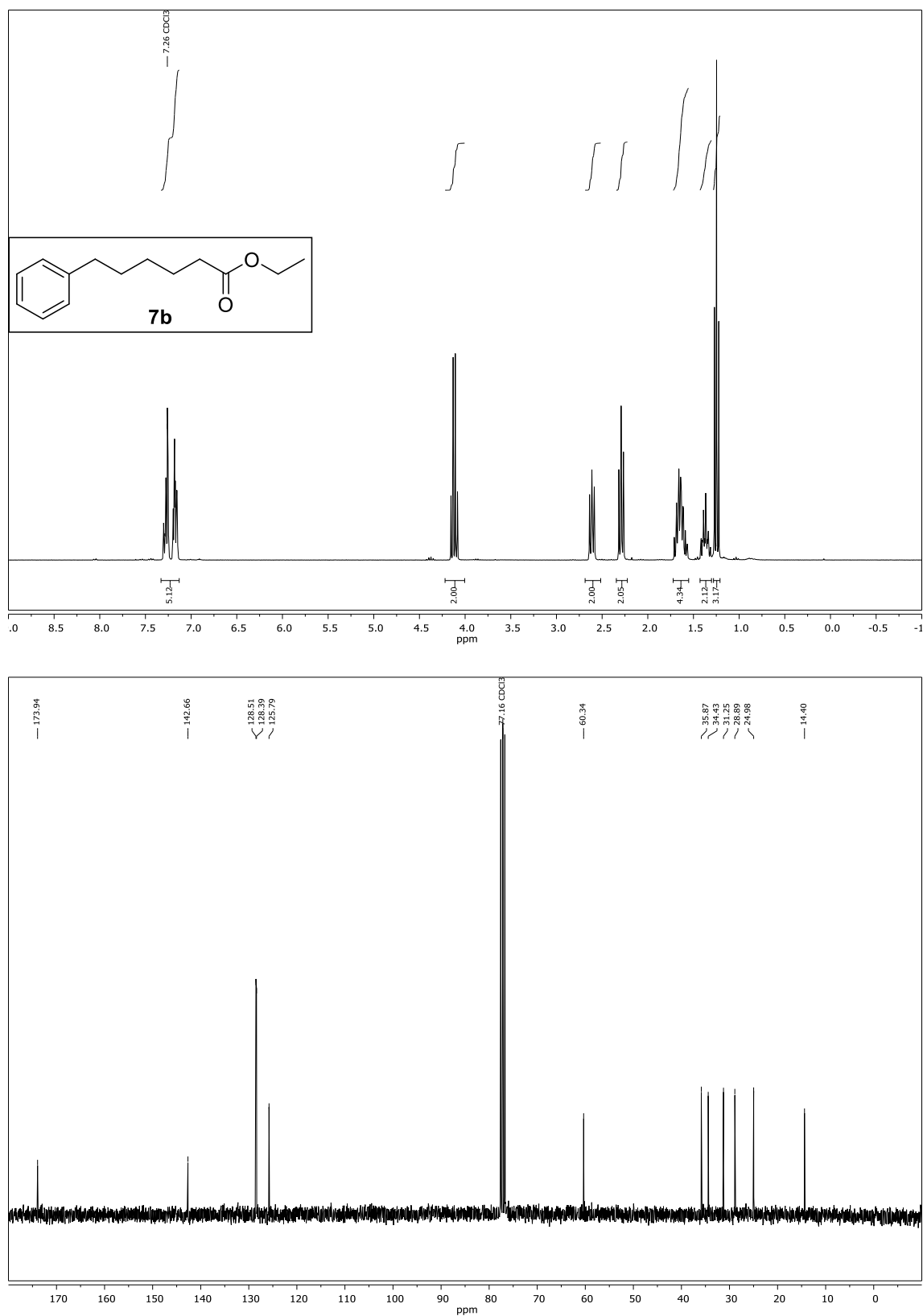


4Cz(pH)BN, ^1H - and ^{13}C -NMR (CDCl_3):

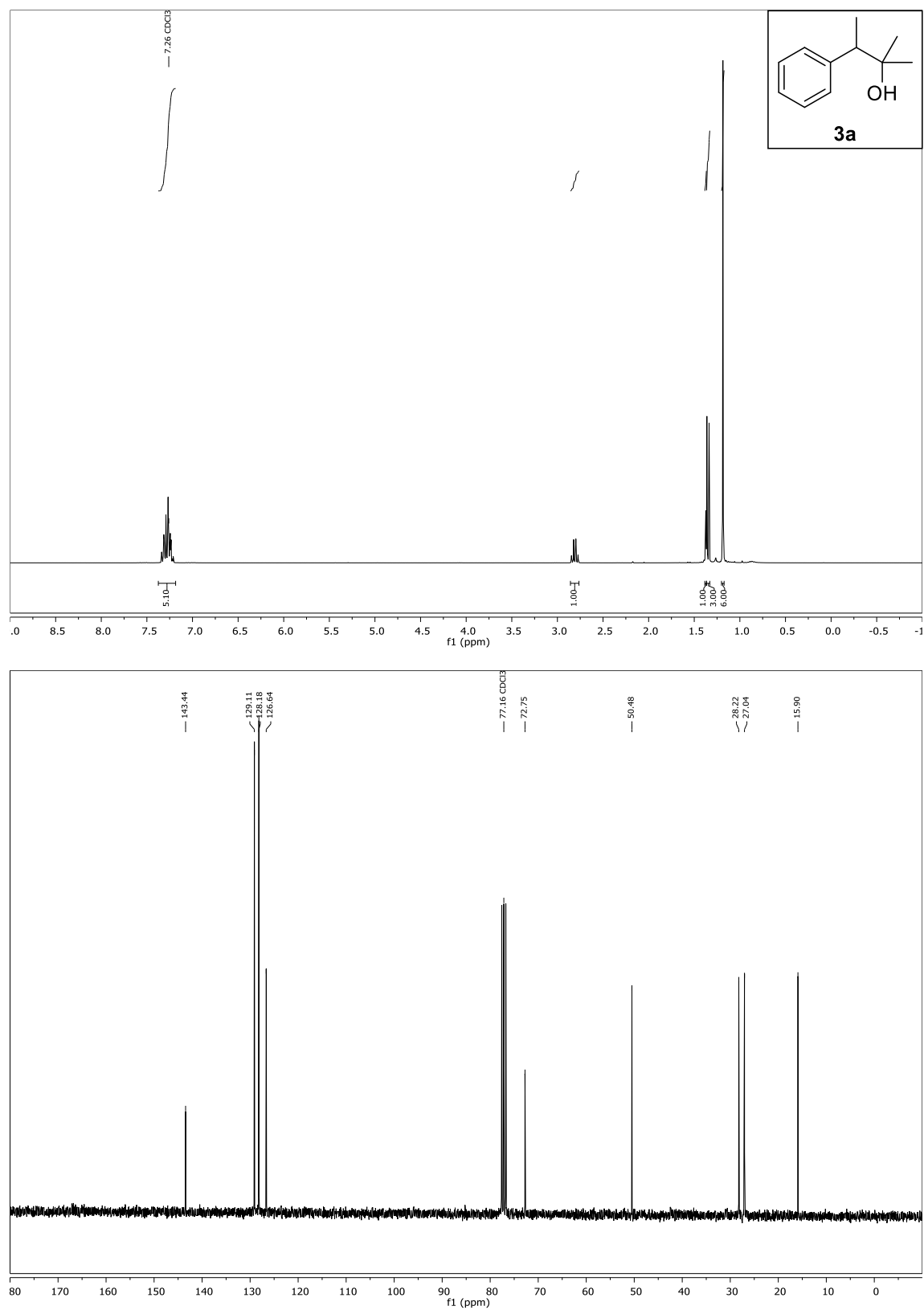


Ethyl-5-phenylpentanoate (7a), ^1H - and ^{13}C -NMR (CDCl_3)

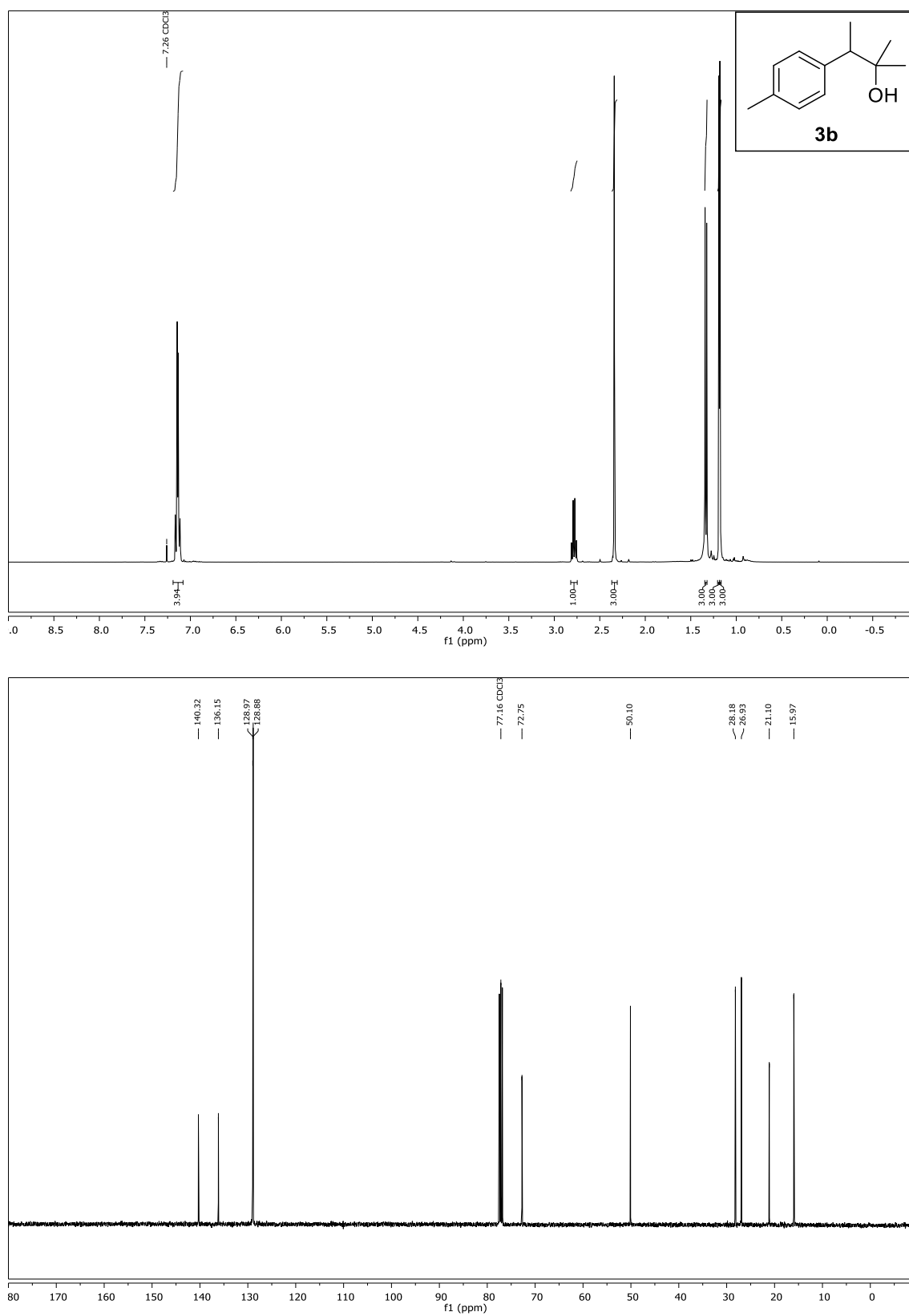
Ethyl-6-phenylhexanoate (7b), ^1H - and ^{13}C -NMR (CDCl_3)

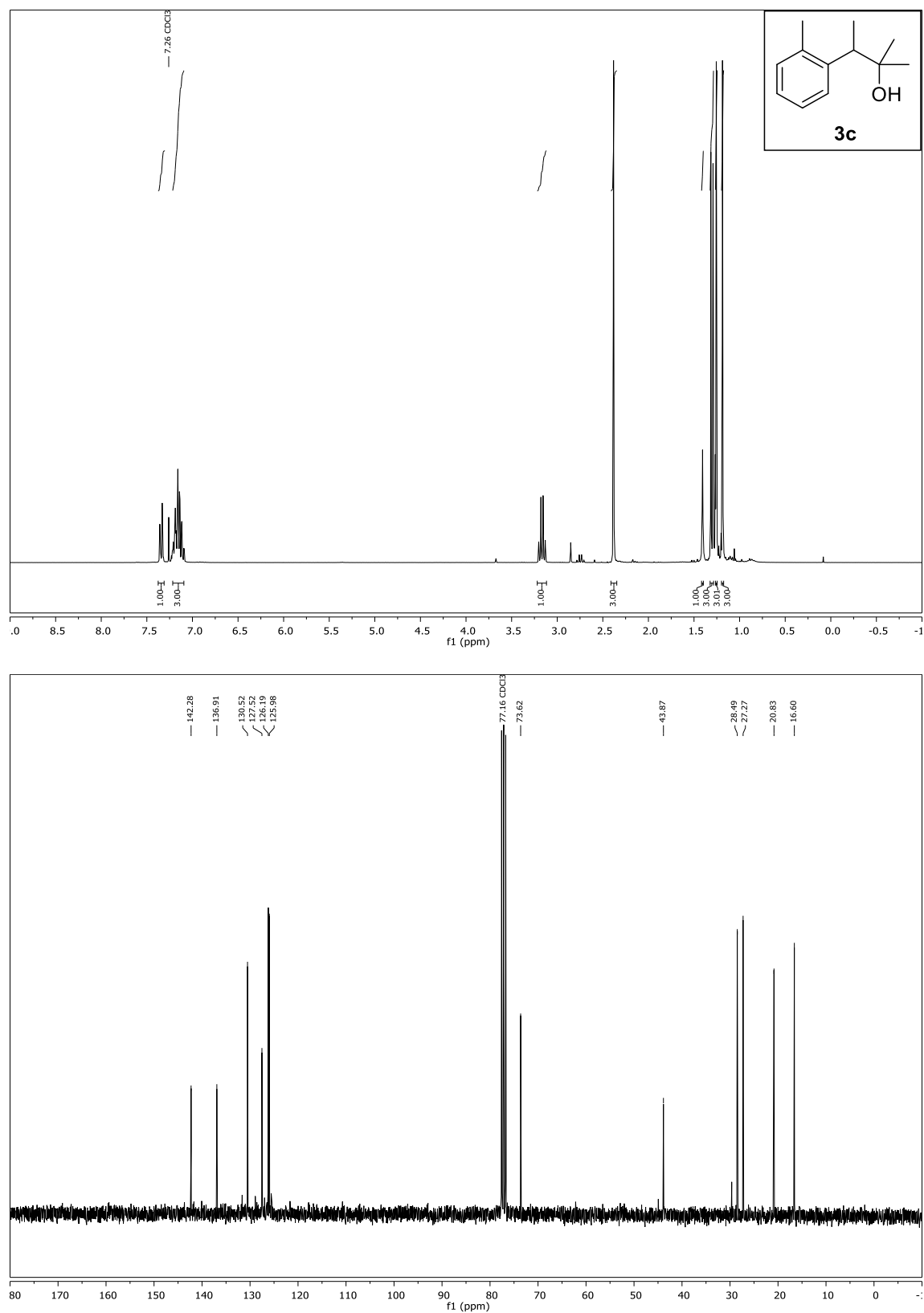


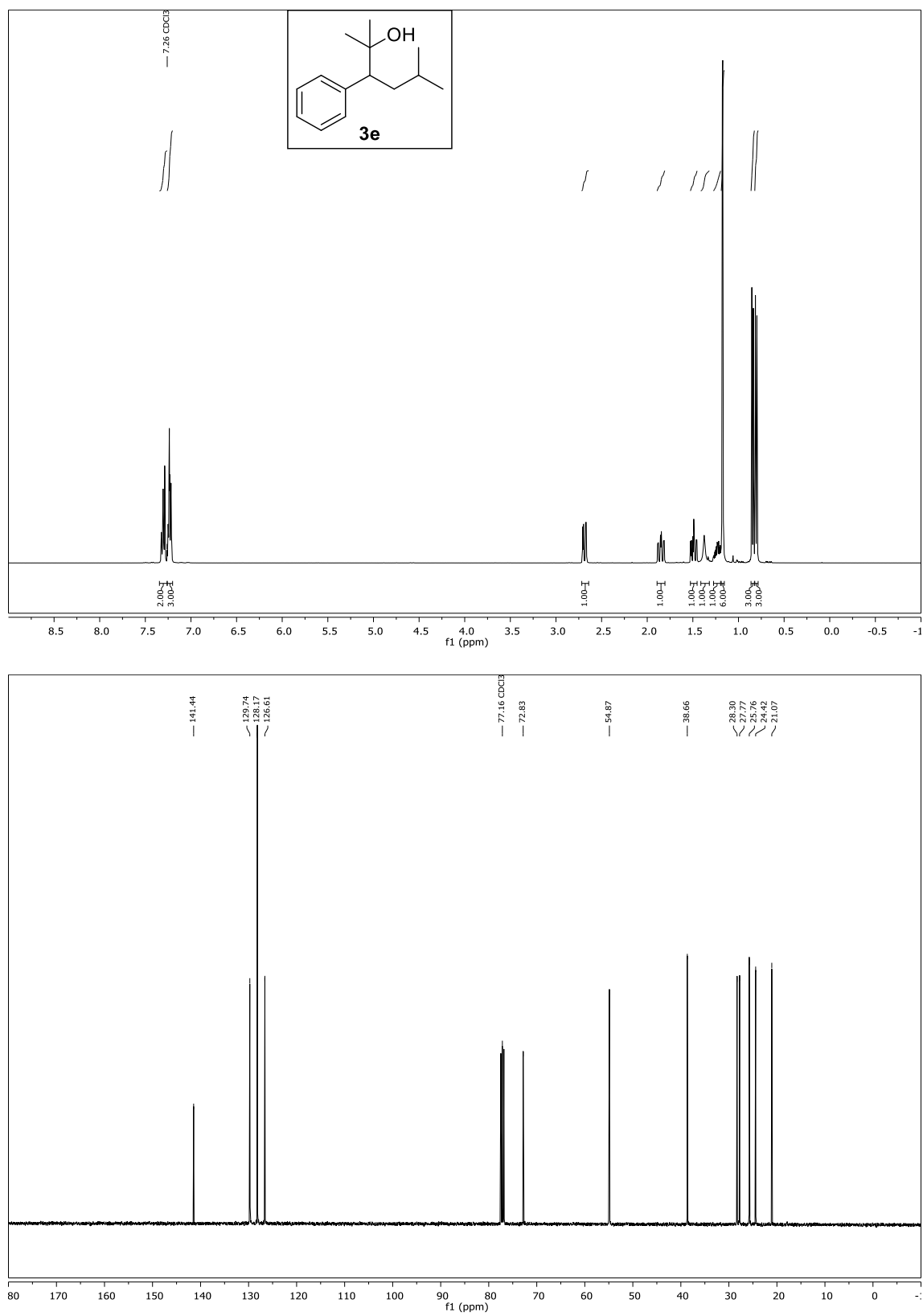
Compound **3a**, ^1H - and ^{13}C -NMR (CDCl_3)



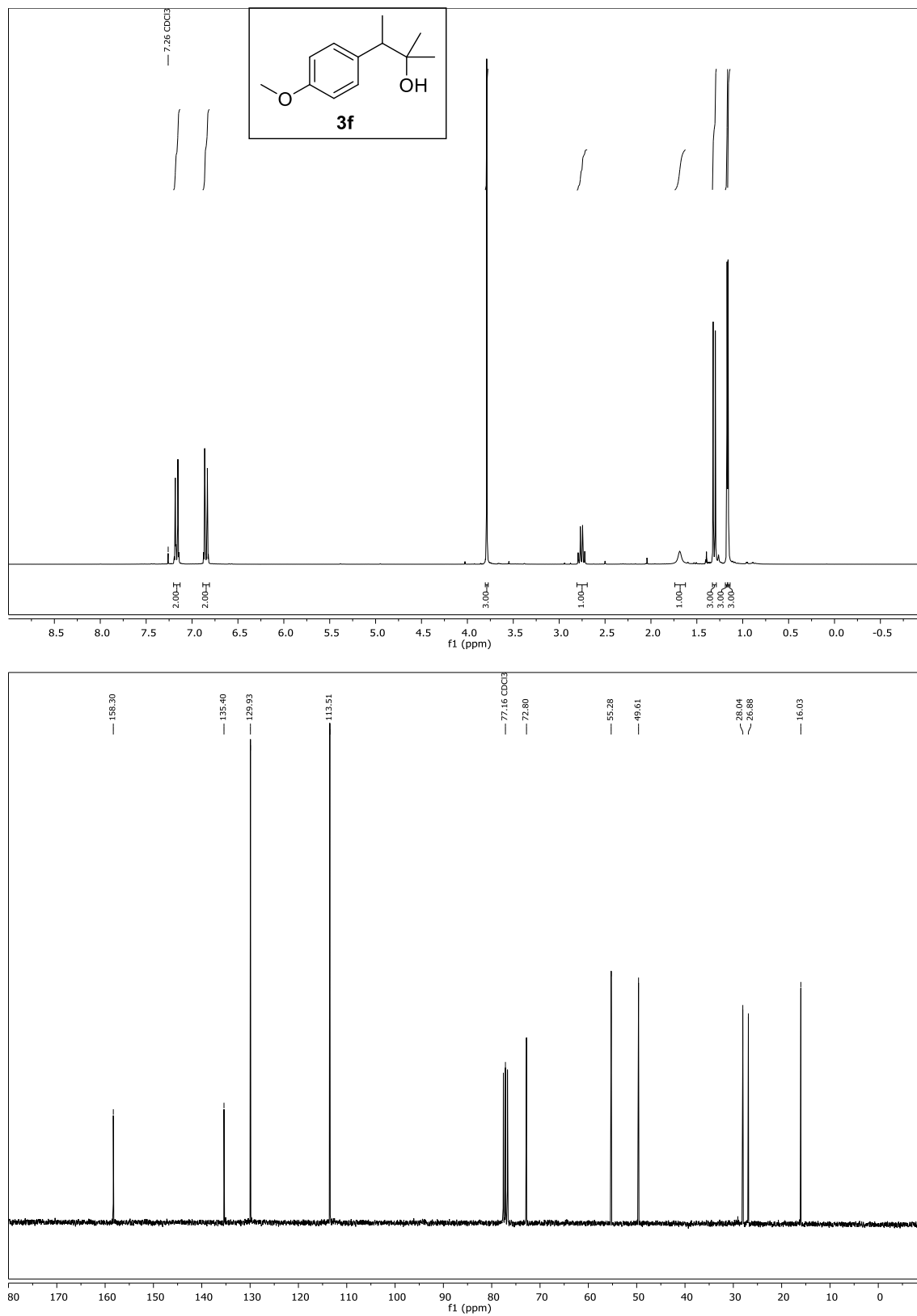
Compound **3b**, ^1H - and ^{13}C -NMR (CDCl_3)



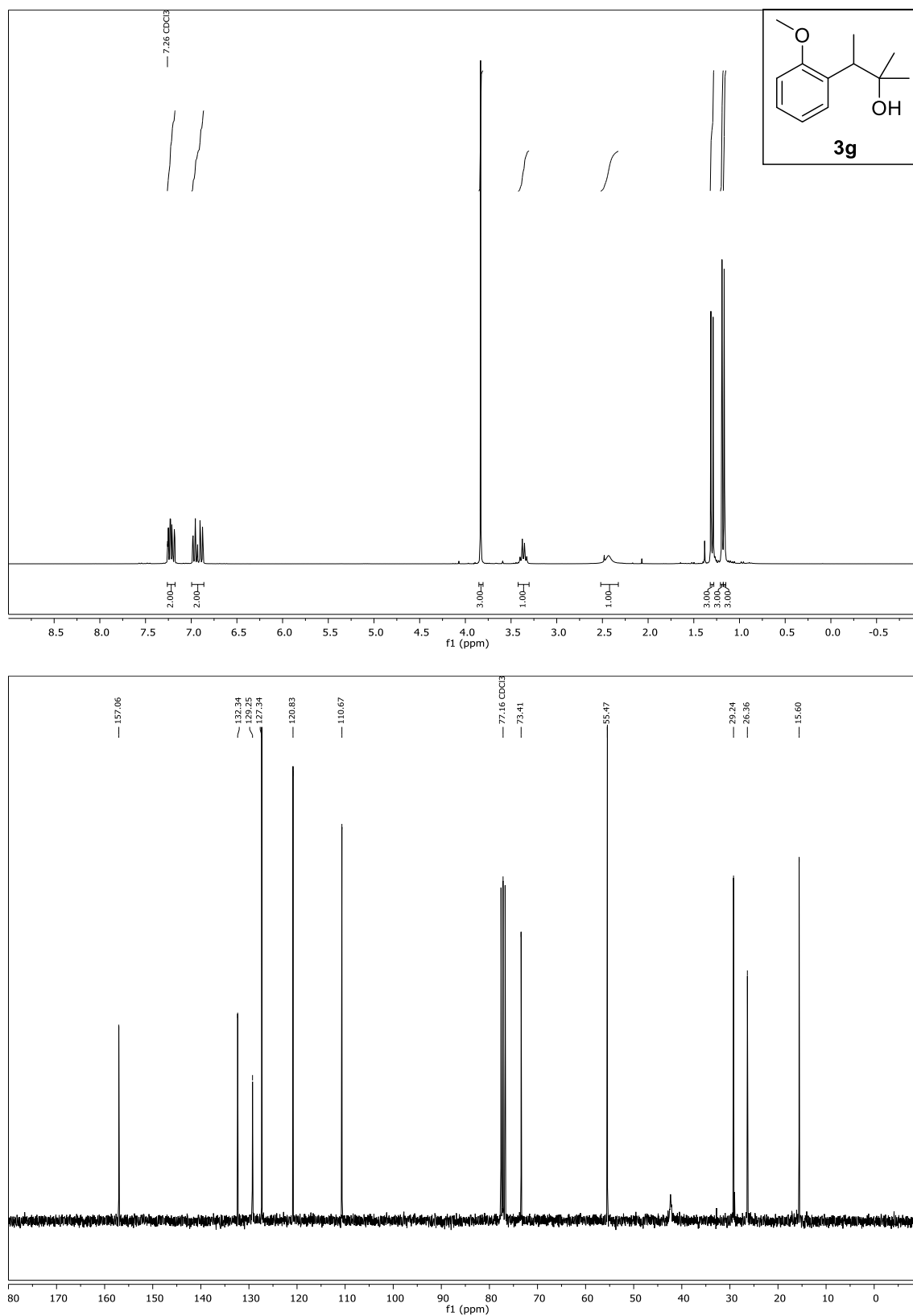
Compound **3c**, ^1H - and ^{13}C -NMR (CDCl_3)

Compound **3e**, ^1H - and ^{13}C -NMR (CDCl_3)

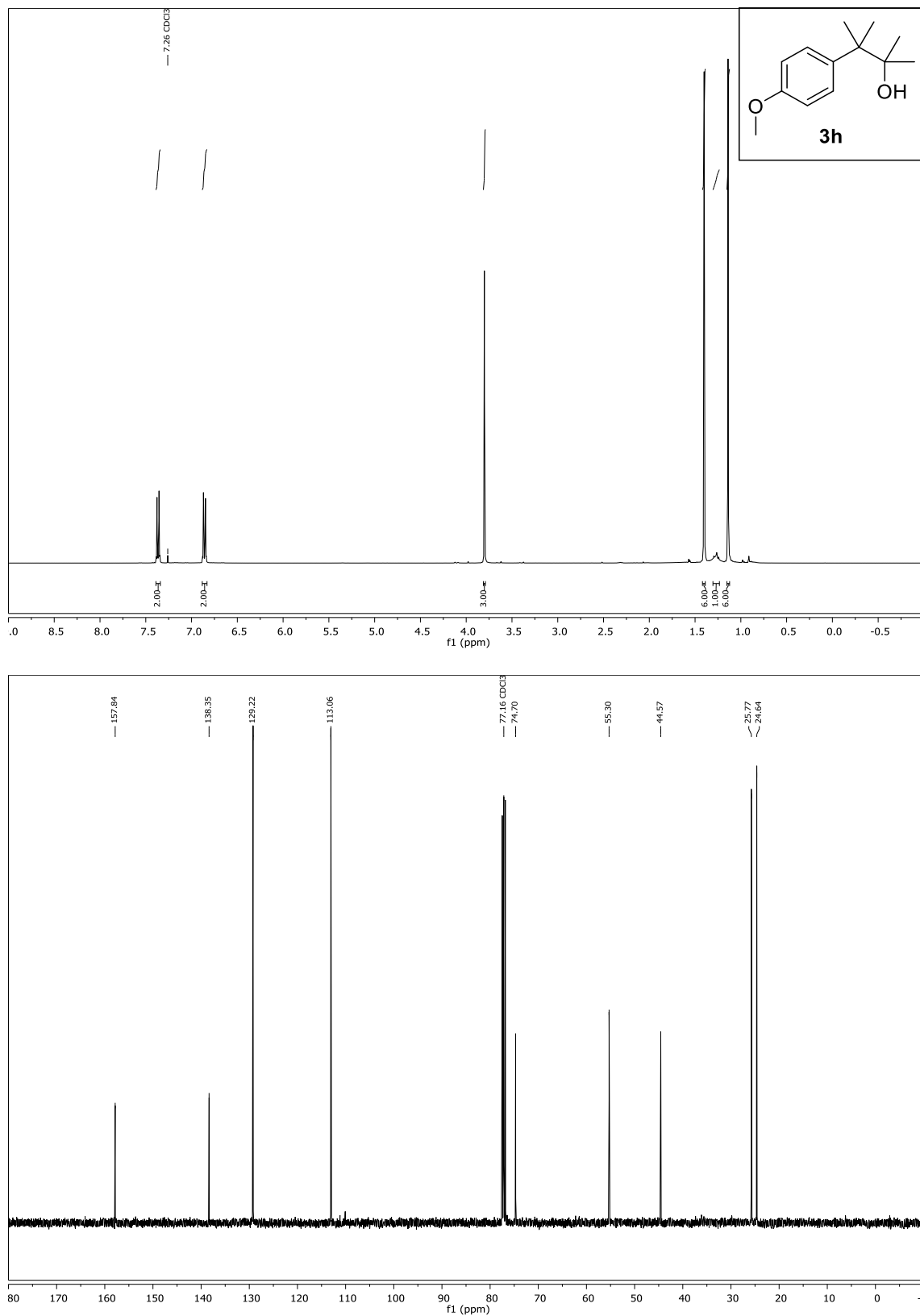
Compound **3f**, ^1H - and ^{13}C -NMR (CDCl_3)

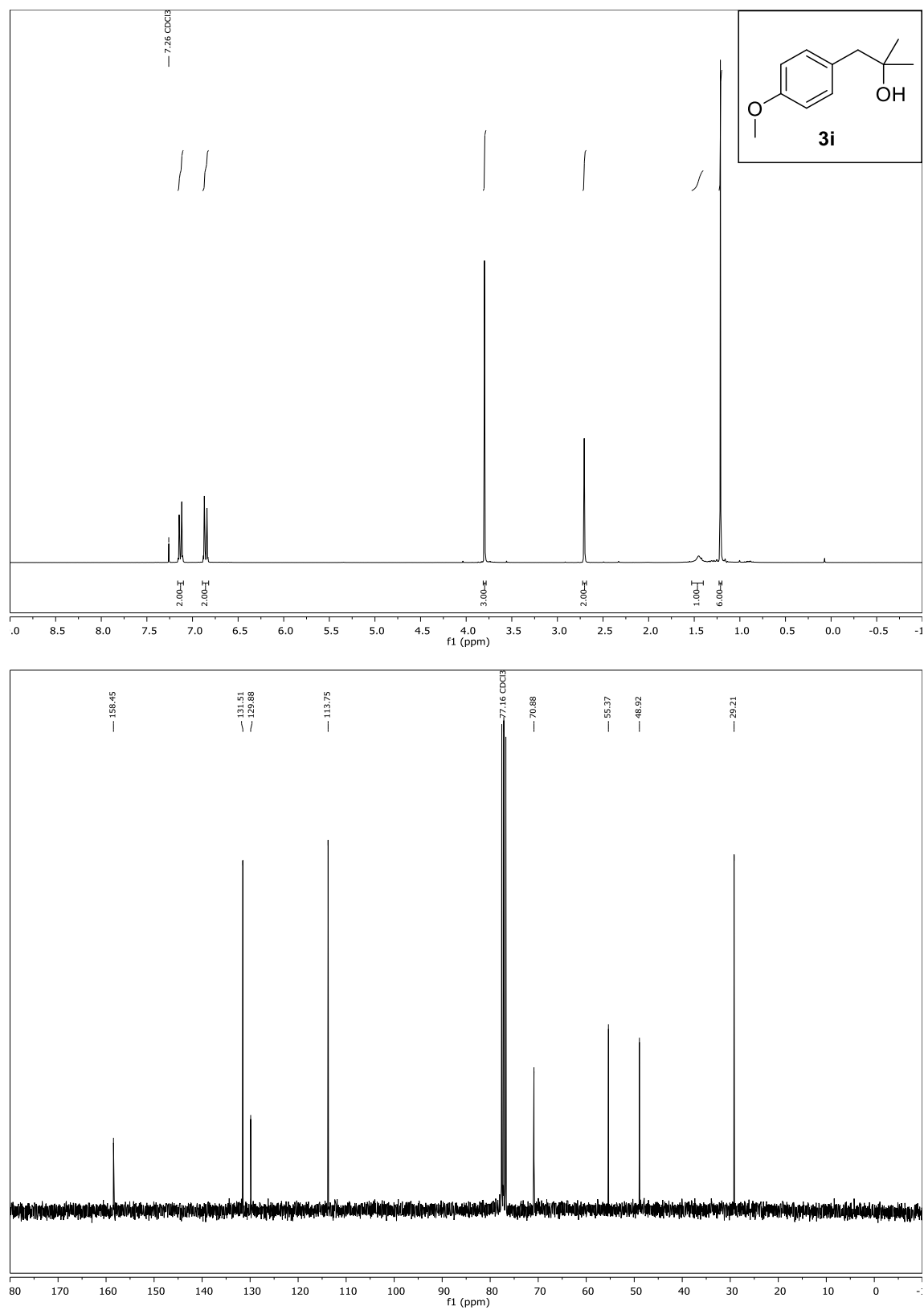


Compound **3g**, ^1H - and ^{13}C -NMR (CDCl_3)

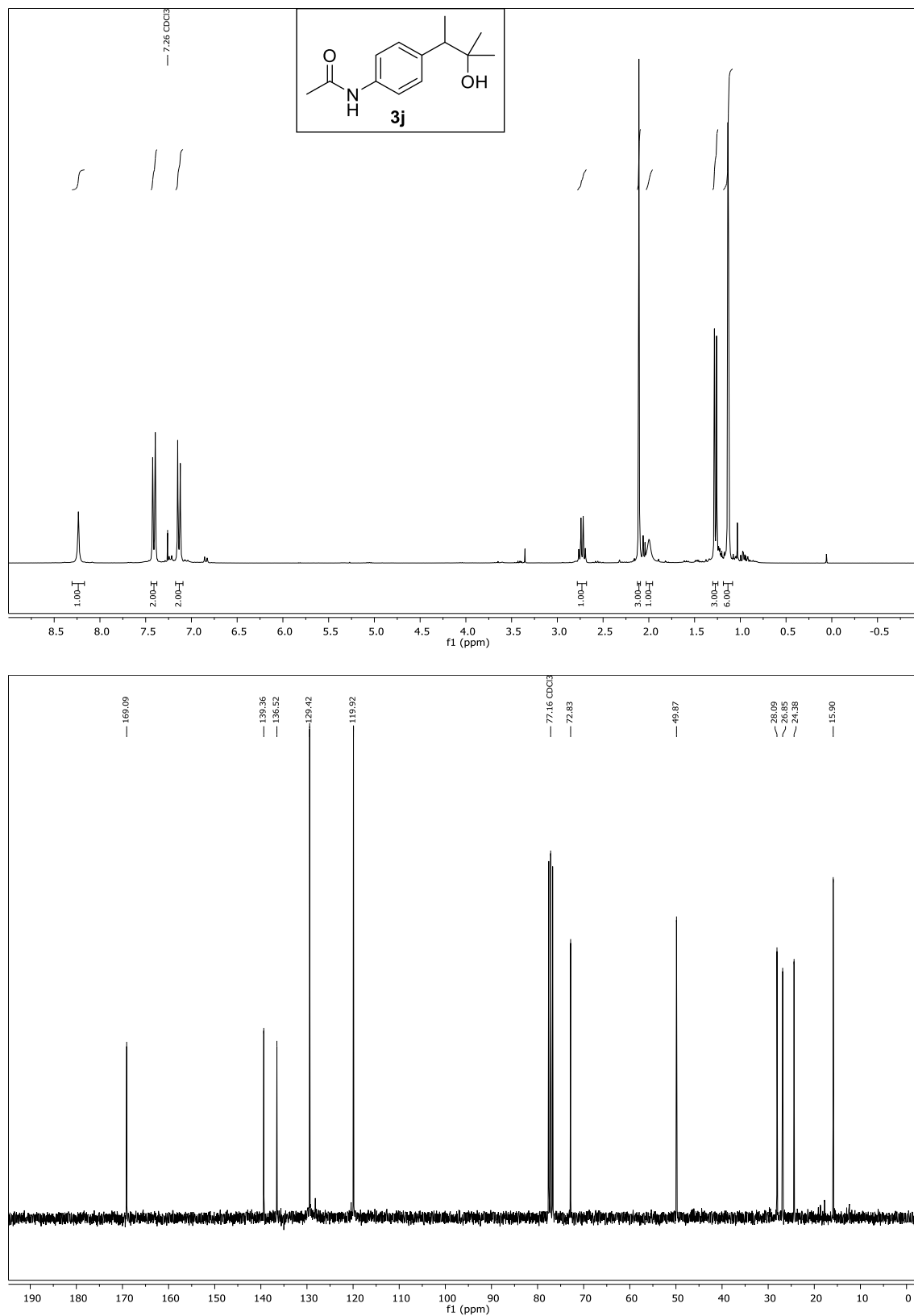


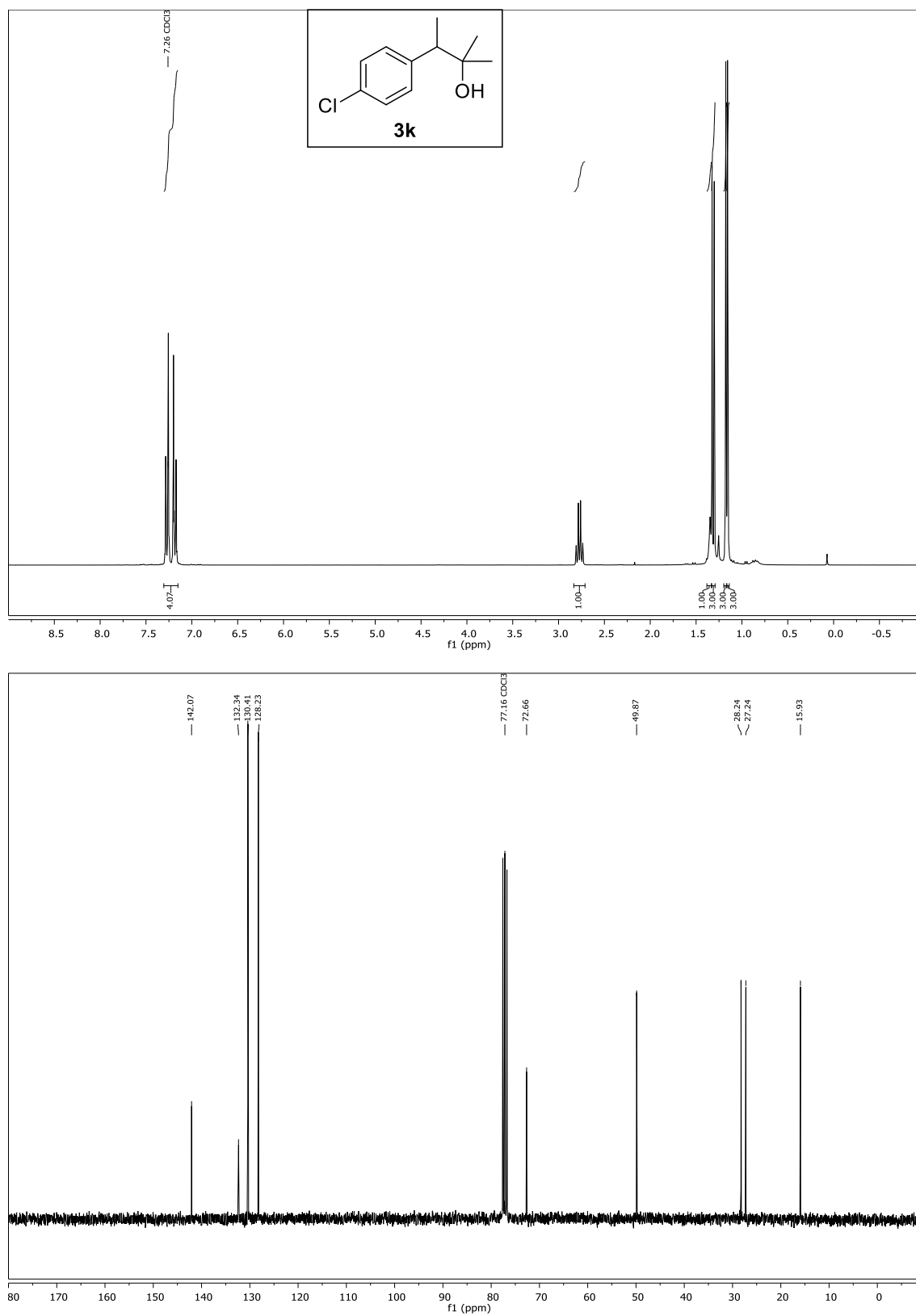
Compound **3h**, ^1H - and ^{13}C -NMR (CDCl_3)



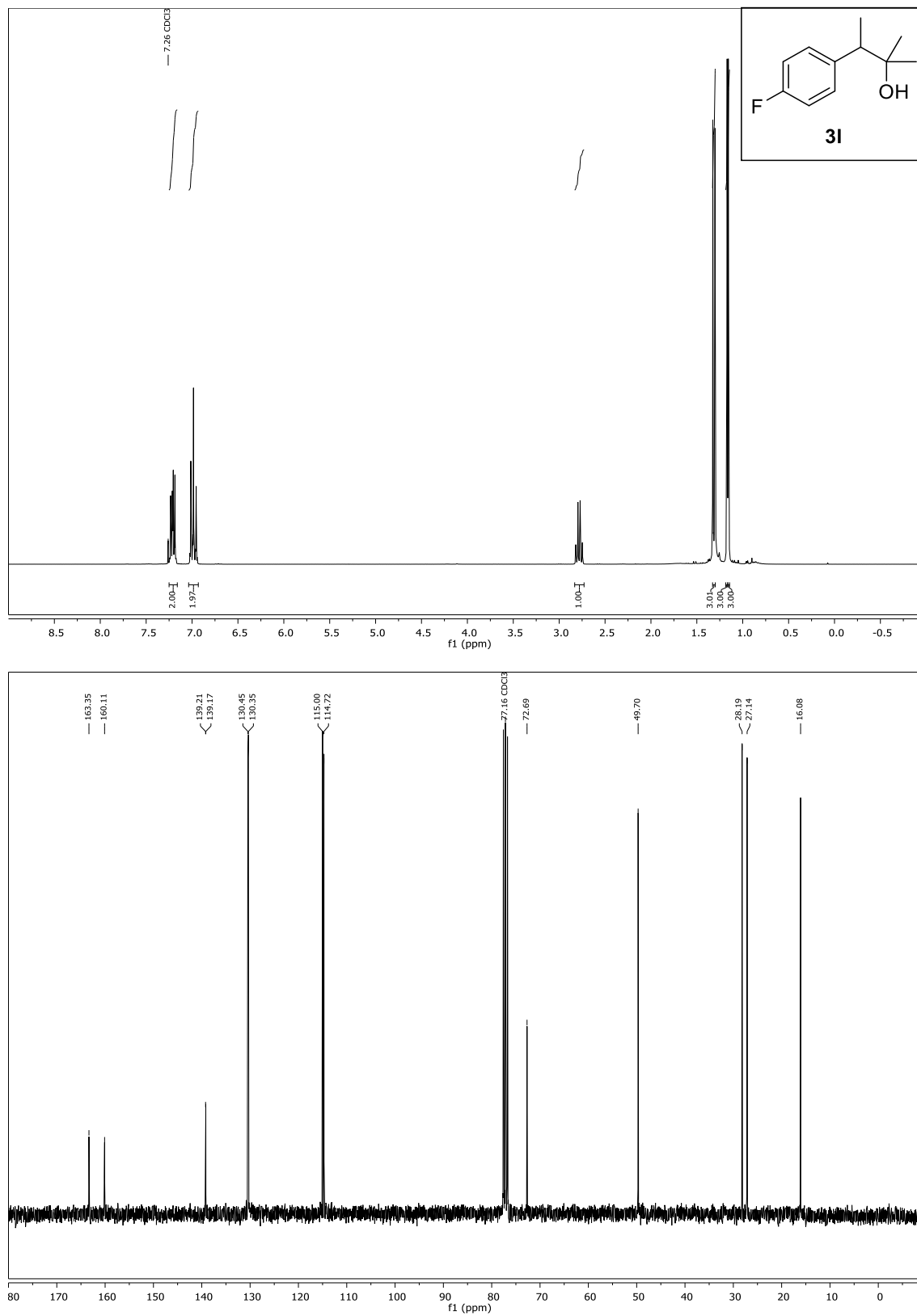
Compound **3i**, ^1H - and ^{13}C -NMR (CDCl_3)

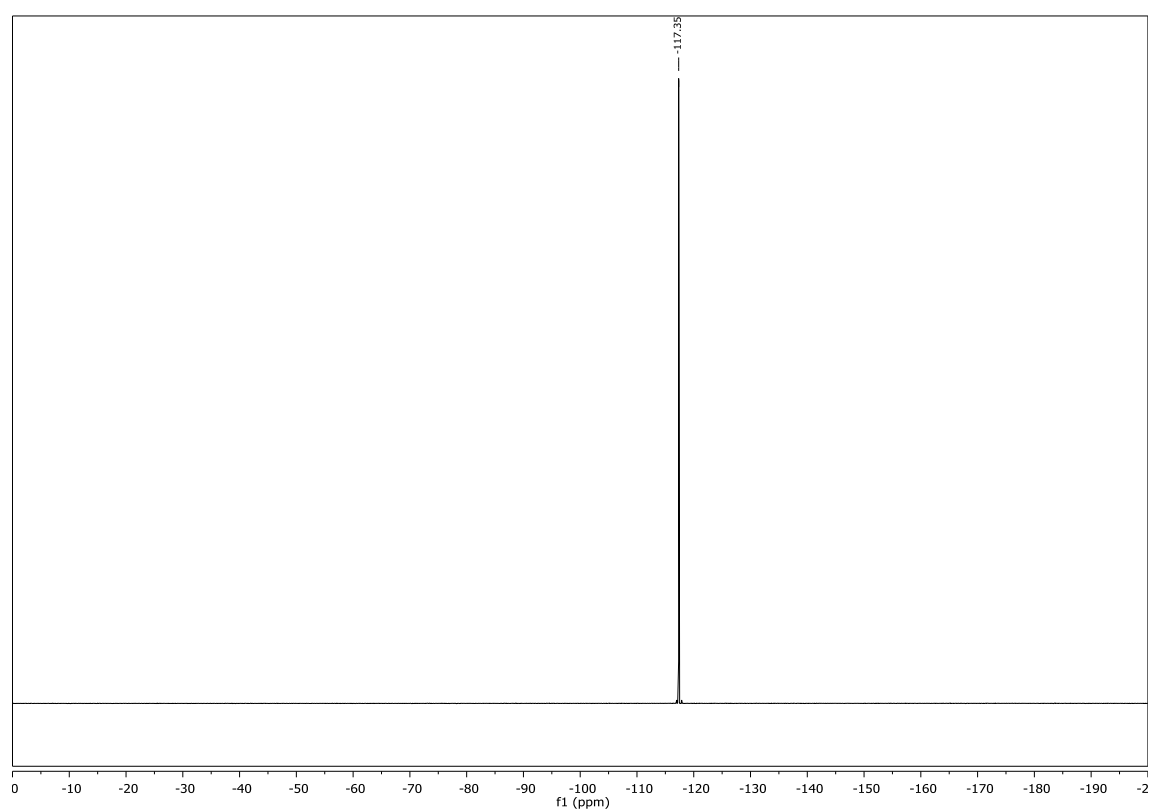
Compound **3j**, ^1H - and ^{13}C -NMR (CDCl_3)



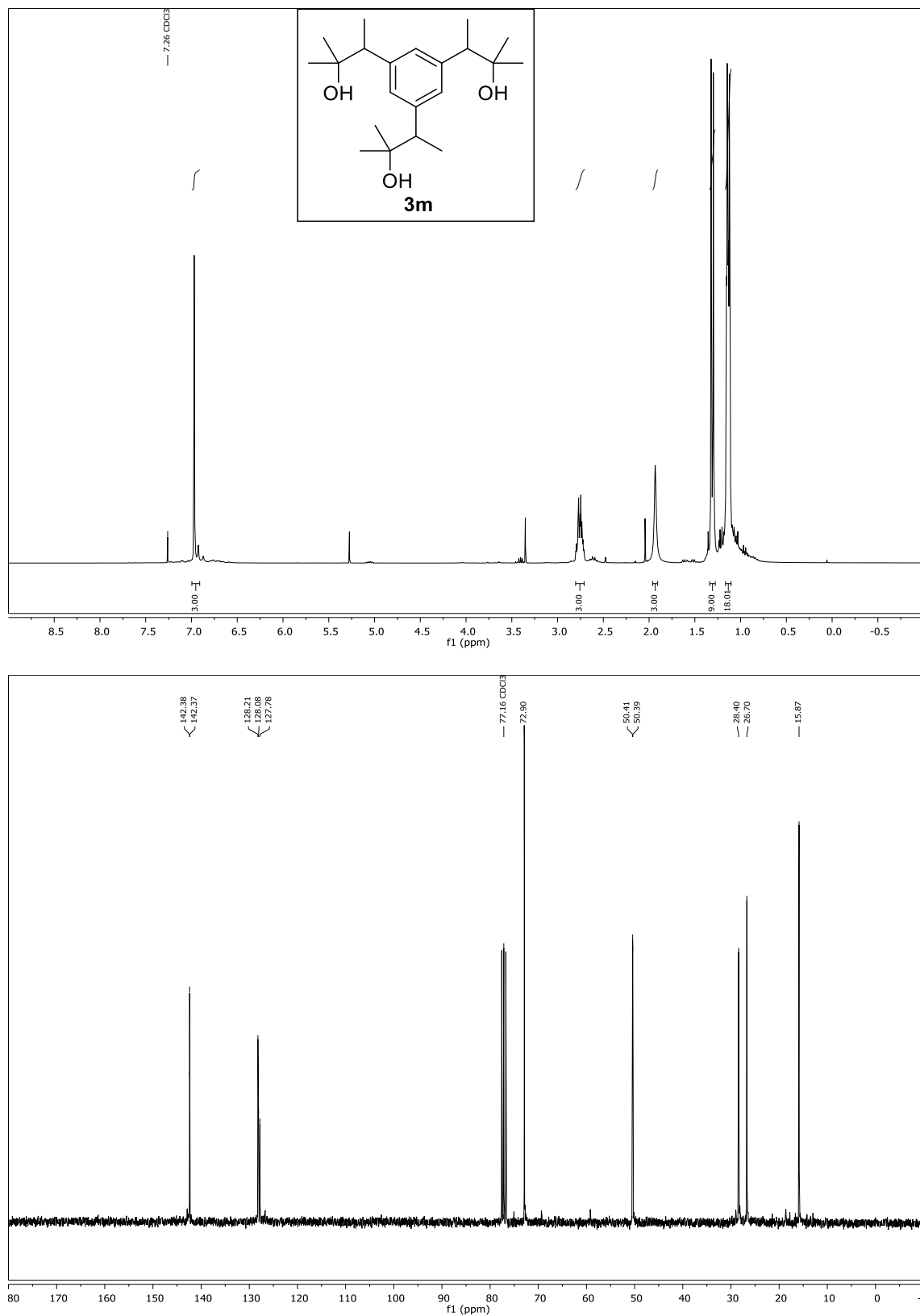
Compound **3k**, ^1H - and ^{13}C -NMR (CDCl_3)

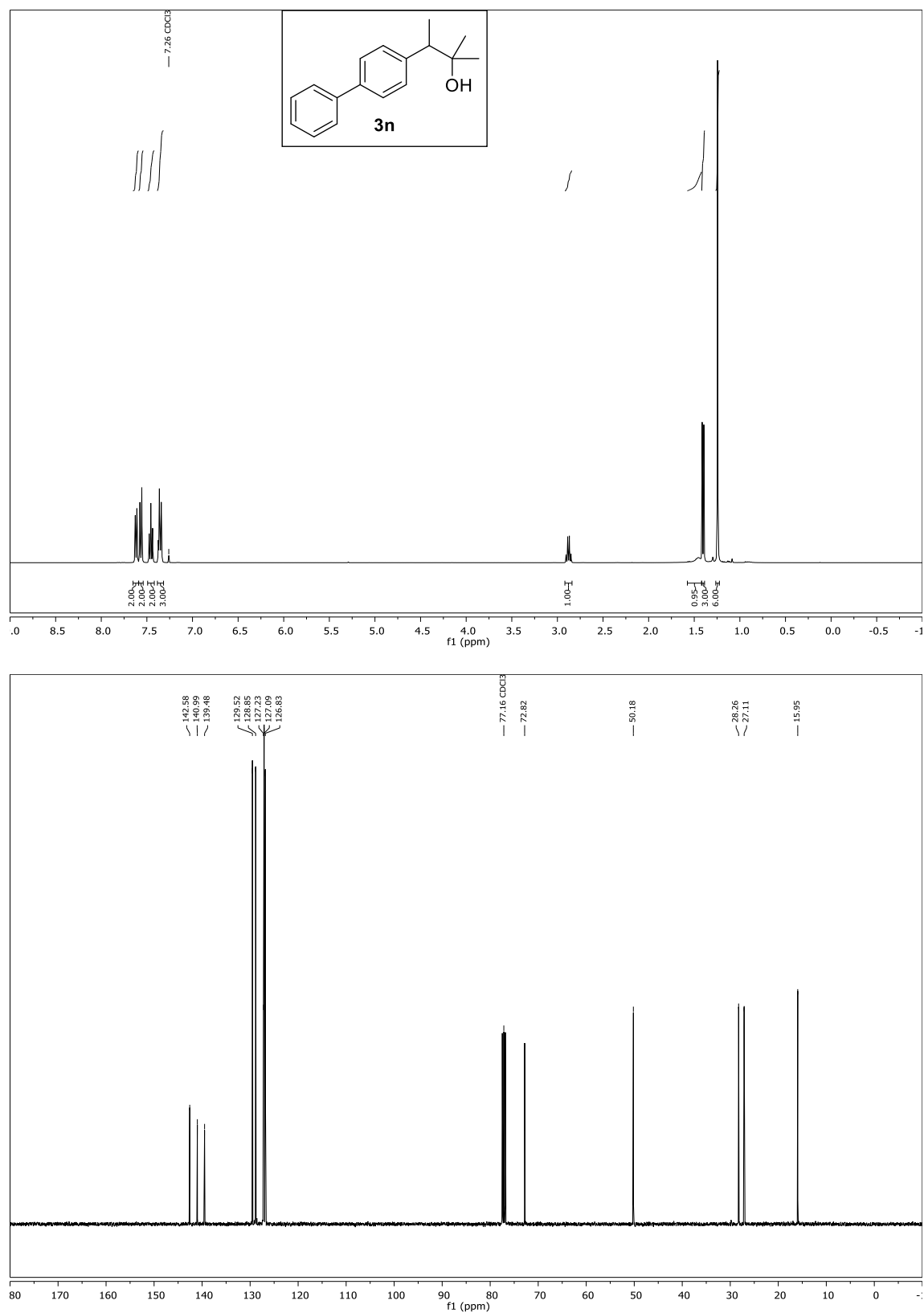
Compound **3l**, ^1H -, ^{13}C - and ^{19}F -NMR (CDCl_3)



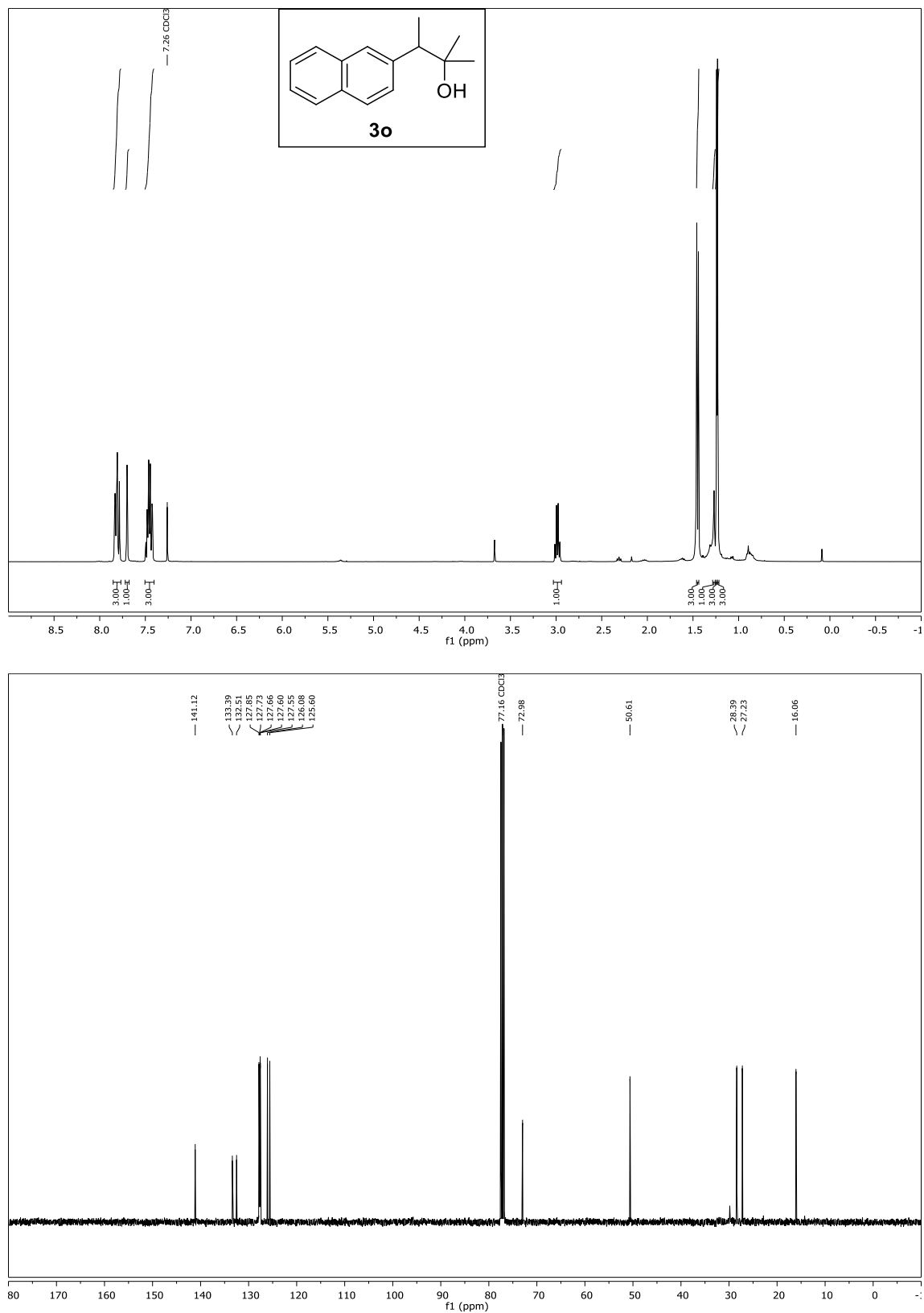


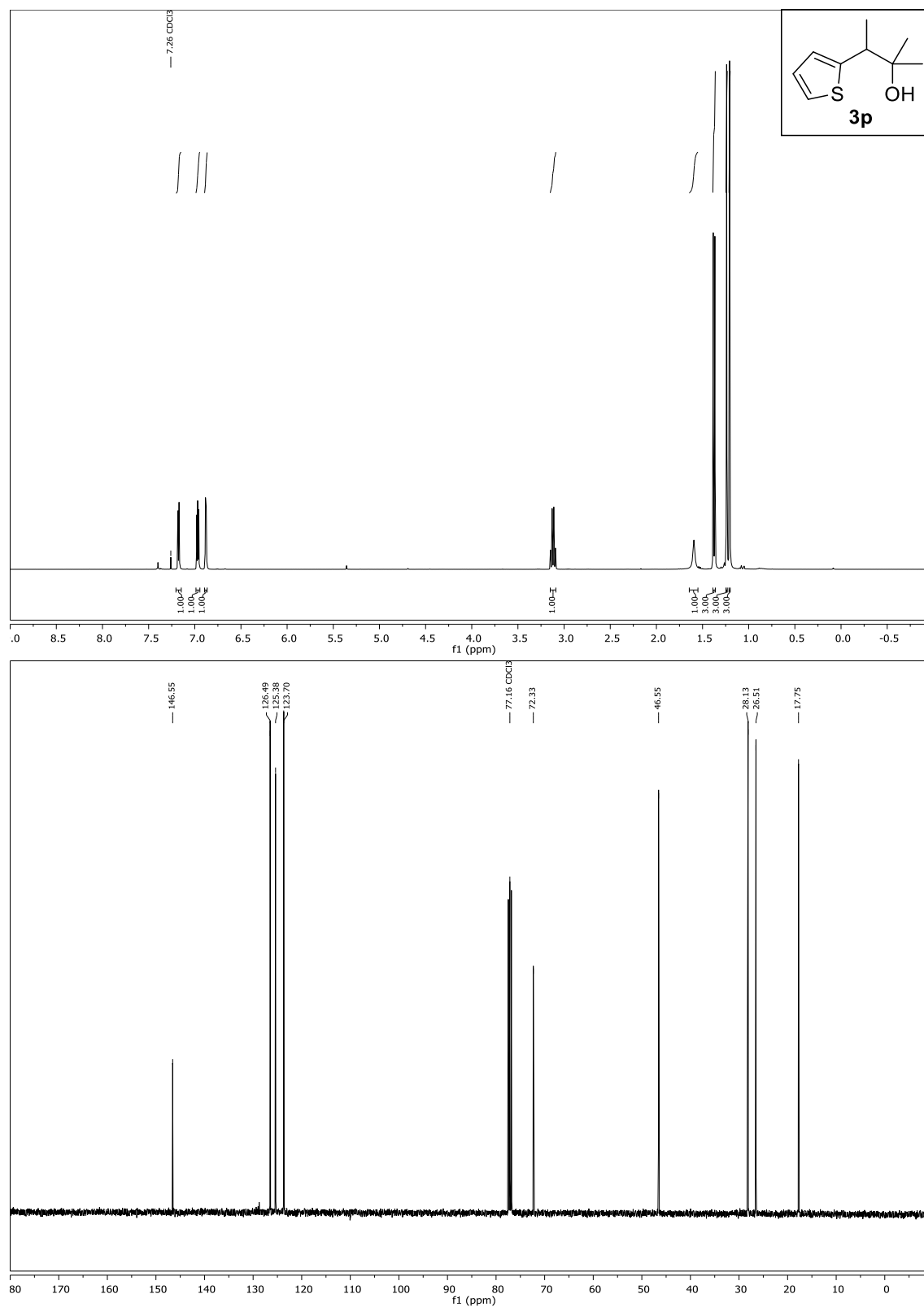
Compound **3m**, ^1H - and ^{13}C -NMR (CDCl_3)



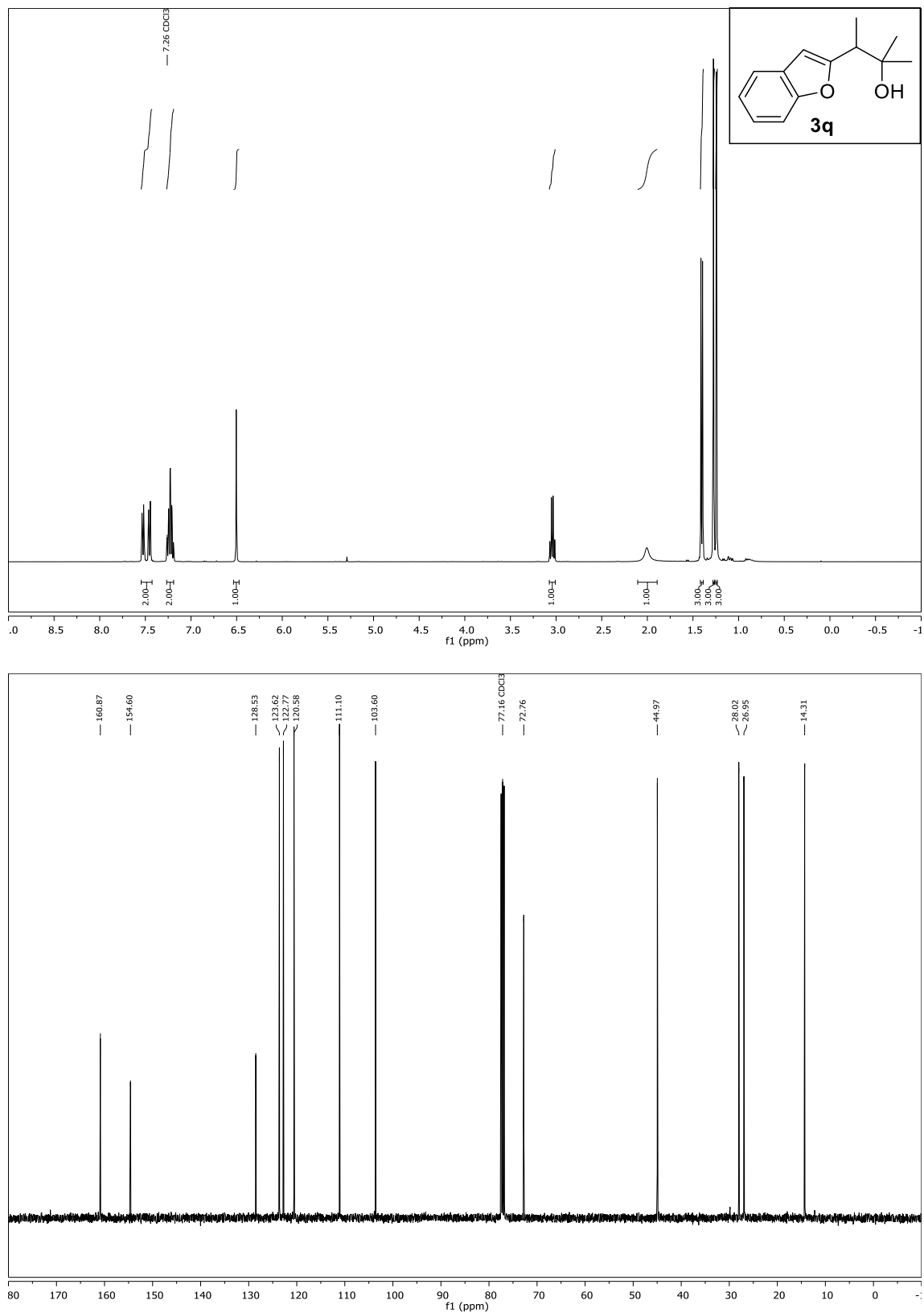
Compound **3n**, ^1H - and ^{13}C -NMR (CDCl_3)

Compound **3o**, ^1H - and ^{13}C -NMR (CDCl_3)

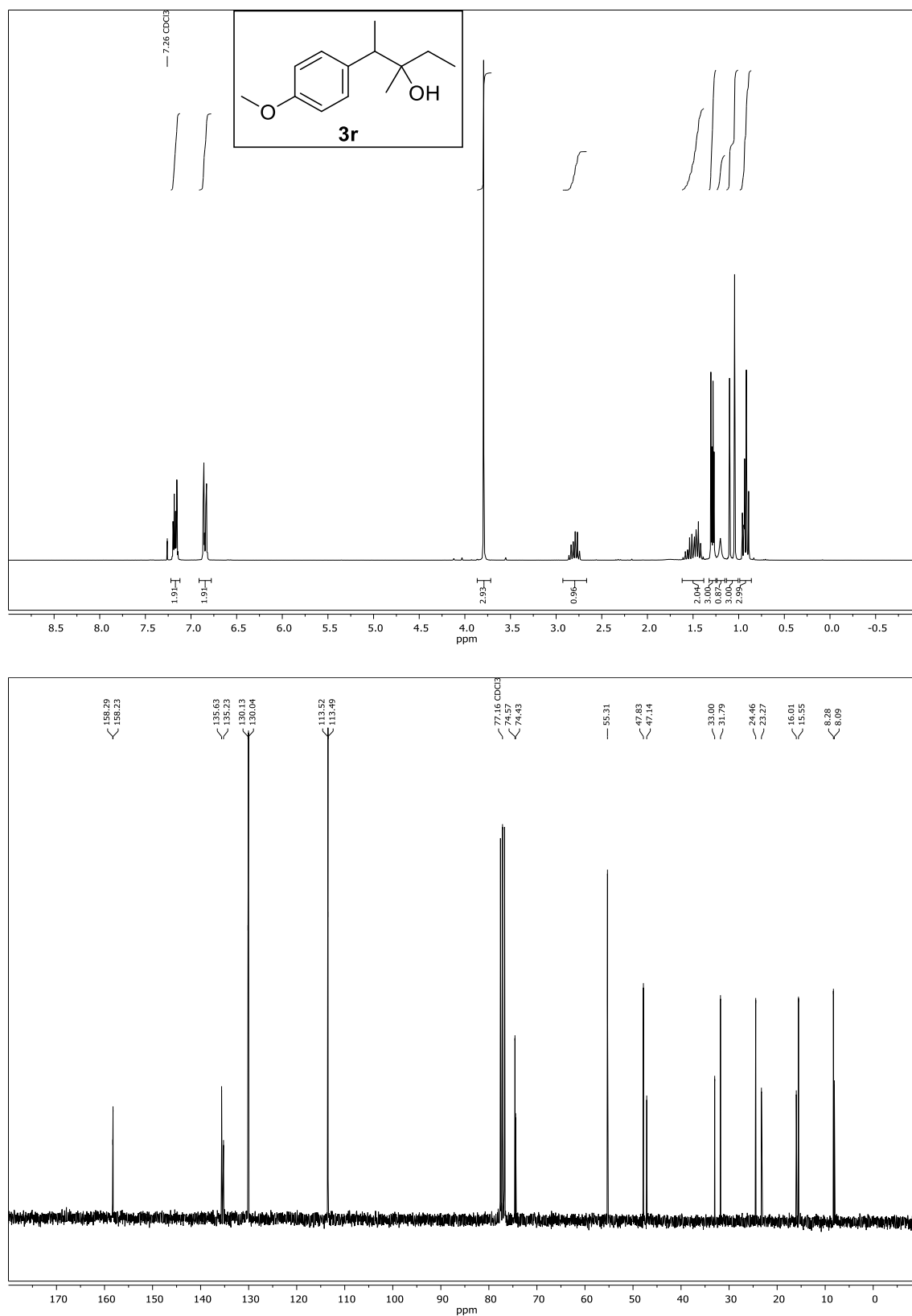


Compound **3p**, ^1H - and ^{13}C -NMR (CDCl_3)

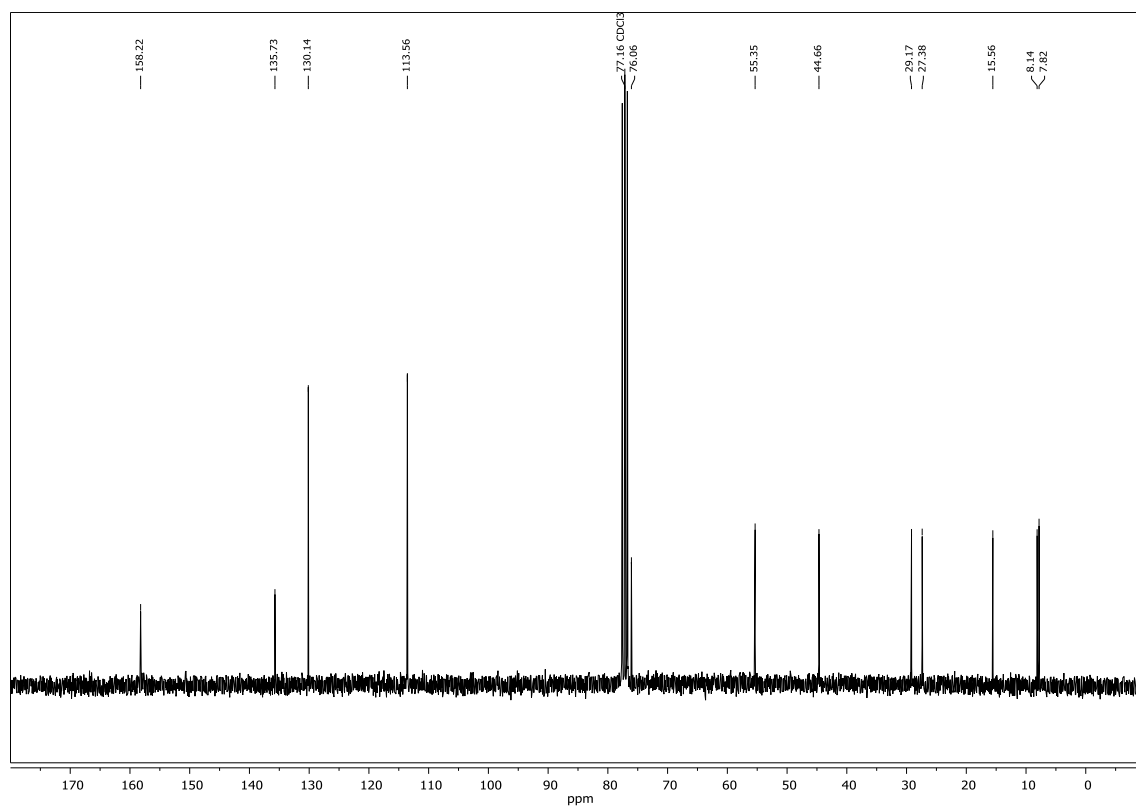
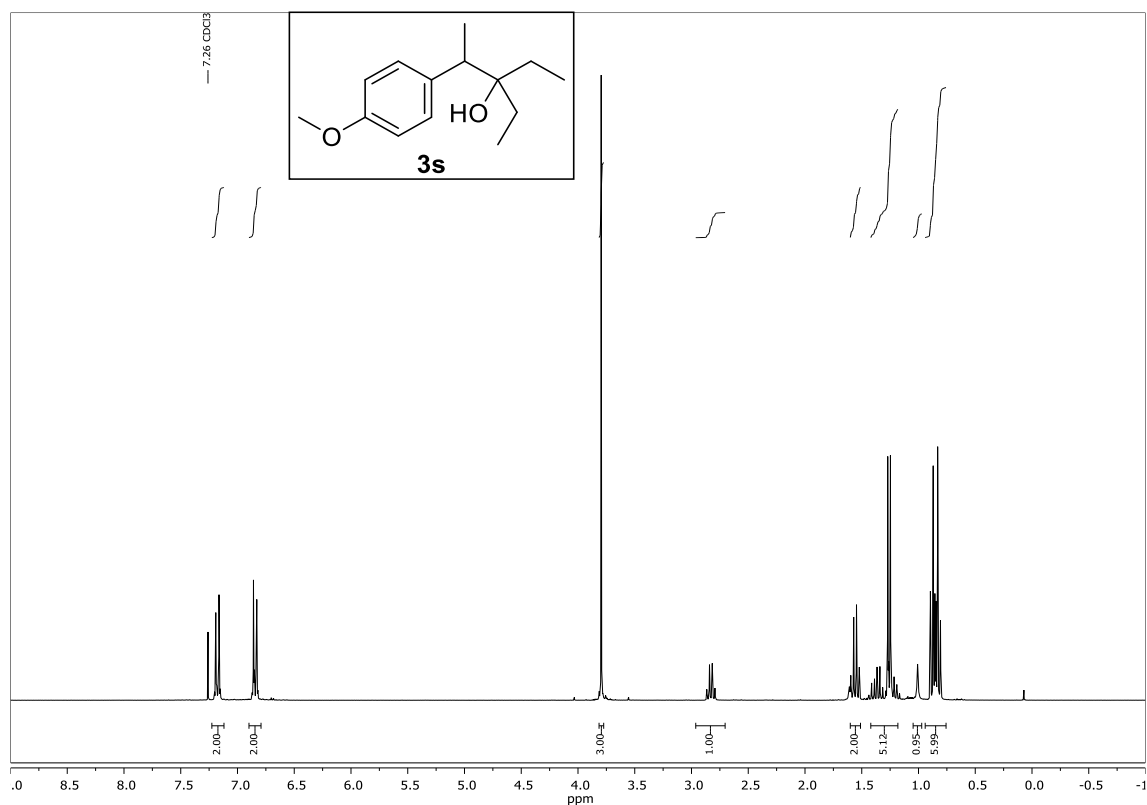
Compound **3q**, ^1H - and ^{13}C -NMR (CDCl_3)



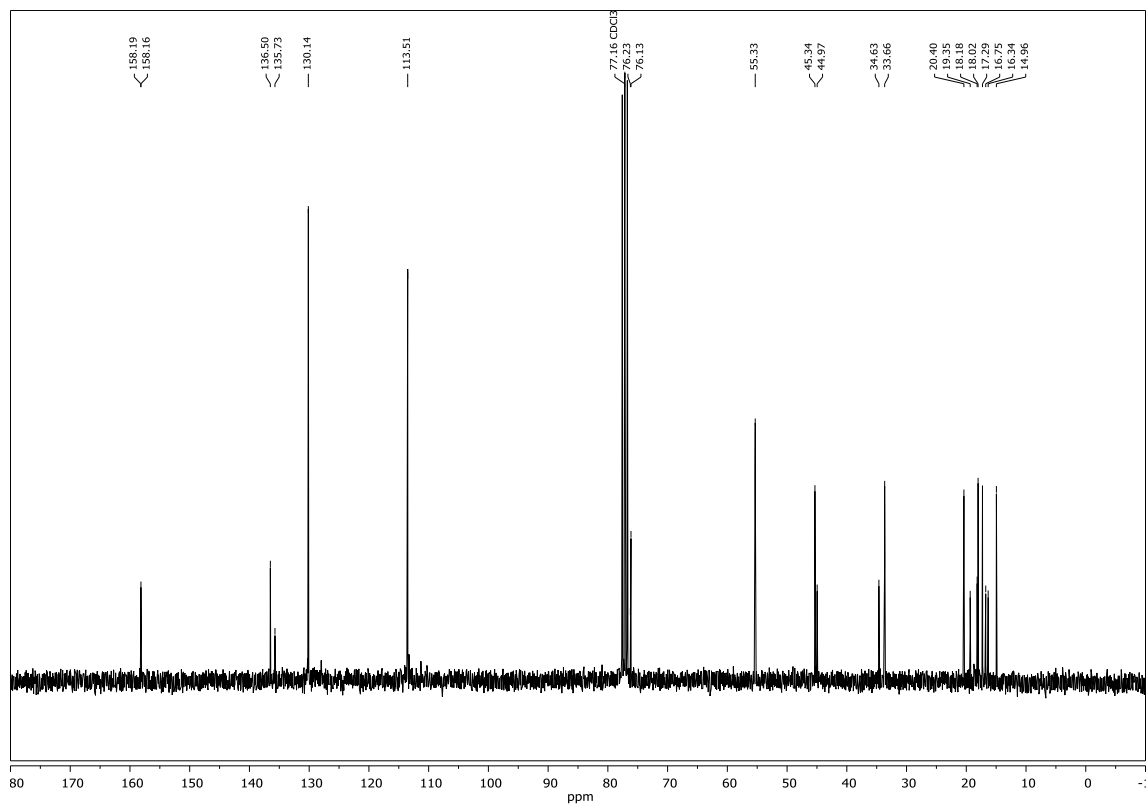
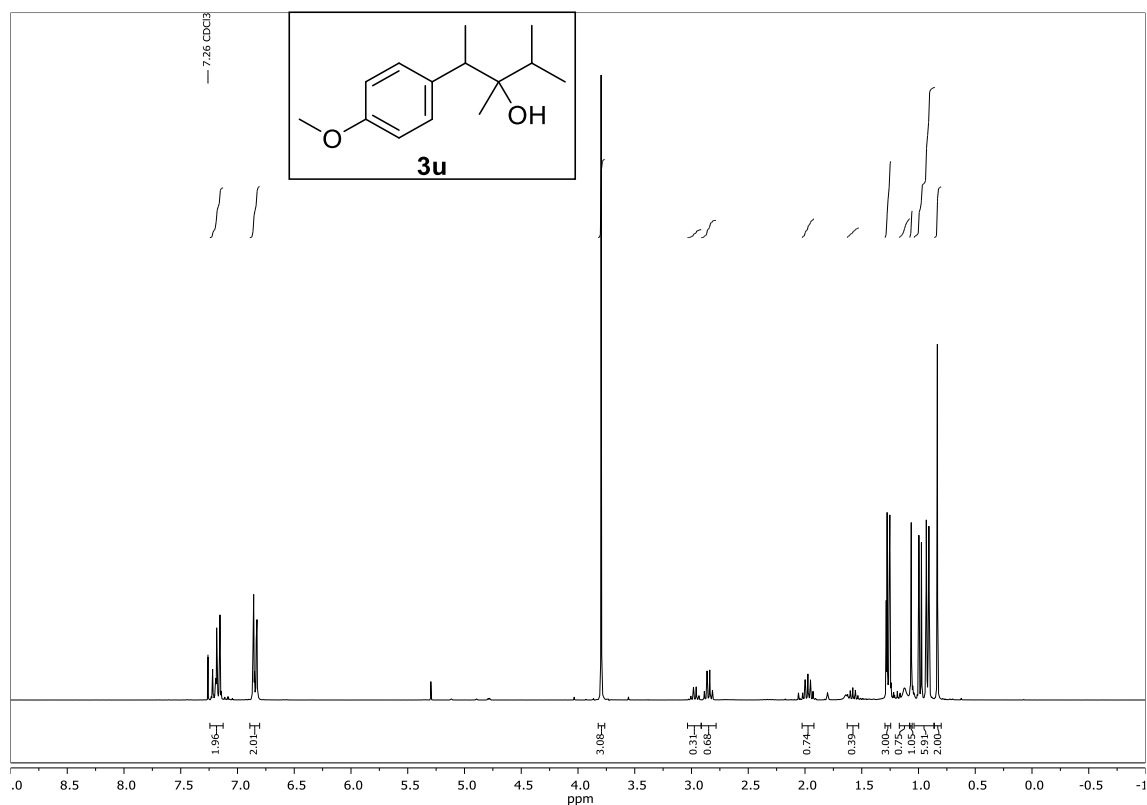
Compound **3r**, ^1H NMR and ^{13}C NMR (CDCl_3):



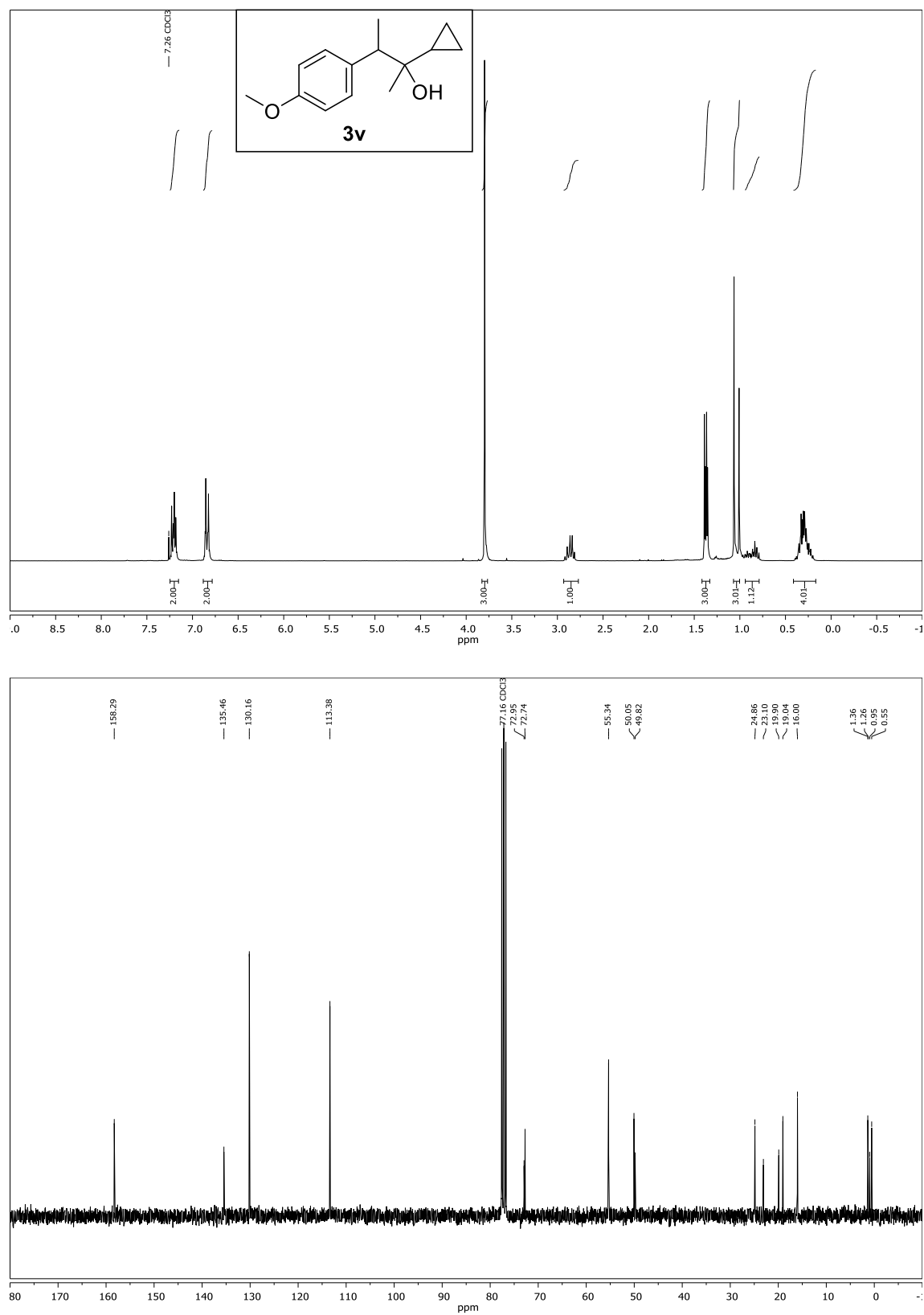
Compound **3s**, ^1H NMR and ^{13}C NMR (CDCl_3):



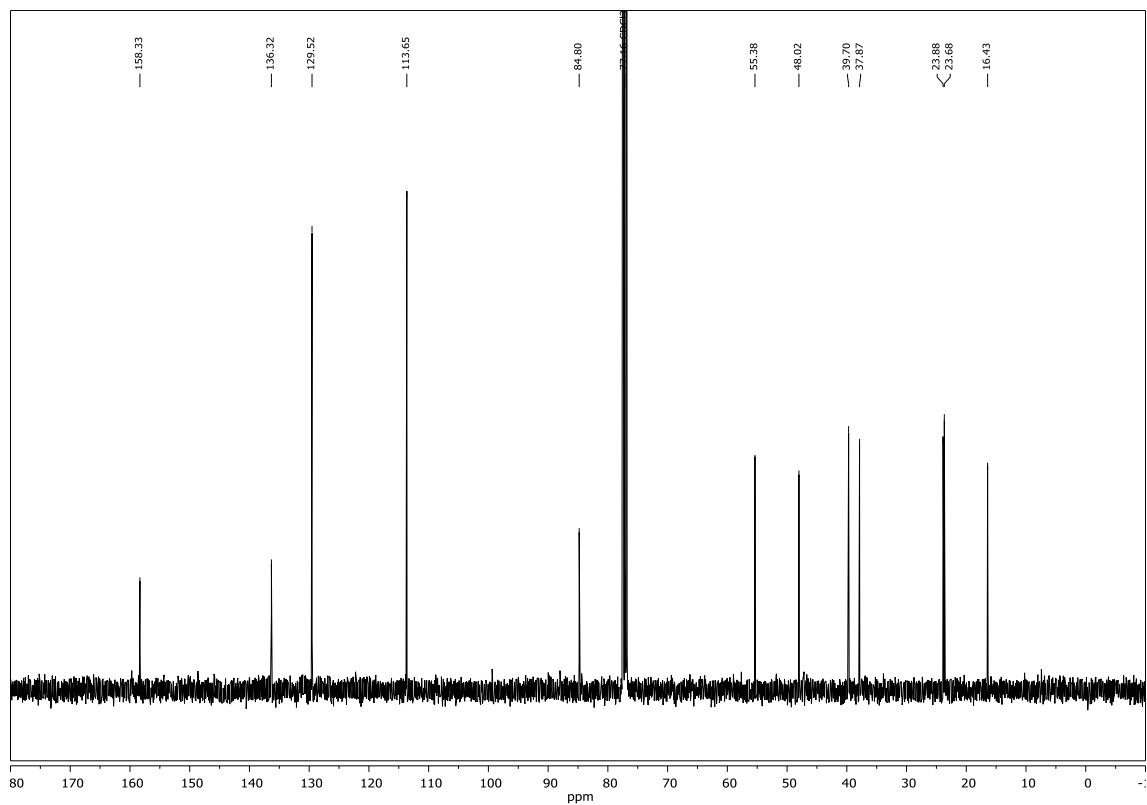
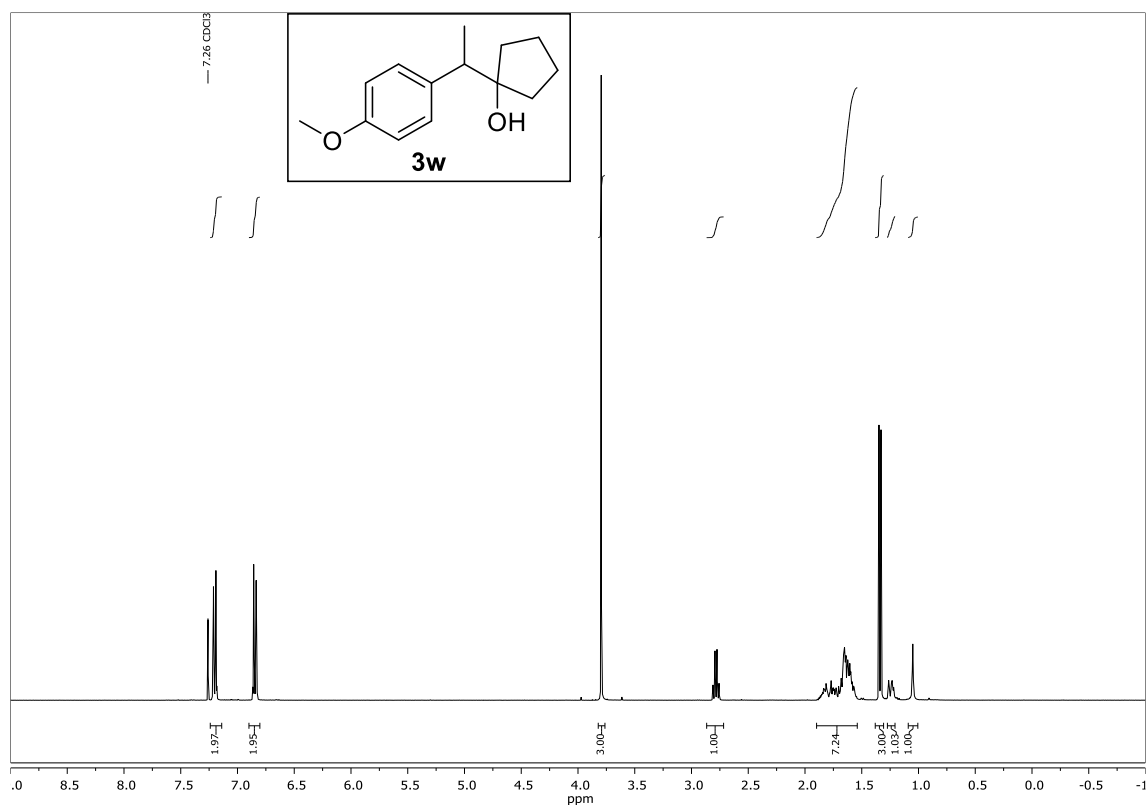
Compound **3u**, ^1H NMR and ^{13}C NMR (CDCl_3):



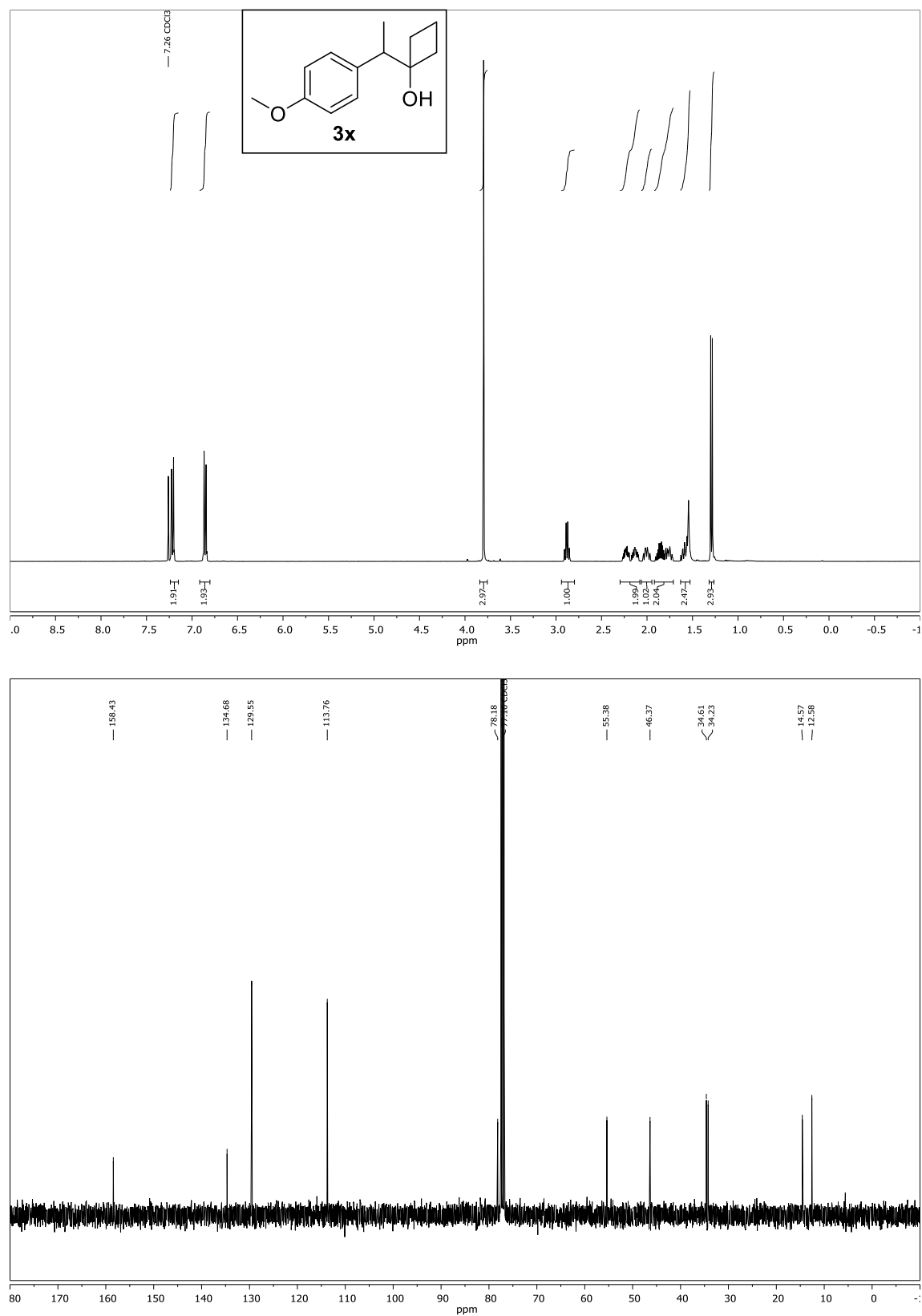
Compound **3v**, ^1H NMR and ^{13}C NMR (CDCl_3):



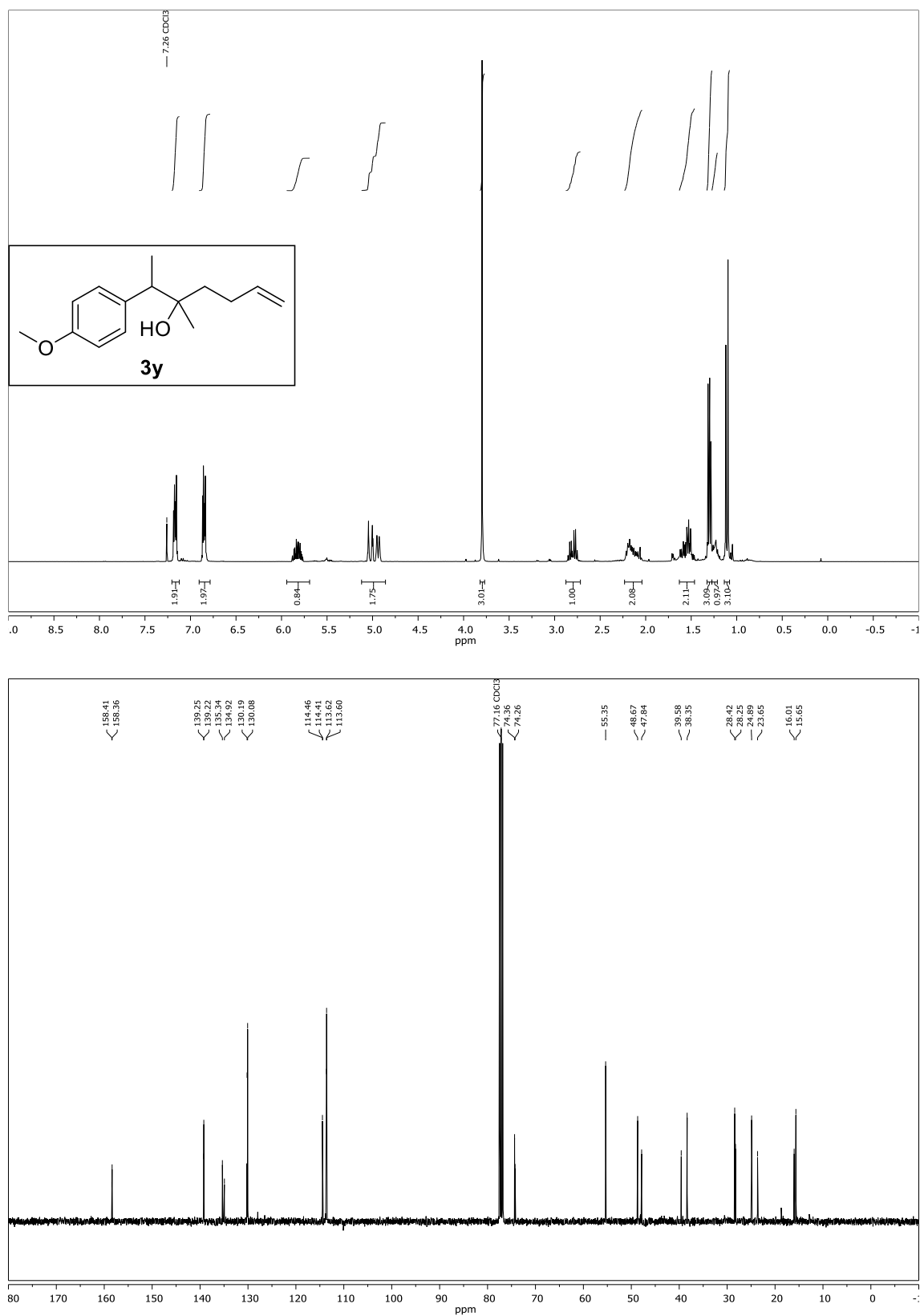
Compound **3w**, ^1H NMR and ^{13}C NMR (CDCl_3):



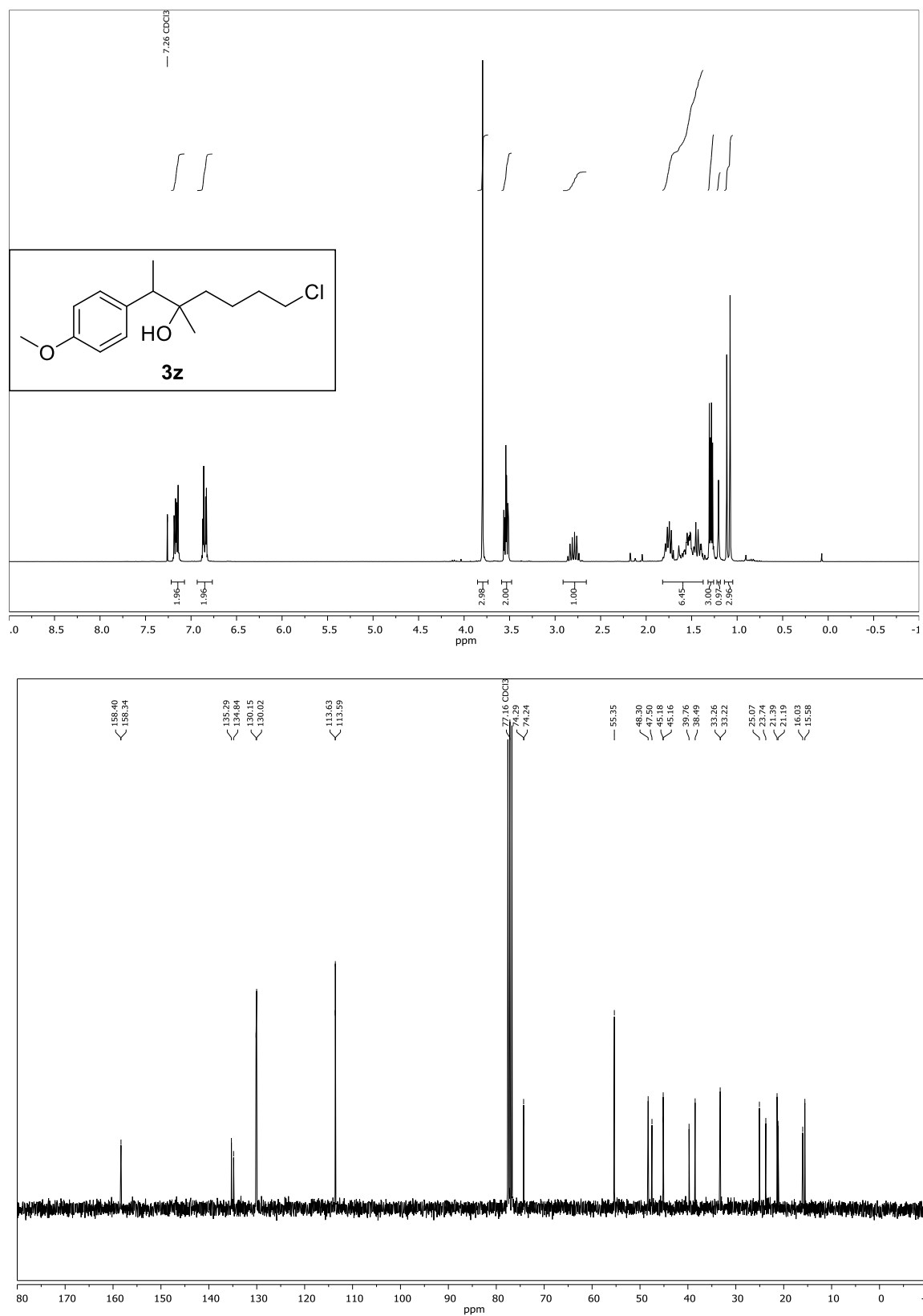
Compound **3x**, ^1H NMR and ^{13}C NMR (CDCl_3):



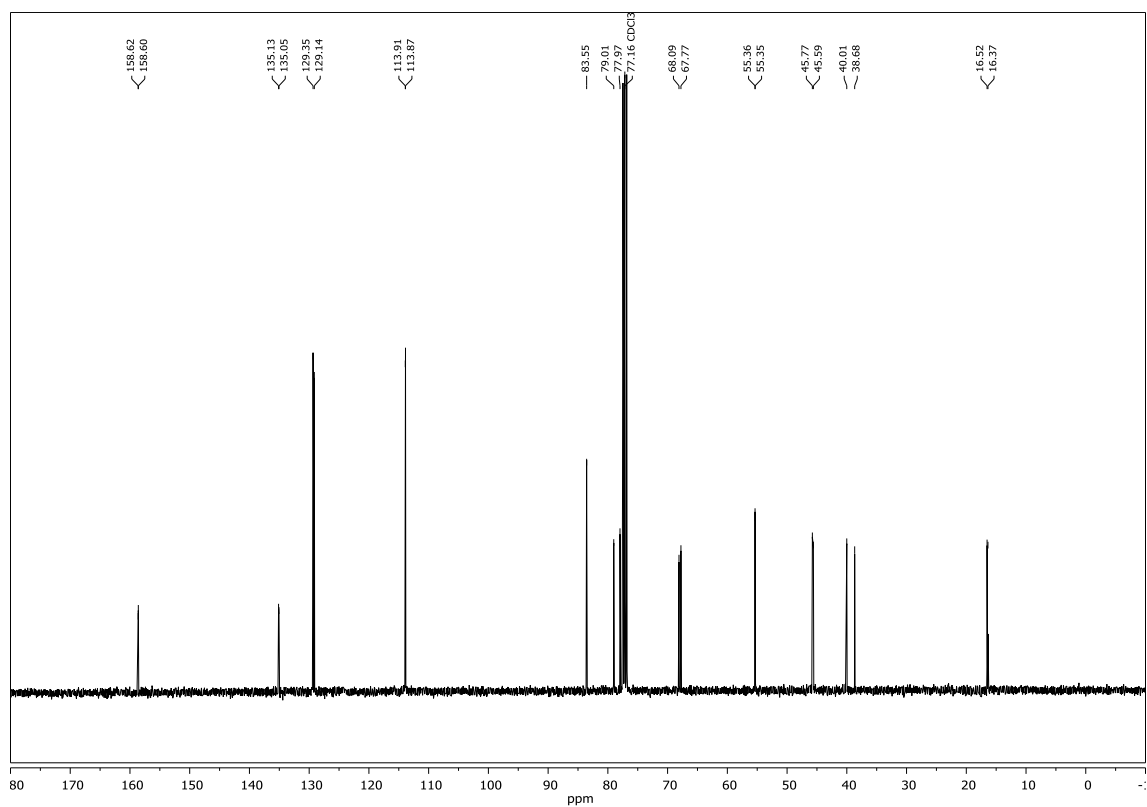
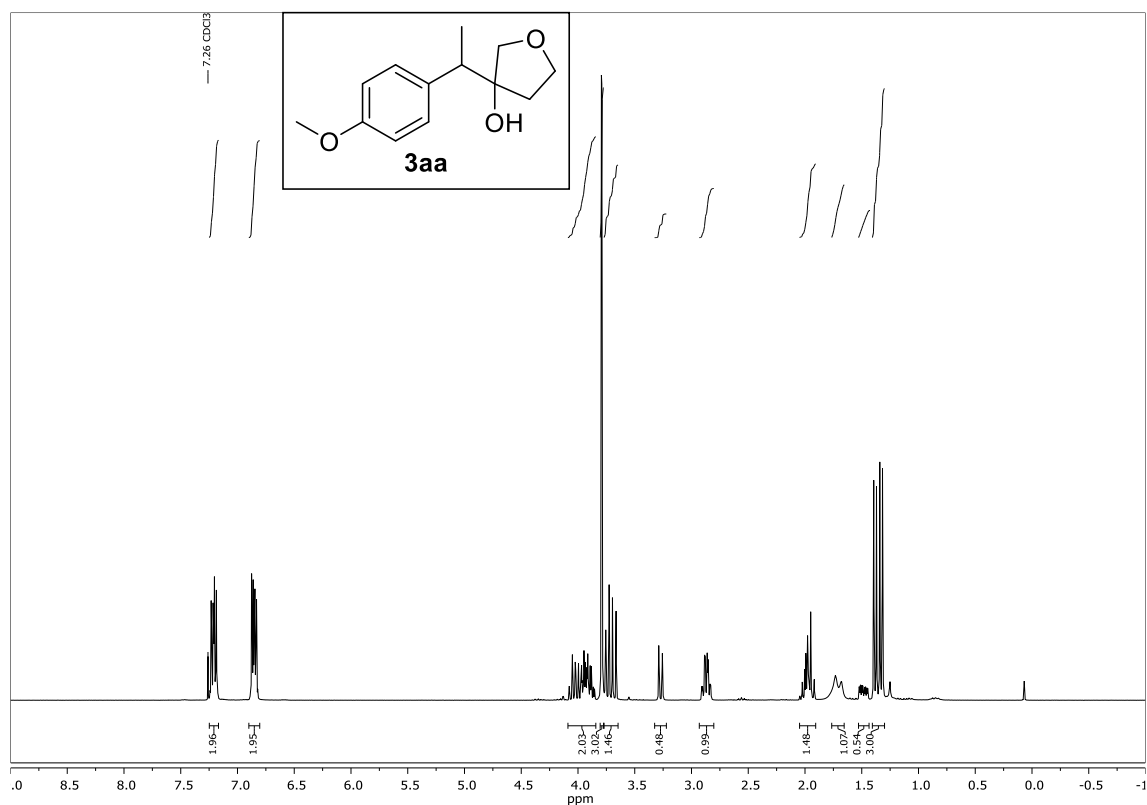
Compound **3y**, ^1H NMR and ^{13}C NMR (CDCl_3):



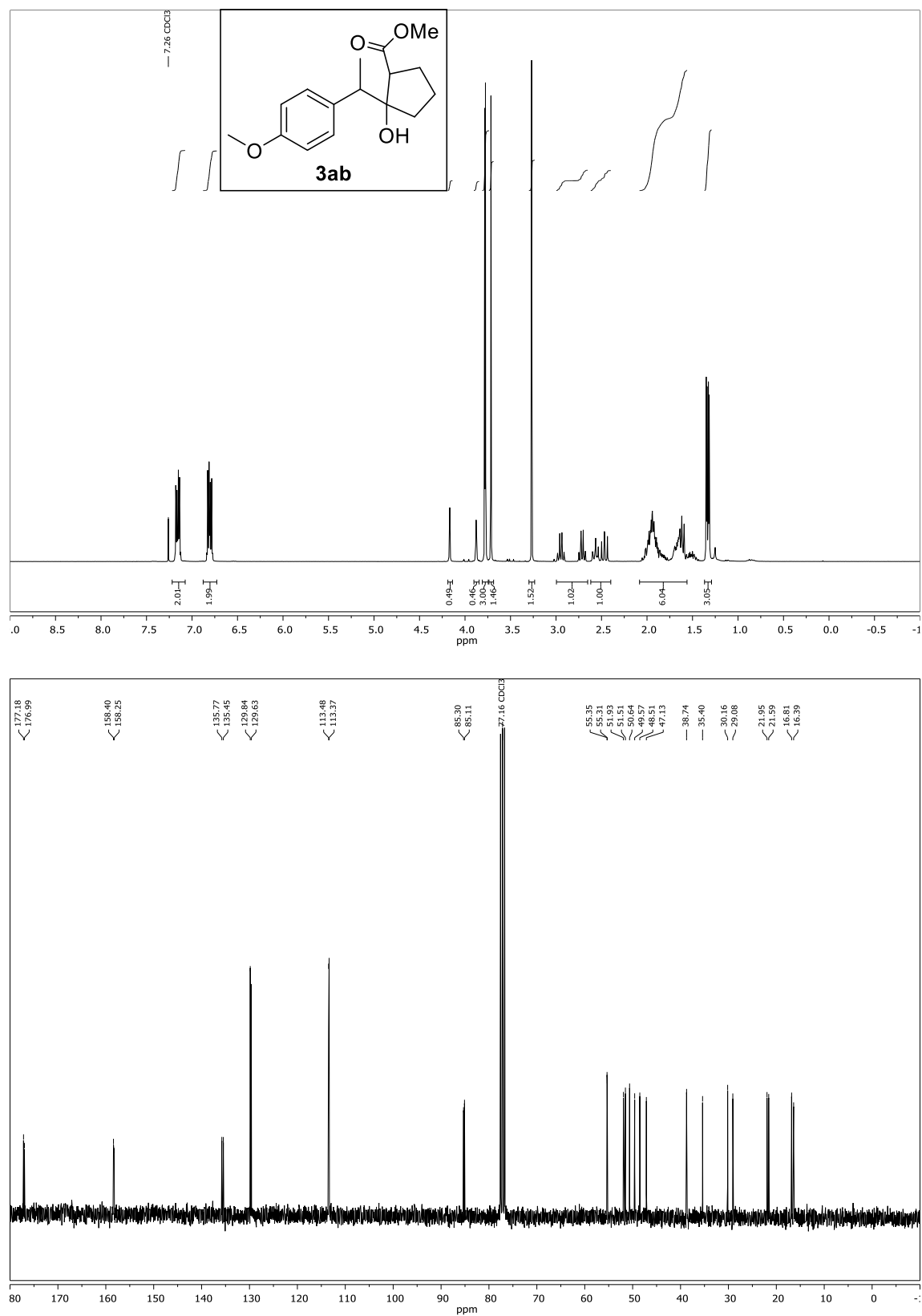
Compound **3z**, ^1H NMR and ^{13}C NMR (CDCl_3):



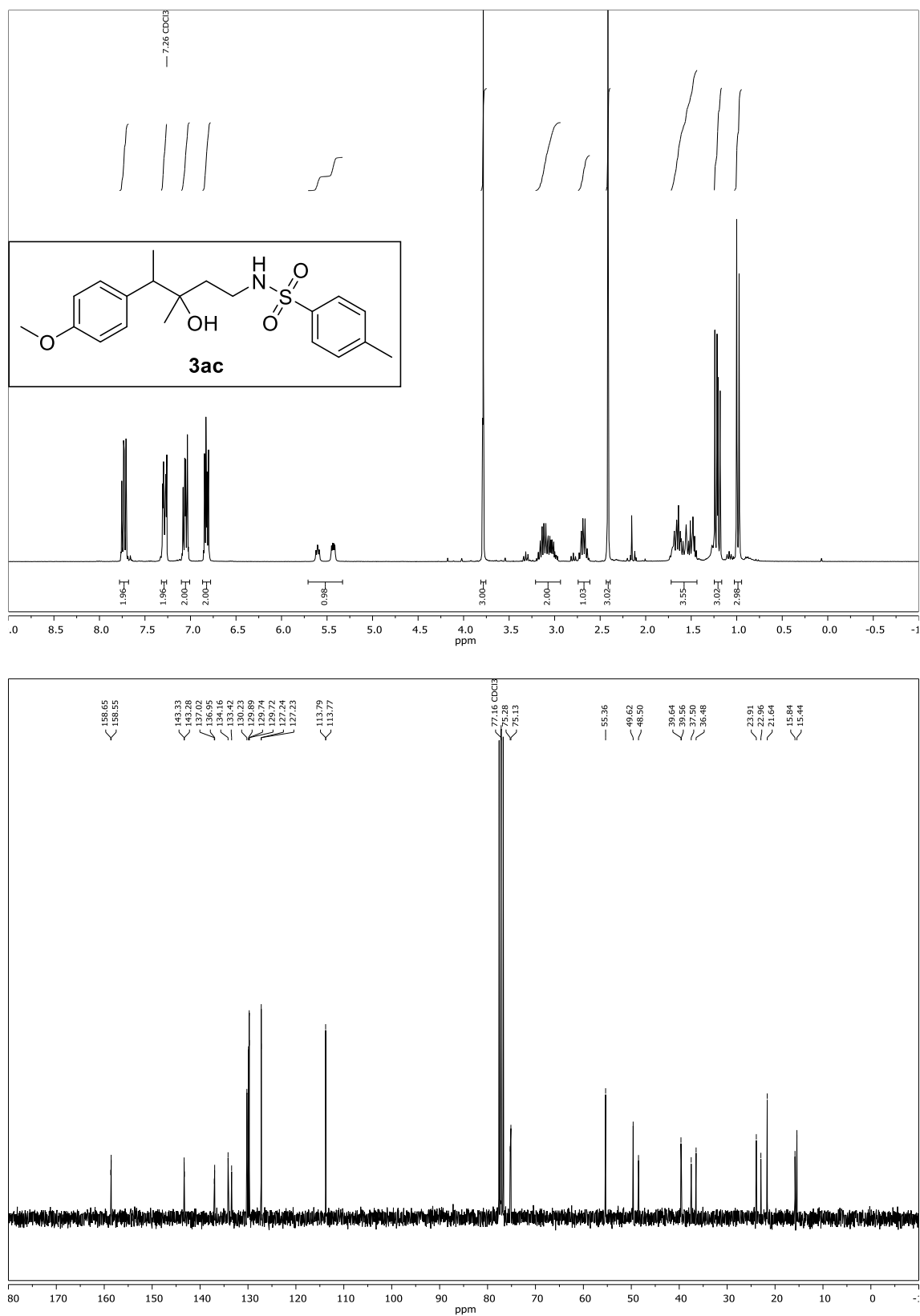
Compound **3aa**, ^1H NMR and ^{13}C NMR (CDCl_3):



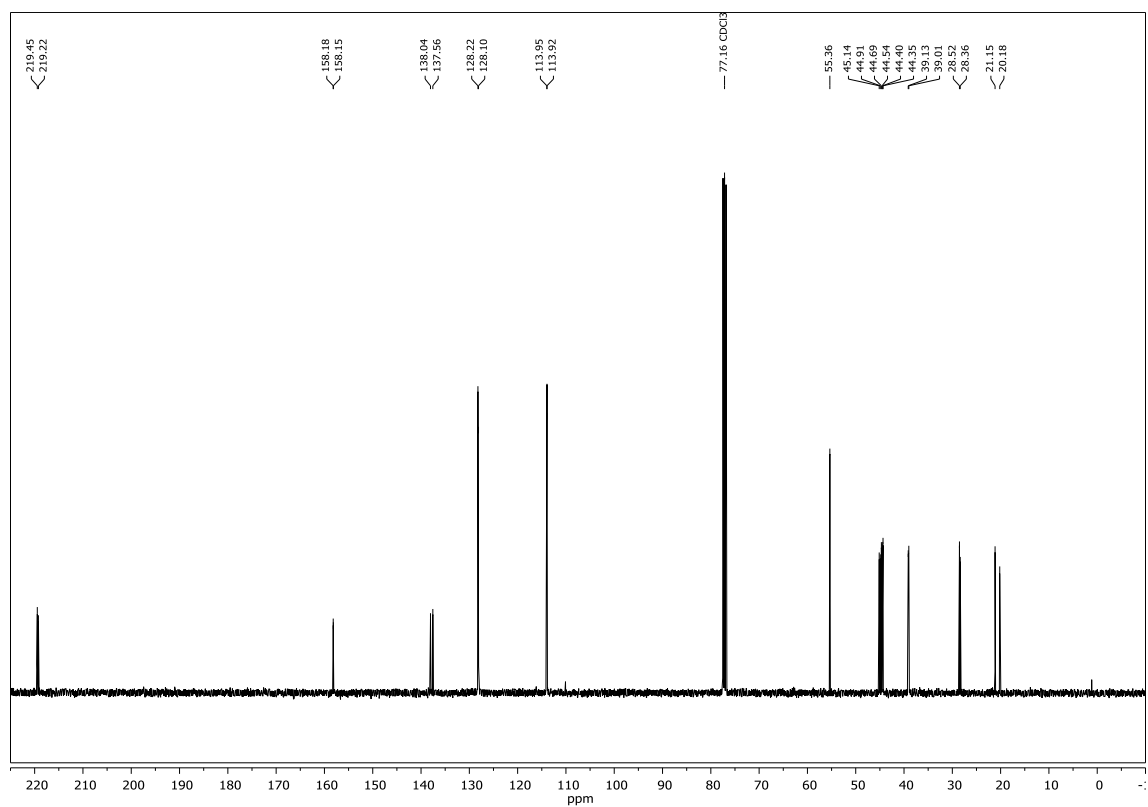
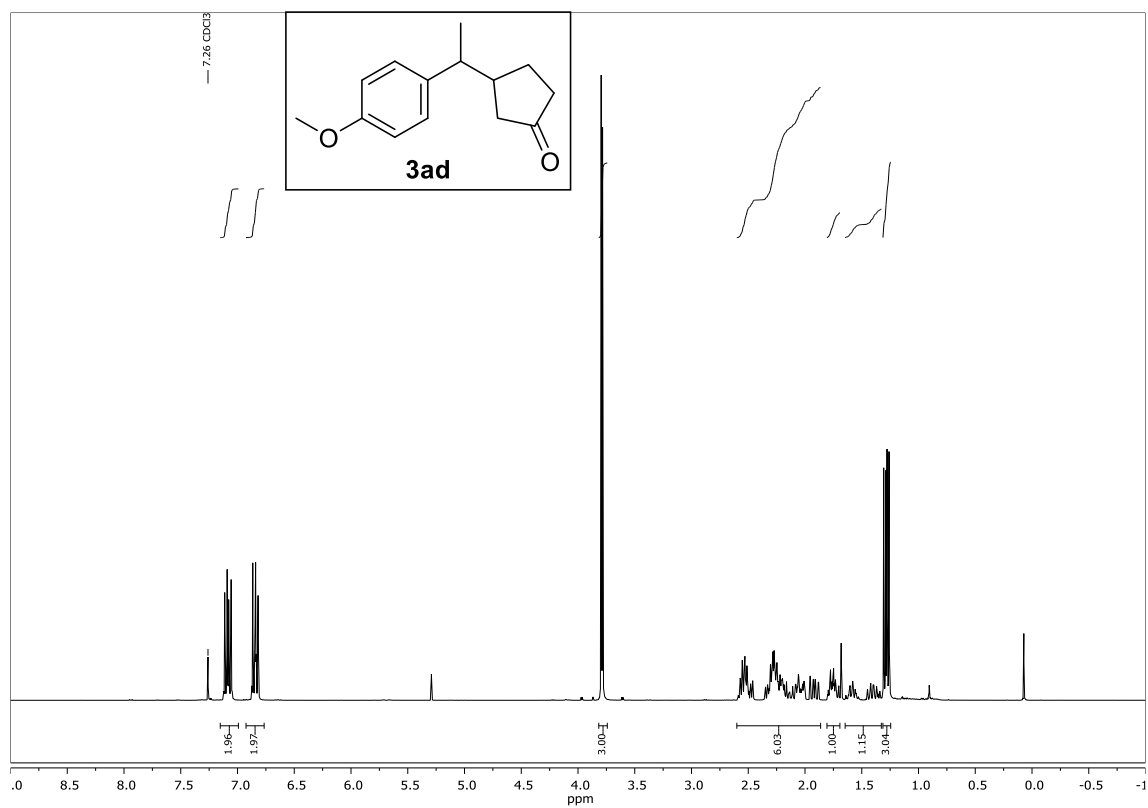
Compound **3ab**, ^1H NMR and ^{13}C NMR (CDCl_3):



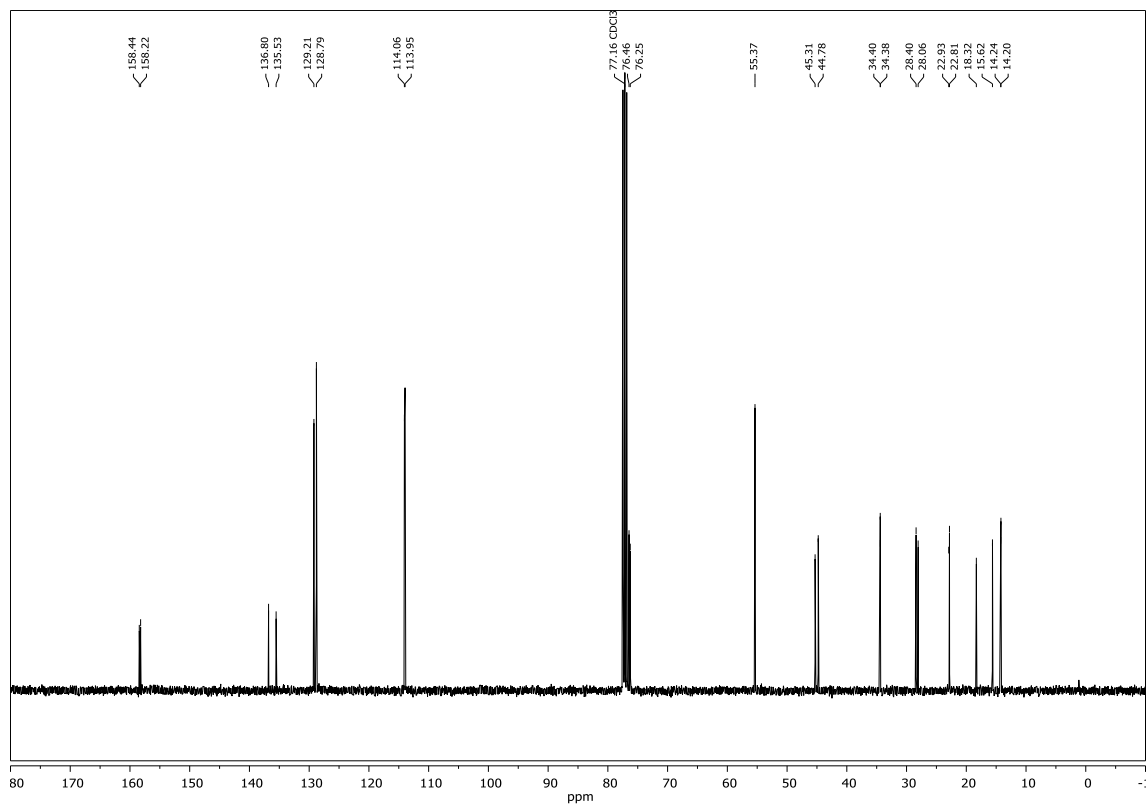
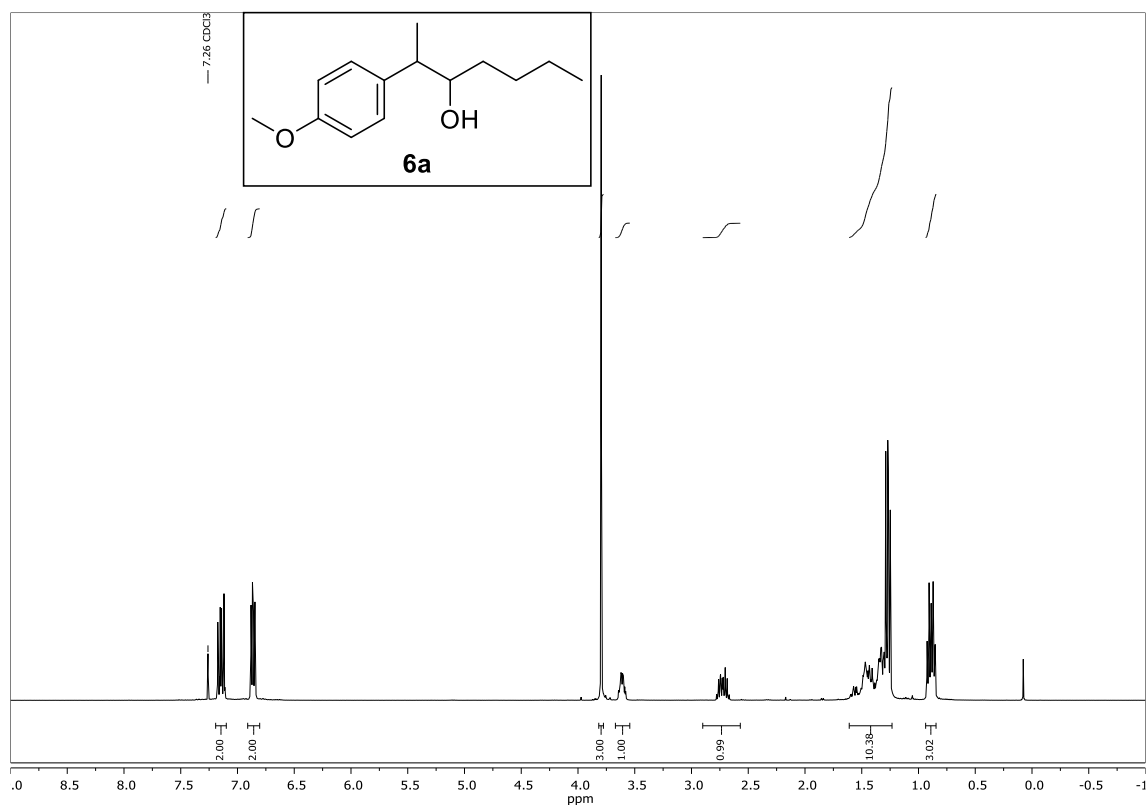
Compound **3ac**, ^1H NMR and ^{13}C NMR (CDCl_3):



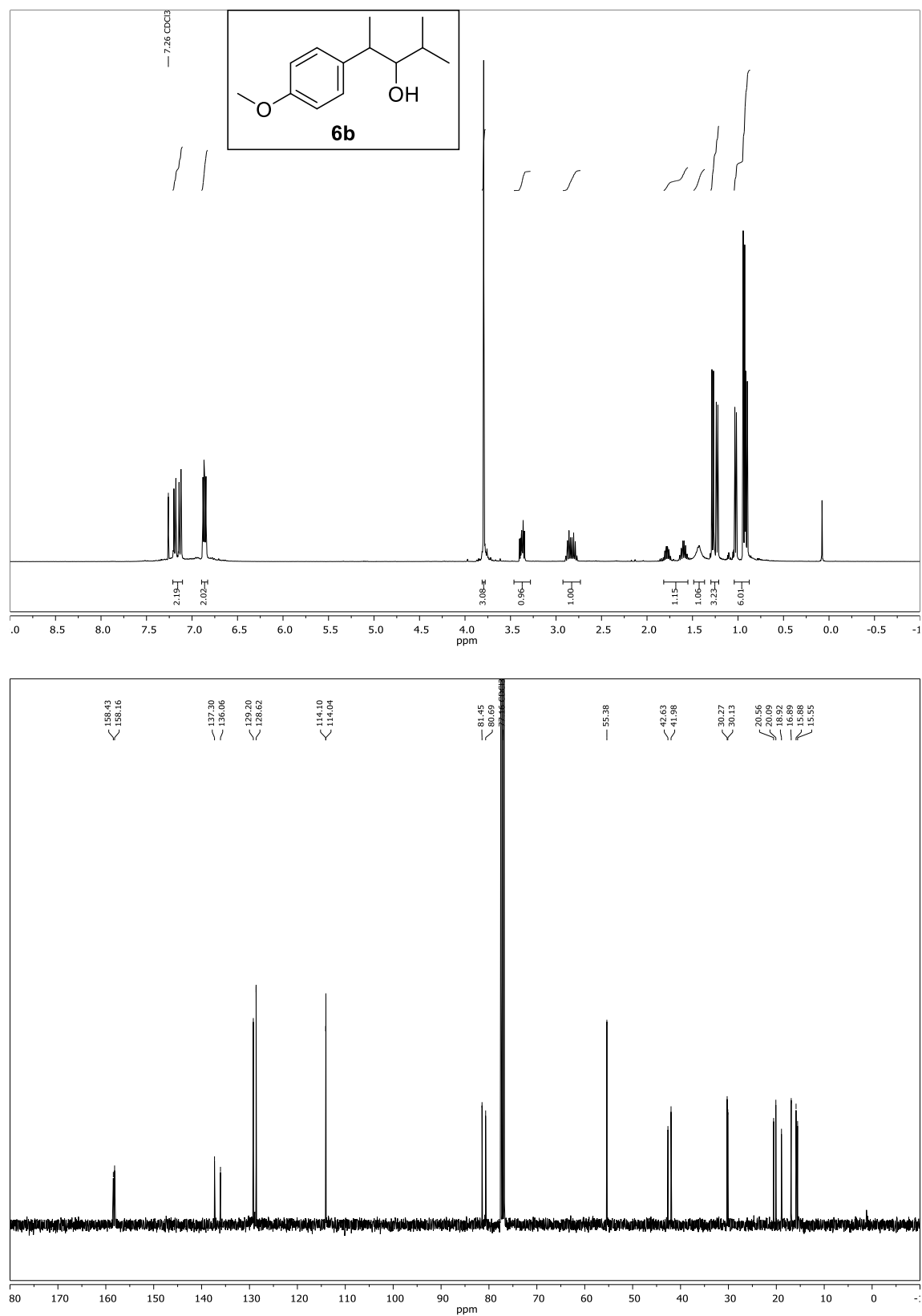
Compound **3ad**, ^1H NMR and ^{13}C NMR (CDCl_3):



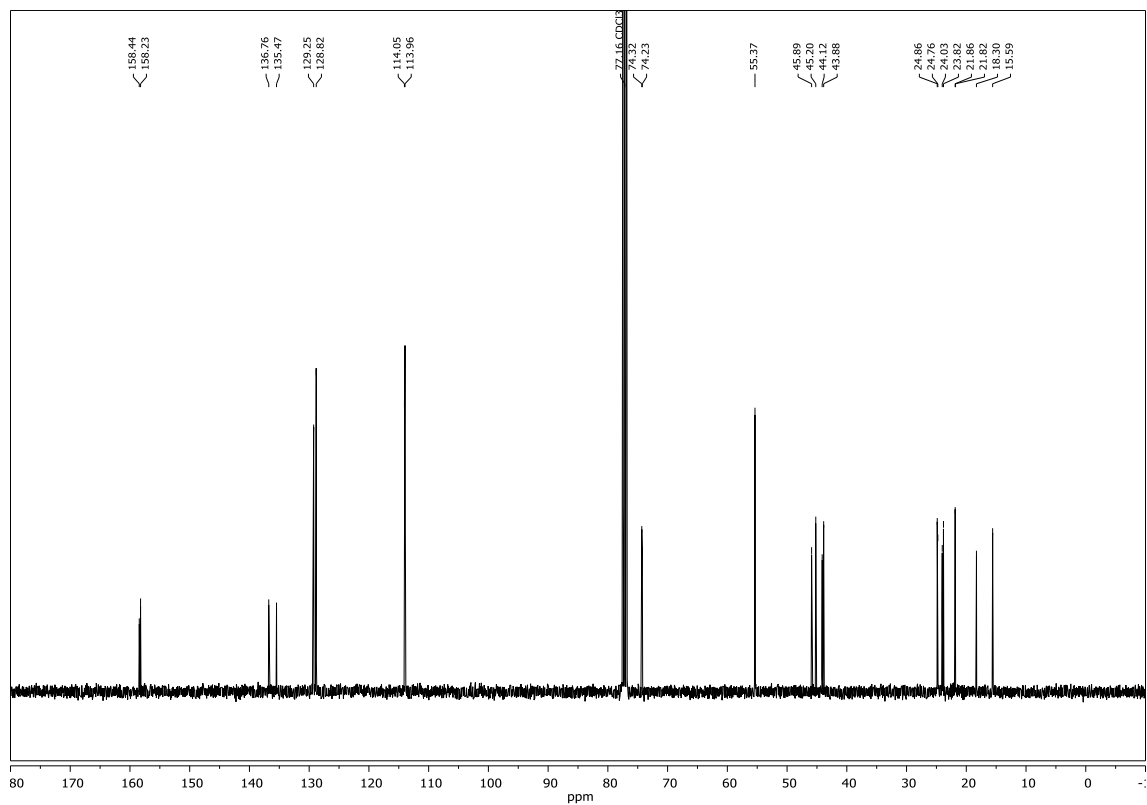
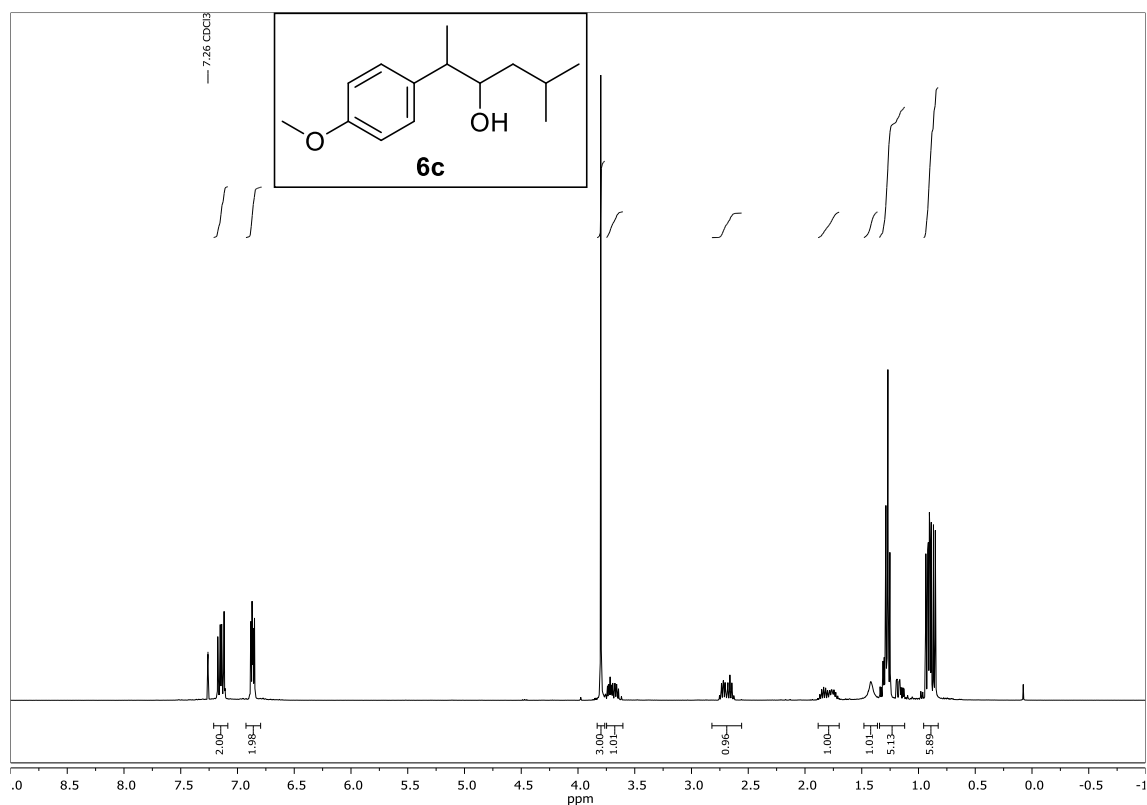
Compound **6a**, ^1H NMR and ^{13}C NMR (CDCl_3):

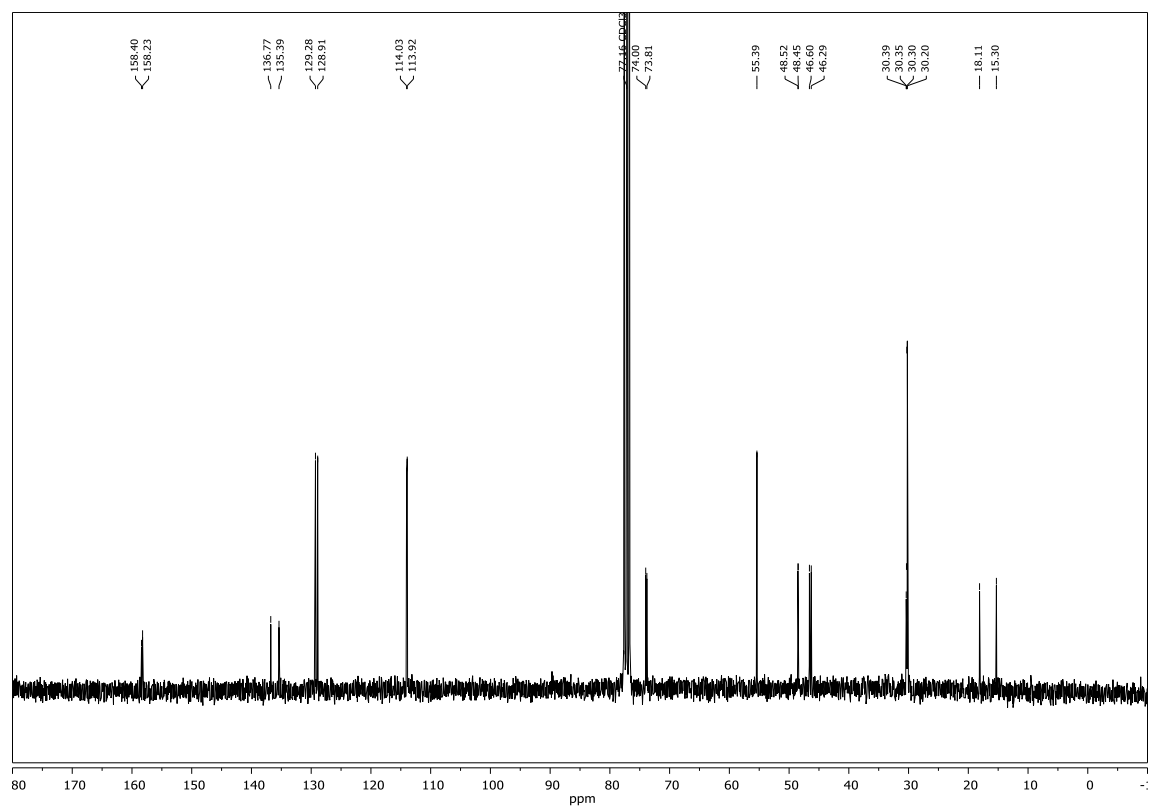
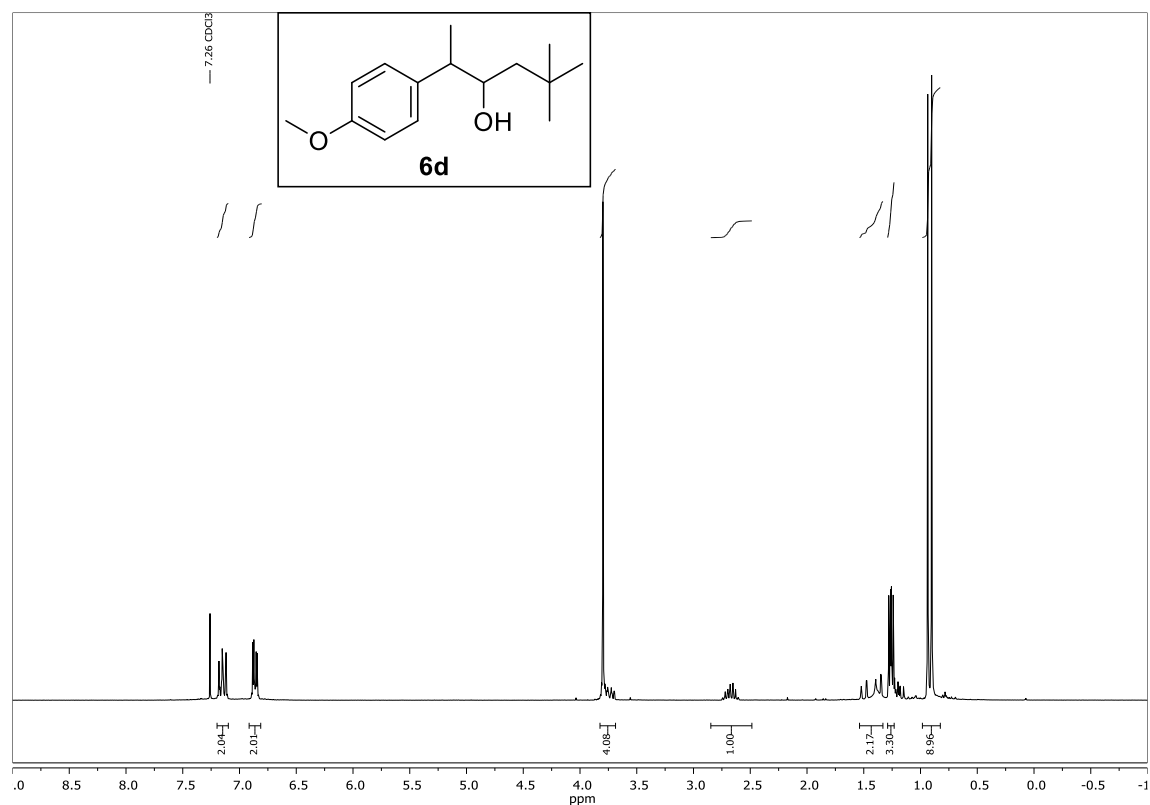


Compound **6b**, ^1H NMR and ^{13}C NMR (CDCl_3):

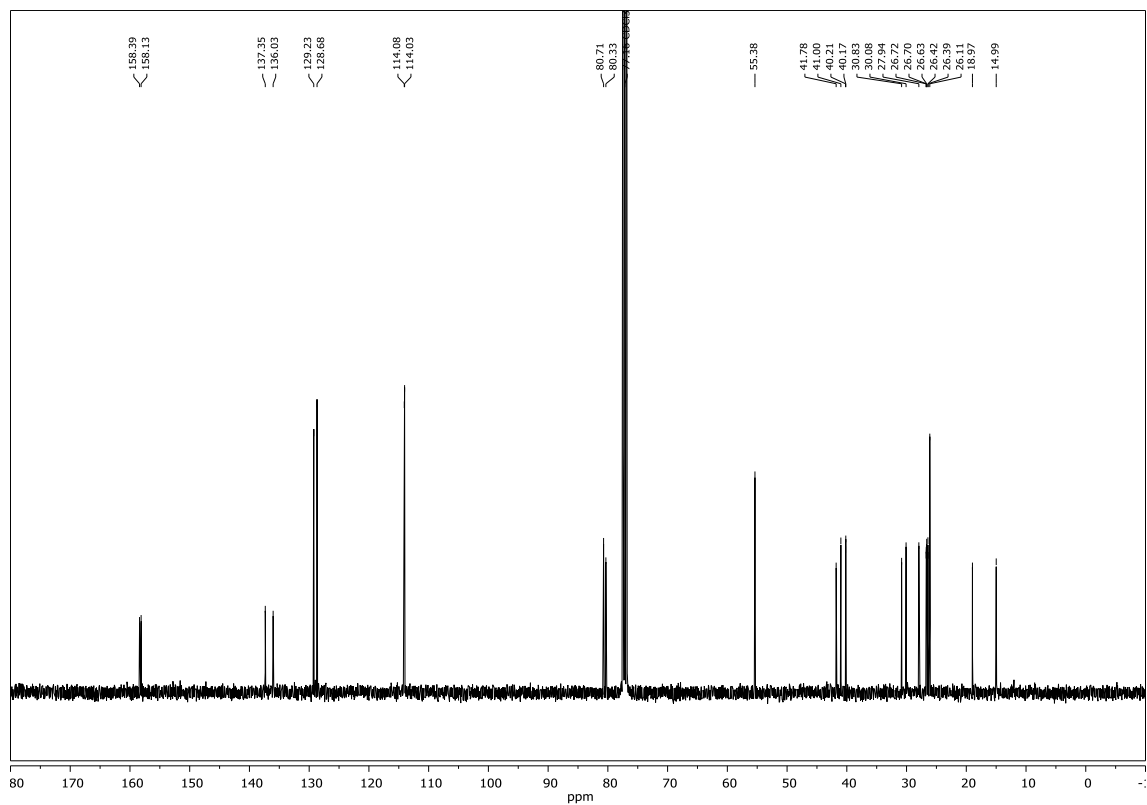
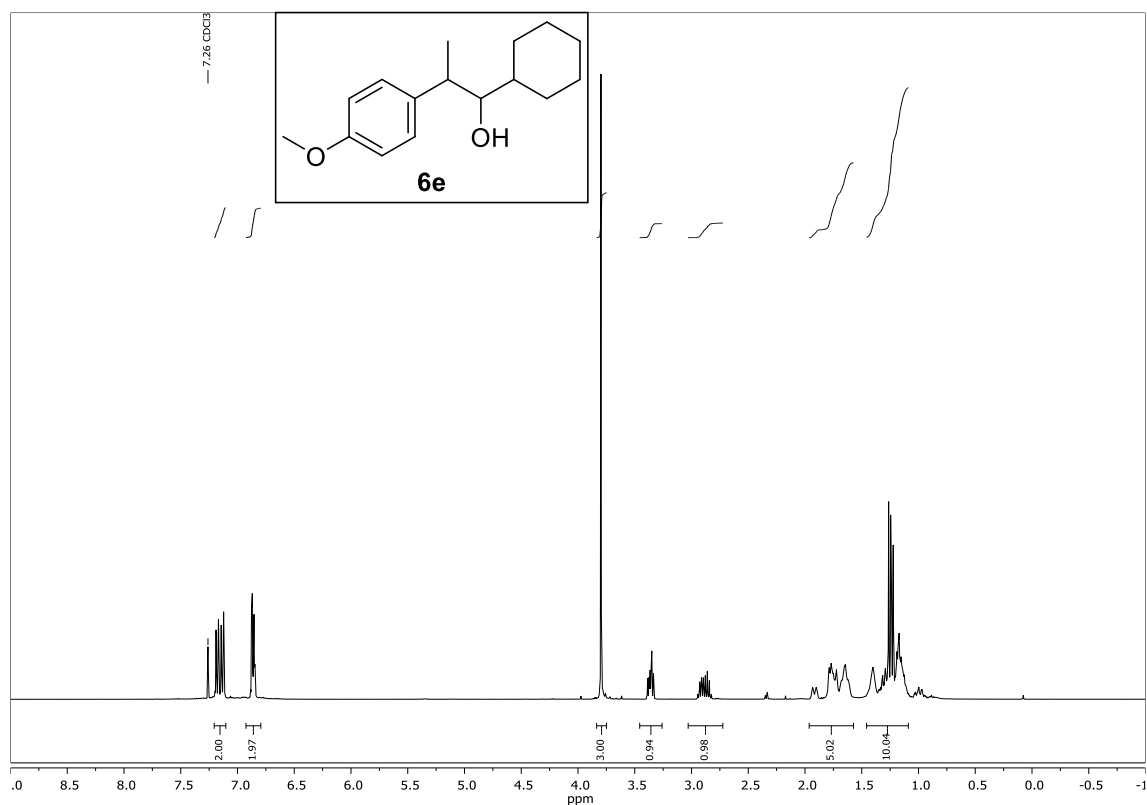


Compound **6c**, ^1H NMR and ^{13}C NMR (CDCl_3):

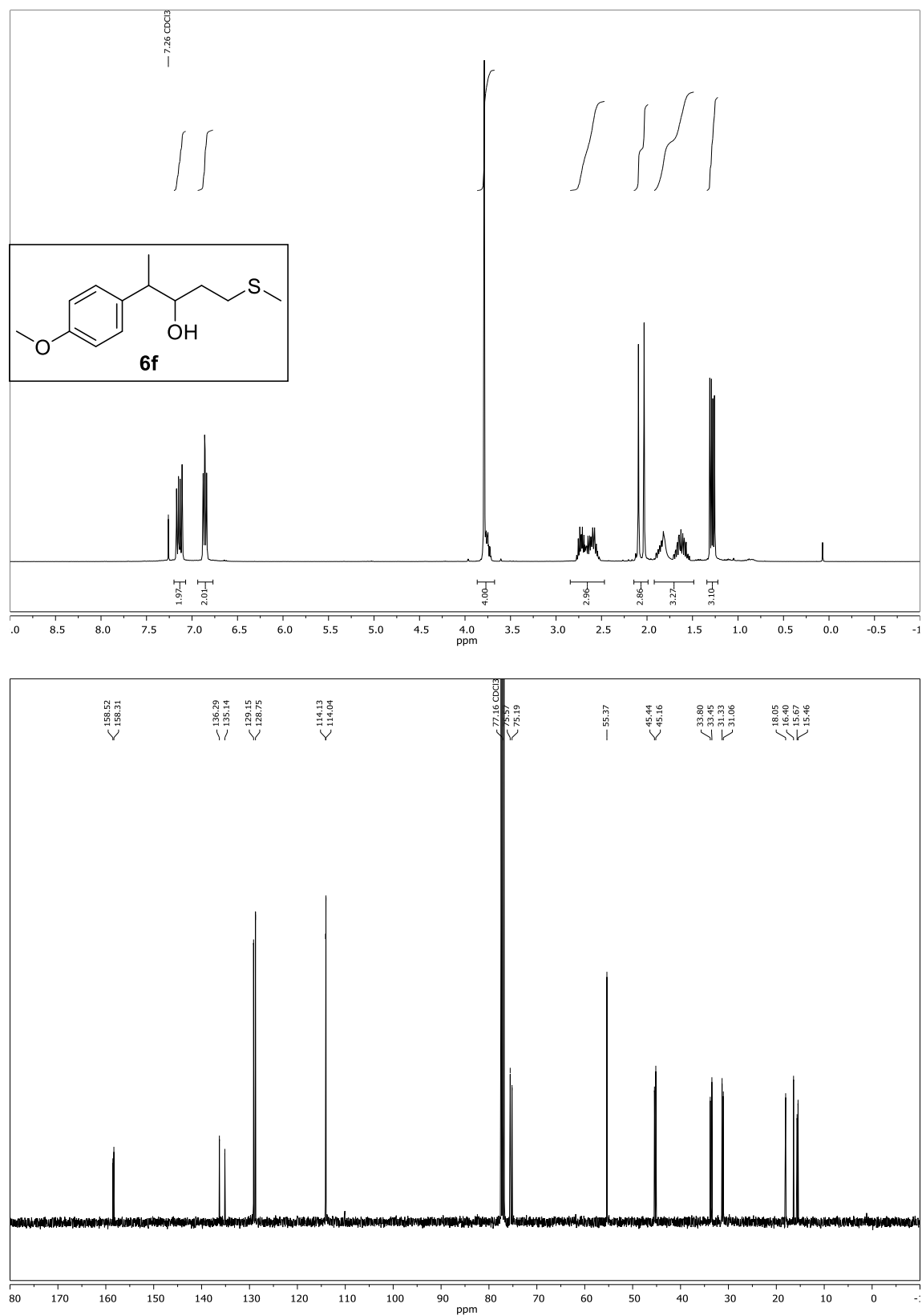




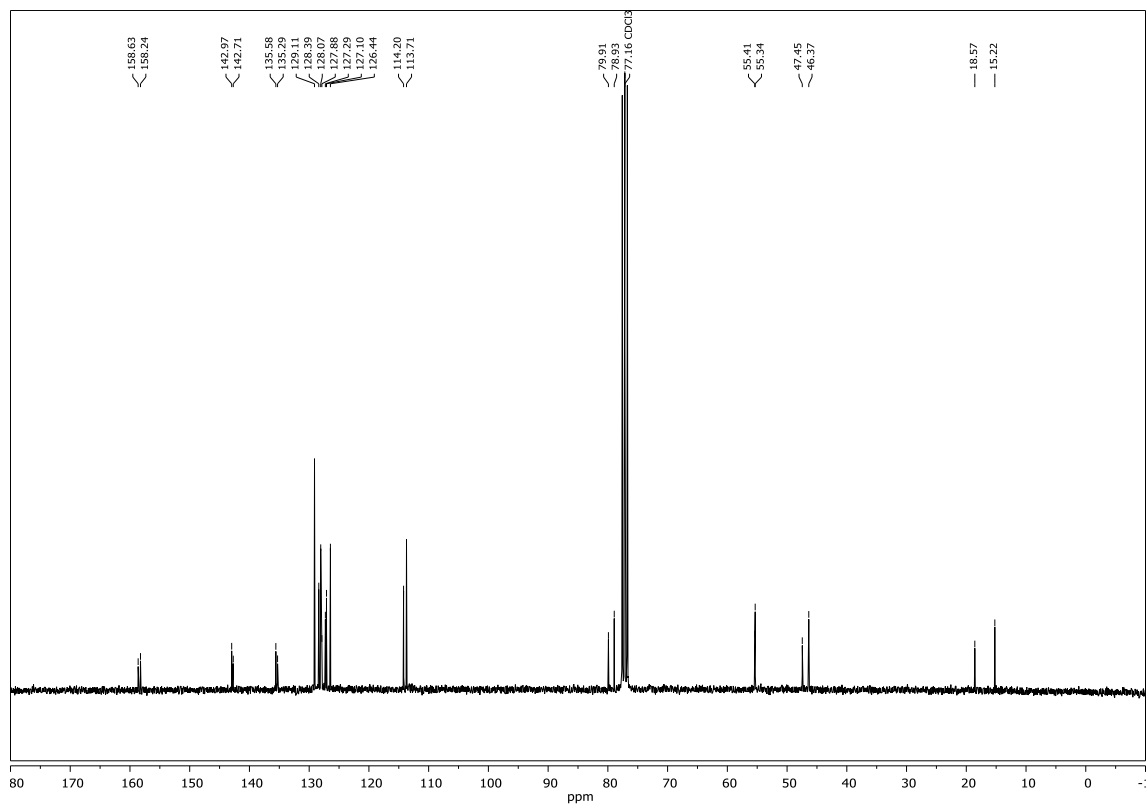
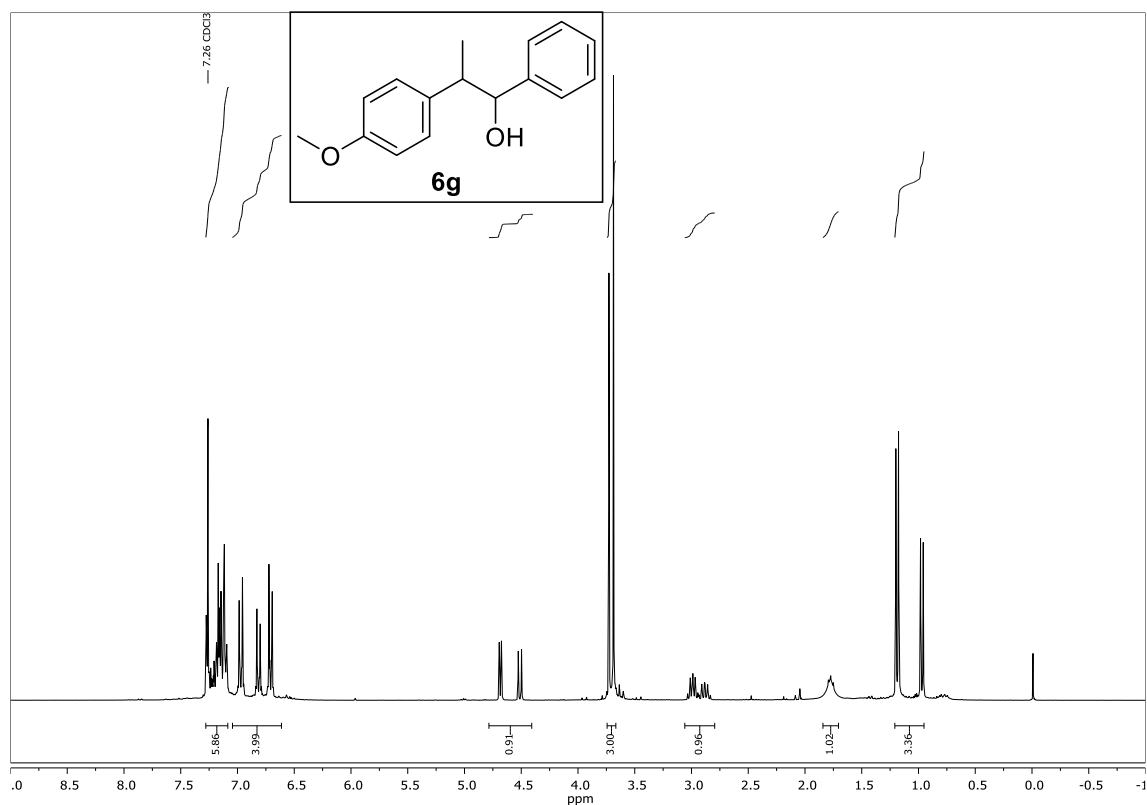
Compound **6e**, ^1H NMR and ^{13}C NMR (CDCl_3):



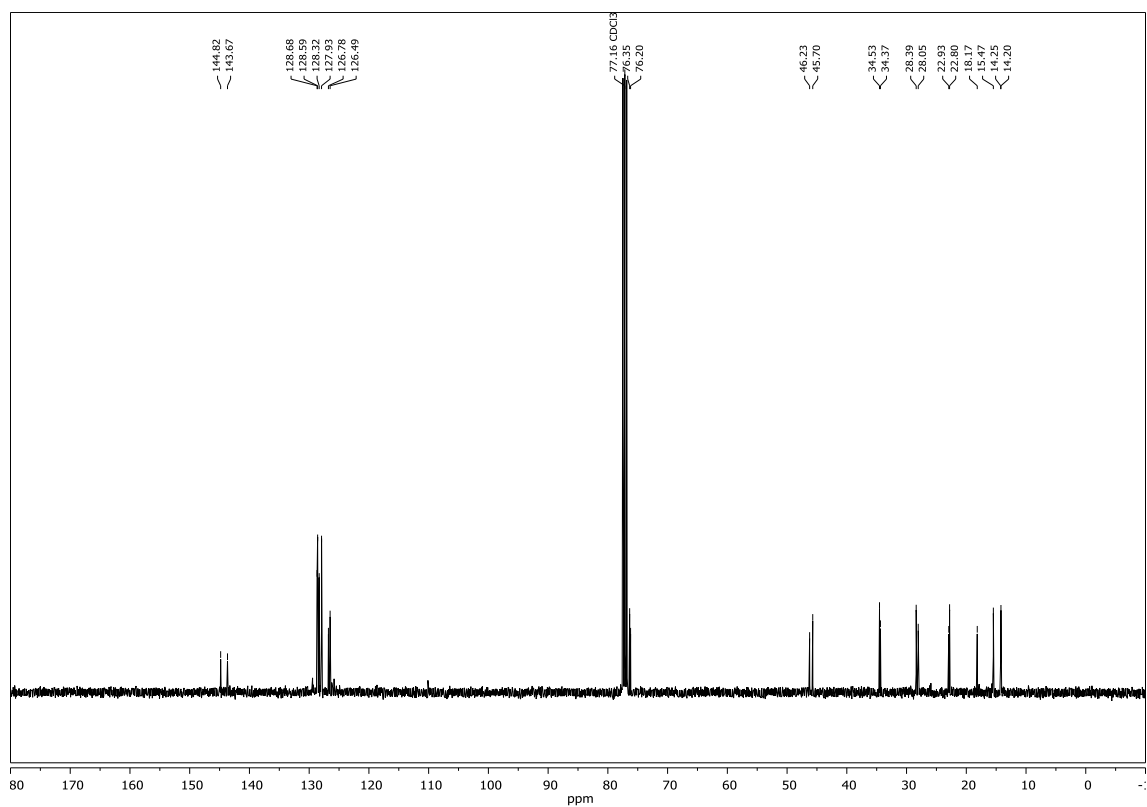
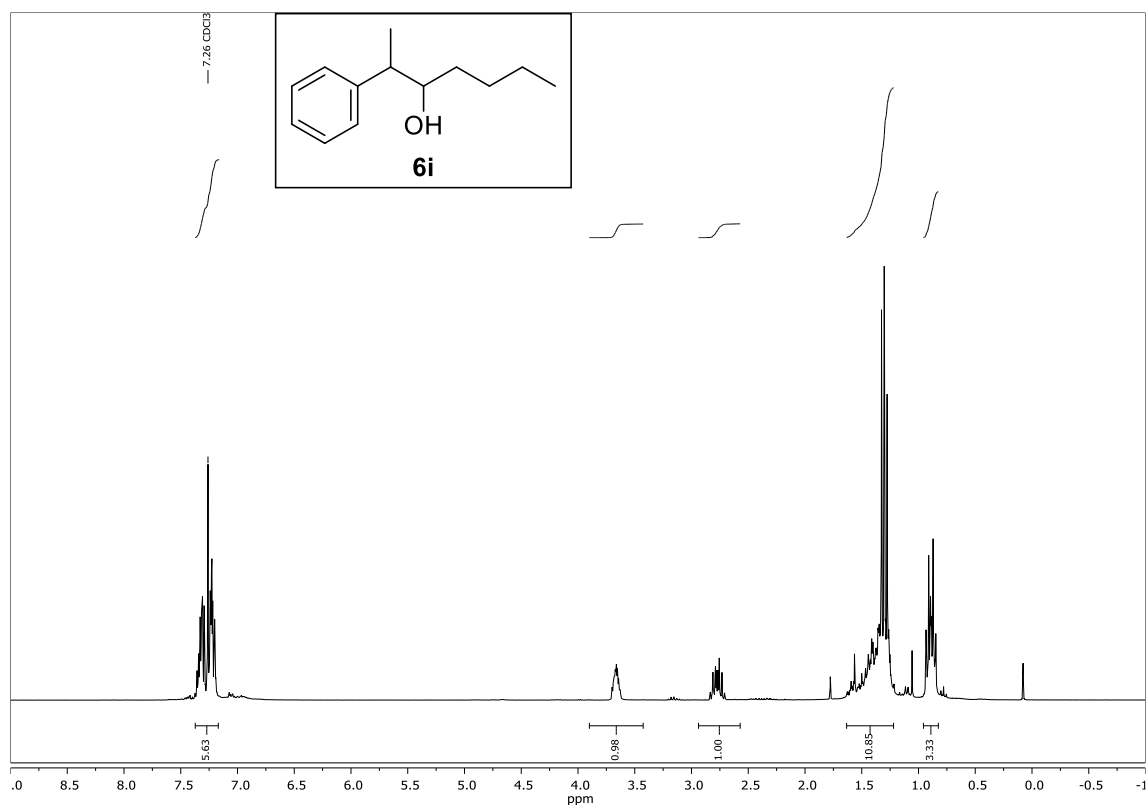
Compound **6f**, ^1H NMR and ^{13}C NMR (CDCl_3):



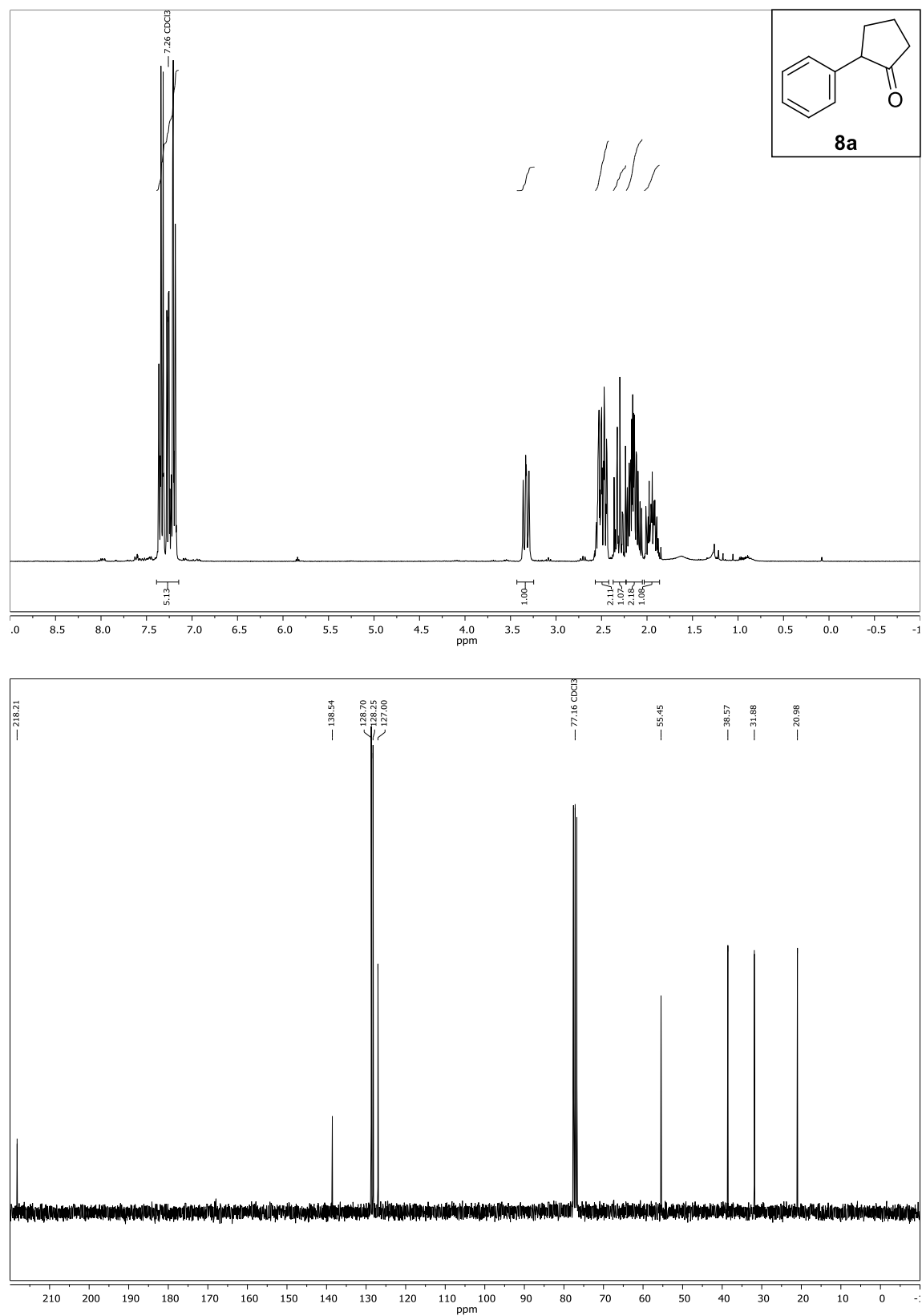
Compound **6g**, ^1H NMR and ^{13}C NMR (CDCl_3):



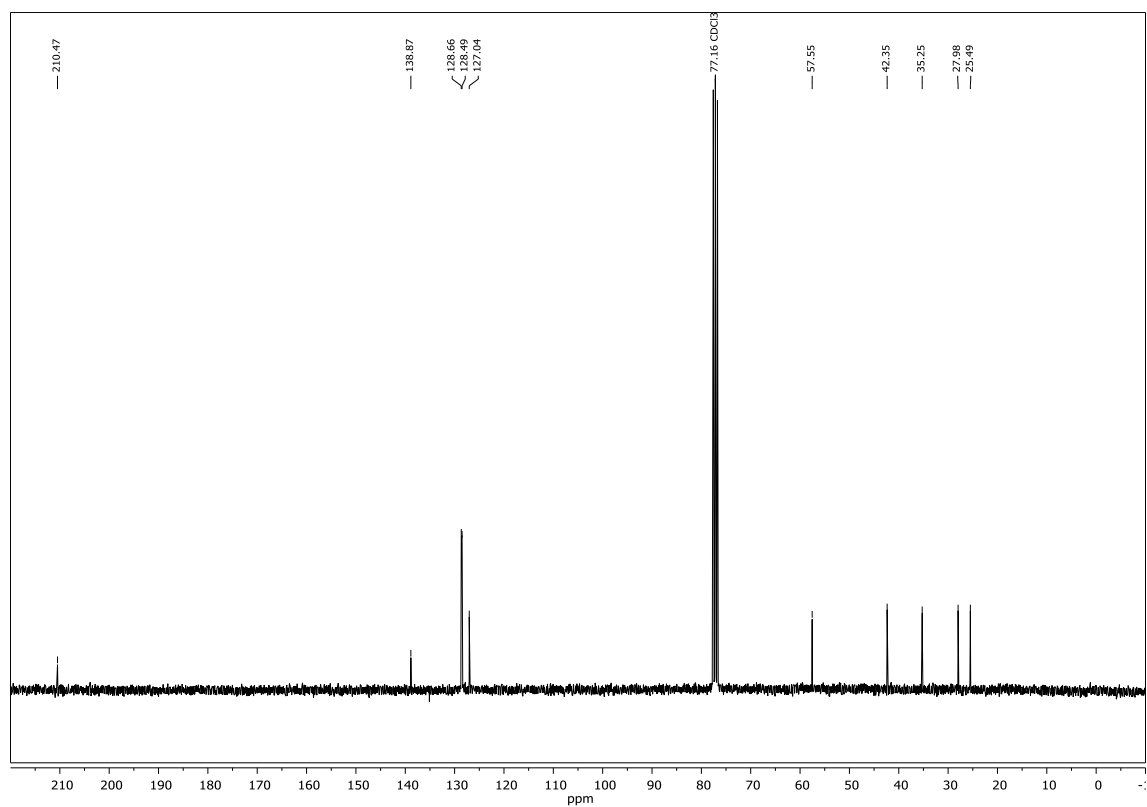
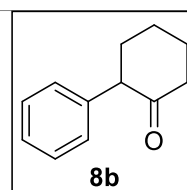
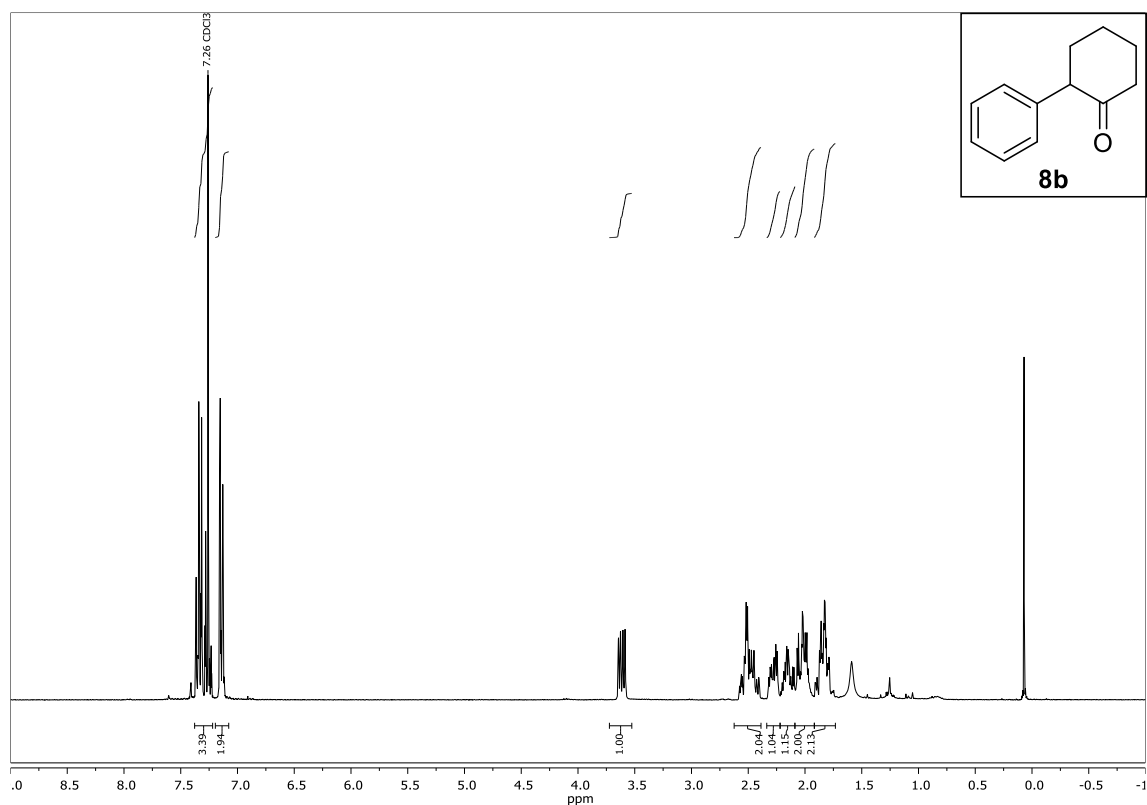
Compound **6i**, ^1H NMR and ^{13}C NMR (CDCl_3):



Compound **8a**, ^1H NMR and ^{13}C NMR (CDCl_3):



Compound **8b**, ^1H NMR and ^{13}C NMR (CDCl_3):



5.6 References

- [1] a) J. B. Hendrickson, *J. Am. Chem. Soc.* **1975**, *97*, 5784-5800; b) J. C. Lewis, P. S. Coelho, F. H. Arnold, *Chem. Soc. Rev.* **2011**, *40*, 2003-2021.
- [2] a) J. Yamaguchi, A. D. Yamaguchi, K. Itami, *Angew. Chem. Int. Ed.* **2012**, *51*, 8960-9009; b) L. McMurray, F. O'Hara, M. J. Gaunt, *Chem. Soc. Rev.* **2011**, *40*, 1885-1898.
- [3] a) T. B. Poulsen, K. A. Jorgensen, *Chem. Rev.* **2008**, *108*, 2903-2915; b) F. Denes, A. Perez-Luna, F. Chemla, *Chem. Rev.* **2010**, *110*, 2366-2447; c) J. He, M. Wasa, K. S. L. Chan, Q. Shao, J. Q. Yu, *Chem. Rev.* **2017**, *117*, 8754-8786; d) Y. Yang, J. Lan, J. You, *Chem. Rev.* **2017**, *117*, 8787-8863; e) Z. Dong, Z. Ren, S. J. Thompson, Y. Xu, G. Dong, *Chem. Rev.* **2017**, *117*, 9333-9403; f) H. M. Davies, D. Morton, *Chem. Soc. Rev.* **2011**, *40*, 1857-1869; g) H. Yi, G. Zhang, H. Wang, Z. Huang, J. Wang, A. K. Singh, A. Lei, *Chem. Rev.* **2017**, *117*, 9016-9085; h) T. Cernak, K. D. Dykstra, S. Tyagarajan, P. Vachal, S. W. Krska, *Chem. Soc. Rev.* **2016**, *45*, 546-576.
- [4] W. Liu, Z. Ren, A. T. Bosse, K. Liao, E. L. Goldstein, J. Bacsá, D. G. Musaev, B. M. Stoltz, H. M. L. Davies, *J. Am. Chem. Soc.* **2018**, *140*, 12247-12255.
- [5] a) S. Protti, M. Fagnoni, D. Ravelli, *ChemCatChem* **2015**, *7*, 1516-1523; b) L. Capaldo, D. Ravelli, *Eur. J. Org. Chem.* **2017**, *2017*, 2056-2071.
- [6] a) D. Hager, D. W. MacMillan, *J. Am. Chem. Soc.* **2014**, *136*, 16986-16989; b) J. C. Chu, T. Rovis, *Nature* **2016**, *539*, 272-275; c) A. Hu, J. J. Guo, H. Pan, H. Tang, Z. Gao, Z. Zuo, *J. Am. Chem. Soc.* **2018**, *140*, 1612-1616; d) M. D. Vu, M. Das, A. Guo, Z.-E. Ang, M. Dokić, H. S. Soo, X.-W. Liu, *ACS Catal.* **2019**, 9009-9014.
- [7] a) Y. Zhang, R. Qian, X. Zheng, Y. Zeng, J. Sun, Y. Chen, A. Ding, H. Guo, *Chem. Commun.* **2015**, *51*, 54-57; b) D. Ravelli, S. Protti, M. Fagnoni, *Chem. Rev.* **2016**, *116*, 9850-9913.
- [8] a) L. L. Liao, G. M. Cao, J. H. Ye, G. Q. Sun, W. J. Zhou, Y. Y. Gui, S. S. Yan, G. Shen, D. G. Yu, *J. Am. Chem. Soc.* **2018**, *140*, 17338-17342; b) Y. Kumagai, T. Naoe, K. Nishikawa, K. Osaka, T. Morita, Y. Yoshimi, *Aust. J. Chem.* **2015**, *68*, 1668; c) V. R. Yatham, Y. Shen, R. Martin, *Angew. Chem. Int. Ed.* **2017**, *56*, 10915-10919; d) W. Kong, H. An, Q. Song, *Chem. Commun.* **2017**, *53*, 8968-8971; e) J. P. Phelan, S. B. Lang, J. S. Compton, C. B. Kelly, R. Dykstra, O. Gutierrez, G. A. Molander, *J. Am. Chem. Soc.* **2018**, *140*, 8037-8047; f) C. Shu, R. S. Mega, B. J. Andreassen, A. Noble, V. K. Aggarwal, *Angew. Chem. Int. Ed.* **2018**, *57*, 15430-15434; g) K. Donabauer, M. Maity, A. L. Berger, G. S. Huff, S. Crespi, B. König, *Chem. Sci.* **2019**, *10*, 5162-5166; h) L. Pitzer, J. L. Schwarz, F. Glorius, *Chem. Sci.* **2019**, *10*, 8285-8291.
- [9] a) V. Grignard, *C. R. Acad. Sci.* **1900**, *130*, 1322-1325; b) C.-J. Li, *Tetrahedron* **1996**, *52*, 5643-5668; c) G. S. Silverman, P. E. Rakita, *Handbook of Grignard Reagents*, Taylor & Francis, **1996**; d) P. Barbier, *C. R. Acad. Sci.* **1899**, *128*, 110-111.
- [10] S. Ni, N. M. Padial, C. Kingston, J. C. Vantourout, D. C. Schmitt, J. T. Edwards, M. M. Kruszyk, R. R. Merchant, P. K. Mykhailiuk, B. B. Sanchez, S. Yang, M. A. Perry, G. M. Gallego, J. J. Mousseau, M. R. Collins, R. J. Cherney, P. S. Lebed, J. S. Chen, T. Qin, P. S. Baran, *J. Am. Chem. Soc.* **2019**, *141*, 6726-6739.
- [11] F. G. Bordwell, D. Algrim, N. R. Vanier, *J. Org. Chem.* **1977**, *42*, 1817-1819.
- [12] K. Chatterjee, M. Miyake, L. M. Stock, *Energy Fuels* **1990**, *4*, 242-248.
- [13] F. G. Bordwell, *Acc. Chem. Res.* **2002**, *21*, 456-463.
- [14] Q. Y. Meng, T. E. Schirmer, A. L. Berger, K. Donabauer, B. König, *J. Am. Chem. Soc.* **2019**, *141*, 11393-11397.
- [15] J. D. Cuthbertson, D. W. MacMillan, *Nature* **2015**, *519*, 74-77.

- [16] a) A. Banerjee, Z. Lei, M. Y. Ngai, *Synthesis* **2019**, 51, 303-333; b) K. Yoshikai, T. Hayama, K. Nishimura, K. Yamada, K. Tomioka, *J. Org. Chem.* **2005**, 70, 681-683; c) B. P. Roberts, *Chem. Soc. Rev.* **1999**, 28, 25-35.
- [17] H. Tanaka, K. Sakai, A. Kawamura, K. Oisaki, M. Kanai, *Chem. Commun.* **2018**, 54, 3215-3218.
- [18] J. A. Murphy, S. Z. Zhou, D. W. Thomson, F. Schoenebeck, M. Mahesh, S. R. Park, T. Tuttle, L. E. Berlouis, *Angew. Chem. Int. Ed.* **2007**, 46, 5178-5183.
- [19] E. Speckmeier, T. G. Fischer, K. Zeitler, *J. Am. Chem. Soc.* **2018**, 140, 15353-15365.
- [20] D. D. M. Wayner, D. J. McPhee, D. Griller, *J. Am. Chem. Soc.* **1988**, 110, 132-137.
- [21] S. Hünig, P. Kreitmeier, G. Märkl, J. Sauer, *Verlag Lehmanns* **2006**.
- [22] R. K. Harris, E. D. Becker, S. M. Cabral de Menezes, R. Goodfellow, P. Granger, *Magn. Reson. Chem.* **2002**, 40, 489-505.
- [23] G. R. Fulmer, A. J. M. Miller, N. H. Sherden, H. E. Gottlieb, A. Nudelman, B. M. Stoltz, J. E. Bercaw, K. I. Goldberg, *Organometallics* **2010**, 29, 2176-2179.
- [24] V. V. Pavlishchuk, A. W. Addison, *Inorg. Chim. Acta* **2000**, 298, 97-102.
- [25] J. Luo, J. Zhang, *ACS Catal.* **2016**, 6, 873-877.
- [26] a) Y. Du, R. M. Pearson, C. H. Lim, S. M. Sartor, M. D. Ryan, H. Yang, N. H. Damrauer, G. M. Miyake, *Chem. Eur. J.* **2017**, 23, 10962-10968; b) J. C. Theriot, C. H. Lim, H. Yang, M. D. Ryan, C. B. Musgrave, G. M. Miyake, *Science* **2016**, 352, 1082-1086; c) R. M. Pearson, C. H. Lim, B. G. McCarthy, C. B. Musgrave, G. M. Miyake, *J. Am. Chem. Soc.* **2016**, 138, 11399-11407.
- [27] A. B. Reitz, E. Sonveaux, R. P. Rosenkranz, M. S. Verlander, K. L. Melmon, B. B. Hoffman, Y. Akita, N. Castagnoli, M. Goodman, *J. Med. Chem.* **1985**, 28, 634-642.
- [28] S. Kathiravan, I. A. Nicholls, *Chem. Eur. J.* **2017**, 23, 7031-7036.
- [29] A. Fürstner, R. Martin, H. Krause, G. Seidel, R. Goddard, C. W. Lehmann, *J. Am. Chem. Soc.* **2008**, 130, 8773-8787.
- [30] D. A. Williams, S. A. Zaidi, Y. Zhang, *J. Nat. Prod.* **2015**, 78, 1859-1867.
- [31] T. Miura, Y. Funakoshi, J. Nakahashi, D. Moriyama, M. Murakami, *Angew. Chem. Int. Ed.* **2018**, 57, 15455-15459.
- [32] Y. Lu, D. Leow, X. Wang, K. M. Engle, J.-Q. Yu, *Chem. Sci.* **2011**, 2, 967.
- [33] J.-L. Zhu, H.-J. Liu, J.-P. Tsao, T.-Y. Tsai, I. C. Chen, S.-W. Tsao, *Synthesis* **2010**, 2010, 4242-4250.
- [34] D. J. Cram, H. L. Nyquist, F. A. A. Elhafez, *J. Am. Chem. Soc.* **1957**, 79, 2876-2888.
- [35] B. G. Ramsey, J. A. Cook, J. A. Manner, *J. Org. Chem.* **1972**, 37, 3310-3322.
- [36] X. Wang, Y. Lu, H. X. Dai, J. Q. Yu, *J. Am. Chem. Soc.* **2010**, 132, 12203-12205.
- [37] O. Piccolo, R. Menicagli, L. Lardicci, *Tetrahedron* **1979**, 35, 1751-1758.
- [38] M. Clarembreau, A. Krief, *Tetrahedron Lett.* **1985**, 26, 1093-1096.
- [39] a) M. T. Reetz, S. Stanchev, H. Haning, *Tetrahedron* **1992**, 48, 6813-6820; b) S.-i. Fukuzawa, K. Mutoh, T. Tsuchimoto, T. Hiyama, *J. Org. Chem.* **1996**, 61, 5400-5405; c) R. D. Rieke, R. M. Wehmeyer, T.-C. Wu, G. W. Ebert, *Tetrahedron* **1989**, 45, 443-454.
- [40] D. C. Moebius, J. S. Kingsbury, *J. Am. Chem. Soc.* **2009**, 131, 878-879.
- [41] M. Shibuya, M. Tomizawa, Y. Sasano, Y. Iwabuchi, *J. Org. Chem.* **2009**, 74, 4619-4622.
- [42] A. Narayanappa, D. Hurem, J. McNulty, *Synlett* **2017**, 28, 2961-2965.
- [43] L. A. Carpino, J. Xia, A. El-Faham, *J. Org. Chem.* **2004**, 69, 54-61.

SUMMARY

6 Summary

This thesis presents different methods for the photocatalytic transfer of two electrons, enabling the generation of twofold reduced carbon–carbon cross coupling products that would classically be generated by the formation of highly reactive and often metal-based carbanionic intermediates. Reactions involving carbanions, e.g. the Grignard- or the Barbier reaction, have been known for more than 100 years and are frequently used in conventional organic synthesis. In contrast, photocatalytic reactions are typically based on the generation of radical intermediates by single electron transfer processes and so far, no photocatalyst that is capable of donating two electrons in one step is known. This work presents three different approaches to mimic carbanionic reactivity using photocatalytic systems.

Chapter 1 gives an overview of recent concepts for the photocatalytic generation of carbanions and their synthetic use.

In **chapter 2**, a combination of classic organometallic chemistry with photocatalysis was attempted by coupling the visible light induced generation of zerovalent zinc from a zinc(II) salt to the formation and subsequent reaction of an organozinc species. Ultimately, this was supposed to enable the catalytic use of Zn(II) salts for various reactions by constantly regenerating the reactive zerovalent zinc in a photocatalytic reaction. The literature reported system for the reduction of Zn^{2+} was improved significantly and a method for a photocatalytic two-step/one-pot Barbier reaction was developed. However, due to the incompatibility of the photocatalytic system with the reaction conditions required for organometallic reactions, it was so far not possible to establish the a dual catalytic one-step cross-coupling reaction.

The Barbier reaction is one of the oldest carbon–carbon bond-forming reactions in synthetic organic chemistry. It is based on the insertion of a zerovalent metal into a carbon–halide bond, generating a nucleophilic carbon center which is capable of reacting with various electrophiles, such as aldehydes and ketones. **Chapter 3** presents a photocatalytic version of this reaction that uses typical substrates for Barbier reactions to generate the same substrates but requires neither the use of metals, nor the formation of carbanionic intermediates. Instead both substrates – an aromatic aldehyde or ketone and an allyl- or benzyl bromide – are reduced once by the photocatalyst *via* a single electron transfer. The generated radical intermediates are capable of recombining in a radical-radical cross-coupling reaction, representing an overall two-electron transfer and forming homoallylic and -benzylic alcohols as products.

A redox-neutral approach for the photocatalytic generation of carbanions is introduced in **chapter 4**. Benzylic carboxylic acids are deprotonated and subsequently oxidized by a photocatalyst, leading to the elimination of CO₂ and the formation of a benzylic radical. Due to the rather high stability of this radical intermediate, it can be reduced in the same photocatalytic cycle, leading to the regeneration of the photocatalyst and the formation of a benzylic carbanion which readily reacts with aliphatic aldehydes forming secondary alcohols which are analog to typical products of the well-known Grignard reaction. However, the use of less reactive electrophiles such as ketones was not possible in synthetically useful yields, due to the competing defunctionalization of the carboxylic acids by protonation of the carbanion intermediate.

Based on the same mechanism, the reaction presented in **chapter 5** uses a combination of photo- and hydrogen atom transfer catalysis to generate carbanions from the corresponding C–H bonds. After photocatalytic oxidation, the thiol-based HAT-catalyst is capable of abstracting a hydrogen atom from the benzylic position of the substrate, generating a radical intermediate. Analogously to chapter 4, this radical is now reduced to the corresponding benzylic carbanion which can undergo reactions with electrophiles. Notably, in addition to aldehydes, this system also enables the use of ketones as electrophiles, as a protonation of the carbanion intermediate does not lead to a termination of the reaction but rather to the regeneration of the starting material.

ZUSAMMENFASSUNG

7 Zusammenfassung

Das Ziel dieser Arbeit war die Entwicklung photokatalytischer Methoden zur Übertragung von zwei Elektronen. Dadurch sollte die Darstellung von zweifach reduzierten Kohlenstoff-Kohlenstoff Kreuzkupplungsprodukten ermöglicht werden. In klassischer organischer Synthese werden diese oft mit Hilfe von hochreaktiven und meist Metall-basierten carbanionischen Intermediaten hergestellt. Reaktionen von Carbanionen, wie zum Beispiel die Grignard- oder die Barbier Reaktion, sind bereits seit über 100 Jahren ein fester Bestandteil der synthetischen organischen Chemie. Im Gegensatz dazu basieren photokatalytische Reaktionen typischerweise auf der Bildung von radikalischen Zwischenstufen, die durch die Übertragung einzelner Elektronen erzeugt werden. Bisher ist kein Photokatalysator bekannt, der zwei Elektronen in einem Schritt abgeben kann. Diese Arbeit stellt drei verschiedene Ansätze vor, um mit photokatalytischen Systemen carbanionische Reaktivitäten zu erreichen.

Kapitel 1 gibt einen Überblick über aktuelle Konzepte zur photokatalytischen Erzeugung von Carbanionen und deren synthetische Anwendung.

In **Kapitel 2** sollte Photokatalyse mit klassischer Organometallchemie kombiniert werden. Hierfür wurde die photokatalytische Reduktion von Zink(II) Salzen zu metallischem Zink genutzt. Aus dem gebildeten $\text{Zn}(0)$ sollte *in situ* eine reaktive Organozink Spezies erzeugt, und für diverse Reaktionen genutzt werden. Die konstante photokatalytische Regeneration von reaktivem nullwertigem Zink sollte letztlich die katalytische Verwendung von Zn(II) Salzen für Reaktionen ermöglichen, die üblicherweise mit stöchiometrischen Mengen von Zinkpulver durchgeführt werden. Das literaturbekannte System für die Photoreduktion von Zn^{2+} wurde deutlich verbessert und eine photokatalytische Barbier Reaktion in zwei Schritten wurde entwickelt. Die gewünschte einstufige Reaktion mit katalytischen Mengen an Zink konnte bisher jedoch nicht entwickelt werden, da sich herausstellte, dass das photokatalytische System nicht mit den für die organometallischen Reaktionen benötigten Bedingungen kompatibel war.

Die Barbier Reaktion ist eine der ältesten Reaktionen zur Bildung von Kohlenstoff-Kohlenstoff Bindungen in der synthetischen organischen Chemie. Sie basiert auf der Insertion eines nullwertigen Metalls in eine Kohlenstoff-Halogen Bindung, wodurch ein nukleophiles Kohlenstoffzentrum gebildet wird, welches mit verschiedenen Elektrophilen, wie zum Beispiel Aldehyden oder Ketonen reagieren kann. **Kapitel 3** stellt eine photokatalytische Version dieser Reaktion vor, in der typische Startmaterialien von Barbier Reaktionen verwendet werden um dieselben Produkte zu erzeugen. Dabei werden jedoch weder Metalle benötigt, noch findet die

Bildung einer carbanionischen Zwischenstufe statt. Stattdessen werden beide Substrate – ein aromatischer Aldehyd bzw. ein aromatisches Keton und ein Ally- oder Benzyl Bromid – vom Photokatalysator durch eine Einelektronen Übertragung reduziert. Die dadurch gebildeten radikalischen Intermediate können nun in einer Radikal-Radikal Kreuzkupplung zu homoallylischen oder -benzyllischen Alkoholen rekombinieren. In der Gesamtreaktion entspricht dies, analog zur klassischen Barbier Reaktion, der Übertragung von zwei Elektronen.

Ein redox-neutraler Ansatz für die photokatalytische Bildung von Carbanionen wird in **Kapitel 4** vorgestellt. Benzyllische Carbonsäuren werden deprotoniert und anschließend vom Photokatalysator oxidiert, wodurch CO₂ abgespalten und ein benzyllisches Radikal gebildet wird. Aufgrund der relativ hohen Stabilität dieser radikalischen Zwischenstufe ist es möglich, diese innerhalb desselben photokatalytischen Zyklus zu reduzieren. Dadurch wird der Grundzustand des Photokatalysators wiederhergestellt und ein benzyllisches Carbanion gebildet. Dieses kann nun an aliphatische Aldehyde addieren, wodurch sekundäre Alkohole erhalten werden welche analog zu den typischen Produkten der weit verbreiteten Grignard Reaktion sind. Die Verwendung von weniger reaktiven Elektrophilen wie Ketonen war jedoch nicht in synthetisch brauchbaren Ausbeuten möglich, da hier die konkurrierende Defunktionalisierung der Carbonsäure durch die Protonierung der carbanionischen Zwischenstufe überwiegt.

Basierend auf diesem Mechanismus wird bei der Reaktion in **Kapitel 5** eine Kombination aus Photo- und Wasserstoffatomtransfer Katalyse verwendet, um aus benzyllischen C–H Bindungen direkt die entsprechenden Carbanionen zu erzeugen. Ein Thiol-basierter Wasserstoffatomtransfer Katalysator kann, nachdem er vom Photokatalysator oxidiert wurde, ein Wasserstoffatom von der benzyllischen Position des Substrats abstrahieren und somit eine radikalische Zwischenstufe bilden. Analog zu Kapitel 4 wird dieses Radikal nun zum entsprechenden benzyllischen Carbanion reduziert, welches wiederum mit Elektrophilen reagieren kann. Beachtenswert an diesem System ist, dass hier zusätzlich zu Aldehyden auch Ketone geeignete Reaktionspartner darstellen, da die Protonierung der carbanionischen Zwischenstufe hier nicht zum vorzeitigen Beenden der Reaktion, sondern lediglich zur Regeneration des Startmaterials führt.

APPENDIX

8 Appendix

8.1 Abbreviations

°C	degrees Celsius
Å	Ångström (10^{-10} m)
Φ_F	fluorescence quantum yield
λ	wavelength
3DPA2FBN	2,4,6-tris(diphenylamino)-3,5-difluorobenzonitrile
3DPAFIPN	2,4,6-tris(diphenylamino)-5-fluoroisophthalonitrile
4CzBnBN	2,4,5,6-tetra(carbazole-9-yl)-3-benzylbenzonitrile
4CzPN	3,4,5,6-tetra(carbazole-9-yl)phthalonitrile
4CzIPN	2,4,5,6-tetra(carbazole-9-yl)isophthalonitrile
anhyd.	anhydrous
APCI	atmospheric-pressure chemical ionization
Ar	arene
BDE	bond dissociation energy
boc	<i>tert</i> -butyloxycarbonyl
bpy	2,2'-bipyridine
BSA	<i>N,O</i> -bis(trimethylsilyl)acetamide
BSTFA	<i>N,O</i> -bis(trimethylsilyl)trifluoroacetamide
cm	centimeter
CV	cyclic voltammetry
DB	double bond
DCM	dichloromethane
DFT	density functional theory
DIPEA	<i>N,N</i> -diisopropylethylamine
DMA	dimethylacetamide
DMF	dimethylformamide
DMSO	dimethyl sulfoxide
DPA	diphenylanthracene
dtbpy/dtbbpy	di- <i>tert</i> -butyl-2,2'-bipyridine
E1cb	elimination unimolecular conjugated base
EDTA	ethylenediaminetetraacetic acid

<i>e.g.</i>	for example (<i>lat. exempli gratia</i>)
eq.	equivalent
EI	electron ionization
ESI	electrospray ionization
<i>et al.</i>	and others (<i>lat. et alii</i>)
EtOAc	ethyl acetate
EtOH	ethanol
eV	electron volt
EWG	electron withdrawing group
fc	ferrocene
FID	flame ionization detector
FT-IR	Fourier-transform infrared spectroscopy
FD-MS	field desorption mass spectrometry
g	gram
GC	gas chromatography
h	hour
HAT	hydrogen atom transfer
HRMS	high resolution mass spectrometry
h ν	incident photon energy
<i>i.e.</i>	that is (<i>lat. id est</i>)
I_0	intensity of the incident light
^t Pr	isopropyl
IR	infrared
L	liter
LDA	lithium diisopropylamide
LED	light emitting diode
M	molar (mol/L)
Me	methyl
MeCN	acetonitrile
MeOH	methanol
mg	milligram
min	minute
mL	milliliter

mM	millimolar (mmol/L)
mmol	millimole
MS	mass spectrometry
<i>n</i> -Bu	<i>n</i> -butyl
NBu ₄ PA	tetrabutylammomium phenylacetic acid
nm	nanometer
NMR	nuclear magnetic resonance
OAc	acetoxy group
OTf	trifluoromethanesulfonate group
p.a.	per analysis
PC	photocatalyst
PE	petroleum ether
Ph	phenyl group
PhCN	benzonitrile
ppy	2-phenylpyridinato
R	alkyl-, aryl- or functional groups
r.t.	room temperature
PTFE	polytetrafluoroethylene
s	second
SCE	saturated calomel electrode
SET	single electron transfer
<i>t</i> -Bu	<i>tert</i> -butyl
TBA	tributylamine
TBATFB	tetrabutylammonium tetrafluoroborate
TEA	triethylamine
THF	tetrahydrofuran
TLC	thin layer chromatography
TMEDA	tetramethylethylenediamine
TMS	trimethylsilyl group
TsOH	toluenesulfonic acid
UV	ultra violet
Vis	visible light
vs.	against (<i>lat.</i> versus)

8.2 Curriculum Vitae

Personal Data

Name: Anna Lucia Berger
Date of birth: 01.12.1991
Marital status: Single
Nationality: German

Education

11/2016 – 12/2018	PhD in Organic Chemistry Institute of Organic Chemistry, University of Regensburg (Supervisor: Prof. Dr. Burkhard König) <i>“Photocatalytic two-electron processes as alternatives to Barbier/Grignard-type reactions”</i>
10/2014 – 09/2016	Master of Science in Chemistry Institute of Organic Chemistry, University of Regensburg Master thesis: <i>“C–H Sulfonamidation of Heteroarenes and Alkenes by Visible Light Photocatalysis”</i> (Supervisor: Prof. Dr. Burkhard König)
10/2011 – 09/2014	Bachelor of Science in Chemistry Institute of Inorganic Chemistry, University of Regensburg Title of thesis: <i>“Kristallisation von Alkalimetallhalogeniden aus flüssigem Ammoniak”</i> Supervisor: Prof. Dr. Nikolaus Korber

Memberships

11/2016 – present	Gesellschaft Deutscher Chemiker (GDCh, German Chemical Society)
11/2016 – 04/2019	DFG – Graduate Training Group GRK 1626 “Chemical Photocatalysis”

Conferences

07/2019	The 29th International Conference on Photochemistry Boulder, Colorado, USA (poster presentation)
11/2018	14th International Kyoto Conference on New Aspects of Organic Chemistry Kyoto, Japan (poster presentation)
09/2018	26. Lecture Conference on Photochemistry Garching/Munich, Germany (poster presentation)
08/2018	Summer School “Advanced Organocatalysis” ADVOCAT Cologne, Germany (poster presentation)
09/2017	26th ISHC Congress (International Society of Heterocyclic Chemistry, Regensburg, Germany)
06/2017	45th ACS National Organic Chemistry Symposium Davis, California, USA (poster presentation)
2016 – 2019	24th – 35th Seminar Days of the GRK 1626 oral contributions and poster presentations

Publications

- Anna Lucia Berger, Karsten Donabauer, Burkhard König, “Photocatalytic carbanion generation from C–H bonds – Reductant free Barbier/Grignard-type reactions”, *Chem. Sci.*, manuscript submitted.
- Qing-Yuan Meng, Tobias E. Schirmer, Anna Lucia Berger, Karsten Donabauer, Burkhard König, “Photocarboxylation of Benzylic C–H Bonds”, *J. Am. Chem. Soc.* **2019**, *141*, 11393-11397.
- Karsten Donabauer, Mitasree Maity, Anna Lucia Berger, Gregory S. Huff, Stefano Crespi, Burkhard König, “Photocatalytic carbanion generation – benzylation of aliphatic aldehydes to secondary alcohols”, *Chem. Sci.* **2019**, *10*, 5162-5166.
- Anna Lucia Berger, Karsten Donabauer, Burkhard König, “Photocatalytic Barbier reaction – visible-light induced allylation and benzylation of aldehydes and ketones”, *Chem. Sci.* **2018**, *9*, 7230-7235.
- Andreas Uwe Meyer, Anna Lucia Berger, Burkhard König, “Metal-free C–H sulfonamidation of pyrroles by visible light photoredox catalysis”, *Chem. Commun.* **2016**, *52*, 10918-10921.

DANKSAGUNG

9 Danksagung

Zunächst danke ich Prof. Dr. Burkhard König dafür, dass er mir die Möglichkeit gegeben hat meine Master- und Doktorarbeit in seinem Arbeitskreis anzufertigen. Ich bedanke mich für die hilfreichen Diskussionen und neuen Denkanstöße, aber auch für die Freiheiten eigene Ideen verfolgen zu dürfen. Außerdem möchte ich mich dafür bedanken, dass er es mir ermöglicht hat zahlreiche Konferenzen in verschiedenen Ländern zu besuchen.

Für die Übernahme des Zweitgutachtens danke ich Prof. Dr. Alexander Breder. Weiterhin danke ich Prof. Dr. Frank-Michael Matsysik dafür, dass er als Drittprüfer eintritt, und Prof. Dr. Patrick Nürnberger für die Übernahme des Vorsitzes meiner Promotionsprüfung.

Für die hervorragende Zusammenarbeit an verschiedenen Projekten, seine zahlreichen kreativen Ideen und seinen nie endenden Optimismus bedanke ich mich bei Karsten Donabauer. Außerdem danke ich Saikat Das für seine Beiträge zur photokatalytischen Zink Erzeugung, Mitasree Maity, Gregory Huff und Stefano Crespi für ihre Unterstützung im Projekt zur photokatalytischen Erzeugung von Carbanionen aus Carbonsäuren, sowie Qing-Yuan Meng für hilfreiche Diskussionen zum Thema der photokatalytischen C–H Aktivierung. An dieser Stelle möchte ich mich auch bei meinen Praktikanten Caroline Gabriel und Jessica Stahl für die Mitarbeit an meinen Forschungsprojekten bedanken.

Ich möchte mich außerdem bei Britta Badzura, Simone Strauß, Julia Zach, Dr. Petra Hilgers und Ernst Lautenschlager für ihre Hilfe bei Problem aller Art, egal ob technischer, bürokratischer oder organisatorischer Art bedanken. Mein besonderer Dank gilt Regina Hoheisel für die CV-Messungen und Dr. Rudolf Vasold für GC/MS-Messungen. Herzlich bedanken möchte ich mich auch bei Katharina Nickl für ihre Unterstützung bei sämtlichen bürokratischen Themen, vor allem aber auch für die zahlreichen gemeinsamen Kletterabende.

Außerdem bedanke ich mich bei allen Mitarbeitern der Zentralen Analytik und der NMR-Abteilung für die schnelle und gewissenhafte Bearbeitung sämtlicher Aufträge.

Für die Finanzierung von Teilen meiner Promotion und den Konferenzbesuchen danke ich dem „GRK 1626 Chemische Photokatalyse“.

Besonders bedanken möchte ich mich bei meinen Laborkollegen Karin, Karsten und Matthias für die hervorragende Stimmung im Labor, die guten Gespräche fachlicher und privater Natur und die tollen gemeinsamen Urlaube. Danke auch dafür, dass ihr meine Launen immer so tapfer ertragen habt. Ohne euch hätte die Zeit im Labor deutlich weniger Spaß gemacht.

Auch bei allen anderen aktuellen und ehemaligen Mitgliedern des AK König möchte ich mich für ihre Hilfsbereitschaft und die angenehme Arbeitsatmosphäre bedanken. Danke vor allem an Alex, Alessa, Andi, Johanna, Karin, Karsten, Matthias, Petzi, Rok, Ranit, Tobi und Ulli für die zahlreichen gemeinsamen Aktivitäten wie Kaffeepausen, Konferenzbesuche, Urlaube, Grillabende, Volleyballspiele oder gemeinsames Bouldern.

Zu Guter Letzt möchte ich meinen Freunden Alex, Isabella und Sabine, meinen Eltern und meinen Schwestern Susi und Sabine dafür danken, dass sie mich immer unterstützt haben. Vielen Dank auch an Emilia und Vincent, die immer für gute Laune in allen Situationen gesorgt haben.

Danke!